

UNIVERSAL
LIBRARY



117 122

UNIVERSAL
LIBRARY

Notice

THIS volume is the eleventh of a series constituting the official proceedings of the Institute of Metals Division of the American Institute of Mining and Metallurgical Engineers. It deals with nonferrous metals and includes papers presented at the Cleveland Meeting, Oct. 20-22, 1936 and the New York Meeting, Feb. 15-19, 1937. The complete list of publications and proceedings, including the present volume, is as follows:

1908-1911 *Transactions* of the American Brass Founders' Association: 1908, Vols. 1 and 2; 1909, Vol. 3; 1910, Vol. 4; 1911, Vol. 5.

1912-1916 *Transactions* of the American Institute of Metals, Vols. 6-10.

1917-1918 *Journal* of the American Institute of Metals, Vols. 11-12.

1919-1926 TRANSACTIONS of the American Institute of Mining and Metallurgical Engineers, Volumes 60, 64, 67, 68, 69, 70, 71 and 73.

1927-1928 PROCEEDINGS of the Institute of Metals Division of the American Institute of Mining and Metallurgical Engineers, two volumes, of which the later is now designated Vol. 78 of the A. I. M. E. TRANSACTIONS.

1929-1937 TRANSACTIONS of the American Institute of Mining and Metallurgical Engineers, Volumes 83, 89, 93, 99, 104, 111, 117, 122 and 124, Institute of Metals Division.

COPYRIGHT, 1937, BY THE
AMERICAN INSTITUTE OF MINING AND METALLURGICAL ENGINEERS
(INCORPORATED)

PRINTED IN THE UNITED STATES OF AMERICA

FOREWORD

It is now ten years since the American Institute of Mining and Metallurgical Engineers started the policy of devoting one volume of its TRANSACTIONS each year to the papers and discussion of the Institute of Metals Division. Including the present one, eleven volumes have now been published, containing 292 papers (approximately 5400 pages). Many of the papers in these volumes are of fundamental importance and the volumes in general constitute a reference library that is indispensable to physical metallurgists.

Of the various papers published in these volumes those on precipitation-hardening constitute a very important classification, for they contribute much to both the theory and practice of the utilization of the phenomenon. The present volume is no exception in this respect, for in it there are four papers dealing with precipitation-hardening, which, together with the discussion, add much to the subject.

Fifteen years ago the Institute of Metals Division listened to its first annual lecture. Since then the roll of lectures has expanded to contain the names of many distinguished men from both this country and abroad. This year we take pleasure in adding the name of Dr. R. S. Hutton, whose lecture on Refractories was presented at our New York meeting.

In 1934 the Division instituted a program of making an annual award for the best paper published during the past three years. This year the award was presented to Arthur Phillips and R. M. Brick for their paper "Effect of Quenching Strains on Lattice Parameter and Hardness Values of High-purity Aluminum-copper Alloys," published in volume 111 of the TRANSACTIONS.

It is customary for the chairman to extend his thanks to the members of the Papers and Publications Committee for their work in caring for the publications of the Divisions and arranging programs for the meetings. These duties have been carried out this year under Dr. R. F. Mehl as Chairman and Dr. D. K. Crampton as Vice-chairman, with the usual sacrifice of personal time and energy that is so often accepted without too much consideration, merely because it is so essential to the office. To Dr. Mehl and Dr. Crampton and their associates on the committee, the Division owes its thanks for this volume.

ALBERT J. PHILLIPS, *Chairman,*
Institute of Metals Division.

PERTH AMBOY, N. J.
June 19, 1937

CONTENTS

	PAGE
Foreword A. J. Phillips	3
Institute of Metals Division Lectures and Lecturers	7
A I.M.E. Officers and Directors	8
Institute of Metals Division Officers and Committees	9
Institute of Metals Division Annual Award Certificate	10

PAPERS

Refractories By R. S. HUTTON	13
The Stereographic Projection. By CHARLES S. BARRETT	29
Solid Solubilities of the Elements of the Periodic Subgroup Vb in Copper. By J. C. MERTZ AND C. H. MATHEWSON	59
Equilibrium Relations in Aluminum-magnesium-zinc Alloys of High Purity. By W. L. FINK AND L. A. WILEY (with discussion)	78
Equilibrium Relations in the Nickel-tin System. By WILLIAM MIKULAS, LARS THOMASSEN AND CLAIR UPTEGROVE (with discussion)	111
Aging Phenomena in a Silver-rich Copper Alloy. By MORRIS COHEN (with discussion).	138
Age-hardening of Aluminum Alloys, II—Aluminum-magnesium Alloy. By WILLIAM L. FINK AND DANA W. SMITH (with discussion)	162
Precipitation-hardening and Double Aging. By R. H. HARRINGTON (with discussion).	172
Notes on Etching and Microscopical Identification of the Phases Present in the Copper-zinc System. By J. L. RODDA.	189
An Investigation to Develop Hard Alloys of Silver for Lining Ring Grooves of Light Alloy Pistons. By CLAUS GUENTER GOETZEL	194
Lead Coating of Steel. By J. L. BRAY (with discussion).	199
Relations between Stress and Reduction in Area for Tensile Tests of Metals. By C. W. MACGREGOR (with discussion)	208
Influence of Temperature on Elastic Limit of Single Crystals of Aluminum, Silver and Zinc. By RICHARD F. MILLER AND W. E. MILLIGAN (with discussion).	229
Equipment for Routine Creep Tests on Zinc and Zinc-base Alloys, and an Exam- ple of Its Application. By J. RUZICKA (with discussion).	252

	PAGE
Fatigue Properties of Five Cold-rolled Copper Alloys. By WILLIAM B. PRICE AND RALPH W. BAILEY (with discussion).	271
Thermal and Electrical Conductivities of Aluminum Alloys. By L. W. KEMPF, C. S. SMITH AND C. S. TAYLOR (with discussion).	287
Primary Crystallization of Metals. By F. R. HENSEL.	300
Segregation in Single Crystals of Solid Solution Alloys. By ARTHUR PHILLIPS AND R. M. BRICK (with discussion)	313
Diffusion of Copper and Magnesium into Aluminum. By R. M. BRICK AND ARTHUR PHILLIPS (with discussion)	331
Effect of Reversed Deformation on Recrystallization. By PAUL A. BECK (with discussion).	351
Studies upon the Widmanstätten Structure, IX—The Mg-Mg ₂ Sn and Pb-Sb Systems. By GERHARD DERGE, ARTHUR R. KOMMEL AND ROBERT F. MEHL	367
Lattice Relationships Developed by the Peritectic Formation of Beta in the Copper-zinc Systems. By ALDEN B. GRENINGER (with discussion)	379
Index	393

THE INSTITUTE OF METALS LECTURE

AN annual lectureship was established in 1921 by the Institute of Metals Division, which has come to be one of the important functions of the Annual Meeting of the Institute. In 1934 the Division established the custom of presenting a certificate to each lecturer.

A number of distinguished men from this country and abroad have served in this lectureship. The roll is quoted below:

- 1922 Colloid Chemistry and Metallurgy. By Wilder D. Bancroft.
- 1923 Solid Solution. By Walter Rosenhain.
- 1924 The Trend in the Science of Metals. By Zay Jeffries.
- 1925 Action of Hot Wall: a Factor of Fundamental Influence on the Rapid Corrosion of Water Tubes and Related to the Segregation in Hot Metals. By Carl Benedicks.
- 1926 The Relation between Metallurgy and Atomic Structure. By Paul D. Foote.
- 1927 Growth of Metallic Crystals. By Cecil H. Desch.
- 1928 Twinning in Metals. By C. H. Mathewson.
- 1929 The Passivity of Metals, and Its Relation to Problems of Corrosion. By Ulick R. Evans.
- 1930 Hard Metal Carbides and Cemented Tungsten Carbide. By S. L. Hoyt.
- 1931 X-ray Determination of Alloy Equilibrium Diagrams. By Arne Westgren.
- 1932 The Age-hardening of Metals. By Paul D. Merica.
- 1933 Present-day Problems in Theoretical Metallurgy. By Georg Masing.
- 1934 Ferromagnetism in Metallic Crystals. By L. W. McKeehan.
- 1935 Gases in Metals. By C. A. Edwards.
- 1936 Diffusion in Solid Metals. By Robert F. Mehl.
- 1937 Refractories. By R. S. Hutton.

A. I. M. E. OFFICERS AND DIRECTORS

For the year ending February, 1938

PRESIDENT AND DIRECTOR
R. C. ALLEN, Cleveland, Ohio

PAST PRESIDENTS AND DIRECTORS
H. A. RUEHLER, Rolla, Mo.
JOHN M. LOVEJOY, New York, N. Y.

VICE-PRESIDENT, TREASURER AND DIRECTOR
KARL EILERS, New York, N. Y.

VICE-PRESIDENTS AND DIRECTORS
HENRY KRUMB, New York, N. Y. H. G. MOULTON, New York, N. Y.
PAUL D. MERICA, New York, N. Y. HARVEY S. MUDD, Los Angeles, Calif.
WILFRED SYKES, Chicago, Ill.

DIRECTORS
W. B. DALY, Butte, Mont. WILLIAM B. HEROY, New York, N. Y.
H. T. HAMILTON, New York, N. Y. FRANK L. SIZER, San Francisco, Calif.
WILBER JUDSON, Newgulf, Tex. L. E. YOUNG, Pittsburgh, Pa.
C. K. LEITH, Madison, Wis. JOHN M. BOUTWELL, Salt Lake City,
R. M. ROOSEVELT, New York, N. Y. Utah
ERSKINE RAMSAY, Birmingham, Ala. ERLE V. DAVELER, New York, N. Y.
SELWYN G. BLAYLOCK, Trail, B. C., W. M. PEIRCE, Palmerton, Pa.
Canada BRENT N. RICKARD, El Paso, Tex.
LOUIS S. CATES, New York, N. Y. GEORGE B. WATERHOUSE, Cambridge,
JOHN L. CHRISTIE, Bridgeport, Conn. Mass.
ELI T. CONNER, Scranton, Pa.

SECRETARY
A. B. PARSONS, New York, N. Y.

DIVISION CHAIRMEN—Acting as Advisers to the Board
A. J. PHILLIPS (Institute of Metals), Maurer, N. J.
M. ALBERTSON (Petroleum), Houston, Tex.
F. B. FOLEY (Iron and Steel), Philadelphia, Pa.
J. B. MORROW (Coal), Pittsburgh, Pa.
W. B. PLANK (Education), Easton, Pa.
CHESTER A. FULTON (Industrial Minerals), Baltimore, Md.

STAFF IN NEW YORK

Assistant Secretaries

E. H. ROBBE
LOUIS JORDAN

Assistant Treasurer
H. A. MALONEY

Assistants to the Secretary

JOHN T. BREUNICH
E. J. KENNEDY, JR.

Manager, "Mining and Metallurgy"
WILLIAM HANDLEY

INSTITUTE OF METALS DIVISION

Chairman, ALBERT J. PHILLIPS, Maurer, N. J.
Past Chairman, E. H. DIX, JR., New Kensington, Pa.
Vice-chairman, R. H. LEACH, Bridgeport, Conn.
Vice-chairman, R. F. MEHL, Pittsburgh, Pa.
Treasurer, W. M. CORSE, Washington, D. C.
Secretary, LOUIS JORDAN, 29 W. 39 St., New York, N. Y.

Executive Committee

W. H. BASSETT, JR., ¹ Hastings-on-the-Hudson, N. Y.	E. E. SCHUMACHER, ³ New York, N. Y.
W. H. FINKELDEY, ² New York, N. Y.	C. S. SMITH, ² Waterbury, Conn.
W. E. REMMERS, ¹ Chicago, Ill.	CARL E. SWARTZ, ³ Cleveland, Ohio
H. J. ROAST, ¹ Montreal, Que.	E. M. WISE, ³ Bayonne, N. J.
	LYALL ZICKRICK, ² Schenectady, N. Y.

Finance

W. M. CORSE	JOHN L. CHRISTIE, Chairman	
	E. H. DIX, JR.	S. SKOWRONSKI
	W. M. PEIRCE	

Data Sheet

	JEROME STRAUSS, Chairman	
W. I. FINK	E. E. SCHUMACHER	E. M. WISE
W. E. REMMERS		LYALL ZICKRICK

Papers and Programs

	D. K. CRAMPTON, Chairman	
	CYRIL S. SMITH, Vice-chairman	
E. A. CAPILLON	E. R. JETTE	E. E. SCHUMACHER
FRANCES H. CLARK	R. F. MEHL	CLAIR UPTHEGROVE
W. L. FINK	ARTHUR PHILLIPS	R. S. WILLIAMS
	CARL H. SAMANS	

Annual Lecture

C. H. MATHEWSON	W. M. CORSE, Chairman	
L. W. MCKEEHAN	R. F. MEHL	GEORG SACHS
		W. P. SYKES

Annual Award

	S. L. HOYT, Chairman	
D. K. CRAMPTON	J. T. NORTON	N. B. PILLING
	A. J. PHILLIPS	

Membership

	E. M. WISE, Chairman	
R. F. MEHL	H. J. ROAST	CARL E. SWARTZ
W. T. MORGAN		K. R. VAN HORN

Nominating

	W. M. PEIRCE, Chairman	
E. H. DIX, JR.	ZAY JEFFRIES	J. W. SCOTT
	L. W. MCKEEHAN	

¹ Until February 1938. ² Until February 1939. ³ Until February 1940.

ANNUAL AWARD CERTIFICATE OF THE INSTITUTE OF METALS DIVISION

In 1933, the Institute of Metals Division of the American Institute of Mining and Metallurgical Engineers established its annual award of an engraved certificate to the author or authors of the paper that in the opinion of the award committee represents the most notable contribution to metallurgical science among the papers that have been accepted by the Division for presentation at one of its meetings and have been published by the Institute within the three years preceding the date of award. The award is made by the Division each February.

There are no restrictions with respect to nationality, age or occupation of the author or authors.

Awards have been made as follows:

- 1934 Robert F. Mehl and Charles S. Barrett: Studies upon the Widmānstätten Structure, I—Introduction. The Aluminum-silver System and the Copper-silicon System. *TRANSACTIONS* (1931) **93**, 78–110.
- 1935 E. A. Anderson, M. L. Fuller, R. L. Wilcox and J. L. Rodda: The High-zinc Region of the Copper-zinc Phase Equilibrium Diagram. *TRANSACTIONS* (1934) **111**, 264–292.
- 1936 Cyril S. Smith and W. Earl Lindlief: A Micrographic Study of the Decomposition of the Beta Phase in the Copper-aluminum System. *TRANSACTIONS* (1933) **104**, 69–105.
- 1937 Arthur Phillips and R. M. Brick: Effect of Quenching Strains on Lattice Parameter and Hardness Values of High-purity Aluminum-copper Alloys. *TRANSACTIONS* (1934) **111**, 94–112.



R. S. HUTTON

Institute of Metals Division Lecturer, 1937

Refractories

By R. S. HUTTON*

(Institute of Metals Division Lecture†)

WHEN I had the honor of receiving an invitation to give the Institute of Metals Lecture, it occurred to me that it might be of interest to review the advances which have been made in refractories, considering how important these materials of construction are in the carrying out of many metallurgical operations and what a large factor they represent in our costs of production. Frankly, I can claim no recent contact with the refractories industry and what little work I myself have been concerned with has been rather unorthodox in character. However, perhaps in consequence of this, I can approach the review without bias and include some suggestions which may prove stimulating or provocative to some of you, who have a more intimate knowledge of refractories and their uses than I possess.

It is neither possible nor necessary for me to survey the progress of industrial refractories, for this has been so thoroughly undertaken by others¹⁻⁷ in recent publications. Perhaps the best way to get a broad picture of this progress is to compare the Faraday Society Symposium on Refractory Materials 20 years ago⁸, containing a report on one of the first attempts at standardized testing, with the American Society for Testing Materials Committee Report of February 1935. Suffice it to say, lest my provocative remarks be misunderstood, that I do appreciate that great advances have been made, particularly by companies that have established their own research laboratories and by universities and cooperative research institutes working for the common weal of groups of manufacturers or for national and international progress.

The scientific study of the constitution diagrams of binary and ternary refractory oxides, which American workers have been foremost in undertaking,† led by the work of the Geophysical Laboratory at Washington, has laid a firm foundation for the whole subject. It should be remembered, however, that to a much greater degree than with the constitution of metal alloys, the equilibrium conditions are so sluggishly arrived at

* Goldsmiths' Professor of Metallurgy, University of Cambridge, England.

† Presented at the New York meeting, February, 1937. Sixteenth annual lecture. Manuscript received at the office of the Institute Feb. 12, 1937.

¹ References are at the end of the paper.

‡ As a typical example, the diagram $\text{SiO}_2\text{-Al}_2\text{O}_3$ of Bowen and Greig is shown in Fig. 1. See also F. P. Hull and H. Inaley⁹.

that, in many practical applications, we may with appreciation accept the definition of this field as covering the "chemistry of frustrated reactions." The applications of petrological and X-ray methods of examination are also proving most fruitful in advancing our knowledge. On the manufacturing side, high-pressure forming, de-airing and electrocasting represent major advances in recent years, as also does the utilization of new materials, both from diligently sought out natural resources or from artificially produced materials such as silicon carbide and fused alumina.

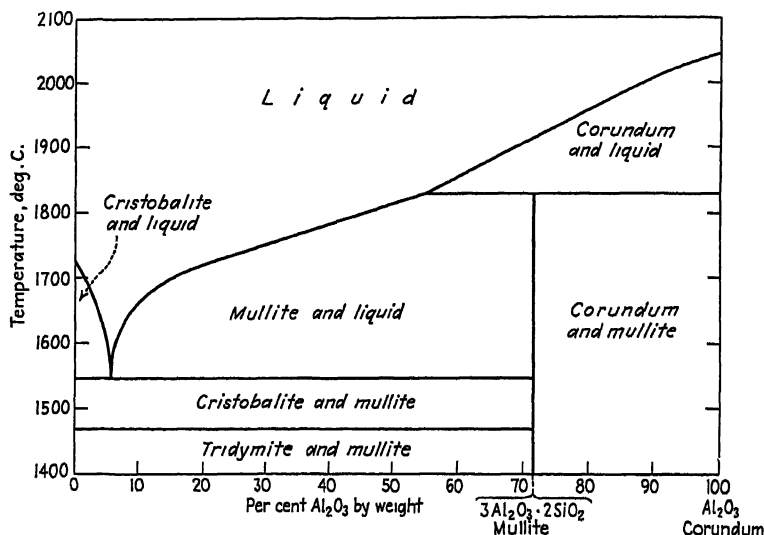


FIG. 1.—SILICA-ALUMINA DIAGRAM (BOWEN AND GREIG).

Above all, the industry has been advanced by the recent cooperative effort for standardization of testing methods in which again America has taken a foremost position.

The insistent call for progress in refractories seems to be due (1) to the urgent demand for more rapid metallurgical production, which entails higher temperatures and the concomitant more severe conditions of service; and (2) to the greater consideration which is being given to the thermal efficiencies of metallurgical processes. In both these directions we are still only on the bottom rungs of our ladder of ascent.

TEMPERATURE CONDITIONS

As an example of the severe conditions which exist let us consider the open-hearth production of steel, of which present-day temperature conditions have recently been investigated with the help of a new form of optical pyrometer^{10,11}:

Temperature of steel, after melting down, 1650° to 1750° C.

Temperature of flame, after melting down, 1800° to 2050° C.

Temperature of refractory roof, after melting down, 1670° to 1720° C.

These temperature measurements were made with a furnace built with a silica roof and the limitation of temperature is entirely due to the fact that any higher temperature would entail the very rapid melting of the roof and destruction of the whole furnace. Whereas it is readily possible, by suitable regeneration, by the selection of combustible gases, and by utilizing recent knowledge of the importance of radiation from luminous and nonluminous gases^{10,12}, to attain flame temperatures of 2700° to 2800° C.—i.e., about 1000° C. higher than the maximum steel temperature of present practice—we are probably limited to an increase of 100° to 200° even if we replace the silica-brick roofs with chrome-magnesia or any other of the better refractories at present available commercially. Although we now know that radiation is far more important than convection for the transmission of heat units from the burning gases to the metal, it is obvious that we need as high a “temperature head” as possible, and the fact that the refractories can only withstand such a low temperature shows how radically they fail to attain any reasonable standard for designing much of our furnace equipment.

It is needless for me to point out, however, that the problem of furnace refractories is not merely one of the melting point of the refractory, for, as we all know, the service requirements are complex and severe, as I shall have occasion to refer to later. On the other hand, it is not widely enough appreciated how vital it is for improvement of our metallurgical production processes to attain higher temperatures than those to which we are limited at the present time. Apart from the prospect of greater throughput and more rapid production, we already know from experience

TABLE 1.—*Thermal Efficiencies of Some Furnaces*

Furnace	Thermal Efficiency, Per Cent	Authority
Open-hearth steel furnace:		
Useful heat in steel (stack losses, 40 per cent; radiation and other losses, 40 per cent).....	20	Haslam and Russell: <i>Fuels and their Combustion</i> , 535, 1926. See also Bone and Himes: <i>Coal, Its Constitution and Uses</i> , 487, 607, 1936; and W. Heiligenstaadt: <i>Wärmetechnische Rechnungen für Bau und Betrieb von Oefen</i> . 1935.
Coke ovens:		
Useful heat (stack losses, 20 per cent; radiation losses, 15 per cent).....	65	
Coke-pit-fired crucible furnaces for brass or steel.....	5-10	
Forging, annealing and rolling-mill furnaces.....	8-48	Trinks: <i>Industrial Furnaces</i> , 3d Ed. 1934.
Electric-arc steel furnaces.....	Up to 67	Robiette: <i>Electric Melting Practice</i> , 51, 178, 1925. (These percentages are on electric energy input.)
Electric coreless induction furnaces...	62	

in electric steel melting how favorably the slag reactions can be influenced and how beneficial from the point of view of reduced inclusions and gases is the attainment of a higher temperature of melting.

If we turn to the problem of thermal efficiency, it is even more obvious how important are the refractories to our metallurgical processes. Whereas in modern steam-boiler practice, despite furnace-chamber temperatures of 1300° C., we have attained a 90 per cent efficiency in the utilization of the thermal units of our fuel, our metallurgical furnaces are still for the most part highly inefficient, as shown in Table 1.

FUEL ECONOMY

It is astonishing how limited is the attention given to fuel economy at the majority of metallurgical works. Except in the most highly organized establishments, a staff of fuel economists engaged to control this major factor of process expenditure is seldom found, and when one has the opportunity of examining a cross section of an industry one finds surprising divergencies between the best and the worst practice of competing firms.

This question of fuel economy is most intimately connected with refractories, for if we analyze out the heat losses they come under one or other of the following headings:

1. Stack losses, mainly sensible heat carried away in the flue gases and primarily due to:
 - a. Excess air and other forms of inefficient combustion.
 - b. Limited temperature gradient; e.g., in high-temperature processes not having the combustion gases hot enough to assure a rapid heat transfer by radiation and convection, which as shown above may be due to limitation of refractories to withstand high temperature.
 - c. Inefficient recuperation or regeneration of the heat in flue gases.
2. Radiation losses primarily due to:
 - a. Inefficient heat insulation.
 - b. Large volume of furnace structure and large exposed surface of furnace.
 - c. Too slow heat transfer, prolonging the duration of the process for any given plant capacity.

If we can visualize such an operation carried out in a proper scientific manner, we should have precise quantitative data of the location and amount of the items of heat loss, and with such a picture before us the crude economic wastefulness would surely offer a powerful incentive to striving for drastic improvements. Some of these are already available, others may need further advance in the quality of the refractories, but I venture to believe that the bugaboo of prime cost of construction has for far too long hindered rapid advance. Does it really pay to construct

furnaces with a life of only a few hundred heats, with high upkeep costs, and with an over-all efficiency of, say, 20 per cent? Does a silica brick at 5¢ really show an over-all economy over a superbrick at 50¢ or even at a dollar? Fuel economy, and above all long life and long runs between repairs of furnace structures, may go far to offset such high costs and render the use and development of super-refractories of real value to the progress of the metallurgical industries.

REQUIREMENTS

What, then, are the requirements? The most difficult of achievement is a high-temperature refractory suitable for use at temperatures well above 2000° C. without melting, of sufficient hot strength, resistant to the wear and tear of the persistent streams of combustion gases and, above all, capable of withstanding attack by slags and fluxes and the clouds or jets of basic or acid discharges projected upon it from the molten metal. Fire clay has given place to silica and to magnesite and recently to chrome-magnesite bricks, each in turn showing important but relatively small advantages¹³, offset to a large extent by the ever-increasing rigor of the operation of the process and fundamentally hampered by all of them having temperature limits below what is really wanted.

Another requirement is for materials and design of our furnaces to reduce the appalling figure of over 40 per cent in the radiation losses. Although this is in part due to the limitation referred to above of refractories for the lining of the furnace, which has necessitated water-cooling and other means to prevent the destruction of the internal surfaces, it is in great measure due to the neglect until recent years of the study of insulating refractories.

I myself remember the day when almost the same fire-clay refractories were used for furnace walls required to box in the heat as for crucibles and muffles required to give optimum conductions of heat to the charge; and in default of any existing information on the thermal conductivity of refractories, I had to undertake the first of such measurements¹⁴. In this work attention was also directed to the necessity for utilizing stratified insulation, so that while the hot internal faces of the furnace could be made of materials stable at high temperatures, progressively less refractory materials of higher insulation properties could be employed for the walls.

This idea of stratification is capable of considerable development and might result in much more than the use of successive layers of different bricks. The temperature slope in furnace walls is sometimes very steep and composite bricks with well graded structures should find most effective applications.

In recent years great advances have been made in heat insulation and we now have a whole range of bricks, some of which can withstand face

temperatures up to 1500° C. The thermal conductivity and the specific heat of refractories are fortunately at last receiving the attention they deserve, for there is tremendous scope for development and for a wise selection and application of improved materials. The requirements of service are so varied that this branch of the subject takes us far beyond merely avoiding heat losses. Whereas in lagging we ask for insulation, in recuperators we need high conductivity and in regenerators both high heat-storing capacity and, if it can be secured at the same time, high thermal diffusivity, so that the brickwork can rapidly take up as much as possible of the thermal units from the momentary glancing contact with the waste gases and give them up again as quickly as possible when the reverse air heating is turned on. It is unfortunate that great discrepancies still exist between the data for thermal conductivity at high temperature, provided by individual investigators—for instance, some results indicate that fused magnesia increases steeply in thermal conductivity and silicon carbide decreases steeply with rise of temperature, whereas others show almost constant or reversed values. (See Fig. 2; also Golla and Laube¹⁵ and Salmang and Frank¹⁶.) Then again there are many cases in which the time factor calls sometimes for the lowest possible "thermal ballast" of the furnace structure, if rapid or intermittent heating is required, and at others for quite the opposite, when slow and continuous processes are sought. Surely in this field there is still much scope for the employment of heat physicists, who seem to be more active in the field of electric heating furnaces^{17,18} than in connection with direct fuel consumers, where much larger aggregate costs are entailed.

No review of refractories could be made without some reference to silicon carbide and the remarkable development work which followed its discovery by E. G. Acheson. Despite its limitations in oxidizing atmosphere, which render it unsuitable for many ordinary furnace refractory bricks, its outstanding properties of stability up to temperatures of 2500° C. and of high thermal conductivity provide it with a prominent position as a constructional material for thermal recuperators, for electric heating resistors, for zinc retorts and in other special applications. The discovery of the late F. A. J. Fitz Gerald of its recrystallization⁴⁵ is perhaps the first example of bonding by sintering, which has lately become so important for oxide refractories. The all too short review of super-refractories by F. J. Tone⁷², and the papers by M. L. Hartmann²⁰ and colleagues, provide indications of some of the properties and uses of silicon carbide.

The ideal high-temperature refractory must be infusible and also possess adequate strength and coherence at the service temperatures; in addition, it should not disintegrate when exposed to pressure or to sudden changes of temperature, and it needs to be highly resistant to attack by any gases, vapors, metals, slags and fluxes with which it may come in contact while forming part of the furnace structure.

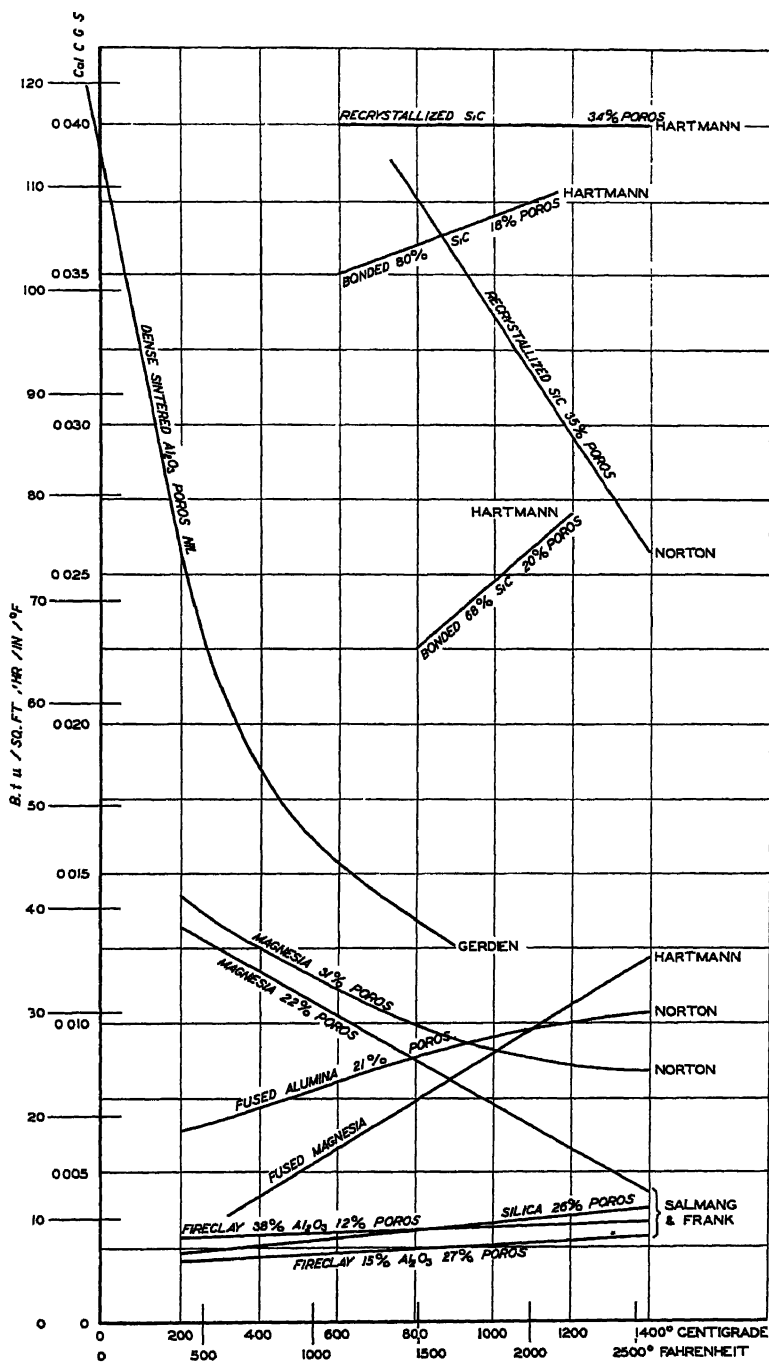


FIG. 2.—THERMAL CONDUCTIVITIES (APPROXIMATE).

These ideals are admittedly difficult of achievement, but considerable progress has been made by systematic study and selection. Fusibility and behavior to chemical attack are basic properties of the individual refractory components and to a certain extent can be foretold from available data. Whether a refractory brick will maintain its form and structure for a long life under load and with cycles of steep temperature change, is by no means so easy to foresee. The struggle against "spalling" has at least demonstrated that it is not simply a question of thermal expansion and contraction with which we have to deal, and even magnesite bricks of superior spalling resistance are now available and depend mainly on improved methods of molding.

DIFFICULTIES IN ATTAINING IDEAL

It seems to me that the major hindrances to the achievement of the ideal refractory in these respects lie in the instability of the components which are utilized and in the fact that we are dependent in most cases upon the cementing together of refractory grains by ceramic bonds, frequently of quite different physical properties, both as regards thermal expansion and melting point, compared with those of the grains themselves.

If this be true (see Fig. 3) even to a partial extent, surely our road lies in the use of more stable and uniform components, fused or thoroughly shrunk refractory grain of as high a purity and uniformity as possible, and the development of autogenous sintering processes for their agglomeration. Metaphorically we may look upon present-day industrial refractory bricks with the same disappointment that we should view a metal made up of granules glued or at the most soldered together, in comparison with metal cast or autogenously welded. It happens that a good deal of laborious study has been devoted to this other aspect of refractories, but so far almost exclusively from the point of view of laboratory vessels, and it may not be amiss to review some of this work in the hope that this may stimulate its application to the major industrial field.

These super-refractories for laboratory work possess two main characteristics: (1) they are fired at such high temperatures that the grains are sintered or fritted together and caused to recrystallize and produce a solid and strong structure, with little if any intermediate ceramic bond; (2) they are made of highly purified and single-phase constituents or purposely chosen admixtures of constituents. I believe that the prime cause of hesitation to develop large-scale production in this direction lies in the fear that costs must necessarily be prohibitive. All new ventures at times need vision to overcome this hindrance. In metallurgy there are countless examples overcome by grim determination, which has made such metals as aluminium, magnesium, and vanadium relatively cheap handmaidens of civilization. No one can surely believe, in this electric age and with oxygen gas available at less than the cost of the cheapest

town gas if we really set out to make it^{21,22}, that high temperatures are out of our reach economically. Again, pure refractory oxides are expensive only when no one has yet developed their large-scale production. Pure alumina is already available on a vast scale for the production of the

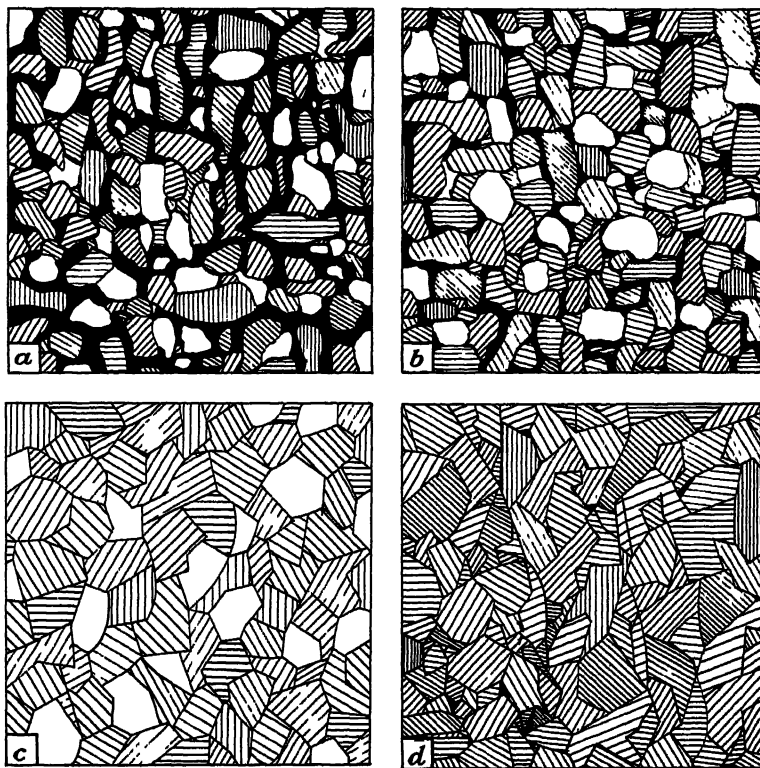


FIG. 3.—STRUCTURE OF REFRACTORIES (DIAGRAMS).

Black regions represent ceramic bond; white regions, pores, and hatched areas grog or granular refractory.

a. Two-phase material made up of grog or refractory grains cemented with relatively large proportion of ceramic bond; 25 per cent porosity.

b. Two-phase material but much smaller proportion of ceramic bond; 25 per cent porosity.

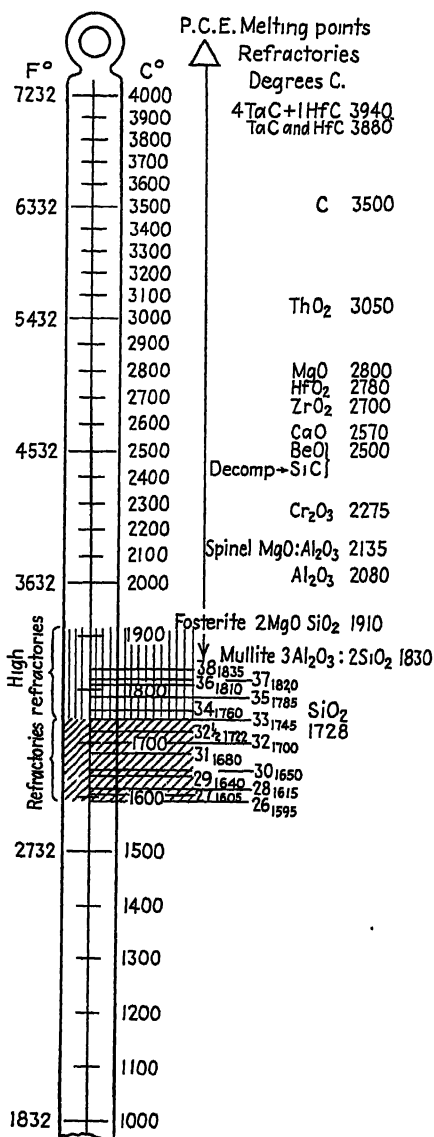
c. Single-phase sintered material but with normal porosity.

d. Dense sintered single-phase material, negligible porosity.

metal, purified zirconia, magnesia and most of the other potential requirements are to be had at a cheap price, if we can muster up the will to make them. So far as the costs of electric energy are concerned, whether this is required for the production of the raw material or for firing of the formed refractories, such data as are available indicate that this factor will certainly not be prohibitive. On a small scale I have produced recrystallized magnesia with 1.17 kw-hr. per kilo, and it is said that fused alumina

can be produced for less than 3 kw-hr. per kilo and silicon carbide for 7 kw-hr. per kilo.

Perhaps an example from the borders of the refractories industry may



serve to drive home my argument. In the year 1903, small fused-silica tubes and vessels made with oxy-hydrogen blowpipe were available in Europe at a price of 1 Mark per gram, equivalent to, say, \$225,000 per short ton, and the makers held out no hopes of a reduction. The application of electric heating which I introduced in 1902 led to the establishment of a flourishing industry in which vessels up to 200 U. S. gallons capacity have been produced, and the price promptly fell to less than one-hundredth of the figure quoted above and is now in some cases as low in Europe as \$60 per short ton²³⁻²⁵.

The extreme limit of every refractory is its melting point, so let us look at the data which we have available. (See Fig. 4.) How great are the possibilities if we could use these pure materials, and not weaken them by inter-crystalline bonds of lower melting points! For instance, as Sosman⁷⁰ has pointed out, pure alumina will not melt below 2040° but if we bond it even with the smallest amount of clay we have merely a cemented agglomerate whose bond becomes fluid at 1545° C.

Next to fusibility, we are concerned with the changes which occur when the grains of the

FIG. 4.—MELTING POINTS OF REFRACTORIES.

refractories are heated up from normal to service temperatures. In most cases it appears undoubted that a high-temperature pretreatment or even a fusion of the raw material affords advantages, not only in limiting subsequent shrinkage but

in rendering the material more resistant to attack by metals, oxides and fluxes.

The recent development of high-pressure molding for ordinary refractories has proved one of the most valuable technical advances and scientific work is throwing light on its mechanism, which appears to be largely due to very localized high temperatures at the frictional contact surfaces of the grains^{26,27}. In this connection, the advantage of rapid repetitive pressings, with momentary intermediate releases, as is adopted in some of the processes of mineral briquetting may be worthy of attention. So far as the sintering process is concerned, there is ample evidence that even with technically pure materials an effective bonding can be secured by raising the temperature of powders, the particles of which are in sufficiently intimate contact.

Tammann, for instance²⁸, found that fritting commences at the following temperatures: CaO, 1112° C.; Al₂O₃, 1160° C.; MgO, 1283° C.; SiO₂, 880° C.; kaolin, 1037° C. Hedvall²⁹ differentiates weak sintering due to shrinkage effects from strong bonding commencing at the recrystallization temperature. Many have been disappointed with such sintering processes of making refractory bricks and vessels because they have not utilized a sufficiently high firing temperature. Ryschkewitz points out the great difference between the structure of formed alumina fired at 1800° and 1900°C. and considers that higher temperatures of at least 2000° C. are essential for magnesia and zirconia.

As shown by some of the earlier experimenters^{30,37} and confirmed by most of those who have worked in this field up to the present time, the sintering is greatly facilitated by the presence of a small proportion of low-fired powder in the agglomerate and by a selected variation in the grain size of the powders, it is also sometimes most helpful to employ "mineralizing" or "activating" agents such as chlorides, fluorides or boracic acid, which after serving this function are volatilized during the high-temperature firing. Another method which sometimes is effective for securing intercrystalline growth is to expose the mass temporarily to a reducing atmosphere or to combine with it a small amount of some organic material, which after incineration has the same action.

All this demonstrates how vital is the recrystallization process; whether this be effected by the well-known propensity of large grains to grow at the expense of small ones, by localized vaporization or by the more occult phenomena of surface activation. The physicochemical work in progress in this field should be of vital interest and importance^{31,32,33}.

Beyond the sintering process itself there remains much stimulating thought in the work of Ruff, von Wartenberg, Bunting and others on the solid solutions of refractory oxides. We are beginning to realize the innate limitations of pure magnesia and have indications of its modification and improvement by spinel formation with such oxides as Cr₂O₃ and

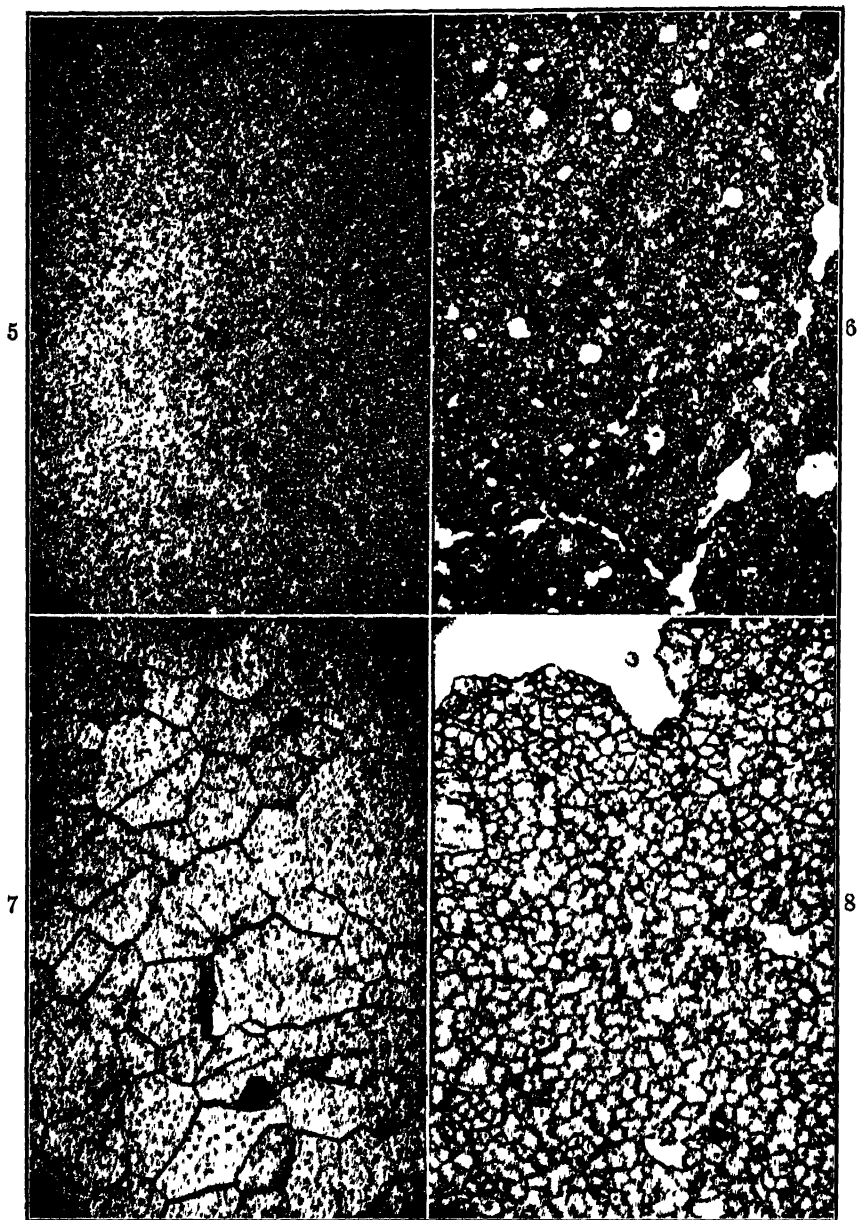


FIG. 5.—DENSE SINTERED PURE Al_2O_3 REFRACTORY.

FIG. 6.—DENSE SINTERED MgO REFRACTORY.

FIG. 7.—SOLID FUSED MAGNESIA.

FIG. 8.—HIGHLY SINTERED MAGNESIA.

All $\times 26$.

I am indebted to Prof. C. E. Tilley, of the Mineralogical Department, University of Cambridge, for the photographs of thin sections of these refractory oxides.

Fe_2O_3 but these also deserve closer scientific study and the properties of sintered masses of such products free from silicate bonding should be determined.

TABLE 2.—*Degussa Refractories*

Material	Melting Point, Deg. C.	Maximum Service Temperature, Deg. C.	Porosity	Hot Strength: Softening Commences 2 Kg per Sq Cm., Deg. C.	Sensitivity to Sudden Change of Temperature
Dense sintered:					
Al_2O_3	2050	1950	Negligible	1730	—
Spinel (= $\text{MgO} \cdot \text{Al}_2\text{O}_3$) ..	2135	2000	Negligible	1730	+
BeO	2500	2200	Negligible	2150	—
ZrO_2	2700	2500	Marked	2000	+
ZrSiO_4	2500 ?	1750	Marked	1500	—
MgO (fused)	2800	2200	High	2000	+
MgO (calcined)	2800	2400	Negligible	2000	+
ThO_2	3000	2700	Negligible over 1900		+

The accompanying tabulation of some of the properties of densely sintered oxide refractories (Table 2) will serve to indicate what has already been accomplished on a relatively small scale. In parallel with these results, which have been achieved by Ryschkewitsch and his co-workers in Germany, both American and English work have largely confirmed the results which have served to provide most useful apparatus for metallurgical research.

ACCOMPLISHMENTS AND OUTLOOK

I have not time to refer to the work of all the pioneers in this field, so must limit myself to the select bibliography on high-temperature refractories attached to this lecture (references 36 to 80). Among these pioneers many have worked purely for the scientific interest of the subject and others in order to provide themselves with research apparatus required for their own metallurgical or other investigations. I may perhaps be allowed to mention such names as: Otto Ruff, H. von Wartenberg, R. Rieke, and E. Ryschkewitsch in Germany, W. H. Swanger and F. R. Caldwell and others at the Bureau of Standards; also H. M. Goodwin, R. B. Sosman, Louis Navias, H. K. Richardson and others in the United States, Donald Turner and others at the National Physical Laboratory, England.

One of the most important considerations, as already pointed out, is the resistance to slag and oxide attack, and there is evidence from the experience with laboratory crucibles made of these oxides (see, for instance, references 34, 69, 71, 80) that the purity and, above all, low

porosity of these products renders them exceptionally resistant. The technical studies of slag and flux attack also demonstrate the importance of structure, the outstanding example being the resistance of electrocast mullite refractories in glass tanks³⁵. One cannot, of course, pretend that the large-scale production of such super-refractories is in sight but I hope that I have not taken up too optimistic an attitude in urging that they are within our reach if we approach the subject from such a standpoint as I have proposed. Let us, at any rate, take more active interest in higher temperatures of pretreatment and firing, in the sintering process, in the provision of purer raw materials, and in the further exploration of the constitution and properties of solid solutions of the refractory oxides, et cetera.

REFERENCES

1. F. H. Norton: Refractories. New York, 1931. McGraw-Hill Book Co.
2. A.S.T.M. Standards on Refractory Materials, 1935, including Industrial Surveys.
3. J. D. Sullivan: Progress in Furnace Refractories. *Min. and Met.* (1936) **17**, 299.
4. L. J. Trostel: New Developments and Trends in Refractory Processes and Materials. *Amer. Inst. Chem. Engrs.* (1935) **31**, No. 3.
5. E. H. Schulz: Refractories, their Testing and Behavior in Metallurgical Practice. *Stahl und Eisen* (1926).
6. L. Litnsky: Developments of Magnesite Refractories. *Ber. deut. Keram. Gesell.* (1935) **16**, 565.
7. J. H. Chesters and L. Lee: Properties of Magnesite and Chrome Magnesite Brick. *Trans. Ceram. Soc.* (Nov. 1936).
8. *Trans. Faraday Soc.* (1917) **12**.
9. F. P. Hull and H. Insley: Phase Rule Diagrams. *Jnl. Amer. Ceram. Soc.* (Oct. 1933).
10. F. Wesemann: Firing of Open Hearth Furnaces in German Steelworks. *Jnl. Iron and Steel Inst.* (Sept. 1936).
11. K. Guttman: Experience with a New Color Pyrometer. *Stahl und Eisen* (1936) **56**, 481.
12. M. Fishenden: Radiation from Nonluminous Combustion Gases. *Engineering* (1936) **142**, 684.
13. F. W. Morawa: Experiences with Special Refractories in Siemens Martin Furnaces. *Stahl und Eisen* (1935) **55**, 201; also A. Heger and others, 265.
14. Hutton and Beard: *Trans. Faraday Soc.* (1905) **1**, 264.
15. Golla and Laube: *Tomind. Ztg.* (1930) **54**, 1431.
16. Salmang and Frank: *Sprechsaal* (1935) **68**.
17. E. F. Collins: *Trans. Amer. Electrochem. Soc.* (1922) **42**, 113.
18. N. R. Stansel: Industrial Electric Heating. New York, 1933. John Wiley & Sons.
19. T. Stassinot: *Stahl und Eisen* (1926) **46**, 1537, 1929.
20. M. L. Hartmann: *Trans. Electrochem. Soc.* (1920-1927).
21. T. Nagel: Low Cost Oxygen. *Min. and Met.* (1935) **16**, 215.
22. E. Karwat: *Stahl und Eisen* (1935) **55**, 860; *Engineering* (1935) **140**, 135.
23. R. Paget: Fused Silica. *Nature* (May 24, 1924) **748**.
24. E. Thomson: *Genl. Elec. Rev.* (1923) **26**, 68.
25. B. Alexander-Katz: Quarzglas und Quarzgut. 1919. Vieweg Braunschweig.
26. J. Johnston and L. H. Adams: *Amer. Jnl. Sci.* (1913) **35**, 205.

27. F. P. Bowden and others: Properties of Surfaces—Kinetic Friction. *Phil. Trans. Roy. Soc.* (1935) **234**, 329; *Proc. Roy. Soc.* (1936) **A-154**, 640.
28. G. Tammann and A. Sworyka: *Ztsch. anorg. Chem.* (1928) **176**, 46.
29. Hedvall: *Ztsch. phys. Chem.* (1926) **123**, 33.
30. T. Schloesing: *Compt. rend.* (1885) **101**, 131.
31. G. Tammann: *Ztsch. angew. Chem.* (1926) **39**, 869.
32. Hedvall: *Ztsch. Elektrochem.* (1935) **41**, 445.
33. Hedvall: *Chem. Rev.* (1934) **15**, 156.
34. Tritton and Hanson: *Jnl. Iron and Steel Inst.* (1924) **110**, 92.
35. F. W. Schroeder: *Ind. and Eng. Chem.* (1931) **23**, 124.

Bibliography on High-temperature Refractory Oxides, Et Cetera

36. K. Arndt: Properties of Magnesia Vessels. *Chem. Ztg.* (1906) **30**, 211.
37. J. B. Austin: Thermal Expansion of Refractory Oxides. *Jnl. Amer. Ceram. Soc.* (1931) **14**, 795.
38. F. Born: Dissociation of Oxides. *Ztsch. Elektrochem.* (1925) **31**, 309.
39. J. Bronn: Fused Magnesia. *Metall. u. Erz* (1926) **23**, 91.
40. E. N. Bunting: Phase Rule in System $\text{Cr}_2\text{O}_3\text{-SiO}_2$. *Nat. Bur. Stds. Jnl. of Research* (1930) **5**, 325.
41. E. N. Bunting: Phase Rule in System $\text{Cr}_2\text{O}_3\text{-Al}_2\text{O}_3$. *Nat. Bur. Stds. Jnl. of Research* (1931) **6**, 947.
42. G. F. Comstock: Some Experiments with Zircon and Zirconia Refractories. *Jnl. Amer. Ceram. Soc.* (1933) **16**, 12.
43. Anon.: Refractory Oxide Vessels (Degussa). *Metallwirtschaft* (June 1, 1934) **13**, 396.
44. W. Fehse: Elektrische Oefen mit Heizkörper aus Wolfram, chap. on Zirconia Refractories for (Tungsten Wire) Furnaces Up to 2650°C ., 28. 1928. Braunschweig.
45. F. A. J. Fitz Gerald: Application of Recrystallized Silicon Carbide. *Trans. Amer. Electrochem. Soc.* (1926) **50**, 141.
46. H. Gerdien: Al_2O_3 as a High-temperature Refractory. *Ztsch. Elektrochem.* (1933) **39**, 13.
47. H. M. Goodwin and R. D. Mailey: Physical Properties of Fused Magnesia. *Trans. Amer. Electrochem. Soc.* (1906) **9**, 89; *Phys. Rev.* (1906) **23**, 22.
48. C. H. Hannon: Fused Magnesia. *Genl. Elec. Rev.* (1933) **36**, 409.
49. J. A. Harker: A New Type of Electric Furnace. *Proc. Roy. Soc.* (1905) **A-76**, 235.
50. L. Jordan, A. A. Peterson and L. H. Phelps: Refractories for Melting Pure Metals. *Trans. Amer. Electrochem. Soc.* (1926) **50**, 155.
51. J. W. Marden and M. N. Rich: Investigations of Zirconium with Especial Reference to the Metal and Oxide. *Nat. Bur. Stds. Bull.* 186 (1921) 20.
52. R. F. Mehl, J. L. Whitten and D. P. Smith: Pure Magnesia Crucibles. *Ind. and Eng. Chem.* (1925) **17**, 1171.
53. G. E. Merritt: Thermal Expansion of Fused Refractory Oxides. *Trans. Amer. Electrochem. Soc.* (1926) **50**, 165.
54. L. Navias: Extrusion of Refractory Oxide Insulators for Vacuum Tubes. *Jnl. Amer. Ceram. Soc.* (1932) **15**, 234.
55. L. Navias: Refractory Shapes for High-temperature Furnaces. *Jnl. Amer. Ceram. Soc.* (1931) **14**, 365.
56. L. Navias: Solid Reactions between MgO or BeO and Fe , Ni , Cr , Mn and their Oxides. *Jnl. Amer. Ceram. Soc.* (1936) **19**, 1.
57. M. Pirani: Elektrothermie, chap. on Sintered Oxide Refractories, 215. Berlin, 1930. Springer.

58. E. Podszus: Zirconia and Furnaces Made with It. *Zisch. angew. Chem.* (1917) **30**, 17 and (1919) **32**, 146.
59. H. K. Richardson: Small Cast Thorium Oxide Crucibles. *Jnl. Amer. Ceram. Soc.* (1935) **18**, 65.
60. F. H. Riddle: Sillimanite Minerals as Refractories. *Trans. Electrochem. Soc.* (1931) **59**, 35.
61. R. Rieke and K. Blicke: Production and Properties of some Spinel. *Ber. deut. Ker. Gesell.* (1931) **12**, 163.
62. P. S. Roller and D. Rittenberg: Impervious Crucibles of Magnesia. *Ind. and Eng. Chem.* (1932) **24**, 436.
63. Otto Ruff: Temperature Limits of Scientific and Technical Work (Refractory Materials). *Metall u. Erz* (1924) **21**, 272.
64. Otto Ruff: Chemistry of High Temperatures. *Angewandte Chemie* (1933) **46**, 1, and 15th Congress of Applied Chemistry, Brussels, 1935.
65. Otto Ruff: An important series of papers on refractory oxide systems and their properties and uses, mostly in *Zisch. anorg. Chem.* (1913 to date).
66. Otto Ruff: Formation and Dissociation of Silicon Carbide. *Trans. Electrochem. Soc.* (1935) **68**, 87.
67. E. Ryschkewitsch: Some New Advances in the Ceramics of Highly Refractory Oxides. *Ber. deut. Ker. Gesell.* (1930) **11**, 619.
68. E. Ryschkewitsch: Single-phase Systems as the Basis for Scientific Ceramic Research. *Ber. deut. Ker. Gesell.* (1935) **16**, 111.
69. H. Salmang and N. Planz: Production of Refractory Oxide Vessels. *Archiv. Eisenhüttenwesen* (1932-1933) **6**, 341.
70. R. B. Sosman: New Tools for High Temperature Research. *Ind. and Eng. Chem.* (1931) **23**, 1369.
71. W. H. Swanger and F. R. Caldwell: Special Refractories for Use at High Temperatures. *Nat. Bur. Stds. Jnl. of Research* (1931) **6**, 1131.
72. F. J. Tone: Super Refractories. *Trans. Electrochem. Soc.* (1935) **68**, 22.
73. F. S. Tritton: Centrifugal Making of Electrically Fused Pots. *Proc. Roy. Soc.* (1925) **A-107**, 287.
74. D. Turner: Special Refractories for Metallurgical Research. *Trans. Faraday Soc.* (1931) **27**, 112; *Trans. Ceram. Soc.* (1934) **33**, 33.
75. H. von Wartenberg: Zirconia Furnace. *Zisch. anorg. Chem.* (1928) **176**, 349. Also an important series of papers on refractory oxide systems, 1928 to date.
76. Weiss and Lehmann: Crucibles of Zirconia. *Zisch. anorg. Chem.* (1910) **65**, 218.
77. Auer von Welsbach: Lanthanum-Zirconia and Thoria-Ceria Incandescent Mantels [See Dr. Franz Sedlacek's biography in *Blätter für Geschichte der Technik*, Heft 2, 20-43. Wien, 1934. J. Springer.]
78. K. Werner: Electrical Resistance of Refractory Materials at High Temperatures. *Sprechsaal* (1930) **63**, 537, 557, 581, 599, 619.
79. H. E. White: Electrical Resistivity of Specialized Refractories. *Jnl. Amer. Ceram. Soc.* (1932) **15**, 598.
80. R. Winzer: Corrosion Resistance of Vessels of Pure Oxides. *Angewandte Chemie* (1932) **45**, 429.

The Stereographic Projection

BY CHARLES S. BARRETT,* Member A.I.M.E.

(New York Meeting, February, 1937)

METALLURGISTS are making use of the stereographic projection to a steadily increasing extent. In the last five years no less than 20 papers in American metallurgical journals alone have employed the stereographic projection; recent books on physical metallurgy, plastic deformation, X-rays and their applications, and crystal structure use it.

Mineralogists have used the stereographic projection for many years in the description of symmetry classes and crystal planes, for it presents an accurate, easily understood plot of any angular relations in crystals with all unessential features eliminated (such as the accidentally determined size and shape of crystal faces). In metallography and physical metallurgy the projection is much used for the analysis of markings appearing on polished grains: slip lines, twins, cracks, structures formed by precipitation, magnetic-powder patterns, etch pits, etc. Data from certain types of X-ray photograms are most conveniently analyzed by its use, particularly those for determining the orientation of single crystals or the preferred orientation of grains in an aggregate. Calculations of how to tilt or cut a crystal parallel to a certain crystallographic plane or to reflect X-rays from a certain plane are rapidly carried out. It has been adopted almost universally to the exclusion of other methods by those studying the deformation of metallic crystals, save where the accuracy required is greater than a few tenths of a degree. Any directional property in a crystal or polycrystalline material can be shown on a stereographic projection; for example, the modulus of elasticity, yield point, etc.

It has been repeatedly called to our attention that there is need of an elementary explanation of the principles and methods of stereographic projection, covering all the common applications in the field of metallography and physical metallurgy. The following contribution is an attempt to fill this need.

The description of each method is supplemented with references to publications in which the method has been used. For convenience to the reader, these illustrative references are chiefly in American journals, particularly the publications of the American Institute of Mining and

Manuscript received at the office of the Institute Jan. 15, 1937.

* Metals Research Laboratory, Carnegie Institute of Technology, Pittsburgh, Pa., Lecturer, Department of Metallurgy.

Metallurgical Engineers. The references are not intended to cover every application that has been made of the methods, nor to refer in every case to the first use of any particular method.

The fundamental principles of the method and the common operations are first explained at some length, for these must be understood before the applications can become clear. In presenting the applications that follow, it has been necessary to discuss numerous details. While it is not expected that these will all be clear in a single reading, nevertheless they involve only simple principles and are readily mastered with study. The sections "Applications to Metallography" and "Preferred Orientations" are independent, so that a reader interested only in one need not read the other.

REFERENCE SPHERE AND ITS STEREOGRAPHIC PROJECTION

Crystallographic planes, axes, and angles are very conveniently represented on a sphere. The crystal is assumed to be very small compared

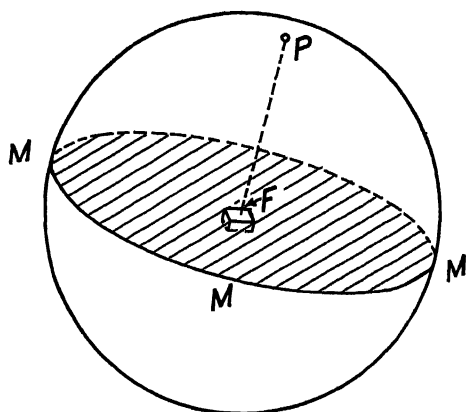


FIG. 1.—PROJECTION OF CRYSTAL PLANE UPON REFERENCE SPHERE.
Plane *F* represented on sphere by great circle *MMM* or pole *P*.

with the sphere (known variously as the reference sphere or polar sphere) and to be located exactly at the center of the sphere. Planes on the crystal can then be represented by extending them until they intersect the sphere, as in Fig. 1, where the plane *F* intersects the sphere at *MMM*.* The crystal is assumed to be so small that each of these planes passes through the center of the sphere, which results in the plane intersecting the sphere in a circle of maximum diameter—a great circle. If all planes of the crystal are projected upon the sphere in this manner, it will be found that the great circles intersect each other at the same angles as

* Assistance in preparing the illustrations for this paper was furnished by the Works Progress Administration and the National Youth Administration.

do the planes of the crystal and so exhibit without distortion all the angular relations of the crystal.

Crystal planes can also be represented on the reference sphere by erecting perpendiculars to the planes. These plane normals are made to pass through the center of the sphere and to pierce the spherical surface at a point known as the pole of the plane. This is illustrated in Fig. 1, where the plane F and its pole P are shown. The array of poles on the sphere, forming a "pole figure," represents the orientation of the crystal

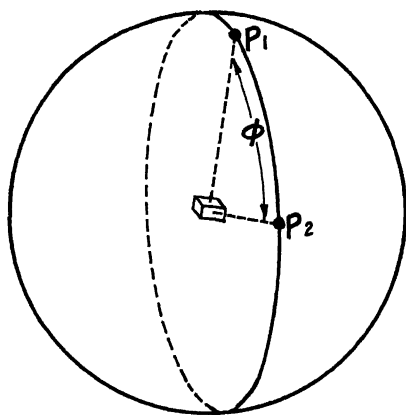


FIG. 2.—ANGLE ϕ BETWEEN POLES P_1 AND P_2 IS MEASURED ON GREAT CIRCLE THROUGH POLES.

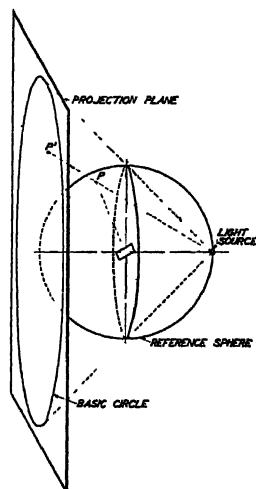


FIG. 3.—STEREOGRAPHIC PROJECTION.

Pole P of crystallographic plane projects to P' on projection plane.

planes without, of course, indicating the size and shape of the crystal planes. The angle between any two planes is equal to the angle between their poles, and this is the number of degrees between the poles measured on a great circle through them, as indicated in Fig. 2.

The applications discussed in this paper can all be carried through by using the spherical projection just described, but in practice it is usually more convenient to use a map of the sphere, so that all the work can be done on flat sheets of paper. The stereographic projection is one of the methods—and the most satisfactory one, generally—by which the sphere may be mapped without distortion of the angular relations between planes or poles.

In Fig. 3 it will be seen that there is a very simple relation between the sphere and its stereographic projection. If the sphere is transparent and a source of light is located *at a point on its surface*, the markings on the surface of the sphere will be projected as shadows upon a plane erected as shown. The plane is perpendicular to the diameter of the sphere that

passes through the light source. The pattern made by the shadows is a stereographic projection of the sphere; the point P' is the stereographic projection of the pole P . The distance of the plane ("projection plane") from the sphere is immaterial, for changing the distance will merely change the magnification of the map and will not alter the geometrical relations (in fact, the plane is frequently considered as passing through the center of the sphere).

Obviously, only the hemisphere opposite the source of light will project within the "basic circle" shown in the figure. The hemisphere containing the source of light will project outside the basic circle and extend to infinity. It is possible, however, to represent the whole sphere within the basic circle if two projections are superimposed, the one for the left-hand hemisphere constructed as in Fig. 3 and the one for the right-hand hemisphere constructed by having the light source on the left and screen on the right. The same basic circle is used for both projections and the points on one hemisphere are distinguished from those on the other by some notation such as plus and minus signs.

Projection of Great and Small Circles

Let us consider how great circles and small circles inscribed on the sphere will appear on the projection (Fig. 4a). Any great circle on the

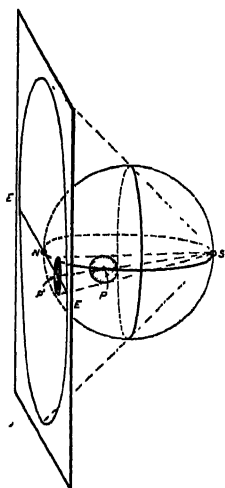


FIG. 4a.

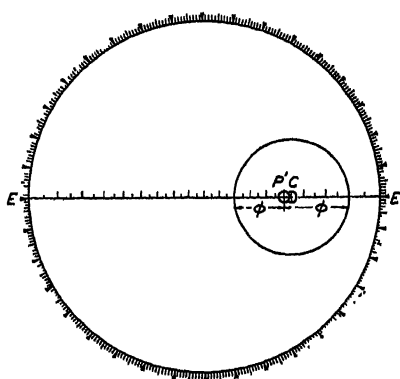


FIG. 4b.

FIG. 4.—STEREOGRAPHIC PROJECTION OF SMALL CIRCLE.

Projection of great circle through N is EE' ; projection of small circle (shaded) is circle having center C displaced from projected center P' .

sphere that passes through the point N will project to form a straight line passing diametrically through the basic circle on the projection; thus SPN projects to EE' . (That this is true will be seen from the fact that

the great circle SPN and its projection EE are, in fact, lines of intersection of a plane with the sphere and projection plane respectively.) If the great circle is graduated in degrees, its projection EE will be a scale of stereographically projected degree points and will be useful for reading off angular distances on the projection; it is shown with 5° graduations in Fig. 4b. Penfield has engraved a scale of this type for a projection of a basic circle of 14-cm. diameter¹, and such a scale is inherent in the stereographic nets that are discussed in the next section.

A small circle inscribed on the sphere about a point such as P that lies on the great circle SPN will cut the great circle at two points, each of which are ϕ° from P . The point P will project to P' . The bundle of projection lines for the small circle will form a cone with its apex at S , and the cone will intersect the plane in a true circle of which the center is on the line EE , either inside or outside of the basic circle. The center of area of this projected circle will not, however, be at P' , but will lie on the line EE at a point distant an equal number of *stereographically projected* degrees from all points of the projected circle. The scale of projected degrees enables the size of the projected circle to be determined quickly, as indicated in Fig. 4b: The scale EE is laid diametrically across the basic circle so as to pass through P' , then two points are laid down at a distance of ϕ° from P' in each direction, and a circle, centered on EE , is drawn through the two points thus located. (In Fig. 4b, $\phi = 30^\circ$ and the center of area on the projected circle is at C .)

If the radius of the small circle about P is increased, it finally becomes a great circle. Since this great circle does not pass through the point N , its projection will not be a straight line. It will be a circle with a large radius of which the center is on EE extended; it will cut the basic circle at two diametrically opposite points, and it will cut the line EE at the point $\phi = 90^\circ$ from P' . Its position and radius will thereby be uniquely determined.*

Ruled Globe and Stereographic Nets

A ruled globe is useful in crystallographic work, just as it is in geography, and the method of ruling is the same in both cases. Great circles are drawn through the north and south poles of the sphere for meridians, connecting all points of equal longitude. Another set of circles is drawn concentric with the north and south poles to connect points of equal latitude (since they have diameters less than the great circles, these are

¹ References are at the end of the paper.

* Penfield's protractors give the radii of stereographically projected small and great circles directly; they may, however, be determined by trial and error in the manner indicated; many will be found on the stereographic nets discussed in the next section and can be traced directly from the nets.

"small circles"). A globe ruled with latitude and longitude lines is shown in Fig. 5.

If the net of latitude and longitude lines on the reference sphere is projected upon a plane, it will form a "stereographic net" much resembling the rulings of the globe in appearance.

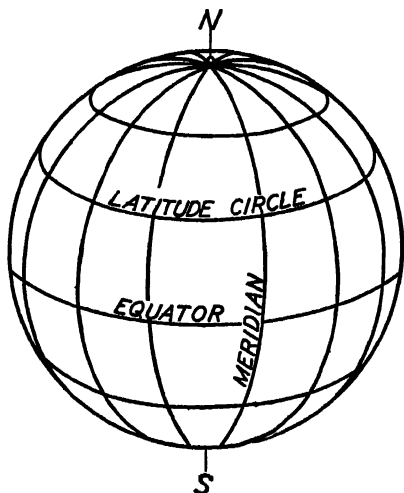


FIG. 5.—RULED GLOBE.
Projections of this form stereographic nets of Figs. 6 and 7.

When the north and south axis of the sphere is *parallel to the projection plane*, the latitude and longitude lines form the stereographic net of Fig. 6, frequently referred to as a "Wulff net." The meridians extend from top to bottom, and the latitude lines from side to side (compare with Fig. 5). If, on the other hand, the north-south axis is *perpendicular to the projection plane*, the net of Fig. 7 will be formed, which is known as the polar net or equatorial net. In this case the meridians radiate from the pole in the center, and the latitude lines

are concentric circles.

The nets reproduced here are graduated in intervals of 5° and are suitable for exercises, but are not accurate enough for research work.

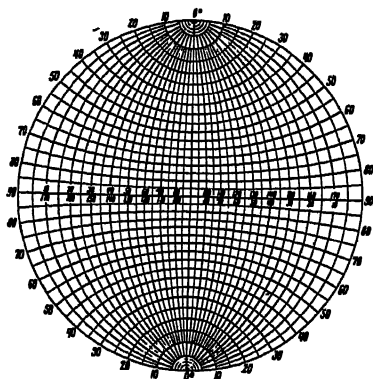


FIG. 6.—STEREOGRAPHIC NET OR WULFF NET.
Used in all stereographic problems.

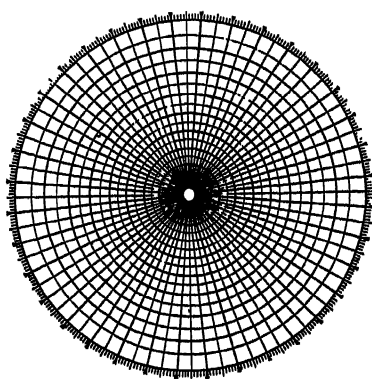


FIG. 7.—POLAR STEREOGRAPHIC NET.
Rotation of data with this net is equivalent to rotation of projection about its center point.

Larger nets of greater precision have been published repeatedly.* Nets

* An accurate stereographic net $15\frac{3}{4}$ in. diameter, of the type reproduced in Fig. 6, was engraved by Admiral Sigsbee and is available on special order from the Hydro-

of reasonable size will enable problems to be solved with an error of a degree or at best a few tenths of a degree; for greater precision it is necessary to resort to mathematical analysis.

MANIPULATIONS WITH STEREOGRAPHIC NETS

Rotation.—For the solution of crystallographic problems on a ruled globe it is necessary to use a device similar or equivalent to the one sketched in Fig. 8, a transparent cap fitting accurately over the globe but free to rotate with respect to it. Poles marked on the cap, such as P_1 and P_2 may then be studied with reference to the underlying net of latitude and longitude lines. Rotating this cap about the north-south axis of the globe will cause each point on the cap to move along a circle of constant latitude on the globe, as shown, and in so doing each point will cross the same number of meridians; i.e., each point will retain its latitude and each will alter its longitude equally.

An exactly analogous rotation may be carried out with stereographic nets. A transparent sheet of tracing paper replaces the transparent spherical cap, and the stereographic net laid under the paper replaces the ruled globe. An array of poles on the tracing paper is rotated with respect to the net by moving each point along the latitude line that passes through it, counting off

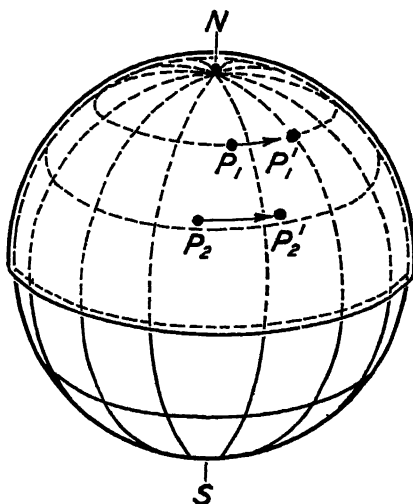


FIG. 8.—RULED GLOBE WITH TRANSPARENT CAP.
Rotation of cap about $N-S$ axis moves P_1 to P_1' and P_2 to P_2' .

graphic Office of the United States Navy, known as No. H. O. Miscellaneous 7736. As a convenience to crystallographers requiring small quantities of these, the Metals Research Laboratory retails them at cost. The author would also undertake the printing and distribution of somewhat smaller nets for rough work and for student use if there were sufficient demand for them. Nets are sold by Penfield Stereographic Supplies, Mineralogical Laboratory, Yale University, New Haven, Conn. (14 cm. dia.); University Press, Cambridge, (12 in. dia.); R. Seifert and Co., Hamburg 13, Germany (50 cm. dia.); Mineralogischen Institut der Universität Leipzig (100 cm. dia.); Schweizerbart'schen Verlag, Stuttgart (20 cm.); reproductions appear in the following references: F. Rinne: *Einführung in die kristallographische Formenlehre*, Leipzig, 1922 (12 cm.); H. E. Boeke: *Die Anwendung der stereographischen Projektion bei kristallographischen Untersuchungszeichnung*, Bornträger, Berlin, 1914 (14 cm.); B. Gossner: *Kristallberechnung und Kristallzeichnung*, Leipzig and Berlin, 1914 (20 cm.); G. Wulff: *Zisch. Krist.* (1902) 36, 14 (20 cm.); F. Rinne: *Zisch. Krist.* (1927) 65, 83 (10 cm.).

along that line the required difference in longitude. Using the Wulff net of Fig. 6, the poles shift to the right or left, whereas with the polar net of Fig. 7 they rotate about the center.

A greater freedom of rotation is possible with the cap and globe device than with the nets, for the axis of rotation in the former case can be chosen at random, while in the latter, rotation must always be done about the north-south axis of a net. But it is possible to rotate first about the axis of one net, and then about the axis of the other, and by thus combining rotations to effect a rotation about an axis inclined to both. In this way, rotations of *any* amount about *any* axis, whatever its inclination to the projection, can always be done. The method amounts to resolving the rotation into components, one component being about the axis parallel to the plane of the paper and carried out by the Wulff net, and the other component being about the axis normal to the paper, and accomplished by using the polar net.

In practice, rotation about an inclined axis can be accomplished without transferring the tracing paper from one net to the other, for obviously the circular rotation with the polar net can be performed simply by rotating the tracing paper about a pin at the center of its basic circle. Rotations of both types can be carried out conveniently with the tracing paper lying on the Wulff net and free to swing about a central pin.

Angle Measurement.—As has been stated in connection with Fig. 2, the angle between two points on a sphere is the number of degrees separating them on the great circle through them. The angle can be read on the spherical cap and ruled-globe apparatus by so rotating the cap that the two points are made to lie on the same meridian of the globe, for all meridians are great circles (they all pass through two diametrically opposite points—the north and south poles). With the two points on the same meridian, the angle between them is their difference in latitude, directly read with the help of the latitude lines ruled on the globe. Angles are measured with a stereographic net in exactly the same way, by bringing the points to the same meridian of the stereographic net and counting their difference in latitude. Any two points can be brought to the same meridian by merely rotating them a certain amount about the center (swinging the tracing paper about the central pin of a Wulff net).

The most frequent source of errors in students' work with the projection comes from misunderstanding or forgetting this principle, that *the angle between two points is equal to their difference in latitude only when they lie on the same meridian*. It is also true, of course, that the angle between two points is equal to their difference in *longitude* when, and only when, they lie on the *equator*, the equator of the Wulff net then serving as the scale of projected degrees that was mentioned earlier.

The operation of angle measurement described above is, of course, identical whether the points on the projection represent poles of crystallographic planes, crystallographic directions, or points on a sphere.

When planes appear in a stereographic projection as great circles, like the circle *MMM* of Fig. 1, it is easy to plot the poles of the planes and then to measure the angle between the poles. To plot the projection of pole *P* (Fig. 1) it is merely necessary to turn the tracing paper about the central pin in a Wulff net until the projection of great circle *MMM* falls on a meridian of the Wulff net; then the point on the equator and 90° from that meridian is the pole *P* of the plane.

Properties of Stereographic Projection.—Elaborate treatises have been written on the properties and uses of the stereographic projection for crystallographic work* and the reader is referred to these for details not mentioned in the present discussion and for mathematical proofs; we are presenting here only items that have been found most useful in metallurgical problems. The properties of the stereographic projection that are of chief importance may be summarized as follows:

1. It is perspective. The reference sphere is projected as it would appear to the eye at a point on the spherical surface. It is also the "shadow projection" when a source of light is on the sphere, as has been discussed above.

2. Small circles on the sphere appear as circles on the projection; however, the centers of these circles on the sphere will not project to the center of the area of the projected circles, but will be displaced radially an amount sufficient to correspond to equal *angular* distances from the center to all points on the circumference.

3. Great circles on the sphere appear on the projection as circles cutting the basic circle at two diametrically opposite points; a great circle lying in a plane perpendicular to the projection plane becomes a diameter on the projection (one of the meridians of a polar net), while great circles in inclined positions on the sphere may be made to coincide with one of the meridians of a Wulff net.

4. Angles between points are measurable and may be read as a difference of latitude on a net so rotated as to give the points the same longitude. The *linear* distance on the projection representing 1° of arc varies from the center to the basic circle by a factor of two.

5. The projection is angle true; the angle between intersecting planes equals the angle at which the projection of the planes intersect. (However, see earlier paragraph for a more suitable method of determining the angle.)

6. Angle relations between points on the projection remain unchanged by rotation of the points about the axis of a stereographic net as described earlier.

7. Half of a sphere is projected within a basic circle; the other half is projected on a plane of infinite extent but is more conveniently projected within the basic circle and distinguished from the first by some notation.

* See footnote on page 34 and references 2 to 5.

Miller Indices.—It will be necessary to introduce here the Miller indices of crystal planes, the notation now universally adopted to signify the orientation of planes with respect to the axes of the crystal. Crystal axes are chosen so as to be parallel to the edges of the unit cell of the space lattice. Distances along these axes are measured in terms of the dimensions of the unit cell (length a , width b and height c); a distance of x cm. along the X axis, that is along the a dimension of the cell, is counted as a distance x/a , a distance y cm. along the Y , or b , axis as y/b and a distance z cm. along the Z , or c , axis as z/c . Planes are described by numbers proportional to the reciprocals of their intercepts on the three axes (Fig. 9). If the intercepts in centimeters are x , y and z , respectively, in terms of unit distances on the axes they are x/a , y/b and z/c , and their reciprocals are a/x , b/y and c/z . The Miller indices are the three smallest integers (hkl) proportional to these numbers.

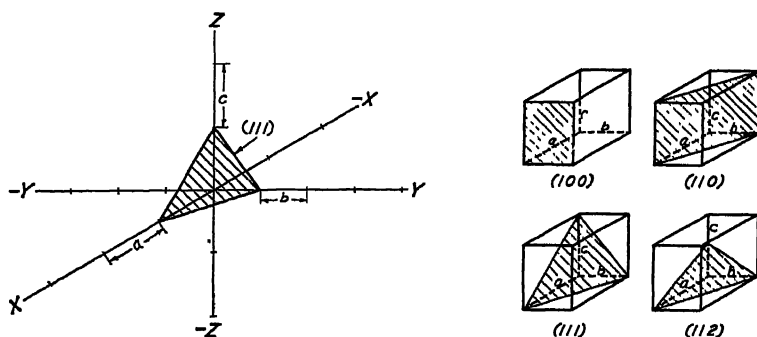


FIG. 9.—MILLER INDICES OF PLANES.
Relation of important planes to unit axial lengths a , b and c .

The plane shown cutting the axes in Fig. 9 has intercepts 1, 1, 1 and therefore indices (111). A plane that has intercepts 2, ∞ (infinity), and 1 times the unit axial lengths, respectively, has for reciprocal intercepts $\frac{1}{2}$, 0, 1 and for Miller indices (102). The figure shows some of the most important planes in relation to the unit cell, but it should be noted that all planes parallel to the crosshatched ones have the same indices. If a plane intercepts the $-X$, $-Y$ or $-Z$ axes, the intercepts are negative numbers and so are the indices. This is indicated by placing a minus sign above the negative indices: ($\bar{h}\bar{k}\bar{l}$). Parentheses, (hkl), are used to signify any single plane or set of parallel planes; braces, $\{hkl\}$, to signify all planes of a "form"—those which are equivalent in the crystal—such as the cube faces $\{100\} = (100), (010), (001), (\bar{1}00), (0\bar{1}0),$ and $(00\bar{1})$.

Somewhat different indices are used for specifying a direction in a crystal. A line in the given direction is passed through the origin, and the coordinates of any other point on the line are determined in terms of the unit axial distances a , b and c . The indices of the direction are the three smallest integers proportional to these coordinates. Indices of a

with (001), (110), (112), (130) and (111) as the projection plane, and most mineralogical textbooks have numerous standard projections.

TABLE 1.—*Angles between Crystallographic Planes in Crystals of Cubic System*⁶

(<i>hkl</i>)	(<i>hkl</i>)	Values of Angle between (<i>hkl</i>) and (<i>hkl</i>)					
100	100	0°	90°				
	110	45°	90°				
	111	54° 44'					
	210	26° 34'	63° 26'	90°			
	211	35° 16'	65° 54'				
	221	48° 11'	70° 32'				
	311	25° 14'	72° 27'				
110	110	0°	60°	90°			
	111	35° 16'	90°				
	210	18° 26'	50° 46'	71° 34'			
	211	30° 1'	54° 44'	73° 13'	90°		
	221	19° 28'	45°	76° 22'	90°		
	311	31° 29'	64° 47'	90°			
111	111	0°	70° 32'				
	210	39° 14'	75° 2'				
	211	19° 28'	61° 52'	90°			
	221	15° 48'	54° 44'	78° 54'			
	311	29° 30'	58° 30'	79° 58'			
210	210	0°	36° 52'	53° 8'	66° 25'	78° 28'	90°
	211	24° 6'	43° 5'	56° 47'	79° 29'	90°	
	221	26° 34'	41° 49'	53° 24'	63° 26'	72° 39'	90°
	311	19° 17'	47° 36'	66° 8'	82° 15'		
211	211	0°	33° 33'	48° 11'	60°	70° 32'	80° 24'
	221	17° 43'	35° 16'	47° 7'	65° 54'	74° 12'	82° 12'
	211	10° 0'	42° 24'	60° 30'	75° 45'	90°	
221	221	0°	27° 16'	38° 57'	63° 37'	83° 37'	90°
311	311	0°	35° 6'	50° 29'	62° 58'	84° 47'	

In the cubic system, and only in the cubic system, can a standard projection of poles of planes also serve as a standard projection of crystallographic directions of similar indices, for only in this system is the direction [*hkl*] perpendicular to the plane (*hkl*) for all values of the indices *h*, *k* and *l*.

Orientation of Single-crystal Wires and Disks.—The orientations of single-crystal wires, rods or disks are conveniently represented with a stereographic projection. It is customary to plot the position of the

axis of the specimen on a standard projection of the crystal. The specimen axis appears on the projection as a point such as *P*, Fig. 10, at the required angular distances from the axes of the crystal. It is not necessary, however, to draw the whole standard projection before plotting the axis *P* in it, for the axis may just as well be referred to the three neighboring poles of (100), (110), and (111) planes. If poles of these three types are joined by great circles, there results (for the cubic system) a pattern of 24 equivalent triangles, one of which is outlined with heavy lines in Fig. 10, and it is common practice to draw only one of these triangles or two adjacent triangles before plotting the specimen orientation.

It is easy to show by means of a projection of this sort (using one triangle or sometimes two adjacent ones) how the orientation of the lattice changes during deformation of the crystal, for deformation causes a certain rotation of the axis with respect to the lattice, and causes the point *P*, Fig. 10, to move along a definite path on the standard projection. For examples of applications of the projection for this purpose, see references 8 to 12. It will be noted that plotting the specimen axis in this way leaves unspecified the orientation of the lattice with respect to rotation around the specimen axis, but in many problems this is unimportant; as, for example, in tensile tests of a wire. A number of investigators have made use of this kind of plot to show the variation of physical properties with lattice orientation; measurements of a physical property of a wire can be written beside the point representing the wire orientation, and points of equal magnitude can be joined by contours.*

APPLICATIONS TO METALLOGRAPHY

The combination of standard projection and stereographic net is particularly convenient for analyzing the crystallographic features of the deformation of crystals by slip, twinning, and cleavage, or the growth habits of crystals precipitated within a crystal. Such studies deal with the orientation of planes in space, the angles between these planes, and the intersections of these planes with one another, which are matters readily visualized and handled on the stereographic projection with the principles that have already been reviewed in this paper. To aid the beginner in acquiring confidence in the solution of problems of this nature it is desirable to list the more common problems and to give the operations by which they are graphically solved, but it should be borne in mind that as soon as one is accustomed to think clearly of the sphere and its "picture," the stereographic net, these operations become self-evident.

* For example see physical tests plotted in this way by W. Fahrenhorst and E. Schmid¹³, and rates of oxidation studied with respect to orientation by R. F. Mehl and E. L. McCandless¹⁴.

Obviously the solutions are independent of the choice of projection plane and are applicable to problems in pure spherical trigonometry. But to make the operations more easily understood by the metallographer, we will present them from his standpoint rather than in the abstract: we will speak of polished surfaces of specimens and the traces (lines of intersection) of crystallographic planes in these surfaces, and we will generally consider the projection plane to lie in one of the surfaces.

1. *Orientation of Planes Causing a Given Trace in a Surface.*—Let us consider the stereographic projection of a polished surface containing the trace of a crystal plane, the projection being made on a sheet of paper laid parallel to the polished surface. The surface will then be represented on the paper by the basic circle, and markings in the surface will be plotted as points on the circumference of this basic circle. A trace in the surface that runs lengthwise of the page ("vertically") will be plotted in the projection as the diametrically opposite points T and T' at the top and bottom of the basic circle, Fig. 11. A trace in any other direction in the surface would be plotted similarly, as the end points of a diameter parallel to the given direction.

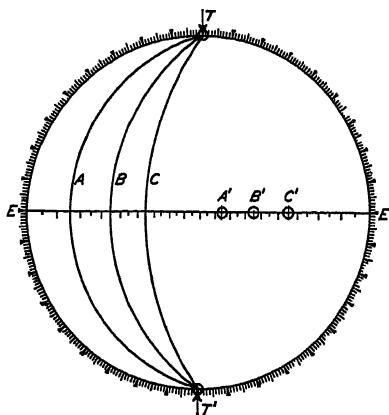


FIG. 11.—PLANES A , B , C , WITH POLES A' , B' , C' , AND ALL OTHERS WITH POLES ALONG EE' INTERSECT PROJECTION PLANE IN TRACE TT' .

To find the planes that would intersect the surface in the direction TT' the points TT' are superimposed on the N and S poles of a Wulff net. It will then be seen that all of the meridians of the net—such as, for example, the meridians A , B and C of Fig. 11—are projections of the required planes, since they intersect the basic circle, which represents the surface, at T and T' . Similarly, any other plane whose pole lies on the equator of the Wulff net will intersect the surface in the direction of the N - S axis.

Conversely, if the pole of a plane is given, such as A' , its trace in the projection plane is readily found. The transparent sheet on which the pole is plotted is laid on a Wulff net and turned until the pole falls on the equator, in which position the required trace will be parallel to the N - S axis of the net.

2. *Trace of One Plane in Another, When Both Are Inclined to the Projection Plane.*—Given two poles A' and B' (Fig. 12), the planes A and B are first plotted by rotating the projection over a Wulff net so that the pole A' lies on the equator E_A , and then tracing on the projection the meridian lying at 90° to the pole A' , then repeating the operation for

the second pole, B' , with the net turned so that its equator is in the position E_B . The point of intersection, C' , of the two planes thus plotted is the projection of the required line of intersection of the planes.

3. *Direction Normal to Two Given Directions (or Zone Axis of Two Planes Whose Poles Are Given).*—Referring again to Fig. 12, let us assume that the directions A' and B' are given and the direction normal to both is required. This may be given by the construction described in the preceding paragraph, for obviously every line in plane A is normal to A' , and every line in B is normal to B' ; hence, the line common to A and B is normal to both A' and B' .

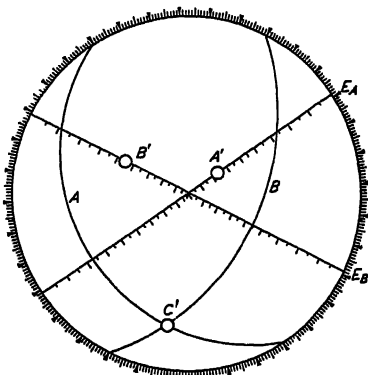


FIG. 12.—PLANES A AND B , WITH POLES A' AND B' , INTERSECT ALONG DIRECTION C' .

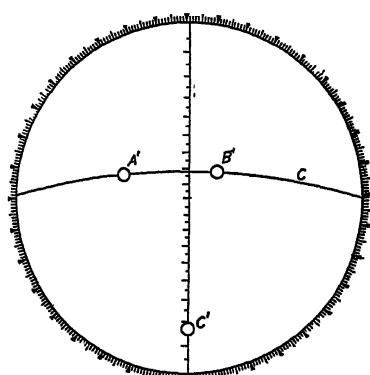


FIG. 13.—ALTERNATIVE METHOD OF LOCATING C' , NORMAL TO A' AND B' .

An alternative solution is shown in Fig. 13. The projection is rotated over a Wulff net until both A' and B' lie on the same meridian, then the point C' on the equator and 90° from this meridian is the projection of the required direction. If A' and B' are poles of planes, C is the zone circle and C' is their zone axis.

4. *Determination of Orientation of Plane from Its Traces in Two Surfaces.*—The surfaces are first plotted on the projection as in Figs. 14a and 14b, one surface lying in the plane of projection and forming the basic circle A of Fig. 14b, the other surface, B , coinciding with the meridian of the stereographic net that lies Φ° from the first about the axis NS . (To draw this meridian the net is rotated so that the direction NS is parallel with the line of intersection of the two surfaces.) On the planes A and B thus plotted in Fig. 14b are then located the points T_A and T_B , which represent the directions of the traces in the two surfaces, respectively; they will lie at angles laid off from the edge NS to correspond with the angles on the specimen, the angles being measured as differences of latitude, ψ_A and ψ_B , on the stereographic net. Having plotted the traces T_A and T_B , the plane that causes them can be drawn in by rotating the net so that some single meridian of the net will pass through both points;

this meridian (the dashed circle C in the figure) is then the projection of the required plane.

5. *Determination of Crystal Orientation from Traces of $\{hkl\}$ Planes When h, k and l Are Known.* (a) *Traces in One Surface Only.*—On tracing

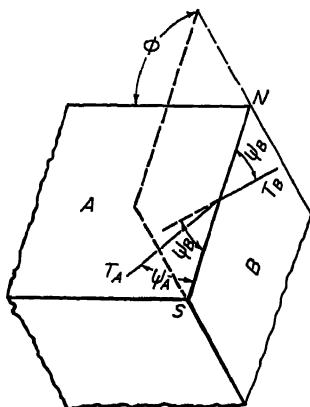


FIG. 14a

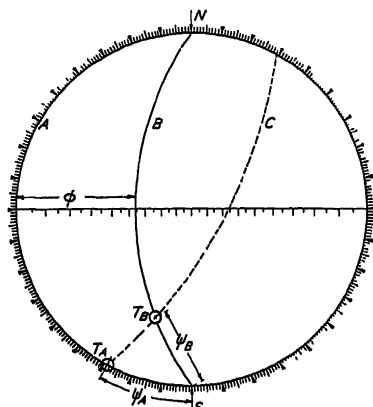


FIG. 14b.

FIG. 14.—DETERMINATION OF ORIENTATION OF PLANE FROM ITS TRACES IN TWO SURFACES.

Traces are T_A and T_B in surfaces A and B , respectively. Plane causing these is C .

paper a basic circle is drawn representing the specimen surface; through this circle are drawn diameters perpendicular to the directions of traces

seen on the specimen surface. These diameters are then the loci of all poles capable of forming the traces. A standard projection of all poles of the given form $\{hkl\}$ on a transparent sheet is then superimposed on this plot and on a Wulff net, and a pin is put centrally through all three sheets. By trial and error, the relative position of the three sheets is found in which each pole of the standard projection may be rotated into coincidence with one of the diameters by the same amount of rotation about the axis of the net. This position of the sheets is illustrated in Fig. 15, in which appear the $\{111\}$ trace normals (diameters), the $\{111\}$ poles of the standard projection (\circ), and the $\{111\}$ poles in orientation explaining traces (\bullet).

FIG. 15.—ORIENTATION OF CUBIC CRYSTAL DETERMINED FROM TRACES OF $\{111\}$ PLANES.

Indicated on projection are normals to traces (diameters); $\{111\}$ poles of standard projection (\circ); $\{111\}$ poles in orientation explaining traces (\bullet).

position of these poles on the trace normals after the rotation with the net (\bullet). This final array of poles (\bullet) describes an orientation of the crystal consistent with the observed traces; it may not, however, be

the only consistent orientation. In fact, if traces on one surface only are studied, the crystal may have the orientation shown or a mirror image of this orientation in the plane of projection, the poles lying in either of the hemispheres.

The example in Fig. 15 is an orientation determination in which a method of this sort was necessary, for the crystal in which the traces originated had decomposed. (The traces were formed by decomposition of a gamma iron crystal into alpha iron crystals which formed lamellae on $\{111\}$ planes¹⁵)

5. (b) *Traces in Two Surfaces.*—The solution is more direct and rigorous if traces can be followed from one surface around the edge to the other surface, thus eliminating any uncertainty as to the proper pairing of traces on the two surfaces. If this is the case, the first operation is to plot the orientation of each plane by method 4 above. The poles thus plotted then give the crystal orientation. If the orientations of other poles of the same crystal are required, they may be obtained by rotation of the standard projection, as in the previous method—the plotted poles on one sheet and the standard projection on another being rotated with respect to the net until a difference of Φ° of longitude and no difference of latitude exists between each $\{hkl\}$ pole of the standard and a corresponding plotted pole. Rotation of Φ° then puts any pole of the standard into its proper position in the plot.

When the pairing of traces on the two surfaces is uncertain, it is necessary to make a plot of poles for all possible pairings. Among this array of poles there will then be one or more groupings having the angular relations appropriate for $\{hkl\}$ planes, and these may be singled out from the whole number by trial and error rotations of the $\{hkl\}$ poles of the standard, possible solutions being those for which Φ° rotation about the net axis brings the standard poles into coincidence with the plotted poles.

6. *Determining Indices of Set of Planes Causing Traces on One or More Surfaces.* (a) *Crystal Orientation Unknown.*—The poles of the planes (or of all possible planes in cases of uncertain pairing) are plotted as in the preceding problem. Trial and error rotations are then performed, using different sets of standard projection poles until a set is brought into coincidence with the plotted poles. For example, traces on two polished surfaces were found to be consistent with $\{111\}$ planes by the analysis

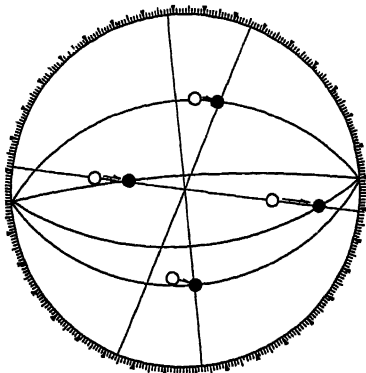


FIG. 16.—ORIENTATION OF CUBIC CRYSTAL DETERMINED FROM TRACES ON TWO SURFACES.

Normals to traces are full lines; standard projection $\{111\}$ poles (O); $\{111\}$ poles in orientation explaining traces (●).

shown in Fig. 16¹⁶. Normals to traces on the plane of projection appear in this figure as diameters, while normals to traces on a second plane of polish appear as great circles. The dots are poles of $\{111\}$ planes that have been rotated from a standard projection, so as to lie at or near the intersections of diameters and circles and that are therefore capable of explaining the traces in both surfaces.

The procedure in this problem is laborious and leads to uncertain results unless traces are measured on two surfaces and unless the planes are of low indices. It is frequently possible to save labor by noting the number of different directions of traces on each surface, for in this way certain planes may be eliminated from further consideration. If, for

example, a single crystal of a cubic metal exhibits more than three directions of traces, they could not have been produced by $\{100\}$ planes alone; if more than four directions are found, neither $\{100\}$ nor $\{111\}$ planes alone could have produced them; if more than six directions, neither $\{100\}$, $\{111\}$, nor $\{110\}$, et cetera.

An example of counting trace directions to determine the indices of planes was a proof by this method that the familiar martensite "needles" in quenched steel are traces of $\{111\}$ planes¹⁷. These needles, when formed from a single grain of austenite, lie parallel or nearly parallel to three directions in some grains and to four directions in others, but never to more

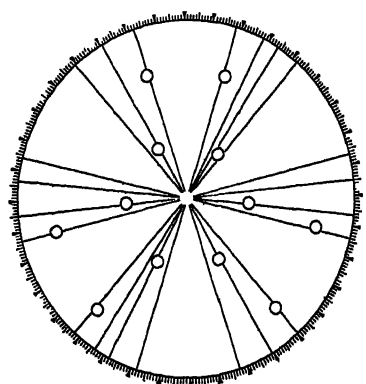


FIG. 17.—DETERMINATION OF INDICES WHEN CRYSTAL ORIENTATION IS KNOWN. TRACES ON ONE SURFACE AVAILABLE.

Diameters are normals to traces of "nitride needles" in polished surface. Circles (○) are $\{210\}$ poles, located by X-rays, that account for traces.

than four; therefore, the needles are traces of $\{111\}$ planes. Numerous applications of this method have been made, particularly in Widmanstätten studies, both for determining the indices of planes and for excluding planes of certain indices. (References 16 and 18 to 21 may be cited as examples.)

6. (b) *Crystal Orientation Known*.—If X-ray data or other observations have already given the orientation of a crystal, a standard projection of all likely planes can be rotated to their positions for this crystal orientation. By the methods presented above, the traces that each set of planes will make in the plane of polish may then be plotted. The coincidence of predicted and observed traces will then single out the set of planes best able to explain the data. (See references 16, 18 to 21 and 22 to 26 for examples.)

Fig. 17 illustrates the method for traces in one surface²⁰. The directions of "nitride needles" in a single crystal of iron were measured and diameters were drawn perpendicular to these directions. The poles of various low-index planes of the matrix crystal of iron were then plotted on the projection in positions determined by X-rays. The poles of {210} planes lay on or near the trace normals without exception and were thus adequate to explain them. One becomes convinced that planes of no other index could be involved, however, only after several individual examples have been analyzed in this way.

That "nitride needles" are plates formed on {210} planes in alpha iron was more rigorously proved by analyzing traces that appeared simultaneously on two surfaces. Poles of the plates could then be plotted by the method of section 4. These are shown as circles in Fig. 18. These observed poles agreed well with the poles of {210} planes located by X-ray diffraction, shown as crosses in the figure.

Methods of Determining Orientation of Crystals.—Space is not available here for an adequate treatment of the numerous methods of determining the orientation of crystals. The reader is referred to some of the recent books for summaries of the more common methods²⁷⁻³⁰. Stereographic projection is particularly useful in the X-ray methods, using Laue photographs of the forward reflection type^{7,31-33} or the back-reflection type (which is frequently more convenient)^{34,35} and using monochromatic rays registered simultaneously on stationary and oscillating films in the technique devised by Davey³⁶ and outlined in detail by Wilson³⁷. When the orientation of a crystal has been determined and plotted on a projection, it is a simple matter to see from the projection how to cut the crystal so as to expose any given crystal face.*

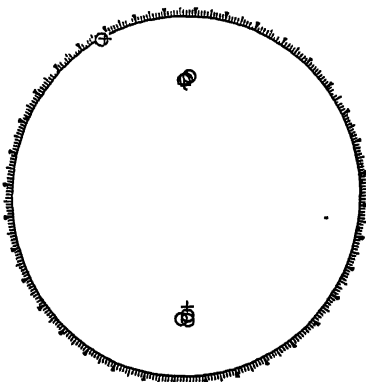


FIG. 18.—DETERMINATION OF INDICES WHEN CRYSTAL ORIENTATION IS KNOWN. TRACES ON TWO SURFACES AVAILABLE.

Circles are poles of "nitride needles" appearing simultaneously on two surfaces; crosses are {210} poles, located by X-rays, that account for traces.

TWINNING

A crystal is said to be twinned if it is made up of sections that are related to each other in pairs, the two individuals of a pair being oriented

* As an example see C. H. Mathewson and K. R. van Horn³⁸, and the description there given of a miter box for cutting to the required angle; also W. C. Elmore and L. W. McKeehan³⁹.

symmetrically with respect to each other. The relation between the individuals may be such that one is the mirror image of the other in the plane of symmetry (the "twinning plane") or it may be such that one is related to the other by a rotation of 180° about some axis of the crystal. Very commonly among the metal crystals, which frequently have a center of symmetry, the first type and the second are equivalent to one another and equivalent to rotations about other axes as well.* Orientation relationships in twinning can be shown conveniently in stereographic projection, as, for example, in Fig. 19. In this projection the cube axes

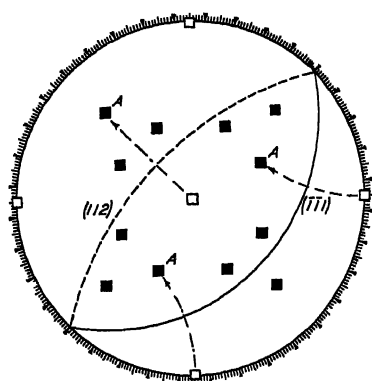


FIG. 19.—TWINNING RELATIONSHIPS IN CUBIC CRYSTALS.

Cube axes of original crystal are hollow squares and of first order twins are black squares; twinning planes are indicated by full and dashed great circles.

of a cubic crystal are plotted as hollow squares, one of the twinning planes, $(\bar{1}\bar{1}1)$, is plotted with a full line (a great circle) and the cube axes of the twinned portion of the crystal are indicated by black squares marked *A*. The axes *A* are mirror images of the hollow squares in the twinning plane $(\bar{1}\bar{1}1)$. One of the several rotations by which the hollow squares can be put into the twinned orientation is indicated in dot-dash lines.

It is also true that the (112) plane, shown by the dashed great circle, could also be a twinning plane and produce the same twinned orientation. If all possible orientations are plotted in a similar way, there will be found to be four new orientations, indicated by the 12 black squares, either twinning mechanism giving the same result. The projection thus illustrates both the orientation of twins in a body-centered cubic crystal, where $\{211\}$ planes are the twinning planes, and the orientation of twins in a face-centered cubic crystal, where $\{111\}$ planes are the twinning planes. While $\{111\}$ and $\{211\}$ types of twinning lead to identical orientations in cubic crystals⁴¹, they are not equivalent with respect to atomic arrangement^{42,43}, nor, of course, are the traces of the twinning planes in a polished surface of the specimen identical. The methods of determining twinning planes and twinning axes will not be treated in this paper, but may be found elsewhere²⁷. Data on twinning in metals have also been adequately summarized^{10,27,44}, together with discussions of the role of twinning in the deformation of metals, and stereographic plots of the orientation relationships occurring.

* A more extended treatment of these and other possible twinning orientations and growth characteristics will be found in N. H. Hartshorne and A. Stuart⁴⁰, and in the textbooks on mineralogy.

PREFERRED ORIENTATIONS

The orientation of grains in a metal following a deforming process, such as rolling, for example, is of fundamental importance because of its influence on the physical properties of the material. Only with a statistically random orientation of the grains will the properties be the same in all directions (isotropic). If certain orientations are preferred by the grains there result—even with cubic metals—directional or anisotropic properties. The stereographic projection or “pole figure” has no equal

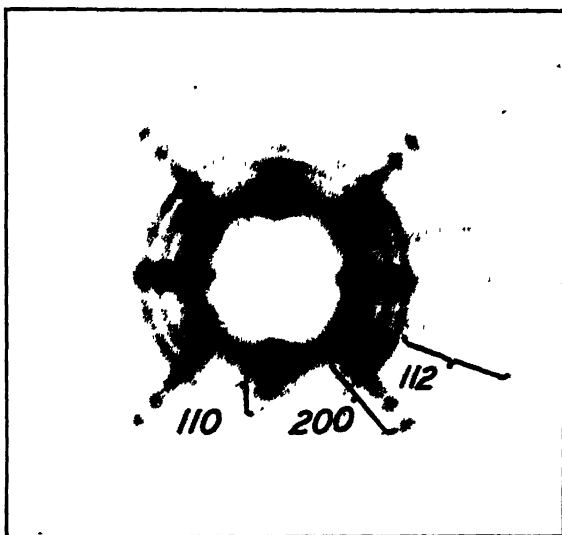


FIG. 20.—DIFFRACTION PATTERN OF COLD-ROLLED STEEL, SHOWING PREFERRED ORIENTATION.

Taken with molybdenum target tube operating at 35,000 volts. Indices of principal Debye rings are indicated.

as a method for interpreting X-ray photographs in terms of the distribution of crystal orientations, and as a means of accurately and quantitatively presenting the data. Since its first use by Wever⁴⁵ for this purpose in 1924, it has been steadily increasing in favor and is now considered by most X-ray workers to be quite indispensable in X-ray studies of the complex deformation structures encountered in rolling and deep drawing.

The pole figures used in preferred orientation studies are stereographic projections of all poles of given indices $\{hkl\}$ in the grains of a sample. Pole figures are plotted only for planes of low indices, either for planes of the form $\{100\}$, $\{110\}$ or $\{111\}$ with cubic metals and usually only for $\{0001\}$ planes of hexagonal metals. In materials with random orientation the normals to $\{hkl\}$ planes pierce the reference sphere with equal frequency all over its surface, but when certain orientations are preferred

by the grains the intersections occur with greater frequency in restricted areas. On the stereographic projection of the sphere, the pole figure, it is customary to represent the areas most densely populated with poles as heavily shaded regions, and to show with lighter shading the regions where poles occur less frequently, thus distinguishing from two to four degrees of relative frequency in the usual case. More quantitative representation is possible by the use of sets of contours drawn through points of constant frequency, just as is the practice in ordinary mapping. The relative frequency of poles is judged by the blackness of the corresponding portion of the rings on the X-ray diffraction pattern (see Fig. 20). Here again there is an opportunity for precise measurements

and careful corrections for absorption effects, but present requirements seem to be met adequately by the simple visual estimation of two to four degrees of blackening. The way in which data from the X-ray patterns are transferred to the pole figure is presented in the following section.

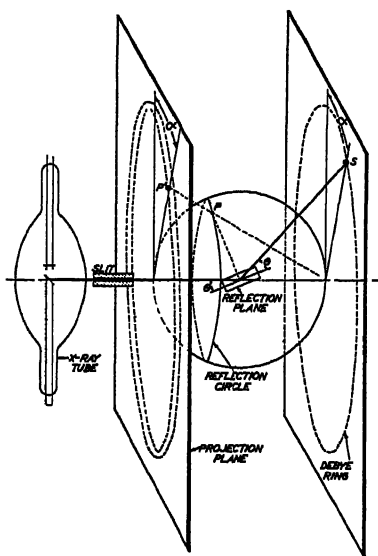


FIG. 21.—RELATION BETWEEN CRYSTALLOGRAPHIC PLANE, DIFFRACTION PATTERN AND STEREOGRAPHIC PROJECTION.

Pole P , diffracted spot S , and projection P' all lie in a plane, which also contains the incident beam.

and projection plane are placed normal to the beam as shown, it will be seen that angular positions about the center of the projection will correspond to angular positions on the film. This azimuth angle is labeled α in the figure.

Since the angle of incidence, θ , of the beam on the crystal plane is determined by the Bragg law $n\lambda = 2d \sin \theta$ whenever reflection occurs, it follows that the poles of all planes capable of reflecting must lie at a constant angle $90 - \theta$ from the incident beam, and must therefore intersect the reference sphere only along the circle known as the "reflection circle,"

Plotting of Pole Figures

There is a simple and direct relation between X-ray diffraction patterns and pole figures, which is illustrated in Fig. 21. A crystal plane is here shown in position to reflect a beam of X-rays to form a spot S on the film. The plane normal intersects the reference sphere, inscribed about it, at the point P , which projects stereographically to the point P' in the projection plane. The incident beam, the reflected beam, and the pole of the reflecting plane all lie in the same plane tipped at an angle α from the vertical. When the film

a circle on the projection $90 - \theta^\circ$ from the centrally located beam. Both the azimuthal and radial position on the pole figure are thus determined.

All of the intensity maxima on a single diffraction ring ("Debye ring") are plotted on a single reflection circle on the pole figure. When the circle cuts through heavily populated regions on the pole figure the diffraction ring will show intense blackening at the same azimuth: when it cuts through lightly populated regions the corresponding arc of the diffraction ring will be weak. To determine the true extent of the areas on the pole figure it is necessary to plot a series of reflection circles that form a network covering the projection. This is accomplished by taking a series of diffraction patterns with the specimen tilted increasing amounts in steps of 5° or 10° . The number of exposures in such a series may vary from 5 to 20 depending upon the detail required in the pole figure.*

We will explain the plotting of the data using rolled steel as an example. If the characteristic radiation ($K\alpha$) from molybdenum is used, the diffraction from the ferrite {110} planes will occur at $\theta = 10^\circ$ and the reflection circle will lie $90 - \theta = 80^\circ$ from the center of the pole figure. If the first photogram is made with the beam normal to the surface of the specimen, the surface will appear on the projection as the basic circle and the reflection circle will lie concentric with it. Let us suppose that the specimen is then rotated about a vertical axis, and a new photogram taken with the specimen turned, say 30° , the near side rotating to the left as we look in the direction of the X-ray beam. We first plot the data as before, with the projection plane again normal to the beam and the reflection circle again concentric. This is illustrated in Fig. 22, where the reflection circle is shown as a dashed circle and an intensity maximum is indicated between the limits A and B. But with this setting of the specimen, its surface will lie at a tilt of 30° from the

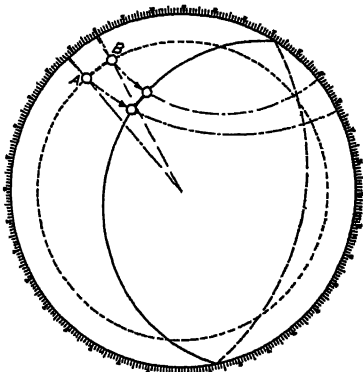


FIG. 22.—PLOTING A POLE FIGURE.
 --- reflection circle with beam normal to projection plane.
 ——— and ——— reflection circle with plane of specimen as projection plane.

* An oscillating film arrangement can be used in plotting pole figures so that one exposure gives the information ordinarily obtained from many individual exposures of the stationary type ^{36,37,46-48}.

The number of exposures can also be reduced by using information from several diffraction rings; for example, by investigating the maxima on the (211) diffraction ring, calculating what positions the {110} or {100} poles must have had to give these maxima, and then plotting the data on a {110} or {100} pole figure. For details of the method see references 28 and 49.

projection plane (the right side tilted up from the projection plane) and all data from this setting must be rotated 30° back to the right in order to plot a pole figure in which the plane of the specimen is the projection plane. The rotation is done with the Wulff net, each point on the reflection circle being moved to the right along its latitude line a distance of 30° of longitude. This is shown in Fig. 22, where the reflection circle with the intensity maximum on it is plotted after rotation as a full line. Part of the rotated reflection circle on the right-hand side passes to the negative hemisphere and is shown as a broken line. The process is repeated with different settings of the specimen and corresponding rotations of the data until the areas on the pole figure are sufficiently well defined.

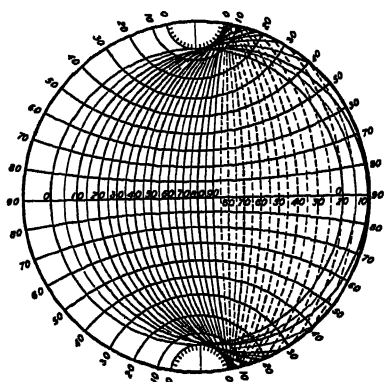


FIG. 23.—POLE-FIGURE CHART FOR MOLYBDENUM $K\alpha$ RADIATION REFLECTING FROM $\{110\}$ PLANES OF IRON. $\theta = 10^\circ$.

charts^{50,51} for copper $K\alpha$ radiation reflecting from $\{001\}$ and from $\{111\}$ planes of aluminum, and for iron $K\alpha$ radiation reflecting from $\{110\}$ of iron. Fig. 23 presents a chart for molybdenum $K\alpha$ radiation reflecting from $\{110\}$ planes of iron ($\theta = 10^\circ$) with reflection circles plotted for every 5° rotation interval from 0° to 90° . The azimuthal positions on all of the circles are given by their intersections with the latitude lines that are drawn on the chart and labeled with values of the angle α (the numbers around the circumference). When the reflection circles lie on the back hemisphere they are shown as dashed lines, but the same lines of constant α apply as on the near hemisphere. This same chart will serve for plotting the $\{200\}$ reflections from iron if one reads the intensity maxima on the broad ring caused by general ("white") radiation, for the most intense portion of the $\{200\}$ reflection of the general radiation from a tube operating at 30 or 40 kilovolts is in the neighborhood of $\theta = 10^\circ$. The maximum intensity of general radiation from $\{110\}$ planes is around $\theta = 7^\circ$, and is particularly suitable for pole-figure work, for it is free from overlapping $\{200\}$ reflections, and shows clearly the slight differences of

Much of the labor of plotting may be eliminated if a chart is made up in which the series of reflection circles are shown in the position they would have after rotation back to the normal setting; i.e., their position with respect to the surface of the specimen as the projection plane. A different chart is required, of course, for every different value of θ that is used, thus for different wave lengths, different specimen materials and different reflecting planes. Wever has published

intensity that are sometimes important. A chart for plotting the {200} reflections of molybdenum $K\alpha$ from iron ($\theta = 14^\circ 20'$) is reproduced in Fig. 24.

Areas near the top and bottom of the pole figure are not crossed by any reflection circles on the chart. To fill in these areas the specimen may be turned 90° in its own plane and then rotated a small amount about the vertical axis, as before. (This requires turning the pole figure plot 90° with respect to the reflection circle chart.) The number of

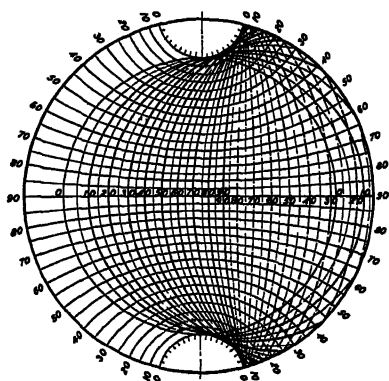


FIG. 24.

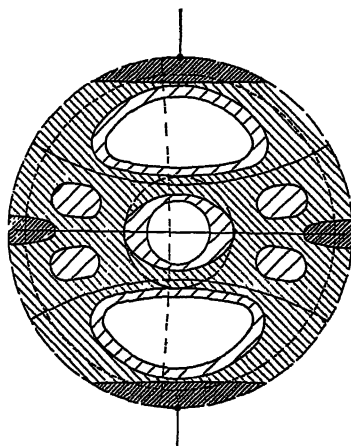


FIG. 25.

FIG. 24.—POLE-FIGURE CHART FOR MOLYBDENUM $K\alpha$ RADIATION REFLECTING FROM {200} PLANES OF IRON. $\theta = 14^\circ 20'$.

FIG. 25⁵².—POLE FIGURE FOR {110} POLES OF MILD STEEL REDUCED 85 PER CENT IN THICKNESS BY COLD-ROLLING⁵³.

* and — — indicate simple tension texture with rolling direction as axis.
 — — — indicates simple compression texture with normal to sheet as axis.
 - - - - shows reflection circle for white radiation incident normal to sheet.
 — — — — shows reflection circle for white radiation incident in transverse direction.

exposures may be reduced by making use of the symmetry of the orientations in the structure; in rolled sheet, for example, a symmetry plane may be anticipated normal to the rolling direction and another normal to the transverse direction in the sheet, but it is always advisable to test for these symmetry planes before assuming them.*

The pole figure for a mild-steel sheet rolled to a reduction of thickness of 85 per cent and etched so that the surface layers are removed is shown in Fig. 25. The rolling plane is parallel to the projection plane, with the rolling direction at the top. This figure illustrates, incidentally, why it is that preferred orientations appear more prominently in photographs made with the beam along or near to the transverse axis of a rolled steel sheet than with the beam normal to the rolling plane. The (110)

* See, for example, M. Gensamer and R. F. Mehl⁵².

reflection circle for a beam of white radiation normal to the rolling plane is shown as a dotted circle near the periphery, and nowhere passes into regions of greatly differing intensity. On the other hand, the reflection circle for a beam along the transverse direction appears as a dotted line extending from top to bottom near the center of the projection, and passes through regions of both maximum and minimum intensity, which would yield more pronounced maxima and minima on the (110) diffraction rings.

Pole Figures in Transformation and Precipitation Studies

Pole figures have been of the greatest usefulness in determining the orientation relationships that almost invariably exist between new metal crystals and the original matrix crystal in which or from which they form by precipitation from solid solution,* by lattice transformations^{15,53,54}, by recrystallization of single crystals^{21,55}, by eutectoid reactions^{54,56}, by peritectic reactions⁵⁷, or by oxidation^{14,58}.

On the Interpretation of Pole Figures†

Ideal Orientations.—The simple preferred orientations such as are encountered in drawn wires and in electrodeposited metals are appropriately called "fiber structures," for they resemble the arrangement of natural fibrous materials and have a crystallographic direction parallel to the "fiber axis," with a random orientation of crystallites about this axis. It is convenient to describe the structure in terms of scattering of a certain number of degrees from an ideal orientation in which a certain crystallographic direction is parallel to the fiber axis. This point of view is frequently used, in fact, for the analysis of the X-ray patterns and is particularly useful in studies of wires. Wever has objected, however, that this method of description may lead to an incomplete and arbitrary analysis of the deformation mechanism, particularly in the more complex cases, and has emphasized that pole figures provide a safer basis for studies of the underlying mechanism, for they represent the observational data in an unprejudiced manner.

The interpretation of pole figures will be illustrated by a brief review of a number of examples.

Rolling Textures appear to be best explained as the superposition of compression and tension textures, with the axis of compression normal to the rolled sheet and the axis of tension in the direction of rolling⁶¹. The compression and tension textures forming the basis for the rolling

* A summary of the various determinations has been published by C. H. Mathewson and D. W. Smith⁵⁸ and by G. Sachs⁵⁴.

† We have not included a discussion of stereographic projection in the analysis of asterism in Laue photograms. This has been summarized in a review of internal stresses⁵⁹.

texture of mild steel are indicated in Fig. 25. The ideal compression texture, with the [111] direction normal to the sheet, is represented on the pole figure by two concentric dashed circles, one at $35^{\circ} 16'$ from the center and the other at 90° . The ideal tension texture (with [110] in the direction of rolling) is represented by the points at the top and bottom of the basic circle, and by the circles drawn as full lines lying 60° and 90° from these. The ideal textures pass through every intense region of the pole figure, and account for most of its principle features.* Several pole figures for rolled iron and its alloys have been published^{51, 52, 62-67} covering different compositions and rolling conditions. Pole figures have also been extensively used for face-centered cubic metals⁶⁸⁻⁷⁰. The structures are complicated in the face-centered cubic metals by the fact that even the simple tension and compression textures are double fiber textures, with two lattice directions in the fiber axis.

Pole figures of the rolling textures of the hexagonal metals and their alloys⁷¹⁻⁷⁸ have been particularly useful in deciphering the role of twinning in the development of the structures, and in comparing the structure at the surface with the structure in the interior of the sheet. The relation of deformation structures to the mechanism of deformation of single crystals is quite direct in the hexagonal metals, but is less clear in the cubic metals. The most successful theories seem to be those in which the principal orientations in a deformation texture are considered as the stable ones that will be approached by a grain whose orientation is changing as a result of deformation on several planes⁷⁷⁻⁷⁸. Boas and Schmid¹¹ have shown by stereographic projection the way in which grains of any initial orientation may be expected to rotate—although there have been some differing opinions on the point—as the result of slip on the two or three slip systems of highest resolved shear stress. These directions of rotation lead to the positions the grains assume in deformation textures, if the restriction is made that only those slip systems operate that will produce the change in specimen shape that is actually observed.

It should be mentioned, however, that wholly different kinds of deforming processes leading to the same change in shape produce identical preferred orientations; as, for example, rolling and drawing through a flat die⁷⁹, or rolling and drawing round wires⁸⁰. There is therefore justification for an interpretation of the preferred orientation in terms of the symmetry of flow of the material²⁷.

Surface Deformation Textures.—A few examples can be given of pole-figure studies of surface textures produced by machining and rolling operations. The surface textures of cold-rolled zinc^{72a} and zinc alloys⁸¹

* There is some divergence of opinion as to whether the compression texture of iron is a single fiber structure⁶⁰ or a double one, with both [111] and [100] in the axis of compression⁶¹. The pole figures published for rolled steels do not require a double texture.

are different from the textures inside of the rolled sheet and are important factors in determining the ability of the sheet to withstand bending. The surface of cold-rolled mild-steel sheet has a texture similar to the recrystallization texture of this material⁶⁴ and it has been suggested that local recrystallization may occur at the surface during the cold-rolling. The outermost layers of a steel block after machining in a shaper have a characteristic texture. A pole figure showing this has been plotted using data from back-reflection patterns⁶².

Textures in Deep Drawing.—Textures of deep-drawing sheet have recently been studied by pole-figure methods⁶⁹. A drawn brass cup was X-rayed at various points from top to bottom and pole figures plotted to show the texture at each point. The texture was found to vary from point to point to correspond with the directions of flow of metal and could be analyzed everywhere as the superposition of ideal tension and compression textures of differing relative intensity. For example, at the center of the bottom of the cup the texture was identical with an ideal compression texture with the compression axis vertical (perpendicular to the bottom of the cup) as would be expected from the movement of metal accompanying the thinning of the sheet during the drawing operation. At the upper rim of the cup, on the other hand, there was nearly an ideal compression texture with the compression axis tangential (produced by the enforced contraction of the sheet to form the rim), and this compression texture persisted throughout the upper part of the side wall with lesser intensity and superimposed on a tension texture having the tension axis vertical (parallel to the axis of the cup).

Recrystallization Textures.—The preferred orientations found in rolled and drawn material after recrystallization are not as yet understood. In rolled metals they are commonly of such complexity that an understanding cannot be hoped for without the use of pole figures, such as have been prepared for recrystallized rolled iron⁶², iron-nickel alloys⁶³, mild steel⁶⁴, iron-silicon alloys⁶⁷, magnesium⁶¹, zinc^{64,65}, and aluminum⁶⁶. The extensive studies in Burgers' laboratory⁶⁵, directed toward a solution of recrystallization textures by the analysis of the simpler case of a single crystal of aluminum recrystallized after homogeneous deformation, were based on pole figures.

REFERENCES

1. S. L. Penfield: *Amer Jnl. Sci.* (1901) **11**, 1–25. The Penfield scales and protractors may be purchased from Penfield Stereographic Supplies, Mineralogical Laboratory, Yale University, New Haven, Conn.
2. S. L. Penfield: *Amer. Jnl. Sci.* (1901) **9**, 1–24, 115–144; (1902) **14**, 249–284; *Ztsch. Krist.* (1902) **35**, 1.
3. E. Boeke: *Die Anwendung der stereographische Projektion bei kristallographischen Untersuchungen*. Berlin, 1911. Bornträger.
4. F. E. Wright: *Jnl. Optical Soc. Amer.* (1930) **20**, 529; *Amer. Mineralogist* (1929) **14**, 251.

5. A. Hutchinson: *Ztsch. Krist.* (1909) **46**, 238, early references.
6. R. M. Bozorth: *Phys. Rev* (1925) **26**, 390.
7. E. Schiebold and G. Sachs: *Ztsch. Krist.* (1926) **63**, 34.
8. G. I. Taylor and C. F. Elam: *Proc. Roy. Soc.* (1923) **102**, 643; (1925) **108**, 28.
9. G. I. Taylor: *Proc. Roy. Soc.* (1927) **116**, 16.
10. H. J. Gough: Edgar Marburg Lecture, Amer. Soc. Test. Mat. (1933) **33**, pt. 2.
11. W. Boas and E. Schmid: *Ztsch. tech. Phys.* (1931) **12**, 71.
12. C. H. Samans: *Trans. A.I.M.E.* (1934) **111**, 119.
13. W. Fahrenhorst and E. Schmid: *Ztsch. Physik* (1932) **78**, 383.
14. R. F. Mehl and E. L. McCandless: *A.I.M.E. Tech. Pub.* 780 (*Metals Tech.*, Feb. 1937).
15. R. F. Mehl and D. W. Smith: *Trans. A.I.M.E.* (1934) **113**, 203. In this work, traces on two surfaces were used, but for simplicity we have shown in the present paper the data from only one surface.
16. R. F. Mehl and C. S. Barrett: *Trans. A.I.M.E.* (1931) **93**, 78.
17. R. F. Mehl, C. S. Barrett and D. W. Smith: *Trans. A.I.M.E.* (1933) **105**, 215.
18. N. T. Belaiew: *Crystallization of Metals*. Univ. of London Press, 1922 and *Jnl. Inst. Metals* (1923) **29**, 379.
19. R. F. Mehl, C. S. Barrett and F. N. Rhines: *Trans. A.I.M.E.* (1932) **99**, 203.
20. R. F. Mehl, C. S. Barrett and H. S. Jerabek: *Trans. A.I.M.E.* (1934) **113**, 211.
21. C. S. Barrett, H. F. Kaiser and R. F. Mehl: *Trans. A.I.M.E.* (1935) **117**, 39.
22. R. F. Mehl and O. T. Marzke: *Trans. A.I.M.E.* (1931) **93**, 123.
23. M. L. Fuller and J. L. Rodda: *Trans. A.I.M.E.* (1933) **104**, 116.
24. D. W. Smith: *Trans. A.I.M.E.* (1933) **104**, 49.
25. C. S. Barrett, G. Ansel, and R. F. Mehl: *Amer. Soc. Metals, Preprint* 17 (October 1936).
26. G. Derge, A. R. Kommel and R. F. Mehl: This volume.
27. E. Schmid and W. Boas: *Kristallplastizität*. Berlin, 1935 Julius Springer.
28. W. P. Davey: *A Study of Crystal Structure and its Applications*. New York, 1934. McGraw-Hill Book Co.
29. Glocker: *Materialprüfung mit Röntgenstrahlen*. Berlin, 1927, 1936. Julius Springer.
30. *Internationale Tabellen zur Bestimmung von Kristallstrukturen*, 2. Berlin, 1935. Bortraeger.
31. E. Schiebold and G. Seibel: *Ztsch. Physik* (1931) **69**, 458.
32. F. Rinne and E. Schiebold: *Ber. Sächs Akad. Wiss. Math.-phys. Kl.* (1915) **68**, 11
33. T. A. Wilson: *A.I.M.E. Tech. Pub.* 210 (1929).
34. W. Boas and E. Schmid: *Metallwirtschaft* (1931) **10**, 917.
35. A. B. Greninger: *Trans. A.I.M.E.* (1935) **117**, 61.
36. W. P. Davey: *Phys. Rev.* (1924) **23**, 764.
37. T. A. Wilson: *Genl. Elec. Rev.* (1928) **31**, 612.
38. C. H. Mathewson and K. R. van Horn: *Trans. A.I.M.E.* (1930) **89**, 59.
39. W. C. Elmore and L. W. McKeehan: *Trans. A.I.M.E.* (1936) **120**, 236.
40. N. H. Hartshorne and A. Stuart: *Crystals and the Polarizing Microscope*. London, 1934. Arnold and Co.
41. A. B. Greninger: *Trans. A.I.M.E.* (1936) **120**, 293.
42. L. S. McKeehan: *Nature* (1927) **119**, 120, 392.
43. G. D. Preston: *Nature* (1927) **119**, 601.
44. C. H. Mathewson: *Trans. A.I.M.E.* (1928) **78**, 1, Inst. Metals Division.
45. F. Wever: *Mitt. Kaiser Wilhelm Inst. Eisenforschung* (1924) **5**, 69; *Ztsch. Physik* (1924) **28**, 69.
46. O. Kratky: *Ztsch. Krist.* (1930) **72**, 529.
47. C. S. Barrett: *Trans. A.I.M.E.* (1931) **93**, 75.

48. C. S. Barrett: *Metals and Alloys* (1937).
49. C. B. Post: *Ztsch. Krist.* (1935) A90, 330.
50. F. Wever and W. E. Schmid: *Mitt. Kaiser Wilhelm Inst. Eisenforschung* (1929) 11, 109.
51. F. Wever: *Trans. A.I.M.E.* (1931) 93, 51.
52. M. Gensamer and R. F. Mehl: *Trans. A.I.M.E.* (1936) 120, 277.
53. C. H. Mathewson and D. W. Smith: *Trans. A.I.M.E.* (1932) 99, 264.
54. G. Sachs: *Praktische Metallkunde*, pt. 3, Wärmebehandlung. Berlin, 1935. Springer.
55. W. G. Burgers and J. C. M. Basart: *Ztsch. Physik* (1928) 51, 545; (1929) 54, 74.
W. G. Burgers and P. C. Louwerse: *Ztsch. Physik* (1931) 67, 605; *Metallwirtschaft* (1932) 11, 251.
W. G. Burgers and J. J. A. Ploos van Amstel: *Ztsch. Physik* (1933) 81, 43.
These are summarized in International Conference on Physics, 2. The Physical Society, London, 1935.
56. R. F. Mehl and D. W. Smith: *Trans. A.I.M.E.* (1935) 116, 330.
57. A. B. Greninger: This volume.
58. R. F. Mehl, E. L. McCandless and F. N. Rhines: *Nature* (1934) 134, 1009.
59. C. S. Barrett: *Metals and Alloys* (1934) 5, 131, 154, 170, 196, 224.
60. F. Wever: *Ztsch. tech. Phys.* (1927) 8, 404.
61. A. Ono: *Mem. Coll. Eng. Kyushu Imp. Univ.* (1925) 3, 195, 267.
62. G. Kurdjumow and G. Sachs: *Ztsch. Phys.* (1930) 62, 592.
63. C. B. Post: *Trans. Amer. Soc. Metals* (1936) 24, 679.
64. M. Gensamer and B. Lustman: *A.I.M.E. Tech. Pub.* 748 (*Met. Tech.* Sept. 1936).
65. M. Gensamer and P. A. Vukmanic: *A.I.M.E. Tech. Pub.* 749 (*Met. Tech.* Sept. 1936).
66. D. McLachlan and W. P. Davey (Fe-Ni alloys): *Amer. Soc. Metals Preprint* (October 1936).
67. C. S. Barrett, G. Ansel and R. F. Mehl (Fe-Si alloys): *A.I.M.E. Tech. Pub.* 813 (1937).
68. E. Schmid and G. Wassermann: *Handbuch der Physikalischen und Technischen Mechanik*, 4, Second Half, 319-350. Leipzig, 1931. Barth.
69. L. Herrmann and G. Sachs: *Metallwirtschaft* (October 1934) 13.
70. G. V. Vargha and G. Wassermann: *Metallwirtschaft* (1933) 12, 511.
71. E. Schmid and G. Wassermann: *Metallwirtschaft* (1930) 9, 698.
72. E. Schmid and G. Wassermann: *Ztsch. Metallkunde* (1931) 23, 87; (1931) 10, 735.
73. M. L. Fuller and G. Edmunds: *Trans. A.I.M.E.* (1934) 111, 147.
74. V. Cagliotti and G. Sachs: *Metallwirtschaft* (1932) 11, 1.
75. M. A. Valouch: *Metallwirtschaft* (1932) 11, 165.
76. W. G. Burgers: *Metallwirtschaft* (1935) 14, 285.
77. M. Polanyi: *Ztsch. Phys.* (1931) 17, 42.
78. G. Sachs and E. Schiebold: *Naturwissenschaften* (1925) 13, 964.
79. W. A. Sisson: *Metals and Alloys* (1933) 4, 192.
80. G. Vargha and G. Wassermann: *Ztsch. Metallkunde* (1933) 25, 310.
81. G. Edmunds and M. L. Fuller: *Trans. A.I.M.E.* (1932) 99, 175.
82. M. Renninger: *Metallwirtschaft* (1934) 13, 889.
83. W. G. Burgers and J. L. Snoek: *Ztsch. Metallkunde* (1935) 27, 158.
84. R. Straumann: *Helv. Phys. Acta* (1930) 3, 463.
85. M. L. Fuller and G. Edmunds: *Trans. A.I.M.E.* (1934) 111, 146 and discussion.
86. E. Schmid and G. Wasserman: *Metallwirtschaft* (1931) 10, 409.

The Solid Solubilities of the Elements of the Periodic Subgroup Vb in Copper*

By J. C. MERTZ,† JUNIOR MEMBER, AND C. H. MATHEWSON,‡ MEMBER A.I.M.E.

(Cleveland Meeting, October, 1936)

ACCURATE knowledge of the solid solubilities of the elements that dissolve in the important base metals is needed for guidance in the preparation and heat-treatment of the alloys derived from these components. While there is still difference of opinion concerning the merits of the X-ray and microscopic methods of determining such solubilities, it is certainly true that the recent extensive use of X-ray diffraction to review the existing constitutional data has revealed many glaring inaccuracies and has brought about a much improved knowledge of phase-boundary locations, which will inevitably come to include all of the important alloy systems. When the work is done with all necessary precautions it appears that in the majority of cases where the solubilities extend beyond a few tenths of a per cent the X-ray back-reflection technique is capable of furnishing the best of information in this field. For the most prolonged and thorough studies it is obviously advisable to combine the results of several methods, in particular, to obtain an agreement between X-ray and microscopic data.

This paper reviews the work previously done on the solubilities of phosphorus, arsenic, antimony and bismuth in copper and, in consideration of the uncertainties thus made apparent, presents new X-ray data obtained with the first three members of this group.

COPPER-PHOSPHORUS SYSTEM

Heyn and Baur¹ found that in slowly cooled alloys phosphorus forms a solid solution with copper up to about 0.175 per cent. Huntington

* From a part of a dissertation presented by J. C. Mertz to the Faculty of the Graduate School of Yale University in partial fulfilment of the requirements for the degree of Doctor of Philosophy. Manuscript received at the office of the Institute June 16, 1936.

† Graduate Student, Department of Metallurgy, Yale University, New Haven, Conn.

‡ Professor of Metallurgy, Yale University.

¹ References are at the end of the paper.

and Desch², by microscopic examination and chemical analysis of slowly cooled alloys, also found 0.175 per cent phosphorus retained in solid solution. Later, Hudson and Law³ stated that a phosphor copper containing 0.9 per cent phosphorus had an almost homogeneous structure after annealing for 2 hr. at 690° C., or 4 hr. at 640° C. Hanson, Archbutt, and Ford⁴ made a thorough microscopic investigation of the solid solubility between 682° and 280° C. Their results indicated that the solubility of phosphorus in copper increases from close to 0.5 per cent at 280° C. to between 0.975 and 1.16 per cent at 682° C. In what we believe to be the latest work published on the copper-phosphorus constitutional diagram, Lindlie⁵ did not investigate the solid solubility, but uses the last mentioned results in his diagram.

The copper used in the experiments described herein was prepared as described by Rhines and Mathewson⁶. Chemical analysis showed 99.99+ per cent copper, and spectrographic analysis* revealed no appreciable quantity of any other element. The lattice parameter of this copper, as determined by the back-reflection method, is 3.6078 Å., which agrees well with the value of Owen and Yates⁷, who give 3.6077 ± 0.0002 Å. Phosphorus was added in the form of a phosphor copper containing about 8.5 per cent phosphorus. Spectrographic analysis showed traces of silver and cobalt to be the only impurities present in recognizable quantities.

Alloys were prepared in 50-gram melts in plain graphite crucibles under molten borax. The crucibles were heated in a high-frequency induction furnace until the borax was liquid and the weighed amount of copper was introduced bit by bit. When the copper was entirely molten, the desired amount of phosphor copper was introduced and the melt stirred by eddy currents for 15 to 30 min.; then the current was stopped and the alloy allowed to solidify and cool in the furnace. The ingots thus produced were quite sound and showed no loss in weight. The ingots were quartered, cold-worked until signs of cracking appeared, then individually sealed under vacuum in Pyrex glass and given a homogenizing treatment at 700° C. for two weeks. At the end of this period they were machined into small rods 0.17 in. in diameter and about one inch long.

Analyses were made electrolytically upon the dust from the quartering operation, the chips from the machining operation, and a section of the X-ray specimen itself. All agreed within ± 0.02 per cent, and the average results are shown in Table 1.

Each specimen was sealed under vacuum in Pyrex glass and annealed for the desired period of time in a nichrome-wound tube furnace with a constant temperature heating zone of 11 in. Two calibrated platinum-

* The authors are indebted to Prof. W. E. Milligan, of the Department of Metallurgy, Yale University, for all spectrographic analyses mentioned.

platinum rhodium thermocouples were used, the hot junctions being placed next to the specimens. One was connected to a Brown recording potentiometer, which gave a control of $\pm 1^\circ \text{C}$., the other to a Leeds & Northrup portable potentiometer for an occasional check on the temperature. Specimens were quenched in cold water, X-rayed immediately, resealed in vacuo, and replaced in the furnace.

The back-reflection method of X-ray analysis used has been described in detail by Phillips and Brick³. The camera used was a modification of the van Arkel type, which enabled specimen to film distance to be

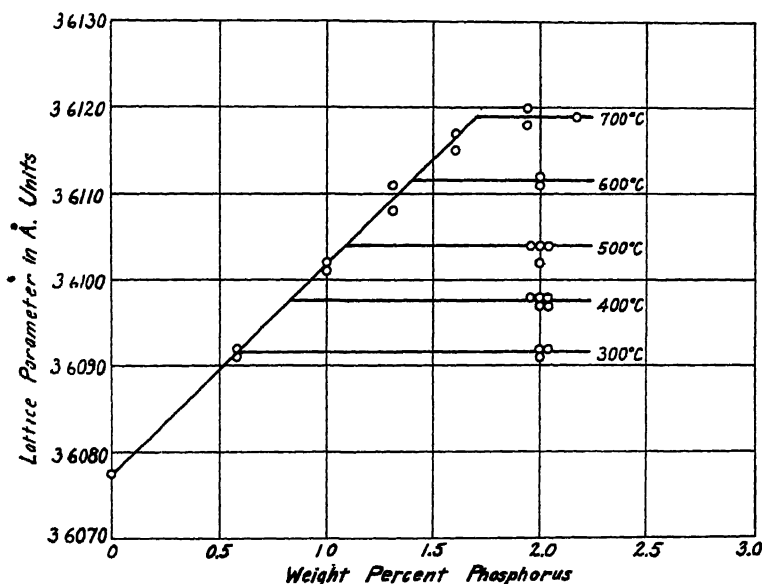


FIG. 1.—CHANGE OF LATTICE PARAMETER OF COPPER-PHOSPHORUS ALLOYS WITH CONCENTRATION AND EFFECT OF ANNEALING TWO-PHASE ALLOYS TO EQUILIBRIUM.

held constant regardless of the specimen diameter. Nickel *K* radiation was employed, operating the Seemann tube at 35 kv. with 20 ma. tube current. Exposure time averaged one hour. The van Arkel extrapolation method was employed to determine corrected a_0 values, and the relative accuracy has been calculated to be approximately $\pm 0.0002\text{\AA}$.

Specimens of each alloy were annealed for 400 hr. at 700°C ., quenched, the parameters determined, annealed at the same temperature for 200 hr. longer, and the parameters again determined. The results are tabulated in Table 1 and are shown graphically in Fig. 1.

Since surface conditions are of primary importance in the X-ray method employed, the surfaces of several specimens were removed, both by a nitric acid etch and by the use of fine emery cloth, and the parameters again determined in an effort to ascertain whether any phosphorus was

lost from the surface by volatilization during heat-treatment. The values obtained were unchanged, the only effect observed being a slight broadening of the lines due to stress produced by these operations.

TABLE 1.—*Lattice-parameter Values of Copper-phosphorus Alloys*
ALL SPECIMENS QUENCHED IN COLD WATER FROM SOLUTION TREATMENT AT 700° C.

Alloy	P, Per Cent by Wt.	a_0 Value, Å.	
		After 400 Hr.	After 600 Hr.
P1	0.58	3.6092	3.6091
P2	1.00	3.6101	3.6102
P3	1.31	3.6107	3.6111
P4	1.60	3.6117	3.6115
P5	1.94	3.6120	3.6118
P6	2.17	3.6119	3.6119

The end of one specimen of each alloy was polished and examined microscopically. Alloys P1, P2, P3 and P4 contained only one phase, while alloys P5 and P6 contained bluish particles of beta, which showed extinction when viewed by polarized light. All had a grain size of approximately 0.20 mm. diameter.

Brick, Phillips and Smith⁹ recently reported marked differences between a_0 values of aluminum-magnesium alloys, depending upon the strain produced by quenching. They found that powders were least subject to strain, while $\frac{1}{2}$ -in. rods quenched in cold water showed the greatest strain and highest a_0 values.

In order to discover whether the a_0 values obtained from our specimens might be anomalously high, because of quenching strains, or approximated the true strain-free parameter values, a powder was obtained from one end of the specimen P5 by means of a fine file, annealed in vacuo at 700° C. for 24 hr., quenched, and a powder photogram taken. The parameter value obtained was 3.6118Å., indicating that quenching strains do not appreciably affect the parameter measurements obtained from our specimens.

Several specimens of the higher phosphorus content alloys were now individually sealed under vacuum in Pyrex glass as before, placed in the furnace side by side, and heat-treated under identical conditions at temperatures between 700° and 300° C., being held at each temperature until successive determinations of parameter values indicated that equilibrium at that temperature had been attained. The results are summarized in Table 2 and also shown in Fig. 1.

The solid solubility curve obtained from these data is shown in Fig. 2, using the eutectic temperature (714° C.) obtained by Lindlie⁵.

For purposes of comparison, the smooth curve drawn by Hanson, Archbutt, and Ford⁴ from the results of their microscopic examination is also shown.

TABLE 2.—*Parameter Values of Copper-phosphorus Alloys after Precipitation Treatment*

Temperature, Deg. C.	Alloy	Time, Hr	a_0 Value, Å.	Temperature, Deg. C.	Alloy	Time, Hr.	a_0 Value, Å
600	P5	200	3.6111	400	P6	200	3.6097
		400	3.6112			400	3.6098
500	P4	150	3.6104	300	P5	200	3.6098
		350	3.6104				
	P6	150	3.6104		P4	200	3.6097
		350	3.6102			400	3.6095
400	P4					600	3.6092
		200	3.6098		P6	200	3.6095
		400	3.6097			400	3.6091
						600	3.6092

In a recent paper, Fink and Freche¹⁰ have shown that thermodynamical equations characterizing the behavior of perfect solutions may be used to generalize the solubility data obtained from many aluminum-base alloys even outside the range of dilute solutions. By plotting solid solubility data of six binary aluminum alloys, employing the reciprocal of the absolute temperature and the logarithm of the atomic per cent of alloying element as coordinates, they obtained curves closely approximating straight lines. It was considered of interest to compare the curves of Fig. 2 in this way.

Corresponding points from these curves were plotted in terms of $\frac{1}{T}$ and log atomic per cent phosphorus, and are shown in Fig. 3, where Centigrade temperatures and weight percentages of phosphorus are indicated for convenience in comparing the two figures.

Inasmuch as Hanson, Archbutt, and Ford⁴ do not report any thoroughly prolonged homogenizing process, but apparently took their alloys as cast and annealed at 685° C. for 96 hr., it seems probable that true equilibrium was not attained. The disappearance of the beta particles visible in all their alloys at first is no guarantee that portions of their specimens were not higher in phosphorus content than others. Upon annealing at lower temperatures it seems conceivable that such localized concentration zones would precipitate particles of phosphide, thereby producing a metastable equilibrium in the zones, while the rest of the

alloy is capable of holding in solution more phosphorus than it has acquired. Our observations indicate that the migration of phosphorus atoms through the copper lattice is a slow process, especially at temperatures below 400° C.

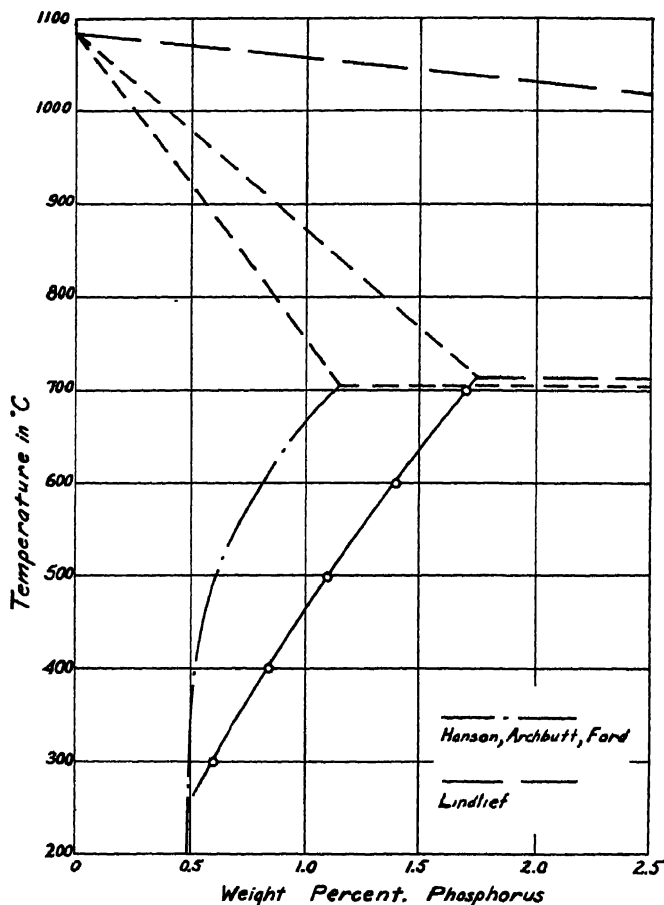


FIG. 2.—SOLID SOLUBILITY OF PHOSPHORUS IN COPPER.

In view of these considerations and the fact that our curve meets the theoretical test outlined above, we feel justified in assuming the results to be more nearly correct, indicating that the solubility of phosphorus in copper increases from about 0.6 per cent phosphorus at 300° C. to approximately 1.7 per cent at 700° C.

COPPER-ARSENIC SYSTEM

Friedrich¹¹ studied copper-arsenic alloys by means of thermal analysis and electrical resistivity measurements, and concluded that at 700° C.

copper may hold 4 per cent by weight of arsenic in solid solution. Bengough and Hill¹², using thermal analysis, micrographic examination and scleroscopic tests, reported that copper holds about 3 per cent arsenic by weight in solid solution at ordinary temperatures with a rate of cooling of approximately 15° to 20° per minute. Pushina and Dishlera¹³ measured electrical conductivity between 0 and 45 per cent arsenic and found a break in the curve at 6 per cent arsenic, indicating a limit of

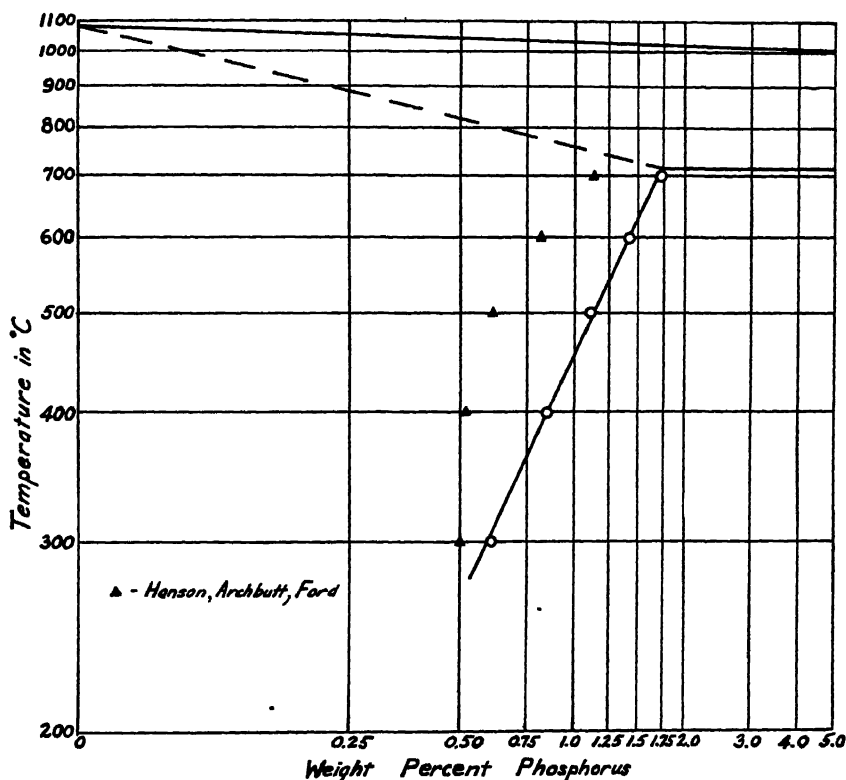


FIG. 3.—DIAGRAM OF FIG. 2 IN WHICH $1/T$ IS PLOTTED AGAINST LOGARITHM OF ATOMIC PER CENT OF PHOSPHORUS, BUT CENTIGRADE TEMPERATURES AND WEIGHT PERCENTAGES ARE SHOWN TO FAVOR COMPARISON WITH FIG. 2.

solid solubility. Hanson and Marryat¹⁴, by microscopic examination, placed the limit of solubility of arsenic in solid copper at close to 7.25 per cent by weight, and stated that it changed very little with fall of temperature. Katoh¹⁵ studied the system copper-arsenic by X-ray methods, but did very little work on the alpha phase. From two powder photograms in this region he concludes that copper dissolves about 4 per cent arsenic by weight at room temperature. Hume-Rothery, Mabbott and Channel-Evans¹⁶ investigated the solid solubility microscopically, and placed the limit between 5.91 and 6.40 atomic per cent

(6.89 to 7.47 weight per cent) arsenic. They found no change with temperature.

The copper previously specified was used in the present experiments along with arsenic "Kahlbaum." A spectrographic analysis of the latter showed traces of antimony, bismuth, silicon, tin, lead, copper and magnesium to be present as impurities.

A hardener alloy containing about 27 per cent arsenic was prepared in the high-frequency furnace, using a graphite crucible and borax flux as before. A series of alloys was then prepared according to the

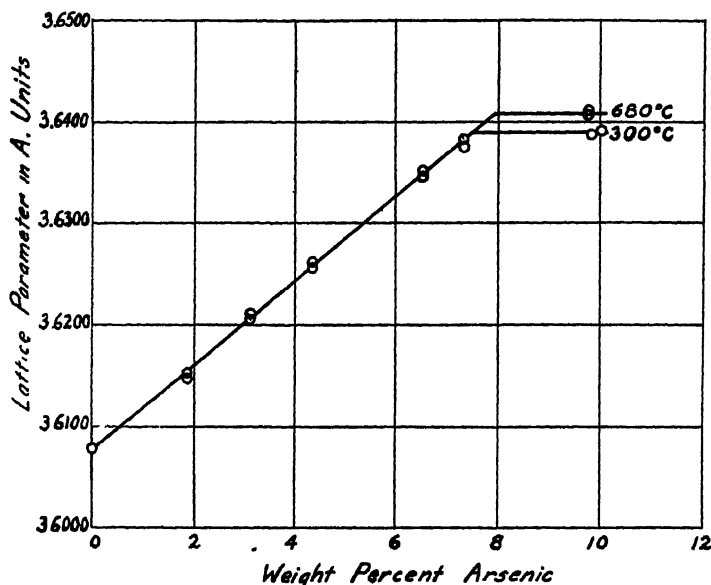


FIG. 4.—CHANGE OF LATTICE PARAMETER OF COPPER-ARSENIC ALLOYS WITH CONCENTRATION AND EFFECT OF ANNEALING TWO-PHASE ALLOYS TO EQUILIBRIUM.

practice followed with the copper-phosphorus alloys. The ingots thus produced were sound and showed no loss in weight. As before, they were quartered, cold-worked, sealed under vacuum in Pyrex glass, homogenized for two weeks at 680° C. and then machined into specimens 0.20 in. in diameter and about one inch long.

Electrolytic analyses of powder, chips and portions of the specimens checked within 0.02 per cent for each alloy. To further check the accuracy of the analyses, the pure copper and arsenic were weighed out in amounts proportional to the percentage composition of the alloys, dissolved and electrolyzed in exactly the same manner as the alloy samples. These determinations checked the weighed amounts to better than 0.02 per cent in every case.

A specimen of each alloy was sealed in evacuated Pyrex tubing, annealed at 680° C. for 800 hr., quenched in cold water, and the parameter

value determined. It was then resealed in vacuo, held an additional 300 hr. at the same temperature, quenched, and the parameter again determined. The results are tabulated in Table 3 and shown graphically in Fig. 4.

Removal of the surface of several specimens by etching and by use of fine emery cloth showed no loss of arsenic in this region.

Microscopic examination of the specimens after the ends were polished showed alloys A1, A2, A3, A4 and A5 to contain only one phase, whereas A6 contained considerable beta in small bluish grains, which showed extinction under polarized light. The average grain diameter was approximately 0.20 mm. A powder obtained from the end of the specimen of A5, annealed in vacuo at 680° C. for 24 hr. and quenched in cold water, gave a parameter value of 3.6376 Å., showing the effect of quenching strains to be negligible in these alloys.

The specimens of alloys A5 and A6 were then individually sealed in evacuated Pyrex tubes and given identical heat-treatments at temperatures between 650° and 300° C., the parameters being determined at

TABLE 3.—*Lattice-parameter Values of Copper-arsenic Alloys Annealed at 680° C. and Quenched in Cold Water*

Alloy	As, Per Cent by Wt.	a_0 Values, Å.	
		After 800 Hr.	After 1100 Hr.
A1	1.85	3.6148	3.6153
A2	3.10	3.6212	3.6208
A3	4.35	3.6257	3.6262
A4	6.50	3.6352	3.6348
A5	7.31	3.6375	3.6378
A6	9.76	3.6407	3.6412

intervals. These data are shown in Table 4 and the values obtained at 300° C. are shown in Fig. 4. The experiments indicate that the solid solubility is about 7.9 per cent arsenic by weight at 680° C. and decreases slowly and approximately linearly to about 7.5 per cent at 300° C. It might be argued that the fall in a_0 values obtained was due to loss of arsenic from the surface of the specimen during the long anneals, but this seems precluded by the fact that the a_0 value of specimen A5, containing 7.31 per cent arsenic, which received identical treatment, and from which no arsenide could precipitate, remained constant within the limit of accuracy of the method.

Fig. 5 shows the solubility curve thus obtained incorporated into the diagram given by Bengough and Hill¹². The uncertain conditions in the vicinity of 30 per cent arsenic have not been subjected to modern investi-

gation, and the early data have been thoroughly discussed by Guertler on pages 842 to 853 of his *Handbuch*.

Friedrich¹¹ cooled his alloys at the rate of 75° per minute to 700° C., quenched, and examined microscopically, hence segregation would account for his low value of 4 per cent arsenic held in solution. Bengough and Hill¹² used the same methods, cooling their alloys more slowly (15° to

TABLE 4.—*Lattice-parameter Values of Alloys A5 and A6 at Various Temperatures, after a Cold-water Quench*

Alloy	Temperature, Deg. C.	Time, Hr.	a_0 Values, Å.	Alloy	Temperature, Deg. C.	Time, Hr.	a_0 Values, Å.
A5	650	500	3.6376	A6	650	500	3.6408
		700	3.6377			700	3.6406
		900	3.6380			900	3.6407
	600	500	3.6379		600	500	3.6403
		700	3.6378			700	3.6405
	500	350	3.6376		500	350	3.6403
		550	3.6379			550	3.6401
	400	400	3.6380		400	400	3.6398
		600	3.6378			600	3.6396
	300	400	3.6378		300	400	3.6393
		600	3.6377			600	3.6389
						800	3.6390

20° per minute) to room temperature, but probable segregation would also account for their figure of 3 per cent. Pushina and Dishlera¹³ prepared no alloys between 6 and 10 per cent arsenic, and if they had done so might have found the break in the conductivity curve at a higher arsenic content than the 6 per cent reported. Katoh¹⁵ gives a_0 values of 3.608 Å. for copper, 3.629 Å. for 2 per cent arsenic and 3.640 Å. for the solubility limit. The last value is in good agreement with ours, but the 3.629 Å. should correspond to about 4 per cent arsenic instead of 2 per cent. How this value was obtained cannot be determined, since no details of heat-treatment, etc., are given. The 7.25 per cent value of Hanson and Marryat¹⁴ and the 7.47 per cent upper limit at 550° C. of Hume-Rothery, Mabbott, and Channel-Evans¹⁶, are in fairly good agreement with our results, especially since they did not anneal for as long periods of time. Furthermore, in all of the investigations outlined above, the copper used was commercial electrolytic, hence inferior in purity to our copper.

COPPER-ANTIMONY SYSTEM

Before 1913 no attempt had been made to determine the solubility of antimony in solid copper in annealed and quenched alloys. In that year

Carpenter¹⁷ reported that such alloys, on micrographic examination, revealed a limit of solubility of antimony in solid copper at 4 atomic per cent

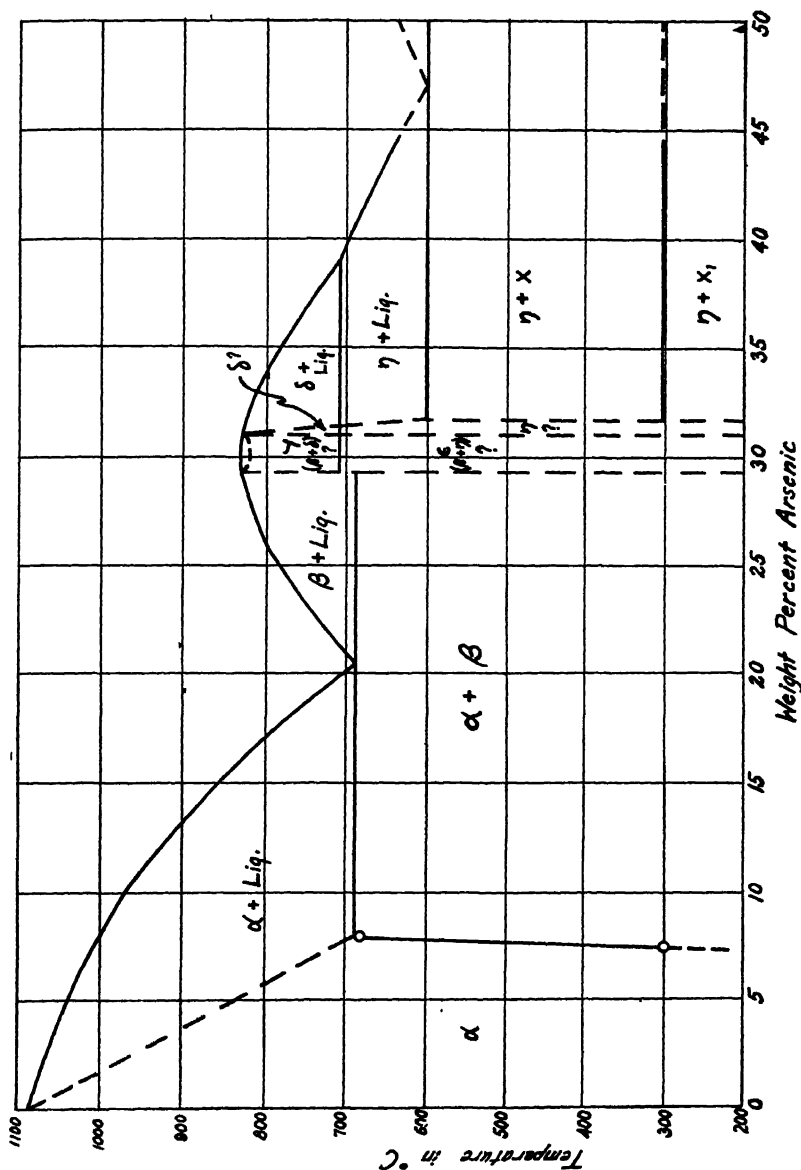


FIG. 5.—COPPER-ARSENIC PHASE DIAGRAM ACCORDING TO BENGOUGH AND HILL, WITH THE ALPHA-PHASE BOUNDARY DETERMINED IN THE PRESENT INVESTIGATION.

(nearly 8 per cent by weight), and stated further that the slope of the line was too steep to be determined by quenching experiments. Westgren, Hägg and Eriksson¹⁸ in 1929 investigated the system by means of X-ray powder photograms and concluded that Carpenter's figure was correct,

although they prepared only one alloy in the alpha-phase region. Howells and Morris-Jones¹⁹ made an X-ray investigation of the copper-antimony system, but also prepared only one alloy in the alpha range. A little later, Archbutt and Prytherch²⁰ prepared a series of alloys between 5 and 10 per cent antimony, annealed in vacuo at temperatures between 400° and 750° C., quenched, and examined the microstructures. They placed the solubility limit at about 9.5 per cent antimony. Finally, Hume-Rothery, Mabbott and Channel-Evans¹⁸ used the same method at temperatures between 200° and 625° C., and found the solubility to be about 5.6 atomic per cent (10.2 per cent by weight) at 600° C., practically unchanged at 550° C., slightly lower at 500° C., followed by a much more marked decrease below 450° to a value of 2.8 atomic per cent (5.23 per cent by weight) at 200° C.

The copper used in our investigation was that previously noted. Antimony "Kahlbaum" was used, a spectrographic analysis showing it to contain traces of arsenic, tin, lead, copper and magnesium.

All melts were made by high-frequency induction melting in pure alundum crucibles in vacuo. A hardener alloy containing 47 per cent antimony was prepared, and when this was used as the addition agent the

TABLE 5.—*Lattice-parameter Values of Copper-antimony Alloys Annealed at 630° C. and Quenched in Cold Water*

Alloy	Sb, Wt. Per Cent	a_0 Values, Å.		
		After 700 Hr.	After 1200 Hr.	After 1600 Hr.
S1	2.36	3.6199	3.6197	3.6198
S2	4.25	3.6330	3.6325	3.6330
S3	6.43	3.6413	3.6455	3.6455
S4	8.40	3.6570	3.6595	3.6591
S5	10.63	3.6706	3.6715	3.6712
S6	12.46		3.6750	3.6754

resulting ingots showed no loss in weight. The ingots were treated exactly as in the previous work, except that the two-week homogenizing treatment was carried out at 630° C. The final specimens were 0.20 in. in diameter by one inch long.

Analyses were made on the dust, chips and a portion of each specimen as before. The copper was electrodeposited, the deposition being carried to a point where gassing and a slight deposit of antimony appeared at the cathode and the electrolyte showed no copper by H₂S test. The electrolyte was then discarded, the deposit dissolved and the copper redeposited at 0.2 amp. per square decimeter. These analyses checked within 0.02 per cent. The same treatment was given weighed amounts of the pure

copper and antimony in proportions similar to the alloy compositions, and the copper checked to within 0.2 mg. or better in a $\frac{1}{2}$ -gram sample in every case. The analyses also checked well with the determination of antimony by the standard permanganate method.

The specimens were sealed in evacuated Pyrex glass tubes and annealed at 630° C., α_0 values being determined at intervals after a cold-water quench. Results are shown in Table 5 and Fig. 6.

Archbutt and Prytherch²⁰ reported traces of a deposit on the tube and thermocouple after vacuum annealing, but their analysis showed that the deposit contained both copper and antimony and that the loss of antimony was too small to be serious. We observed a copper-colored deposit on the inside of the Pyrex tubes at the higher temperatures, but removal of the specimen surfaces by etching and mechanical means showed no change in parameter value, nor did the value drop after re-annealing. Consequently it seems apparent that the slight sublimation does not affect the equilibrium in the solid metal.

Microscopic examination of the specimens showed S1, S2, S3, S4 and S5 to consist entirely of one phase, while S6 showed bluish grey particles of beta, generally diamond-shaped. These particles showed extinc-

TABLE 6.—*Parameter Values of Alloys S5 and S6 Annealed in Vacuo at Various Temperatures and Cold-water Quenched*

Alloy	Temperature, Deg. C.	Time, Hr.	α_0 Values, Å	Alloy	Temperature, Deg. Hr.	Time, Hr.	α_0 Values, Å.
S5	600	800	3 6708	S5	400	200	3.6565
		1000	3 6712			400	3.6562
		1200	3 6710			600	3.6566
S6	600	800	3.6744	S6	400	200	3 6567
		1000	3 6742			400	3 6563
		1200	3.6744			600	3 6564
S5	500	150	3.6706	S5	300	400	"
		350	3 6710			600	3 6305
		550	3.6708			800	3 6302
S6	500	150	3.6719	S6	300	400	"
		350	3 6712			600	"
		550	3.6712			800	3 6307
S5	450	200	3 6677	S6	211	200	"
		450	3.6659			500	"
		600	3.6661			750	"
						1050	3.6200

" Denotes equilibrium not attained. Lines too broad for accurate measurement. tion under polarized light. Average grain size was approximately 0.25 mm. diameter.

A powder prepared from the specimen of S6 was vacuum-annealed for 24 hr. at 630° C., cold-water quenched and X-rayed. The a_0 value obtained was 3.6749 Å., indicating that quenching strains have no appreciable effect on the parameters of these alloys.

Specimens were now annealed in vacuo at temperatures between 630° and 211° C., the latter heat-treatment being carried out in a constant-boiling bath of nitrobenzene. The results are shown in Table 6, also in Fig. 6.

The solubility curve obtained from the data is shown in Fig. 7, together with the curves of Archbutt and Prytherch²⁰ and Hume-Rothery, Mab-

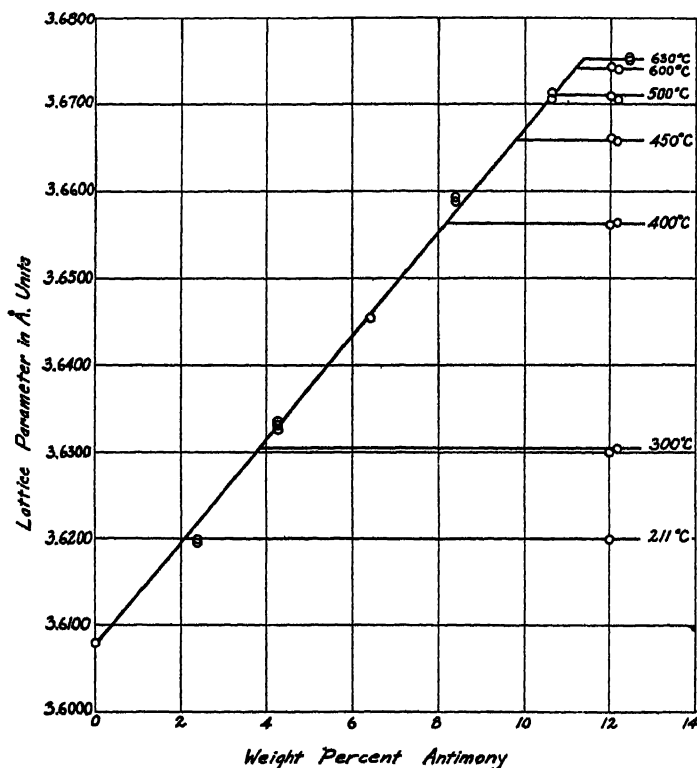


FIG. 6.—CHANGE OF LATTICE PARAMETER OF COPPER-ANTIMONY ALLOYS WITH CONCENTRATION AND EFFECT OF ANNEALING TWO-PHASE ALLOYS TO EQUILIBRIUM.

bott and Channel-Evans¹⁶. The data of the latter authors were given in atomic per cent but have been recalculated to weight per cent for this comparison.

Fig. 8 shows an attempt to apply to our data and those of the last-mentioned investigators, the thermodynamical treatment previously cited, in which log atomic per cent antimony is plotted against the reciprocal of the absolute temperature. For comparison with Fig. 7

the coordinates shown are degrees Centigrade and weight per cent antimony. The plot of our data closely approximates two straight lines intersecting at about 450°C ., which is to be expected from theoretical considerations, inasmuch as above that temperature we are measuring the solubility of beta in alpha, and below it that of gamma in alpha. (The nomenclature used is that of Carpenter¹⁷.) Archbutt and Prytherch²⁰ and Hume-Rothery, Mabbott and Channel-Evans¹⁶ determined one

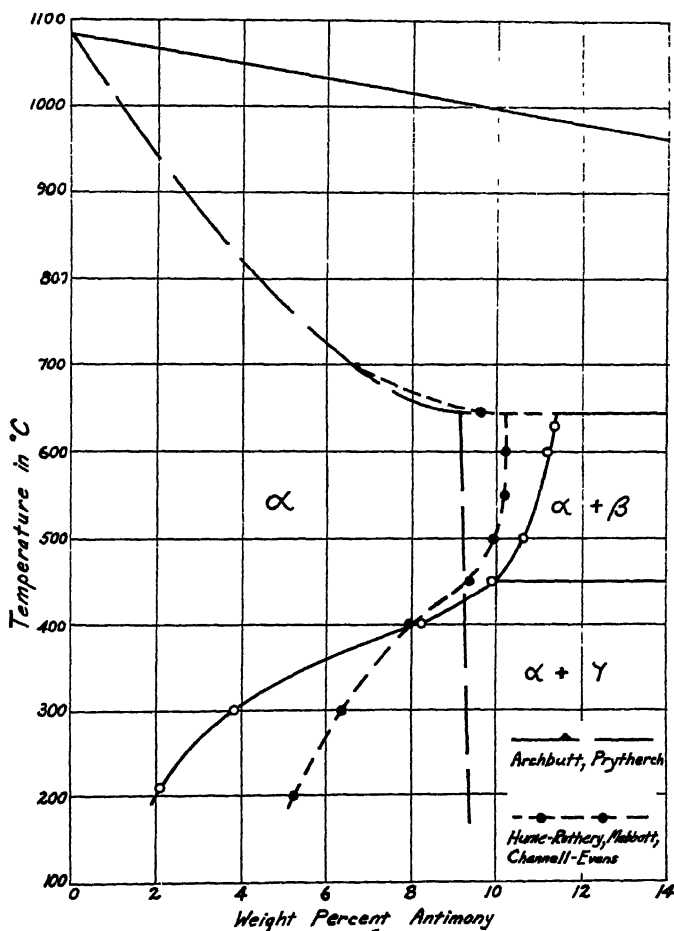


FIG. 7.—SOLID SOLUBILITY OF ANTIMONY IN COPPER.

point on the solidus. A straight line drawn from the melting point of pure copper to the intersection of our upper solubility line and the eutectic horizontal falls between these two points, as shown.

Westgren, Hägg and Eriksson¹⁸ took powder photographs of alloys containing 3 and 6 atomic per cent antimony. Both revealed lines

of the gamma phase, but the authors decided that in the case of the former alloy the faint lines would disappear if the alloy were annealed to equilibrium. From measurements on the latter photogram they reported the parameter of the saturated alpha phase to be 3.66\AA . This result is low, showing a failure to attain true equilibrium.

Howells and Morris-Jones¹⁹ took powder photograms of alloys containing 4 and 20 weight per cent antimony. For the first they give a parameter of 3.644\AA , which should correspond to about 6 per cent

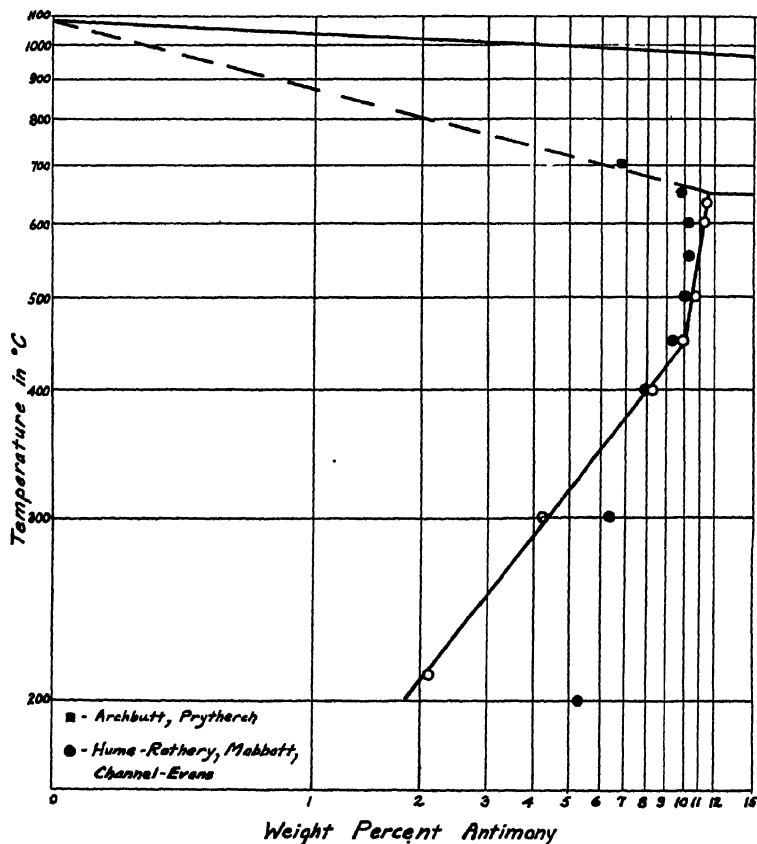


FIG. 8.—DIAGRAM OF FIG. 7 IN WHICH $1/T$ IS PLOTTED AGAINST LOGARITHM OF ATOMIC PER CENT OF ANTIMONY, BUT CENTIGRADE TEMPERATURES AND WEIGHT PERCENTAGES ARE SHOWN TO FAVOR COMPARISON WITH FIG. 7.

antimony and indicates a failure to get a representative powder or an error in analysis. From their 20 per cent antimony photogram a value of 3.670\AA was obtained for the saturated alpha phase. They give no details of heat-treatment, but this approximates our value at 600°C . They draw a straight line between their values for pure copper (3.610\AA .) and the 4 per cent alloy as plotted against percentage of antimony, and

find that 3.670\AA . corresponds to about 7 per cent antimony. Had their middle point been correct they might have obtained a fair approximation of the solubility limit at whatever temperature the 20 per cent alloy was annealed, although the location of a line by two points only is always a questionable procedure. Archbutt and Prytherch²⁰ obviously did not anneal long enough to attain equilibrium.

Hume-Rothery, Mabbott and Channel-Evans¹⁶ have done a fine piece of work, especially considering the limitations of the microscopic method and the fact that melting under charcoal permitted oxygen to enter their melts to the extent of 0.3 to 0.4 per cent. They annealed for several weeks at the higher temperatures but obviously were mistaken in assuming that equilibrium was attained in 30 hr. at the lower temperatures. Our alloy S6, after annealing for 750 hr. at 211°C . had not reached a true state of equilibrium, as indicated by the very diffuse bands on the X-ray photograms. It might be argued that this was due to the large amount of material to be precipitated, but alloy S2, containing about 4 per cent Sb, showed the same broad bands after 300-hr. anneal at the same temperature.

COPPER-BISMUTH SYSTEM

In 1907 Portevin²¹ published a constitutional diagram for the copper-bismuth system based on thermal and microscopic data, which showed no solid solution formation. In the same year Jeriomin²² reported inability to see bismuth in an alloy containing 0.25 per cent, and concluded that it was in solid solution in the copper. More recently Hanson and Ford²³ have prepared a series of oxygen-free alloys containing 0.001 to 0.36 per cent of bismuth by melting in an atmosphere of hydrogen. Small specimens cut from these alloys were polished and examined microscopically, sealed in silica tubes, heated at 980°C . for four days, water-quenched, and re-examined. In all their specimens particles of bismuth were visible before heat-treatment, and the same was true after the anneal except for the 0.001 per cent alloy, hence they concluded that the solid solubility of bismuth in copper is less than 0.002 per cent.

Ehret and Fine²⁴ examined a series of alloys covering the range from pure copper to pure bismuth by the powder method, using the General Electric equipment. All photograms showed the superimposed patterns of copper and bismuth. The mean error of their lattice-parameter measurements was 0.004\AA . and they reached the conclusion that a solid solubility of bismuth in copper of about 0.5 atomic per cent would have been detected. This low solubility of bismuth in copper is to be expected from theoretical considerations, since Hume-Rothery, Mabbott and Channel-Evans¹⁶ have shown that inasmuch as the atomic diameter of bismuth is more than 14 per cent greater than that of copper, conditions are unfavorable for solid solution.

In view of the foregoing evidence to the effect that bismuth can be only slightly soluble in solid copper, it was considered unnecessary to attempt any experimental work upon this system.

SUMMARY

1. By means of the X-ray back-reflection method the following solid solubilities in copper were determined:

Phosphorus; about 1.7 per cent by weight at 700° C., decreasing to about 0.6 per cent by weight at 300° C.

Arsenic; about 8 per cent by weight at 680° C., decreasing slowly to about 7.5 per cent by weight at 300° C.

Antimony; the curve for beta in alpha falling slowly from about 11.3 weight per cent at 630° C. to about 10 weight per cent in the neighborhood of 450° C., that for gamma in alpha falling rapidly from this point to about 2.1 weight per cent at 211° C.

2. Experimental evidence indicates that the effect of quenching strains on lattice-parameter values is practically, if not entirely negligible in these alloys.

3. The application of the Law of Dilute Solutions generalizes the solubility data, indicating that the experimental observations define a true state of equilibrium.

REFERENCES

1. E. Heyn and O. Bauer: Kupfer und Phosphor. *Ztsch. f. anorg. Chem.* (1907) **52**, 129
2. A. Huntington and C. Desch: The Planimetric Analysis of Alloys, and the Structure of Phosphor-Copper. *Trans. Faraday Soc.* (1908) **4**, 51.
3. O. Hudson and E. Law: A Contribution to the Study of Phosphor Bronze. *Jnl. Inst. Metals* (1910) **3**, 161.
4. D. Hanson, S. L. Archbutt and G. W. Ford: Investigation of the Effects of Impurities on Copper, VI.—The Effect of Phosphorus on Copper. *Jnl. Inst. Metals* (1930) **43**, 41.
5. W. E. Lindlief: Melting Points of Some Binary and Ternary Copper-rich Alloys Containing Phosphorus. *Metals and Alloys* (1933) **4**, 85.
6. F. N. Rhines and C. H. Mathewson: Solubility of Oxygen in Solid Copper. *Trans. A.I.M.E.* (1934) **111**, 337.
7. E. A. Owen and E. L. Yates: Precision Measurements of Crystal Parameters. *Phil. Mag.* (1933) [vii] **15**, 472.
8. A. Phillips and R. M. Brick: Grain Boundary Effects as a Factor in Heterogeneous Equilibrium of Alloy Systems. *Jnl. Franklin Inst.* (1933) **215**, 557.
9. R. M. Brick, A. Phillips and A. J. Smith: Quenching Stresses and Precipitation Reaction in Aluminum-magnesium Alloys. *Trans. A.I.M.E.* (1935) **117**, 102.
10. W. F. Fink and H. R. Freche: Correlation of Equilibrium Relations in Binary Aluminum Alloys of High Purity. *Trans. A.I.M.E.* (1934) **111**, 304.
11. K. Friedrich: Kupfer und Arsen. *Metallurgie* (1905) **2**, 477.
Neure Untersuchungen über das Schmelzdiagramm des Systemes Kupfer-Arsen und den elektrischen Leitungswiderstand von arsenhaltigen Kupfer. *Metallurgie* (1908) **5**, 529.

12. G. Bengough and B. P. Hill: The Properties and Constitution of Copper-Arsenic Alloys. *Jnl. Inst. Metals* (1910) **3**, 34.
13. N. A. Pushina and E. G. Dishlera: Conductivity of Alloys of Copper and Arsenic. *Jnl. Russian Phys. Chem. Soc.* (1912) **44**, 125, *Ztsch. anorg. Chem.* (1913) **80**, 65.
14. D. Hanson and C. B. Marryat: Investigation of the Effects of Impurities on Copper, III.—The Effect of Arsenic on Copper. *Jnl. Inst. Metals* (1927) **37**, 121.
15. N. Katch: X-Ray Investigations on Copper-Arsenic Alloys. *Ztsch. Kristallog.* (1930) **76**, 228.
16. W. Hume-Rothery, G. W. Mabbott and K. M. Channel-Evans: The Freezing Points, Melting Points, and Solid Solubility Limits of the Alloys of Silver and Copper with the Elements of the B Sub-Groups. *Phil. Trans. Roy. Soc.* (1934) **A233**, 1.
17. H. C. H. Carpenter: The Copper-Antimony Equilibrium. *Int. Ztsch. Metallog.* (1913) **4**, 300.
18. A. Westgren, G. Hagg, and S. Eriksson: Röntgenanalyse der Systeme Kupfer-Antimon und Silber-Antimon. *Ztsch. Physik. Chem.*, Section B (1929) **4**, 453.
19. E. V. Howells and W. Morris-Jones: An X-Ray Investigation of the Copper-Antimony System of Alloys. *Phil. Mag.* (1930) [vii] **9**, 993.
20. S. L. Archbutt and W. E. Prytherch: Investigations of the Effects of Impurities on Copper, VII—The Effect of Antimony on Copper. *Jnl. Inst. Metals* (1931) **45**, 265.
21. A. Portevin: Les Alliages Cuivre-Bismuth. *Rev. de Mét.* (1907) **4**, 1077.
22. K. Jeriomin: Über Kupfer-Wismutlegierungen. *Ztsch. anorg. Chem.* (1907) **55**, 412.
23. D. Hanson and G. W. Ford: The Effects of Impurities on Copper, V—The Effect of Bismuth on Copper. *Jnl. Inst. Metals* (1927) **37**, 169.
24. W. F. Ehret and R. D. Fine: Crystal Structure in the System Copper-Bismuth. *Phil. Mag.* (1930) [vii] **10**, 551.

Equilibrium Relations in Aluminum-magnesium-zinc Alloys of High Purity

BY WILLIAM L. FINK,* MEMBER A.I.M.E., AND L. A. WILLEY†

(Cleveland Meeting, October, 1936)

THIS paper is the nineteenth of a series from the Aluminum Research Laboratories, presenting the results of the investigations of equilibrium relations in aluminum-base alloys made from electrolytically refined aluminum. In previous papers equilibrium relations have been determined and correlated for 12 binary systems. Equilibrium relations have also been determined for portions of the aluminum corners of three ternary systems (aluminum-iron-silicon, aluminum-magnesium-silicon and aluminum-copper-magnesium). The object of the present paper and those to follow is to increase our knowledge of the aluminum corner of the more important ternary systems.

In 1926 Dix and Keith† suggested a new method for designating the phases encountered in alloy systems. The system has been used to a very limited extent^{1,2,3}. The system has since been slightly modified and will be used in this and future papers. In the system as modified, a phase is designated by placing in parentheses the chemical symbols of the elements essential to the formation of that phase. The symbols in the parentheses are separated by dashes in order to clearly distinguish them from a chemical formula. Elements that are not necessary to the formation of the phase in question, but which may be present in solid solution, are not indicated in the designation. If two or more phases would have the same designation according to these rules, they are distinguished by prefixing Greek letters, and are definitely identified by X-ray diffraction patterns.

PREVIOUS INVESTIGATIONS

The solid solubility of magnesium in aluminum has been well established by the work of Dix and Keller⁴, Schmid and Siebel⁵, and Saldau and Sergeev⁶. There is no agreement as to the composition of the magnesium constituents at the aluminum end of the binary aluminum-magnesium system. Hanson and Gayler⁷ report Mg_2Al_3 ; Boyer⁸ found that the alloy

Manuscript received at the office of the Institute Aug. 14, 1936.

* Aluminum Research Laboratories, New Kensington, Pa.

† References are at the end of the paper.

having a composition corresponding to Mg_2Al_3 was not a single phase. Kauakami⁹ reports Mg_3Al_8 . The present authors, in accordance with the system outlined above and the designation used by Keller and Wilcox in their paper on Polishing and Etching of Constituents of Aluminum Alloys³ will refer to this constituent as $\beta(Al-Mg)$.

The equilibrium relations at the aluminum end of the aluminum-zinc system have been reported by Fink and Willey¹⁰. The zinc terminal solid solution which in that paper was called α will now be called (Zn). The aluminum terminal solid solution which was referred to as β will be designated as (Al). β_1 and β_2 will become (Al) and (Al)'.

On the basis of a critical review of previous work on the magnesium-zinc system (by Chadwick¹¹ and by Hume-Rothery and Rounsefell¹²), Botschwar and Welitschko¹³ published what they considered to be the most probable equilibrium diagram for the magnesium-zinc alloys. There are three binary constituents in this system, one of which, $MgZn_2$ - $[\beta(Mg-Zn)]$, is stable up to its melting point.

The compound $\beta(Mg-Zn)$ forms a binary system with aluminum. This system was investigated by Sander and Meissner¹⁴; Saldau and Zamotorin¹⁵; and by Nishihara¹⁶. It is a eutectic system with the eutectic at approximately 475° C. and approximately 75 weight per cent of $\beta(Mg-Zn)$. These investigations do not agree on the solid solubility at the aluminum end of the diagram.

There have been two investigations of the ternary aluminum-magnesium-zinc system; one by G. Eger¹⁷ and the other by Botschwar and Kuznetsov¹⁸. Eger was interested in the solidus and liquidus curves; Botschwar and Kuznetsov devoted themselves principally to the (Al)-phase boundary in solid alloys.

ALLOYS

Materials Used.—Electrolytically refined aluminum was used in preparing the alloys for the work reported in this paper. Chemical analysis showed the following impurities: 0.004 to 0.005 per cent silicon, 0.004 to 0.006 per cent iron and 0.005 to 0.006 per cent copper. The zinc was triply distilled zinc supplied by the New Jersey Zinc Co., which showed by analysis the following impurities: 0.001 per cent iron and less than 0.001 per cent each of aluminum, silicon, copper, lead, cadmium and sodium. Distilled magnesium furnished by the American Magnesium Corporation was used for most of the alloys, including all those used in the determination of the solid solubility curves. This magnesium showed by analysis the following impurities: silicon, 0.004 per cent; iron, 0.004; copper, 0.001; manganese, 0.0002. Some of the alloys used in determining the phase boundaries were made from commercial magnesium which contained by analysis 0.005 per cent silicon, 0.05 per cent iron, 0.006 per cent copper and 0.002 per cent manganese.

Preparations of Alloys.—The aluminum was melted in a small Hoskins electric crucible furnace. All alloys were prepared by the direct addition of zinc and/or magnesium to aluminum at 690° to 700° C. in an alundum-lined plumbago crucible. The alloys that were to be rolled into sheet were cast in an iron mold into small ingots 10 by 75 by 75 mm. The alloys to be used in the cast form were cast in a graphite mold into rods 12 mm. in diameter and 250 mm. long. The procedure used in rolling the ingots into sheet was varied somewhat, depending upon the alloy. The ingots were all given a homogenizing anneal at temperatures ranging

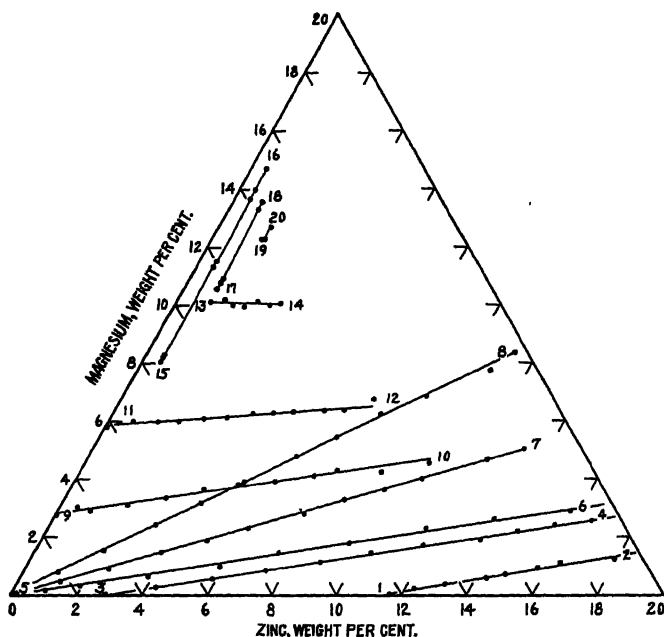


FIG. 1.—SECTIONS AND LOCATIONS OF SAMPLES CONTAINING MORE THAN 80 PER CENT ALUMINUM.

from 400° to 425° C. These alloys were immediately hot-rolled (usually with intermediate anneals) to approximately 3 mm. They were then cold-rolled to a thickness of 1 mm. (18 B.&S. gauge). The specimens for resistivity determinations at elevated temperatures, and for metallographic examination after heat-treatment, were cut from the cold-rolled sheet. The specimens for resistivity determinations were 1 by 23 cm., and for metallographic determinations 2 by 2 centimeters.

Chemical Analyses.—The specimens that had been used for resistivity measurements were later used for chemical analyses. Sometimes the results so obtained were checked by analyzing the sheet adjacent to the resistivity specimens. For cast specimens the analyses were made on small chill-cast slabs poured just before the specimens were poured. Zinc

was determined by the mercuric thiocyanate method¹⁹, and magnesium was determined by the usual method of precipitating as magnesium ammonium phosphate and ignition to pyrophosphate¹⁹. The results of the analyses are given in Table 1 and the locations of the alloys in the ternary system in Figs. 1 and 2.

METHODS

The principal methods used in this investigation were microscopic examination of quenched samples and the measurement of electrical resistivity at elevated temperatures. For the definite identification of the phases, X-ray diffraction patterns were used.

Electrical Resistivity Measurements.—The electrical resistivities were determined by measuring the potential drop across each specimen and

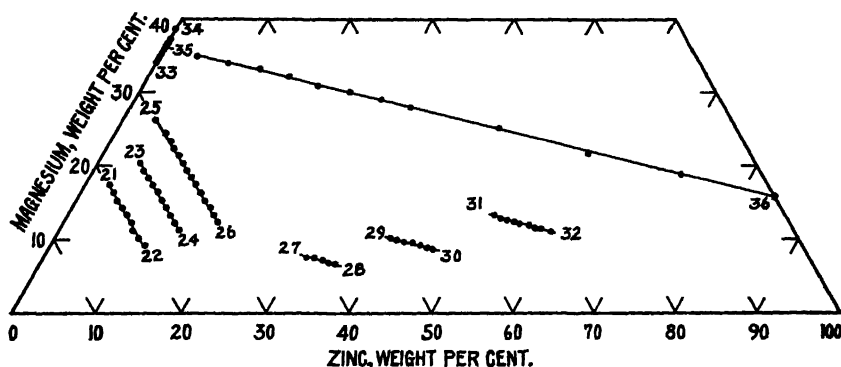


FIG. 2.—SECTIONS AND LOCATIONS OF SAMPLES CONTAINING 80 PER CENT OR LESS OF ALUMINUM.

across a standard 0.001-ohm resistance when the same current was flowing through them in series. The apparatus has been described in a previous paper¹⁰. The temperature of the specimens was held constant within 1° C. of any desired temperature.

Microscopic Methods.—The results of the electrical resistivity methods were checked at numerous points by microscopic examination of specimens heat-treated as described later, and polished and examined as described in previous papers. In certain sections of the diagram where the electrical resistivity method was relatively insensitive (for example, some of the boundaries between two-phase and three-phase fields) it was necessary to rely almost entirely upon microscopic examination.

X-ray Methods.—Debye-Scherrer patterns were prepared from some of the alloys used in this investigation. The patterns so obtained were used as a primary method of identification of the phases present and as a check on the etching procedures used. Most of the specimens for X-ray analysis were small rods approximately 0.5 to 1 mm. in diameter. The samples were rotated during exposure in order to obtain more nearly

TABLE 1.—*Analysis of Alloys Investigated*

Section	Alloy No	Weight Percentage					Atomic Percentage	
		Si	Fe	Cu	Mg	Zn	Mg	Zn
1-2	S13926	0 006	0 004	0 006		11.62		5 15
	S13927				0 20	12 30	0 24	5 47
	S13928				0 36	13 18	0 43	5.90
	S13929				0 57	14 36	0 69	6 47
	S13930				0 72	14 80	0 87	6 69
	S13931				0.91	15 72	1 11	7 15
	S13932				1.07	16.35	1 31	7.46
	S13933				1.21	17.97	1 50	8 28
	S13934				1 43	18.74	1 78	8 68
	S13935				1 58	19.46	1 98	9 05
	S13936				1 76	20.52	2 22	9.61
	S13937	0.006	0 004	0 006	1.99	21 27	2 52	10.01
	S22128	0 005	0.002	0 006		2.87		1.21
	S22129				0 25	4.31	0 29	1 82
3-4	S22130				0 56	5.85	0 64	2 50
	S22131				0.82	7.39	0 95	3.19
	S22132				1.07	8 95	1.25	3 90
	S22133				1 41	10.37	1.67	4 55
	S22134				1 67	11.83	1 99	5.24
	S22135				1 92	13 46	2 31	6 01
	S22136				2 18	14 45	2 64	6.50
	S22137				2 39	15 48	2 91	7.01
	S22138				2 57	16 54	3.16	7 54
	S22139	0 008	0.002	0.006	2.78	17 53	3.42	8.05
5-6	S12556	0.005	0.006	0.006				
	S12557				0 16	0 96	0 18	0 40
	S12558				0.32	1 96	0 36	0 82
	S12559				0.62	3 86	0.70	1.63
	S12560				0 96	5 87	1.10	2 51
	S12561				1 42	7 51	1.65	3 24
	S12562				1.75	9 53	2 05	4.16
	S12563				2.26	11.62	2 68	5 14
	S12564				2 59	13 55	3 11	6.06
	S12565				2 85	15.74	3.47	7 14
	S12566				3.34	18 07	4.13	8 32
5-7	S12511	0.004	0 004	0.006	3.71	19.97	4.64	9 31
	S13078	0.005	0.005	0.006				
	S13080				0 46	1 27	0.51	0.53
	S13082				0.92	2 55	1.04	1.07
	S13084				1.44	3 83	1 63	1.62
	S13086				1.84	5 04	2.10	2 14
	S13088				2.27	6 13	2.61	2 62
	S13090				2 77	7 60	3.21	3 23
	S13092				3 25	8.61	3 78	3.73
	S13094				3.61	9 66	4.23	4.21
	S13096				3.98	10 60	4.69	4 65
	S13098				4.65	12 30	5 53	5.45
	S13100	0.005	0 004	0.006	5 00	13.23	5.98	5 90
5-8	S13214	0.005	0 006	0 006				
	S13215				0 78	1.03	0.87	0 42
	S13216				1 52	2.09	1.71	0 87
	S13217				2.39	3 18	2 70	1.33
	S13218				3 15	4.21	3.57	1 78
	S13219				3.92	5.20	4.47	2.21
	S13220				4.77	6 37	5.47	2.72
	S13221				5.41	7 29	6 24	3.12
	S13222				6 13	8.24	7 10	3.55
	S13223				6.84	9 35	7.97	4.06
	S13224				7.74	10.84	9.09	4.74
	S13225	0.005	0.004	0.006	8.37	11 27	9 85	4 94
9-10	S12668	0.005	0.005	0.006	2.75		3 04	
	S12669				3.02	0.51	3.35	0 21
	S12670				2.89	1 00	3.22	0.41
	S12671				3.10	2.01	3.47	0.84
	S12672				3.34	3 06	3 76	1.28
	S12673				3.63	4 07	4 11	1 72
	S12674				3.79	5.02	4.32	2 13
	S12675				3 88	6 14	4 46	2.62
	S12676				4.10	7 24	4 73	3.11
	S12677				4.26	7.91	4.94	3.41
	S12678				4.22	9 27	4 93	4.04
	S12679	0.006	0.004	0.007	4.56	10 59	5 37	4 63

TABLE 1.—(Continued)

Section	Alloy No.	Weight Percentage					Atomic Percentage	
		Si	Fe	Cu	Mg	Zn	Mg	Zn
11-12	S13577	0 006	0 004	0 006	5 80		6 40	
	S13578				5 98	0 73	6 62	0 30
	S13579				5 96	1 47	6 63	0 61
	S13580				5 98	2 11	6 68	0 87
	S13581				6 06	2 83	6 80	1 18
	S13582				6 09	3 54	6 86	1 48
	S13583				6 24	4 27	7 06	1 79
	S13584				6 25	4 88	7 09	2 06
	S13585				6 28	5 51	7 15	2 34
	S13586				6 37	6 43	7 30	2 74
	S13587				6 38	7 05	7 34	3 01
	S13588	0 007	0 004	0 006	6 75	7 78	7 79	3 34
13-14	S13745	0 007	0 004	0 006	10 10	1 04		
	S13746				10 19	1 42		
	S13747				9 98	1 79		
	S13748				9 94	2 16		
	S13749				10 08	2 51		
	S13750				9 97	2 98		
	S13751	0 007	0 004	0 007	10 03	3 21		

Section	Alloy No.	Weight Percentage						
		Si	Fe	Cu	Mg	Zn		
15-16	S15570				8 05	0 56		
	S15571				8 19	0 58		
	S15572				8 25	0 55		
	S15700				11 32	0 50		
	S15701				11 50	0 49		
	S15408				13 67	0 46		
	S15409				13 99	0 45		
17-18	S15410				14 70	0 43		
	S15704				10 56	1 00		
	S15705				10 75	0 99		
	S15706				10 87	1 00		
	S15416				13 30	0 94		
	S15417				13 33	0 92		
	S15418				13 56	0 90		
19-20	S15422				12 27	1 55		
	S15423				12 28	1 61		
	S15424				12 68	1 59		
21-22	S17225	0.005	0 009	0 007	17 24	3 00		
	S17226				16 17	4 01		
	S17227				15 09	4 96		
	S17228				14 27	6 02		
	S17229				13 25	7 06		
	S17230				12 17	8 05		
	S17231				11 03	8 88		
23-24	S17232				10 13	10 01		
	S17233				9 21	11 17		
	S17207	0 005	0 008	0 006	20 28	5 02		
	S17208				19 22	6 01		
	S17209				18 23	7 05		
	S17210				17 31	8 04		
	S17211				16 27	9 09		
25-26	S17212				15 20	10 05		
	S17213				14 16	11 09		
	S17214				13 16	12 13		
	S17215				12 12	13 11		
	S17216				11 17	14 19		
	S17181	0 006	0 010	0 007	26 08	3 98		
	S17183				24 38	6 01		
25-26	S17184				23 19	7 00		
	S17185				22 24	7 97		
	S17186				21 33	8 98		
	S17187				20 25	10 02		
	S17188				19 18	10 93		

TABLE 1.—(Continued)

Section	Alloy No.	Weight Percentage				
		Si	Fe	Cu	Mg	Zn
25-26	S17189				18.24	11.97
	S17190				17.24	12.96
	S17191				16.13	14.11
	S17192				15.12	15.06
	S17193				14.25	16.22
	S17194				13.17	17.14
	S17195				12.12	18.06
27-28	S21803	0.004	0.002	0.002	7.53	31.06
	S21804				7.33	32.19
	S21805				7.07	33.21
	S21806				6.76	34.26
	S21807				6.63	35.09
29-30	S21816				10.03	40.00
	S21817				9.87	40.87
	S21818				9.55	41.89
	S21819				9.31	43.20
	S21820				9.14	44.10
	S21821				8.79	45.16
	S21822				8.59	45.94
31-32	S21832				13.19	51.00
	S21833				12.84	52.01
	S21834				12.59	52.91
	S21835				12.29	54.00
	S21836				12.08	54.84
	S21837				11.83	56.05
	S21838				11.51	56.94
	S21839				11.31	57.88
	S21840	0.003	0.003	0.002	10.95	59.10
33-34	S16365				34.09	
	S16366				35.57	
	S16367				37.12	
	S16368				38.65	
	S17538	0.006	0.011	0.007	34.49	
	S17539				34.80	
	S17540				35.31	
	S17541				35.37	
	S17542				35.73	
	S17543				35.75	
	S17544				36.34	
	S17545				36.45	
	S17546				36.82	
	S17547				36.92	
	S17548	0.006	0.011	0.006	37.13	
35-36	S17583	0.006	0.011	0.006	34.96	4.19
	S17584				33.95	8.37
	S17585				33.15	12.48
	S17586				32.15	16.57
	S17587				30.90	20.72
	S17588				29.99	25.04
	S17589				29.00	29.18
	S17590				27.95	33.41
	S17591				25.07	45.68
	S17592	0.003	0.007	0.003	21.78	58.25
	S17593				18.81	71.20
	S17594				15.65	84.35 By diff

continuous diffraction circles. Usually unfiltered copper radiation was used.

INVESTIGATIONS OF BINARY SYSTEMS

Binary Aluminum-zinc System

The portion of the aluminum-zinc diagram that is directly concerned with the present investigation has been previously determined¹⁰. It is reproduced in Fig. 3.

Binary Aluminum-magnesium System

Since previous investigators do not agree on the composition of the aluminum-magnesium phase β (Al-Mg) occurring in aluminum-rich aluminum-magnesium alloys, it became a part of the present investigation to determine the homogeneous-phase field occupied by this constituent.

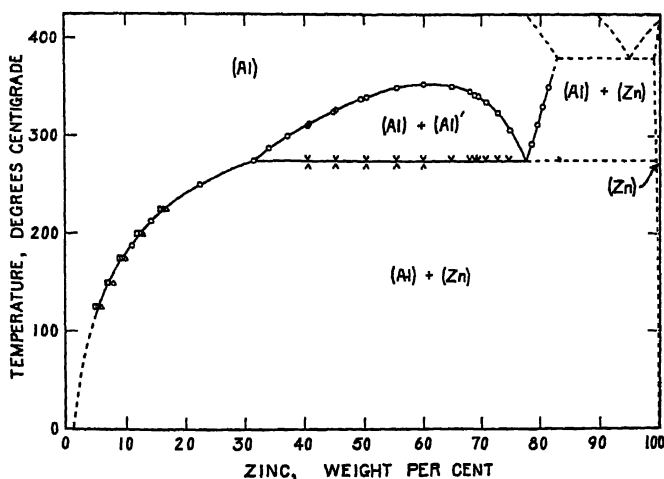


FIG. 3.—ALUMINUM-ZINC DIAGRAM.

Cast specimens of alloys, containing from approximately 34 to 37 per cent magnesium, were heated at 350°, 400° or 440° C. for sufficient time to effect equilibrium, and quenched in water. To protect the specimens from oxidization, they were buried in calcined alumina during the heating. The thermal treatments given to each of these specimens are given in Table 2. The results of microscopic examination of these specimens are

TABLE 2.—Heat-treatments for Determination of β (Al-Mg) Phase Limits

GROUP No.	SECTION 33-34
1	47 hr. at 400° C., cooled to 300° C., held 21 hr., heated to 350° C., held 165 hr. and quenched in cold water.
2	120 hr. at 400° C. and quenched in cold water.
3	72 hr. at 440° C. and quenched in cold water.

shown in Fig. 4. The solid solubility of magnesium in aluminum has been determined by previous investigators and is shown in Fig. 5.

Binary Magnesium-zinc System

The equilibrium diagram for the binary magnesium-zinc system taken from data in the literature is reproduced in Fig. 6.

Phases and Phase Fields in Aluminum Corner of Aluminum-magnesium-zinc System

Since it has been reported that the section β (Al-Mg)- β (Mg-Zn) is a binary system²⁰, and since no other binary system or ternary compound

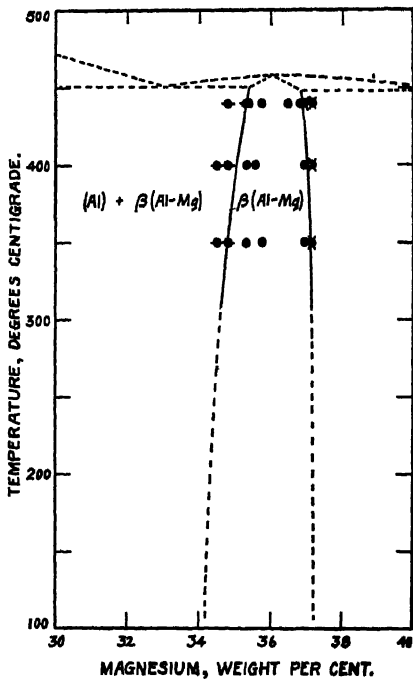


FIG. 4.

FIG. 4.—ALUMINUM-MAGNESIUM DIAGRAM. HOMOGENEITY RANGE OF $\beta(\text{Al-Mg})$.

For legenda see Fig. 7.

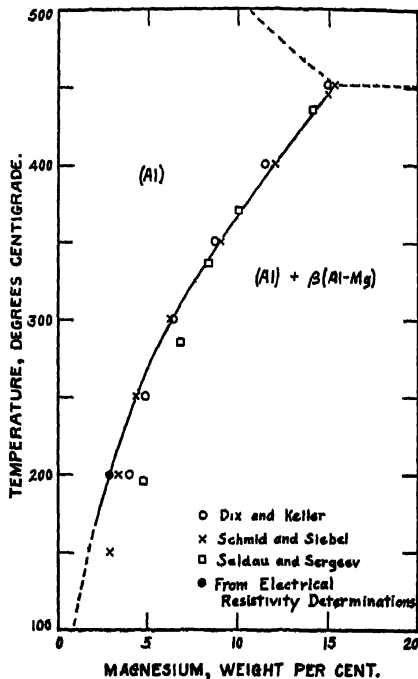


FIG. 5.

FIG. 5.—ALUMINUM-MAGNESIUM DIAGRAM. SOLID SOLUBILITY OF MAGNESIUM IN ALUMINUM.

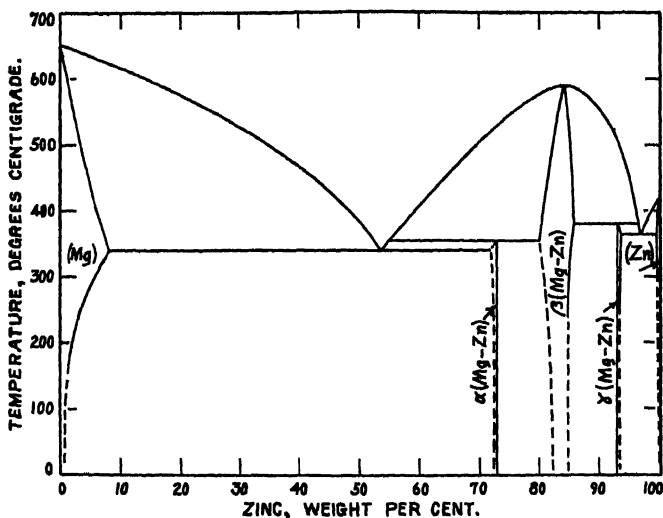


FIG. 6.—MAGNESIUM-ZINC DIAGRAM: CONSTRUCTED FROM DATA IN THE LITERATURE.

has been reported between this line and the aluminum corner of the diagram, it seemed that the phases occurring in the aluminum corner of the system could be identified by a study of the phases occurring along the binary line $\beta(\text{Al-Mg})$ - $\beta(\text{Mg-Zn})$. Consequently, the alloys of section 35-36 in Fig. 2 were prepared. These alloys were all examined microscopically after annealing at various temperatures, as shown in Table 3.

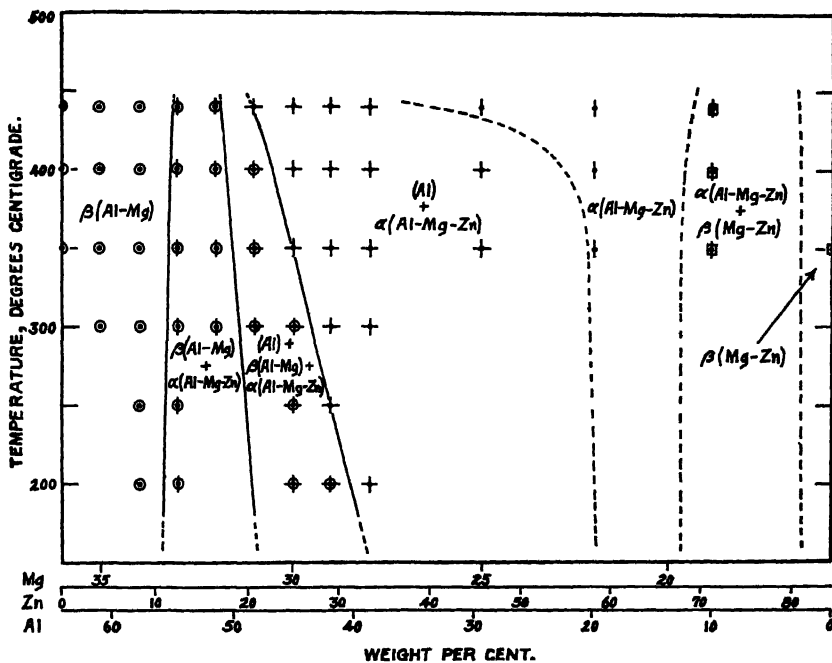


FIG. 7.—DIAGRAM OF SECTION 35-36.

Legenda:

- (Al)
- ⊙ $\beta(\text{Al-Mg})$
- ⊥ $\alpha(\text{Al-Mg-Zn})$
- ⊠ $\beta(\text{Mg-Zn})$
- × Other phases
- ⊙ Electrical resistivity determination.

The phases determined in this way were also checked by X-ray diffraction analysis of selected samples. The section so determined is shown in Fig. 7. The presence of (Al) in two of the phase fields makes it very doubtful that this is a binary section. Nevertheless, this section serves the purpose of showing the phases that occur in the aluminum corner of the diagram between the aluminum-magnesium binary line and the (Al)- $\beta(\text{Mg-Zn})$ line. The phase fields in order (reading from the binary aluminum-magnesium line) are as follows: the first field contains (Al) and $\beta(\text{Al-Mg})$; the next field contains (Al), $\beta(\text{Al-Mg})$ and $\alpha(\text{Al-Mg-Zn})$;

the next phase field contains (Al) and $\alpha(\text{Al-Mg-Zn})$; the next field contains (Al), $\alpha(\text{Al-Mg-Zn})$ and $\beta(\text{Mg-Zn})$; the last phase field contains (Al) and $\beta(\text{Mg-Zn})$.

Obviously the study of the section $\beta(\text{Al-Mg})$ - $\beta(\text{Mg-Zn})$ gives no information concerning the phases in the aluminum corner of the system between the sections (Al)- $\beta(\text{Mg-Zn})$, and (Al)-(Zn). In order to identify the phases in this region, two samples, Nos. 13928 (0.42 Mg, 13.9 Zn) and 13930 (0.72 Mg, 14.8 Zn) were subjected to X-ray diffraction analysis. These specimens were given a solution heat-treatment at 425° C.,

TABLE 3.—*Heat-treatments for Determination of Phases and Phase-field Limits on Section 35-36*

GROUP No.	HEAT-TREATMENT
1	120 hr. at 425° C., air-cooled, 522 hr. at 200° C. and quenched in cold water.
2	120 hr. at 425° C., air-cooled, 353 hr. at 250° C. and quenched in cold water.
3	120 hr. at 425° C., air-cooled, 167 hr. at 300° C. and quenched in cold water.
4	47 hr. at 400° C., 21 hr. at 300° C., 165 hr. at 350° C. and quenched in cold water.
5	120 hr. at 400° C. and quenched in cold water.
6	72 hr. at 440° C. and quenched in cold water.

quenched, cold-rolled and then aged at 200° C. The X-ray diffraction pattern of both of these samples revealed the phases (Al), $\beta(\text{Mg-Zn})$ and (Zn). Since both of these samples consisted entirely of aluminum solid solution at 425° C., the phases $\beta(\text{Mg-Zn})$ and (Zn) obviously precipitated during the aging. Above the eutectoid temperature, of course, no (Zn) would exist in the aluminum corner.

In the zinc corner of the diagram one would expect to find other phases such as $\gamma(\text{Mg-Zn})$, previously referred to as MgZn_8 , (Zn) and (Al)*. However, it was the object of this investigation to determine the aluminum corner of the system, and accordingly the phase fields in the zinc corner were not investigated.

DETERMINATION OF PHASE-FIELD BOUNDARIES

Boundaries of Ternary Field Containing Single Phase (Al)

The boundaries of the (Al)-phase field have been determined by electrical conductivity and microscopic examination of the samples along the sections numbered as follows in Fig. 1: 1-2, 3-4, 5-6, 5-7, 5-8, 9-10, 11-12. The heat-treatments of the specimens are listed in Table 4 and electrical resistivity-concentration curves for these sections are given in Figs. 8 to 14. The results of both electrical resistivity measurements and microscopic examination are given in Table 5. The sections of the equilibrium diagram so determined are given in Figs. 15 to 21.

* Since this paper was written, an article²¹ on the aluminum-magnesium-zinc system, including the zinc corner, has come to the authors' attention.

TABLE 4.—Heat-treatments for Determination of (Al)-phase Limits

Section	Temperature Deg. C.		Time to Reach Temperature, Hr.	Resistivity Specimens		Metallographic Specimens	
	From	To		Total Time at Temperature, Hr.	Resistivity Measurements, Time after Reaching Tem- perature, Hr.	Group No.	Quenched in Cold Water, Time after Reaching Tem- perature, Hr.
1-2	Room	200	Quench	48		1	1512 ^a
	200	Room		17	16		
	Room	200		21	3-20	2	21
	200	250		22	4-21	3	22
	250	300		4	4	4	4
	300	350		14	13	5	14
3-4	350	400	Quench	4	4	6	4
	400	440		70		1	315 ^a
	Room	200		135	113-134		
	200	Room		44	22-43	2	44
	Room	250		22	4-21	3	22
	250	300		22	4-21	4	22
5-6	300	350	Quench	22	4-21	5	22
	350	400		22	4-21	6	22
	400	440		122		1	624 ^a
	Room	200		112	39-63-111		
	200	Room		42	1-18-42	2	42
	Room	250		21	2-21		
5-7	250	300	Quench	45	1-20-43		
	300	350		43	20-42	3	43
	350	400		24	2-22	4	24
	400	430		187	18-144-167	5	167
	430	450		137	16-39-67-136	6	137
	450	350		68		1	2735 ^a
5-8	Room	200	Quench	39	15-38		
	200	Room		91	2-19-90	2	91
	Room	250		21	2-20	3	21
	250	300		20	2-20	4	20
	300	350		22	4-22	5	22
	350	400		22	3-22	6	22
9-10	400	440	Quench	22	3-22		
	Room	200		408		1	3648 ^a
	200	Room		88	64-88		
	Room	250		21	2-20	2	21
	250	300		20	2-19	3	20
	300	350		28	4-26	4	26
11-12	350	400	Quench	66	18-65	5	66
	400	430		93	2-22-92	6	93
	430	450		69	2-22-67		
	Room	200		74		1	2040 ^a
	200	Room		43	42		
	Room	250		20	2-19	2	20
11-12	250	300	Quench	21	3-20	3	21
	300	350		22	4-21	4	22
	350	400		21	3-20	5	21
	400	440		22	4-21	6	22
	Room	200					
	200	Room					

^a Group No. 1 of the metallographic specimens was heat-treated separately. All other specimens of each alloy group were subjected consecutively to the treatments in the order indicated.

In addition to the above, chill-cast alloys along additional sections were used for microscopic examination only. These sections are indicated

TABLE 5.—*The (Al)-phase Limits*

Section	Temperature Deg. C.	From Electrical Resistivity-concentration Curves				From Microscopic Examination Limit Between			
		Atomic Per Cent		Weight Per Cent		Weight Per Cent		Weight Per Cent	
		Mg	Zn	Mg	Zn	Mg	Zn	Mg	Zn
1-2	200	0.04	5.08	0.03	11.50	0	11.62	0.20	12.30
	250	0.06	5.12	0.05	11.60	0	11.62	0.20	12.30
	300	0.16	5.32	0.13	12.00	0	11.62	0.20	12.30
	350	0.40	5.80	0.33	13.00	0.20	12.30	0.36	13.18
	400	0.95	6.90	0.78	15.20	0.72	14.80	0.91	15.72
	440					1.07	16.35	1.43	18.74
3-4	200	0.15	1.50	0.13	3.56		2.87	0.25	4.31
	250	0.25	1.70	0.22	4.02		2.87	0.25	4.31
	300	0.50	2.20	0.44	5.17	0.25	4.31	0.56	5.85
	350	0.95	3.10	0.82	7.19	0.56	5.85	0.82	7.39
	400	1.60	4.40	1.36	10.04	1.07	8.95	1.41	10.37
	440	2.80	5.80	1.92	13.00	1.67	11.83	1.92	13.46
5-6	200	0.23	0.47	0.21	1.13	0.16	0.96	0.32	1.96
	250	0.47	0.93	0.42	2.22	0.32	1.96	0.62	3.86
	300	0.80	1.60	0.70	3.79				
	350	1.30	2.60	1.13	6.08	0.96	5.87	1.42	7.51
	400	1.97	3.93	1.68	9.03	1.42	7.51	1.75	9.53
	430	2.45	4.90	2.07	11.11	1.75	9.53	2.26	11.62
5-7	450	2.80	5.60	2.34	12.59	2.26	11.62	2.59	13.55
	200	0.32	0.32	0.29	0.78			0.46	1.27
	250	0.65	0.65	0.58	1.56	0.46	1.27	0.92	2.55
	300	1.12	1.12	1.00	2.68	0.92	2.55	1.44	3.83
	350	1.85	1.85	1.63	4.37	1.44	3.83	1.84	5.04
	400	2.80	2.80	2.43	6.54	2.27	6.13	2.77	7.60
5-8	440	3.75	3.75	3.22	8.65	2.77	7.60	3.61	9.60
	200	0.47	0.23	0.42	0.56			0.78	1.03
	250	0.93	0.47	0.83	1.13	0.78	1.03	1.52	2.09
	300	1.60	0.80	1.43	1.92	0.78	1.03	1.52	2.09
	350	2.60	1.30	2.30	3.10	1.52	2.09	2.39	3.18
	400	3.93	1.97	3.46	4.66	3.15	4.21	3.92	5.20
9-10	440	5.27	2.63	4.60	6.17	3.92	5.20	4.77	6.37
	200					2.75		3.02	0.51
	250	3.21	0.13	2.90	0.32	2.75		3.02	0.51
	300	3.35	0.40	3.01	0.97	3.02	0.51	3.10	2.01
	350	3.62	0.93	3.23	2.23	3.10	2.01	3.34	3.06
	400	4.08	1.87	3.59	4.43	3.63	4.07	3.79	5.02
11-12	430	4.48	2.67	3.91	6.25	3.88	6.14	4.10	7.24
	350	6.58	0.47	5.92	1.14	5.98	0.73	5.96	1.47
	400	6.79	1.17	6.06	2.80	5.98	2.11	6.06	2.83
	440	7.05	2.00	6.22	4.74	6.24	4.27	6.25	4.88

on Fig. 1, with the numbers: 13-14, 15-16, 17-18 and 19-20. The thermal treatments of these specimens are given in Table 6. The results of

TABLE 6.—*Heat-treatments for Determination of (Al)-phase Limits*

Group No	Section	Heat-treatment
1		64 hr. at 200° C. quenched, slowly heated to 400° C., held 24 hr. and quenched in cold water.
2	13-14	64 hr. at 200° C. quenched, slowly heated to 420° C., held 20 hr. and quenched in cold water.
3		64 hr. at 200° C. quenched, slowly heated to 440° C., held 21 hr. and quenched in cold water.
1	15-16 17-18 19-20	120 hr. at 440° C. and quenched in cold water.
2	15-16 17-18	4 hr. at 425° C., rapidly cooled to 250° C., held 2 hr., rapidly heated to 400° C., held 88 hr. and quenched in cold water.
3	15-16	44 hr. at 400° C., cooled to 350° C., held 116 hr. and quenched in cold water.

TABLE 7.—*The (Al)-phase Limits*

Temperature, Deg. C.	Section	From Microscopic Examination Limit Between			
		Weight Per Cent		Weight Per Cent	
		Mg	Zn	Mg	Zn
400	13-14	10.10	1.04	10.19	1.42
420		9.98	1.79	9.94	2.16
440		10.08	2.51	9.97	2.93
350	15-16	8.19	0.56	8.25	0.55
400		11.32	0.50	11.50	0.49
440		13.67	0.46	14.70	0.43
400	17-18	10.56	1.00	10.87	1.00
440		13.30	0.94	13.56	0.90
440	19-20	12.27	1.55	12.68	1.59

the examination are given in Table 7. The sections of the equilibrium diagram are shown in Figs. 22 to 24.

Boundaries of Phase Field Containing (Al), β (Al-Mg) and α (Al-Mg-Zn)

The boundaries of this phase field were determined by microscopic examination of chill-cast samples along three sections: 21-22, 23-24 and 25-26 shown in Fig. 2. The thermal treatments of these alloys are given

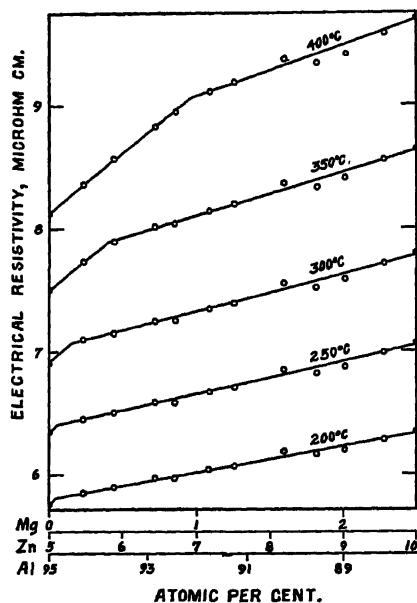


Fig. 8, Section 1-2.

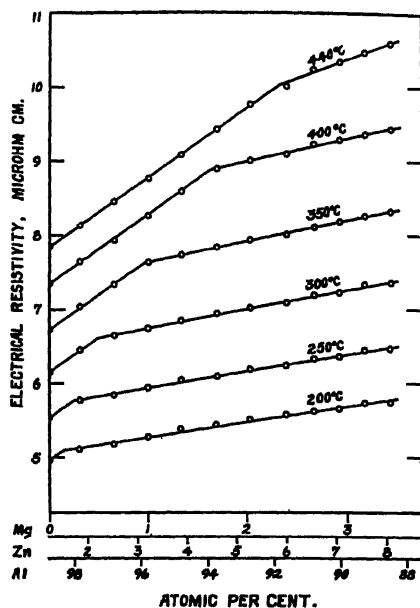


Fig. 9, Section 3-4.

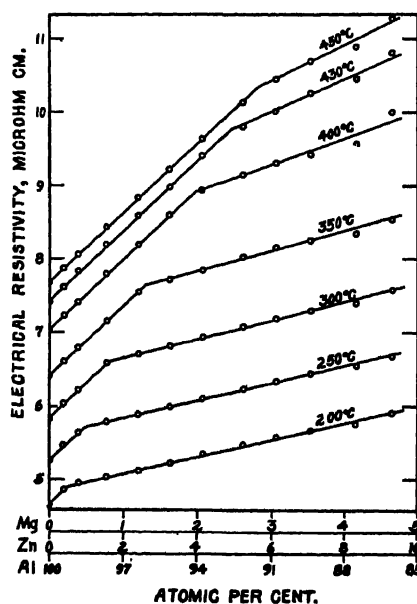


Fig. 10, Section 5-6.

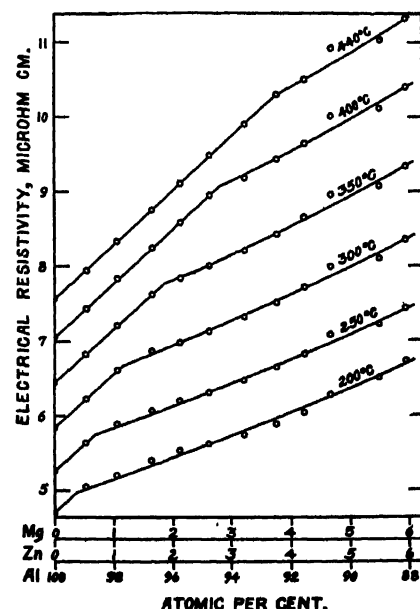


Fig. 11, Section 5-7.

FIGS. 8-11.—ELECTRICAL RESISTIVITY-CONCENTRATION CURVES.

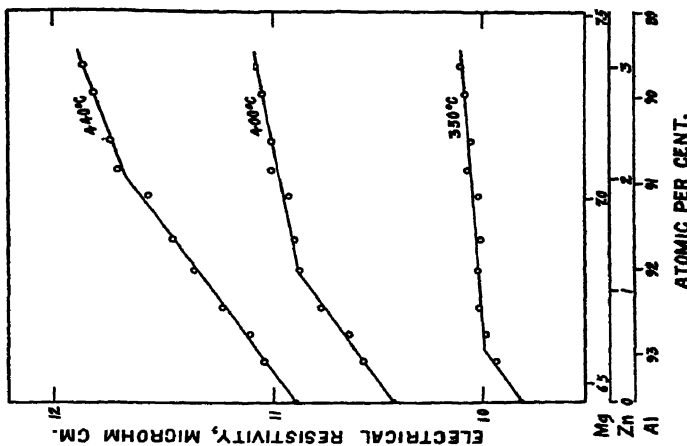


Fig. 14, Section 11-12.

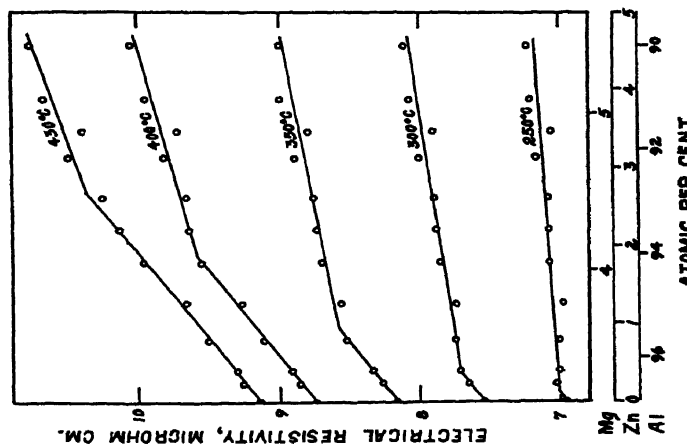


Fig. 13, Section 9-10.

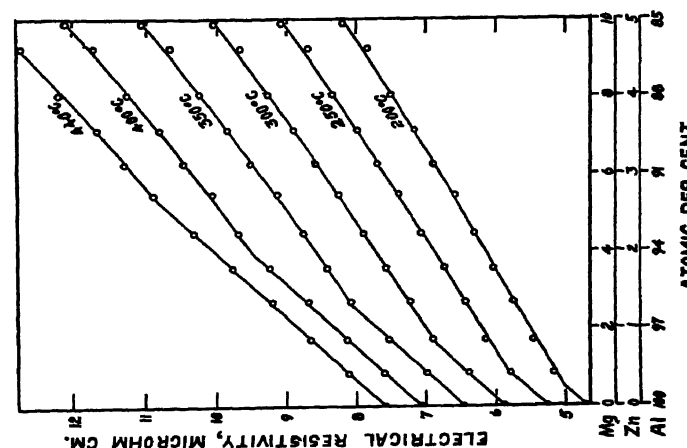


Fig. 12, Section 5-8.

Figs. 12-14.—ELECTRICAL RESISTIVITY-CONCENTRATION CURVES.

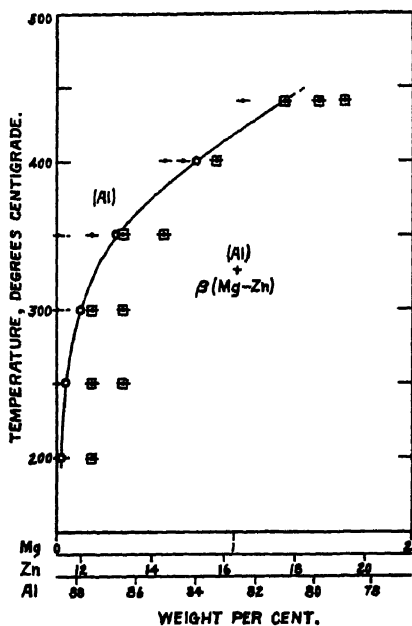


Fig. 15, Section 1-2.

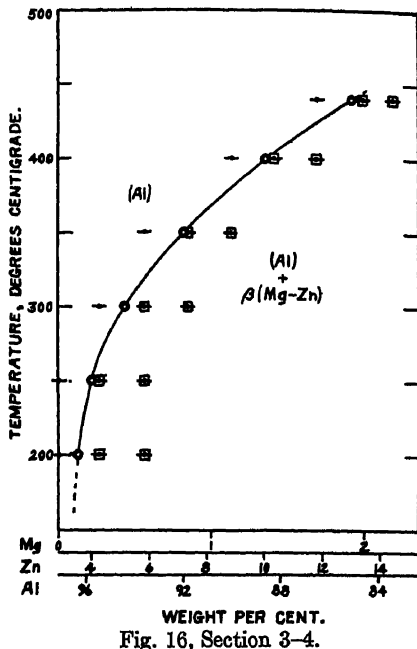


Fig. 16, Section 3-4.

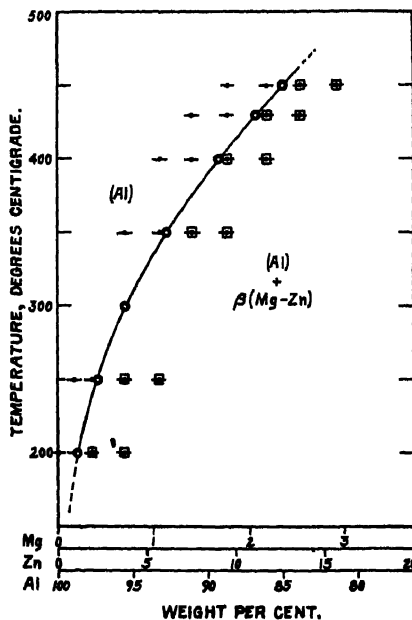


Fig. 17, Section 5-6.

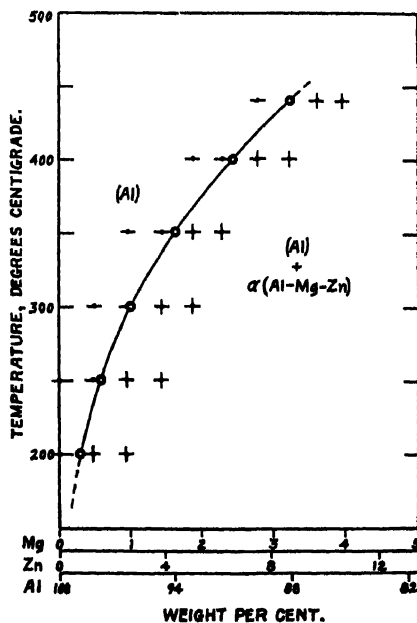


Fig. 18, Section 5-7.

FIGS. 15-18.—SECTIONS OF EQUILIBRIUM DIAGRAM.

For legenda see Fig. 7.

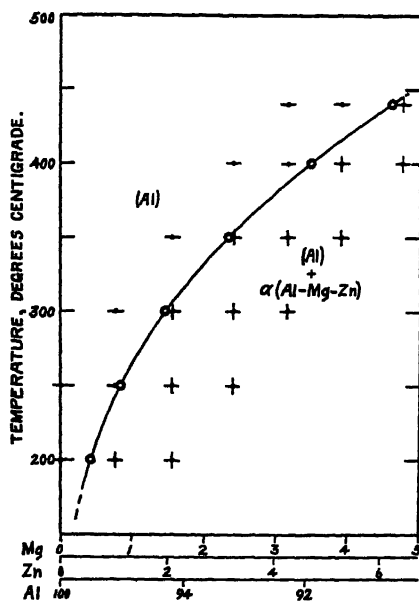


Fig. 19, Section 5-8.

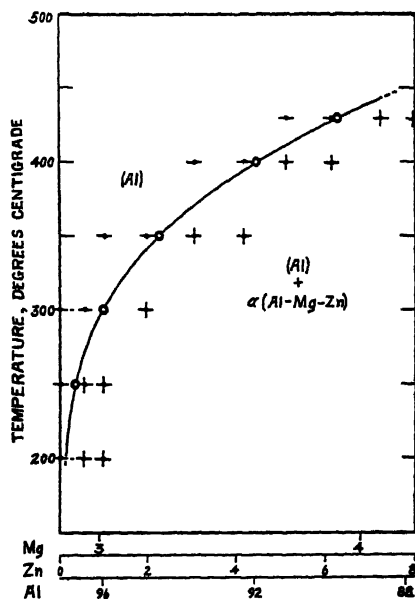


Fig. 20, Section 9-10.

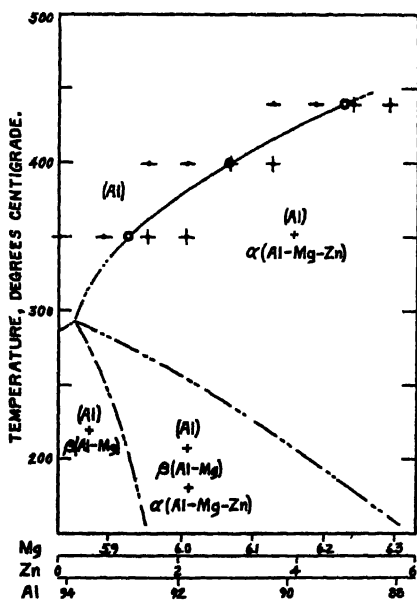


Fig. 21, Section 11-12.

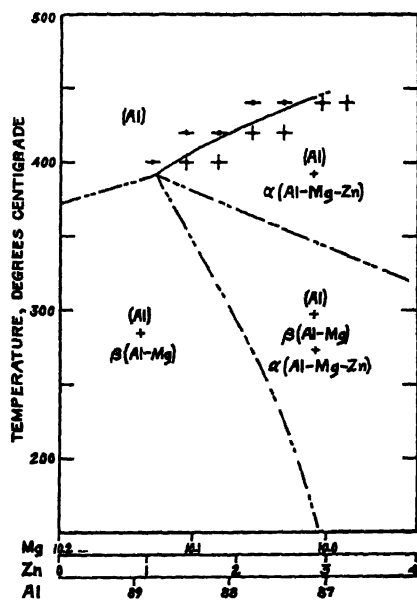


Fig. 22, Section 13-14.

FIGS. 19-22.—SECTIONS OF EQUILIBRIUM DIAGRAM.

For legenda see Fig. 7.

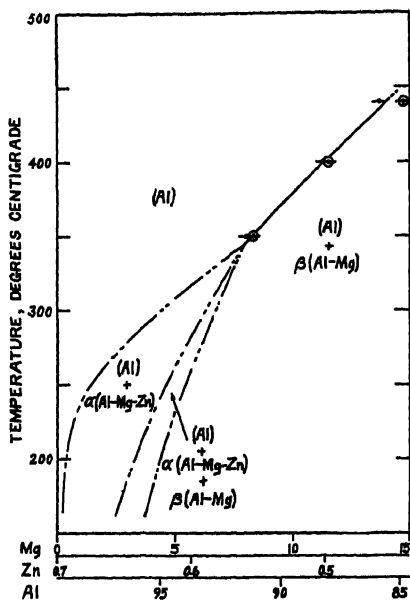


Fig. 23, Section 15-16.

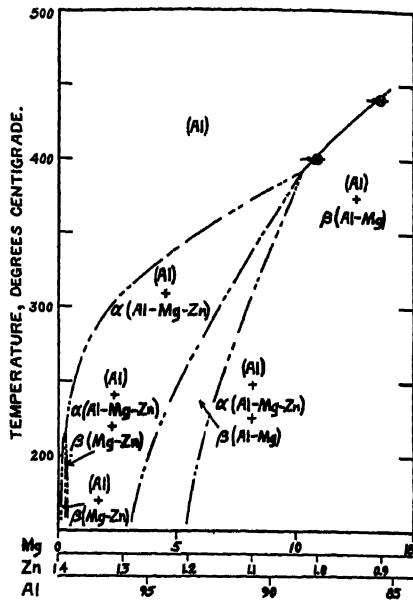


Fig. 24, Section 17-18.

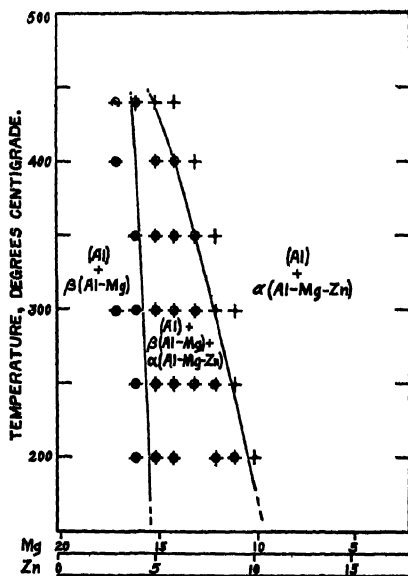


Fig. 25, Section 21-22.

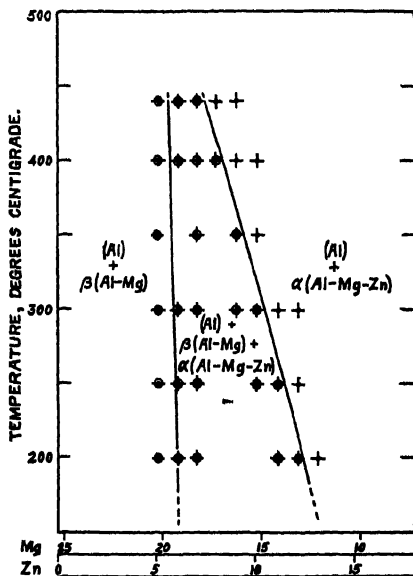


Fig. 26, Section 23-24.

FIGS. 23-26.—SECTIONS OF EQUILIBRIUM DIAGRAM.

For legends see Fig. 7.

in Table 8. The results of the examination are given in Table 9, and the sections of the equilibrium diagram in Figs. 25 to 27.

TABLE 8.—*Heat-treatments for Determination of Limits of Field Containing (Al), β (Al-Mg) and α (Al-Mg-Zn)*

GROUP No.	ALLOYS OF SECTIONS 21-22, 23-24 AND 25-26
1	120 hr. at 425° C., air-cooled, 522 hr. at 200° C. and quenched in cold water.
2	120 hr. at 425° C., air-cooled, 353 hr. at 250° C. and quenched in cold water.
3	120 hr. at 425° C., air-cooled, 167 hr. at 300° C. and quenched in cold water.
4	18 hr. at 350° C., 22 hr. at 300° C., 22 hr. at 350° C., 22 hr. at 300° C., 46 hr. at 350° C., 22 hr. at 300° C., 190 hr. at 350° C. and quenched in cold water.
5	18 hr. at 400° C., 22 hr. at 350° C., 22 hr. at 400° C., 22 hr. at 350° C., 94 hr. at 400° C. and quenched in cold water.
6	72 hr. at 440° C. and quenched in cold water.

TABLE 9.—*Limits of Field Containing (Al), β (Al-Mg) and α (Al-Mg-Zn)*

Temperature, Deg. C.	Section	From Microscopic Examination							
		Limit Between				Limit Between			
		Weight Per Cent		Weight Per Cent		Weight Per Cent		Weight Per Cent	
		Mg	Zn	Mg	Zn	Mg	Zn	Mg	Zn
200	21-22	16 17	4 01	15.09	4 96	11.03	8.88	10.13	10.01
250		16.17	4 01	15.09	4.96	12 17	8.05	11.03	8.88
300		16.17	4.01	15 09	4.96	13 25	7.06	12.17	8.05
350		16 17	4 01	15.09	4 96	13.25	7.06	12.17	8.05
400		17.24	3.00	15.09	4.96	14.27	6.02	13.25	7.06
440		17.24	3.00	16.17	4.01	16.17	4.01	15.09	4.96
200	23-24	20.28	5.02	19.22	6.01	13.16	12.13	12.12	13.11
250		20.28	5.02	19.22	6.01	14.16	11.09	13.16	12.13
300		20.28	5.02	19.22	6.01	15.20	10.05	14.16	11.09
350		20.28	5.02	18.23	7.05	16 27	9 09	15.20	10.05
400		20.28	5.02	19.22	6.01	17.31	8.04	16.27	9.09
440		20 28	5.02	19.22	6.01	18 23	7.05	17.31	8.04
200	25-26	23.19	7.97	22.24	7.97	15.12	15.06	14.25	16.22
250		23.19	7.97	22.24	7.97	16.13	14.11	15.12	15.06
300		23.19	7.97	22.24	7.97	17.24	12.96	16.13	14.11
350		23.19	7.97	22.24	7.97	18.24	11.97	17.24	12.96
400		23.19	7 97	22.24	7.97	19.18	10.93	18.24	11.97
440		23.19	7.97	22.24	7.97	21.33	8.98	20.25	10.02

Boundaries of Phase Field Containing Phases (Al), α (Al-Mg-Zn) and β (Mg-Zn)

The boundaries of this phase field were determined by microscopic examination of chill-cast samples along three sections: 27-28, 29-30 and

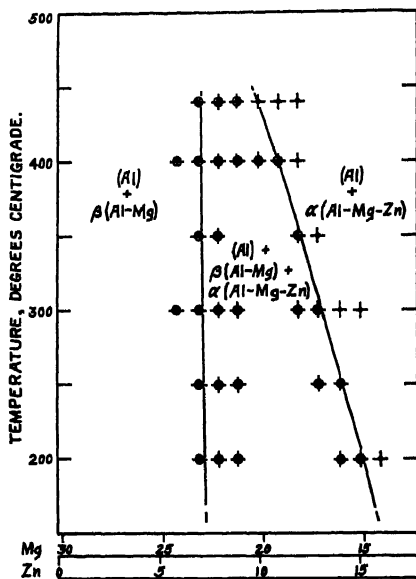


Fig. 27, Section 25-26.

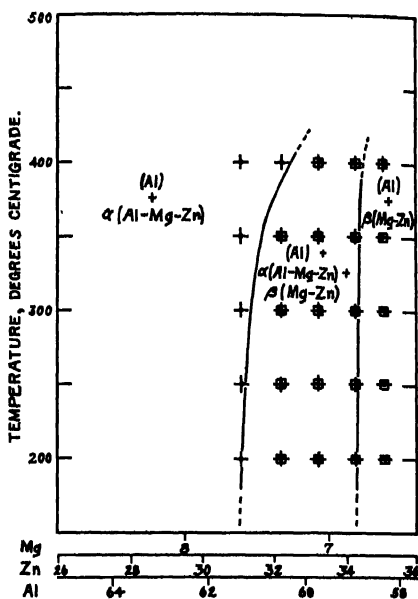


Fig. 28, Section 27-28.

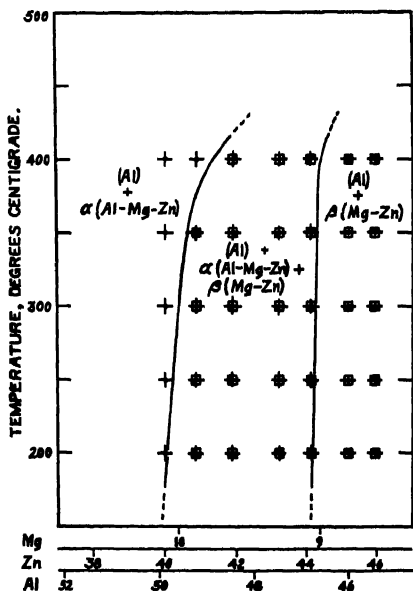


Fig. 29, Section 29-30.

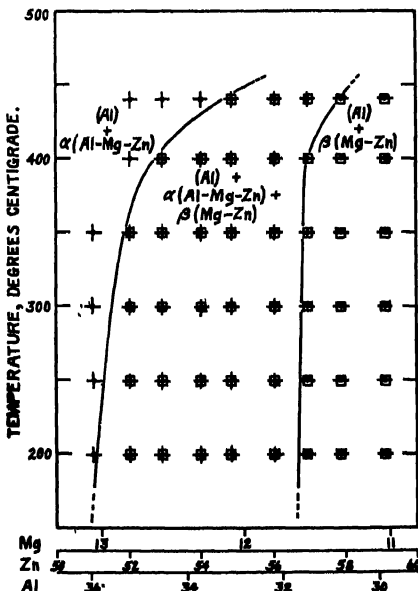


Fig. 30, Section 31-32.

FIGS. 27-30.—SECTIONS OF EQUILIBRIUM DIAGRAM.

For legenda see Fig. 7.

TABLE 10.—*Heat-treatments for Determination of Limits of Field Containing (Al), α (Al-Mg-Zn) and β (Mg-Zn)*

GROUP NO.		ALLOYS OF SECTIONS 27-28, 29-30 AND 31-32	
1	120 hr. at 400° C., air-cooled, 359 hr. at 200° C. and quenched in cold water.		
2	120 hr. at 400° C., air-cooled, 359 hr. at 200° C., quenched, 336 hr. at 250° C. and quenched in cold water.		
3	120 hr. at 400° C., air-cooled, 192 hr. at 200° C., air-cooled, 288 hr. at 300° C. and quenched in cold water.		
4	120 hr. at 400° C., air-cooled, 359 hr. at 200° C., quenched, 240 hr. at 350° C. and quenched in cold water.		
5	120 hr. at 400° C., air-cooled, 192 hr. at 400° C. and quenched in cold water.		
6	120 hr. at 400° C., air-cooled, 144 hr. at 200° C., air-cooled, 144 hr. at 440° C., and quenched in cold water.		

TABLE 11.—*Limits of Field Containing (Al), α (Al-Mg-Zn) and β (Mg-Zn)*

Temperature, Deg. C.	Section	From Microscopic Examination							
		Limit Between				Limit Between			
		Weight Per Cent		Weight Per Cent		Weight Per Cent		Weight Per Cent	
		Mg	Zn	Mg	Zn	Mg	Zn	Mg	Zn
200	27-28	7.53	31.06	7.33	32.19				
250		7.53	31.06	7.33	32.19	6.76	34.26	6.63	35.09
300		7.53	31.06	7.33	32.19	6.76	34.26	6.63	35.09
350		7.53	31.06	7.33	32.19	6.76	34.26	6.63	35.09
400		7.33	32.19	7.07	33.21				
200	29-30	10.03	40.00	9.87	40.87	9.14	44.10	8.79	45.16
250		10.03	40.00	9.87	40.87	9.14	44.10	8.79	45.16
300		10.03	40.00	9.87	40.87	9.14	44.10	8.79	45.16
350		10.03	40.00	9.87	40.87	9.14	44.10	8.79	45.16
400		9.87	40.87	9.55	41.89	9.14	44.10	8.79	45.16
200	31-32	13.19	51.00	12.59	52.91	11.83	56.05	11.51	56.94
250		13.19	51.00	12.84	52.01	11.83	56.05	11.51	56.94
300		13.19	51.00	12.84	52.01	11.83	56.05	11.51	56.94
350		13.19	51.00	12.84	52.01	11.83	56.05	11.51	56.94
400		12.84	52.01	12.59	52.91	11.83	56.05	11.51	56.94
440		12.29	54.00	12.08	54.84	11.51	56.94	11.31	57.88

31-32 as shown in Fig. 2. The thermal treatments of these alloys are given in Table 10. The results of this examination are given in Table 11, and the sections of the equilibrium diagram so determined are given in Figs. 28-30.

CHARACTERISTICS OF PHASES

Etching Characteristics.—Table 12 shows the reaction of each phase to the usual etches (1-6) and two special etches that were used in this investi-

TABLE 12.—*Etching Characteristics*

No	Reagent	Constituents in Presence of (Al) Phase					
		β (Al-Mg) Containing No Zinc	β (Al-Mg) with Zinc in Solid Solution	β (Al-Mg) and α (Al-Mg-Zn)	α (Al-Mg-Zn) Magnesium Rich	α (Al-Mg-Zn) Zinc Rich	α (Al-Mg-Zn) and β (Mg-Zn)
1	0.5 per cent HF swab for 15 sec., wash in cold water.	Outlined. Un-colored. Attacked by pitting.	Outlined. Colored dark brown to black.	Not clearly distinguished.	Outlined. Attacked, resulting in severe pitting.	Outlined. Unattacked. Clear to light brown.	Outlined. Unattacked. Colored unevenly, clear to light brown.
2	1 per cent NaOH swab for 10 sec., wash in running water.	Not outlined. Unattacked. Uncolored.	Not outlined. Unattacked. Uncolored.	Not clearly distinguished.	Not outlined. Unattacked. Slightly darkened.	Not outlined. Unattacked. Slightly darkened.	Not outlined. Unattacked. Uncolored.
3	20 per cent H_2SO_4 at 70° C., immerse specimen for 30 sec., quench in cold water.	Heavily outlined. Attacked. Colored brown.	Heavily outlined. Colored light brown.	Not clearly distinguished.	Mostly dissolved, that remaining is black.	Dissolved.	Dissolved.
4	25 per cent HNO_3 at 70° C., immerse specimen for 40 sec., quench in cold water.	Heavily outlined. Partially dissolved, that remaining colored brown.	Heavily outlined. Partially dissolved, that remaining colored brown.	Both dissolved.	Dissolved.	Dissolved.	Dissolved.
5	10 per cent NaOH at 70° C., immerse specimen for 5 sec., rinse in cold water.	Heavily outlined. Slightly attacked. Uncolored. (Al) attacked.	Heavily outlined. Slightly attacked. Uncolored. (Al) attacked.	Not clearly distinguished.	Heavily outlined. Unattacked. Uncolored. (Al) attacked.	Outlined. Unattacked. Colored. (Al) blackened.	Outlined. Unattacked. Colored. (Al) blackened.
6	0.5 per cent HF, 1.5 per cent HCl , 2.5 per cent HNO_3 , immerse specimen for 15 sec., rinse in warm water.	Heavily outlined. Roughened by attack.	Heavily outlined. Roughened by attack.	Both dissolved.	Dissolved.	Dissolved.	Dissolved.
7	Concentrated HNO_3 , immerse specimen for 10 sec., rinse in warm water.	Outlined. Colored blue to brown.	Outlined. Colored blue to brown.	Clearly distinguished.	Outlined. Colored dark gray.	Dissolved.	Dissolved.
8	1 per cent H_2SO_4 , immerse specimen for 3 sec., immerse for 60 sec. in a 0.1 per cent H_2SO_4 solution saturated with H_2S , rinse in warm water.	Not outlined. Unattacked. Uncolored.	Not outlined. Unattacked. Uncolored.	Distinguished.	Outlined. Colored light brown.	Outlined. Colored blue to very dark brown.	Outlined. Uncolored or slightly discolored.

gation (7 and 8). The etching characteristics of some of the phases change with composition. Typical photomicrographs (Figs. 31 to 40) are

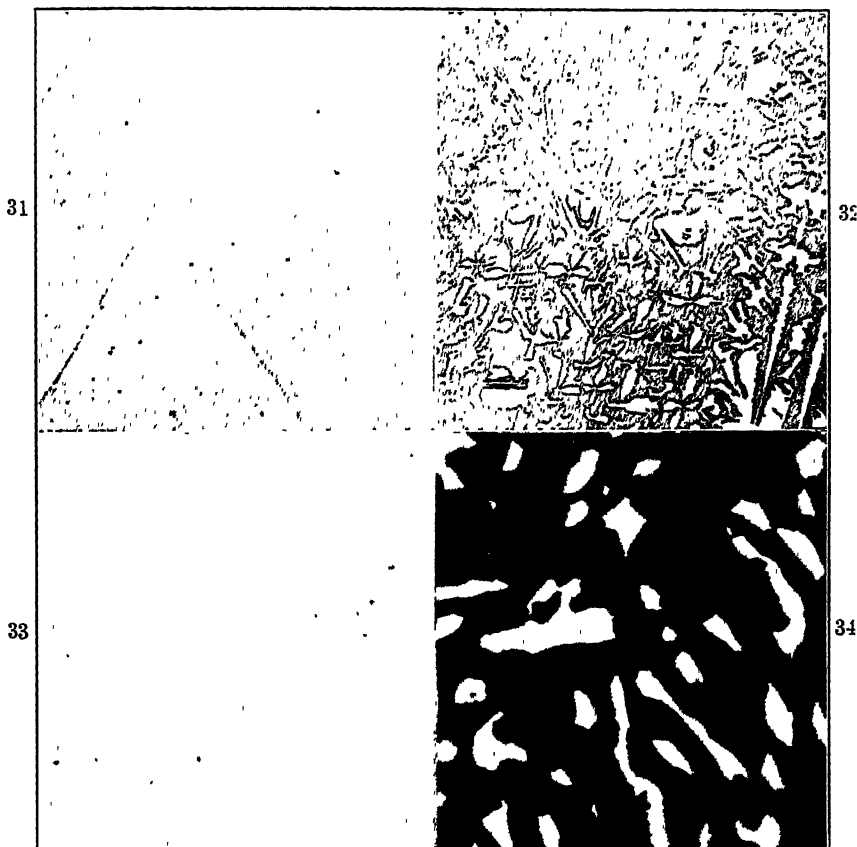


FIG. 31.—ALLOY OF 33.95 PER CENT MAGNESIUM, 8.37 PER CENT ZINC (S17584-2—A9919D). $\times 500$.

Specimen heat-treated 120 hr. at 400° C. and quenched. Shows a single-phase structure. Zinc is in solid solution in β (Al-Mg). Etched with concentrated HNO_3 .

FIG. 32.—ALLOY OF 32.15 PER CENT MAGNESIUM, 16.57 PER CENT ZINC (S17586-2—A9920D). $\times 500$.

Specimens heat-treated 120 hr. at 400° C. and quenched. Shows particles of α (Al-Mg-Zn) in β (Al-Mg). Etched with concentrated HNO_3 .

FIG. 33.—ALLOY OF 29.99 PER CENT MAGNESIUM, 25.04 PER CENT ZINC (S17588-2—A9921D). $\times 500$.

Specimen heat-treated 120 hr. at 400° C. and quenched. Shows small particles of (Al) in α (Al-Mg-Zn). Etched with concentrated HNO_3 .

FIG. 34.—ALLOY OF 18.81 PER CENT MAGNESIUM, 71.20 PER CENT ZINC (S17593-2—A14298D). $\times 500$.

Specimen heat-treated 120 hr. at 400° C. and quenched. Shows particles of β (Mg-Zn) in α (Al-Mg-Zn) matrix. Etched with 1 per cent H_2SO_4 and 0.1 per cent H_2SO_4 solution saturated with H_2S .

given to illustrate the structures in the various phase fields and the use of etches 7 or 8 to distinguish between the coexisting phases β (Al-Mg) and

$\alpha(\text{Al-Mg-Zn})$, or $\alpha(\text{Al-Mg-Zn})$ and $\beta(\text{Mg-Zn})$ respectively. The locations of samples used for Figs. 31 to 40 are shown in Fig. 41. The numbers on the diagram refer to the corresponding figure number.

X-ray Patterns.—The Debye-Scherrer patterns of $\beta(\text{Al-Mg})$, $\alpha(\text{Al-Mg-Zn})$ and $\beta(\text{Mg-Zn})$ are shown in Fig. 42. These patterns,

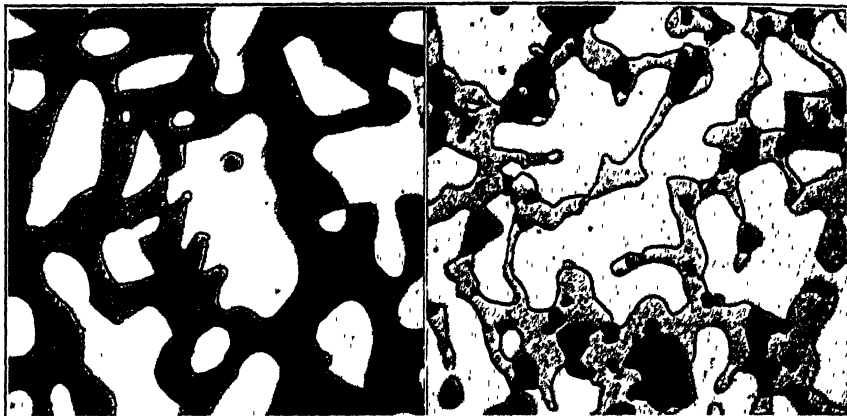


FIG. 35.

FIG. 36.

FIG. 35.—ALLOY OF 23.19 PER CENT MAGNESIUM, 7.0 PER CENT ZINC (S17184-2—A9912D). $\times 500$.

Specimen heat-treated 18 hr. at 400°C ., 22 hr. at 350°C ., 22 hr. at 400°C ., 22 hr. at 350°C ., 94 hr. at 400°C . and quenched. Shows $\beta(\text{Al-Mg})$ (dark) and (Al) (light). Etched with concentrated HNO_3 .

FIG. 36.—ALLOY OF 20.25 PER CENT MAGNESIUM, 10.02 PER CENT ZINC (S17187-2—A9914D). $\times 500$.

Specimen heat-treated 18 hr. at 400°C ., 22 hr. at 350°C ., 22 hr. at 400°C ., 22 hr. at 350°C ., 94 hr. at 400°C . and quenched. Shows (Al) (light), $\alpha(\text{Al-Mg-Zn})$ (gray) and $\beta(\text{Al-Mg})$ (dark). Etched with concentrated HNO_3 .

together with the well-known patterns of (Al) and (Zn), were used as the primary identification of the phases in the various phase fields.

DISCUSSION OF RESULTS

Probably the best way to visualize the results of this investigation is to construct isothermal sections of the ternary system. A section of the diagram at 440°C . constructed from the results given above is shown in Fig. 43. The phase boundaries shown by solid lines are those definitely determined by the above data. The phase boundaries indicated by dotted lines have been only approximately located by these data.

The corresponding section at 200°C . is shown in Fig. 44. A comparison of this figure with Fig. 43 shows the way in which phase boundaries change with temperature between 440° and 200°C .

Since the principal object of this investigation was to determine equilibrium relations in the aluminum corner of the aluminum-magnesium-zinc system, the results from aluminum = 100 per cent to aluminum =

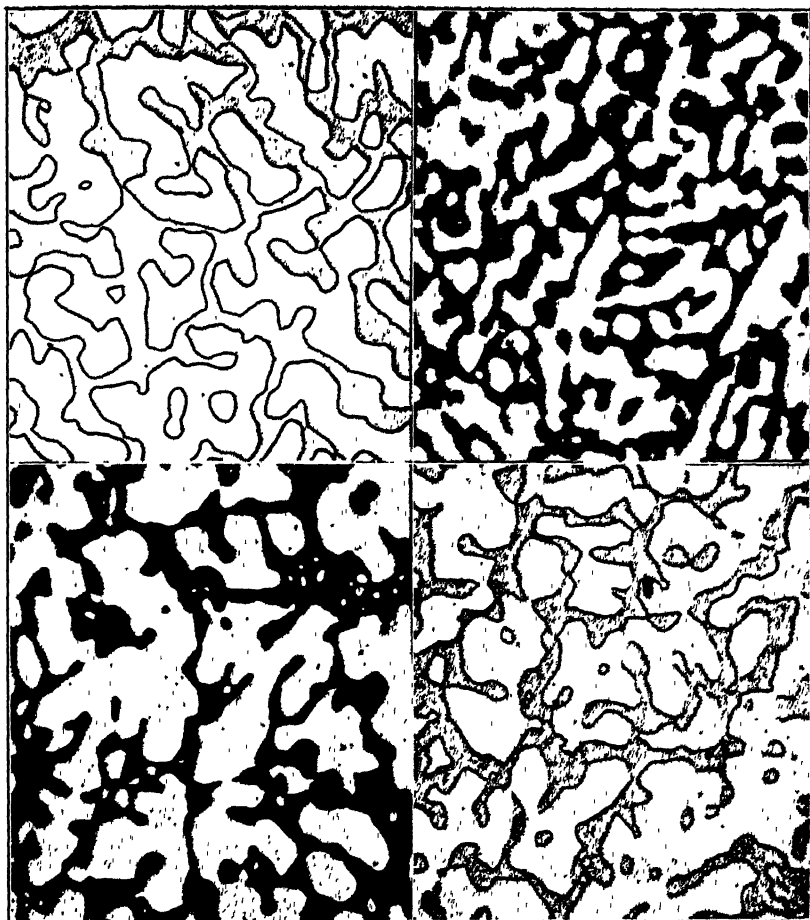


FIG. 37.—ALLOY OF 18.24 PER CENT MAGNESIUM, 11.97 PER CENT ZINC (S17189-2—A9916D). $\times 500$.

Specimen heat-treated 18 hr. at 400°C ., 22 hr. at 350°C ., 22 hr. at 400°C ., 22 hr. at 350°C ., 94 hr. at 400°C ., and quenched. Shows (Al) (light) and $\alpha(\text{Al-Mg-Zn})$ (gray). Etched with concentrated HNO_3 .

FIG. 38.—ALLOY OF 9.87 PER CENT MAGNESIUM, 40.87 PER CENT ZINC (S21817-400—A13333D). $\times 500$.

Specimen heat-treated 312 hr. at 400°C and quenched. Shows (Al) (light) and $\alpha(\text{Al-Mg-Zn})$ (dark). Etched with 1 per cent H_2SO_4 and 0.1 per cent H_2SO_4 solution saturated with H_2S .

FIG. 39.—ALLOY OF 9.31 PER CENT MAGNESIUM, 43.20 PER CENT ZINC (S21819-400—A13334D). $\times 500$.

Specimen heat-treated 312 hr. at 400°C and quenched. Shows (Al) (light), $\alpha(\text{Al-Mg-Zn})$ (dark) and $\beta(\text{Mg-Zn})$ (gray). Etched with 1 per cent H_2SO_4 and 0.1 per cent H_2SO_4 solution saturated with H_2S .

FIG. 40.—ALLOY OF 8.79 PER CENT MAGNESIUM, 45.16 PER CENT ZINC (S21821-400—A13335D). $\times 500$.

Specimen heat-treated 312 hr. at 400°C and quenched. Shows (Al) (light) and $\beta(\text{Mg-Zn})$ (gray). Etched with 1 per cent H_2SO_4 and 0.1 per cent H_2SO_4 solution saturated with H_2S .

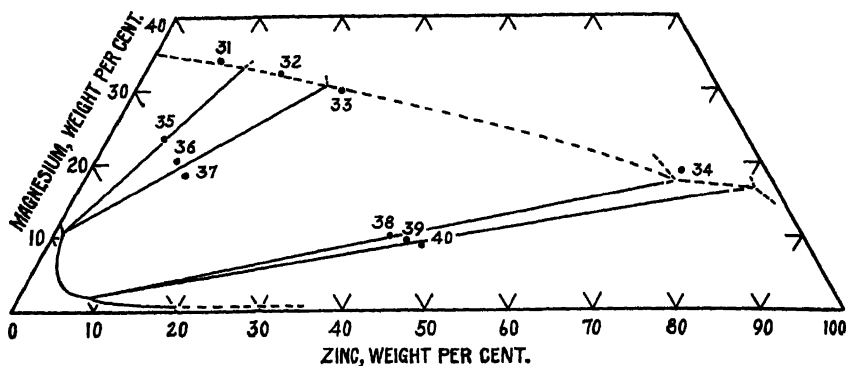


FIG. 41.—SECTION OF DIAGRAM AT 400° C.
Shows locations of samples used for the preparation of Figs. 31 to 40 inclusive.

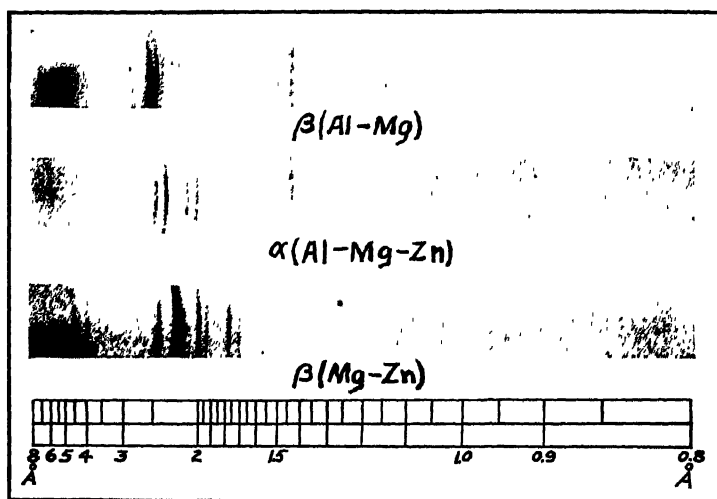


FIG. 42.—DEBYE-SCHERRER PATTERNS OF $\beta(\text{Al-Mg})$, $\alpha(\text{Al-Mg-Zn})$ AND $\beta(\text{Mg-Zn})$.

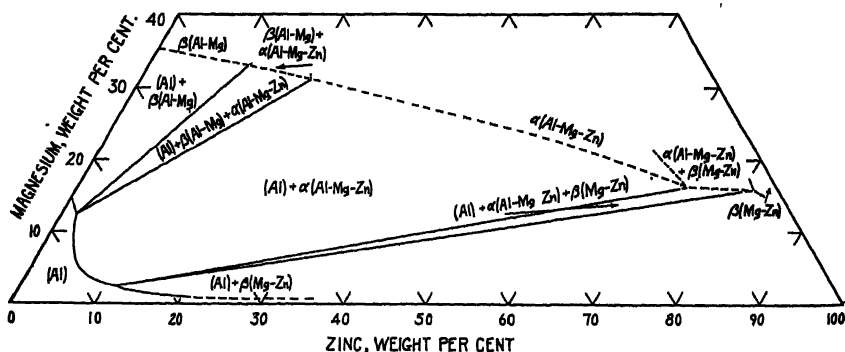


FIG. 43.—EQUILIBRIUM RELATIONS AT 440° C. IN ALUMINUM-MAGNESIUM-ZINC SYSTEM.

80 per cent are presented in the form of six isothermal sections, Figs. 45 to 50. These six figures summarize the principal results of this investigation—the equilibrium relations in the aluminum corner of the diagram from 200° to 440° C.

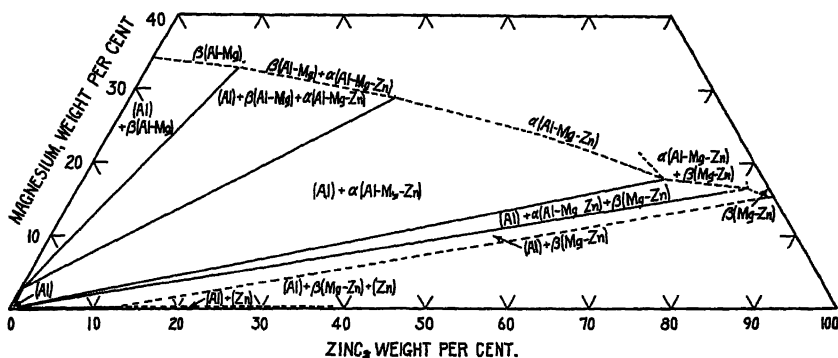


FIG. 44.—EQUILIBRIUM RELATIONS AT 200° C. IN ALUMINUM-MAGNESIUM-ZINC SYSTEM.

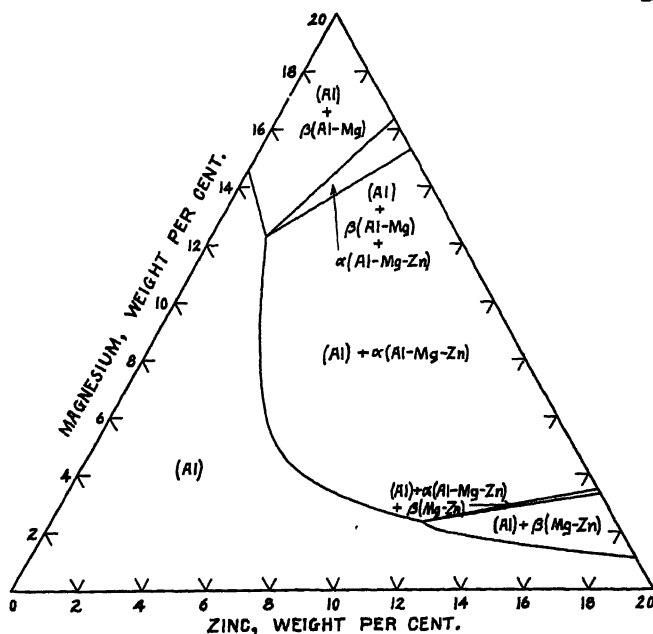


FIG. 45.—EQUILIBRIUM RELATIONS AT 440° C. IN ALUMINUM CORNER OF ALUMINUM-MAGNESIUM-ZINC SYSTEM.

ACKNOWLEDGMENT

The authors express appreciation to Mr. C. J. Walton and Mr. C. W. Cline, who assisted with the metallographic work, to Dr. D. W. Smith, who did the X-ray diffraction work, and to

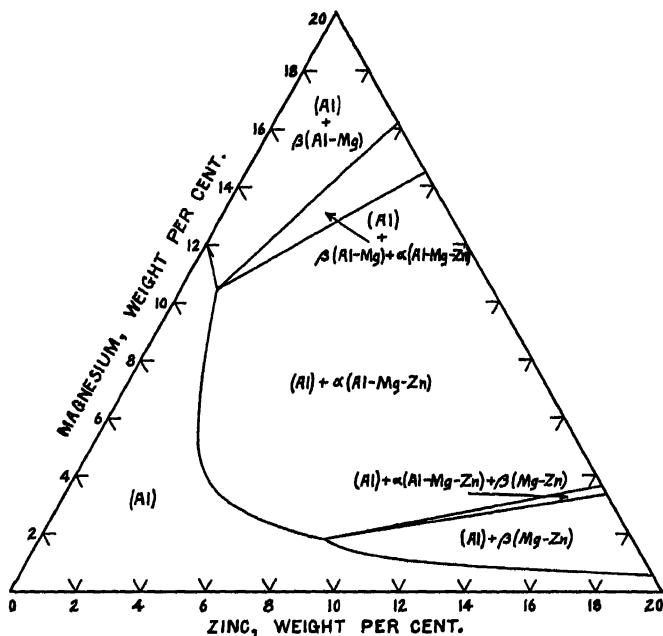


FIG. 46.—EQUILIBRIUM RELATIONS AT 400° C. IN ALUMINUM CORNER OF ALUMINUM-MAGNESIUM-ZINC SYSTEM.

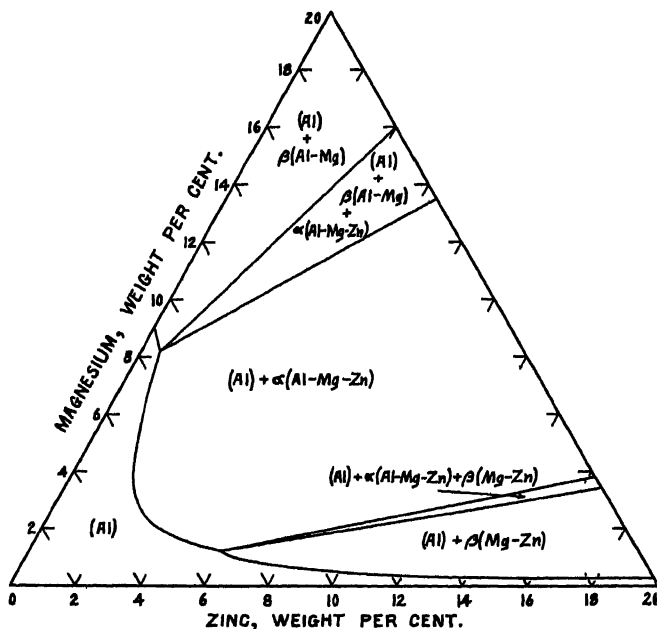


FIG. 47.—EQUILIBRIUM RELATIONS AT 350° C. IN ALUMINUM CORNER OF ALUMINUM-MAGNESIUM-ZINC SYSTEM.

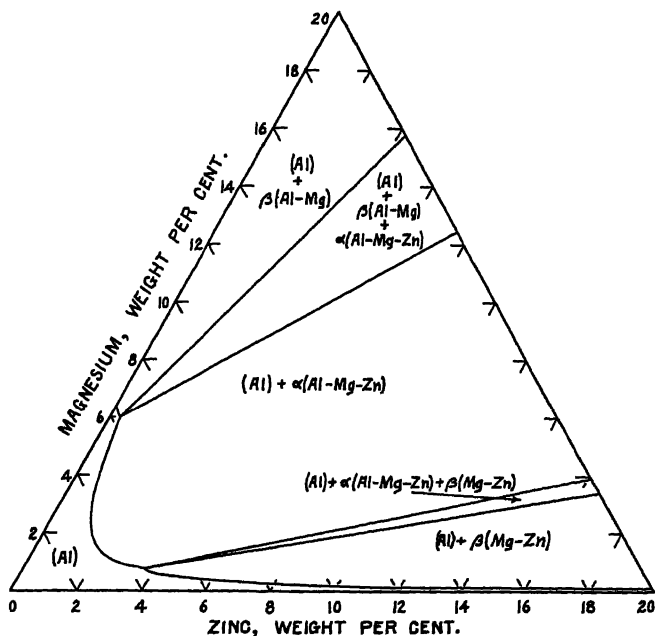


FIG. 48.—EQUILIBRIUM RELATIONS AT 300° C. IN ALUMINUM CORNER OF ALUMINUM-MAGNESIUM-ZINC SYSTEM.

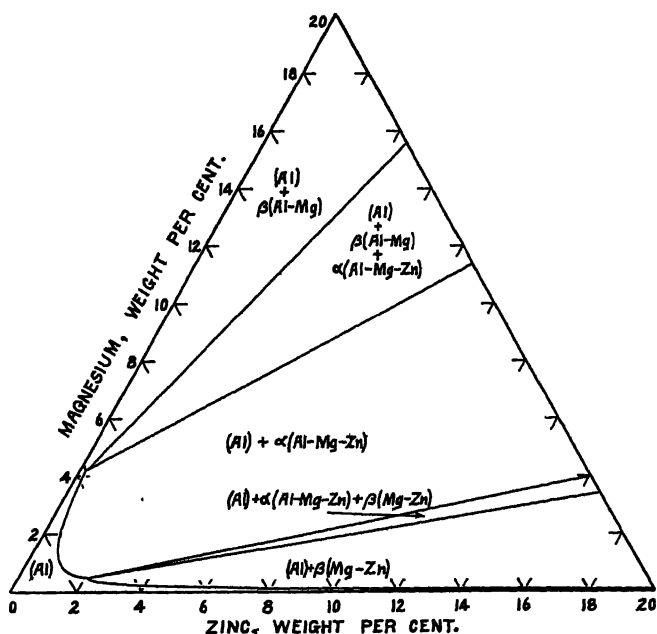


FIG. 49.—EQUILIBRIUM RELATIONS AT 250° C. IN ALUMINUM CORNER OF ALUMINUM-MAGNESIUM-ZINC SYSTEM.

Mr. H. V. Churchill, under whose direction the chemical analyses were made.

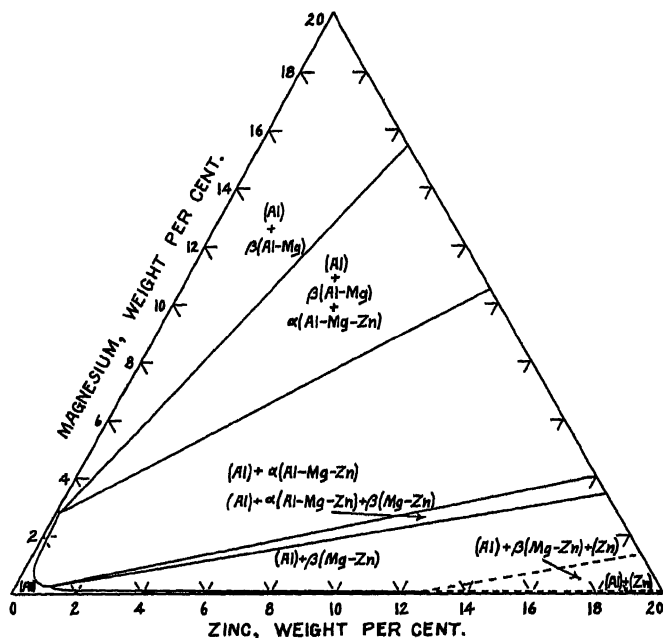


FIG. 50.—EQUILIBRIUM RELATIONS AT 200° C. IN ALUMINUM CORNER OF ALUMINUM-MAGNESIUM-ZINC SYSTEM.

REFERENCES

1. E. H. Dix, Jr. and W. D. Keith: Etching Characteristics of Constituents in Commercial Aluminum Alloys. *Proc. Amer. Soc. Test. Mat.* (1926) **26**, pt. II, 317.
2. E. H. Dix, Jr. and A. C. Heath, Jr.: Equilibrium Relations in Aluminum-silicon and Aluminum-iron-silicon Alloys of High Purity. *Trans. A.I.M.E.* (1928) **78**, 164.
3. F. Keller and G. W. Wilcox: Polishing and Etching of Constituents of Aluminum Alloys. *Metal Progress* (1933) **23**, 45.
4. E. H. Dix, Jr. and F. Keller: Equilibrium Relations in Aluminum-magnesium Alloys of High Purity. *Trans. A.I.M.E.* (1929) **83**, 351.
5. E. Schmid and G. Siebel: Röntgenographische Bestimmung der Löslichkeit von Magnesium in Aluminium. *Ztsch. Metallkunde* (1931) **23**, 202.
6. P. J. Saldau and L. M. Sergeev: Solid Solubility of Magnesium in Aluminum at Different Temperatures. *Metallurgie* (1934) **4**, 67. *Met. Abs., Inst. of Met.* (1934) **1**, 563.
7. D. Hanson and M. L. V. Gayler: Constitution of Alloys of Aluminum and Magnesium. *Jnl. Inst. Metals* (1920) **24**, 201.
8. Reference 4, page 11.
9. M. Kawakami: On the Equilibrium Diagram of the Aluminum-magnesium System. *Kinzoku no Kenkyu* (1933) **10**, 532. *Abs., Metals and Alloys* (1934) **5**, MA217.
10. W. L. Fink and L. A. Willey: Equilibrium Relations in Aluminum-zinc Alloys of High Purity, II. *Trans. A.I.M.E.* (1936) **122**, 244.

11. R. Chadwick: Constitution of the Alloys of Magnesium and Zinc. *Jnl. Inst. Metals* (1928) **39**, 285.
12. W. Hume-Rothery and E. O. Rounsefell: The System Magnesium-Zinc. *Jnl. Inst. Metals* (1929) **41**, 119.
13. A. A. Botschwar and I. P. Welitschko: Über das Zustandsdiagramm der Magnesium-Zinklegierungen. *Ztsch. anorg. Chem.* (1933) **210**, 164.
14. W. Sander and K. L. Meissner: Der Einfluss der Verbindung $MgZn_2$ auf die Vergutbarkeit von Aluminiumlegierungen. *Ztsch. anorg. Chem.* (1926) **154**, 144.
15. P. Saldau and M. Zamotorin: Löslichkeit der Chemischen Verbindung $MgZn_2$ in Aluminium im festen Zustande bei verschiedenen Temperaturen. *Ztsch. anorg. Chem.* (1933) **213**, 377.
16. Seiren Nishihara: The Ternary System: Aluminum-magnesium-zinc. *Suiryo-kaishi* (1929) **5**, 783. *Chem. Abs.* (1930) **24**, 1608.
17. G. Eger: Studie Über die Konstitution der Ternären Magnesium-Aluminium-Zink-Legierungen. *Int. Ztsch. Metallg.* (1913) **4**, 29.
18. A. A. Botschwar and M. O. Kuznetsov: Transformations in Solid Alloys of Aluminum with up to 30 per cent Zinc and 12 per cent Magnesium. *Metal-lurgie* (1933) **8**, 7.
19. Chemical Analysis of Aluminum. Aluminum Company of America.
20. W. Guertler: Zur Fortentwicklung der Konstitutionsforschungen bei ternären Systemen. *Ztsch. anorg. Chem.* (1926) **154**, 439.
21. W. Köster and W. Wolf: Das Dreistoffsystem Aluminium-Magnesium-Zink. *Ztsch. Metallkunde* (1936) **28**, 155

DISCUSSION

(O. W. Ellis presiding)

G. EDMUNDS,* Palmerton, Pa.—A statement was made that with certain of the alloys that were workable, the rich aluminum alloys, the procedure was to cast and then to roll the alloys. I should like to know whether any of the alloys in the intermediate fields are workable, because I think it is of general interest to know whether there are workable alloys in the fields where two or more different microscopic constituents are observed. Of course, most of our common alloys are solid solution alloys, with a few very important exceptions.

The other point that I wish to bring out is to ask the authors whether they have attempted, as did Dr. Fink and Miss Freche two or three years ago, in working with binary alloys, to apply the thermodynamic methods of analyzing the solubility relations that they have found.

W. L. FINK.—In regard to the range of workability, I think the first two figures will assist in the explanation. In Fig. 1 the portion of the section below about 11 per cent magnesium represents workable alloys; i.e., alloys that can be rolled. Most of the alloys in the upper portion of this section of the diagram are very difficult to roll (i.e., alloys containing more than about 11 per cent magnesium) and we usually use them in the cast form. In the portion of the diagram shown in Fig. 2, all the alloys were used in the cast form. It might have been possible to roll some of the alloys with lowest magnesium contents under section 21-22, but considerable difficulty would have been encountered.

A great deal of work was done with a number of etches, from two points of view. First, we were trying to build up information on the etching of various phases with certain standard etches. This will permit the identification of phases by running a series of etches much as one would run a qualitative chemical analysis. Mr. Dix

* Investigator, Research Division, New Jersey Zinc Co.

and Mr. Keith¹ started this work several years ago, and Mr. Keller and Mr. Wilcox² have made a further contribution. As we work on the various new systems, we determine the action of these same etching reagents.

The second portion of the etching studies was conducted to develop new etches to differentiate coexisting phases in this particular system. One of the best of these was a double etch. The specimen was first immersed for a short time, about 3 sec., in a 1 per cent sulphuric acid solution, then immersed again for 60 sec. in a solution containing 0.1 per cent sulphuric acid saturated with hydrogen sulphide. I do not know why that etch works, but it does. Table 12 gives the etching characteristics of the various constituents in the different phase fields, and directs attention to one of the difficulties encountered in using an etching method for the identification of phases. Sometimes the effect of the etch is altered by the presence of other phases. This is one reason why we used X-ray diffraction patterns for initial positive identification and then determined the etching characteristics.

In regard to the correlation between electrical-conductivity measurements and microscopic observation, there were two or three points in the diagram where there was some question, but it always involved a sample very close to a phase boundary. I would say that the correlation was as good as could be expected. In the paper itself the curve is drawn through the points shown by breaks in the electrical-resistivity concentration curves, and the results of the microscopic examinations are indicated for each sample, so that one can follow through sample by sample and see how good the correlation is.

There is a considerable variation in the time required for reaching equilibrium. Ordinarily with sheet specimens that previously have reached equilibrium at a lower temperature, equilibrium is obtained rapidly—usually in a few hours; certainly within two or three days. Approach to equilibrium can be followed readily. That is one of the advantages of the electrical-conductivity method. The electrical conductivity of all of the specimens can be measured, the specimens can be left in the furnace for another day then measured again. Only a short time is required to measure the whole group. Measurements can be continued at the same temperature until no further change occurs. For cast specimens, a much longer time is required to obtain equilibrium. In some tests we have left samples in the furnace for weeks.

I believe that electrical-conductivity measurements at temperature are destined to be used more and more. It is such a convenient method and so much information can be obtained in a relatively short time. In studying ternary systems, where one deals with so many specimens for each section, and so many sections, something must be done to decrease the time required for the investigation. The preparation of the samples so that equilibrium can be obtained in a short time is also important. The best procedure we have found is to start with cold-rolled specimens with a very fine structure and approach equilibrium at very low temperatures. We usually do this by cold-rolling the samples, putting them in a bath at 200° C., and forgetting about them for a while. Measurements are made first at 200° C. and then at successively higher temperatures. The particles that precipitate at 200° C. are very fine and consequently go into solution readily. At higher temperatures the particles become larger, but this is compensated by the higher rates of solution and diffusion. If the procedure is reversed, the higher temperature produces large particles, and excessive time is required to obtain equilibrium at lower temperatures.

Equilibrium Relations in the Nickel-tin System

BY WILLIAM MIKULAS,* JUNIOR MEMBER A.I.M.E., LAARS THOMASSEN† AND
CLAIR UPTEGROVE,‡ MEMBER A.I.M.E.

(Cleveland Meeting, October, 1936)

LITTLE work has been done in the field of the nickel-tin binary system. The complete diagram has been investigated on two occasions, but the results are in very poor agreement. The structure of a compound NiSn and the solubility of tin in nickel have been determined by X-ray methods. Several investigations have been made of the liquidus curve, and the compositions of the eutectics have been determined. A study of the literature, however, shows that there is no satisfactory agreement between the data presented in the various papers.

The present investigation was undertaken in an attempt to determine the equilibrium conditions, and to correlate X-ray with metallographic data. The equilibrium diagram was determined by thermal and metallographic means, and the solubility of tin in nickel further investigated with X-rays. Powder diagrams were made of the intermetallic compounds, and three of the structures were partly determined. No attempt was made to determine the range of homogeneity of the intermetallic compounds.

REVIEW OF THE LITERATURE

Vigouroux¹ prepared alloys of tin and nickel containing 74 and 92 per cent of tin. By treating these alloys with very dilute nitric acid or with sodium hydroxide he was able to separate residues, both of which analyzed 66.7 per cent tin. This corresponds to the compound NiSn and was reported as such.

Guillet² made the first investigation of the complete binary diagram (Fig. 1). The maximum point of the liquidus is at 43.5 per cent nickel. Several solid solution areas were found, and the compound NiSn was included on the strength of Vigouroux's work. The investigation was

This paper is based on a dissertation submitted in partial fulfillment of the requirements for the degree of Doctor of Science at the University of Michigan. Manuscript received at the office of the Institute July 20, 1936; revised January, 1937.

* Metallurgist, Kelvinator Corporation, Detroit, Mich.

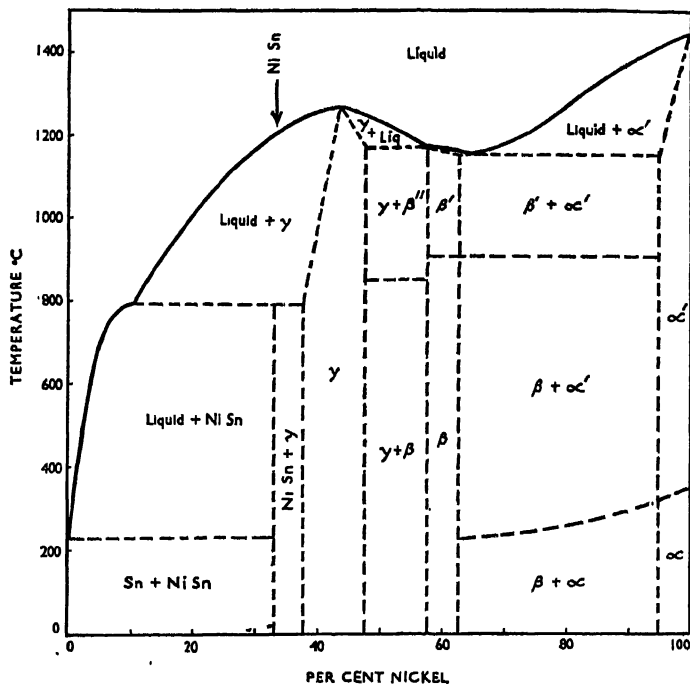
† Assistant Professor of Chemical Engineering, University of Michigan, Ann Arbor, Mich.

‡ Professor of Metallurgical Engineering, University of Michigan.

¹ References are at the end of the paper.

primarily thermal, with microscopic examination of certain of the alloys.

Voss³ published the diagram that is reproduced in Fig. 2. There is very little similarity between this diagram and that of Guillet. Voss found compounds of the formulas Ni_3Sn_2 , Ni_3Sn , and Ni_4Sn . The solid solutions, except Guillet's alpha, are absent.



Temp. °C.	Nature of transformation	Range of composition per cent nickel
1266	Melting point of γ	43.5
1170	Peritectic: $\gamma + \text{liq} \rightleftharpoons \beta'$	47.5-58.0 ($\beta' = 57.5$)
1150	Eutectic: $\text{liq} \rightleftharpoons \beta' + \alpha'$	62.5-95.0 (Eutectic point = 64)
910	Polymorphic: $\beta' \rightleftharpoons \beta$	57.5-95.0
850	Polymorphic: $\beta'' \rightleftharpoons \beta$	47.5-57.5
790	Peritectic: $\text{liq} + \gamma \rightleftharpoons \text{Ni}_3\text{Sn}$	10.0-37.5
351-227	Magnetic: $\alpha' \rightleftharpoons \alpha$	62.5-100
230	Eutectic: $\text{liq} \rightleftharpoons \text{Sn} + \text{Ni}_3\text{Sn}$	0.33.0 (Eutectic point = 0.1)

The figures in italics were obtained from the diagram by measurement.

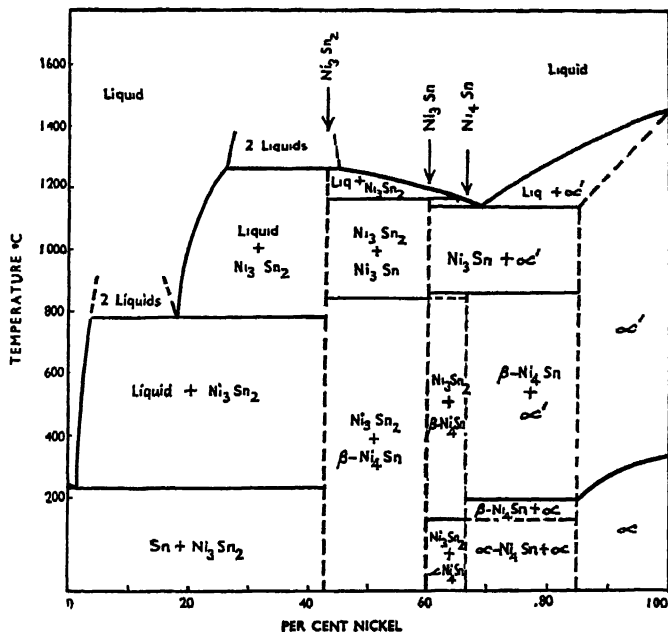
FIG. 1.—NICKEL-TIN SYSTEM ACCORDING TO GUILLET².

Reproduced from Tech. Pubs., Ser. B., No 2, International Tin Research and Development Council.

Oftedal⁴ calculated from the powder diagram that the compound Ni_3Sn has a nickel arsenide structure with values for a_0 of 4.08\AA . and for c_0 5.17\AA . Very little description of the preparation of the alloy is given.

Hanson, Sandford and Stevens⁵ found the eutectic on the high-tin side of the diagram to contain 0.18 per cent nickel. They used segregation

methods to determine this point and also the liquidus curve for alloys up to 4 per cent nickel. A microscopic examination showed that the solubility of nickel in tin was less than 0.005 per cent. Their results are shown in Fig. 3.



Temp. °C	Nature of transformation	Range of composition per cent nickel
1263	2 liquids \rightleftharpoons Ni ₃ Sn ₂ + liq.	26-45
1162	Peritectic: Ni ₃ Sn ₂ + liq. \rightleftharpoons Ni ₃ Sn	42-63-65
1135	Eutectic: liq. \rightleftharpoons Ni ₃ Sn + α'	60-85 (Eutectic point = 68.5)
855	Peritectic: Ni ₃ Sn + α' \rightleftharpoons β-Ni ₄ Sn	60-85
837	Ni ₃ Sn \rightleftharpoons Ni ₃ Sn ₂ + β-Ni ₄ Sn	42-63-66.5
775	2 liquids \rightleftharpoons Ni ₃ Sn ₂ + liq.	3.5-18
330-190	Magnetic: α' \rightleftharpoons α	66.5-100
229	Eutectic: liq. \rightleftharpoons Sn + Ni ₃ Sn ₂	0-42.63 (Eutectic point 1.3)
130	Magnetic: β-Ni ₄ Sn \rightleftharpoons α-Ni ₄ Sn	60-85

The figures in italics were obtained from the diagram by measurement

FIG. 2.—NICKEL-TIN SYSTEM ACCORDING TO VOSS³.

Reproduced from Tech. Pubs., Ser. B., No 2, International Tin Research and Development Council.

Fetz and Jette⁶ determined the solubility of tin in nickel by means of X-ray methods. They found that the solubility at 1100° C. was 20 per cent and that it dropped to 2.5 per cent at 500° C. The excess constituent was stated to be Ni₃Sn.

For purposes of discussion, the results are considered in two parts. The first part, which deals primarily with the equilibrium relations found in the nickel-tin system, presents the procedure, results and interpretation

of the thermal and metallographic work; also, supporting data from the X-ray work in as far as they are necessary in the interpretation of the results. The second part presents the procedure, complete results and the interpretation of the X-ray studies.

PART I. EQUILIBRIUM RELATIONS IN THE NICKEL-TIN SYSTEM

Procedure

The alloys were prepared from "Chempur" tin analyzing 99.99 per cent tin and electrolytic nickel having a purity of 99.95 per cent (including 0.2 per cent cobalt). They were melted, usually in charges of 500

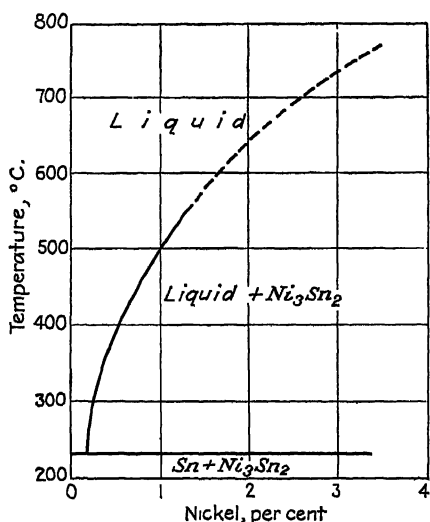


FIG. 3.—HIGH-TIN EUTECTIC ACCORDING TO HANSON, SANDFORD AND STEVENS.

Eutectic composition, 0.18 per cent nickel; eutectic temperature, 232° C.

Reproduced from Tech. Pubs., Ser. B., No. 2, International Tin Research and Development Council.

grams, in an Ajax-Northrup induction furnace. Alloys containing up to 43 per cent nickel (the composition of Ni₃Sn₂) were melted under hydrogen and poured into a cold graphite mold. While the alloys between 20 and 43 per cent nickel were porous because of absorbed hydrogen, vacuum melting could not be successfully used to remedy this condition because of the tendency for segregation of Ni₃Sn₂. The low-nickel alloys were made by melting a master alloy containing 19.3 per cent nickel and adding tin. Alloys containing over 20 per cent nickel were made by melting pure nickel and adding the tin.

Alloys containing from 43 to 70 per cent nickel were melted in a vertical quartz-tube vacuum furnace. For alloys over 70 per cent nickel the method of melting reported by Fetz and Jette⁶ was

used. The nickel was given a preliminary annealing of 72 hr. at 1000° C. in purified hydrogen. Charges of 250 grams were melted in a small vacuum furnace under hydrogen. When the charge was completely molten the chamber was evacuated with a mechanical pump, and when solidification was completed the vacuum was broken and the metal removed. The ingots were cut in two and annealed for 120 hr. at 1000° C. in purified hydrogen.

All of the ingots were annealed for a period of 72 hr., those containing less than 30 per cent nickel at 200° C. and the others at 500° C. One inch was discarded from the top and ½ in. from the bottom of each of

the ingots cast in the graphite mold. Metallographic samples of about five grams were cut from the remaining portions, where possible, so as to give a section representative of a half section of the ingot.

Table 1 lists the alloys prepared, their analysis and the thermal critical points as determined by cooling curves.

TABLE 1.—*Analytical and Thermal Data*

Per Cent Ni	Analysis, Per Cent		Liquidus, Deg. C	Solidus, Deg. C.	Phase Change, Deg. C.
	Sn	Ni			
0				231-232	
½	99.5	0.47	390	231	
1	99.0	1.04	490	231	
2	98.0		590	231	
3	97.1		680	231	
5	95.0		793	230	
8	91.9		793		
12	88.2				
19.3	80.7	19.36	930, 793		
21	78.9		1110, 793		
25	75.0		1252, 793		
27.1	72.7	27.22			
30	69.8		1254		
33	67.1		1252		
40	59.8		1252	790, 230	
43	57.0	42.92		1253	902
45	55.0		1253	1166	
47	53.1		1246	1166	902
55	45.1		1232	1163	904
60	40.0		1220	1163	
62.5	37.3		1204	1164, 1144	941
65	35.0		1188	1164, 1142	940
66.4	33.4	66.50			
67.5	32.4		1151	1141, 1125	940
70	30.0		1153	1124	941
75	25.1		1233	1127	942
80	19.9		1299	1122	941
82	18.0				
84	15.9	83.95			
85	15.0		1354		
86	14.0				
88	12.1				
90	10.0		1404	1239	
92	8.0	92.11			
94	6.1				
95	5.0		1440	1333	
96	4.0				
98	2.0				
100			1453		

The annealing furnace and the method of heat-treatment followed the plan previously used by Rowland and Upthegrov⁷. For temperatures below 850° C. the samples were annealed in a furnace fitted with a

Nichrome block. The temperature was automatically maintained and held to a variation of $\pm 2^\circ$ C. during the annealing period. Temperature gradients within the furnace block were kept to less than 2° C. by means of a heating element within the door. For temperatures above 850° C. an automatically controlled Nichrome tube furnace and a manually controlled Globar furnace were used. The Globar was a six-element tube furnace and could be readily maintained at temperature for the short-time anneals.

After annealing the samples were ground, polished and etched. The final polishing, especially of the high-tin alloys, required the use of magnesia on a silk broadcloth wheel. Etching was accomplished through the use of three different solutions. Alloys up to 30 per cent nickel were etched with a 5 per cent water solution of ferric chloride. Alloys containing 30 to 80 per cent nickel were etched by the usual acid ferric chloride. The high-nickel alloys were etched either with a 1 to 1 mixture of nitric and glacial acetic acids or electrolytically in a solution containing 10 per cent nitric and 5 per cent acetic acids.

The determinations of the liquidus and solidus were carried out according to the usual procedure except that for temperatures above 1000° C. a vertical Globar furnace was used. Inverse-rate curves were obtained for 24 alloys, using a platinum-platinum rhodium thermocouple and a type K precision potentiometer. Samples of 150 grams were melted in alundum crucibles and cooled at a rate of 2° to 4° C. per minute. With the nickel content of the alloy over 50 per cent, it was necessary to introduce hydrogen just above the melt to minimize the tendency for the melt to react with the crucible.

Inverse-rate thermal analyses were conducted upon 10 different samples to determine the temperature at which solid phase changes occurred. These alloys could not be machined, so specimens were cast in a graphite mold giving cylinders $1\frac{1}{4}$ in. long, $\frac{1}{2}$ in. in diameter, with a hole for the thermocouple $\frac{1}{4}$ in. in diameter and $\frac{1}{2}$ in. deep. The sample and couple were enclosed in a closed-end protection tube and supported in a vertical electric tube furnace. The results of the thermal analyses are given in Table 1.

Discussion of Previous Investigations

Figs. 1 and 2 show that the results of the investigations carried out by Guillet and Voss are in almost complete disagreement. Guillet worked with nickel containing about 2 per cent of cobalt, iron and copper, while Voss reported an analysis of 1.86 per cent cobalt, 0.47 per cent iron and a trace of copper. Neither reported an analysis of the tin. Guillet combined metallographic examination with the thermal investigation. Voss made his alloys in a porcelain tube and used the whole ingot in the determination of the critical points.

Guillet determined metallographically the solubility of tin at room temperature to be about 5 per cent, while Voss placed the solubility at the eutectic temperature at 15 per cent. Voss' figure was based on observation of the decreasing length of time required for the alloys of eutectic, 70, 75 and 80 per cent nickel to cool through the eutectic temperature. Both assumed no change in solubility with change in temperature.

Guillet indicated the presence of several solid solutions, other than the alpha, but failed to give any satisfactory explanation for their location or identification. The compound Ni_3Sn as found by Vigoroux was

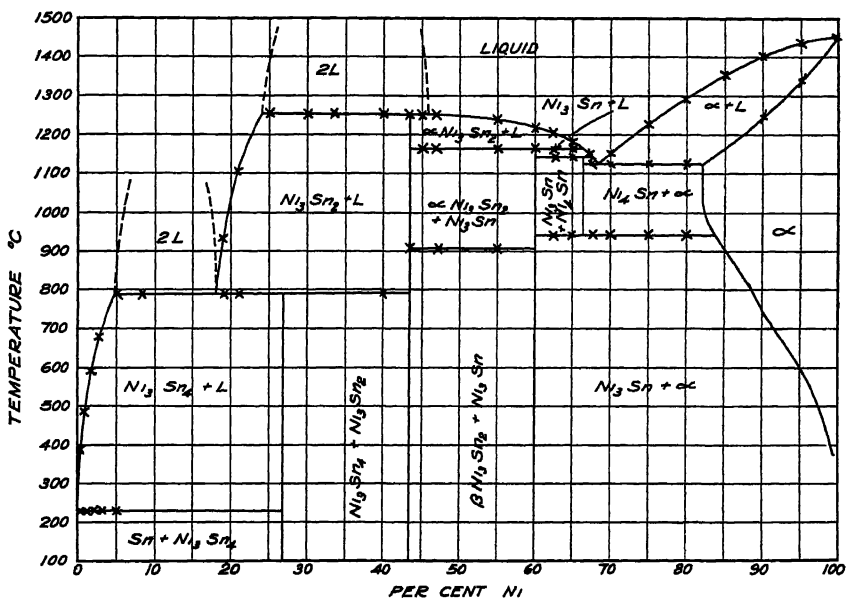


FIG. 4.—NICKEL-TIN EQUILIBRIUM DETERMINED IN PRESENT INVESTIGATION.

included. Voss introduced the compounds Ni_3Sn_2 , Ni_3Sn and Ni_4Sn , and failed to find any areas of solid solubility between any of them. He found no evidence of Ni_3Sn . Ni_3Sn_2 formed from the liquid at 1264° C. and remained unchanged down to room temperature. Ni_3Sn was formed by a peritectic reaction at 1162° C., and in time reacted with alpha solid solution to form Ni_4Sn . Ni_3Sn decomposed at 837° C. to form Ni_3Sn_2 plus Ni_4Sn . Voss' thermal data cannot be considered sufficiently accurate to justify the assumption of the decomposition of the Ni_3Sn .

Both found a high-tin eutectic at about one per cent nickel and melting at 230° C. Guillet assumed that it was made up of tin and Ni_3Sn , while Voss considered that it was a mixture of tin and Ni_3Sn_2 .

Results

The nickel-tin equilibrium diagram as determined by the results of this investigation is shown in Fig. 4. The thermal data of Table 1 constituted the basis for much of the form of the diagram.



FIG. 5.—NICKEL, 0.5 PER CENT. TIN + Ni_3Sn_4 . $\times 250$.

FIG. 6.—NICKEL, 1 PER CENT. TIN + Ni_3Sn_4 . $\times 250$.

FIG. 7.—NICKEL, 8 PER CENT. TIN + Ni_3Sn_4 . $\times 250$.

FIG. 8.—NICKEL, 12 PER CENT. TIN + Ni_3Sn_4 . $\times 250$.

Starting from a composition of zero per cent nickel and 232°C ., the liquidus rises rapidly as a smooth curve to 793°C . at about 4.5 per cent

nickel. There was no indication of the presence of a eutectic alloy, and the solidus showed no appreciable variation from the melting point of tin. Ni_3Sn_4 is formed at 793°C . and for compositions between 4.5 and

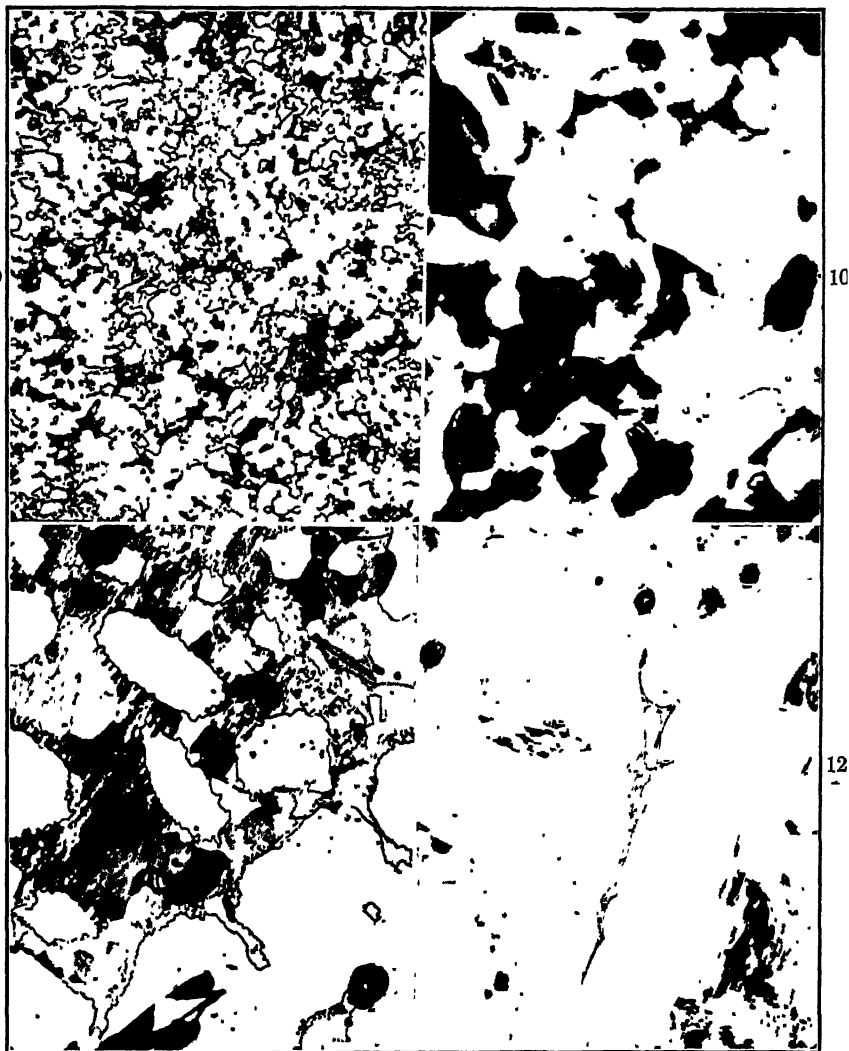


FIG. 9.—NICKEL, 19 PER CENT. $\text{TIN} + \text{Ni}_3\text{Sn}_4$. $\times 250$.
 FIG. 10.—NICKEL, 27 PER CENT. Ni_3Sn_4 . $\times 250$.
 FIG. 11.—NICKEL, 33 PER CENT. $\text{Ni}_3\text{Sn}_4 + \text{Ni}_3\text{Sn}_2$. $\times 100$.
 FIG. 12.—NICKEL, 40 PER CENT. $\text{Ni}_3\text{Sn}_4 + \text{Ni}_3\text{Sn}_2$. $\times 100$.

43 per cent nickel as the result of a peritectic reaction. In much the same way Ni_3Sn_2 is formed at 1253°C . for alloys between 24 and 46 per cent nickel. As the nickel content passes 46 per cent the liquidus

temperature decreases to that of the eutectic at 1124°C . and 68.5 per cent nickel.

Ni_3Sn forms as the result of a peritectic reaction at 1164°C . between Ni_3Sn_2 and the liquid phase. Ni_7Sn then forms at 1143°C . from the



FIG. 13.—NICKEL, 47 PER CENT. $\text{Ni}_3\text{Sn}_2 + \text{Ni}_7\text{Sn}$. $\times 250$.

FIG. 14.—NICKEL, 55 PER CENT. $\text{Ni}_3\text{Sn}_2 + \text{Ni}_7\text{Sn}$. $\times 250$.

FIG. 15.—NICKEL, 60 PER CENT, QUENCHED FROM 1100°C . Ni_3Sn . $\times 100$.

FIG. 16.—NICKEL, 60 PER CENT, ANNEALED AT 500°C . Ni_3Sn . $\times 100$.

reaction between Ni_3Sn and liquid. As the nickel content exceeds 68.5 per cent, the liquidus gradually rises to the melting point of nickel at 1452°C .



FIG. 17.—NICKEL, 70 PER CENT. Ni_3Sn
PLUS SOLID SOLUTION. $\times 250$.

FIG. 18.—NICKEL, 80 PER CENT. Ni_3Sn
PLUS SOLID SOLUTION. $\times 250$.

FIG. 19.—NICKEL, 90 PER CENT.
 Ni_3Sn PLUS SOLID SOLUTION. $\times 250$.

Thermal analysis of alloys containing between 5 and 43 per cent nickel indicated the existence of a compound Ni_3Sn_4 at 27.1 per cent nickel. Figs. 5 to 10 show the increasing amounts of this compound in alloys having 0.5 to 27 per cent nickel, the tin constituent having completely disappeared at 27 per cent. Fig. 11 illustrates the two-phase structure of the 33 per cent alloy. It was found impossible to prevent the breaking out of the compound in the polishing operations, particularly in the higher percentages of this range, as is evident from the photo-

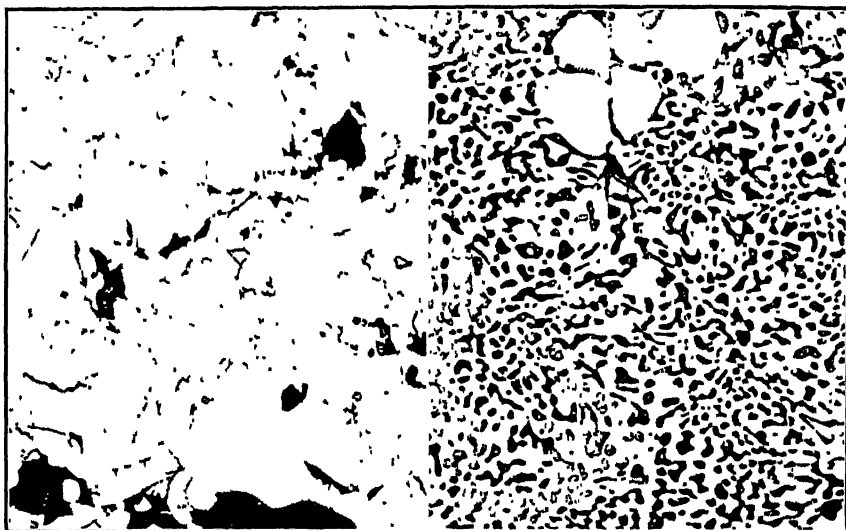


FIG. 20.

FIG. 21.

FIG. 20.—NICKEL, 66.4 PER CENT, QUENCHED FROM 1100° C. Ni_3Sn_4 . $\times 250$.

FIG. 21.—NICKEL, 66.4 PER CENT, QUENCHED FROM 900° C. Ni_3Sn PLUS SOLID SOLUTION. $\times 250$.

micrographs. An X-ray investigation of the crystal structure of Ni_3Sn_4 showed it to have a complex structure, which was not determined.

Ni_3Sn_2 undergoes a transformation at 902° C. Studies of X-ray diffraction patterns show that at temperatures below 902° C. the structure appears hexagonal, and of the nickel-arsenide type, with one molecule per unit cell. Above 902° C. the structure is tetragonal with an axial ratio of 0.94 and containing 10 molecules per unit cell.

Figs. 12, 13 and 14 show alloys of 40, 47 and 55 per cent nickel, after annealing at 500° C. Fig. 12 shows Ni_3Sn_2 with a small amount of Ni_3Sn_4 . Fig. 13 shows Ni_3Sn_2 with a very small amount of Ni_3Sn , while Fig. 14 shows increasing amounts of Ni_3Sn . The somewhat striated appearance of the Ni_3Sn_2 in Fig. 13 is apparently due to a pitting or breaking out of the compound, the markings developing partly during the etching of the alloys.

Figs. 15 and 16 show the alloy containing 60 per cent nickel after quenching from 1100° and 500° C., respectively. Examination of this alloy after quenching from 1100°, 1000° and 500° C., respectively, showed it to be composed of one phase, Ni_3Sn . Thermal analysis also showed the absence of any transformation in the solid state. The structure of this compound was not determined.

Figs. 17 and 18 illustrate the eutectic type of structure found in the annealed alloys of 70 and 80 per cent nickel. Fig. 19 represents the solid solution and excess constituent Ni_3Sn of the 90 per cent alloy.

Ni_4Sn forms at 1142° C. and decomposes at 941° C. Its structure appeared to be tetragonal with two molecules per unit cell. Figs. 20 and 21 show the 66.4 per cent nickel alloy quenched from 1100° and 900° C. At 1100° C. only the single phase Ni_4Sn is shown, while at 900° C. two phases are present, Ni_3Sn and the solid solution.

Table 2 gives the results of the metallographic examination of a series of alloys from 80 to 92 per cent nickel that were subjected to annealing and quenching treatments to determine the solubility of tin in nickel.

TABLE 2.—*Results of Annealing and Quenching Experiment*

Temperature. Deg. C.	Two-phase Alloys, Per Cent Ni	Single-phase Alloys, Per Cent Ni
1100	80, 82	84, 86, 88
1000	80, 82	84, 86, 88
900	82, 84	86, 88, 90
800	84, 86, 88	90, 92
700	90	92, 94, 96, 98
500	92, 94	96, 98
25	92, 94	96, 98

The metallographic study of the solubility of tin in nickel was supplemented by an X-ray investigation. The results of the X-ray and metallographic determinations are presented in Fig. 23 with the X-ray determinations of Jette and Fetz.

Discussion of Results

The solidus temperature of the high-tin alloys was found to be very close to the melting point of tin. Solidus-temperature determinations gave variations from 231° to 232° C. The same variations were obtained in calibrating the thermocouple used against Chempur tin. The results confirm the conclusions of Hanson, Sandford and Stevens that the addition of nickel does not lower the melting point of tin.

In determining the composition of the high-tin eutectic, a method similar to that of the aforementioned authors was used. Samples of the 0.5, 1, 3, and 5 per cent nickel alloys each weighing 250 grams were heated to 800° C. for 24 hr., cooled to 240° C. and held for 24 hr., and

quenched in water. Analysis of drillings taken from the tops of the specimens showed the presence of only a trace of nickel, certainly less than 0.01 per cent, indicating that the eutectic contains practically zero per cent nickel.

In the present diagram the first compound to show up on adding nickel to tin is Ni_3Sn_4 . This is not in agreement with the works of Vigoroux¹ and Oftedal⁴ on NiSn . Vigoroux treated alloys containing 8 and 26 per cent nickel with very dilute reagents, and obtained a residue that corresponded to NiSn in composition. A description of the preparation of Vigoroux's alloys could not be found, and it is possible that the samples may not have been in equilibrium when the chemical treatment was performed. Also, the presence of Ni_3Sn_2 , which later was shown to exist, may have thrown off the result through its relative insolubility, for it was almost certain to have been present in the as-cast 26 per cent alloy and may have been in the other.

Oftedal determined the crystal structure of what he claimed to be NiSn , as hexagonal and of the nickel arsenide type. An X-ray investigation of the compound Ni_3Sn_2 showed, however, that the powder diagram of one of its forms was identical with the diagram that Oftedal had obtained for what he considered to be NiSn .

Metallographic examination of alloys corresponding to Ni_3Sn_4 and NiSn after annealing for 72 and 500 hr. at 200° and 500° C. showed that the Ni_3Sn_4 composition had a single phase while the NiSn composition had two.

Voss found neither NiSn nor Ni_3Sn_4 . He noticed that all of the alloys containing up to 43 per cent nickel had a break in their cooling curves at 230° C., thus indicating that the eutectic extended from pure tin to Ni_3Sn_2 . Voss's cooling data were shown to be correct in so far as the breaks at 230° C. are concerned, but his interpretation is believed to be incorrect. If an alloy of 40 per cent nickel is cooled according to the usual procedure, some Ni_3Sn_2 separates out at 1253° C. As the cooling continues down to 793° C., Ni_3Sn_2 continues to separate. At this point, if sufficient time elapses the liquid should be entirely used up in the reaction with the solid. Under ordinary conditions, however, sufficient time is not provided and the alloy finally freezes as if the nickel content were under 4.5 per cent. Therefore, the breaks in the cooling curve at 230° C. are not, in these alloys, an indication that eutectic is present under equilibrium conditions. This is further confirmed by the fact that alloys containing more nickel than required for Ni_3Sn_4 when annealed at 500° C. showed no signs of a liquid phase.

There are two ranges of alloy composition where the liquid consists of two immiscible phases, from 4.5 to 18 per cent nickel and from 24 to 46 per cent nickel. The solid separating out in the first is Ni_3Sn_4 and in the second Ni_3Sn_2 . This condition, as indicated above, contributed to

Voss' inability to find a compound of lower nickel content than Ni_3Sn_2 . The boundaries in the liquid phases were not investigated.

The left end of the horizontal line at 1253°C. was determined at 24 per cent nickel by analyzing the tops of three alloys, 25, 33, and 40 per cent nickel, which had been melted in the vacuum furnace. The density of the compound Ni_3Sn_2 caused it to settle to the bottom of the crucible as soon as it had formed. Drillings from the tops of these ingots showed the following compositions: 24.3, 22.6 and 24.3 per cent nickel. A second sample of the 40 per cent alloy, melted as before but cooled very slowly by keeping a low current on until solidification started, showed 24.2 per cent nickel at the top and 43.0 per cent nickel at the bottom, the latter being the composition of Ni_3Sn_2 .

Voss' explanation of the decomposition of Ni_3Sn and the formation of Ni_3Sn is shown to be in error. The transformation was placed at 837°C. by Voss on the basis of retardations observed in alloys of 60, 55 and 50 per cent nickel at 837° , 782° and 760°C. In the present study no transformation was found at these temperatures; instead, alloys of 43 to 60 per cent nickel showed a thermal change at 902°C. corresponding to the transformation of the Ni_3Sn_2 . Voss considered Ni_4Sn as forming at 855°C. from Ni_3Sn and the solid solution. Present thermal studies indicated that Ni_4Sn is formed at 1143°C. from Ni_3Sn and the liquid, and that it decomposes at 941°C. into Ni_3Sn and the solid solution, the latter being confirmed by the metallographic examination. It may be assumed, therefore, that Voss' 855°C. horizontal line represented the decomposition of Ni_4Sn and not Ni_3Sn .

Reference has been made to the solubility determinations of tin in nickel and the methods used by Guillet and Voss. Voss' solubility at the eutectic temperature is shown to be low, while Guillet's figure for room temperature corresponds to the value determined metallographically at 500°C. X-ray results indicate lower solubilities at the lower temperatures.

PART II. X-RAY STUDIES OF THE NICKEL-TIN SYSTEM

Crystal Structure of the Compounds

Preliminary to the X-ray investigation, samples of the compounds were carefully polished and examined under polarized light in order to determine whether or not any of the compounds had cubic structures. The evidence indicated that none of them had.

The possibility of developing single crystals of the compounds had been considered but was dropped because of the experimental difficulties involved. Therefore, the powder method only was used and the results carried out as far as was reasonably possible. Samples of the alloys prepared as previously indicated were pulverized in an agate mortar and

annealed in purified hydrogen at 700° C. for 24 hr. As it was desired to investigate the structures of the alloy compositions corresponding to Ni_3Sn_2 and Ni_4Sn at elevated temperatures, samples of these materials were sealed in thin-walled, evacuated quartz tubes. These were then heated for 2 hr., the Ni_4Sn at 1100° C. and the Ni_3Sn_2 at 1050° C. and quenched in ice water, the quartz tubes being broken when they reached the water.

A Siegbahn-Hadding gas tube with an iron target was used. The rod made of powdered compound, NaCl and Duco cement, was mounted in a Debye-Scherrer type of X-ray camera having a film diameter of 57.65 mm. The films were measured and the probable structures determined by use of the graphical charts developed by Hull and Davey. The possibility of tetragonal and hexagonal lattice was investigated.

Ni_3Sn_4 .—The powder diagram of this compound was unusually faint, even after relatively long exposures, and many lines could barely be distinguished. Attempts to fit the calculations to any of the simpler lattices were unsuccessful, and it is fairly certain that the structure was not hexagonal nor tetragonal. The faintness of the lines points toward the presence of a structure of low symmetry. The density of the compound is 8.78.

Ni_3Sn_2 below 902° C.—Calculations of the powder diagram indicated that the structure of the material that Oftedal had considered to be NiSn and that of Ni_3Sn_2 are identical. The structure of NiSn had been found by him to be hexagonal, of the nickel-arsenide type with $a = 4.081\text{\AA}$, $c = 5.174\text{\AA}$, $c/a = 1.268$; and assuming two molecules to the unit cell, Oftedal had calculated a probable density of 7.915. The present metallographic studies proved that NiSn does not exist. Carrying out the calculations for the structure of Ni_3Sn_2 , the results of the present investigation are found to be: $a = 4.092\text{\AA}$, $c = 5.186\text{\AA}$, $c/a = 1.267$, with a probable accuracy of 0.005 \AA . Assuming four atoms per unit cell, the probable density is 7.25. However, actual experimental determination of the density of Ni_3Sn_2 shows it to be 8.99, thus verifying indications during the melting that the compound was heavy. The density calculated from the lattice dimensions, assuming one molecule Ni_3Sn_2 per unit cell, gives a density of 9.07.

The assumption that a unit cell of a material having the nickel-arsenide structure should contain five atoms does not agree with work reported on such compounds as Fe_3Sb_2 , Mn_3Sb_2 and others having that structure. Oftedal determined the lattice parameters of Fe_3Sb_2 and reported³ the values $a = 4.122\text{\AA}$, $c = 5.163\text{\AA}$, $c/a = 1.252$. He assumed that the unit cells contained four atoms in an average molecular configuration of $\text{Fe}_{1.2}\text{Sb}_{0.8}$, and on that basis calculated a probable density of 7.11. However, no experimental determination was made of the density. Since the ratios of the atomic radii, as found by Gold-

schmidt, of Fe/Mn and Sb/Sn in the nonionic condition are the same, it may be assumed that Ni_3Sn_2 and Fe_3Sb_2 would have the same structure and the empirical formula of $\text{Fe}_{1.2}\text{Sb}_{0.8}$ may be open to question. The lattice parameters are very similar and the observed intensities of the lines were in fair agreement. Table 3 gives the values used in making the computations.

TABLE 3.—X-ray Data for Ni_3Sn_2 at Room Temperature

Observed Intensity	Double Line Displacement		Double Angular Displacement, 2θ	NaCl	2θ Correction	$\sin^2 \theta$	n	Calculated $\sin^2 \theta$
	Mm	Minus 0.15 Mm ^a						
2	3 58	3 43	34 09	200 α	34 84	0 08963	β 101	0 08980
4	3 96	3 81	37.87		38 63	0 1094	101	0.1092
1	4.12	3 97	39.46		40 20			
4	5.06	4.91	48.79		49.57	0.1757	β 102	0.1755
4	5.19	5.04	50.09		50.86	0.1846	β 110	0 1838
10	5 61	5 46	54.27		55 06	0.2136	102	0 2135
10	5.75	5 60	55.66	220 α	56.45	0.2237	110	0.2234
1	5.92	5.77	57.34		58.16			
3	7.15	7.00	69.57		70.41	0.3323	201	0.3326
7	7.51	7.36	73.15		74.99	0.3621	112	0 3624
6	7 80	7.65	76.03		76.86	0 3863	103	0.3863
9	8.39	8.24	91.90		82.74	0.4368	202	0.4368
2	9.61	9.46	94.02	420 α	94.88	0.5425	212	0.5430
6	9.77	9.62	95.61		96.47	0.5562	004	0.5562
3	10.16	10.01	99 49		100.42			
5	10.40	10.25	101.87		102 74	0.6103	203	0.6106
4	10.77	10.62	105.55		106.43	0.6414	β 114	0.6406
10	10 99	10.84	107.73		108.61	0.6596	212	0.6602
7	11 10	10.95	108.83	422 α	109.72	0.6687	300	0.6700
1	11.60	11 45	113 80		114.66			
10	12.54	12.39	123.13		124 04	0.7799	114	0.7796
3	13.32	13.17	130 13		131.79	0.8332	213	0.8340

$$\sin^2 \theta = 0.07445(h^2 + k^2 + hk) + 0.03476(l^2)$$

$$a = 4.092\text{\AA}, c = 5.186\text{\AA}, c/a = 1.267.$$

Density is 8.99, and number of molecules per unit cell is 0.99.

The structure appears to be a modification of the NiAs type.

^a Divergence correction.

Ni_3Sn_2 above 902° C.—The powder diagram indicated the presence of a body-centered tetragonal structure containing 10 molecules per unit cell. The parameters were calculated to be: $a = 9.199\text{\AA}$, $c = 8.578\text{\AA}$, $c/a = 0.933$, with a probable accuracy of 0.005\AA . The density of the material is 9.36.

Attention is called to the agreement between this compound and the theory of Hume-Rothery on the formation of intermetallic compounds.

According to that theory, one of the factors affecting the structure and composition of intermetallic compounds is the ratio of the free valence electrons to the number of atoms per molecule. This rule has been substantiated by numerous compounds, including several with a ratio of 1.62. These include Cu_9Al_4 , $\text{Cu}_{31}\text{Sn}_8$, Cu_5Zn_8 , $\text{Fe}_3\text{Zn}_{10}$, and many others, all of which have a cubic structure containing 52 or $8 \times 52 = 416$ atoms per unit cell. The compound Ni_3Sn_2 , on the other hand, has eight free valence electrons and five atoms to give a ratio of 1.60. The probable structure was seen to be tetragonal with an axial ratio close to unity and containing 50 atoms per unit cell. The measurements and figures used in the computations are shown in Table 4.

TABLE 4.—*X-ray Data for Ni_3Sn_2 Quenched from 1050° C.*

Observed Intensity	Double Line Displacement		Double Angular Displacement, 2θ	NaCl	2θ Correction	$\sin^2 \theta$	n	Calculated $\sin^2 \theta$
	Mm.	Minus 0.15 Mm.						
1	3 54	3 39	33.69	200 α	34.58	0.08833	220	0.08840
3	3 95	3 80	37.77		38.67	0.1096	130	0.1105
1	4.12	3.97	39.46		40.20			
2	4.47	4.32	42.92		43.82	0.1392	222	0.1392
1	5 05	4.90	48.68		49.58	0.1758	400	0.1763
1	5.17	5.02	49.49		50.39	0.1812	β 240	0.1815
10	5.61	5.46	54.07	220 α	55.97	0.2130	303	0.2138
10	5.70	5.55	55.16		56.06	0.2209	240	0.2210
2	5 87	5.72	56.85		57.75	0.2332	421	0.2337
1	5 91	5.76	57.25		58.16			
3	6 78	6.63	65.90		66.80	0.3030	304	0.3028
4	7.08	6.93	68.89		69.79	0.3281	432	0.3271
6	7.50	7.35	73.05	400 α	73.95	0.3618	205	0.3620
3	7.81	7.66	76.13		77.03	0.3878	531	0.3884
6	8 36	8.21	81.60		82.50	0.4347	523	0.4348
1	8 80	8.65	85.97		86.84			
1	9.54	9.37	93.31		94.21	0.5367	β 731	0.5368
1	9.67	9.52	94.62		95.52	0.5481	β 713	0.5477
1	9.77	9.62	95.61	422 α	96.51	0.5567	623	0.5564
2	10.75	10.60	105.35		106.25	0.6399	β 644	0.6390
7	10.91	10.76	106.94		107.84	0.6532	731	0.6536
3	11 06	10.91	108.43		109.33	0.6656	713	0.6669
1	11 60	11.45	113.80		114.66			
10	12.52	12.37	122.94		123.84	0.7784	644	0.7780

$$\sin^2 \theta = 0.01105(h^2 + k^2) + 0.01271(l^2)$$

$$a = 9.199\text{\AA}, c = 8.578\text{\AA}, c/a = 0.933.$$

Density = 9.36, and number of molecules per unit cell is 9.92.

The structure as calculated is tetragonal.

Ni_3Sn .—The structure of Ni_3Sn could not be determined. Although several possible structures were found, which contained close to an integral

number of molecules, attempts to compute values of $\sin^2 \theta$ showed very great differences between computed values and those resulting from measurement of the film. The density of Ni_3Sn was found to be 9.62.

Ni_4Sn .—The probable structure of this compound was found to be tetragonal, with two molecules per unit cell. The parameters are: $a = 5.111\text{\AA}$, $c = 4.881\text{\AA}$, $c/a = 0.955$. The accuracy of this determination is somewhat less than in the two former calculations, one line, that of (322), being considerably in error. The density of the compound is 9.15. Table 5 shows the values used in making the calculation for Ni_4Sn .

TABLE 5.—X-ray Data for Ni_4Sn

Observed Intensity	Double Line Displacement		Double Angular Displacement, 2θ	NaCl	2θ Correction	$\sin^2 \theta$	n	Calculated $\sin^2 \theta$
	Mm.	Minus 0.15 Mm.						
1	3 74	3 59	35.68	200 β	36 32			
3	4 13	3 98	39.56	200 α	40.20			
1	4.78	4 63	46 00		46 70	0 1571	002	0 1570
3	5 10	4 95	49.19		49.93	0.1782	120	0 1789
3	5 26	5.11	50 79		51.53	0.1890	β 112	0.1877
4	5.66	5.51	54.76		55.54	0.2171	121	0.2182
9	5.82	5.67	56.35		57.14	0.2287	112	0.2286
2	5.92	5.77	57 35	220 α	58 16			
7	6 59	6.44	64.01		64 85	0 2876	220	0.2862
1	6.98	6.83	67.89		68.76	0.3189	β 103	0.3187
1	7.41	7.26	72.16	222 α	73 06			
6	7.81	7.66	76.13		77.07	0.3881	103	0.3880
3	8.80	8 65	85.97		86 98	0 4737	β 400	0.4702
10	9.95	9 80	97.40		98.50	0.5739	400	0.5725
3	10.14	9.99	99.28	420 α	100.42			
10	10.83	10 68	106.14		107.31	0.6488	411	0.6475
9	11.64	11.49	114.11		115 43	0.7147	420	0.7156
7	12.15	12.00	119.26		120.53	0 7540	421	0.7549
6	12.32	12.17	120.96		122.23	0.7666	412	0.7653
10	12 70	12.55	124 73		126.03	0.7941	332	0.8010

$$\sin^2 \theta = 0.03578(h^2 + k^2) + 0.03925(l^2)$$

$$a = 5.111\text{\AA}, c = 4.881\text{\AA}, c/a = 0.955.$$

Density is 9.15 and number of molecules per unit cell is 2.01.

Structure as calculated is tetragonal.

Solubility of Tin in Nickel

Filings of the 82, 84, 88, 92 and 94 per cent nickel alloys were sealed under vacuum in quartz tubes, and heated for 2 hr. at 1000°C . The tubes were quenched in ice water, the tubes being broken as soon as they reached the water.

Eight portions of filings from the 75 per cent nickel alloy were sealed as before in quartz tubes, and the tubes heated to temperatures of 1100°, 1085°, 1040°, 1000°, 900°, 800°, 700°, 600° and 450° C. The lengths of time for annealing at the various temperatures, which are much the same as those used by Fetz and Jette, are listed in Table 6. After completion of the annealing treatment, the tubes were quenched and broken as described above.

TABLE 6.—*Solubility of Tin in Nickel as Determined by X-rays*

Temperature, Deg. C.	Time at Temperature, Hr.	α , Å.	Atomic Per Cent Sn	Weight Per Cent Sn
SOLID SOLUBILITY AS DETERMINED BY FETZ AND JETTE				
1102	1	3.6084	10.80	19.8
1008	1	3.6025	10.13	18.6
1000	1	3.6028	10.15	18.6
962	1	3.6006	9.90	18.2
910	1	3.5971	9.51	17.5
865	1	3.5911	8.81	16.4
740	4	3.5622	5.45	10.5
707	4	3.5558	4.72	9.1
600	65	3.5322	1.93	3.8
557	120	3.5289	1.60	3.1
506	700	3.5237	0.98	2.0
SOLID SOLUBILITY AS DETERMINED BY PRESENT INVESTIGATION				
1100	2	3.6033		18.4
1085	2	3.6033		18.4
1040	2	3.6020		18.3
1000	2	3.5987		17.7
900	2	3.5844		14.8
800	4	3.5699		12.1
700	9	3.5499		9.3
600	72	3.5347		4.8
450	700	3.5222		1.6

The investigation was carried out with two back-reflection cameras having a 6-in. film diameter. The X-ray beam entered through a slit system, which projected radially through the circumference of the camera. Brass slits were used with a spacing of 0.015 in. The powdered sample was placed on a plane surface located tangentially to the circumference of the camera, and diametrically across and perpendicular to the slit system. The sample was rotated during the exposure, in order to insure a more uniform set of lines on the film. A Siegbahn-Hadding gas tube with a copper target was used.

The plane surface upon which the powdered samples were mounted was that of a carefully polished and etched piece of nickel that had been

annealed in purified hydrogen. It had been etched deeply enough to remove all evidence of cold-work. A thin film of oil was spread over the nickel and the powdered sample sprinkled on this. The excess powder was shaken off, leaving a thin uniform layer of the sample on a backing of pure nickel. The result on the X-ray film was the presence of lines from both the sample and the nickel with almost equal intensities. The lines from the nickel were used in correcting the calculations of the parameters of the face-centered cubic solid solution.

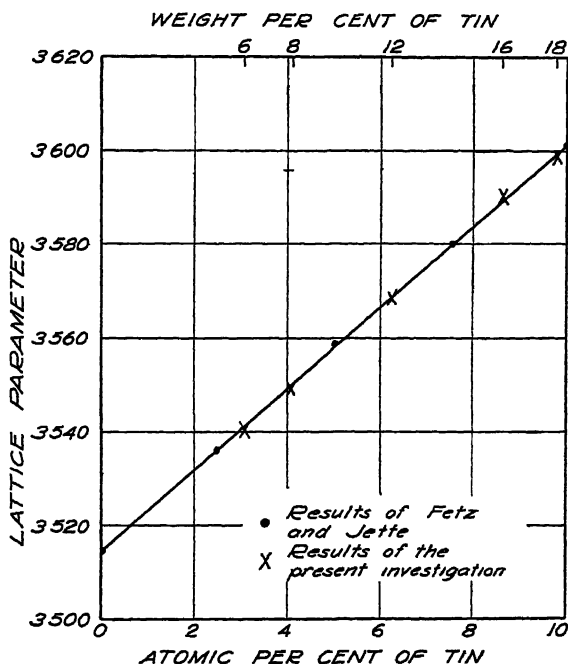


FIG. 22.—EFFECT OF TIN UPON LATTICE PARAMETER OF SOLID SOLUTION.

Measurements were made on lines reflected from the (331) and (420) planes of both the nickel and the samples. The values for the wave lengths of the copper radiation used are: 1.5412 and 1.5373 Å.

Table 6 contains the solubility data of Fetzer and Jette and the present investigation. Fig. 22 represents the effect of the solution of tin upon the lattice parameter, and Fig. 23 reproduces the solubility of tin in nickel. The data plotted in Fig. 23 indicate a good agreement between the present X-ray and metallographic results, on the solubility of tin in nickel. The agreement is most marked above 600° C., while below that temperature the X-ray results show a smaller solubility.

The difference can be explained to some extent by the fact that the rate of diffusion of metals at the lower temperatures may be very slow, and with the slow diffusion there is much less chance that the precipitating

phase will agglomerate in particles large enough to be resolvable under a microscope. The metallographic method, therefore, for these lower temperatures, should indicate higher solubility than the X-ray method, as the X-ray determination is not affected by the particle size of the second phase. A close agreement exists between the results of Fetz and Jette and those of the present investigation in regard to the effect of tin upon

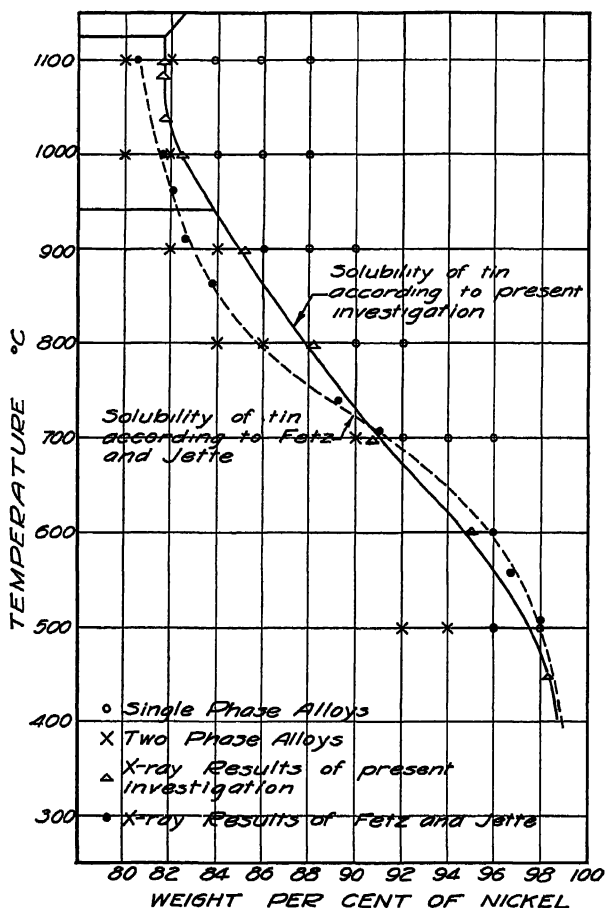


FIG. 23.—SOLUBILITY OF TIN IN NICKEL.

the lattice dimensions of the solid solution. The preparation of the alloys and the procedure in the two experiments had been the same. The agreement on the solubility boundary, as shown in Fig. 23, was not as good as that obtained in the effect of tin on the lattice parameter.

Since the results of the two determinations agreed so well on the effect of tin on the lattice parameter, it would have been expected that the results on the solubility would show better agreement. In so far as pos-

sible, the methods followed in the two determinations were the same, the only differences being that in the present one larger heats were made, and the powders were heated for slightly longer periods of time at the higher temperatures. The matter is further complicated in that the results given by Fetz and Jette are not uniformly higher or lower over the range 1100° to 500° C. than those obtained by the present investigators.

In the results of the present investigation the solid solubilities as determined by the X-ray and metallographic methods are in agreement between 1100° and 600° C. This confirmation of X-ray results by metallographic means gives the authors confidence in the accuracy of the determinations. Further experimentation, however, is considered necessary to determine the cause of the difference between these results and those of Fetz and Jette.

ACKNOWLEDGMENTS

The authors desire to express their appreciation to the International Nickel Co. and the International Tin Research and Development Council, which kindly furnished the nickel and tin used in this investigation.

REFERENCES

1. E. Vigoroux: *Compt. rend.* (1907) **144**, 712.
2. L. Guillet: *Rev. de Métallurgie* (1907) **4**, 531.
3. G. Voss: *Ztsch. anorg. Chem.* (1908) **57**, 34.
4. I. Oftedal: *Ztsch. phys. Chem.* (1928) **132**, 208.
5. D. Hanson, E. J. Sandford and H. Stevens: *Jnl. Inst. Metals* (1934) **55**, 115.
6. E. Fetz and E. R. Jette: *Metallwirtschaft* (1935) **14**, 165.
7. E. S. Rowland and C. Upthegrove: *Trans. A.I.M.E.* (1935) **117**, 190.
8. I. Oftedal: *Ztsch. phys. Chem.* (1927) **128**, 135; *idem* (1929) **4B**, 67.

DISCUSSION

(Lyall Zickrick presiding)

E. R. JETTE* AND E. FETZ,† New York, N. Y. (written discussion).—The nickel-tin system is one on which we have made extensive investigations and have already published one article on the solubility of tin in nickel,⁶ which was referred to by the authors, and a very recent preliminary note on the phase relationships.⁹ Our results differ in a number of important aspects from those reported in the article under discussion. Thirty years ago the two independent investigations of Voss and Guillet yielded widely different results; the comparison of the two new investigations again leaves us in a similarly confused state. While Voss and Guillet used essentially the same experimental methods, the two new investigations were made with quite different methods. Mikulas and his co-workers used the conventional methods of thermal analysis and microscopic examination combined with some X-ray determinations for checking the solubility of tin in nickel and the existence of certain phases where the other methods had indicated their possible presence. In our work only X-ray methods were used.

* Associate Professor of Metallurgy, School of Mines, Columbia University.

† Columbia University.

⁹ E. Fetz and E. R. Jette: *Jnl. Chem. Physics* (1936) **4**, 537.

In comparison with the method of thermal analysis the main disadvantage of the X-ray method is that, in general, the X-ray examination must be done at room temperature. Therefore, if a phase that exists only at high temperatures transforms very rapidly, the X-ray examination will give no indication of its existence except in special cases, which need not be entered into at this time. It should be emphasized that there is no conflict between the thermal analysis and X-ray methods on this point and there can be none until X-ray methods have been developed for working at higher temperatures than is possible today. Little work of any kind and no precision X-ray determinations have been performed at temperatures over 600° C. It should also be observed that small amounts of a phase in a mixture cannot be detected.

Both microscopic and X-ray work may suffer from inadequate technique in the preparation of the sample. One of the writers¹⁰ has already discussed this matter for X-ray work and similar considerations apply to samples for microscopic examination. Annealing times long enough (perhaps several months) to obtain equilibrium, and quenching rates sufficiently rapid to retain the high-temperature situation are absolutely essential for either method. The use of powders in X-ray work makes it possible to secure quenching rates far greater than on the comparatively massive samples used in microscopic investigation.

The main advantages of the X-ray method are due primarily to the extreme care that *must* be used in the preparation of the sample. The character of the diffraction lines (their sharpness, etc.) generally gives unmistakable indications of the degree to which equilibrium conditions have been obtained during heat-treatment and retained during quenching. In addition, the marked differences in the diffraction patterns give evidence of the existence of solid phases which in definiteness is unequaled by any other method.

Needless to say, the full advantages of any method and the minimizing of its disadvantages are secured only when it is properly applied. Each method, however, has its own characteristic ways of checking its own results. While metallographers are generally familiar with these checks as far as thermal analysis and microscopic examination are concerned, a word here as to the methods used in X-ray investigations may be appropriate.

When an investigator relies upon X-ray methods for determining an equilibrium diagram for the solid state, three conditions must be fulfilled:

1. There must be a complete series of films showing in consecutive order with composition the diffraction lines of the several phases. If the order of phases is A, A + B, B, B + C, C, etc., there must be a film for each of these phase regions. The only generally permissible exception is when one of the phases (e.g., B) has such a narrow homogeneity range that it is difficult to secure an alloy of that precise composition. In this case, the film sequence corresponding to A, A + B, B + C, C, etc., would be accepted without question. As a check on this, the positions of the diffraction lines from phase B must be identical in the A + B and B + C regions.

2. In two-phase regions (in binary system) there must be a systematic change in the relative intensities of the diffraction lines of the two phases corresponding to the change in the relative amounts of these phases.

3. In determining homogeneity ranges the diffraction lines of the phase-changing composition (in some cases, two phases) with temperature must be sharp and/or independent of annealing time. In careful work both conditions are generally satisfied. Lack of sharpness indicates change of composition during quenching or failure to anneal for sufficient time to establish equilibrium. In some cases it may be impossible to eliminate such effects and it is then incumbent upon the investigator to state

¹⁰ E. R. Jette et al.: *Trans. A.I.M.E.* (1936) 111, 372.

E. R. Jette and F. Foote: *Jnl. Chem. Physics* (1935) 3, 605.

either that the lines were not sharp or to give some other information that the results are open to question.

Experience has shown (for example, see the many reports from Westgren's laboratory in Stockholm) that, when these conditions are fulfilled and the limitations of the method duly recognized, the phase relationships in the solid state disclosed by X-ray investigations are usually more nearly correct than those indicated by the commoner methods of physical metallurgy. The inherent difficulties of the latter methods seem more troublesome to overcome than those of the X-ray method.

The conditions outlined above were fulfilled, except in one very narrow region, in our X-ray investigation. The conclusions reported in our preliminary note on the phase relationships thus had a sound experimental basis. Mikulas did not attempt to make a complete X-ray investigation and hence did not fulfill these conditions. He relied mostly on other types of methods.

For purposes of comparison, we quote the conclusions in the preliminary note mentioned above:

"1. The investigation of the Ni-Sn system has been extended beyond the solubility limit of Sn in Ni already reported by the authors.

"2. The next phase to the nickel solid solution phase occurs at the composition Ni_3Sn . This phase has a very narrow composition range.

"3. The Ni_3Sn phase is in equilibrium with a phase having a typical nickel arsenide structure between approximately 25.0 and 37.5 atomic per cent tin.

"4. The nickel arsenide structure first appears alone at about 37.5 atomic per cent Sn but extends as a homogeneous phase only up to 45 atomic per cent Sn. It thus requires excess nickel atoms to stabilize the lattice.

"5. At 40 atomic per cent Sn or the composition Ni_2Sn_3 , a new phase forms from the nickel arsenide-like phase at temperatures below 500°C . Its diffraction pattern appears to be closely related to the nickel arsenide structure and it may be a deformed modification. The range of homogeneity must be quite small since it is not found at 38.0 nor at 42.5 atomic per cent Sn.

"6. The homogeneity range of the NiAs structure is independent of temperature on the high-tin side but increases slightly at higher temperatures on the high-nickel side.

"7. In the remainder of the system there are three new phases provisionally called eta, theta and zeta. The first two have very narrow homogeneity ranges at approximately 51 and 54 atomic per cent Sn, respectively. The eta phase forms by a peritectoid reaction between the NiAs structure and theta. The zeta phase extends between approximately 56 and 62 atomic per cent Sn although this range may possibly be more complicated.

"8. The zeta phase coexists with the tin phase from 62 per cent up to practically 100 per cent Sn. The diffraction patterns indicate that the solubility of nickel in tin is very low."

The two investigations agree: (1) on the existence of a phase at or near the composition Ni_3Sn_4 which was previously unknown, (2) on the existence of Ni_3Sn , (3) that the NiAs structure does not occur at the composition NiSn , (4) on the variations of the lattice constant of the nickel-rich phase with tin content and (5) to a limited extent on the position of the solubility curve for tin in nickel. We have not been able to find the high-temperature tetragonal modifications of Ni_3Sn_2 but it may be mentioned in passing that if a transformation at 906°C . exists, their diagram needs correction in the region labeled liquid + Ni_3Sn_2 .

The authors raise the question of the reason for the difference between their solubility curve and the one given in our earlier publication. It may be of interest to compare solubility curves from a somewhat uncommon point of view. The excellent agreement between the two sets of results on the effect of tin on the lattice constant of nickel fortunately enables us to discuss the differences on the basis of sample prepara-

tion. In this case, the predominating factor is the quenching rate, and it should be pointed out at once that this factor is of even greater importance in the preparation of samples for microscopic examination. It may be stated with a great deal of assurance that the rate of cooling of a solid block of alloy is less than that of a fine powder (through 100 or 200 mesh) quenched by our method. The confirmation of a solubility curve obtained from X-ray studies by means of microscopic examination is therefore not necessarily evidence of correctness in either determination.

In our quenching method for powders, the quartz sample tube is torn loose from the wire suspending it in a vertical furnace by a heavy plunger, which crushes the tube under water automatically on the instant of immersion. As far as can be determined, Mikulas pulled the sample tube from the furnace, thrust it into ice water and then crushed it. Such a series of operations may easily consume several seconds, and furthermore, this time is not uniform in different quenchings. We have mentioned in an earlier article⁶ an experiment in which a quartz sample tube being quenched from 1060° C. failed to break. Experience in this laboratory has been that under such conditions the glow in the tube disappears within about five seconds, depending somewhat upon the original temperature and the wall thickness and diameter of the tube. This means that the sample was over 700° C. within that time. Obviously accurate estimates of such times is impossible. The lines obtained were still fairly sharp but the lattice constant indicated a solubility corresponding to a temperature approximately 100° C. below that of the furnace.

Comparing the two solubility curves shows that the agreement at 600° and 700° is very good. At 450° a recently finished determination on a sample that had been annealed over 10,000 hr. is appreciably less than that given by Mikulas.

Above 700° C. the two curves deviate considerably. Ordinarily such curves are compared by taking the differences in composition at selected temperatures. In view of the importance of quenching rates, the proper way to compare these results here is in terms of temperature differences. Thus, instead of stating that Mikulas obtained solubilities in the range 800° to 1100° C. from 1 to 2 per cent (by weight) lower than ours, it is more correct to say that his solubility curve lies from 50° to 100° higher than ours. We believe that our solubility curve is essentially correct, especially since two new results at 900° and 1100° C. were in excellent agreement with the curve. We believe, therefore, that we are justified in interpreting the authors' results in the following way: The actual solubility values in the range 800° to 1100° C. correspond to temperatures 50° to 100° C. lower than the furnace temperature. On this basis the five solubility values at 900° and over average close to 90° below the furnace temperature. Finally, it may be noted that the general form of the Mikulas curve is very much influenced by the two points at 800° and 900° C.

The other differences between the results of the two investigations are important but the full treatment of them is beyond the scope of the present discussion. A critical review will be included in our final publications on this system.

W. MIKULAS.—It was not our purpose to perform a complete X-ray investigation of the nickel-tin system. We conducted our research with the usual thermal and metallographic methods, then used the X-rays to further define certain points. We feel that the tone of the discussion by Dr. Jette and Dr. Fetz is to the effect that in determining equilibrium conditions it is necessary to carry out an investigation such as they describe. This may well be true when the only purpose of the work is to determine the nature of the phases occurring at, or slightly above, room temperature. In our work we felt justified in using thermal and metallographic methods, since we were interested in the liquidus, solidus, and phase changes occurring at elevated temperatures, as well as the conditions at room temperatures. We intended to locate the single-phase areas by means of the microscope and then investigate their structures by means of X-rays.

That the X-ray method can have certain advantages is shown by the fact that in the area where the present authors found Ni_3Sn_4 , Dr. Fetz reports the presence of three phases, eta, theta and zeta, which have not as yet been defined. The advantage, however, is not due to the greater accuracy of the method so much as to the mechanical difficulty found in preparing the metallographic specimens. On the other hand, the authors, by means of thermal and metallographic methods, were able to show the existence of the compound Ni_4Sn and the transformation of Ni_3Sn_2 . These points had escaped Dr. Jette and Dr. Fetz.

Our method of representing the transformation of Ni_3Sn_2 at 902°C. was occasioned by an adherence to the phase rule. Since we could not, as the result of our investigation, indicate the compound Ni_3Sn_2 by any other means than a vertical line, it became impossible to continue the horizontal line at 902°C. into the area marked $\text{Ni}_3\text{Sn}_2 + L$.

The differences in the X-ray determinations of the solid solubility of tin in nickel appear still to be open to question. Although no mechanical devices were used in our work, the manual operation was synchronized to effect as rapid a quench as possible. In every test the quartz tube was shattered as it entered the water. The heat content of the quartz tube should have been ample protection to keep the metal powder from cooling during the small interval of time required for quenching. Jette and Fetz point out that when one of the tubes was not broken the result indicated a drop in temperature of 100°C. before the quench was effective. This would indicate that a solubility difference interpreted as a 90°C. difference in temperature must be explained on a different basis.

C. UPTHEGROVE.—There is just one point I should like to make. We have no quarrel in any sense with the use of the X-ray, because we would like to take advantage of that in every way possible. On the other hand, I do not believe that everybody is so fully convinced of the infallibility of the X-ray. I believe Dr. Fetz is familiar with the report of the three X-ray investigations of the solubility of tin and copper, all made by X-ray, but not in agreement.

Aging Phenomena in a Silver-rich Copper Alloy*

By MORRIS COHEN, † JUNIOR MEMBER A.I.M.E.

(Cleveland Meeting, October, 1936)

It has been known for several years that in certain age-hardenable alloys precipitation of finely divided particles occurs simultaneously with the changes in physical properties; while, in other alloys, these changes take place prior to, or without any, precipitation. The silver-copper alloys are generally considered to be the classical example of the first group, and the aluminum-copper alloys (duralumin) are typical of the second group. The two types of aging are explained by the *precipitation theory* and the *knot theory* respectively.‡ It is well recognized now that these theories do not conflict with each other; the one used for a given aging system depends upon which way the alloy in question happens to age-harden.

However, previous work on the aluminum-copper alloys^{1,2} has shown that if the aging temperature is raised sufficiently the hardening will be accompanied by actual precipitation. In fact, it is quite probable that all of the so-called knot-hardening alloys will harden by precipitation at elevated temperatures. Therefore, a combination of the knot and precipitation theories is necessary to give a complete picture of the age-hardening of these alloys, and indicates that knot formation and precipitation are not independent processes.

To test the generality of this concept, it is necessary to show that the alloys that commonly harden by precipitation will harden prior to precipitation if the aging temperature is sufficiently lowered. For this reason, it would be well to carefully re-examine the aging characteristics of the silver-copper alloys at aging temperatures somewhat below those used by previous investigators. If hardening can be detected prior to precipitation in these alloys, it will lend great weight to the idea that knot forma-

* This work represents a portion of a thesis submitted in partial fulfillment of the requirements for the degree of Doctor of Science at the Massachusetts Institute of Technology, June, 1936. Manuscript received at the office of the Institute July 6, 1936.

† Instructor, Department of Mining and Metallurgy, Massachusetts Institute of Technology, Cambridge, Mass.

‡ For a full discussion of these theories, see P. D. Merica: The Age-hardening of Metals. *Trans. A.I.M.E.* (1932) 99, 13.

¹ References are at the end of the paper.

tion must precede precipitation and that they form two consecutive steps in a general mechanism of age-hardening.

To this end, the aging phenomena in a silver-copper alloy containing 8.72 per cent copper by weight were studied by means of hardness, X-ray, microscopic, electrical resistance, and dilatometric measurements. Aging temperatures between 100° and 200° C. were used.

PREVIOUS WORK

The silver-copper equilibrium diagram shows a simple eutectic system with limited solid solubility at either end. Both the eutectic temperature and the solid solubility of copper in silver have been carefully determined by previous workers. Roesser³ reports the eutectic temperature to be $779.4 \pm 0.1^\circ \text{C.}$, while the solid solubility curve has been checked by several independent investigators using the microscopic^{4,5}, electrical resistance⁵, and X-ray^{6,7} methods.

The curve shown in Fig. 1 is taken from the National Metals Handbook⁸ and is a compromise of the work of Stockdale⁵ and of Ageew and Sachs⁶. The maximum solubility at the eutectic temperature is 8.8 per cent copper by weight, and decreases to 0.1 per cent copper at room temperature.

The previous work on the aging of the silver-copper alloys indicates that the age-hardenability of these alloys is definitely due to precipitation.

Fraenkel and Schaller^{9,10} showed by means of electrical resistance measurements on an 8 per cent copper alloy that the changes in hardness, tensile strength, and ductility were caused by precipitation (of the copper-rich solid solution) at all the temperatures at which age-hardenability could be detected. These results were confirmed by Norbury¹¹ with microscopic and density studies on a 7.5 per cent alloy, by Haas and Uno^{12,13} with dilatometric studies on a series of alloys containing up to 13 per cent copper, and by Ageew, Hansen and Sachs¹⁴ with X-ray as well as electrical resistance studies on a series of alloys containing up to 7.5 per cent copper.

The latter work showed that when precipitation occurred the lattice parameter did not change progressively, as it would if the precipitation were gradual. Instead, the diffraction lines of the supersaturated solid solution remained fixed; but soon after the beginning of aging a new set of lines appeared, which corresponded to the lattice of the stable (completely decomposed) solid solution. As the precipitation continued, the position of the two sets of lines did not change, but the intensity of the lines of the

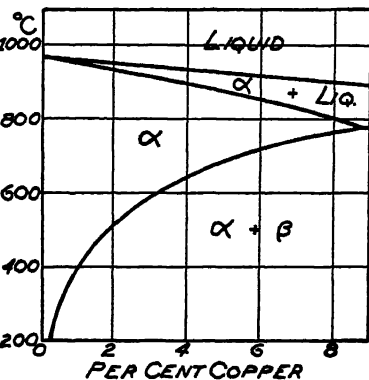


FIG. 1.—SOLID SOLUBILITY OF COPPER IN SILVER.

stable phase increased while that of the supersaturated phase decreased until the latter disappeared completely. The conclusion drawn from these results was that the precipitation does not take place gradually and uniformly, but suddenly goes to completion in localized areas. This was confirmed by Norbury's¹¹ photomicrographs, which indicated that the precipitation occurs at the grain boundaries first and then progresses inward toward the centers of the grains.

O'Neill, Farnham and Jackson¹⁵ found by means of X-rays that the age-hardening was accompanied by gradual precipitation, not the sudden localized type discussed in the preceding paper.

EXPERIMENTAL DETAILS

Preparation of the Alloys for Aging

The fine silver used in this investigation analyzed 99.98+ per cent silver, the total amount of impurities other than copper being 0.014 per cent. The copper used was of the oxygen-free high-conductivity variety and contained 99.985 per cent copper. The total impurities other than silver were about 0.013 per cent.

The alloys were prepared by melting down the necessary amounts of pure copper and silver in a graphite crucible under a cover of charcoal. The molten metal was bottom-poured under reducing conditions into a heavy iron mold. Chill casting was found desirable to prevent undue segregation. The ingots were then homogenized by cold-rolling to a 50 per cent reduction in area followed by an anneal at 750° C. for 160 hr. in a purified nitrogen atmosphere.

The alloys were analyzed for both copper and silver, and for all specimens the sum of the two was equal to 100 per cent within the experimental error. The composition of the ingot used in this work was 8.72 per cent copper and 91.28 per cent silver. The composition aimed at was 8.8 per cent copper, the maximum solid solubility at the eutectic temperature, in order to obtain the greatest degree of age-hardenability.

The ingot was then cut up into appropriate sizes for the aging studies. The specimens for the hardness, X-ray and microscopic investigations measured 1 by $\frac{1}{2}$ by $\frac{3}{16}$ in. The dilatometer specimens consisted of rods $\frac{1}{4}$ in. square and 4 in. long. The specimens for the electrical resistance measurements were in the form of wires, which were reduced from a portion of the ingot by means of rolling, swaging and drawing.

The solution heat-treatment prior to the aging was carried out in a purified nitrogen atmosphere, and consisted of a 2-hr. heating at $765^{\circ} \pm 2^{\circ}$ C. followed by water quenching. The grain size was sufficiently small to give consistent hardness readings. The oxidation of the specimens was negligible.

Aging of the Alloys

Aging experiments were performed at temperatures of 100°, 125°, 150°, 175° and 200° C. Hardness and X-ray measurements made on a quenched sample aged for several days at room temperature indicated no change. Therefore the aging at the higher temperatures could be interrupted, if necessary, by quenching in water and the measurements made at room temperature. The aging was carried out in boiling liquids. The required boiling points were obtained by the addition of the proper amount of carbital to water. By continuously returning the vapors with the aid of a reflux condenser, the temperature could be easily adjusted and maintained to within $\pm 0.5^\circ$ C. These boiling solutions were very satisfactory in that they did not attack the alloys, so that the specimens could be immersed directly without any protective covering. In this way, they could be brought up to temperature almost instantaneously, and so the actual time of aging at temperature was accurately known even though the aging had to be frequently interrupted for obtaining hardness, X-ray or microscopic data.

The hardness measurements were made with a Rockwell hardness tester using a load of 60 kg. and a $\frac{1}{16}$ -in. steel ball indenter (giving the so-called Rockwell F hardness). The impressions were large enough to give an average value over many grains, and yet were small enough so that all the hardness readings for a given run could be made on one surface of the same specimen. Thus the measurement of hardness was certainly a most satisfactory method for disclosing small changes in the physical properties of the alloy on aging.

The X-ray measurements were made at appropriate intervals on the reverse side of the same specimens that furnished the hardness data. These surfaces were polished through No. 00 emery prior to the solution heat-treatment, and thereafter were not polished or etched in any way, in order to eliminate the possibility of premature decomposition of the super-saturated solid solution at the surface. The lattice-parameter measurements were made with a back-reflection camera using copper radiation from a Hagg tube. Both the camera and X-ray tube, as well as the technique employed, are completely described elsewhere by Norton¹⁶. The experimental error was about $\pm 0.0002\text{\AA}$. for the sharp diffraction lines produced by the alloys when in the quenched condition and early stages of aging. This corresponds to a change of composition of approximately ± 0.03 per cent copper. However, in the later stages, when the lines become broader, the precision decreased correspondingly.

The samples for the microscopic investigation were given a metallographic polish and etch prior to the solution heat-treatment. The aging runs were made with duplicate samples; one was examined after definite intervals without further polishing or etching, while the other was lightly

polished and reetched each time for photographing. Although the former showed the general course of precipitation, it was not well defined, hence it was impossible to determine whether the light polishing and etching from time to time had any effect on the rate of precipitation on the surface. The chromic acid etching reagent recommended by Leach and Chatfield¹⁷ was found most satisfactory.

The wires for the electrical resistance measurements were wound into helical coils on a $\frac{1}{4}$ -in. mandril, and were heat-treated and aged in this form. The resistance measurements were made at the aging temperatures with a Leeds & Northrup Kelvin bridge having an accuracy of ± 0.1 per cent.

The dilatometer was built according to the specifications of the American Society for Testing Materials¹⁸. The dial gage, which directly indicated the changes in length of the specimen, could be read to $\pm \frac{1}{10}$ of a division or ± 0.00001 inch.

EXPERIMENTAL RESULTS

All of the following data were obtained on an alloy containing 8.72 per cent copper that was water-quenched from 765° C.

Hardness Results

Table 1 gives the Rockwell F hardness values obtained on specimens aged at 100°, 125°, 150°, 175° and 200° C. In order to represent all the values in a single graph without unduly suppressing the initial aging

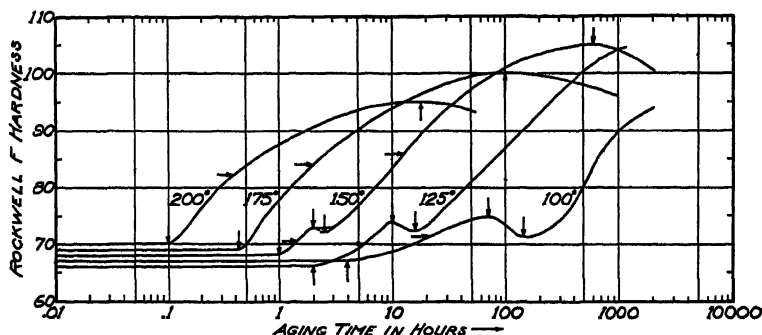


FIG. 2.—CHANGES IN HARDNESS DURING AGING.

effects, it was necessary to plot the aging time on a logarithmic scale. This permits a more exact determination of the beginning of hardening at all temperatures and yet shows the entire course of hardening in sufficient detail. Fig. 2 shows the hardness results at all five aging temperatures. The curves indicate a definite incubation period at all temperatures; that is, the hardness remains constant for a finite length of time after quenching. At 100° and 125° C., the hardness then rises in a normal fashion to a

TABLE 1.—*Hardness and X-ray Data on Aging Alloy*

Aging Time, Hr.	Rockwell F Hardness	Unstable Phase		Stable Phase	
		Appearance of X-ray Lines	Lattice Parameter	Appearance of X-ray Lines	Lattice Parameter
100° C.					
0	67	Sharp	4.0314	Diffuse lines faintly visible ^b	4.075-4.080
½	67				
1	67	Sharp	4.0313		
5	68	Sharp	4.0314		
21	71	Sharp	4.0314		
70	75	Sharp	4.0315		
100	73				
140	71	Sharp	4.0316		
288	74	Sharp	4.0319		
576	83	Sharp	4.0324		
624	85	Sharp	4.0326		
720	88	Sharp	4.0330		
864	89	Very slight broadening ^a	4.0334		
1008	90				
1440	92	As above ^a	4.0340		
2160	94	As above ^a	4.0348		
125° C.					
0	66	Sharp	4.0309	Diffuse lines faintly visible ^b	4.075-4.079
½	66				
1	66	Sharp	4.0308		
1.5	65				
2	67				
3	67				
5	69				
8	72				
10	74	Sharp	4.0308		
12	73				
16	72	Sharp	4.0311		
24	74	Sharp	4.0312		
36	79	Sharp	4.0313		
60	83	Very slight broadening ^a	4.0315		
108	88	As above ^a	4.0323		
156	91				
208	93	As above ^a	4.0328		
304	97	Slightly broader ^a	4.0336		
512	101	Broader ^a	4.035	Diffuse lines darker ^b	4.075-4.079

^a Doublet still resolved.^b Doublet not resolved.

TABLE 1.—(Continued)

Aging Time, Hr.	Rockwell F Hardness	Unstable Phase		Stable Phase	
		Appearance of X-ray Lines	Lattice Parameter	Appearance of X-ray Lines	Lattice Parameter
125° C. (continued)					
750	103	Very broad ^a	4.036	As above ^b	4.075-4.079
1000	104	Doublet barely resolved ^a	4.036	As above ^b	4.075-4.079
150° C.					
0	68	Sharp	4.0306	Diffuse lines faintly visible ^b Diffuse lines darker ^b As above ^b Diffuse lines still darker ^b As above ^b	4.074-4.079 4.074-4.079 4.074-4.079 4.074-4.079 4.074-4.079
½	68	Sharp	4.0305		
1	68	Sharp	4.0306		
2	73	Sharp	4.0305		
3	73	Sharp	4.0309		
4	75	Sharp	4.0309		
5	77	Very slight broadening ^a	4.0320		
6	78				
12	86				
26	92				
48	96				
100	101	As above ^a	4.0331		
		Broad ^a	4.0336		
144	102.5	Very broad ^a	4.034		
192	103	Very faint ^a	4.035		
288	104	Disappeared			
432	104.5	Disappeared			
576	105				
720	105				
912	104				
1200	102.5				
1920	101				
175° C.					
0	69	Sharp	4.0310		
5 min.	69	Sharp	4.0310		
10 min.	68	Sharp	4.0310		
15 min.	69				
30 min.	70				
42 min.	74				
1	78				
1.5	81				
2	83				
3	87	Very slight broadening ^a	4.0316		

^a Doublet still resolved.^b Doublet not resolved.

TABLE 1.—(Continued)

Aging Time, Hr	Rockwell F Hardness	Unstable Phase		Stable Phase	
		Appearance of X-ray Lines	Lattice Parameter	Appearance of X-ray Lines	Lattice Parameter
175° C (continued)					
6	92	As above ^a	4 0319		
12	95				
18	96	Broad ^a	4.0330	Diffuse lines faintly visible ^b	4.073-4.078
24	98	Broad ^a	4.033	Diffuse lines darker ^b	4.073-4.078
36	98 5	Broad and faint ^a	4.034	Diffuse lines darker ^b	4.073-4.078
60	99	Faint unresolved ^b	4.035	As above ^b	4.073-4.078
108	100	Disappeared		Diffuse lines very dark ^b	4.073-4.078
204	99	Disappeared		As above ^b	4.073-4.078
630	97	As above		As above ^b	4.073-4.078
1000	96	As above		As above ^b	4.073-4.078
200° C.					
0	69	Sharp	4 0311		
2 min.	70				
4 min.	70	Sharp	4 0310		
6 min.	70	Sharp	4.0310		
8 min.	72	Sharp	4.0312		
12 min.	76	Very slight broadening ^a	4.0313		
18 min.	79				
30 min.	84	Slightly broader ^a	4.0315		
1	88	As above ^a	4 0316		
2	91	Broader and fainter ^a	4 0318	Diffuse lines faintly visible ^b	4.073-4.077
4	93	Very broad and faint ^a	4.032	Diffuse lines darker ^b	4.073-4.077
6	94	Faint and unresolved ^b	4.032	As above ^b	4.073-4.077
10	94	As above ^b	4.033	As above ^b	4.073-4.077
18	95	Too faint to measure ^b		Diffuse lines very dark ^b	4.073-4.077
30	92	Disappeared		As above ^b	4.073-4.077
54	91	As above		As above ^b	4.073-4.077
100		As above		As above ^b	4.073-4.077
500		As above		Beginning of resolution ^a	4.076
1000		As above		Lines definitely resolved ^a	4 0757
2000		As above		Sharp ^a	4.0759

^a Doublet still resolved.^b Doublet not resolved.

low maximum with subsequent softening. This is not the usual overaging, because on continued aging the hardness finally increases again to a

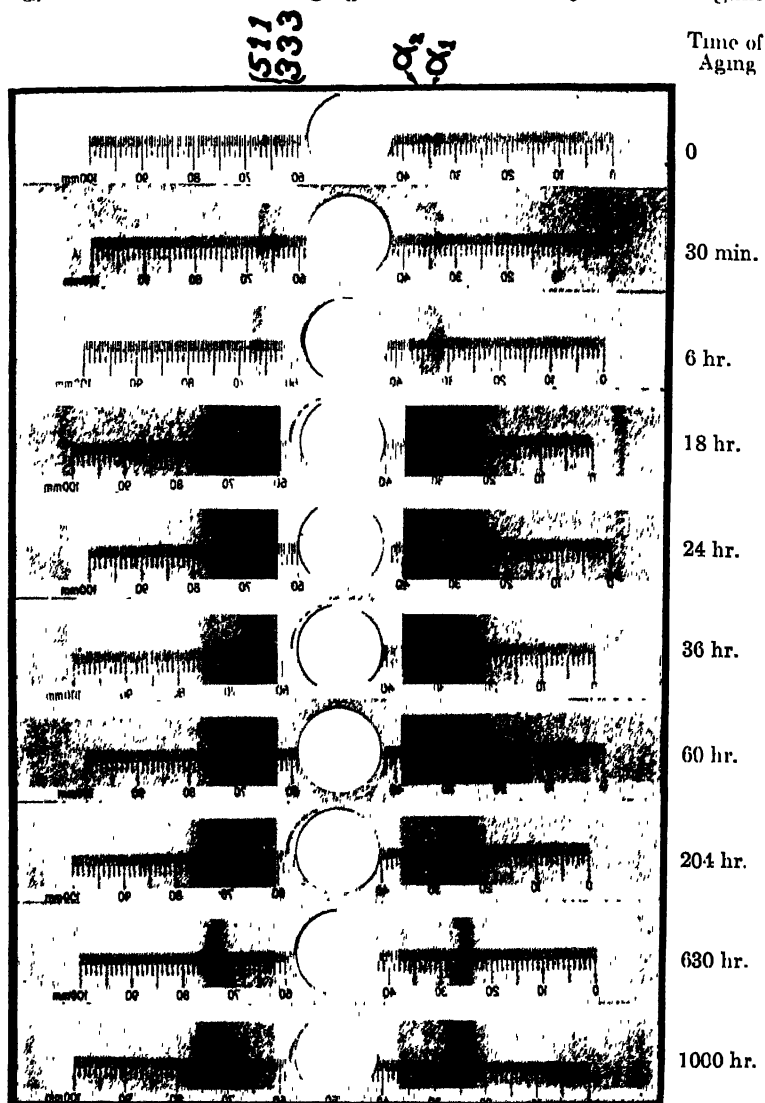


FIG. 3.—CHANGES IN DIFFRACTION PATTERN DURING AGING AT 175° C.

value far above the hardness at the initial peak.* At 150°, a positive primary peak was not detected, although the hardness curve flattens out

* The term *initial* or *primary* hardness peak will be used to distinguish it from the higher hardness maximum that just precedes overaging. The intermediate softening that follows the initial peak will be spoken of as the *hardness valley*, to distinguish it from the softening due to overaging

for an interval of 1 hr. at the end of 2 hr. of aging, after which the hardness continues to rise again. In view of the results at 100° and 125° , it is believed that a small primary peak does exist in the 150° aging curve, but not enough readings were made in this interval to detect it. The probable peak is shown in dotted lines. At 150° , the aging was prolonged sufficiently to attain maximum hardening with subsequent softening (actual overaging). At 175° and 200° , the aging curves are normal, each showing a single hardness maximum. The arrows on the curves indicate obvious stages in the hardening process, which will be referred to later.

X-ray Results

The X-ray data obtained on the aging alloys are given in Table 1. A typical set of diffraction patterns is shown in Fig. 3. At all aging temperatures, the first change to be noted is a gradual displacement of the

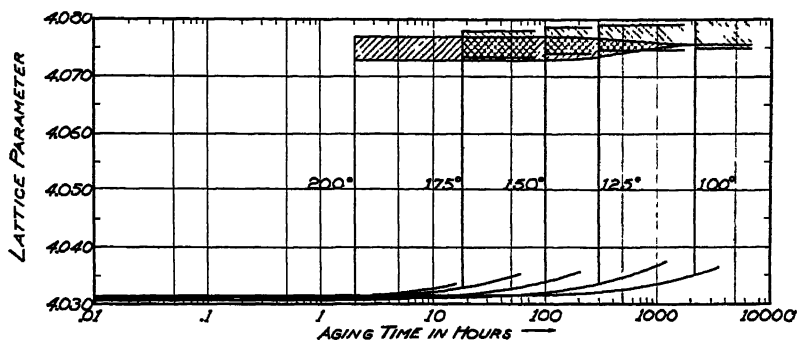


FIG. 4.—CHANGES IN LATTICE PARAMETER DURING AGING.

diffraction lines of the supersaturated solid solution, indicating that the initial precipitation is progressive. However, the precipitation does not progress uniformly to completion. While the lines of the supersaturated solid solution are shifting gradually, a new set of faint broad lines appears, which corresponds to the stable solid solution—that is, the silver-rich solid solution from which all the excess copper has precipitated. As the aging proceeds, the original lines continue to shift, but become fainter and broader. The new lines do not shift, but become relatively more intense. Finally, the original lines disappear.

These results are shown graphically in Fig. 4. The gradual changes in lattice parameter denote the initial general precipitation. The vertical lines indicate the first appearance of the stable-phase diffraction lines, and the shaded bands represent very roughly the lattice parameters corresponding to these broad lines. After prolonged aging at 200° , these lines finally sharpen and an accurate value of the lattice parameter of the stable solid solution can be determined. The mean lattice parameter is lower, the higher the aging temperature. This is because of the increase in the solid solubility of copper in silver with temperature.

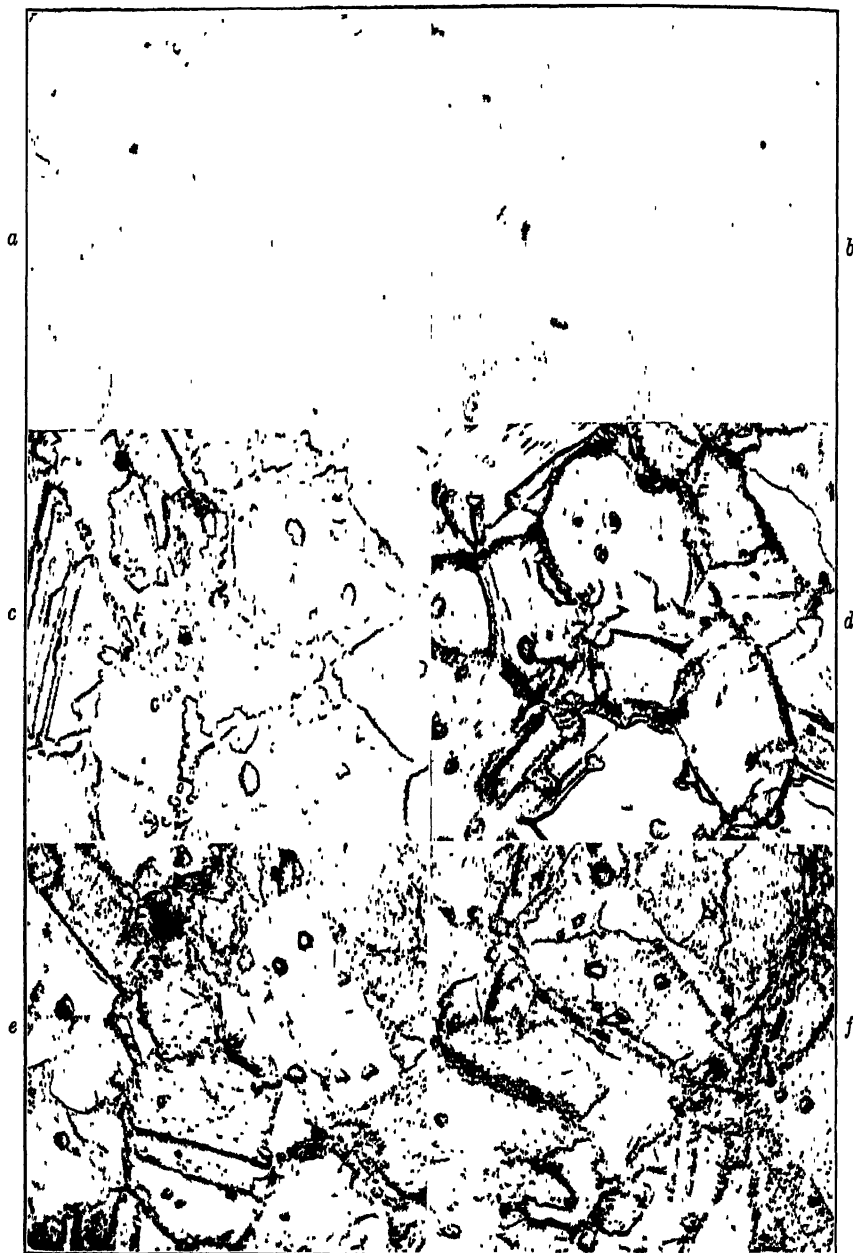


FIG. 5.—CHANGES IN MICROSTRUCTURE DURING AGING AT 200° C. $\times 500$. ETCHED WITH CHROMIC ACID.

a. As quenched.

b. Aged 4 hours.

c. Aged 12 hours.

d. Aged 18 hours.

e. Aged 24 hours.

f. Aged 48 hours.

Microscopic Results

The changes in microstructure were observed on aging at 150° and 200°. A representative series of photomicrographs is shown in Fig. 5. There is no visible change under the microscope that corresponds to the

TABLE 2.—*Electrical Resistance Data on Aging Alloy*

100° C		150° C.		200° C.	
Aging Time, Hr.	Per Cent of Initial Value	Aging Time, Hr.	Per Cent of Initial Value	Aging Time, Hr.	Per Cent of Initial Value
0	100 0	0	100 0	0	100 0
15 min.	100.0	5 min.	100.0	3 min.	100 0
30 min.	100.1	20 min.	100 2	5 min.	100 1
2	100 4	30 min.	100.3	8 min.	100 2
5	100 4	45 min.	100 3	10 min.	100 1
7	100 3	1	100 2	15 min.	99 9
12	100 3	2	100 0	20 min.	99.8
24	100.4	4	99 6	30 min.	99 4
36	100 5	6	99 3	1	98 4
48	100 6	9	98 9	2	97.6
60	100 6	25	97 8	4	95.7
80	100 4	48	97 1	6	94 4
100	100 2	74	96 2	12	91.2
150	99 9	92	96 1	24	88 3
168	99 8	141	94 8	36	87 3
216	99 6	212	94.0	62	86.5
264	99.4	260	93.1	80	86.1
300	99 2	300	92.7	90	86 0
				100	86 0

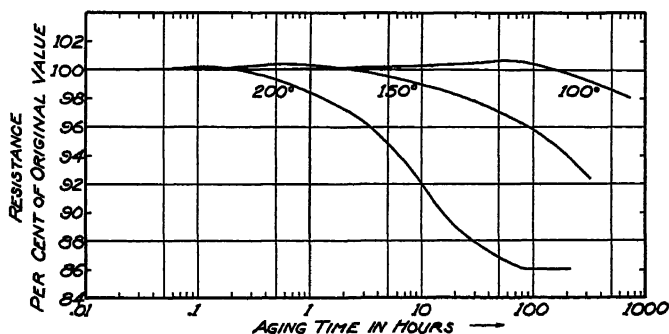


FIG. 6.—CHANGES IN ELECTRICAL RESISTANCE DURING AGING.

beginning of the gradual precipitation indicated by the X-ray. However, the microscope does show the sudden precipitation in the form of darkened areas at the grain boundaries and twinning planes. These areas grow until the precipitation is complete.

Electrical Resistance Results

The resistance measurements, made at 100°, 150° and 200° C., are tabulated in Table 2 and plotted in Fig. 6. The general trends of the

TABLE 3.—*Dilatometric Data on Aging Alloy*

150° C		200° C	
Aging Time, Hr.	Dilation in 4 In. 0.0001 In.	Aging Time, Hr.	Dilation in 4 In. 0.0001 In.
0	0	0	0
15 min.	0.1	6 min.	0
30 min.	0.7	10 min.	+ 0.1
1	0.7	20 min.	- 0.7
1.5	0.7	30 min.	- 1.3
2	0.6	45 min.	- 1.9
2.5	0.4	1	- 3.5
3	0.3	1.5	- 4.8
6	- 1.4	2.5	- 9.2
12	- 2.4	3	-11.1
24	- 4.3	3.5	-13.3
36	- 5.2	5.5	-19.4
48	- 6.4	6.5	-21.5
60	- 7.6	7	-23.6
72	- 7.5	12	-29.1
96	- 9.6	24	-32.5
125	-10.0	48	-32.5
170	-10.9	72	-32.5
211	-12.4		
255	-13.7		
300	-15.0		

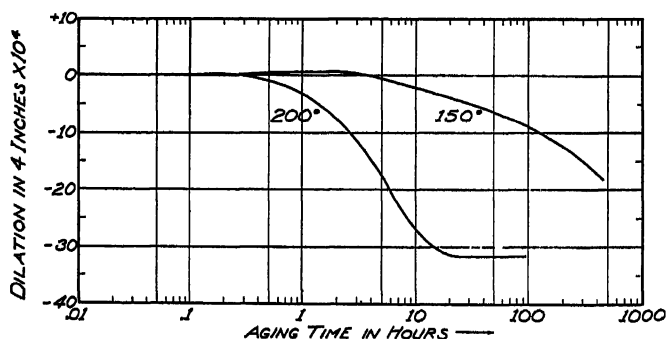


FIG. 7.—CHANGES IN LENGTH DURING AGING.

curves are the same at all the aging temperatures, in that the resistance first increases and then decreases. The initial increase evidently is due to changes going on within the supersaturated solid solution prior to pre-

cipitation while the subsequent decrease indicates the decomposition of the supersaturated solid solution and, hence, precipitation.

Dilatometric Results

The dilatometric data at 150° and 200°, given in Table 3 and plotted in Fig. 7, show the same trend as the electrical resistance values. The normal contraction that accompanies precipitation is preceded by a slight expansion. It is to be noted that in both sets of curves the magnitude of the abnormal reverse effect increases with decreasing aging temperature.

INTERPRETATION OF RESULTS

Pre-precipitation Behavior of the Alloy

From the hardness curves in Fig. 2, it is obvious that the simple precipitation theory might be adequate to explain the changes in hardness at 175° and 200° C., but it certainly cannot explain the small initial hardness peaks found at 100°, 125° and 150°.

In order to determine the mechanism of the aging process, it is first necessary to find out whether the beginning of hardening occurs prior

TABLE 4.—*Comparison of the Beginning of Hardening and of Precipitation*

Aging Temperature, Deg. C	Beginning of Hardening	Beginning of Precipitation
100	4 hr.	70-140 hr.
125	2 hr.	10- 16 hr.
150	1 hr.	2- 3 hr.
175	27 min.	15- 30 min.
200	6 min.	6- 8 min.

to, or simultaneously with, precipitation. This comparison is shown in Table 4. The times for the beginning of precipitation are taken from the X-ray results in Table 1. These values are preferred to those indicated by the electrical resistance and dilatometric measurements because the lattice-parameter values show no abnormal reverse effects prior to precipitation. Furthermore, the hardness and X-ray measurements were made simultaneously on the same specimens, so that a better correlation between the hardening and precipitation processes can be obtained if the X-ray results are used.

Table 4 shows that at 100°, 125° and 150°, the hardening definitely precedes precipitation; but at 175° and 200°, the hardening occurs simultaneously with precipitation. This points to the possibility of knot formation at the same temperatures at which the initial hardness peaks occur, and no knot formation at the aging temperatures at which these hardness peaks do not occur.

Further evidence along these lines is given in Table 5, in which the times for the beginning of precipitation are compared with the times for the attainment of the primary hardness peak and of the intermediate hardness valley. This table shows that precipitation does not set in until

TABLE 5.—*Comparison of Times for Beginning of Precipitation with Attainment of Primary Hardness Peak and Intermediate Valley*

Aging Temperature, Deg. C.	Beginning of Precipitation, Hr.	Primary Hardness Peak, Hr.	Intermediate Hardness Valley, Hr.
100	70-140	70	140
125	10- 16	10	16
150	2- 3	2	2 5

just after the primary hardness peak. We may assume, therefore, that at these three temperatures the initial hardness peak is caused by the formation of knots (which eventually precipitate into discrete particles). At 175° and above, however, the initial hardening is due to precipitation.

Further evidence in support of knot formation in these alloys is obtained from the electrical resistance and dilatometric curves in Figs. 6 and 7. The abnormal reverse effects prior to precipitation are certainly not due to the relief of quenching strains during the initial stages of aging. The resistance would decrease, and not increase, under such circumstances, and the magnitude of the effect would probably not be a function of the aging temperature. Since knot formation causes lattice distortion, it should cause an increase in resistance, and may result in a change in length that is the reverse of that caused by actual precipitation. Furthermore, as the hardness curves show, the knot-formation stage becomes relatively more important with lower aging temperatures, which accounts for the increased magnitude of the abnormal resistance and dilation effects before precipitation at the lower aging temperatures. It should be noted, however, that the resistance and dilation curves indicate knot formation even at 200°, although there is no pre-precipitation-hardening at this temperature. This anomaly will be discussed later.

The fundamental mechanism of aging of the silver-copper alloys, therefore, appears to be quite similar to that of the aluminum-copper alloys, in that both will age-harden by knot formation and by precipitation. The detection of these pre-precipitation effects in the silver-copper alloys, which have been generally considered to harden by precipitation only, is sufficient to indicate that perhaps we are no longer justified in classifying age-hardenable systems as either knot-hardening or precipitation-hardening. Such a classification seems both arbitrary and unnecessary.

Effect of Aging Temperature on Mechanism of Age-hardening

Jenkins and Bucknall¹⁹ demonstrated that, for many age-hardenable systems, the logarithm of the time required to attain maximum hardness or tensile strength varies inversely as the absolute aging temperature. To ascertain whether this relationship holds for the silver-copper alloys, the reciprocal of the absolute aging temperature was plotted against the logarithm of the time necessary to attain maximum hardness. The result is given by straight line *FP* in Fig. 8, which indicates the validity of the above relationship. This is further proved by the straight line *ER* which demonstrates the relationship as applied to the time required to attain one-half of the maximum hardening.

When the time for the beginning of hardening is plotted in this fashion, the linear relationship no longer holds throughout, although the three

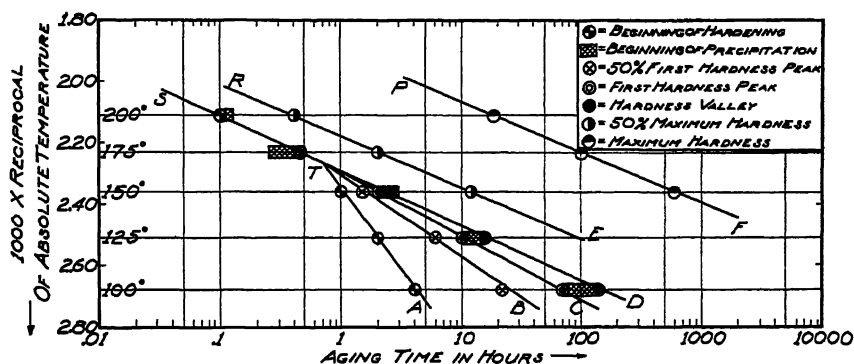


FIG. 8.—GRAPHIC REPRESENTATION OF EFFECT OF AGING TEMPERATURE ON MECHANISM AND RATE OF AGING.

points for 100°, 125° and 150° lie on a straight line that intersects the straight line drawn through the two points for 175° and 200°. The broken line *ATS* offers striking proof that the beginning of hardening is not due to the same phenomenon at all aging temperatures. By plotting the times for the attainment of one-half the initial hardness peak, the attainment of the initial hardness peak, and the attainment of the intermediate hardness valley, point *T* assumes greater significance because all three give straight lines that intersect at *T* (169° C.). Since the horizontal distance between lines *AT* and *DT* may be taken as a measure of the time of duration of the initial hardness peak, this peak actually disappears at 169° C.

Finally, plotting the time for the beginning of precipitation gives an answer to these unusual results. These values fall roughly on a straight line that is a continuation of *ST*. Hence, above 169°, the hardening occurs simultaneously with precipitation, and the broad hardness maxima are caused by the coalescence of the precipitated particles through and beyond the critical size necessary for maximum hardness. Below 169° C.,

however, the primary hardening takes place prior to precipitation and is due to knot formation. When the precipitation sets in, the intermediate softening occurs, presumably because the initial particles are too small to be very effective in hardening, and so they do not counterbalance the softening caused by the relief of distortion as the knots leave the matrix lattice to form discrete particles. However, as the particles grow in size, the hardness begins to increase again; and if the aging is prolonged sufficiently, the particles pass through the critical size for maximum hardening just as they do above 169° C.

It is believed that the disappearance of the initial hardness peak above 169° is due to a nonuniformity of the initial precipitation, which increases with the aging temperature and results in an overlapping of the knot and precipitation processes.* At 150°, for example, when hardness readings are taken at times between the occurrence of the primary hardness peak and the intermediate hardness valley, some submicroscopic regions in the structure are undergoing precipitation while others are still in the knot-formation stage. The hardness values, therefore, really result from these two effects. That is why the primary hardness peak at 150° is so indistinct. As the aging temperature is lowered to 125° and 100°, where the initial precipitation becomes more uniform, there is less overlapping of the two stages; the hardness valley becomes deeper, and the primary peak more pronounced. On the other hand, above 150° the extent of the overlapping increases and, at 169°, finally becomes complete as far as the hardness is concerned. The intermediate softening disappears and the primary peak no longer exists. Furthermore, above 169°, because of the nonuniformity of the initial precipitation, sporadic precipitation sets in before the knots can build up in sufficient numbers to affect the hardness, and so the entire hardening is due essentially to precipitation, although the knot-formation stage is still a vital part of the aging mechanism. This explains why the abnormal reverse effects (prior to precipitation) in the more sensitive electrical resistance and dilatometric measurements persist even above 169°, but become progressively smaller in magnitude as the aging temperature is raised.

Thus, it is believed that the mechanism of aging (not of hardening) in these alloys is actually the same at all temperatures. It is only the increased overlapping of the knot and precipitation stages as the aging temperature is raised that gives rise to the different hardening effects above and below 169°.

* The fact that the maximum hardness due to precipitation decreases as the aging temperature is raised indicates that the higher the aging temperature, the fewer the number of particles that simultaneously attain the critical size for maximum hardening, and hence the more nonuniform the precipitation. This inference is confirmed by the X-ray measurements in Table 1, which show that the higher the aging temperature, the relatively sooner do the diffraction lines become broad, and the greater is the broadening by the time the stable-phase lines appear.

Mode of Precipitation

The beginning of precipitation is gradual, as indicated by the progressive shift of the diffraction lines of the supersaturated solid solution.* After a while these lines begin to broaden. Evidently, then, in the later stages, precipitation becomes less uniform because of more rapid precipitation in some particular regions, which gives rise to a nonuniform composition of the remaining supersaturated solid solution. As the broad lines continue to shift, a new set of diffuse lines appear, which belong to the stable silver-rich phase from which all the excess copper has precipitated. This indicates that in localized areas precipitation must rapidly go to completion. The microscope shows that this rapid precipitation always starts at the grain boundaries and twinning planes, and works its way into the interior of the grains. Hence, for a certain length of time, the two sets of diffraction lines are obtained simultaneously on the film. However, as the regions of rapid precipitation overtake those of gradual precipitation, the lines due to the latter become broader and fainter and, finally, disappear. The diffuseness of the new set of lines is due either to extreme fragmentation or distortion of the silver-rich matrix. The sharpening of the diffraction lines after long aging at 200°C., therefore, indicates ultimate coalescence or removal of the lattice distortion.

It is believed that the precipitation in the vicinity of the grain boundaries and twinning planes takes place gradually, as in the interior of the grains, but at an accelerated rate. Eventually, a stage is reached at which diffusion is not rapid enough to supply copper atoms to these depleted regions, and a sufficient amount of the completely decomposed silver-rich solid solution accumulates to produce its own set of interference lines.

SUMMARY

1. The existence of pre-precipitation phenomena in a silver-copper alloy has been established by means of hardness, X-ray, electrical resistance, and dilatometric measurements. It is believed that knot formation plays an important part in the fundamental aging mechanism of silver-copper alloys.

2. The linear relationship between the reciprocal of the absolute aging temperature and the logarithm of the time required to attain some definite point in the aging process, such as maximum hardness, has been found to hold for these alloys.

3. For the particular alloy containing 8.72 per cent copper, 169° C. is the critical aging temperature below which the beginning of hardening

* The fact that Ageew et al. did not detect this initial gradual precipitation in their work above 200° C. is explained by Fig. 4, which shows that as the aging temperature is raised the change in lattice parameter prior to the appearance of the stable-phase lines becomes vanishingly small.

(as measured by the Rockwell F scale) occurs prior to precipitation, and above which the beginning of hardening occurs simultaneously with precipitation.

4. Below 169°, double hardness peaks occur in the aging curves. The results indicate that the first peak is due to knot formation, that the intermediate softening is caused by the relief of strain when precipitation takes place, and that the secondary hardening is due to the growth of the precipitated particles as they approach the critical size distribution necessary for maximum hardening.

5. Above 169°, the hardness curves consist of the usual single peak, the entire hardening being due to precipitation.

6. The electrical resistance and dilatometric results indicate that the mechanism of aging (not of hardening) is the same at all temperatures: knot formation followed by precipitation. However, above 169°, it is believed that scattered precipitation occurs before the knots become numerous enough to affect the hardness as measured in this investigation.

7. The mode of precipitation is the same at all temperatures. The initial precipitation is gradual, but becomes more and more nonuniform as precipitation goes rapidly to completion in localized regions at the grain boundaries and twinning planes. These regions grow at the expense of the progressively precipitating areas until the precipitation process is complete.

8. It is concluded that additional evidence has been accumulated to show that knot formation and precipitation are two consecutive stages, which permit a more generalized picture of the mechanism of age-hardening.

ACKNOWLEDGMENTS

The author is deeply indebted to Prof. John T. Norton, and to other members of the Department of Mining and Metallurgy, at the Massachusetts Institute of Technology, for their friendly cooperation and many helpful suggestions.

REFERENCES

1. F. Göler and G. Sachs: Die Veredelung einer Aluminiumlegierung im Röntgenbild *Metallwirtschaft* (1929) 8, 671.
2. W. Stenzel and J. Weerts: Die Anlasswirkungen in abgeschreckten Kupfer-Aluminiumlegierungen. *Metallwirtschaft* (1933) 12, 353, 369.
3. W. F. Roesser: Thermoelectric Temperature Scales. *Nat. Bur. Stds. Jnl. of Research* (1929) 3, 343.
4. M. Hansen: Die Löslichkeit von Kupfer in Silber. *Ztsch. Metallkunde* (1929) 21, 181.
5. D. Stockdale: The Solid Solutions of the Copper-Silver System. *Jnl. Inst. Metals* (1931) 45, 127.
6. N. Ageew and G. Sachs: Röntgenographische Bestimmung der Löslichkeit von Kupfer in Silber. *Ztsch. Physik* (1930) 63, 293.

7. E. A. Owens and J. Rogers: X-ray Study of Copper-Silver Alloys. *Jnl. Inst. Metals* (1935) **57**, 257.
8. C. S. Smith: Constitution of Copper-Silver Alloys. *National Metals Handbook* (1933) 1170.
9. W. Fraenkel: Zur Kenntnis der Vorgänge bei der Entmischung übersättigter Mischkristalle. *Ztsch. anorg. Chem.* (1926) **154**, 386.
10. W. Fraenkel and P. Schaller: Vergütbare Silberlegierungen. *Ztsch. Metallkunde* (1928) **20**, 237.
11. A. L. Norbury: The Effect of Quenching and Tempering on the Mechanical Properties of Standard Silver. *Jnl. Inst. Metals* (1928) **39**, 145.
12. M. Haas and D. Uno: Über die Vergütung von Standardsilber. *Ztsch. Metallkunde* (1929) **21**, 94.
13. M. Haas and D. Uno: Beitrag zum Härtungsproblem von Kupfer-Silber-, Beryllium-Kupfer-, Und Zink-Kupfer-Legierungen. *Ztsch. Metallkunde* (1930) **22**, 154.
14. N. Ageew, M. Hansen and G. Sachs: Entmischung und Eigenschaftsänderungen übersättigter Silber-Kupferlegierungen. *Ztsch. Physik* (1930) **66**, 350.
15. H. O'Neill, G. S. Farnham and J. F. B. Jackson: An Investigation of the Heat-treatment of "Standard Silver." *Jnl. Inst. Metals* (1933) **52**, 75.
16. J. T. Norton: Simplified Technique for Lattice Parameter Measurements. *Metals and Alloys* (1935) **6**, 342.
17. R. H. Leach and C. H. Chatfield: Manufacture of Sterling Silver and Some of its Physical Properties. *Trans. A.I.M.E.* (1928) **78**, 743.
18. Tentative Method of Test for Linear Expansion of Metals. *Proc. Amer. Soc. Test. Mat* (1934) **34**, pt. I, 33.
19. C. H. M. Jenkins and E. H. Bucknall: The Interrelation of Age-Hardening and Creep Performance. *Jnl. Inst. Metals* (1935) **57**, 141.

DISCUSSION

(E. R. Darby presiding)

M. L. V. GAYLER,* Teddington, England (written discussion).—Mr. Cohen's paper is of particular interest to me because several months ago I finished writing a paper (which now—Nov. 2, 1936— is awaiting publication) on a theory of age-hardening practically identical with that of Mr. Cohen's. I congratulate the author on the excellence of his paper as well as on the fact that he has explained facts hitherto considered as anomalous. It is particularly pleasing that the author and I have come to the same conclusions independently and from entirely different experimental data. My deductions have been based primarily on data on the age-hardening of alloys of the duralumin type, taken from my own published and hitherto unpublished researches and also from those of many other investigators. Substantial proof of the theory has also been shown to exist in the published data on the aging of beryllium-copper as well as silver-copper alloys.

I am in complete agreement with the author's statements that (1) the mechanism of aging (not hardening) is the same at all temperatures, (2) the mode of precipitation is the same at all temperatures; (3) the two stages of aging are consecutive, but I am not in entire agreement with the statement that the stages are due to (a) knot formation and (b) precipitation, for I consider that the first state is due to diffusion of solute atoms and that the formation of groups of molecules, which Merica calls "knots," are the indication that the second stage of the aging process (precipitation) is starting. The first stage, therefore, consists of the diffusion of the solute atoms to planes in the lattice of the solid solution about which precipitation ultimately occurs.

* National Physical Laboratory.

This diffusion will cause an increasing concentration of solute atoms about these planes of precipitation and will result in an increase in resistance to deformation and electrical resistivity, etc. X-ray evidence is in support of this idea. The second stage of the aging process directly follows the first and takes place nearly simultaneously; it begins when some of the diffusing atoms form molecules or groups of molecules with neighboring atoms of the solvent or other solute atoms. This group formation results in an increase of stresses in the lattice and consequent increase in the rate of hardening, until they become so great that rejection of a group takes place and precipitation proper sets in.

Mr. Cohen regards the softening that occurs intermediate between the two stages of hardening as due to "the relief of strain when precipitation takes place," and it is here that my conception of the aging process differs again from his. I have put forward evidence to show that the first stage of the aging process (as well as the second) increases to a maximum and then decreases. The entry of the second stage tends to overlap the first until at some stage in the age-hardening process it entirely balances the first. This point is indicated by the minimum softening and maximum resistivity and it is not essential that precipitation proper shall have taken place, but that groups of molecules shall be forming in the space lattice, increasing in amount and size. That precipitation proper is not the cause is shown by that fact that the softening takes place with no change in lattice parameter.

I have suggested forms of curves that will represent the general theory of age-hardening applicable to any system and have submitted typical curves showing: (1) the relation between hardness and time for all temperatures within what I have termed the "temperature range"; (2) the relationship between the time of attaining maximum hardness and the aging temperature; (3) the relationship between maximum hardness and temperature of both stages of age-hardening.

It is impossible to go more fully into the general application of the theory at the moment, but I hope that Mr. Cohen will understand that full discussion cannot be made until my paper is in print.

W. L. FINK* AND D. W. SMITH,* New Kensington, Pa. (written discussion).—Mr. Cohen's paper contributes interesting information on the process of age-hardening in a high-purity binary alloy. Many data of this kind will be required to clearly elucidate all of the details in the process of age-hardening.

The data in this paper show clearly that for aging temperatures of 150° C. or below the beginning of hardening is different from the beginning of hardening at higher temperatures. The aging time required for initial hardening is shorter than would be expected as shown in Fig. 8, and there is a small hardness peak before any change in lattice parameter and before the main portion of the hardening curve appears. In this same region there is an increase in electrical conductivity and an increase in volume.

Mr. Cohen assumes that these low-temperature aging phenomena are caused by the formation of knots prior to precipitation. We believe that these data can be explained without assuming the formation of knots, and that exhaustive experiments to determine whether or not the early hardening at low temperatures is accompanied by precipitation would be warranted. The polishing and etching technique was obviously not suited for revealing the first stages of precipitation, because even in the advanced stages the precipitate was not resolved but its presence inferred from darkened areas. The fact that a transition phase has been found to precipitate at low temperatures in the three aluminum-base alloys investigated up to the present time leads us to believe that the formation of such phases during aging may be general. This is in accordance with the law of physical chemistry that when two phases are possible of formation under given conditions the less stable phase forms first. The

* Aluminum Research Laboratories.

epireptation of a transition phase in this silver-copper alloy might persist for a time at 150° C. and below, and so produce the changes in electrical conductivity, volume, and hardness that have been reported.

It was assumed in the paper that the aging of aluminum-copper alloys is due to knot formation. Recently it has been found and reported by us that the aging of aluminum-copper alloys can be explained satisfactorily by the formation of precipitate. Precipitation was observed microscopically after room-temperature aging.

R. PHILLIPS,* Cleveland, Ohio.—I should like to ask Mr. Cohen whether he has done any work on the solubility of copper and silver. The diagram he used indicated a solubility of about 8.8 per cent, and his paper gives an alloy of 8.7 in order to insure the maximum hardenability due to aging. Experimenters have been consistent in getting data on the other end of the diagram of approximately 8 per cent solubility of silver and copper, but on the end we are interested in, during that same period, experimentation has shown values every place from 1 per cent to approximately 9 per cent. It seems rather queer that experimental error should be so great on one end of the diagram and almost perfect on the other.

I believe there is something that influences this in the rate of cool of the specimens. I have found that on slow cool with silver that is only 7.5 per cent copper it is possible to obtain a eutectic, and even on very slow cooling through the range between a liquidus and a solidus I have obtained a constituent that compares with the high-copper constituent on the other end of the diagram. That time was approximately 5 hr. between the two ranges. I should like to know whether Mr. Cohen has any ideas regarding this effect.

E. M. WISE,† Bayonne, N. J.—I am not sure that the examination of rather slowly cooled samples is altogether satisfactory. There may be some complicating effects. It seems to me that for precise determinations of solubility it is essential to chill-cast, drastically work and thoroughly homogenize the alloys and approach equilibrium from both sides. I have no doubt that some of the recent determinations of solid solubility are close enough for practical purposes.

A. J. PHILLIPS,‡ Maurer, N. J.—In Fig. 2, the flat horizontal line has four different values. Will the author explain why those four different values exist? They cannot be errors in Rockwell determinations, because if they are there is no significance in plotting the humps shown there. If they are initial aging effect, why is it the 100° curve is a little higher than the 125° curve?

M. COHEN.—The different values of the initial hardness are not due to experimental error in the Rockwell determinations. Probably they are caused by a slight variation in quenching temperature. The solid solubility of copper in silver varies rapidly with temperature in the particular quenching range used, hence a slight difference in the quenching temperature of $\pm 1^\circ$ or 2° would put more or less copper into solid solution. This, of course, would have a material effect on the initial hardness values.

A. J. PHILLIPS.—Then the samples were not all cut from the same material and quenched the same?

M. COHEN.—The samples were cut from the same material, but were heated and quenched individually.

A. J. PHILLIPS.—They did not all have the same quench?

* Case School of Applied Science.

† Assistant Manager, Research Laboratory, International Nickel Co.

‡ Superintendent of Research, Central Research Laboratory, American Smelting & Refining Co.

M. COHEN —That is correct. However, I might say that the aging results were checked individually at least two or three times.

In answer to the question on the solid solubility of copper in silver, I have done no work on that solubility curve. However, in reviewing the literature on that subject, it seemed to me that the curves as determined by independent investigators using independent methods are in very good agreement. The methods used were the microscopic, the electrical resistance, the dilatometric and the X-ray method. Considering only the more recent work on this solubility curve, the maximum variation at any temperature is only a matter of 1 or 2 per cent copper, certainly nothing like the 8 per cent that was suggested.

It is true that the older work on this system showed widely varying curves, but this work was done before the importance of long-time homogenization was appreciated. I fully agree that the proper way to determine this solid solubility curve is to suppress the precipitation by quenching from a high temperature, and then to reheat to the given temperature for a sufficiently long time to attain equilibrium. It appears that this is a more reliable method for reaching equilibrium than by slow cooling to the temperature in question.

It may be that Mr. Robert Phillips' alloy was not cooled slowly enough from the liquid state, and the resultant coring in the primary particles of the silver-rich solid solution caused these particles to have lower average copper contents than the equilibrium values indicated by the solidus curve. This means that at each successively lower temperature the remaining liquid would have a higher copper content than the equilibrium value indicated by the liquidus curve. Hence, the last drops of liquid to solidify may actually have the eutectic composition, and thus, due to coring, a eutectic structure may appear in an alloy containing only 7.5 per cent copper.

In answer to the comments of Dr. Fink, I really believe that the existence of the double-hardness peak in the aging curves below 169° is indicative of pre-precipitation phenomena. I do not think that break in the curves can be explained simply on the basis of an intermediate phase. However, I will refer to that in greater detail later.

With respect to the age-hardening of the aluminum-copper alloys, I believe Dr. Fink refers to his recent work in which he showed that there is a visible precipitation at room temperature. So far as I know, this was the first piece of work that showed room-temperature precipitation. An enormous amount of work has been done on aluminum-copper alloys, both pure and commercial, in which no precipitation could be detected at room temperature, either by use of the microscope or the X-ray. For this reason, it seems to me that the particular alloy used by Fink and Smith was different in some way from the alloys used by previous investigators.

The precipitation in dural or pure aluminum-copper alloys is well known at elevated temperatures, but wherever it has been found it has been shown that this precipitation is reasonably uniform and that the changes in lattice parameter are gradual. With Dr. Fink's alloy, the changes in lattice parameter were not gradual. The precipitation was decidedly nonuniform. As I showed in my work, when the precipitation becomes so nonuniform that it goes to completion in some areas of the specimen before it begins in others, there is what amounts to complete overlapping of the knot and precipitation processes, assuming that knot formation does exist. If the precipitation is very nonuniform, we can visualize that in some particular region the alloy will be in the knot-formation stage; in another region, the alloy will be in the process of precipitation; in still another region, the precipitation will be complete; and in a fourth region, the knot-formation stage may not even have begun. Hence, even if knot formation does exist, it cannot be detected as a pre-precipitation phenomenon when the initial precipitation is nonuniform.

M. COHEN (written reply).—Messrs. Fink and Smith agree with me in the concept of a two-stage aging process for the silver-rich copper alloys. They will admit, I

think, that the second stage of this process is the formation or precipitation of a copper-rich equilibrium phase as dictated by the equilibrium diagram. We differ only when it comes to giving a name to the transition stage between the initial supersaturated solid solution and the final equilibrium state. They feel that the transition stage, which becomes so important at low aging temperatures, is due to the precipitation of an unstable phase, while I believe that the transition represents the formation of nuclei within the solid solution just prior to the direct precipitation of the stable phase.

If the initial hardening found during the low-temperature aging of silver-copper alloys is due to the precipitation of an unstable phase, the change in lattice parameter of the matrix solid solution should occur simultaneously with the initial hardening. Actually this change in parameter takes place after the initial hardness peak. Therefore, it seems more logical to attribute this initial hardening to a diffusion process within the solid solution prior to precipitation rather than to the formation of an unstable precipitate. Furthermore, it would be expected that the transformation of the precipitate from the unstable to the stable state, as proposed by Messrs. Fink and Smith, would simply result in a difference in the rate of hardening, and not to a definite intermediate softening such as was actually found. Finally, in my opinion, it is very unlikely that the precipitation of a transition phase would result in a decrease in electrical conductivity. If this precipitation occurred, it would decrease the copper content of the matrix solid solution, and this tendency toward an increase in conductivity would probably be considerably greater than the opposing tendency caused by internal stresses due to precipitation. Thus, one would expect that the precipitation of even an unstable phase would cause an increase in electrical conductivity, whereas the silver-copper alloys showed a decrease in conductivity during the initial stage of aging.

I am pleased to note the close agreement between Dr. Gayler's concept of the general mechanism of age-hardening and my own ideas as deduced from the aging of silver-copper alloys. Dr. Gayler recognizes the necessity for an initial diffusion process taking place within the supersaturated solid solution in preparation for precipitation. This results in segregation of solute atoms in certain regions of the solvent lattice which cause the initial hardening. I have used the word "knot" to describe these segregations. Dr. Gayler, however, uses the word "knot" to indicate a molecule-formation stage which she regards as the beginning of the second-stage process and hence the cause of the secondary hardening. Thus, it appears that Dr. Gayler's picture of the two-stage process is very different from the ideas suggested by Messrs. Fink and Smith. The latter believe that the double hardening is due to the formation of two types of precipitate; the former is of the opinion that the double hardening takes place before precipitation proper. I differ with Dr. Gayler on only one point. I do not believe that it is necessary to postulate the formation of solute molecules before precipitation. If, as Dr. Gayler states, the formation of molecules or groups of molecules causes the secondary hardening by increasing stresses in the lattice, there should be a third stage in the hardening process corresponding to subsequent formation of an actual precipitate and the growth of the precipitated particles to the critical size distribution for maximum (precipitation) hardening. Yet Dr. Gayler agrees with me that the aging is only a two-stage process.

I am gratified to note that in spite of the disagreement as to the exact mechanism of the aging process, the contributors to this discussion all recognize that aging is not a simple precipitation process. It is hoped that further efforts along these lines on other pure binary systems will lead to a clearer and more universal picture of age-hardening.

Age-hardening of Aluminum Alloys, II—Aluminum-magnesium Alloy

BY WILLIAM L. FINK,* MEMBER A.I.M.E., AND DANA W. SMITH,* JUNIOR MEMBER A.I.M.E.

(Cleveland Meeting, October, 1936)

APPROXIMATELY two years ago the authors obtained data that indicated that initial precipitation could not be detected by change of lattice parameter in the aluminum-rich aluminum-magnesium alloys. Some of these data were first published in a brief note in MINING AND METALLURGY¹. Cast specimens were used at that time and they showed initial precipitation relatively sooner than sheet material of the same composition. For this reason a more thorough investigation has been carried out using a homogenized aluminum-magnesium sheet containing approximately 10 per cent magnesium.

Materials.—The aluminum used in the preparation of the aluminum-magnesium alloy was of high purity, containing less than 0.01 per cent each of iron, silicon and copper. The magnesium was high-purity sublimed magnesium.

Preparation of Alloy.—Approximately 4 kg. of the aluminum was melted in a plumbago crucible in an electric furnace and the magnesium was added. The melt was thoroughly stirred with a graphite rod and fluxed with chlorine gas before casting. The alloy was cast in the form of a sheet ingot in a cold iron tilting mold (approximately 200 by 165 by 40 mm.) and into small chill-cast slabs for chemical analysis (75 by 40 by 5 mm.).

The chemical analyses were made upon drillings from the analysis slabs. The analytical methods were those described in "Chemical Analysis of Aluminum," published by the Aluminum Company of America. The composition of the alloy was found to be: magnesium 10.30, silicon 0.013, iron 0.008 and copper 0.005 per cent.

In order to insure homogeneity the alloy was given two intermediate anneals at 430° C. for a total time of 36 hr. The ingot was hot-rolled

Paper received at the office of the Institute Aug. 20, 1936.

* Aluminum Research Laboratories, New Kensington, Pa.

¹ References are at the end of the paper.

to a thickness of 6.4 mm., and then cold-rolled to a thickness of 3.2 mm., at which point small specimens approximately 12 by 12 mm. were cut out for microscopic examination and lattice-parameter measurements. The remainder of the sheet was further cold-rolled to a thickness of approximately 1 mm. and cross-grained tensile specimens were machined with a formed milling cutter.

All of the specimens were heated for 16 hr. at 450° C., quenched in cold water and subsequently aged at various temperatures for various periods of time.

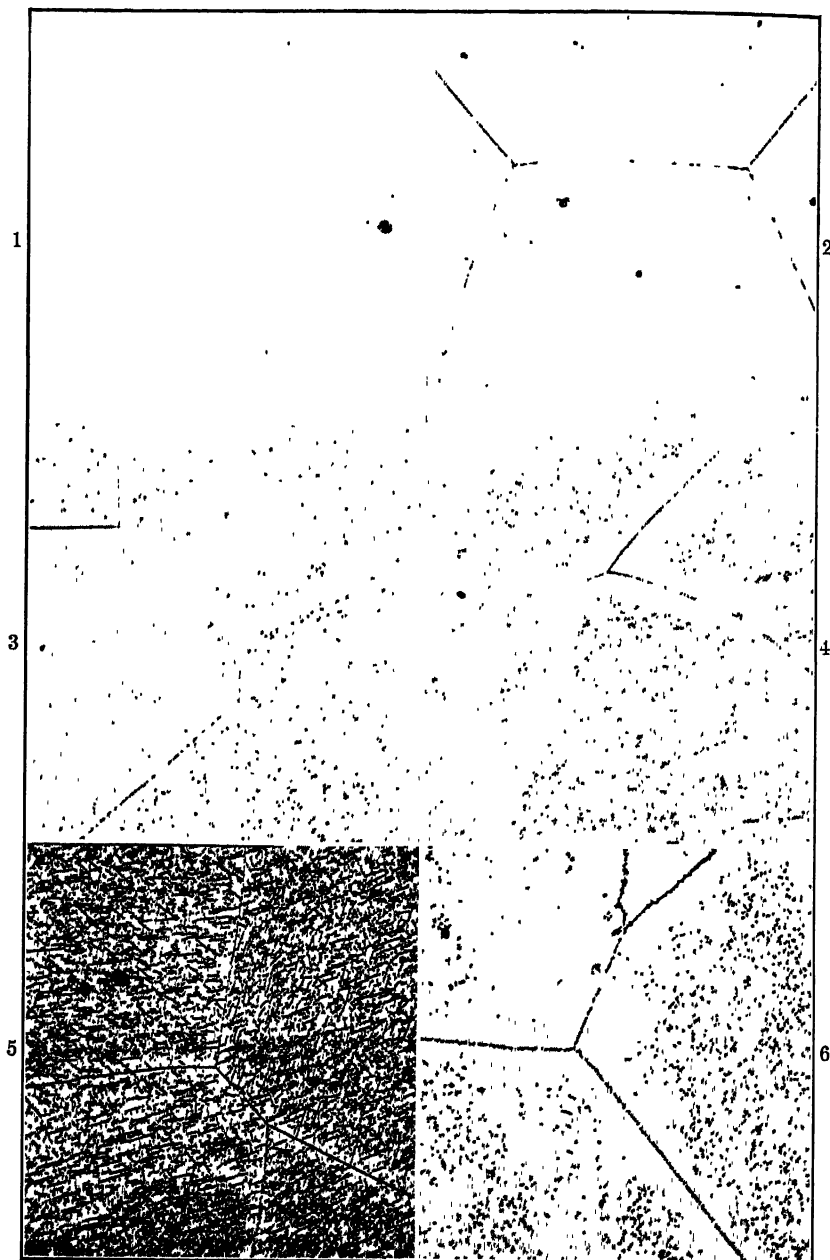
Microscopic Examination.—All of the specimens for microscopic examination were polished with unusual care to avoid defects such as polishing pits and surface flow. They were then etched in an aqueous solution containing 0.5 per cent hydrofluoric acid. The time required for etching varied with the aging treatment that the sample had received.

Specimens of the as-quenched alloy and the specimen aged 1 hr. at 100° C. revealed the polyhedral grain structure typical of solid solutions, with a few small particles of Mg_2Si (Fig. 1). Specimens aged for longer periods of time at 100° C. revealed small amounts of precipitation at the grain boundaries (Fig. 2), but no apparent precipitation within the grain until the specimen had been aged 604 hr. at this temperature, when appreciable precipitation is visible within the grains (Fig. 3).

Upon aging specimens at 200° C. for short periods ($\frac{3}{4}$ hr. and $1\frac{1}{2}$ hr.) grain-boundary precipitation and a small amount of precipitation within the grains are visible and by the time a specimen is aged for $3\frac{1}{2}$ hr. a rather large amount of precipitation has occurred within the grains (Fig. 4). The type of precipitation is Widmanstätten in nature and becomes more clearly defined as the aging time increases (Fig. 5).

Aging at 300° C. resulted in very rapid precipitation at grain boundaries as well as within the grains (Fig. 6). Aging for long times agglomerates the precipitate into large particles.

Lattice-parameter Measurements—The same polished surfaces that were used for microscopic examination were also used for the measurement of lattice parameter by the X-ray back-reflection method. No change in lattice parameter could be detected until after substantial precipitation within the grains was visible microscopically. The very first evidences of lattice-parameter change were observed after 1 hr. at 300° C., or 8 hr. at 200° C., and no change was observed in specimens aged at 100° C. even after 604 hr. The lattice parameter did not change uniformly throughout the entire specimen; that is, the first evidence of any change in parameter was shown by the diffraction circles becoming more diffuse in the direction of decreasing lattice dimension. With continued aging the diffraction circles became more diffuse and at approximately the midpoint of the decomposition of the solid solution the circles were so diffuse as to make them practically unmeasurable. This was



FIGS. 1-6.—ALUMINUM-MAGNESIUM ALLOY (10.30 PER CENT MAGNESIUM) HEATED 16 HR. AT 450°C., QUENCHED AND AGED. ETCHED IN AQUEOUS SOLUTION OF 0.5 PER CENT H_2F_2 . $\times 500$.

Fig. 1. Aged 1 hr. at 100° C.

Fig. 2. Aged 8 hr. at 100° C.

Fig. 3. Aged 604 hr. at 100° C.

Fig. 4. Aged 3½ hr. at 200° C.

Fig. 5. Aged 64 hr. at 200° C.

Fig. 6. Aged ½ hr. at 300° C.

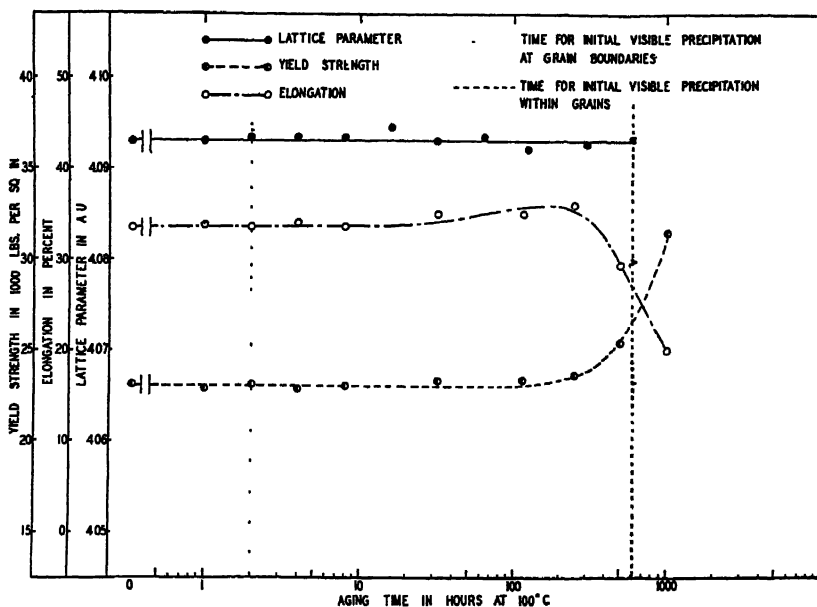


FIG. 7.—PLOT OF AGE-HARDENING DATA OF AN ALUMINUM-MAGNESIUM ALLOY (10.30 PER CENT MAGNESIUM).

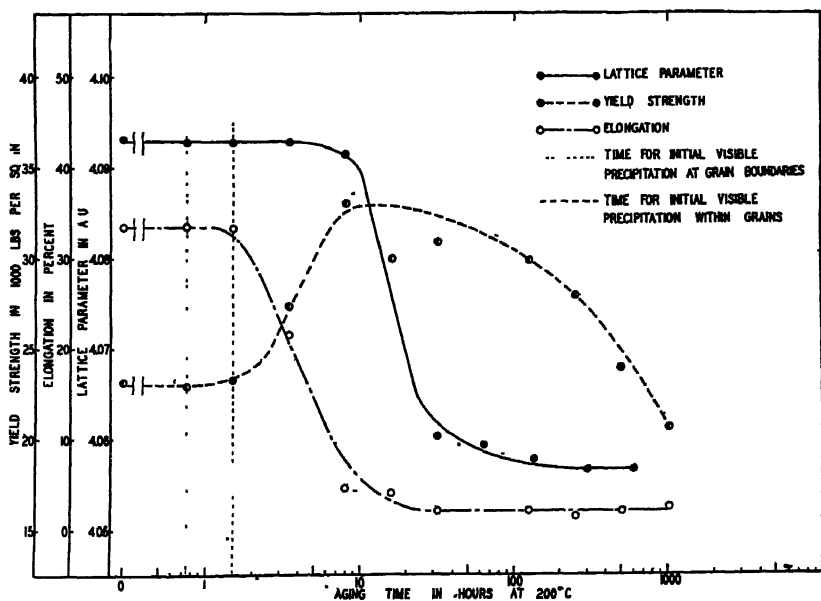


FIG. 8.—PLOT OF AGE-HARDENING DATA OF AN ALUMINUM-MAGNESIUM ALLOY (10.30 PER CENT MAGNESIUM).

especially true of the specimen aged 16 hr. at 200° C. The lattice-parameter data are summarized in the curves of Figs. 7, 8 and 9.

Tensile Tests.—Previous tests have shown that the most reliable criteria of the extent of age-hardening are yield strength and elongation. Consequently, these properties were determined as a function of the aging time. The test data are summarized in the curves of Figs. 7, 8 and 9. The specimens were tested in an Amsler testing machine equipped with self-aligning grips². The yield strength was determined from the stress-strain curve drawn by an electric recording extensometer³.

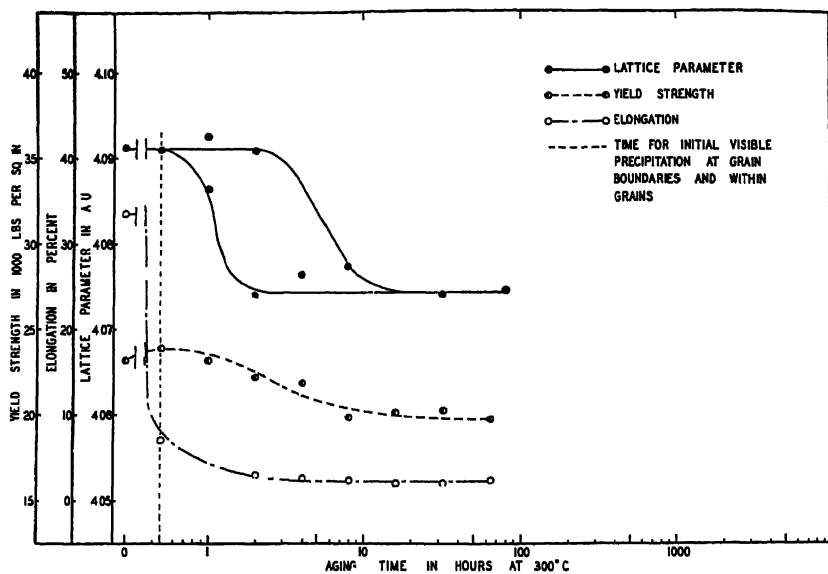


FIG. 9.—PLOT OF AGE-HARDENING DATA OF AN ALUMINUM-MAGNESIUM ALLOY (10.30 PER CENT MAGNESIUM).

Identification of Precipitating Phase.—Debye-Scherrer X-ray patterns made from aged samples of the 10 per cent magnesium alloy used in this work yielded reflections showing that the precipitating phase in specimens aged 80 hr. at 300° C. is the equilibrium phase β (sometimes referred to as Mg_2Al_3) while in specimens aged 136 hr. at 200° C. the precipitating phase was found to have a lattice arrangement different from the equilibrium phase. This new phase will be called β' . This same phenomenon has been previously observed and reported^{4,5} in connection with age-hardening of aluminum-copper alloys.

Discussion of Results.—The curves of Figs. 7, 8 and 9 summarize the data on elongation, yield strength, lattice parameter and the time required for precipitation as revealed under the microscope. It is evident that precipitation has occurred before any change in lattice parameter can be detected and before the yield strength or elongation have suffered

any substantial change. It should be noted that the first particles of precipitate appear at the grain boundaries but that these particles have no measurable effect on the yield strength or elongation. For example, aging for 8 hr. at 100° C. produces many particles of precipitate at the grain boundaries but no measurable change in yield strength or elongation. However, as soon as precipitation occurs within the grain some change can be detected in both yield strength and elongation. The lattice parameter, however, does not change measurably until the aging has been carried further.

The occurrence of a different crystal structure (β') in the particles precipitated at lower aging temperatures is of considerable interest. The same phenomenon has been observed in the aluminum-copper system. It has also been observed that the precipitate in the aluminum-magnesium-silicide alloys has a crystal structure different from the equilibrium phase Mg_2Si^6 . The authors suggest that the precipitate that forms in age-hardenable aluminum-base alloys at the usual aging temperatures may frequently, or even generally, have a structure different from the equilibrium phase.

CONCLUSIONS CONCERNING AGING OF ALUMINUM-MAGNESIUM ALLOY

1. Lattice parameter is not changed by precipitation of minute particles during age-hardening as it is by precipitation under equilibrium conditions.
2. Precipitation at grain boundaries can be observed microscopically before the aging has progressed far enough to change the yield strength and elongation measurably.
3. Changes in yield strength and elongation are coincident with the appearance of precipitation within the grains.
4. The phase β' , which precipitates at normal aging temperatures, has a crystal structure different from the equilibrium phase β .

ACKNOWLEDGMENT

The authors express their appreciation to Mr. C. J. Walton, who prepared all the specimens for microscopic examination; to Mr. H. V. Churchill, under whose direction the chemical analyses were made; and to Mr. R. L. Templin, under whose direction the tensile tests were made.

REFERENCES

1. Lattice Parameter No Criterion. *Min. and Met.* (May, 1935) 228.
2. R. L. Templin: *Proc. Amer. Soc. Test. Mat.* (1926) 26, II, 378 and A.S.T.M. Stds. (1933) I, 949.
3. R. L. Templin: *Proc. Amer. Soc. Test. Mat.* (1932) 32, II, 783.
4. W. L. Fink and D. W. Smith: *Trans. A.I.M.E.* (1936) 122, 284.
5. G. Wassermann and G. Weerts: *Metallwirtschaft* (1935) 14, 605.
6. R. F. Mehl, C. S. Barrett and F. N. Rhines: *Trans. A.I.M.E.* (1932) 99, 203.

DISCUSSION

(E. R. Darby presiding)

J. T. NORTON,* Cambridge, Mass.—This system is a typical example of the non-uniform type of precipitation. It is a phenomenon found also in the other end of this same system, the magnesium-rich alloys. In this paper the authors have suggested that the measurement of yield strength and tensile strength are very sensitive methods of determining the progress of the age-hardening phenomena. In our experience the measurement of the dilation or change in volume and of the electrical resistance are also very sensitive measurements of the beginnings of the changes that take place. It would be interesting if such experiments could be made on these alloys to see how changes in these properties compare with the visible precipitation the authors have indicated.

I might say just a word in defense of the X-ray method, which the authors have indicated as unsuitable for the study of this particular problem. In that statement I agree. In a system in which there is the nonuniform type of precipitation, obviously the measurement of the parameter, which is an average effect, is unsuited. I think we can say, however, that where the lines remain sharp and indicate gradual change in parameter that evidence is positive. Negative X-ray evidence is not conclusive, but positive X-ray evidence of a continuous change in parameter is definitely indicative of precipitation.

M. COHEN,† Cambridge, Mass.—It is rather amusing to note that Dr. Fink and Dr. Smith in the past have used the aluminum-copper alloys, upon which the knot theory was originally based, to show that there is no need for the knot theory, while I have used the silver-copper alloys, which ordinarily have been considered to harden by precipitation only, to show that there does seem to be a need for the knot theory.

To establish whether or not precipitation is taking place, it is important to select sensitive properties by measurement of which the course of aging can be followed. I feel, with Professor Norton, that the electrical resistance and dilation, and also the Rockwell hardness, are more sensitive properties for this purpose than the yield strength and the elongation.

Again, where the precipitation is uniform, I still believe that the X-ray method offers a more sensitive means for detecting the beginning of precipitation than the microscopic method; but where the precipitation is nonuniform, as indicated in the aluminum-magnesium alloys, it is true that the microscopic method is superior to the X-ray method. Whereas the precipitation in the aluminum-magnesium alloys and also in the authors' aluminum-copper alloys is decidedly nonuniform, there is the possibility of masking out or overlapping the knot-formation stage, so that even if knot formation did take place it could not be detected. Therefore I feel that unless the precipitation can be made to occur uniformly there is no point in too much theorizing.

I hoped that Professor Norton would say a little more about his work on the magnesium-rich aluminum alloys. As he stated, he also found the nonuniform type of precipitation, but in addition he found a very significant fact: the longer the time of homogenization prior to the age-hardening—i.e., the longer the time of solution heat-treating—the greater tendency there was for precipitation during aging to become uniform. In the present paper the solution treatment, as I remember it, was a homogenizing treatment of about 16 hr. It may be that if 16 days or 16 weeks had been used, a general trend toward more and more uniform precipitation could have been established. I really do not know, but there is that possibility.

* Associate Professor, Physics and Metals, Massachusetts Institute of Technology.

† Assistant Instructor, Massachusetts Institute of Technology.

W. L. FINK (written discussion).—We agree with Professor Norton that measurements of electrical conductivity or volume change are very desirable and sensitive, and we have a program lined up now in which those measurements will be made.

Mr. Cohen evidently overlooked a part of the description of the treatment. It was repeatedly cold-rolled and annealed at high temperature until it had had 36 hr. at temperature prior to the 16-hr. treatment to which he referred. We have found, in a number of systems, that repeated cold-work and heating is much more effective than one homogenizing treatment of the same duration, so we feel confident that these alloys were adequately homogenized.

In regard to the question of knots, I should like to recall the origin of that theory. It was believed that there were certain substantial changes in the properties—hardness, strength, and so forth—before there was any precipitation. That being the case, it became necessary to assume some mechanism to account for interference with slip before precipitate particles formed. Therefore, the presence of precipitate experimentally revealed during that interval eliminates all necessity for assumption of knots. Of course, crystal nuclei must form in some manner or other (probably by a Widmanstätten mechanism) before visible particles form, and it is possible that this formation of nuclei is preceded by the formation of knots. However, there is no evidence that those knots, if they exist, contribute anything to the hardening, and certainly in the systems we have studied there is no measurable effect on the properties measured, from the formation of any nuclei prior to precipitation. It seems to me, therefore, that consideration of what happens in very early stages prior to the formation of nuclei has a very slight effect upon our theory of age-hardening.

J. T. NORTON.—Dr. Fink has spoken of the formation of nuclei before actual precipitation forms. Perhaps that is the same thing that we are talking about when we speak of knots. Perhaps the origin of the term "knots" was unfortunate. If, however, we can show that something happens, regardless of what we may desire to call it, before we have any indication of precipitation, we must have a theory to explain it. In this particular system there seems to be little evidence that anything has happened before precipitation, but there is a tremendous amount of evidence in the literature that does suggest that possibly something happens before we can detect precipitation by any other means that we have now. That has been the reason for all of the controversy.

Whether the knot formation or pre-precipitation behavior is a necessary antecedent to the formation of the precipitate is still open to question. If we can show later that it is a necessary antecedent of the actual precipitation, one theory will cover the whole situation beautifully, but it does not seem to me that has been definitely established as yet. It certainly seems to be true in some systems, and there is still some doubt in other systems. Until there is a great deal more experimental evidence, it seems as though the whole question should be held in abeyance.

W. L. FINK.—I might say just a word in regard to the amount of data in the literature indicating changes in properties before any precipitation has been observed. That is perfectly true, but I think it should be kept in mind also that the precipitate during the early stages is necessarily very fine and very difficult to observe. It requires very careful work and very sensitive methods. There must be precipitation long before it can be observed under the microscope.

We selected the aluminum-copper system to work on because that seemed to be the outstanding system regarding which there was a great deal of work to show that there were changes in properties before precipitation occurred, but after working on it for a while we were able, microscopically, to show precipitation at such an early stage that it left no room for any appreciable change in properties due to the formation of knots or any other pre-precipitation phenomena.

I am inclined to think, therefore, that all that is necessary in order to reveal precipitation in some of the other systems described in the literature is sufficiently sensitive methods and accurate work.

E. H. DIX, JR.,* New Kensington, Pa.—I believe the principal thing that caused Dr. Merica to propose his knot theory was the very exact work done by Dr. Sachs, using the new X-ray tool with which, as nearly as anybody could see, should be shown changes that were taking place inside the metal sooner than in any other way. Dr. Sachs' measurements did not show a change in the lattice parameter at the time to account for the change in mechanical properties.

It seems to me that the principal point in the work of Fink and Smith is that they have definitely shown in two systems, aluminum-copper and aluminum-magnesium, that visible precipitation takes place prior to any change they have been able to find in lattice parameter.

M. COHEN.—Do you feel that you have detected this precipitation process simply by more sensitive methods than have been used previously, or do you think that your alloy is different in some way or other from those used by previous investigators? I want to call attention to the fact that an enormous amount of work by Goler and Sachs, Fraenkel, and others, has not detected any room-temperature precipitation either by means of X-rays or by the microscope. On the other hand, they have detected reverse effects in the electrical resistance and dilation curves.

W. L. FINK.—It is true that the alloys we use are made from higher purity material than much of the material used for reported investigations, but I feel that the principal factors are more careful work and a better etch. The surface must be prepared very carefully. Even a slight surface flow either obliterates or makes indistinct the microscopic evidence of precipitation. Moreover, it is difficult to find a satisfactory etch. We have been working on the problem of suitable etches for aluminum-copper alloys for a long time, and only since Mr. Keller, of our laboratories, developed an etch capable of revealing the precipitate in the commercial alloy 17-S have we had an etch good enough to allow us to reveal clearly the precipitation in these binary aluminum-copper alloys. After we did reveal the precipitation with this etch, it was possible to use older etches on an alloy that was known to have precipitate and get some faint, hazy indications of it, but the difference is striking. If the indications with the older etches were the only evidences, one would be inclined to pass it over as some sort of superficial effect due to improper polishing or etching technique or something of that sort. In other words, a better etch was necessary before we could feel sure of our ground. I think the same thing will probably occur in the study of other systems.

M. COHEN.—What do you think of the possibility of premature precipitation at the very surface of your alloys caused by the polishing and etching operation? Previous investigators of silver-copper alloys have found, even after careful polishing and etching, that the supersaturated solid solution at the surface would decompose, either from the effect of the cold-working or the chemical attack.

W. L. FINK.—The specimens we used were polished in the same way, regardless of aging time. The as-quenched material showed no precipitation, but after enough aging this same polishing and etching would reveal evidence of precipitation. I feel that there is no chance of the precipitation having been caused by the polishing operation.

J. T. NORTON.—Suppose, Dr. Fink, you were to examine the electrical resistance and the dilation in these alloys and find the reverse effects of time prior to the first

* Aluminum Company of America.

visible precipitation; in other words, that the actual resistance would increase and the volume changes would be in the abnormal direction. Would that in any way modify your opinion as to the nature of the precipitation?

W. L. FINK.—No. I should rather expect that they would be in the "wrong" direction. We know that when two phases are possible the least stable forms first, and that usually it is the less dense or more voluminous. Moreover, I should be very much surprised if very minute particles should behave in the same way and give the same results as large crystals. In other solutions, for example, liquid solutions, the change from the true solution to a typical two-phase system is not abrupt. Small colloidal particles have many of the properties of molecules; that is, they may be considered as large molecules. So I think we are on very dangerous ground if we assume the same properties for a two-phase system with large particles and the same system with very minute particles that contain relatively few solute atoms.

J. T. NORTON.—Then our only difference in opinion is as to what we shall call these. It seems to me it stays between a solid solution and a precipitated situation, which we can recognize as a result of our experiments on considerable amounts of precipitate; that is, if we observe these reverse effects they must be due to something different from the precipitates that are ordinarily recognized. That is the situation which perhaps we have suggested as knots, perhaps incorrectly, because the situation is entirely changed since the original knot system was developed. The real nub of the problem seems to be in the explanation of these abnormal effects of one sort or another.

Precipitation-hardening and Double Aging

By R. H. HARRINGTON*

(Cleveland Meeting, October, 1936)

THE definition of precipitation-hardening¹ is well understood and its principles have been subjected to study for some time. However, the variation of properties with double aging, combined with strain-hardening, gives promise of new and useful phenomena. Properly to understand these distinctions, definitions of these terms are necessary.

*Precipitation-hardening*¹.—This reaction usually depends upon an alloy having such a composition that it consists only, or in major part, of but one phase, a solid solution, at a high temperature, so that, upon slow cooling, this solution breaks down into two phases, the solid solution and a compound. By heating the alloy to the temperature for maximum solution of the compound, quenching, and reheating to a suitable lower temperature for critical dispersion precipitation of the compound, useful properties of the alloy may be developed to a maximum.

Double Aging.—Double aging in part is similar to the process for precipitation-hardening, consisting of heating a precipitation-hardening alloy to the solution temperature, quenching, reheating to the suitable dispersion precipitation temperature, strain-hardening, and again reheating to a suitable temperature to develop certain useful properties to a maximum. The strain-hardening may be induced by two methods: (1) a rate of cooling from the first reheat may suffice to strain the solid solution lattice of the alloy; or (2) the alloy may be cold-worked to a suitable degree between the two reheats.

PRECIPITATION-HARDENING OF COPPER-COBALT-BERYLLIUM ALLOYS^{1,2}

The composition of principal interest is that of 2.6 per cent Co, 0.4 per cent Be, 97 per cent Cu. The alloy has been developed commercially and, with certain reasonable precautions, ordinary brass-foundry practice suffices to produce an alloy of high quality.

Preliminary Precipitation-hardening Study.—Samples were cut from a 1-in. round rod cast in a graphite mold. These samples were then

Manuscript received at the office of the Institute Aug. 27, 1936.

* Research Laboratory, General Electric Co., Schenectady, N. Y.

¹ R. H. Harrington: The Present Status of Age-Hardening. *Trans. Amer. Soc. for Metals*, **22**, 505-531.

² U.S. Patents 1847929 and 1957214.

quenched from the solution temperature and drawn at different temperatures to determine the heat-treatment necessary to develop maximum precipitation hardness. The results are shown in Table 1. The electrical conductivities, referred to 100 per cent for copper, are also in Table 1. The hardness and conductivity values are clear indications that precipitation-hardening has taken place. It is to be noted that the ratio of cobalt to beryllium in this analysis is the ratio of atomic weights of the two elements in the compound formula CoBe; also that, in the absence of cobalt, up to 1 per cent beryllium is soluble in copper at room temperature. The correct hardening heat-treatment of this alloy is, therefore, to heat 1 hr. at 900° C., quench in water, reheat 2 to 4 hr. at 500° C., and cool in air or a reducing atmosphere.

TABLE 1.—*Hardness and Electrical Conductivity*

Condition of Alloy	As Cast	900° C. Water Quench	Temperature of Draw, Deg. C.							
			200	300	400	500	600	700	800	900
Brinell hardness.....	80	69	69	74	120	220	130	92	80	80
Electrical conductivity, per cent.....	26.3	19.6				45-50				

Tensile Properties.—The tensile properties are shown in Table 2. The proportional limit is unusually high for such an alloy.

TABLE 2.—*Physical Properties*
TENSILE PROPERTIES

Condition of Alloy	Tensile Strength, Lb per Sq. In.	Proportional Limit, Lb per Sq. In.	Elongation, Per Cent in 2 In.	Reduction in Area, Per Cent	Brinell Hardness
Cast and heat-treated...	90,000	45,000	10	20	220
Forged and heat-treated	100,000	45,000	20	24	220

ADDITIONAL PHYSICAL PROPERTIES

Modulus of elasticity in tension..... 17,000,000

Modulus of elasticity in torsion: 20° C..... 7,192,000

400° C..... 6,961,000

Effect of temperature on tensile properties, cast bars, heat-treated:

	At 20° C.	At 350° C.	At 475° C.
Tensile strength..	90,000	68,000	56,000
Elongation, per cent.....	10	4	1
Reduction of area, per cent.....	20	4	2

Once precipitation-hardened, the alloy may be reheated to about 500° C. without affecting the room-temperature properties. Cold-rolling

to four numbers hard between the quench and the draw results in a small increase in tensile strength to a value of about 110,000 lb. The hardness and toughness of this alloy in the heat-treated state prevent any practical results from attempts to cold-work the heat-treated alloy. The alloy is easily worked hot, before heat-treatment, or cold-worked between quench and draw.

The torsional modulus of elasticity values indicate an unusual maintenance of spring properties at temperatures up to 400° C. The fatigue properties are also unusually good.

DOUBLE AGING WITH INTERMEDIATE THERMAL STRAIN-HARDENING

A few alloys, by their phase constitution, may have their properties appreciably affected by strain-hardening a solid solution phase by cooling rates from aging temperatures that are not at all so effective in this way for the majority of the known alloys. Thus, abnormal grain growth in high-speed steel³ may be caused by simply air-cooling the alloy from 800° to 850° C. and subsequently hardening the steel without intermediate anneals. This was ascribed to the strain-hardening of the retained austenite during cooling from the lower temperature. It is also known that usually strain-hardening (as by cold-working) between the quench and the draw tends to increase somewhat the amount and degree of precipitation that takes place in a precipitation-hardening alloy.

Bearing this in mind, the benefits ascribed to the "double aging" of high-speed steel may be considered. Although the details and exact conclusions will be the subject of another publication, some of the conclusions from tests on a high-speed steel of the 18 W, 4 Cr, 1 V type are as follows:

Heat Treatment.—Test tools were preheated at 900° C., heated 5½ min. at 1300° C. and oil-quenched. A number were then drawn 2 hr. at 550° C. and air-cooled for a single aging. Others were drawn 1 hr. at 550° C., air-cooled and reheated 1 hr. at 550° C., followed by air-cooling.

Tool Life.—The double-aged tools had about twice the life of those with single aging.

Transverse Strength.—The double-aged tools had more than twice the strength of the single-aged tools.

Structures.—At a magnification of 2000, the structure of the double-aged tools showed a greater amount of precipitation of the hardening particles and an appreciable increase in the amount of troostitic structure.

Conclusion.—One conclusion may therefore be that lattice straining of the retained austenite, accomplished by air-cooling from the first 550° C. draw, favored two reactions during the second draw as would be

³ G. R. Brophy and R. H. Harrington: Nature of Abnormal Grain Growth in High Speed Steel. *Trans. Amer. Soc. for Metals*, **19**, 385-402.

expected: (1) Further transformation of some of the gamma phase (austenite) to the alpha (troostite); and (2) more precipitation of tungstides and complex carbides that form the critically dispersed hard particles.

DOUBLE AGING WITH INTERMEDIATE COLD-WORKING, COPPER-CHROMIUM-BERYLLIUM ALLOYS²

Most precipitation-hardened alloys of practical value are too tough, hard, or brittle to be cold-worked to any appreciable degree following complete heat-treatment. Had it not been for the unusually high electrical conductivities of the precipitation-hardened alloys of copper-chromium-beryllium they could easily have been overlooked.

The preferred analysis is that of 0.4 per cent Cr, 0.1 per cent Be, 99.5 per cent Cu. The alloy has been developed commercially and, with certain reasonable precautions, ordinary brass-foundry practice suffices to produce alloy of high quality.

Preliminary Precipitation-hardening Study.—Two compositions, one with chromium and beryllium balanced in the ratio to form CrBe, and one with excess chromium, were used for melts. Samples were cut from 1-in. round rods cast in graphite molds. These were quenched from a high temperature to retain the solid solution and then reheated at successively higher temperatures for drawing treatments. Rockwell B hardness tests were made after each treatment. Electrical conductivity tests were made on cast rods heat-treated to the maximum hardness. The data are shown in Table 3.

TABLE 3

Composition, by Analysis Per Cent	As Cast	925° C. Water Quench	Temperature of Draw, Deg C							
			200	300	400	450	475	500	525	550
0.08 Be	+22	-12	-10	-2	+15	+30	+35	+40	+33	+29
0.38 Cr... ..										
Balance Cu.....										
Electrical conductivity, 73.2 per cent										
0.095 Be.....	+20	- 5	- 6	-1	+16	+30	+35	+40	+33	+27
1.18 Cr... ..										
Balance Cu.....										
Electrical conductivity, 71.4 per cent										

In general, the accepted heat-treatment consists of: (1) Heat 1 to 2 hr. at 900° to 925° C.; (2) quench in water; (3) reheat 1 to 4 hr. at 500° C. The heat-treatment may be given in either air or reducing atmospheres.

Chromium in excess of the amount to form with beryllium the compound CrBe is to be avoided, as no benefits accrue and there is a tendency toward a lower electrical conductivity.

Physical Properties of Heat-treated Cast Rod.—Standard tensile specimens were machined from 1¼-in. and 1-in. dia. heat-treated cast rods. All proportional limits as reported were derived from load extension data, of which the extension values were obtained by use of the Sayre extensometer. Physical properties (average of three or more test specimens) are as follows: tensile strength, 30,000 to 35,000 lb. per sq. in.; proportional limit, 15,000 to 16,000 lb. per sq. in.; elongation, 10 to 15 per cent; hardness, 35 to 40 Rockwell B; electrical conductivity, 72 to 75 per cent of that of copper.

Size of casting and pouring procedure give the ranges indicated for tensile strength and elongation. These room-temperature tensile properties are unaffected by reheating the fully heat-treated cast or forged bars to temperatures up to 500° C. and recoiling.

The conductivity of the heat-treated alloy decreases less than does that of pure copper with increasing temperature. The data are as follows:

Temperature, Deg. C	Resistivity, Micro-ohms per Cu Cm.		Conductivity, Per Cent of That of Cu
	Cu-Cr-Be	Cu	
21	2.433	1.73	71.2
125	3.142	2.44	77.6

Effect of Cold-working between Quench and Draw.—Rods, 1¼ in. in diameter, were cast in graphite molds, all rods tested being from the same melt. All rods were heated 1 hr. at 900° C. and quenched in water, then cold-swaged to 1-in. dia. Small samples were then heated 1 hr. at each of various drawing temperatures and Rockwell B hardness values were measured. Results are shown in Table 4.

TABLE 4.—Hardness

Condition of Metal	Quenched	Swaged	Temperature of Draw, Deg. C.							
			100	200	300	400	450	500	550	600
Hardness, Rockwell B.....	-12	59	50	53	50	53	59	61	47	41

Cold-swaged bars 1 in. in diameter were then reheated 1½ hr. at each of the temperatures: 450°, 475° and 500° C. The reheated bars were machined into standard tensile specimens, the electrical conductivities,

hardness values, and tensile properties were determined and photomicrographs were taken. The physical properties are indicated in Table 5.

TABLE 5.—*Physical Properties*

Treatment	Structure ^a	Tensile Strength, Lb per Sq. In.	Proportional Limit, Lb per Sq. In.	Elongation, Per Cent in 2 In.	Hardness, Rockwell B	Electrical Conductivity, Per Cent
Quenched and swaged, 450° C. draw.....	Fig. 2	47,900	30,000	26	59	71.2
Quenched and swaged, 475° C. draw.....	Fig. 3	47,700	30,000	27	63	70.6
Quenched and swaged, 500° C. draw	Fig. 4	46,200	27,000	20	61	73.6

^a Fig. 1 shows the structure of the alloy as quenched and swaged.

The data of Tables 4 and 5 and the photomicrographs of Figs. 1 to 4 lead to the following conclusions:

1. The effect of cold-work between the quench and the draw has lowered the critical dispersion precipitation temperature from 500° to 475° C. for maximum hardness.

2. The maximum hardness achieved by cold-working the alloy between quench and precipitation reheat is 63 Rockwell B, as compared to 35 Rockwell B after the simple precipitation-hardening treatment.

3. Similarly, the proportional limit has been doubled with an increase of only 60 per cent in the tensile strength, and the elongation has been appreciably increased to 27 per cent.

4. The improvement in tensile properties is combined with the high electrical conductivity obtained by the simple precipitation heat-treatment.

5. Since the electrical conductivities of the alloy for both treatments are practically the same, it seems probable that the actual amount of the precipitated phase is the same following both treatments. Therefore it would seem that cold-work between the quench and the draw has exercised a preferential effect as to the location of the dispersed phase, so as to more effectively key the slip planes most readily affected by cold deformation during the tensile tests.

6. Fig. 1, showing the structure of the quenched and cold-swaged alloy, pictures the typical slip-banded grains for such a treatment. Fig. 2 shows the alloy with the same treatment followed by a 450° C. draw. There has been no apparent change from the structure of Fig. 1 other than a possible slight decrease in the number of slip bands. Drawing at a temperature of 475° C. appears to have caused a further decrease in the number and width of the slip bands as shown in Fig. 3, compared to Figs. 1 and 2. Fig. 4 shows the structure of the alloy with the same base

treatment of quench followed by cold-work but with a succeeding draw at 500° C. There is an apparent marked decrease of slip bands as compared to Figs. 1 and 2, and some indication of the beginning of recrystallization. The preferential precipitation, caused by cold-working between the quench and the draw, appears to have blocked the diffusion conditions ordinarily prevailing when no precipitation occurs upon reheating, so that recrystallization, if at all appreciable, must take place at some tempera-

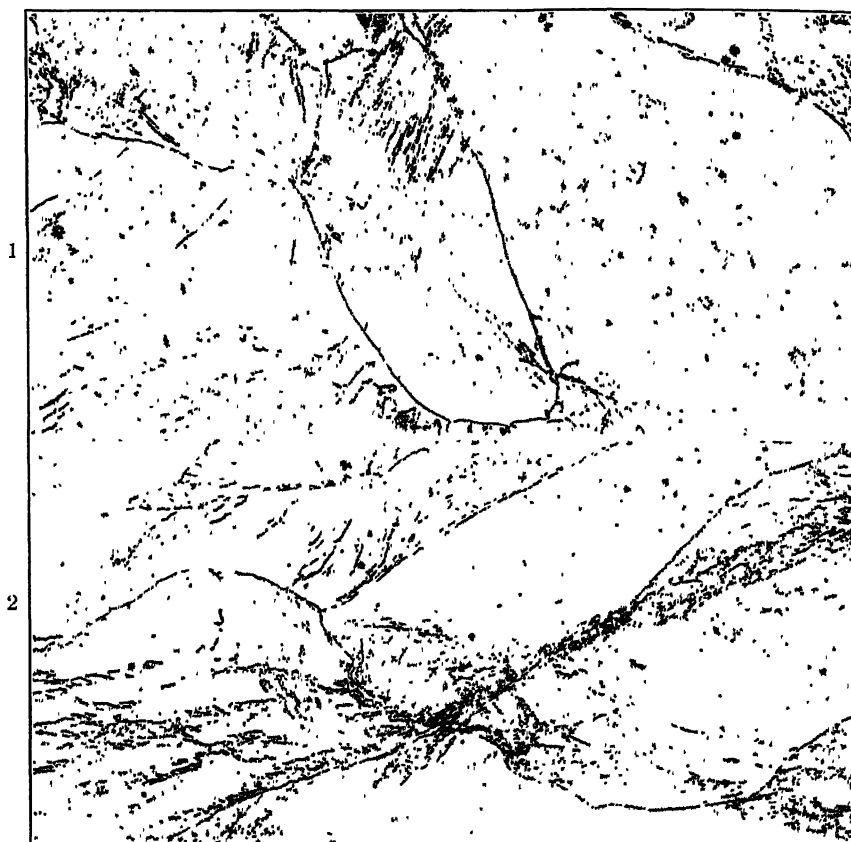


FIG. 1.—AS QUENCHED AND SWAGED.

FIG. 2.—SAME AS FIG. 1, DRAWN AT 450° C.
× 100. Etch, sulphuric dichromate.

ture above 500° C., when coalescence of the precipitated phase would decrease its blocking effect.

Effect of Cold-work Intermediate to Double Aging.—Alloy of the same composition was cast in graphite molds into rods of $1\frac{1}{4}$ -in. dia. These rods were heated 1 hr. at 900° C., quenched in water and reheated 1 hr. at 500° C. They were then cold-swaged to 1-in. dia. (giving them about the same amount of reduction as was given the rods that were cold-

swaged between the quench and the draw). For a preliminary "age-hardening" study, samples of the heat-treated and cold-worked rod were reheated at various drawing temperatures for 1 hr. and air-cooled. The

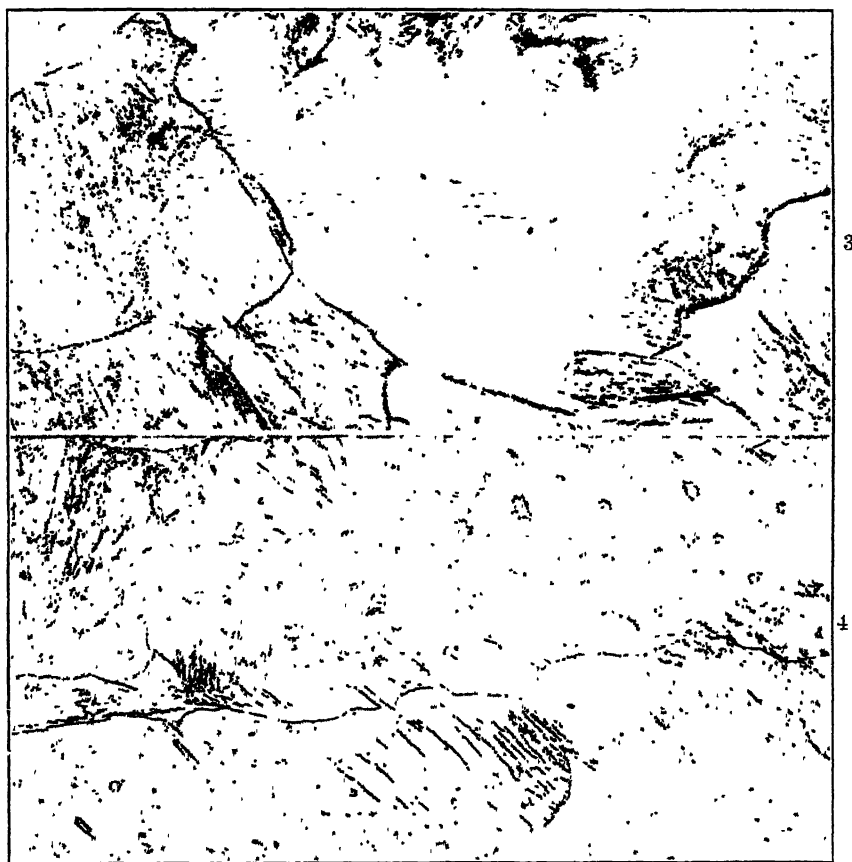


FIG. 3.—SAME AS FIG. 1, DRAWN AT 475° C.

FIG. 4.—SAME AS FIG. 1, DRAWN AT 500° C.

× 100. Etch, sulphuric dichromate.

Rockwell B hardness values were then determined. The results are given in Table 6.

TABLE 6.—*Hardness*

Treatment, Deg. C.	Heat-treated and Cold-worked	Temperature of Draw, Deg. C.							
		100	200	250	300	350	400	450	500
Rockwell B hardness.....	69	74	72	72	70	69	68	64	60

These results indicate a substantial increase in hardness over the effect of cold-work between the quench and the draw as indicated in Table 4. Since the fully precipitation-hardened alloy is more hard and tough than the simply quenched alloy, more work was necessary to cold-reduce the hardened alloy to the same degree as was the soft-quenched alloy.

Stock for standard tensile bars, $1\frac{1}{4}$ -in. dia., was then treated to represent the following conditions: (1) as cast; (2) cast and water-quenched after 1 hr. at 900°C .; (3) same, drawn $1\frac{1}{2}$ hr. at 500°C .; (4) remaining rods cold-swaged to 1-in. dia. after complete precipitation-hardening: (a) as swaged; (b) several swaged bars reheated $1\frac{1}{2}$ hr. at each of the following drawing temperatures: 100° , 200° , 300° , 350° , 400° , 450° , and 500°C . Standard tensile specimens were machined from the processed rods. Electrical conductivity of the tensile bars was measured, as was also the Rockwell B hardness. The tensile properties were then determined and photomicrographs were taken of the structures. The results are shown in Table 7.

TABLE 7.—*Tests on Stock for Standard Tensile Bars*

Treatment	Structure	Tensile Strength, Lb per Sq. in.	Proportional Limit, Lb. per Sq. in.	Elongation, Per Cent 2 in.	Hardness, Rockwell B	Electrical Conductivity, Per Cent of That of Cu
As cast.....	Fig. 5	27,900	9,000	16	13	44.6
900°C . quench.....	Fig. 6	26,300	6,000	34.5	-15	47.4
900°C . quench, 500°C . draw..	Fig. 7	35,200	15,000	22	33	69.0
900°C . quench, 500°C . draw, cold-swaged.....	Fig. 8	49,400	35,200	12	70	67.0
Heat-treated, cold-swaged, re-drawn 100°C	Fig. 9	50,600	35,300	11	73	66.4
Heat-treated, cold-swaged, reheated 200°C	Fig. 10	47,200	35,200	9	69	68.9
Heat-treated, cold-swaged, reheated 300°C	Fig. 11	49,400	33,000	12	69	67.7
Heat-treated, cold-swaged, reheated 350°C	Fig. 12	49,000	31,500	20	67	67.2
Heat-treated, cold-swaged, reheated 400°C	Fig. 13	48,000	30,000	21	65	70.8
Heat-treated, cold-swaged, reheated 450°C	Fig. 14	44,750	29,200	8	65	71.2
Heat-treated, cold-swaged, reheated 500°C	Fig. 15	38,000	24,000	12	58	71.7

Conclusions

Photomicrographs.—Comparing Figs. 8, 9 and 10 with Fig. 1, and Figs. 13, 14 and 15 with Figs. 2, 3 and 4, showing structures developed by similar heat-treatments, but with the difference that Figs. 1, 2, 3 and 4

are photomicrographs of the alloy with cold-work between the quench and the draw, whereas Figs. 8 through 15 show structures developed by cold-work superimposed upon the fully hardened alloy, the comparative absence of slip bands is noted for the latter. Hardness is also constant across the transverse section of a rod cold-swaged from $1\frac{1}{4}$ -in. dia. to 1-in. dia. after complete precipitation, whereas ordinary cold-worked



FIG. 5.—ROD $1\frac{1}{4}$ INCHES IN DIAMETER, AS CAST.

FIG. 6.—SAME AS FIG. 5, 900° C. QUENCH.

× 100. Etch, sulphuric dichromate.

material usually shows a harder surface and a softer interior. It appears, therefore, that the strain of cold-working is transmitted entirely through the cross section with general uniformity. Since precipitation has keyed the slip planes, the superimposed cold-work does not appear to have caused slip for a sufficient distance or of sufficient degree along any slip plane to effect the etching of the slip bands usually characteristic of cold-worked metal. Several of the samples did show a very few grains with



FIG. 7.—SAME AS FIG. 6, 500° C. DRAW.

FIG. 8.—SAME AS FIG. 7, COLD-SWAGED.

FIG. 9.—SAME AS FIG. 5, HEAT-TREATED, COLD-SWAGED, REDRAWN 100° C.
× 100. Etch, sulphuric dichromate.



FIG. 10.—SAME AS FIG. 9, REDRAWN 200° C.
FIG. 11.—SAME AS FIG. 9, REDRAWN 300° C.
FIG. 12.—SAME AS FIG. 9, REDRAWN 350° C.
× 100. Etch, sulphuric dichromate.

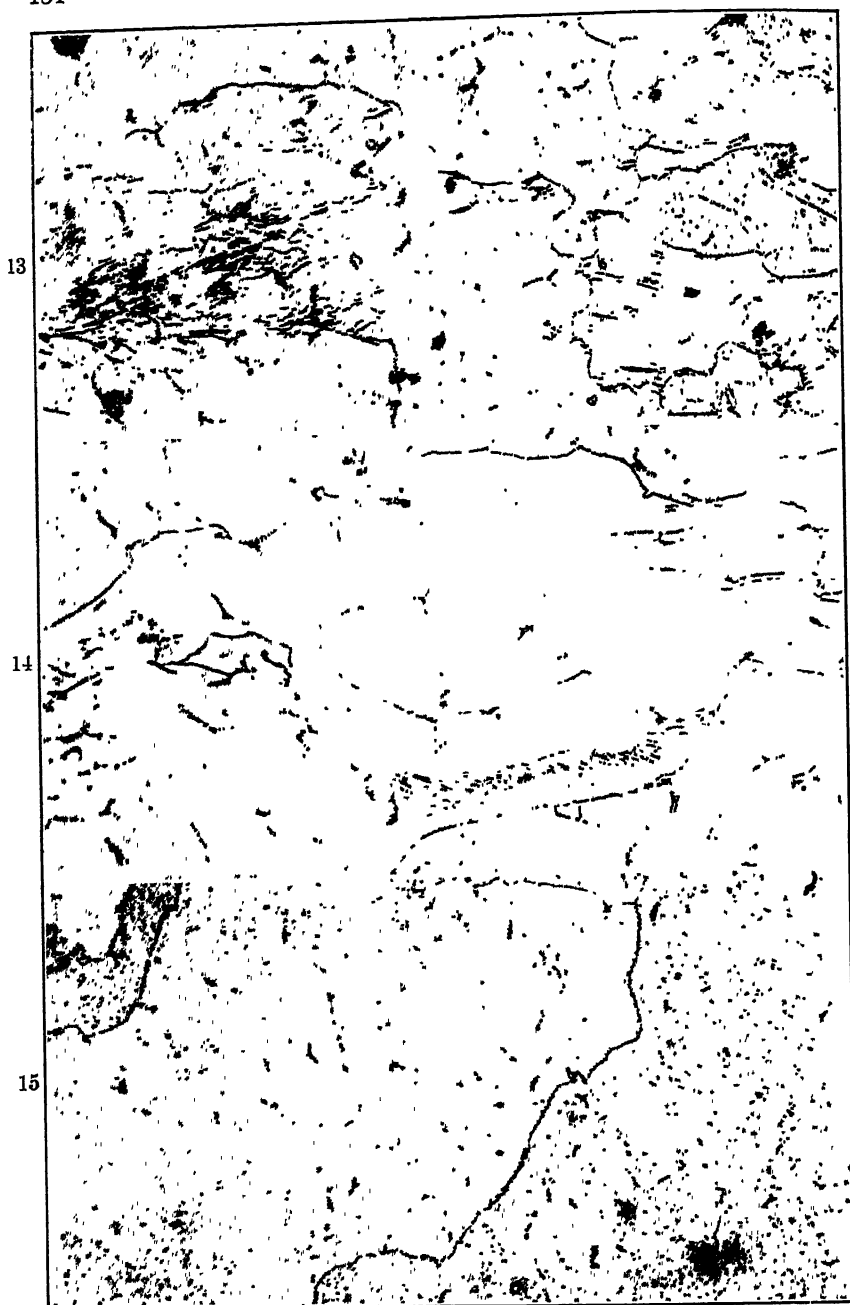


FIG. 13.—SAME AS FIG. 9, REDRAWN 400° C.
FIG. 14.—SAME AS FIG. 9, REDRAWN 450° C.
FIG. 15.—SAME AS FIG. 9, REDRAWN 500° C.
× 100. Etch, sulphuric dichromate.

slip bands. Possibly these few were lower in quantity of the precipitated phase due to possible nonhomogeneity of the solid solution retained by the quench.

Although in the samples studied there was no indication of any recrystallization from the cold-work involved in the double aging, there did appear to be local segregations of precipitate in a faint tracing of an incomplete secondary network in samples with a secondary aging at 400°, 450° and 500° C. (Figs. 13, 14, 15). This was accompanied by a decrease in hardness and tensile properties, as might be expected. This coalescence of the precipitated phase was accompanied also by a slight increase in the electrical conductivity.

The photomicrographs of the cast, quenched, and precipitation-hardened conditions (Figs. 5, 6, 7) show the expected structures.

Physical Properties.—The alloy, cold-worked after complete precipitation-hardening, yields appreciably better physical properties than it possesses in the cold-worked-between-quench-and-draw condition. Double aging at 100° C. develops the tensile properties and hardness to a maximum accompanied by a slight decrease in the electrical conductivity. The unusually high proportional limit is maintained up to a secondary aging temperature of 300° C.

The properties developed by double aging are superior to those developed by cold-work between the quench and the draw up to a secondary aging temperature of 400° C., above which they become inferior.

The tensile strength and proportional limits show regular variations with the increase in the secondary aging temperature, whereas the elongation, hardness and electrical conductivities exhibit minor vagaries that remain unexplained at this time.

GENERAL CONCLUSIONS

1. An alloy of 2.6 per cent Co, 0.4 Be, 97 Cu is cited as a typical precipitation-hardening alloy combining high proportional limit, ductility and hardness with unusually high electrical conductivity, 50 per cent of that of copper. No practical improvements of considerable degree are effected in the physical properties of this alloy by cold-working between the quench and the draw and cold-workability is very limited after the alloy is completely precipitation-hardened.

2. Double aging with intermediate straining is defined, for the purposes of this publication, as distinct from simple precipitation-hardening.

3. The effects of double aging of high-speed steel are cited as a probable example of double aging with an intermediate thermal strain.

4. The simple precipitation-hardening of an alloy of 0.4 per cent Cr, 0.1 Be, 99.5 Cu alloy is described. As a heat-treated casting alloy, this composition combines good tensile properties with an electrical conductivity of 75 per cent of that of copper.

5. The tensile properties of the Cu-Cr-Be alloy are markedly improved by cold-working between the quench and the precipitation reheat.

6. The tensile properties of the Cu-Cr-Be alloy are still further improved by a double-aging treatment, including a cold reduction, between the two reheats following the solution quench. By this means, for example, a proportional limit of 35,000 lb. per sq. in. and good ductility are combined with an electrical conductivity of about 70 per cent of that of copper.

7. The room-temperature properties of the two copper alloys are unusually stable for reheat temperatures up to 400° to 500° C.

8. The investigation was chiefly concerned with the variation of physical properties for treatments that result in maximum hardness, or its retention, in the alloys cited. It is evident that, in many precipitation-hardening alloys, the precipitation reaction may be subject to accurate control to produce specific combinations of physical properties as may be desired.

ACKNOWLEDGMENTS

The writer is deeply indebted to the following metallurgists and engineers of the General Electric Co.: L. L. Wyman for the photomicrographs; J. E. Erb for the data concerning the double aging of high-speed steel; G. R. Brophy, C. H. Hannon, F. G. Benford, E. H. Horstkotte, F. M. Kirkpatrick, E. R. Spittler, W. B. Kruse, R. G. Thompson, D. Basch, and others for developmental and application work; and to Mr. T. S. Fuller for advice and consultation. The fine cooperation of Mr. R. J. Wheeler, chief metallurgist of the Riverside Metal Co., in the processing of the copper alloys is also deeply appreciated.

DISCUSSION

(E. R. Darby presiding)

E. E. SCHUMACHER,* New York, N. Y.—In the telephone industry, binary and ternary alloys of beryllium are utilized in limited amounts in special applications where their superior properties justify their use despite the higher cost. These uses would undoubtedly be extended if the cost of the alloys could be considerably reduced. We would, for example, be interested in a nonferrous alloy in the cost range of brass and phosphor bronze with tensile strengths of the order of 150,000 lb. per sq. in. and an electrical conductivity of from 35 to 40 per cent of that of copper. This cost condition would be difficult to meet at present for alloys containing beryllium, but I wonder if Mr. Harrington in his studies has found any of the copper-cobalt-beryllium alloys possessing the properties I have mentioned and costing considerably less than the 2.25 per cent beryllium-copper alloy now in general use.

R. H. HARRINGTON.—Mr. Schumacher has emphasized tensile strength and electrical conductivity. We have come to depend more upon the electrical conductivity and the *proportional limit* for our uses. The alloy of 2.6 Co, 0.4 Be, 97 Cu will give a proportional limit of 45,000 to 50,000 lb. per sq. in. and an electrical conductivity of 45 to 55 per cent of that of copper. Thus this alloy is about equivalent to the

* Metallurgist, Bell Telephone Laboratories.

standard 2.25 per cent Be-Cu alloy in the matter of proportional limit; it is superior in conductivity and appreciably lower in cost. The alloy of 0.4 per cent Cr, 0.1 per cent Be, 99.5 per cent Cu combines a proportional limit of 35,000 lb. per sq. in. with an electrical conductivity of 70 per cent of that of copper and its cost is only a little more than that of phosphor bronze as compared to the standard 2.25 per cent Be-Cu alloy.

B. W. GONSER,* Columbus, Ohio.—Several years ago Dr. van Wert (Harvard University) and I did some similar work on copper-nickel-silicon alloys. We found the same general reaction to a double aging treatment. After normal precipitation-hardening, then strain-hardening by cold-work, we found that appreciable further hardening would result on reheating between 200° and 300° C. This was reported in the December 1934 issue of *Metals and Alloys*.

R. H. HARRINGTON.—It is planned in the future to correlate the few references in the literature on double aging with more new data with the hope of establishing a practical theory for the phenomena.

J. L. CHRISTIE,† Bridgeport, Conn.—I can add nothing to the meat of this paper. I should like to ask one question about strain-hardening. It comes down to a question of just what we mean by strain-hardening and I am really looking for information.

Is not "cold-work hardening" a better term than strain-hardening? To me the term "strain" implies only that part of the deflection or deformation that is accompanied by stress in the metal. For instance, while a piece of metal is being rolled, the external forces produce stresses in the metal and corresponding strains. As the metal leaves the rolls, there is a slight elastic recovery resulting in a complete or partial reduction of stress and of corresponding strain. The metal remains in the cold-worked condition, however, and it is the amount of cold-work that determines the hardening effect of the operation, and not any residual stress and strain. Am I correct in this conception?

R. H. HARRINGTON.—I believe that "cold-work hardening" is not a better term than "strain-hardening" because they are not synonymous: strain-hardening is always a part of cold-work hardening but cold-work hardening includes also the effects of plastic deformation along slip planes as well as the attendant elastic "strain-hardening" of the areas (usually solid solution) along and between the affected slip planes. These areas are affected by stress gradients or the setting up of internal pressures and tensions of elastic nature but permanent in cold-worked material until the temperature is raised sufficiently to accomplish the "strain anneal" usually at a temperature somewhat below the temperature of recrystallization. It might be that "stress-hardening" would be a better term than strain-hardening if it were generally adopted.

Consider, then, Mr. Christie's example of a piece of metal being rolled. The factors involved in altering the nature of the material between the rolls are three in number: (1) plastic deformation along certain slip planes; (2) elastic strain gradients of the areas along and between the affected slip planes; (3) elastic deformation of the cross section of the piece between the rolls. As the material leaves the rolls, the constraining forces of the rolls are removed from the material cross section, thus eliminating factor 3 and leaving factors 1 and 2 to constitute the cold-work hardening of the metal.

In double aging, it appears that factor 2 determines whatever additional changes may take place.

* Battelle Memorial Institute.

† Metallurgist, Bridgeport Brass Co.

E. M. WISE,* Bayonne, N. J.—The term “proportional limit” has been used here. How has that been defined? What was the sensitivity of the extensometer? In other words, why should that indicate the value to such a large extent?

R. H. HARRINGTON.—All of our proportional limits are determined with the Sayre extensometer. This is probably the most sensitive type of practical instrument and we are well satisfied with the consistent and reproducible results from its use. The use of a standardized “proof stress” is also very satisfactory but perhaps not absolutely indicative of the property of elasticity. This is because different compositions and different heat-treatments result in varying the rate of curvature of the plastic deformation from the straight line of practical elasticity. The proof stress involves this difference in curvature while the proportional limit, accurately determined in a practical test, denotes the limit of practical elasticity beyond which practically measurable plastic deformation takes place.

* Assistant Manager, Research Laboratory, The International Nickel Co.

Notes on Etching and Microscopical Identification of the Phases Present in the Copper-zinc System

By J. L. RODDA,* MEMBER A.I.M.E.

(Cleveland Meeting, October, 1936)

A large amount of time has been devoted to the microscopical study of the copper-zinc alloys, emphasis naturally being placed upon the commercially important alloys of the system. Suitable methods are available for microscopically recognizing the two phases richest in copper,

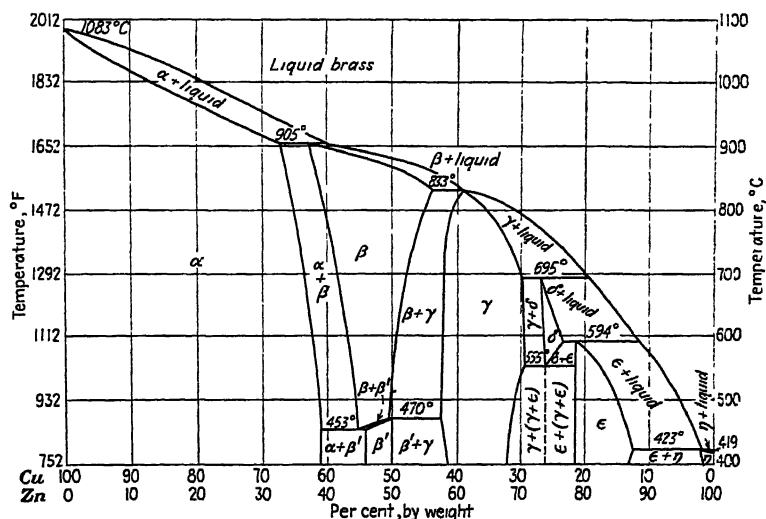


FIG. 1.—COPPER-ZINC EQUILIBRIUM DIAGRAM. (From *National Metals Handbook*, 1933.)

but none appear to have been developed for the positive identification of the other phases. This is, however, accomplished, for the phases normally encountered, by an electrolytic method described in the following pages.

Five phases of the copper-zinc diagram (Fig. 1) are considered for the purpose of this paper: the solid solution of zinc in copper, alpha (α); the intermediate phases, beta (β), gamma (γ), and epsilon (ϵ); and the solid solution of copper in zinc, eta (η). Beta prime is not considered a separate

Manuscript received at the office of the Institute June 26, 1936.

* Investigator, Metal Section, Research Division, The New Jersey Zinc Company, Palmerton, Pa.

phase, since, according to Phillips and Thelin¹, it is probably not a true polymorphic modification of beta. Delta is stable only between the temperatures of 555° and 695° C., and has not been observed in this work.

Identification of Alpha and Beta.—Unstained alpha and beta are easily recognized by their natural colors. The color of alpha varies under the microscope, according to zinc content, from that of pure copper to what may be described as a light flesh color. Beta is pure lemon yellow. The other phases are all white and identification by color is not possible.

Identification of Gamma, Epsilon and Eta.—In some early work (1928) on annealed copperplated zinc, mixtures of Superoxol (30 per cent H₂O₂) and ammonia were partially successful in developing the structure of the alloy layers. Attention was therefore turned to this reagent as a possible means of identifying the white copper-zinc phases. It was found that

the staining that occurred could be somewhat reduced by pouring a mixture of one part of Superoxol and five parts of ammonia over the specimen; washing; rinsing in a 17 per cent solution of chromic anhydride (200 grams CrO₃, 1000 c.c. H₂O), then washing in running water. The chromic rinse reduces staining somewhat but does not etch the specimen. Where staining does not occur, this etchant reveals the alloy layers (Fig. 2). When tried upon specimens containing but one or two phases, however, the action was found to depend upon the associated phases, even when various proportions of Superoxol and ammonia were used.

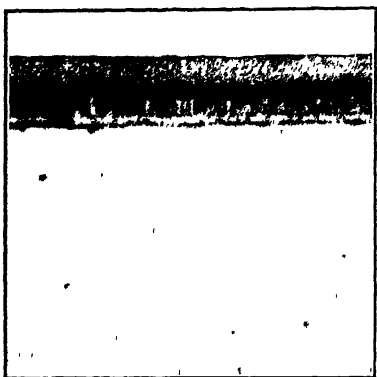


FIG. 2.—COPPERPLATED ROLLED ZINC CONTAINING ONE PER CENT OF COPPER, ANNEALED 21 MONTHS AT 40° C. X 500.

Etched with 1 part Superoxol + 5 parts ammonia. Rinsed in 17 per cent CrO₃.

Although this (as well as Vilella's reagent², which was also tried) is useful in developing the microstructures of known alloys, it does not help in identifying the white phases. Etching methods were therefore sought to make this identification possible.

Electrolytic etching in a 17 per cent aqueous solution of chromic anhydride was found to be a positive means of distinguishing between gamma and epsilon. The polished specimen is made the anode while a small coil of platinum wire in the bottom of the dish or beaker serves as the cathode. The specimen is connected to the source of current before immersion in the etching solution³. At 1.5 amp. per square inch, gamma

¹ A. Phillips and L. W. Thelin: An X-ray Study of the Beta Transformation in Copper-Zinc Alloys. *Jnl. Franklin Inst.* (1927) 204, 359-368.

² J. R. Vilella: Delving into Metal Structures. *Iron Age* (1926) 117, 834-836.

³ The apparatus finally adopted for this work consisted of a 12-volt storage battery, connected through a rheostat and ammeter to the specimen. The specimen

and epsilon are about equally attacked. At higher current densities⁴, gamma is preferentially attacked; at lower current densities, epsilon is

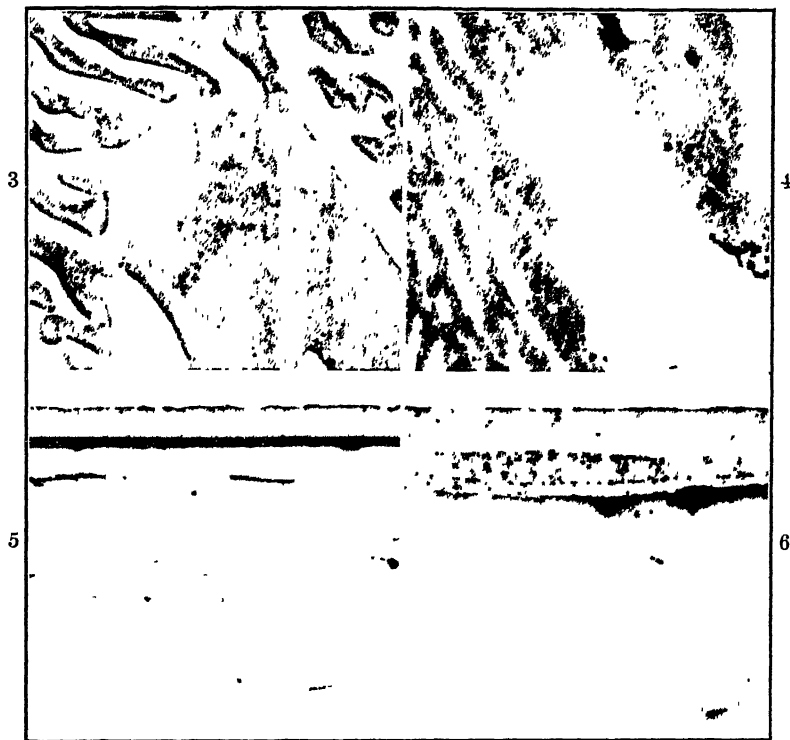


FIG. 3.—27.2 PER CENT CU + ZN, SLOWLY COOLED FROM MELT.

Anodically etched in 17 per cent CrO_3 at about 5 amp. per sq. in. for 5 seconds. Gamma (dark) + epsilon (light).

FIG. 4.—SAME AS FIG. 3.

Anodically etched in 17 per cent CrO_3 at about 0.4 amp. per sq. in. for 10 seconds. Gamma (light) + epsilon (dark).

FIG. 5.—COPPERPLATED ROLLED ZINC CONTAINING 1 PER CENT CU ANNEALED 2 YEARS AT 40°C .

Anodically etched in 17 per cent CrO_3 at about 5 amp. per sq. in. for 3 seconds.

FIG. 6.—SAME AS FIG. 5 ANNEALED 3 YEARS AT 40°C .

Anodically etched in 17 per cent CrO_3 at about 0.4 amp. per sq. in. for one minute.

All $\times 500$.

preferentially attacked. The recommended procedure for identification is as follows:

Polish, and etch anodically at 5 amp. per sq. in. Gamma, if present, will be attacked, but epsilon will not be attacked. Repolish, and etch at

was grasped with a pair of crucible tongs, which are permanently connected to the positive side of the battery. The separation between the platinum wire cathode and the specimen was generally about one inch. The resistance of the solution was then about one ohm.

⁴ Current densities over about 10 amp. per sq. in. were not tried in this work.

1 amp. per sq. in. (Current densities less than 0.4 amp. per sq. in. are not recommended, because of uneven etching.) The effects will be reversed (Figs. 3 and 4). The reversal serves as a positive identification. No confusion with eta (η), the solid solution of copper in zinc, should occur, since it is attacked under both conditions.

The effect of anodic etching at high current densities in 17 per cent CrO_3 on annealed copperplated rolled zinc, containing 1 per cent copper, is shown in Fig. 5. Four phases are visible, alpha, gamma (dark due to strong etching), epsilon, and eta (the base material). The effect of low current density on this same specimen is shown in Fig. 6. The four first mentioned phases are again visible, but epsilon, which is etched this time, is seen to be made up of two layers. A faint line, indicating the double layer, will also be seen in Fig. 5, and the effect is quite marked in Fig. 2. The reason for the double layer is not understood, although it is possible that one layer may indicate diffusion of copper into zinc, the other of zinc into copper. The beta phase has not been observed microscopically on this type of specimen, although X-ray studies by M. L. Fuller, of this laboratory, on similar material have revealed its presence along with the other four phases. It seems that the amount of beta formed must be very small, since the structure of alpha-beta brasses is nicely revealed by this etching method (although on pure alpha brass grain boundaries are not well developed).

DISCUSSION OF RESULTS

At low current densities the five phases are attacked roughly in the order of their zinc contents. At high current densities, epsilon is not attacked. The suggestion is made that this reversal may be explained by a selective polarization of epsilon at high current densities.

Electrolytic methods of etching deserve wider application than they have enjoyed in the past. G. A. Ellinger⁵, working in the National Bureau of Standards, has found electrolytic etching in oxalic acid a superior method of developing stainless-steel structures. A mild reagent, oxalic acid, is used instead of strong mixed acids, which are difficult to handle. W. A. Mudge⁶ has recommended electrolytic etching for obtaining contrast with nickel. In the present work, a high-copper phase (gamma) may be etched in the presence of high-zinc phases (epsilon and eta). Other problems that might possibly be solved by electrolytic etching with a suitable reagent suggest themselves. It is difficult to etch steel structures adjacent to a galvanized coating, because of the strong reactivity of the coating. Etching of nickel or chromium plate on zinc

⁵ G. A. Ellinger: Oxalic Acid as an Electrolytic Etching Reagent for Stainless Steels. *Trans. Amer. Soc. for Metals* (1936) 24, 26-35.

⁶ W. A. Mudge: Etching Solutions for Nickel and Nickel Alloys. *National Metals Handbook* (1933) 1360-1361.

is almost impossible, owing to the strong selective etching action on zinc. It is for such problems as these that electrolytic etching may provide an answer.

SUMMARY

The alpha and beta phases of the copper-zinc system are easily identified by their distinctive colors. A method has been described whereby gamma and epsilon may be identified by anodic etching in 17 per cent CrO_3 . At current densities over 1.5 amp. per sq. in., gamma is attacked, epsilon not attacked. At low current densities the reverse is true. Eta is attacked under both conditions. Positive identification of the five important phases is thus secured.

The flexibility of electrolytic etching as a method and its possible wide application are stressed.

ACKNOWLEDGMENT

Acknowledgment is made to Mr. D. C. Jillson, who was responsible for the preparation of the alloys used in checking these tests.

An Investigation to Develop Hard Alloys of Silver for Lining Ring Grooves of Light Alloy Pistons

By CLAUD GUENTER GOETZEL*

(New York Meeting, February, 1937)

THE object of this investigation was to determine whether silver alloys could be used instead of the currently employed insert of high-expansion

	AVERAGE COEFFICIENT PER DEG. C. OVER RANGE 20° to 200° C.
Pure aluminum.....	24.6×10^{-6}
Cast low-expansion Si-Cu-Ni-Al piston alloy.....	20.0×10^{-6}
High-expansion austenitic Cu-Ni cast iron	19.3×10^{-6}
Cast steel (0.25-0.35 C, 0.40-1.0 Mn).....	12.6×10^{-6}
Cast iron (3.15 total C, 2.16 Si)....	12.8×10^{-6}
Pure silver.....	18.9×10^{-6}

austenitic ferronickel alloy, to reduce the wear of ring grooves in light metal pistons. A typical example of a piston containing a ferronickel insert is shown in Fig. 1. The high coefficient of expansion of silver made it worthy of consideration, while the small size of the insert would render its use feasible in Germany as an emergency measure.



FIG. 1.—PISTON CONTAINING FERRONICKEL INSERT.

The coefficients of linear expansion of several metals and alloys are as shown in the table above.

Obviously the melting point of the insert must be high enough to prevent it from melting when the light alloy is cast around it. This imposes a lower limit of about 850° C. for the solidus of the silver alloy. Pure silver melts at about 961° C., so that the tolerable depression in the solidus is rather small. To avoid deformation of the insert during use a Brinell hardness number of at least 60 appears necessary.

Manuscript received at the office of the Institute Oct. 1, 1936. Extract from a report of work done by the author at the Institut für Angewandte Metallkunde of the Technische Hochschule, Charlottenburg, Berlin, Germany, under Prof. W. Guertler and Prof. L. Dreibholz.

* Metallurgist, Hardy Metallurgical Co., New York, N. Y.

Fig. 2 depicts the alloying behavior of silver with a number of metals. The solid areas correspond to solid solution ranges at low temperatures while the crosshatched areas represent the solid solution ranges at high temperatures. The dotted areas correspond to regions of heterogeneity and the clear areas to gaps in miscibility. An examination of this dia-

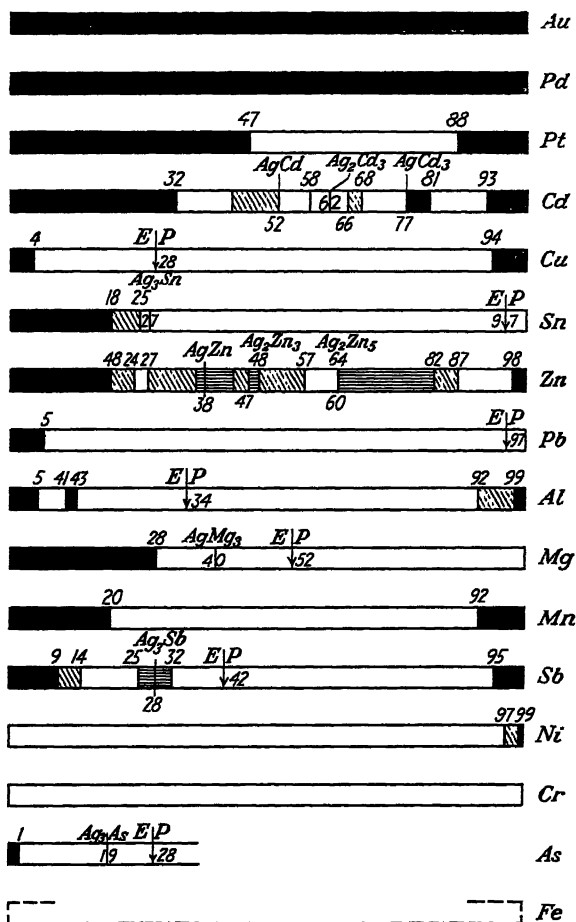


FIG. 2.—ALLOYING BEHAVIOR OF SILVER WITH VARIOUS METALS.

gram suggests that the magnesium, manganese and antimony offer promise. Therefore the binary magnesium-silver, manganese-silver alloys, ternary alloys based on manganese-silver and antimony-silver, and quaternary alloys based on manganese-silicon-silver alloys were studied.

EXPERIMENTAL PROCEDURE

All of the metals employed except the manganese (98.5 per cent) and chromium (98 per cent) were at least 99 per cent pure. Melts ranging in

weight from 40 to 160 grams were made in sand or porcelain crucibles protected with suitable fluxes. Some were cast into a small iron mold while the remainder were permitted to solidify in the crucible. The melting was done in granular, gas and high-frequency furnaces. The heating and cooling curves were obtained with a Pt-Rh Pt thermocouple.

Brinell hardness measurements were made on ground surfaces employing a 5-mm. ball, 250-kg. load and 30-sec. loading.

EXPERIMENTAL RESULTS

Magnesium-silver.—The liquidus and solidus of the silver-rich alloys as determined by W. Guertler* and the Brinell hardness values obtained in the present investigation are presented in Fig. 3. The hardening effect increases rather rapidly with the magnesium content and is about 60 for the 7 per cent alloy and about 115 for the 10 per cent alloy. The solidus temperature of the alloy containing 7 per cent Mg is about 770° C. which is lower than desirable. The castability, ductility and machinability of the alloys containing up to 10 per cent Mg are satisfactory.

Manganese-silver.—Manganese apparently forms solid solutions with silver up to about 20 per cent Mn; beyond this a wide

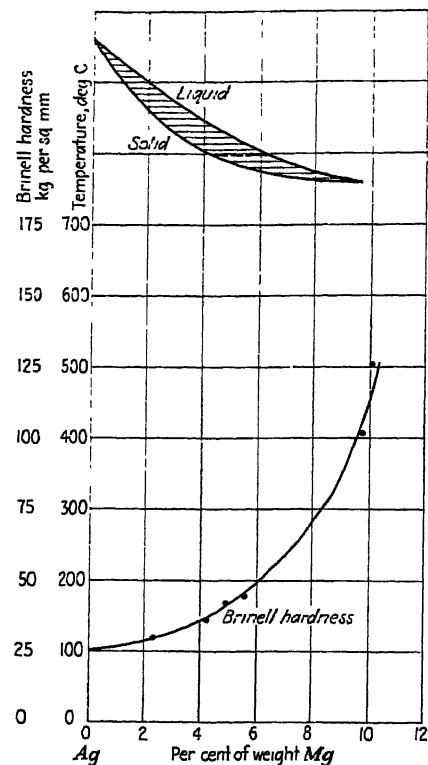


FIG 3.—LIQUIDUS AND SOLIDUS OF SILVER-RICH ALLOYS DETERMINED BY GUERTLER, WITH HARDNESS VALUES OBTAINED BY AUTHOR.

gap in miscibility occurs. In the solid solution range only a slight change occurs in melting point. Alloys containing 10 and 15 per cent Mn cast well, could be rolled and machined. The latter alloy had a hardness of but 40.9, which is less than that required. The 20 per cent alloy was only moderately ductile and machinable, owing to lack of miscibility, which may have been due to impurities in the manganese.

Ternary Alloys Based on Manganese Silver. *Manganese, Magnesium and Silver.*—Two alloys containing 15 per cent Mn and 0.2 and 1 per cent Mg were prepared. Their castability was fair, machinability and ductil-

* W. Guertler: *Ztsch. Metallkunde* (1927) 19, 68.

ity good, but their structure was duplex. The solidus was estimated to be about 960° C. The hardness of the 0.2 Mg alloy was 47 and that of the 1 per cent alloy was 49, both too low for the requirements.

Manganese, Aluminum and Silver—One alloy containing 15 per cent Mn and 5 per cent Al was prepared. The pouring properties were bad, the machinability and ductility moderate. The structure showed a lack of miscibility. The solidus was estimated to be about 900° C. while the Brinell hardness was 53.6.

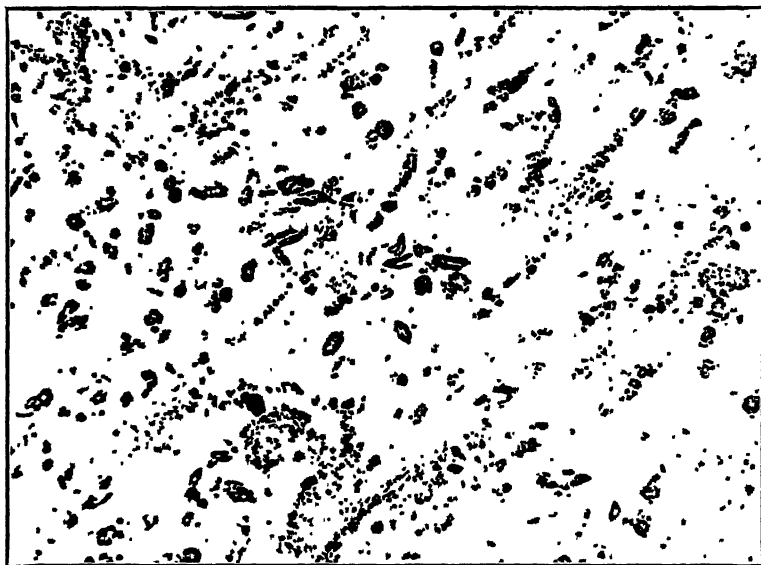


FIG. 4.—SILICIDES IN MANGANESE-SILICON-SILVER ALLOY. $\times 150$.

Manganese, Zinc and Silver.—One alloy containing 15 per cent Mn and 2 per cent Zn was made. The castability, machinability and ductility were good. The alloy was a solid solution, of which the solidus was estimated to be about 930° C. The Brinell hardness was 41.5.

Manganese, Silicon and Silver.—An attempt was made to secure higher hardness by producing alloys containing manganese silicide. Alloys containing 15 per cent Mn with 1 and 3 per cent Si and one with 11 per cent Mn and 1.5 Si were made. The first was a solid solution free from silicides, but poured well and was ductile and machinable. The second contained silicides but showed a lack of miscibility and its other properties were unsatisfactory. The third alloy contained silicides as shown in Fig. 4, and possessed good castability, machinability and ductility. The solidus was estimated to be about 960° C. The hardness of the latter alloy was 57.3 as cast and 58.5 when cooled in the crucible.

Quaternary Alloys Based on Manganese, Silicon and Silver.—Attempts were made to prepare alloys containing 11 per cent Mn, 1.5 per cent Si,

with 1.5 per cent Fe and 1.5 per cent Cr, respectively. Both were wholly unsatisfactory, owing to lack of miscibility.

Ternary Alloys Based on Antimony-silver.—The addition of antimony to silver causes a rapid depression in solidus temperature, whereas the effect of zinc is milder. A ternary alloy containing 14 per cent Sb, 12 per cent Zn, had a hardness of 56.8, but the melting point was only 450° C.

Cadmium depresses the melting point of silver less rapidly than does zinc, so that some possibility existed in alloys containing it. Alloys containing 20 per cent Cd and 5 per cent Sb and alloys containing 10 per cent Cd and 7.5 per cent Sb were made. Both showed good casting and physical properties. The hardness of the former was 54.4 when cast into a warm mold and 87.3 when cast into a cold mold, while the latter alloy had a hardness of 59.6. The liquidus of the 20 per cent Cd, 5 per cent Sb alloy was about 880° C. and the solidus in the neighborhood of 720° C. The corresponding data for the 10 per cent Cd, 7.5 per cent Sb alloy were 855° and 700° C.

CONCLUSIONS

While none of the alloys possessed the properties required, it is thought that the data may be of some interest in other connections. The manganese-silver and cadmium-antimony-silver alloys showed properties approaching those desired.

Lead Coating of Steel

By J. L. BRAY,* MEMBER A.I.M.E.

(New York Meeting, February, 1937)

LEAD has often been suggested as a protective coating for iron and steel. Such a protective coating should possess: (1) good adhesion, (2) durability, (3) ease of application, (4) freedom from pinholes, (5) good appearance and (6) low cost, but, unfortunately, lead coatings so far produced do not have all of these characteristics. Because of the necessity of carrying out the coating process cheaply, and because lead solutions have poor plating characteristics, most of the efforts have been directed toward the hot-dipping process rather than electroplating.

The hot-dipping processes using lead have not been successful chiefly because of the lack of adherence between iron and lead. In any coating process involving iron a bond can be obtained only by the formation of an intermetallic compound, the formation of a solid solution, or mechanical means. Lead forms with iron two immiscible liquid solutions, and in the solid state no intermetallic compounds or solutions. It is necessary, therefore, to employ some other element or elements as a binding agent. Tin may be used as in terneplate, or copper in the form of a thin film of electrolytically deposited metal to which the lead will adhere.

Because of its physical and chemical properties, lead as a coating medium would undoubtedly be limited in its use to sheet and wire and then only when the article is not subject to abrasion or wear. A very large tonnage of these products is being used under such conditions and a successful lead-coating process should be a valuable contribution to the science. Two other difficulties stand in the way of successful lead coating—that of poor appearance of the weathered surface and the tendency of the lead to form pinholes during solidification. Since lead is commonly accepted as cathodic to iron, these exposed areas are ones of accelerated corrosion.

Use of Zinc.—The method under consideration involves zinc as a binding agent on both the steel sheet and in the molten bath. This

A part of the work described was done as a thesis in partial fulfillment of the requirement for the degree of Doctor of Science from the Massachusetts Institute of Technology. Manuscript received at the office of the Institute Nov. 27, 1936.

* Head, School of Chemical Engineering, Purdue University, Lafayette, Ind.

method has often been suggested, and tried before, but these methods have all been unsuccessful because of the rough surfaces obtained as well as the presence of pinholes. The writer proposes to show that this failure has been caused by a lack of knowledge of the fundamentals involved in the coating process.

Lead-zinc Equilibrium Diagram.—Preliminary experiments cast some doubt on the accuracy of the commonly accepted lead-zinc equilibrium diagram. The eutectic composition of this system has been determined by various investigators as 0.74, 1.2, and 2.3 per cent Zn. This is at variance with the writer's experience in lead refining where desilver-

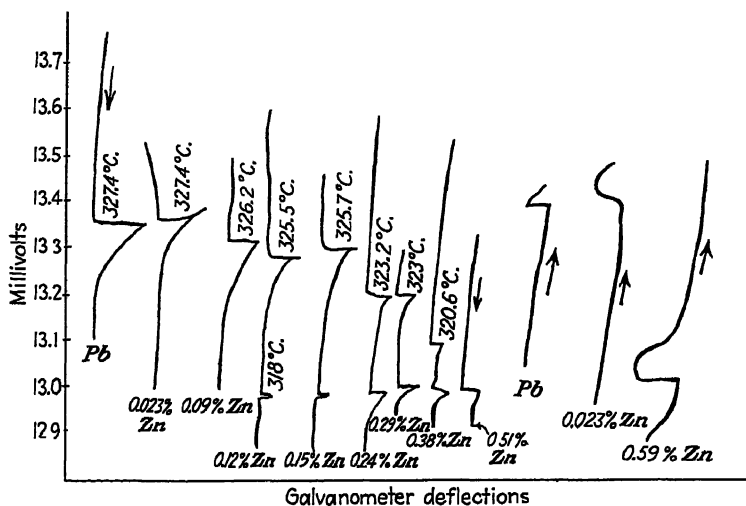


FIG. 1.—TYPICAL COOLING CURVES OF MATERIALS USED IN EXPERIMENTS ON LEAD COATING OF STEEL.

ized lead, saturated with zinc at its melting point, will consistently contain about 0.55 per cent Zn.

In order to verify this diagram a series of alloys was made up from pure materials, using specially prepared electrolytic lead and zinc¹. The zinc was determined, in triplicate, by the phosphate method. Thermal analyses were very carefully carried out by the differential cooling method using three thermocouples in series. Care was taken to prevent oxidation by passing a reducing gas through the melting system. Typical cooling curves are shown in Fig. 1 and photomicrographs in Figs. 2 to 7. Fig. 3 shows the first appearance of the lead-zinc eutectic around the grain boundaries, Fig. 5 considerable amounts of this eutectic and in Fig. 6 an alloy close to the eutectic composition. Fig. 7 shows the large needles of excess zinc. Incidentally, because of their extreme softness, great difficulty was experienced in preparing the specimens for

¹ J. M. Hodge and R. H. Heyer: *Metals and Alloys* (November, 1931) 297.

FIGS. 2-7.—LEAD AND LEAD-ZINC ALLOYS. $\times 100$.

Fig. 2, pure lead.

Fig. 3, 0.06 per cent Zn.

Fig. 4, 0.08 per cent Zn.

Fig. 5, 0.17 per cent Zn.

Fig. 6, 0.55 per cent Zn.

Fig. 7, 1.30 per cent Zn.

microscopic examination. Samples were cut vertically from the ingots by a sharp, oiled hack saw. They were then ground on numbers 1, 0 and 00 French emery papers using a solution of paraffin in kerosene as a lubricant. They were then cleaned with alcohol and naphtha, and rough-polished on felt or broadcloth wheels using a fairly coarse suspension of levigated alumina in distilled water containing a few drops of liquid soap. This polishing was continued until all emery particles were removed from the surface of the metal. This required from fifteen minutes to half an hour or more. A black smudge, which forms first, must be entirely removed by the end of this process so that the surface has the appearance of a roughly polished piece of steel. After washing,

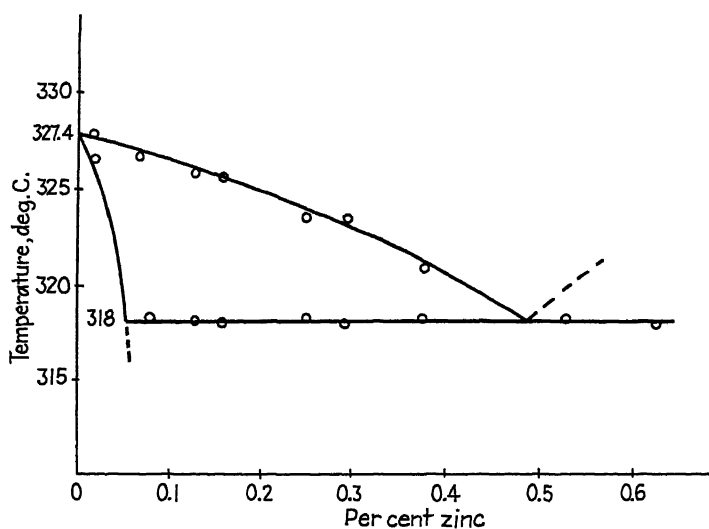


FIG. 8.—EQUILIBRIUM DIAGRAM OF LEAD-RICH LEAD-ZINC ALLOYS.

the specimens were polished on a silk-velvet wheel using a very fine suspension of alumina in a soap solution. Very light polishing pressure had to be used to prevent further smudging. When the scratches were apparently removed the following etchant was used: glycerin, 60 cc.; glacial $\text{HC}_2\text{H}_3\text{O}_2$, 20 c.c.; concentrated HNO_3 , 20 c.c. It should be made up fresh for best results. Excessive dilution of the etching reagent with water must be avoided. By repeated polishing and etching the structures of the alloys were clearly brought out as shown in the preceding photomicrographs.

The lead-rich end of the new diagram, as indicated by the data above, is shown in Fig. 8. It differs from the old one in the presence of a solid solution containing up to 0.05 per cent Zn and a more accurate determination of the eutectic proportions. The function and importance of the solid solution, heretofore unrecognized, will be discussed later.

Dipping Experiments.—A small sheet-dipping machine, similar in principle to those employed in conventional galvanizing, in which sheets 4 in. wide and 20 in. long were employed was constructed for these experiments. It was heated by resistance units clamped to the outside of the tank and the temperature of the bath automatically controlled. A great deal of difficulty was encountered in adapting this to the experiments because of:

1. Crusting of the bath, which interfered with the driving gears.
2. Difficulty in preparing and maintaining a proper working surface on the stripping rolls.
3. Difficulty in maintaining the molten bath at the proper composition with intermittent operation.

The importance of these factors was early recognized for it was found that successful coating could be carried out only over a relatively narrow range of composition and temperature. Variations in zinc content are brought about by (1) diffusion of zinc from the zinc-coated sheet to the bath, (2) volatilization from the flux bath, (3) drossing

Diffusion of Zinc.—A careful determination was made of the rate of diffusion of zinc from sheets, electrolytically coated with zinc, to the bath under conditions to be met with in practice. This was found to be of the order of 0.015 gram per sq. in. of sheet with an immersion of 30 sec. In plant operation this would probably be more than sufficient to maintain the zinc content of the bath at the proper point, but in these experiments, because of oxidation and volatilization, it was not. The necessity for maintenance of the zinc content has already been referred to. It was necessary to devise some method by which the zinc could be rapidly determined, since precipitation as the phosphate was too time-consuming. The method finally adopted was one using the electrical resistance, since the specific resistances of zinc and lead at 20° F. are very different, being, respectively, 5.8 and 22.0 ohms per cm. cube. Samples were cast in chilled molds in the form of slugs 4 in. long by $\frac{1}{2}$ in. in diameter. These were inserted in the chamber of a special extrusion apparatus, which was placed in an ordinary tensile machine. A section about $\frac{1}{4}$ in. in diameter was extruded at the rate of about 12 in. per minute. At first hopes were held of using the total pressure on the plunger as a measure of the zinc content, since this varied almost linearly with the zinc content but the method proved to be not sensitive enough. As soon as the lead wire had cooled to room temperature it was placed in a modification of the bridge used in measuring the conductivity of copper wire, and the conductivity was determined. Careful measurements of a series of alloys of which the zinc content had been determined by gravimetric analysis furnished a curve from which the composition of the alloy in question could be estimated. The accuracy of this method is indicated in Table 1.

The total elapsed time from the taking of the sample to the estimation of the zinc need not exceed 25 min., as compared with 3 to 6 hr. using the gravimetric method. In this way the composition of the bath can be kept within the narrow limits required.

TABLE 1.—*Estimation of Zinc Content*

Alloy No.	Per Cent Zinc Predicted	Per Cent Zinc by Analysis
545-2	0 38	0.38
546-2	0 61	0 65
547-2	0 71	0.72
549-2	1 00	0 98
550-2	1 28	1.31
551-2	1 46	1.51

Coating Experiments.—Nearly 300 runs were made over a period of two years, in which the bath composition, bath temperature, flux composition, construction and composition of the stripping rolls, sheet speed, stripping-roll pressure, etc. were varied. Within the narrow range of temperature and composition referred to smooth, adherent coatings of lead could be obtained. It was possible to produce, under certain conditions, a particularly attractive sheet with a spangle similar to that obtained in galvanizing, but not, of course, to so pronounced a degree.

Coating of Wire.—This method of coating was also extended to wire on a semicommercial scale. By modifying the method commonly used in galvanizing, much less difficulty was experienced in coating the wire.

Corrosion Tests.—In order to determine the relative life of these lead coatings under the commonly accepted testing conditions, a large number of tests were run with the salt spray and Weatherometer. Samples have also been under atmospheric exposure in racks for three years at Key West, Galveston and a seaside location in Maine. The details of these tests are omitted, because there appears to be a lack of correlation between such tests and actual atmospheric weathering. Suffice it to say that in no test, save with wire, or sheet purposely made under poor conditions, was the life of the article less than that of a control sample of high-grade galvanized stock, and frequently it was 40 to over 100 per cent longer.

Function of the Zinc.—Because of the differences in hardness between the various alloy layers, great difficulty was experienced in examining the coatings at high magnification. Figs. 9 and 10 are typical of these sections. The binding agent is undoubtedly the needles of zinc (Fig.

11)² which can attach themselves to the lead through a solid solution of zinc in lead, and to the sheet that has been previously coated with zinc,



FIGS 9-10.—TYPICAL COATINGS. $\times 500$.

Fig. 9, iron-zinc contact. Steel base, top left; zinc along the bottom.

Fig. 10, zinc-lead contact. Steel base at top; zinc in middle and lead at bottom.

by a series of solid solutions of the zinc-iron intermetallic compound in zinc. There will obviously be a limiting size to these needlelike particles, which will in turn be determined by the composition and

* From U. S. Patent 1948505.

temperature of the coating alloy. If the zinc content is too low, there will be lack of adhesion between the lead coat and the base metal. If the zinc content is too high, the zinc particles tend to agglomerate, intersect, and the large particles thus formed cause not only a rough surface on the sheet but, since zinc is notably soluble in atmospheric water, they form channels through which corrosion can go on. If, however, they are below the limiting value referred to, not only will capillarity cut down convection currents and thus slow up solution,

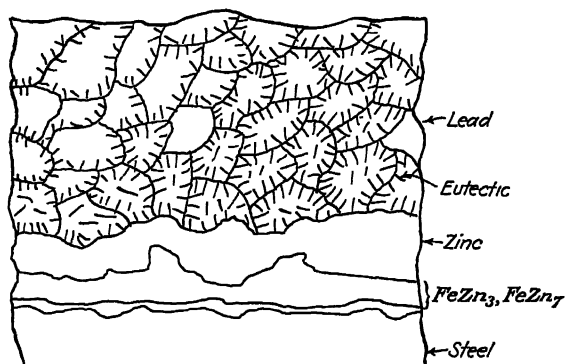


FIG. 11.—ZINC NEEDLES. (U. S. Patent 1948505.)

but the needles of zinc will not intersect and solution will be slowed up at the lead surface.

ACKNOWLEDGMENTS

The author desires to express his appreciation and gratitude to Dr. R. S. Williams, of the Massachusetts Institute of Technology, for his advice and counsel; to Mr. J. M. Hodge and Mr. R. H. Heyer for data and photographs; and particularly to Mr. J. L. Schueler and his associates of the Continental Steel Corporation of Kokomo, Ind., who by contributing material, funds, laboratory and plant facilities, made possible a great deal of this work.

CONCLUSIONS

1. Steel or iron can be coated with lead by using zinc as a binding alloy if the temperature and composition of the bath are held within narrow limits.
2. The resistance to corrosion of such lead-coated sheets is apparently superior to that of ordinary galvanized material.

DISCUSSION

(E. E. Schumacher presiding)

L. FERGUSON,* New York, N. Y.—One of the incidental parts of Mr. Bray's paper is interesting to me and I am sure it interests Mr. Schumacher also. That is the

* Bell Telephone Laboratories.

method of analyzing for zinc and lead by electrical-conductivity measurements. Some years ago, we had the problem of analyzing for antimony in lead in about the same range of compositions; that is, from about 0.4 to 1.1 per cent antimony. We developed a conductivity method, also, and estimated that, if necessary, results could be obtained in about ten minutes with about the same precision given by Mr. Bray's method. We published our results in 1935 (*Metals and Alloys*, 6, 150) but the work was done about five years ago. The coincidences of analysis of lead alloys by a conductivity method the same range of compositions analyzed, and the same precision interests me greatly.

J. L. BRAY.—Incidentally, this has some possibilities for a more complex alloy. Of course, iron is being introduced over a long period of time; copper and other impurities present in the iron will accumulate in the bath. Nevertheless, you can always have a master slug, making it simply a question of comparison—that is, if the bath is working nicely and you do not care particularly what the composition is or what small amounts of impurities there are. A comparison can always be made. You are not going to actually measure the resistance.

L. FERGUSON.—This matter of the effect of impurities in the lead alloys was one of the important points that concerned us, too. Instead of having representative slugs for comparison, however, we constructed one calibration curve for, say, a grade II A.S.T.M. lead, containing copper, and another calibration curve for copper-free so-called pure lead. We did not go into Omaha and Grant or other bismuth-bearing leads, but I imagine they could be handled in the same way. As long as the impurities are known, I believe the percentage of the antimony or of the zinc in lead can be determined accurately by conductivity measurements. If the impurities are unknown, the method would have to be based on comparisons with standard slugs, as explained by Mr. Bray.

Relations between Stress and Reduction in Area for Tensile Tests of Metals

By C. W. MACGREGOR*

(New York Meeting, February, 1937)

IN the testing of materials there exist various methods of recording graphically the behavior of a material subjected to tensile stress. Probably the most common method is to plot the tensile stress S_0 , obtained by dividing the load P by the original area of cross section A_0 at the start of the test, as a function of the strain ϵ_0 , which is obtained by dividing the ΔL_0 or the change in the gauge length by the original gauge length L_0 . A list of the symbols used here is given in Table 1. This method, while it has proved useful in the routine testing and comparison of various materials, does not have a very sound physical basis, as was first pointed out by P. Ludwik¹, and consequently does not afford a very deep insight into the true physical behavior of the material under stress. Among the objections to this method may be mentioned: (1) that by dividing the load P at any stage of the test by the original area A_0 a fictitious stress is obtained, which does not actually exist; (2) that the strain $\epsilon_0 = \frac{\Delta L_0}{L_0}$ is not an exact expression for the true strain for large values of ΔL_0 in per cent of L_0 ; (3) that when necking starts the strain varies considerably along the gauge length and the above expression no longer gives the true strain existing at any point on the outside of the bar; and (4) that the axial strain varies over the cross section of the necked portion and ϵ_0 does not represent an average of these strains over the cross section. Stresses taken from such a diagram would be only approximate and, if used to compare results of a test on a given material under simple tension with results obtained under combined stresses, certain errors would be thus introduced.

In order to overcome some of these objections, various methods have been suggested, both as to the quantities to be measured and as to their graphical representation. In some cases the so-called "true stress," obtained by dividing the load P by the actual area of cross section A existing when the load P was applied, is plotted as a function of the strain

Manuscript received at the office of the Institute Dec. 1, 1936.

* Instructor of Mechanical Engineering, Massachusetts Institute of Technology, Cambridge, Mass.

¹ References are at the end of the paper.

ϵ_0 . After necking has begun, however, a complicated three-dimensional stress distribution is set up in the necked region of the tensile bar and hence the stress obtained by dividing the load P by the area at the bottom of the necked portion no longer represents the true stress², but only the *average of the true stresses* acting in the axial direction along the bar. Further, objections 2, 3 and 4 listed above also apply to this method.

It has been suggested by Ludwik¹, based on the fact that the expression for the strain $\epsilon_0 = \frac{\Delta L_0}{L_0}$ holds only for small ΔL_0 values as compared to L_0 , that a more correct definition of strain would be

$$\epsilon = \int_{L_0}^L \frac{dL}{L} = \log \frac{L}{L_0} \quad [1]$$

It can be shown that this definition of strain holds for strains both small and large, and hence is a better physical definition. For small values of ΔL_0 , it can be seen that equation 1 approaches $\epsilon_0 = \frac{\Delta L_0}{L_0}$. The above expression for the strain is based on the fact that the change in length is always referred to the length from which that change was produced, and not to the original length. Using this definition of strain, then, a tensile stress-strain curve may be drawn with $S = \frac{P}{A}$ or the average true stress plotted as a function of $\epsilon = \log \frac{L}{L_0}$. Such a curve might be called a *true stress-true strain curve* as long as necking has not begun at any point of the bar. If, however, necking has begun, $S = \frac{P}{A}$ becomes the average true axial stress, and if the strain is measured over a gauge length of about

TABLE 1.—*Symbols*

S_0, S	Tensile stresses where load is divided by original area and actual area, respectively.
$P, \Delta P, P_{\max}$	Axial loads.
L_0, L	Original and final lengths.
A_0, A	Original and final areas.
e	Base of natural logarithms.
ϵ_0, ϵ	Strains $\frac{\Delta L_0}{L_0}$ and $\log \frac{L}{L_0}$, respectively.
q, q'	Reduction in area $\frac{A_0 - A}{A_0}$ and $\log \frac{A_0}{A}$, respectively.
q'_b, q'_u	Reduction in area at breaking and maximum loads, respectively.
S_b, S_u	Average true stresses at breaking and maximum loads, respectively.
d_0, d, D_0, D	Bar diameters. Those having subscripts refer to original diameters; the others to actual diameters.
S_t	Average true stress obtained by prolonging $(S - q')$ curve to axis $q' = 0$.
m	Slope of $(S - q')$ curve.

four times the diameter of the bar, as is the usual custom, the strain $\epsilon = \log \frac{L}{L_c}$ loses its physical significance, since it holds only for a bar of uniform section. The value of ϵ would then vary both along the bar axis and perpendicular thereto, as in the former cases. If the strain is measured, not over a large gauge length as above, but over a comparatively small length, which could be followed through during the necking stage at the bottom of the notch (even though considerable experimental difficulties might be encountered), the true strain $\epsilon = \log \frac{L}{L_0}$ in the outside fibers could be determined throughout the test. The strain probably varies over the cross section of the necked-down portion, and the curve thus plotted during the necking stage would be the average true stress over the cross section as a function of the true strain in the outside fibers. It would perhaps be more rational, since we do not know the true stress distribution in the notched portion, and are plotting the average of the true stresses, to plot also the average of the true strains over the cross section if such could be determined.

J. Stead³ suggested that the average true stress $\frac{P}{A}$ be plotted as a function of the decreasing diameter. In this case a convenient linear relationship was obtained between the true stress and the diameter of the test piece for the portion of the curve between the stress corresponding to the maximum load and that corresponding to fracture. This method appears to be free from many of the disadvantages of the former methods mentioned. For some steels, especially those that were hardened and tempered, the linear relation suggested did not hold for the entire region of the curve between the stress corresponding to the maximum load and that of fracture. It is also not quite clear whether this method holds for flat bars as well as for round bars. This procedure will be discussed more fully later.

Because of the difficulties mentioned above of plotting average true stress as a function of strain, various investigators⁴⁻¹¹ have found it convenient to plot $S = \frac{P}{A}$ or the average true stress as a function of $q = \frac{A_0 - A}{A_0}$ or the so-called reduction in area. This method is easy to carry out for round bars and with proper procedure can also be applied to flat bars. It has a decided advantage over most of the methods previously mentioned in that measurements can be taken at one cross section, which simplifies matters during the necking stage. However, this method is open to the same objection as mentioned before in connection with the definition of strain, in that for large reductions in area the expression $q = \frac{\Delta A_0}{A_0} = \frac{A_0 - A}{A_0}$ does not represent the true reduction in area.

The purpose of this paper, then, is not only to suggest a method of representing the behavior of metals under tensile stress which has a better physical basis than former methods, but also to present, as far as the author is aware, a new law for the average true stress-reduction in area relations in the region of test from the ultimate strength to fracture. In searching the literature, no reference to the use of such a law in connection with the tensile test could be found. Further, tensile tests at normal temperatures on various materials will be described, which substantiate such a relation. The advantages of this method of representation and its application to the actual drawing of wires and tubes will also be discussed.

RELATIONS BETWEEN STRESS AND REDUCTION IN AREA

Suppose a uniform bar of original length L_0 and area of cross section A_0 has small increments of load ΔP_i successively applied to it, so that the bar is stressed in pure tension only. There will then result a series of small increments of length ΔL_i and decrements in area ΔA_i . Provided each small value of ΔL_i and ΔA_i is referred to the length or area from which it was produced, we get for a large number of loading steps

$$P = \sum_{i=0}^n \Delta P_i, \quad \epsilon = \sum_{i=0}^n \frac{\Delta L_i}{L_i}, \quad q' = \sum_{i=0}^n \frac{\Delta A_i}{A_i} \quad [1a]$$

where P , ϵ and q' are the total load, the true strain, and the true reduction in area, respectively. If L and A represent the final length and area of the bar, we get, by passing to the limit as $n \rightarrow \infty$ and ΔL_i and ΔA_i approach zero, the true strain ϵ and true reduction in area q' given by

$$\epsilon = \int_{L_0}^L \frac{dL}{L} = \log \frac{L}{L_0} \quad q' = - \int_{A_0}^A \frac{dA}{A} = \log \frac{A_0}{A} \quad [2]$$

The reduction in area commonly used in the testing of materials is $q = \frac{A_0 - A}{A_0}$ from which it may be seen that

$$q' = -\log (1 - q) \quad [3]$$

The method suggested here for the representation of stress-reduction in area data in the tensile test is to plot the average true stress $S = \frac{P}{A}$ as a function of q' instead of as a function of q , as is usually done. We are then using a more rational expression for reduction in area, which holds for both large and small reductions. It is felt that this method has perhaps fewer objections than those previously mentioned.

For round bars equation 2 may be replaced by

$$q' = 2 \log \frac{d_0}{d} \quad [4]$$

and the entire curve of $(S - q')$ plotted from load and diameter readings.

Tensile tests with round bars were made on various materials in a Southwark-Emery 30-ton machine in which the diameters of the standard 0.505-in. test pieces were measured by means of a specially designed clamp and dial gauge throughout the entire test. Knife edges were

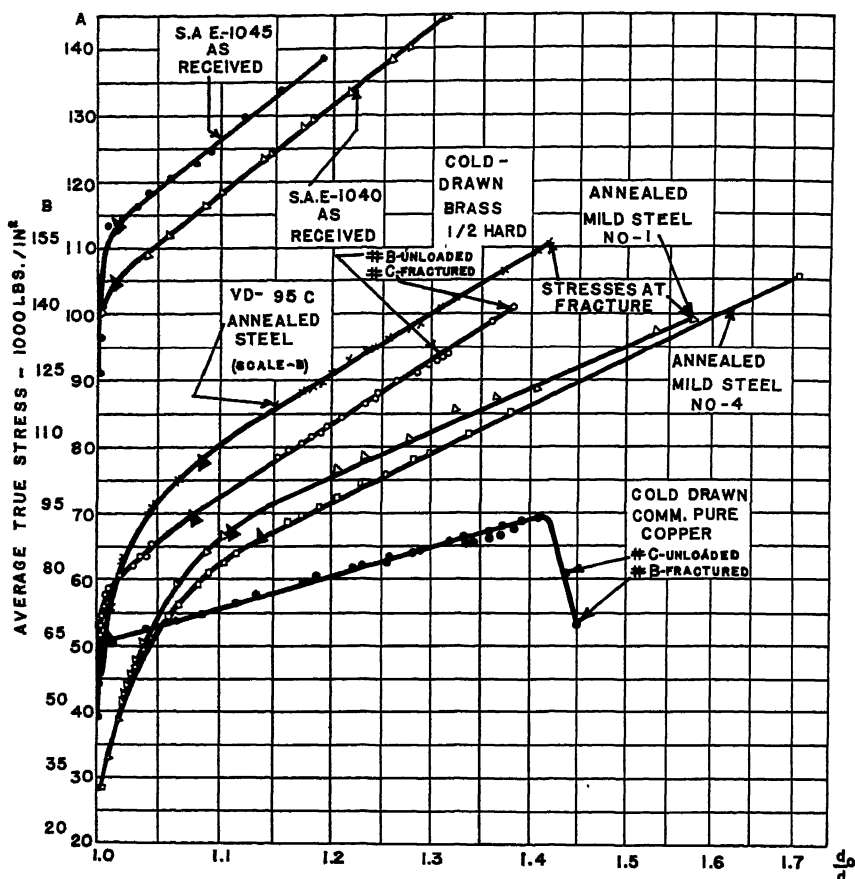


FIG. 1.—AVERAGE TRUE STRESS PLOTTED ON SEMILOGARITHMIC PAPER VS. d_0/d FOR TENSILE TESTS TO FRACTURE OF VARIOUS MATERIALS.

provided so that the diameter could be determined accurately during the necking stage.

Certain preliminary tests were made to determine the effect of speed of testing on the values measured, and it was found that for the mild steel tested no appreciable effect either on the breaking stress or on the diameter of the bar at fracture could be detected for a speed ratio of 20 to 1. With commercially pure aluminum, a speed ratio of 3 to 1 showed no appreciable effect on these values. This coincides with the general effects of speed of testing that have been found by various other investigators

for ductile metals. Tests were also made to determine the relative suitability of the hydraulic and the beam type of testing machines for

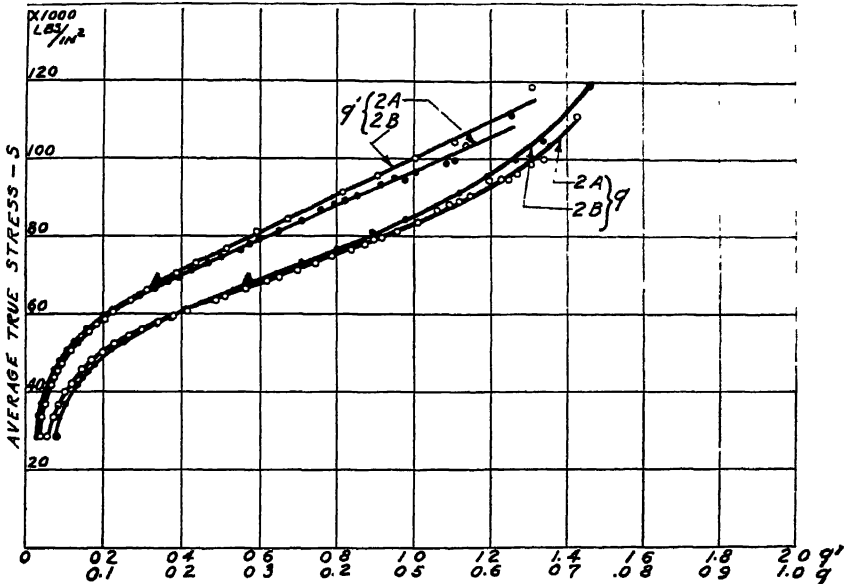


FIG. 2.—COMPARISON OF $(S - q)$ AND $(S - q')$ CURVES FOR TENSILE-TEST PIECES 2A AND 2B OF ANNEALED BOILER-RIVET STEEL.

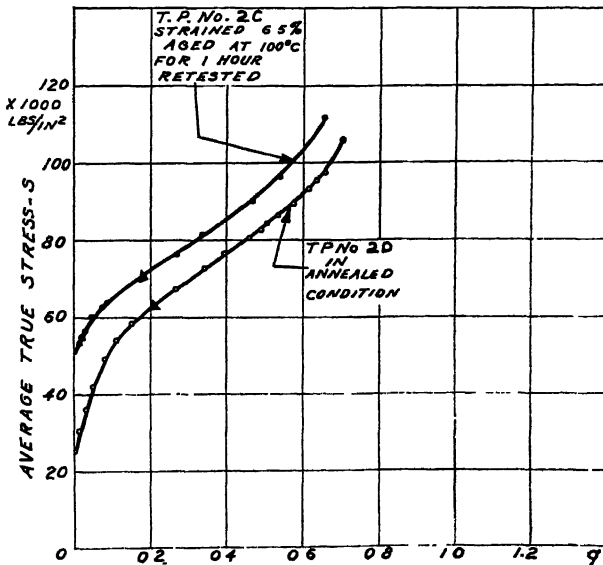


FIG. 3.— $(S - q)$ CURVES FOR BOILER-RIVET STEEL.

this investigation. Slow tests were carried through on both types and it was found that although the $(S - q')$ curves obtained were of the same

shape on both machines, the hydraulic machine appeared to be in general more satisfactory. There was a difference of only a few pounds on the

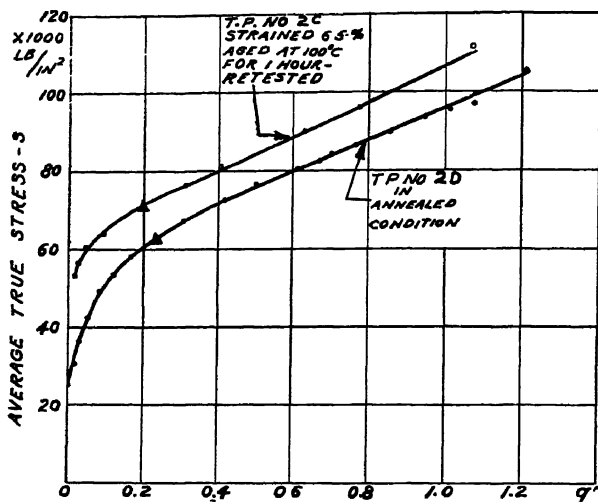


FIG. 4.—($S - q'$) CURVES FOR BOILER-RIVET STEEL.

hydraulic machine between the load for complete cessation of flow and that for slow flow as read by the dial gauge.

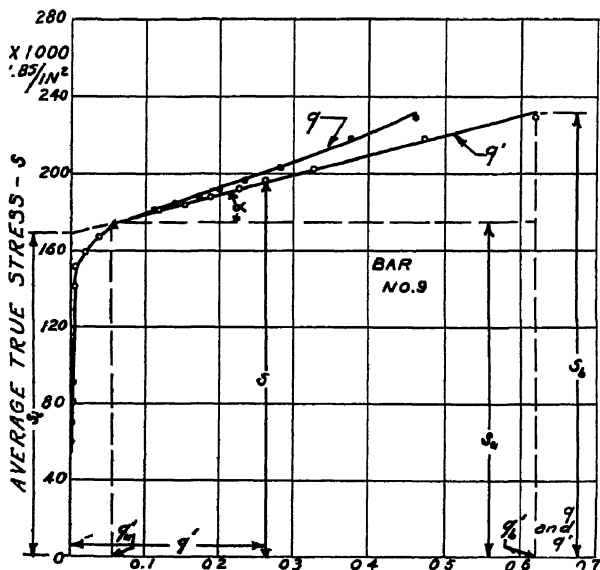


FIG. 5.—($S - q$) AND ($S - q'$) CURVES FOR S.A.E. 6150 STEEL OIL-QUENCHED (1575° F.) AND DRAWN (1200° F.).

Fig. 1 shows the stress-reduction in area data for tensile tests on several materials plotted on semilog paper in which the true reduction

in area q' was used as given in equation 4. The heat-treatment and approximate composition of these materials is listed in Table 2.

Fig. 1 is essentially equivalent to plotting the average true stress $\frac{P}{A}$ as a function of q' on regular coordinate graph paper. The point on the curves marked with a solid triangle near the junction of the straight and the curved portions indicates the position of the true stress corresponding to the maximum load. For each material, with the exception of the copper tested, the curve becomes a straight line from the point

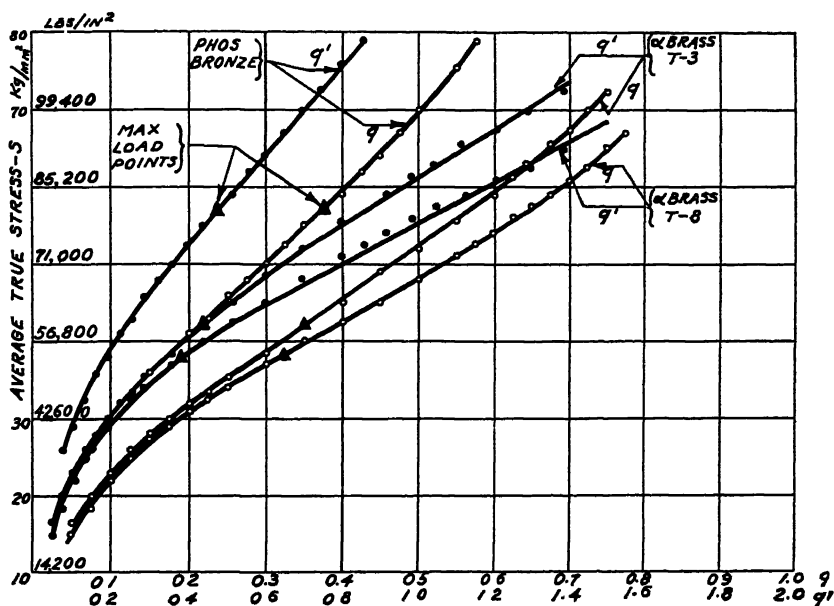


FIG. 6.—COMPARISON OF $(S - q)$ CURVES AS PLOTTED IN TENSILE TESTS BY KÖRBER AND ROHLAND⁶ FOR BRASS AND BRONZE WITH $(S - q')$ CURVES.

of maximum load to fracture. Even for copper, a straight line was obtained almost to fracture. The load dropped off rapidly near rupture, causing a drop in the curve. The reason for this anomalous behavior of copper will be explained later.

In Fig. 2 a comparison is made between the former method of plotting the $(S - q)$ curves for two test pieces of annealed boiler-rievet steel with the suggested $(S - q')$ method. Figs. 3, 4 and 5 show a similar comparison for annealed boiler-rievet steel, a prestrained and aged test piece of the same material, and a test piece of S.A.E. 6150 steel, which was quenched in oil from 1575° F. and drawn at 1200° F. In each case the $(S - q)$ curves show a curvature upward after necking has begun, whereas the $(S - q')$ curves show a linear relationship of average true stress and true reduction in area q' from the beginning of necking to fracture. This

is further substantiated by data obtained by Körber and Rohland⁵ for phosphor bronze and brass, which is shown plotted in Fig. 6 by both the $(S - q)$ and $(S - q')$ methods.

Fig. 7 compares the shapes of the curves obtained for 20° C. annealed mild steel by plotting both the average true stress S as a function of q and q' and also by plotting the average stress based on the original area

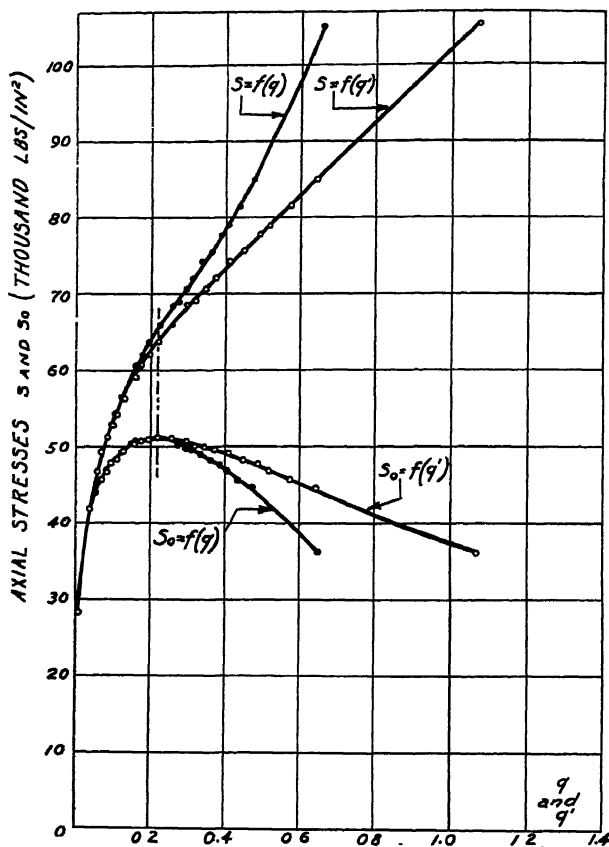


FIG. 7.—CURVES FOR STRESS AND REDUCTION OF AREA FOR 20 C. ANNEALED MILD STEEL (BAR NO. 4).

or S_0 as a function of q and q' . It is to be noted again that only the curve $s = f(q')$ is linear after necking has begun. Similar relationships were found for duralumin, which for the sake of brevity are not included here.

For all of the ferrous and for most of the nonferrous materials tested this linear relationship from the beginning of necking to fracture was obtained. An exception to this rule, however, was also found in soft, annealed, commercially pure aluminum, which is shown in Fig. 8. Bar 8A is shown as it was carried through to fracture, the average true stress being plotted as a function of both q and q' to different scales. The

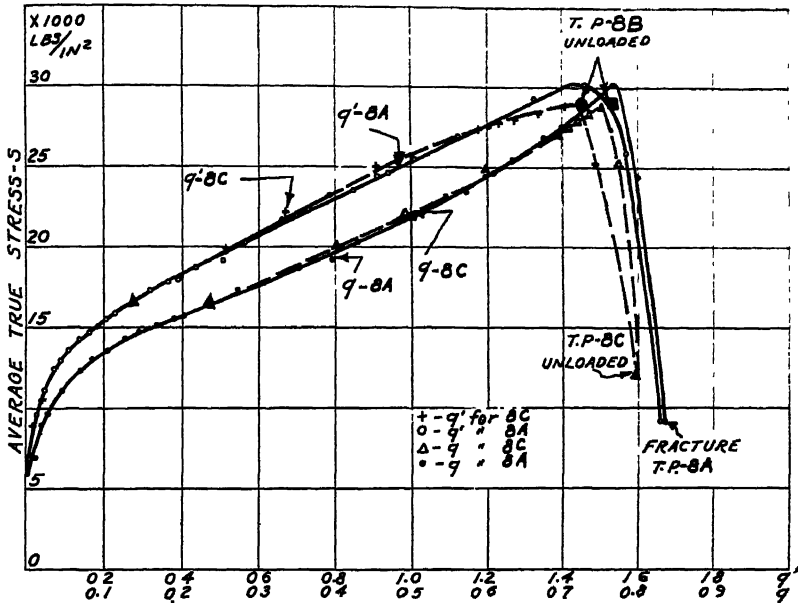


FIG. 8.—($S - q$) CURVES FOR TENSILE TESTS ON PURE ALUMINUM IN SOFT ANNEALED CONDITION.

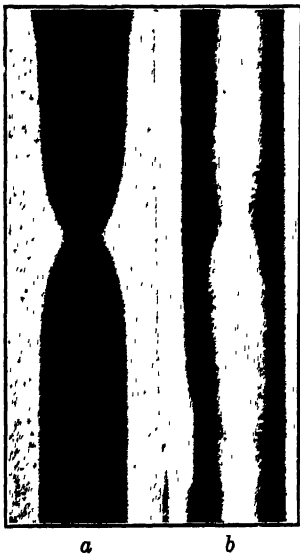


FIG. 9.

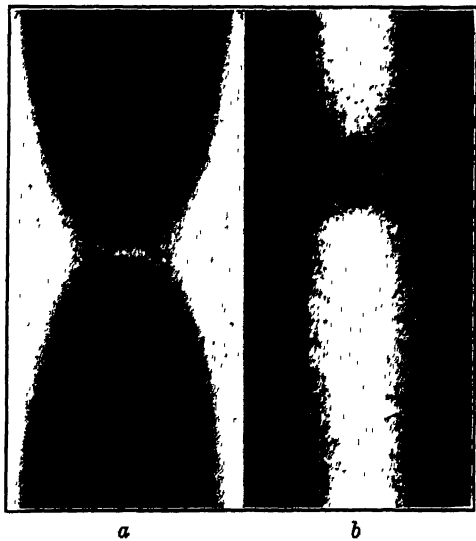


FIG. 10.

FIG. 9.—(a) X-RAY (POSITIVE) OF BAR 8C OF SOFT, ANNEALED, COMMERCIALY PURE ALUMINUM, SHOWING CRACK IN NECKED PORTION. (b) TEST PIECE 8C AFTER UNLOADING.

FIG. 10.—ENLARGED VIEWS ($\times 2.6$) OF BAR SHOWN IN FIG. 9, TAKEN AT 90° .

linear relationship of S and q' apparently held in this case for a considerable region after the maximum load was reached, and then the load dropped off rapidly as shown. In order to investigate the reason for this anomalous behavior, two additional specimens 8B and 8C were tested and unloaded before fracture at the points shown on the curves in Fig. 8.

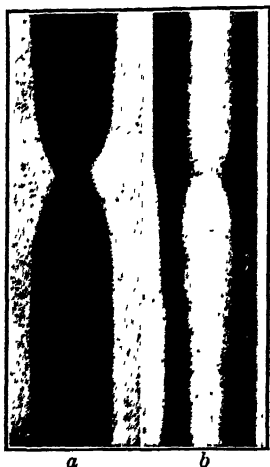


FIG. 11.

FIG. 11.—(a) X-RAY OF TEST PIECE 8B SHOWING VERY SMALL CRACK AT CENTER OF NECKED PORTION. (b) SIDE VIEW OF SAME PIECE AFTER UNLOADING.

X-rays were then made of these two test pieces, with the results as indicated in Figs. 9, 10 and 11. A large crack* is to be seen in the necked portion in Figs. 9 and 10, while a very small crack can be noticed in Fig. 11. In view of the position of the unloading points on the curves, it is seen that this crack formation is closely connected with the shape of the $(S - q')$ curves, indicating the reason for this departure from the

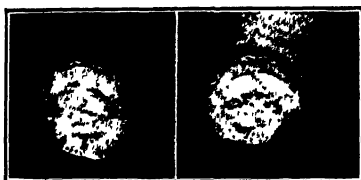


FIG. 12.

FIG. 12.—END VIEWS OF FRACTURED BAR OF SOFT, ANNEALED, COMMERCIAL PURE ALUMINUM SHOWING SPIRAL OR DOUBLE CUP AND CONE FRACTURE.

usual linear relationship found. Fig. 12 shows a typical tensile fracture of this material with an unusual spiral cup and cone formation.

As shown in Fig. 1, a similar $(S - q')$ curve was obtained for commercially pure copper in the hard-drawn condition. Although an X-ray of test piece C, which was unloaded at the point indicated in Fig. 1, gave no clear indication of a crack, possibly because of greater difficulties in X-ray technique with this material than with the aluminum, the same unusual spiral cup and cone fracture was obtained. It is felt, therefore, probable that a crack had already formed in this test piece. A cold-drawn brass specimen B unloaded at the point shown in Fig. 1 showed no crack when photographed with X-rays.

Referring to Fig. 5, the equation of the $(S - q')$ curve in the region where $q'_u \leq q' \leq q'_b$ becomes

$$S = S_i + mq' = S_i + m \log \frac{A_0}{A} \quad [5]$$

where $m = \frac{S_b - S_u}{q'_b - q'_u}$. In this equation S_b and q'_b are the average true

* Similar effects were found by P. Ludwik⁶.

stress and true reduction in area at fracture, S_u and q'_u the average true stress and true reduction in area corresponding to the maximum load, and S_b the average true stress obtained by continuing the curve to the average true stress axis. The value of S_b is given by

$$S_b = S_u - \frac{S_b - S_u}{q'_b - q'_u} \cdot q'_u \quad [6]$$

Equation 5 indicates that if areas $A, A_1, A_2 \dots$ are chosen in terms of a geometric progression, the corresponding stresses change in an arithmetic progression. Table 2 gives the equation for the average true stress in the region $q'_u \leq q' \leq q'_b$ for a number of the materials tested.

RELATION BETWEEN BREAKING STRENGTH AND ULTIMATE STRENGTH

From Fig. 5 we may also derive the relation between the ultimate strength based on the original cross-sectional area and the average true breaking stress. We see that

$$S_b = S_u + m(q'_b - q'_u) \quad [7]$$

Since $\frac{A_0}{A} = e^{e'}$

and $\begin{aligned} S_b A &= S_0 A_0 \\ S &= S_0 e^{e'} \end{aligned}$

We then have $S_u = \frac{P_{\max}}{A_0} \cdot e^{e'_u}$ [8]

Substituting in equation 7, we obtain

$$S_b = \frac{P_{\max}}{A_0} \cdot e^{e'_u} + m(q'_b - q'_u) \quad [9]$$

From this equation the *average true breaking stress* S_b can be calculated from the ultimate tensile strength $\frac{P_{\max}}{A_0}$, the true reductions in area corresponding to the maximum load q'_u and to the breaking load q'_b , and the slope of the curve m . It is often difficult to determine the actual breaking load, especially if the test is carried out on a beam machine. Equation 9 provides a method for calculating this average true breaking stress from data that can be easily measured. For purposes of approximate calculation, equation 9 may be simplified by placing

$$e^{e'_u} \cong 1 + q'_u$$

when the equation reduces to

$$S_b \cong \frac{P_{\max}}{A_0} (1 + q'_u) + m(q'_b - q'_u) \quad [10]$$

Table 2 compares the breaking stress observed with that calculated from equation 9. The agreement is very close when the actual slope in each

case is used. If for the six mild-steel test pieces the average slope of $m = 46,000$ is used, the agreement between calculated and observed values is still within a maximum error of 2.5 per cent. The above equations do not hold, of course, for the anomalous cases of the pure aluminum and copper tested.

In most specifications, the tensile strength is given with no mention of the breaking strength. With the tendency today to inquire further into the fundamental behavior of metals under stress, the breaking strength will probably assume a gradually increasing importance, especially, perhaps, in its relation to fatigue problems. P. Ludwik¹² has shown that the breaking strength helps to bring out certain material

TABLE 2.—Results of Calculations by Means of Equations 5 and 9

Material	Equation 5 S	Breaking Stress Measured from Curve S_s Lb per Sq. In.	Breaking Stress Calculated by Equation 9 Using Actual m , Lb per Sq. In.	Heat-treatment
Boiler-rivet steel 2A.	$51,430 + 44,900q'$	108,000	107,800	Annealed 1700° F. for 1 hr. Slow cool.
Boiler-rivet steel 2B.	$50,300 + 49,000q'$	115,000	115,200	Annealed 1700° F. for 1 hr. Slow cool.
Boiler-rivet steel 2C.	$61,800 + 46,000q'$	111,000	111,400	Same anneal as No. 2A prestrained 6.5 per cent aged 1 hr. at 100° C.
Boiler-rivet steel 2D.	$52,400 + 44,400q'$	106,000	106,000	Same anneal as No. 2A.
Mild steel No. 1.....	$59,120 + 43,500q'$	98,700	99,300	Annealed 1700° F. for 1 hr. Slow cool.
20C Mild steel No. 4.	$53,900 + 48,200q'$	105,300	105,400	Annealed 1700° F. for 1 hr. Slow cool.
S.A.E. 1040.....	$103,000 + 75,400q'$	145,000	145,050	As received.
S.A.E. 1045.....	$111,500 + 78,000q'$	138,100	138,400	As received.
95C vanadium steel.	$95,000 + 86,100q'$	156,000	154,500	Annealed at 1450° F. Cooled in furnace.
S.A.E. 6150.....	$167,000 + 104,800q'$	232,000	232,200	Oil-quenched 1575° F. Drawn 1200° F.
½ hard-drawn brass C (Cu, 65 per cent, Zn, 35).....	$61,500 + 60,800q'$	100,600	99,700	As received.
Cold-drawn commercially pure copper (Cu, 99.9 per cent)	$50,000 + 28,340q'$			As received
Aluminum, commercially pure.....	$13,750 + 11,610q'$			Annealed 5 hr. at 700° F., cooled in furnace.

properties which the tensile strength does not. For example, it was shown that for some materials the breaking strength values brought out effects of overheating, chemical influences, etc., which were not detectable by any change in the tensile strength.

ADVANTAGES OF THE METHOD AS APPLIED TO THE TENSILE TEST

In carrying out the details of the method, either semilog graph paper such as is shown in Fig. 1 or ordinary graph paper may be used. In either case, since it has been observed that during the necking stage the $(S - q')$ curve is linear, the entire curve from the stress corresponding to the maximum load to the breaking stress can be drawn in by observing only the loads at the maximum and fracture points as well as the corresponding diameters. This means that the number of points necessary to be plotted and the number of observations necessary to be made are very much reduced. In all the materials tested here it was found that the $(S - q)$ curves were concave upward and linear extrapolation of the tangent at the maximum load point of such a curve (as is very frequently done⁵⁻¹¹) does not appear to be justified. By the $(S - q')$ method the tangent coincides with the curve at this point and follows the curve to fracture.

As was observed in the previous section, the $(S - q')$ procedure not only provides the possibility of deriving the equation of the curve in a simple manner but also of determining an analytical relation between the tensile strength and the breaking strength.

The coefficient m in equation 5 might be called the modulus of work-hardening for the tensile test during the necking stage. Both S , and m are probably greatly influenced by certain metallurgical and mechanical conditions, as can be seen in Table 2, and it is conceivable that they might serve as useful indices of these effects, although this particular question was not investigated here.

The fact that the reduction in area q' is a logarithmic expression should not be a drawback, since either semilogarithmic paper may be used or a large curve may be constructed from which for a given $\frac{A_0}{A}$ the logarithm may be read. The latter procedure should not be any more laborious than the computation of q .

COMPARISON WITH STEAD'S METHOD

Since, as was mentioned earlier, Stead² found a linear relationship for the average true stress plotted as a function of decreasing diameter between the points corresponding to the maximum load and fracture, it was deemed of interest to replot the data for a number of the materials tested here according to his method. It was found that for all of the

materials considered a straight line was obtained for this portion of the curve, as was suggested by Stead. Since the same data also gave a linear relationship when plotting the average true stress S as a function of $q' = 2 \log \frac{d_0}{d}$ for the portion of the curve between the point corresponding to the maximum load and fracture, this result at first appeared somewhat contradictory. If the one method gives a straight line, theoretically the other should yield a curve over the same region. On further investigation, however, it was found that if $\frac{d}{d_0}$ was plotted as a function of $2 \log \frac{d}{d_0}$, a very flat curve was obtained, departing very little from a straight line over a considerable portion of its length. It was thus found possible for the range of values of $\frac{d}{d_0}$ and $2 \log \frac{d}{d_0}$ which occur in tensile tests to replace the curve $\frac{d}{d_0}$ vs. $2 \log \frac{d}{d_0}$ so obtained by a straight line. In this manner $2 \log \frac{d}{d_0}$ could be expressed as a linear function of $\frac{d}{d_0}$ and when substituted in equation 5 a linear equation in $\frac{d}{d_0}$ was obtained for the average true stress S of a form identical with that given by Stead. When numerical values were substituted in this derived equation, a close check with Stead's equation was obtained for various values of the average true stress. This procedure was carried through on several materials. It is thus apparent why both methods yield a straight line for the materials tested with sufficient accuracy for most engineering purposes.

The data available so far are not sufficient to determine whether the $(S - q')$ or the Stead method gives a *theoretically exact* straight line for the necking stage of the tensile test. It is hoped that further tests will clear up this point. For practical purposes, however, the materials tested here yield a straight line for this portion of the $(S - q')$ curve.

The $(S - q')$ procedure possesses certain advantages over the Stead method. The abscissa of the $(S - q')$ curves, or the true reduction in area, has a greater physical meaning than the quantity $\frac{d}{d_0}$. Further, the $(S - q')$ method is not restricted to round bars.

APPLICATION OF $(S - q')$ METHOD TO DRAWING OF METALS

The problem of the drawing of metals through dies is very complicated and there are many fundamental facts concerning the process about which we know very little today. It is not the intention here to consider this field in general but to confine the discussion to the use of the $(S - q')$ method in problems of this kind.

The distribution of stress over the cross section of a round wire that is being drawn through a conical die is not known for a section of the wire passing through the die. For this reason the usual procedure is to consider only the average value of the axial stress S , to assume that the pressure p of the material on the die wall is a principal stress and to use the maximum shear theory for the plasticity condition, or $S + p = k$ where k is the average resistance to deformation during the reduction.

As this solution for the average axial stress in the drawing operation is given completely elsewhere¹³ the details will not be repeated here. It can be mentioned, however, that when the equilibrium equation of the stresses acting in the axial direction is combined with the plasticity condition and integrated, making use of the boundary conditions, an expression for the axial draw stress S_s is obtained as follows

$$S_s = k \left(1 + \frac{\tan \varphi}{\mu} \right) \left[1 - \left(\frac{D}{D_0} \right)^{\frac{2\mu}{\tan \varphi}} \right] \quad [11]$$

where μ is the coefficient of friction of the material on the die wall, φ is half the die angle, D_0 and D are the initial and final diameters, respectively. If the equilibrium equation is integrated making use of the plasticity condition above but assuming the coefficient of friction $\mu = 0$, the axial draw stress becomes

$$S_s = k \log \frac{A_0}{A} \quad [12]$$

where A_0 is the original area and A the final area of the drawn wire. In the derivation it was assumed that the die angle was small. The assumptions made in deducing these equations are by no means fulfilled exactly; however, tests by Sachs have shown that the above expressions give satisfactory results for small die angles.

Equation 12, for the draw stress under frictionless conditions so derived by Sachs, is very similar to the expression for the average true stress during the necking of a tensile-test piece used in this investigation. The latter expression may be put in the form

$$S - S_u = m \log \frac{A_u}{A} \quad [13]$$

where $S - S_u$ represents the increase in the average true stress during the necking of the bar.

It has been shown by Sachs and Linicus¹⁴ that for a given reduction in area the material passing through a die work-hardens more than that stretched to the same reduction in area by a tensile test. Also, it appears that the steeper the die, the stronger is the work-hardening for a given reduction, owing to the nonuniform flow of the material through the

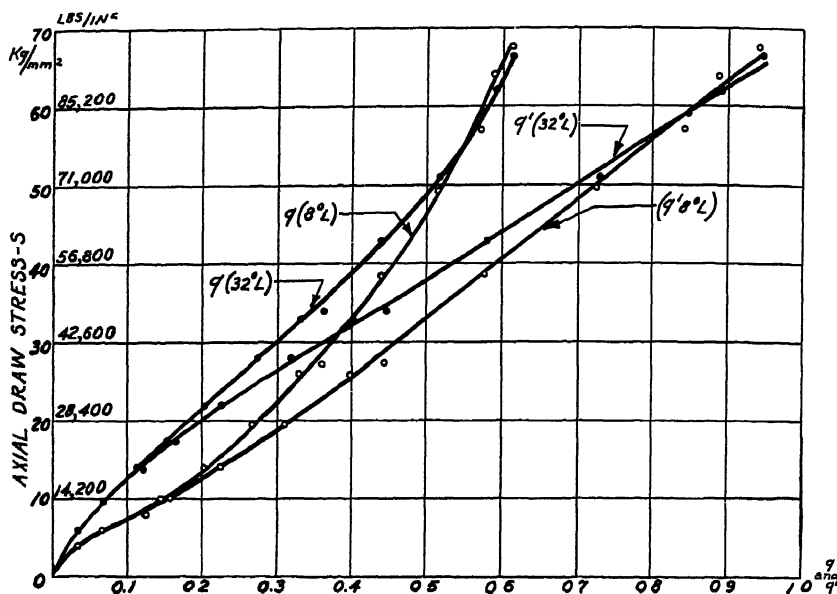


FIG. 13.—COMPARISON OF ($S - q$) CURVES FOR BRASS WIRE DRAWN THROUGH DIES OF DIFFERENT WALL SLOPE, AS OBTAINED BY SACHS AND LINICUS¹⁴ WITH ($S - q'$) METHOD SUGGESTED HERE.

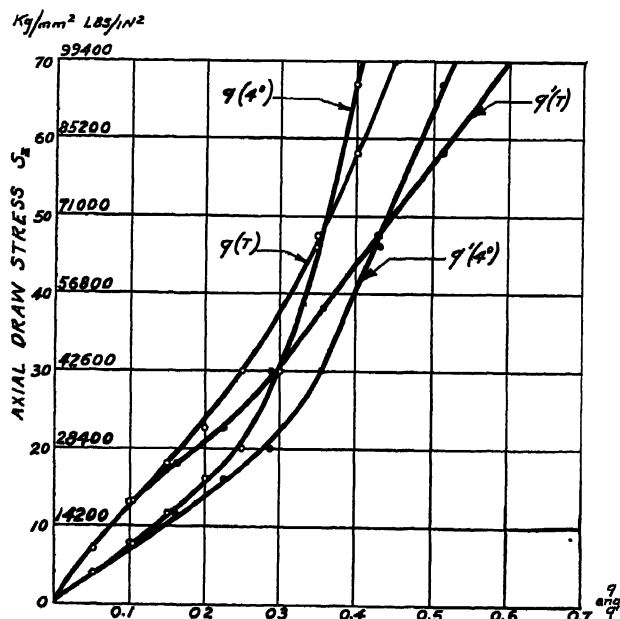


FIG. 14.—DRAWING OF BRASS TUBES THROUGH A 4° AND A TRUMPET-SHAPED DIE (ACCORDING TO G. SACHS).

Draw stress plotted also by new method vs. q' .

die. For large reductions, however, the work-hardening as obtained in the tensile test and in the drawing operation appear to approach coincidence. Consequently in equation 12 it is necessary to use the average flow resistance during the reduction, which can be taken from a curve of the actual yield point plotted as a function of q or q' as determined from tensile tests on bars drawn through dies of various wall slopes. Drawing tests were made by Sachs and Linicus on brass wire using dies of various wall slopes, which could be rotated to minimize the friction. The test results checked well with equation 12.

Heretofore, the axial draw stress obtained from drawing tests has usually been plotted as a function of the reduction in area q . Fig. 13 shows a comparison of the $(S - q)$ curves plotted for brass wire drawn through dies of different wall slope as obtained by Sachs and Linicus with the $(S - q')$ method suggested here for the tensile test. It is apparent that after a reduction of $q' = 0.45$ the $(S - q')$ curves are essentially straight lines instead of possessing a continuous curvature, as illustrated by the $(S - q)$ graphs. Similar effects were found in the tensile tests described in this investigation. Fig. 14 makes a similar comparison for brass tubes drawn through dies of different shape, according to Sachs. In the latter figure, although the reductions were not carried nearly as far as in Fig. 13, the $(S - q')$ curves became straight lines after a reduction in area of $q' = 0.35$.

SUMMARY

A critical discussion was made of certain methods of plotting stress-strain and stress-reduction in area curves for metals cold-worked in tension. Based on certain physical considerations, a different method of representing these relations was suggested in which the average true stress $\frac{P}{A}$ is plotted as a function of the true reduction in area $q' = \log \frac{A_0}{A}$ where A_0 is the original area and A the area at any load P . Tensile tests were made on various metals and such curves were plotted. For all of the steels tested and for most of the nonferrous metals as well, the curve became a straight line from the point corresponding to the maximum load up to fracture, as distinguished from the curve usually obtained for $\frac{P}{A}$ plotted as a function of $q = \frac{A_0 - A}{A_0}$. This fact permitted the formulation of a new law giving the relation between the average true stress and the true reduction in area within the necking region of the tensile test. It also provided a relation between the tensile strength and the breaking strength such that one may now be easily calculated from the other. Various important advantages of this method of plotting were brought out.

The anomalous behavior of the commercially pure aluminum and copper tested was explained by means of X-rays, which showed a crack formed inside the necked portion of the test piece.

A comparison was made between the expression for the axial drawing stress for frictionless drawing as obtained by Sachs with the corresponding expression for the increase in stress during the necking stage of a tensile test. Further, the application of the $(S - q')$ method of plotting to the drawing of brass wires and tubes was illustrated.

ACKNOWLEDGMENTS

The author desires to express his appreciation for the interest and support of this work by Professors J. C. Hunsaker and C. E. Fuller, of the Massachusetts Institute of Technology. Acknowledgment is also due Prof. J. T. Norton for taking the X-ray photographs and Messrs. A. R. Peel, H. B. Leslie and A. G. Strom for assistance in the preparation of the curves and in the calculations.

REFERENCES

1. P. Ludwik: *Elemente der technologischen Mechanik*. Berlin, 1909. Julius Springer.
2. A. Nádai: Discussion of Zur Analyse der Zerreiversuches, by G. Sachs. *Mitt. Material-prüfungsamt* K. W. Inst. Metallforschung, Berlin-Dahlem (1926) S. No. 11. Also cf. *Plasticity*. New York, 1931. McGraw-Hill Book Co.
3. J. Stead: The Cold-Working of Steel with Reference to the Tensile Test. *Jnl. Iron and Steel Inst.* (1923) 107, 377-416.
4. F. Körber: Verfestigung und Zugfestigkeit-Ein Beitrag zur Mechanik des Zerreiversuches plastischer Metalle. *Mitt. K. W. Inst. Eisenforschung zu Düsseldorf* (1922) 2, Bd. 3.
5. F. Körber u. W. Rohland: Über den Einfluss von Legierungszusätzen und Temperaturänderungen auf die Verfestigung von Metallen. *Ibid.* (1924) 2, Bd. 5, 55-68.
6. P. Ludwik: Bestimmung der Reissfestigkeit aus der gleichmässigen Dehnung. *Ztsch. Metallkunde* (1926) 9, 269-272.
7. E. V. Crane: Plastic Drawing of Sheet Steel into Shapes. *Amer. Soc. Steel Treat.*, Sept. 1931.
8. R. L. Kenyon and R. S. Burns: Autographic Stress-Strain Curves of Deep-Drawing Sheets. *Trans. Amer. Soc. Steel Treat.* (1933) 577-612.
9. G. Sachs and F. Saefel: Festigkeitseigenschaften und Struktur einiger begrenztes Mischkristallreihen. *Mitt. K. W. Inst. Metallforschung, Berlin-Dahlem* (1926) S. No. 11.
10. W. v. Moellendorf: *Ztsch. Ver. deut. Ing.* (1913) 57, 931-935.
11. J. Czocharski: Die Grundlagen der Verfestigungsvorgänge. *Ztsch. Metallkunde* (1923) 15, 7.
12. P. Ludwik: Die Bedeutung des Gleit- und Reisswiderstandes für die Werkstoffprüfung. *Ztsch. Ver. deut. Ing.* (1927) 7, 1532-1538.
13. G. Sachs: Zur Theorie des Ziehvorganges. *Ztsch. ange. Math. Mech.* (1927) 7, 235-236.
14. G. Sachs and W. Linicus: Versuche über die Eigenschaften gezogener Drähte und den Kraftbedarf beim Drahtziehen. *Mitt. deut. Materialprüfungsanstalt* (1931) S. 16, 38-67.

DISCUSSION

(S. L. Hoyt presiding)

A. V. DE FOREST,* Cambridge, Mass.—Is the slope of this new curve a measurement of hardening that is going on during the necking portion of the diagram? Can we hope to get a measurement from this method of plot that we cannot from the ordinary one, which involves the strain-hardening behavior of the material, and from which work-hardening capacity can be readily determined?

D. K. CRAMPTON,† Waterbury, Conn.—In the $S - q'$ curves shown, if the straight-line portion is extrapolated back to zero strain, would the value of stress so obtained be the value ordinarily given as maximum tensile strength; in other words, the maximum load divided by *original* area? It would seem that it might be.

Another point I wish to make is that the length and slope of this same straight portion of the curve should be an excellent indication of the capacity for work-hardening and would, therefore, be an excellent way of comparing materials or treatments from that standpoint and possibly a better way than we have had in other methods heretofore used.

W. L. FINK,‡ New Kensington, Pa.—We have been doing some work on the rolling of aluminum and plotting our results very much in this same way. In plotting the yield strength against the logarithm of the ratio of the initial to final cross-sectional (i.e. $\int \frac{dA}{A}$) a linear relation is obtained above approximately 50 to 60 per cent reduction.

L. W. KEMPF,§ Cleveland, Ohio.—I wonder if the authors would care to make any remarks regarding the variation in slope of the straight portion of the line from material to material, or even within a certain family, say in iron-base alloys. Is the slope fairly constant for iron-base alloys and different from that for copper-base alloys?

S. L. HOYT,|| Milwaukee, Wis.—I think several of the discussers have picked on a rather interesting point here—the slope of the curve and its use as a measure of work-hardening. The slope changes continuously up to the maximum point on the ordinary tensile curve, and from there on remains constant. It is a very interesting point but it suggests a change in the mechanism of work-hardening at that point.

C. W. MACGREGOR (written discussion).—Dr. Crampton's remarks on the use of the slope of the $S - q'$ curves as a measure of work-hardening coincide with the author's own convictions that the length and slope of these curves past the maximum load point should prove to be a convenient means of comparing the work-hardening characteristics of various materials. This also answers the question raised by Professor de Forest.

If the straight-line portion of an $S - q'$ curve is extrapolated back to zero q' , the stress value so obtained is called S , in the paper itself and it is the first term in the right-hand side of equation 5. Values of S , for the various materials investigated are listed in Table 2. When compared with the ordinary tensile strength, which is defined as the quotient of the maximum load and the original area, it was found that

* Associate Professor of Mechanical Engineering, Massachusetts Institute of Technology.

† Director of Research, Chase Brass & Copper Co.

‡ Aluminum Research Laboratories.

§ Aluminum Research Laboratories.

|| A. O. Smith Corporation.

the values of S_b , although different slightly from the ordinary tensile strengths, were rather close to the latter in value in most cases, as suggested by Dr. Crampton.

Dr. Kempf asked about the variation from material to material in the slope of the $S - q'$ curves after the maximum load has been reached. This is an interesting point and it is hoped that further tests will throw additional light on the question. Although it was not the purpose of the paper to investigate this phase of the problem, the establishment of a linear relation between S and q' with a large variety of materials being the primary object, certain effects have been noted. Table 2 shows that slope m for the various mild steels tested remained fairly constant. It was found that if an average value of $m = 46,000$ is used for the six mild-steel test pieces, the calculated and observed values of breaking stress checked within 2.5 per cent. The q' values took care of any differences in ductility in the individual cases. Further, for higher carbon and alloy steels the value of m is much greater than for the mild steels investigated. It is also apparent that the slope m is in general different for iron-base alloys and copper-base alloys.

Dr. Fink's statement more or less bears out some of the test results we have found.

Influence of Temperature on Elastic Limit of Single Crystals of Aluminum, Silver and Zinc

BY RICHARD F. MILLER* AND W. E. MILLIGAN,† MEMBERS A.I.M.E.

(New York Meeting, February, 1937)

WORK was undertaken two years ago at the Hammond Laboratory for the purpose of determining the magnitude of the elastic range in single crystals of pure metals by means of creep tests, the assumption being made that if a true elastic range exists, the elastic limit represents the maximum stress for no creep. A sensitive extensometer was constructed, and creep tests were made on zinc single crystals at a variety of loads and temperatures¹. It was soon discovered that there is no measurable elastic limit in ductile zinc single crystals at, or above, room temperature.

The inference that pure metallic single crystals may not possess a definite elastic range was not justified, however, since zinc had been tested in creep only above its recrystallization temperature, and several investigators^{2,3,4} had already shown that above the recrystallization temperature polycrystalline metals will flow under very small stresses, while below that temperature stresses of a much larger magnitude are required.

For that reason, it was decided to extend the study of the elastic limit to other metals having a higher recrystallization temperature than zinc. Aluminum and silver were selected, because of the ease of obtaining pure materials and of preparing large single crystals, and because the crystallographic glide system of these metals is well known. Owing to the limited time available, the elastic range was investigated by slow tensile tests rather than by creep tests.

PRODUCTION OF SPECIMENS ·

Aluminum

Recrystallized single crystals were prepared from 99.95 per cent aluminum supplied by the Aluminum Company of America. The ingots were melted in an Acheson graphite crucible in a gas furnace, and cast

This paper describes the results of an investigation carried out at the Hammond Laboratory, Yale University. Manuscript received at the office of the Institute Dec. 1, 1936.

* United States Steel Corporation, Research Laboratory, Kearny, N. J.

† Assistant Professor of Metallurgy, Hammond Laboratory, Yale University, New Haven, Conn.

¹ References are at the end of the paper.

into a preheated graphite ingot mold, $1\frac{1}{2}$ in. in diameter by 6 in. long. Care was taken to avoid pipes by cooling from bottom to top. Subsequently these ingots were forged cold to bars $\frac{5}{8}$ in. in diameter and machined to tensile specimens having a diameter of 0.475 in. and a gauge length of 6 in. These polycrystalline specimens were then recrystallized to single crystals by a modification of the strain-annealing method, described by Vaughan H. Stott⁵. Of the 15 specimens treated in this manner, 11 became single crystals, and four were composed of two or three grains each.

Thirteen specimens of cold-rolled 99.90 per cent aluminum rod were similarly treated. Five of these were found to be single crystals, while the others contained from two to six grains apiece.

For the sake of comparison, two aluminum single crystals of the 99.90 per cent purity were grown by gradual solidification from the melt, in the same manner as that employed for the silver and zinc single crystals (Bridgman method)⁶. All the aluminum specimens were etched with Tucker's solution (25 per cent H_2O , 15 per cent conc. HF , 15 per cent conc. HNO_3 , and 45 per cent conc. HCl) to reveal the number of grains present.

Silver

The silver was donated for research use in the Hammond Laboratory by the Committee on Industrial Uses of Silver, through the courtesy of Mr. Lawrence Addicks and Dr. H. S. Rawdon. It was supplied in ingot form, accompanied by chemical and spectrographic analyses, and was of 99.999 per cent purity. Since the authors had had little experience in handling high-purity silver, they requested assistance from Handy and Harman, of Bridgeport. The silver was melted by that company in zircon crucibles, in 25-oz. melts, in a gas furnace, and poured into an open graphite mold 6 in. long by 1 in. wide by $\frac{3}{4}$ in. thick. The ingot was then hot-rolled on wire rolls at 1200° to 1300° F., to $\frac{5}{8}$ -in. squares, which were drawn cold through round dies to $\frac{3}{8}$ -in. dia. Etching in 1:1 HNO_3 and H_2O removed surface contamination. At Hammond Laboratory, the $\frac{3}{8}$ -in. silver rods were pointed at one end, cut to 10-in. lengths, and inserted in graphite molds. The rods were then changed into single crystals by the Bridgman method⁶. A Kanthal wound resistance furnace was employed at a temperature of 1020° C. A nickel muffle permitted the specimens to be melted in a nitrogen atmosphere. A lowering rate of $\frac{1}{2}$ in. per hour produced single crystals in every instance. After cooling, the specimens were etched with 40 per cent aqueous HNO_3 .

Zinc

Zinc single crystals of 99.999 per cent purity were produced by the Bridgman method⁶, in the manner previously described¹.

ANALYSIS OF PURITY OF SPECIMENS

Because of the great effect of minute amounts of impurity on the strength of single crystals, materials of the highest obtainable purity were employed, and spectrographic analyses were made to investigate the possibility of contamination during the process of manufacture of the crystals. The large Bausch & Lomb Littrow-type spectrograph at the Hammond Laboratory was used in making the analyses. The sources of excitation were the manufacturer's standard 220-volt d.c. arc, and a locally assembled condensed spark equipment. A nonrecording densitometer was used for measuring the plates.

Analysis of Aluminum

A survey of the literature on aluminum indicated the difficulty of obtaining reproducible results with arcing methods of excitation, because of interference from the large quantity of oxide formed, a defect absent when condensed sparks are employed. Smith⁷ reported successful use of the spark in analyzing commercial grades of aluminum, and his procedure was followed in the present work. Comparison was made between the impurity lines in the spectrum of the specimen and the selected nickel lines appearing in the spectrum of an auxiliary alloy of aluminum with 1 per cent of nickel added, both spectra recorded on adjacent portions of the same plate and produced under similar conditions. Control of electrical conditions was evidenced when equality was obtained in the blackening of the aluminum spark line 2816.2Å. and the arc line 2575.1Å.

Pairs of electrodes of the single crystal (99.90 per cent) and of ingot and single crystal (99.95 per cent) aluminum were made up in lengths of $2\frac{1}{2}$ by $\frac{3}{8}$ -in. dia., with chisel-shaped ends $\frac{3}{16}$ in. long.

The auxiliary alloy was prepared from 99.95 per cent aluminum and small pellets of Mond nickel, by melting in a crucible of Acheson graphite and casting in rod form in a mold of the same material. The rod was cut into two portions, and millings were made from the new surfaces for the chemical determination of nickel. The alloy contained 0.97 per cent nickel.

Standard conditions having been established, a series of exposures of the three types of electrodes was made, each exposure with an exposure of the auxiliary alloy immediately adjacent. After development, the various comparison lines were identified on the dry plate, and readings of total blackening of the lines were made in the densitometer. The readings were not corrected for general background, as all line pairs were relatively narrow, and all comparisons were made of line pairs produced under similar conditions and registered immediately adjacent on the same plate. The analytical results appear in Table 1.

TABLE 1.—*Spectrographic Analysis of Aluminum*

Element ^a	Aluminum 99.90 Per Cent, Single Crystal	Aluminum 99.95 Per Cent, Ingot	Aluminum 99.95 Per Cent, Single Crystal
Fe, per cent.....	0.05	^b	^b
Cu, per cent.....	0.01	0.015	0.015
Si, per cent.....	^b	^b	^b
Ti, per cent.....	0.01	0.007	0.007
Mn, per cent.....	0.01	^c	^c

^a Magnesium was present in all three samples in minute quantity.

^b Present but in smaller amounts than the lower limits of the analytical tables of Smith⁷.

^c Barely visible; appears to be of the order of 0.001 per cent.

The incomplete character of these results was recognized and chemical analysis was undertaken to fill some of the gaps. Ten-gram portions of millings of the 99.95 per cent samples were analyzed in duplicate for copper, silicon and iron, by a modification of the procedures outlined on pages 19, 20 and 21 of "Chemical Analysis of Aluminum⁸". The modifications consisted of variation in the quantity of acid due to the large amount of metal under test, although retaining the same basic acidity, weighing the silicon by difference after fuming with hydrofluoric and sulphuric acid, and the use of correction blanks for all reagents. The results are given in Table 2.

TABLE 2.—*Chemical Analysis of Aluminum*

Element	Aluminum 99.95 Per Cent, Ingot	Aluminum 99.95 Per Cent, Single Crystal	Aluminum 99.90 Per Cent, Single Crystal
Fe, per cent.....	0.013	0.012	0.060
Cu, per cent.....	0.012	0.010	0.007
Si, per cent.....	0.004	0.004	0.040

These tabulated results indicate that no appreciable contamination of the metal occurred during the manipulation incident to the preparation of the single crystals. This conclusion was further substantiated by the close agreement of the densitometer readings of the 99.95 per cent material.

Analysis of Silver

No attempt was made to determine the definite amounts of impurities present in the silver. It was considered sufficient to compare spectrographically the ingot with the single-crystal silver, since a complete spectrographic and chemical analysis had been supplied with the ingots by the U. S. Metals Refining Co. through the courtesy of the Committee on Industrial Uses of Silver (Table 3). This comparison was broadened

TABLE 3.—*Analysis of High-purity Silver*

Element	U. S. M. R. Co. Ingot Silver		Handy & Harman High-purity Silver	
	Chemical	Spectrographic	Chemical	Spectrographic
Au, per cent.....	0 001	0 001		N.D.
Ag, per cent.	99.993			
Cu, per cent.	0 0017	0.0020		Tr.
Fe, per cent.	0.0004	0.0008 ^a	0 0004	
Pb, per cent.	0 0003	0.001		Tr.
Bi, per cent.	Nil	N.D. ^b		Tr.?
Se, per cent.	Nil			N.D.
Te, per cent.	Nil			N.D.
Sn, per cent.		0.001		N.D.
Ni, per cent.		Tr. ^c		N.D.
Mn, per cent.		Tr.		N.D.
Mg, per cent.		P ^d		N.D.

^a Less than.^b Not detected.^c Less than 0.0001 per cent is present.^d Less than 0.005 per cent is present.

somewhat by the study of a sample of high-purity silver (999.90 fine or better) obtained from Handy & Harman, which had already been spectrographically analyzed by them (Table 3).

Pairs of electrodes of similar dimensions to those used for aluminum were prepared of ingot, single-crystal and high-purity silver. All were given a short etch in cold 10 per cent hydrochloric acid, washed in dilute ammonia and in distilled water. These were arced at a current of 5.0 amp. Comparisons were always made of spectral lines on the same plate. The blackening of similar lines of the impurities, in general the *raies ultimes*, was compared through densitometer readings. These readings confirmed the absence of elements chromium, cobalt, cadmium, zinc, indium, aluminum, osmium, iridium, platinum, rhodium and ruthenium, which were not detected spectrographically by the U. S. Metals Refining Co. The readings indicated that with the exception of iron and magnesium, the single crystal was similar to or purer than the ingot metal with respect to copper, lead and gold. The increase in iron content was negligible. The magnesium readings were not decisive.

A desire to clarify the question of magnesium content prompted the use of the condensed spark in a manner similar to that employed with the aluminum. The plate obtained under these conditions showed the presence of the magnesium spark lines at 2795.54Å. and 2802.7Å. in all three spectra. The ingot silver was definitely lower in this element than either the single-crystal or the high-purity silver. The difference in densi-

tometer readings did not indicate any large increase. The magnesium content was estimated to be of the order of 0.005 per cent.

The spectrographic work on the silver confirmed the purity of the original metal, and indicated that the single-crystal silver contained slightly more iron and magnesium than the ingot metal.

Analysis of Zinc

The spectrographic analysis of the zinc employed in these tests has been given in a previous publication¹.

DETERMINATION OF ORIENTATION AND STRESS CALCULATIONS

The method used for the determination of the orientation of the ductile zinc single crystals has been previously described¹.

The orientation of the silver and aluminum crystals was determined by the back-reflection Laue method described by Greninger⁹. A Seeman demountable, hot-cathode, X-ray tube was employed, utilizing a 25 milli-ampere filament current, a tungsten target, a 3-cm. specimen to film distance, and a 2-hr. exposure. The indices of the planes giving rise to the spots on the X-ray films were ascertained by measuring the interfacial angles with Greninger's⁹ hyperbolic coordinate plat. The azimuth and polar angles of these planes were then measured with the plat, and transferred to a stereographic projection. Suitable rotations gave the angle x between the axis of the specimen and the glide plane, and the angle λ between the glide directions [110] and the axis of the specimen with an error of less than $\pm 0.5^\circ$.

For each one of the four possible glide planes {111}, there were three possible glide directions [110]. By rotating each one of the four glide planes into the plane of the projection, and then projecting the axis of the specimen onto this plane, it was possible to pick out which one of the three possible [110] directions made the smallest angle (e) with the direction of action of the shearing force in the glide plane. This reduced the number of calculations necessary to determine the active glide directions from twelve to four. The formula for calculating the shearing stress acting in the glide plane and glide direction is given by Elam¹⁰:

$$S = \sigma \sin x \cos \lambda$$

where $\sigma = P/A$, tensile stress in specimen,

S , resolved shearing stress in grams per sq. mm.,

P , applied load in grams,

A , area of cross section of specimen in sq. mm.,

x , angle between {111} and axis of specimen,

λ , angle between [110] and axis of specimen.

Assuming that the active glide plane will be the one on which the greatest fraction (F) of the tensile stress will be acting in shear, it is

immediately possible to pick out from the tabulation of X-ray data for each specimen, such as that shown in Table 4, which one of the four

TABLE 4.—*X-ray Data Regarding Specimen IV*

{111} Plane	α , Deg.	θ , Deg	e , Deg	λ , Deg.	F
1	2	88	21.5	22	0.034
2	37	53	12.5	38	0.474
3	66.5	156.5	7	67	0.358
4	20.5	69.5	5.5	21.5	0.325

α , angle between specimen axis and {111}.

θ , $90^\circ \pm \alpha$.

e , angle between selected [110] and projection of specimen axis on glide plane (direction of maximum shear on glide plane).

λ , angle between [110] and specimen axis.

F , fraction of tensile stress acting in shear = $\sin \alpha \cos \lambda$. (F can vary from 0 to 0.5.)

possible glide planes will first act in shear. In that specimen, plane No. 2 is the active glide plane. The active glide planes for each specimen are given in Table 5. Traces of the glide plane on the surface of the speci-

TABLE 5.—*Tensile Tests of Aluminum and Silver Single Crystals*

Specimen No.	Purity, Per Cent Al	Testing Temperature, Deg. C.	Critical Shearing Stress, Grams per Sq. Mm.	Critical Shearing Stress, Lb. per Sq. In.	Diameter, In.	α , Deg.	e , Deg.	λ , Deg.	F
ALUMINUM									
I	99.90	27	138	196	0.506	34.	13.5	36.5	0.449
II.....	99.90	250	185	262	0.507	32	14.	35.	0.433
IV.....	99.95	23	50	71	0.419	37.	12.5	38.	0.474
IX.....	99.95	300	60	85	0.420	50	19.5	53.5	0.456
X.....	99.95	250	80	113	0.420	49.	3.	49.	0.496
XII.....	99.95	150	60	85	0.420	32.	23.5	39.	0.411
XIII.....	99.95	100	55	78	0.396	34	25.5	41.5	0.419
XIV.....	99.95	200	65	92	0.421	29.5	14.	33.	0.412
XVI.....	99.90	300	134	190	0.404	44.	2.5	44.5	0.496
XVIII.....	99.90	250	213	302	0.402	39.	8.	39.5	0.486
XXI	99.90	100	115	163	0.400	32.	3.	32.	0.449
XXIV.....	99.90	24	113	160	0.403	41.5	4.	42.	0.493
XXVII.....	99.90	200	145	206	0.405	51.	11.	52.	0.479
XXVIII.....	99.90	150	90	128	0.400	34.	20.	39.5	0.432
SILVER									
2 Ag.....	99.99	250	31	44	0.373	33.5	14.5	36.5	0.444
5 Ag.....	99.99	300	55	78	0.377	48.5	3.	49.	0.492
6 Ag.....	99.99	200	23	33	0.373	35.	15.5	37.5	0.455
7 Ag.....	99.99	100	47	67	0.373	40.	26.5	47.	0.439

men after the tensile test permitted the predicted angle α to be checked by the observed angle; close agreement was found.

When a tensile test was carried out, the observed values were the amount of load in pounds* and the simultaneous amount of extension in microns. Knowing the load and the cross-sectional area of the round specimen, it was possible to calculate the corresponding shearing stress, using the formula given above. None of these tests were carried to a sufficient extension to cause double glide by rotation of the next most favorable glide plane into a position where it also would begin to slip.

TENSILE TESTS

The tensile tests were carried out with the creep-testing apparatus previously described¹. The specimen was suspended from a heavy steel framework and connected at the bottom to a 6:1 lever. Loading was caused by allowing sand to flow from a reservoir into a loading bucket attached to the end of the lever. A uniform rate of loading of 3 lb. per minute was used in all the tests. The rate of extension was so slow that it was possible to measure the distance between the reference marks every minute with no appreciable error caused by alternate readings of the two microscopes. An electric furnace surrounded the specimen, keeping it at the desired temperature during the test.

Extension of Aluminum Single Crystals

Single crystals of 99.95 per cent aluminum were tested at 23°, 100°, 150°, 200°, 250° and 300° C. The results of the tests are shown in Fig. 1, in which the resolved shearing stress is plotted against the amount of extension. Owing to the sensitivity of the extensometer employed, the strain coordinate is highly magnified, thereby revealing the early stages of plastic deformation. Most unexpected features are disclosed between 0 and 1.5 per cent extension, a region totally blind in the previously published curves of the effect of temperature on the plasticity of aluminum single crystals. (See, for example, Fig. 127, p. 162, "Kristallplastizität" by E. Schmid and W. Boas¹¹.)

The shapes of all the curves in Fig. 1 are similar, but their relative positions are drastically modified by the testing temperature. In order to clarify the discussion of the curves, each will be divided into three zones. Zone 1 is the elastic range; zone 2 is the range of "yield-point elongation" lying between the elastic range and zone 3, where abundant plastic deformation begins to occur. Taking the curve for specimen IV tested at 23° C., for example, as the load is increased, only elastic deformation (zone 1) is noted until a critical shearing stress of about 50 grams per sq. mm. is exceeded. Rapid extension then appears (zone 2), followed by a sharply decreasing rate of flow. Zone 3 commences when fur-

* Data available in this field have been expressed in grams per square millimeter, which is close to the figure used in American engineering practice. (Conversion factor, 1 gram per sq. mm. = 1.42 lb. per sq. in.)

ther increase of stress causes the flow rate to again increase (at a shear stress of about 170 grams per sq. mm.).

Analysis of the curves shows that as the temperature of the test is increased, the magnitude of zone 1 increases up to 250° C.; i.e., the critical shearing stress increases with increasing temperature (Table 5). The magnitude of zone 2 decreases with increasing temperature, and the rate

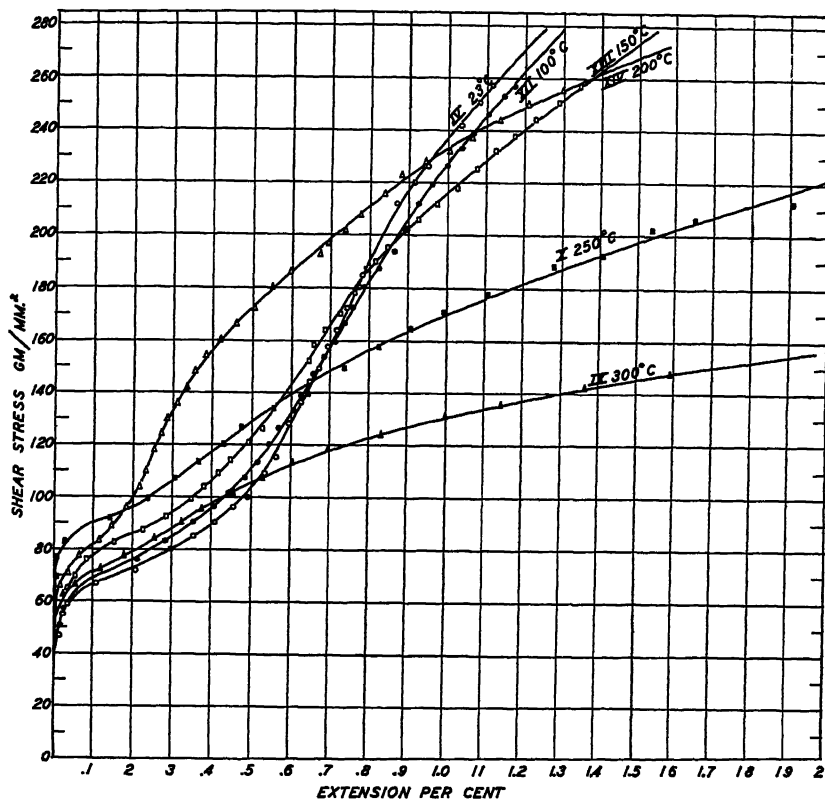


FIG. 1.—INFLUENCE OF TEMPERATURE ON STRESS-STRAIN CURVES OF RECRYSTALLIZED ALUMINUM SINGLE CRYSTALS OF 99.95 PER CENT PURITY.
Load added at rate of 3 lb. per minute.

of deformation in this range becomes slower the higher the temperature (up to 200° C.). Zone 3 begins at smaller amounts of deformation the higher the temperature, and in this region the normal effect of temperature is observed—the higher the testing temperature, the more rapid the ultimate rate of flow.

In an effort to ascertain whether or not this peculiar temperature effect is confined to recrystallized aluminum single crystals of this degree of purity, tests were made with the same loading rate and testing temperatures on recrystallized single crystals of 99.90 per cent aluminum. The

results are shown in Fig. 2. The same configuration is apparent, although markedly displaced toward higher temperatures and stresses, presumably

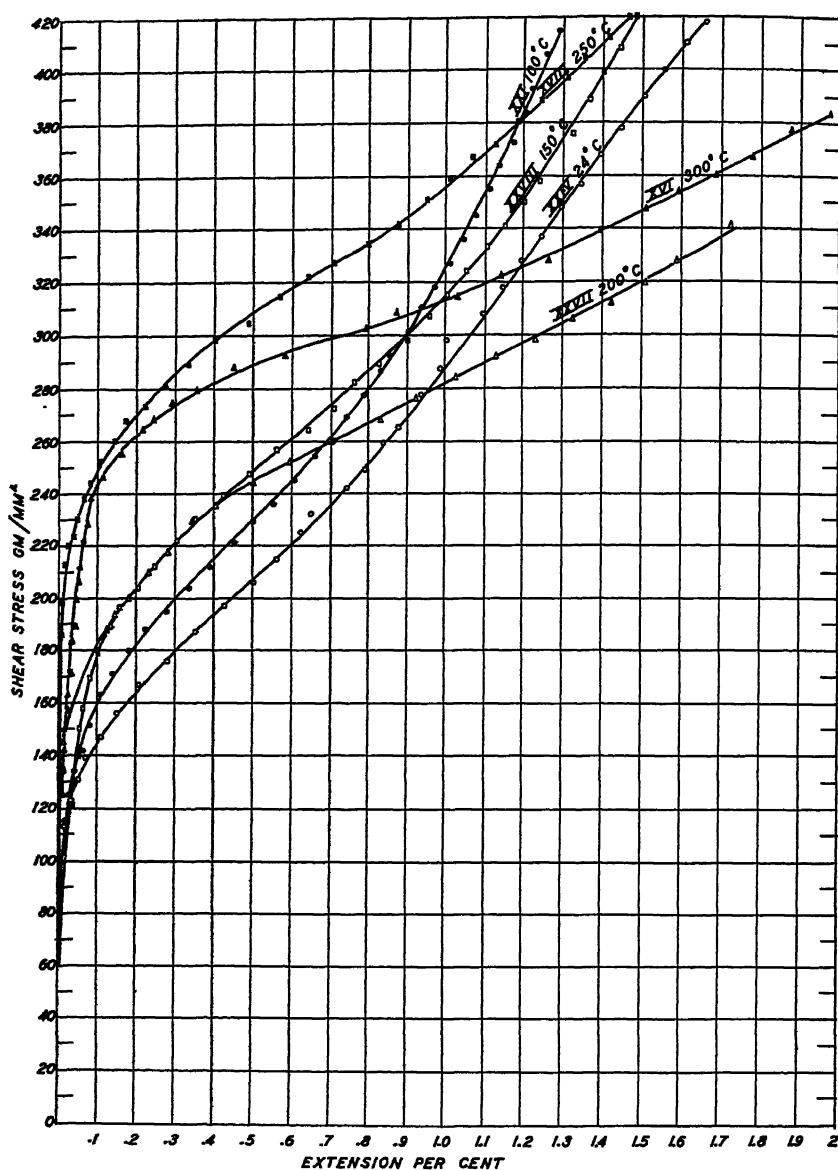


FIG. 2.—INFLUENCE OF TEMPERATURE ON STRESS-STRAIN CURVES OF RECRYSTALLIZED ALUMINUM SINGLE CRYSTALS OF 99.90 PER CENT PURITY.
Load added at rate of 3 lb. per minute.

by the presence of the greater amount of impurity. The specimens did not behave as uniformly, but in the early stages of the plastic deformation

the curves are in the same order, except that the specimen tested at 300° C. did not begin to deform quite as readily as the similar specimen of

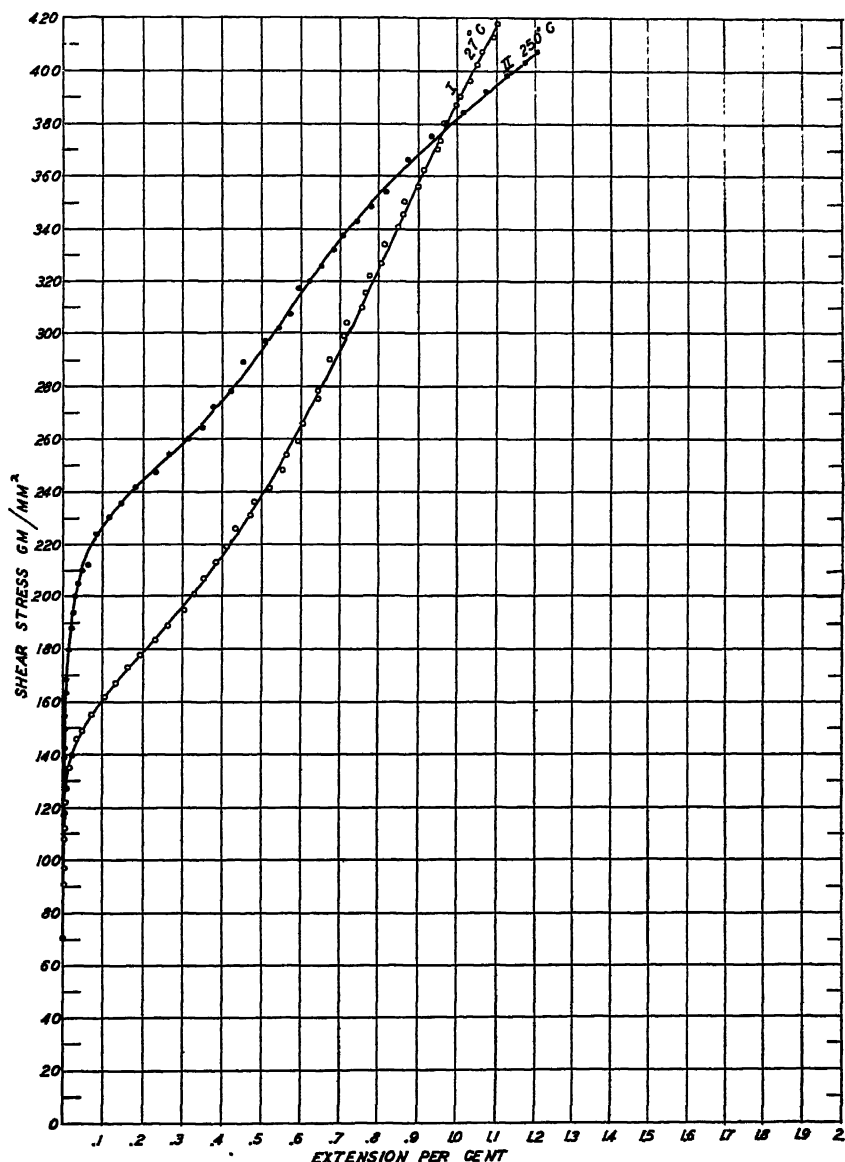


FIG. 3.—INFLUENCE OF TEMPERATURE ON STRESS-STRAIN CURVES OF GRADUALLY SOLIDIFIED ALUMINUM SINGLE CRYSTALS OF 99.90 PER CENT PURITY.

Load added at rate of 3 lb. per minute.

higher purity. Also, in the later stages of deformation, the reversal of the curves was not as regular, and larger amounts of deformation than

were possible with the apparatus employed seemed to be necessary to cause them to fall into the correct order. It should also be noticed that the increased amount of impurity seemed to mask almost entirely the "yield-point elongation" effect. However, the elastic limit is noticeably raised up to 250° C. by increasing temperature (Table 5). Two distinct

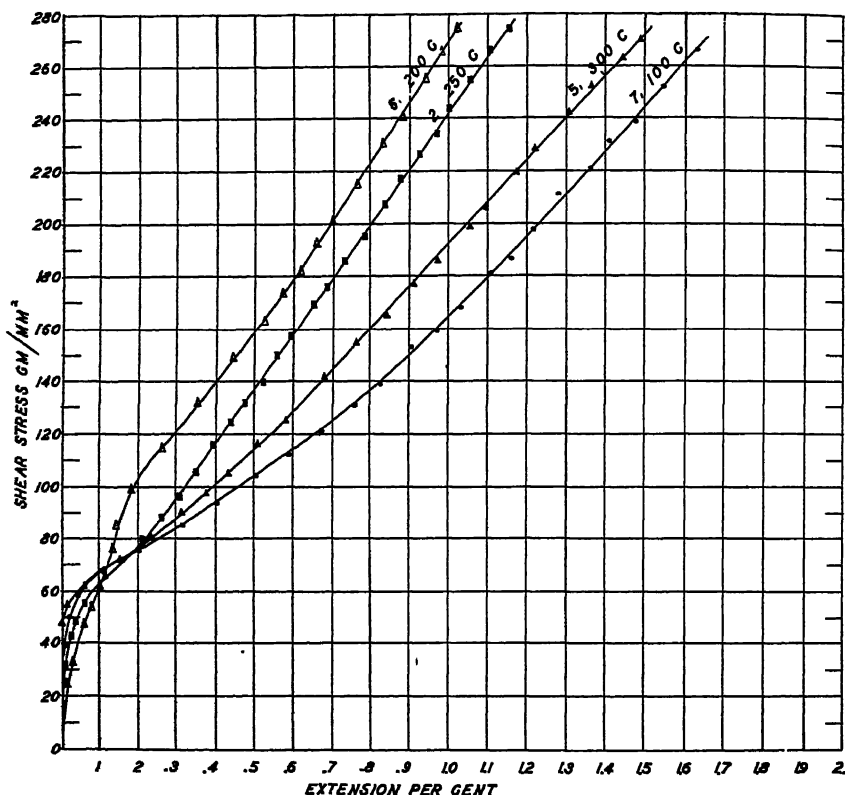


FIG. 4.—INFLUENCE OF TEMPERATURE ON STRESS-STRAIN CURVES OF GRADUALLY SOLIDIFIED SILVER SINGLE CRYSTALS OF 99.99 PER CENT PURITY.
Load added at rate of 3 lb. per minute.

sets of curves are evident in Figs. 1 and 2; one set, consisting of specimens tested at 23°, 100° and 150° C., and the other set, showing much more rapid flow, consisting of specimens tested at 200°, 250° and 300° C.

Tests were also made on two 99.90 per cent aluminum single crystals (I and II) grown by gradual solidification from the melt (Bridgman method⁶). The results of the tensile tests at 27° and 250° C. on these specimens are shown in Fig. 3. Here also the elastic range is raised by increase of testing temperature (Table 5), and the same crossing of the curves is noted, showing that in the early stages of plastic deformation the specimen tested at the lower temperature deformed more readily.

The curves are similar to those of the strain-annealed single crystals of the same purity tested at the same temperature.

Extension of Silver Single Crystals

Similar tests were made on silver, which could be obtained in a state of much higher purity than could aluminum. Silver was selected also because of the similarity of its glide system and recrystallization range to those of aluminum. The data concerning the specimens are shown in Table 5, and the results of the tensile tests at different temperatures are seen in Fig. 4. The same reversal of curves is noted here. The critical shearing stress is higher the higher the temperature. The specimen tested at 100° C. was accidentally bent before testing, accounting for its confused position. The silver crystals had a noticeably lower yield point (Table 5) than the aluminum crystals, but showed more rapid strain-hardening even though the purity was higher.

TABLE 6.—*Tensile Tests of Zinc Single Crystals*

Specimen No.	Testing Temperature, Deg. C.	Diameter, In.	α , Deg.	ϵ , Deg.	λ , Deg.	F
R-4.	250	0.490	70.2	30.	73.	0.274
R-14.	25	0.405	22.2	17.5	28.	0.332
R-19.	300	0.481	81.	22.2	81.7	0.143
R-20.	20	0.495	66.5	4.7	66.6	0.363
R-21.	150	0.480	24.8	27.4	36.2	0.339

α , angle between specimen axis and (0001).

ϵ , angle between selected [11 $\bar{2}$ 0] and projection of specimen axis on glide plane (direction of maximum shear on glide plane).

λ , angle between glide direction [11 $\bar{2}$ 0] and specimen axis.

Extension of Zinc Single Crystals

Several ductile zinc single crystals were tested in a manner similar to that employed for the aluminum and silver single crystals except that the load was added at a rate of $\frac{1}{2}$ lb. per min. The data concerning the zinc crystals are in Table 6, and the results of the test are shown in the solid curves in Fig. 5. It was noted in a previous investigation¹ that there was no measurable critical shearing stress in ductile zinc single crystals tested in creep at or above room temperature. The presence of an apparent elastic range in the solid curves in Fig. 5 may be attributed to the fact that these are stress-strain curves, the speed of testing being much more rapid than it was in the creep tests. The effect of the increase of rate of straining is demonstrated by the dotted curve in Fig. 5, which is intermediate between a creep curve and a stress-strain curve. In testing this specimen, the load was added in small increments separated by intervals of one day.

The crystals behave in a manner consistent with the observations on aluminum above its recrystallization temperature; no crossing of the curves is noted, and an increase in testing temperature causes increase in the ease of flow.

DISCUSSION OF RESULTS

The purpose of the present work was to investigate the influence of temperature on the elastic range in metallic single crystals of high purity. Previous work¹ had shown that there was no measurable elastic range in

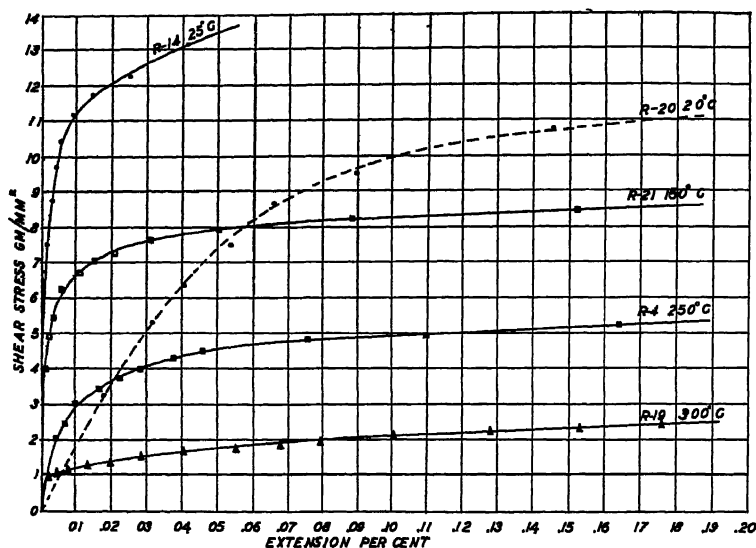


FIG. 5.—INFLUENCE OF TEMPERATURE ON STRESS-STRAIN CURVES OF GRADUALLY SOLIDIFIED ZINC SINGLE CRYSTALS OF 99.999 PER CENT PURITY.

Load added at rate of $\frac{1}{2}$ lb. per min., except in test shown by dotted curve, in which increments of load were applied at intervals of one day.

ductile zinc single crystals when tested in creep at or above room temperature. The slow tensile tests made on zinc in the present investigation confirmed this conclusion, and showed that the presence of an elastic range above the recrystallization temperature is apparent only when the rate of testing is rapid enough to make the rate of strain-hardening more rapid than the rate of relief of strain.

The results of the tests on aluminum single crystals show that above 250°C . the elastic limit drops sharply. This is known to be near the temperature at which cold-worked polycrystalline aluminum of this degree of purity will begin to show visible recrystallization in the length of time occupied by this test—about 2 hr. Such a drop in the elastic limit was expected, since a marked change in the creep properties of aluminum occurs at about this temperature³. Whether the critical shearing stress of 60 grams per sq. mm. shown by specimen IX tested at

300° C. (Fig. 1 and Table 5) is a definite quantity, or whether the elastic range for this specimen is only apparent (similar to the elastic range in zinc single crystals tested at or above room temperature) is not known, since no variation in testing speed was employed in studying the aluminum crystals.

The appearance of a larger and seemingly definite critical shearing stress near the lowest temperature of recrystallization of polycrystalline aluminum seems to be consistent with evidence derived from creep tests on aluminum single crystals³. Also, it is in harmony with Taylor's¹² theory of plastic deformation, which states that below a certain critical temperature (perhaps the recrystallization or recovery temperature) a finite stress is required to cause the atoms on the glide planes to jump the first potential barriers and for plastic deformation to commence.

No reason is known for the apparent increase of elastic limit with increase of temperature below the recrystallization temperature. It has been suggested that this increase of strength with increase of testing temperature may be due to age-hardening resulting from the precipitation of the 0.05 per cent impurity present. This seems hardly likely, however, since the crystals were all furnace-cooled from just below the melting point of aluminum after their production, giving ample opportunity for the precipitation of any solutes that might be present. To eliminate this argument completely, and also to discover whether this peculiarity is confined to aluminum, tests were made as described above on high-purity (99.99 per cent) silver. The possibility of contamination of the material during the production of the single crystals was thoroughly examined by spectrographic analysis, and the conclusion was reached that there had been little if any loss in purity.

The silver showed the same increase of elastic range with increase of temperature up to 300° C. The limited time available did not permit the extension of the studies on silver, but it is to be expected that at some higher temperature, corresponding to the lowest temperature of recrystallization for the speed of testing employed, there would be a sudden decrease in the elastic limit.

The presence in the aluminum single crystals of a marked "yield-point elongation," which is more marked the lower the temperature of the test and the purer the metal, is not so surprising as the increase of the elastic limit with increase of temperature. The "yield-point elongation" is a characteristic of annealed low-carbon steel, and has been noted by Schoenmaker¹³ at low temperatures in copper and brass. Perhaps the behavior of the aluminum single crystals below their recrystallization temperature could be considered in the following manner.

The strain-free crystals do not begin to slip plastically until a certain critical stress has been reached, but when this stress is exceeded they may glide a small amount before enough strain-hardening has been produced

to retard the deformation to the normal amount. The face-centered cubic metals, being softer than the body-centered (iron) may show this behavior only at low temperatures and in the very early stages of plastic deformation. It may be that at lower temperatures the glide planes have less tendency to rumple, and for that reason the "yield-point elongation" takes place more readily at lower temperatures. The argument that the gradual disappearance of the "yield-point elongation" with increase of temperature may be due to age-hardening may be dismissed for the same reasons as were stated above in the discussion of the possibility of age-hardening affecting the elastic range.

In the foregoing discussion, the word "recrystallization" has been freely used. That visible recrystallization, using the term in the sense commonly employed when discussing polycrystals, does not occur in the single crystals is evidenced by the fact that the crystallographic laws for glide are obeyed in all three metals at all temperatures and up to the highest amounts of extension used. However, a decided change in the behavior of aluminum is apparent between 200° and 300° C., and it is known from the literature and from tests on the metal used that the first visible recrystallization does occur in this range for cold-worked polycrystalline aluminum in the length of time occupied by the test. The significance of this temperature in the study of aluminum single crystals seems to be that somewhere in this range, for the given speed of testing, the rate of relief of strain (rate of recovery) begins to exceed the rate of strain-hardening, and marked flow takes place with much lower stresses. The evidence shown by the silver seems to indicate that even 300° C. is below the critical range for the purity of metal and speed of testing used.

The fact that the zinc used in the present work will recrystallize at room temperature has also been experimentally observed. The recrystallization temperature of zinc is not definitely known, and no tests on zinc were carried out below room temperature.

In an attempt to discover whether or not the crossing of the stress-strain curves and the increase of strength of the aluminum and silver crystals up to the recrystallization temperature might be due to the manner of plotting the results of the tensile tests, curves were drawn showing the tensile stress instead of the resolved shearing stress plotted against the amount of extension, and curves were also drawn showing the resolved shearing stress plotted against the amount of shear. (The amount of shear (s) in the single crystal may be derived from the amount of strain by use of the formula $s = \frac{1}{2} \sin \alpha (\sqrt{d^2 - \sin^2 \lambda} - \cos \lambda)^{11}$.) In both these methods of plotting, all salient features of the curves remained in evidence, but slightly displaced in each case.

It is noteworthy that the temperature range and small amounts of extension studied in the present work are of about the same magnitude as those important in the creep studies of steel and other metals. The

similarity in behavior of the aluminum single crystals and mild steel in regard to the yield-point elongation has already been mentioned, and it is possible that some of the other phenomena found in the present work may be encountered in commercial metals in the early stages of their extension, such as the reversal of the effect of temperature on the yield-point elongation (zone 2), and the increase of the elastic range with increase of temperature up to the recrystallization temperature.

CONCLUSIONS

1. Slow tensile tests on ductile zinc single crystals at or above room temperature show that the magnitude of the apparent elastic range depends on the speed of testing, and the conclusion drawn from creep tests, that in this temperature range there is no measurable critical shearing stress, is supported.

2. Slow tensile tests on aluminum and silver single crystals show that there is a small but definite elastic range below the recrystallization temperature; this elastic range is smaller the lower the temperature. Above the recrystallization temperature the critical shearing stress decreases rapidly. Time was not available for creep tests on aluminum and silver, but it is expected that above the recrystallization temperature they would behave in a manner similar to zinc (no measurable critical shearing stress would be encountered).

3. A marked yield-point elongation was noted in the aluminum single crystals, which was more marked the lower the temperature of the test and the purer the metal. During this period, increase of temperature decreased rather than increased the rate of flow. Following this period, the stress-strain curves crossed, and the temperature effect was normal; i.e., increase of temperature increased the rate of flow.

ACKNOWLEDGMENTS

The authors are indebted to Dr. C. H. Mathewson and other members of the Department of Metallurgy at Yale University for their assistance, criticisms and suggestions.

REFERENCES

1. R. F. Miller: Creep and Twinning in Zinc Single Crystals. *Trans. A.I.M.E.* (1936) **118**, 176.
2. C. L. Clark and A. E. White: Influence of Recrystallization Temperature and Grain Size on Creep Characteristics of Non-ferrous Alloys. *Proc. Amer. Soc. Test. Mat.* (1932) **32**, pt. 2, 492-506.
3. D. Hanson and M. A. Wheeler: Deformation of Metals under Prolonged Loading, 1.—The Flow and Fracture of Aluminum. *Jnl. Inst. of Metals* (1931) **45**, 229.
4. C. L. Clark and A. E. White: Creep Characteristics of Metals. *Amer. Soc. Metals Preprint* 2 (1936.)

5. V. H. Stott: A Modification of Carpenter and Elam's Method of Producing Single Crystals of Aluminum by Deformation and Annealing. *Trans. Faraday Soc.* (1935) **31**, 998-1000.
6. P. W. Bridgman: Certain Physical Properties of Single Crystals of Tungsten, Antimony, Bismuth, Tellurium, Cadmium, Zinc, and Tin. *Proc. Amer. Acad. Arts and Sci.* (1925) **60**, 305.
7. D. M. Smith: Spectrographic Analysis of Aluminum. *Jnl. Inst. of Metals* (1935) **56**, pt. 1, 257.
8. H. V. Churchill and R. W. Bridges: Chemical Analysis of Aluminum. Aluminum Research Laboratories, New Kensington, Pa.
9. A. B. Greninger: Determination of Orientations of Metallic Crystals by Means of Back-reflection Laue Photographs. *Trans. A.I.M.E.* (1935) **117**, 75-89.
10. C. F. Elam: Distortion of Metal Crystals. Oxford, 1935. Clarendon Press.
11. E. Schmid and W. Boas: Kristallplastizität. Berlin, 1935. Verlag von Julius Springer.
12. G. I. Taylor: Mechanism of Plastic Deformation. *Proc. Roy. Soc.* (1934) **A145**, 362-404.
13. P. Schoenmaker: Tensile and Impact Tests at Low Temperature. First Comm. New Int. Ass. Test. Mat. (1930) [A], 237-250.

DISCUSSION

(S. L. Hoyt presiding)

G. EDMUNDS,* Palmerton, Pa.—I congratulate Dr. Miller and Mr. Milligan on a very well done job, both from the standpoint of the experimental technique and Dr. Miller's presentation, which has been excellent.

In Table 5 the authors have given the values of F , the fraction of the tensile stress that acts in shear. These are taken as the maximum values of F for any one of the $\{111\}$ planes that are in position for slip. By calculations I have made, I notice that for certain directions of applied stress the value of F will be a great deal below the values that have been given in Table 5 for both the aluminum and silver crystals. For example, if the axis of the specimen is parallel to a $[111]$ direction, the angle between the direction of stress and the only $\{111\}$ slip planes that could possibly act would be about $19\frac{1}{2}^\circ$. At the same time the angle between the crystal axis and the direction of shear would be about $35\frac{3}{4}^\circ$, which means that the value of F would amount to 0.272. That, of course, indicates that there have been no crystals examined that had anywhere near that orientation. Dr. Fink has told me that the $[111]$ direction lies parallel to the wire axis in a drawn aluminum wire. Were all of the specimens concerned here rolled rods which had been machined and recrystallized?

Aside from crystals 1 and 2, throughout Table 5, including both the aluminum and silver, a mode of preparation was used that would have tended to align a $[111]$ direction with the crystal axis. Yet the recrystallized structures have departed rather widely from that, which is a point of possible interest.

The authors state on page 236 that none of these tests were carried to a sufficient extension to cause double glide by rotation of the next most favorable glide plane into a position where it would also begin to slip. It may be pointed out, however, that slip might occur in two directions in one of the zinc crystals; namely, specimen No. R-4 of Table 6 of the preprint, since it is so oriented that the projection of the rod axis on the slip plane makes an angle of 30 degrees with each of two slip directions on that plane. This would mean that slip would as likely start in one as the other direction.

* Investigator, Research Division, New Jersey Zinc Co.

Having started in a given direction it would so continue unless affected by changes in the relative resistance to slip in the directions concerned. If it so happened that the slip resistance increased enough more rapidly in the active than in the inactive direction slip in the second direction might then take place. By this mechanism slip might occur in two directions in this particular crystal.

I might also point out in regard to the zinc crystals that the F values reach a minimum of 0.143. The minimum value of F in the zinc crystals is dependent upon the position of the crystal with reference to the direction of stress at which slip takes place in preference to twinning or at which slip will take place in preference to cleavage. It is possible to have values of F , such as Dr. Miller has given us, much lower than any that could be encountered in connection with the aluminum crystals.

A. V. DE FOREST,* Cambridge, Mass.—This piece of work is illuminating a very important corner of the age-hardening reaction. The reaction that occurs when a piece of cold-worked material is reheated in most cases is an increase in its elastic behavior. In other words, the perfection of elasticity goes up and the damping capacity goes down; the material becomes a better spring as there is lower creep at room temperature. The reason for that is still considerably obscure, but I think that it is a little clearer from this work than it has been in the past. The usual explanation, or at least one of the usual explanations of that behavior has called for some form of precipitation-hardening. The old idea of aging has gradually shaded off into a precipitation reaction. When precipitation became a powerful explanation for a great many mechanical behaviors of material, this idea of precipitation fitted the case very nicely except for the fact that it also worked on very pure materials.

I believe Chevenard published results on damping capacity of pure gold in which cold-worked and reheated gold had an elastic behavior exactly similar to that of a very impure copper-silver alloy.

In the case before us, not only a pure material but also a single-crystal material is doing the same thing, so we have to get rid of the idea of the ordinary form of precipitation. Dr. Miller's remarks about the roughening effect may be a point of a good deal of importance. I should like to look at this as a galling effect on the slip plane, that instead of having a foreign material required to do the hardening, perhaps a fragment can be rolled up between the slip planes exactly as a fragment is rolled up in the ordinary galling behavior of screwing a pipe into a coupling. Perhaps something of the same kind is happening along even these very slight deformations in single crystals.

Another thing adds to that picture a little. Using a very sensitive recording strain measurement on the early stages of creep at room temperature, Mr. Carson has shown steps in the creep rate exactly similar to the steps in the plastic deformation of many materials especially at elevated temperature, in other words, discontinuous creep, as we have discontinuous extension in the plastic range. That would indicate that again creep is not a matter of extension elastically throughout the whole mass of the material, but is a very local effect. This observation tends to improve the possibility of explaining strain-hardening by this galling reaction, because if all the creep takes place on one plane there is a considerable amount of deformation available to do the required work.

C. STARR,† Cambridge, Mass.—The difference in behavior of the single crystals above and below the recrystallization temperature may have a simple explanation. It is debatable whether a single crystal that has been strained remains a single crystal. The stress-strain curves below the recrystallization temperature are probably those of

* Associate Professor, Mechanical Engineering, Massachusetts Institute of Technology.

† Harvard University.

gradually produced polycrystalline material. Above the recrystallization temperature, the condition of self-anneal sets in, so that the single-crystal structure tends to be preserved and the resultant stress-strain curves approach that of true single crystals. The low-temperature production of polycrystals from the single crystal might occur most rapidly at that part of the stress-strain curve called the "yield-point elongation." The decrease of this "yield-point elongation" with rising temperature follows from this hypothesis, since the production of polycrystals would decrease with increasing rate of self-anneal. Since recrystallization is an exponential function of time and temperature, the stress-strain curves should be functions of both rate of loading and temperature. The dotted curve of Fig. 5 for zinc is consistent with this analysis, as it shows a typical self-anneal curve at a very low temperature and at a greatly decreased rate of loading.

A. J. PHILLIPS,* Maurer, N. J.—I should like to defend the old precipitation idea, not that I have any data to prove that it is correct but merely because I do not feel that ample evidence has been presented here today to rule out the precipitation theory. My contention is based merely upon the fact that in working with lead alloys we have been able to demonstrate, we feel quite definitely, that certain alloying elements in values as low as 0.005 per cent will produce precipitation-hardening in lead of a considerable magnitude—enough to raise the tensile strength between 10 and 20 per cent. Therefore I contend that until we are sure that the elements or impurities in the alloy in the third decimal place are of no importance, we cannot rule out the possibility of precipitation-hardening even though the alloy is made from 99.99 per cent pure metals.

T. E. NORMAN,† Toronto, Ont.—We had some experience regarding purity. We ran a series of corrosion tests with two types of zinc, one manufactured by the electrolytic process and one made by the retort process, both supposed to be as pure as it is possible to get commercial zinc. They were "both four nines plus." The marked difference in the rate of corrosion between the electrolytic zinc and the retort zinc indicated that the type of impurity in the zinc certainly had some effect. It might be interesting to try out the two types of zinc on such tests as these.

J. WINLOCK‡ AND R. W. E. LEITER,§ Philadelphia, Pa. (written discussion).—As to whether any departure from the ordinary load-deformation relations shown by polycrystalline aluminum, copper, etc. is a "yield-point elongation" may, of course, be partly a matter of definition. If a yield-point elongation is taken simply to mean any such departure, the load-deformation curves of the single crystals of aluminum obtained by the authors may certainly be considered as having yield-point elongations. It does not seem to us, however, that the same phenomenon is taking place in the authors' single crystals as occurs in the load-deformation curves of annealed polycrystalline iron and low-carbon steel, which more generally conform to our conception of a yield-point elongation. As we will attempt to explain, it is possible that this view might be changed if autographic load-deformation curves were obtained.

In annealed polycrystalline iron and low-carbon steel, the existence of the kind of nonuniform deformation generally referred to as "yield-point elongation" appears, as we see it, to depend upon the ability of the metal to support a greater load before the initiation of plastic deformation than it can support (without further plastic deforma-

* Superintendent of Research, Central Research Laboratory, American Smelting and Refining Co.

† Research Fellow, Department of Engineering and Metallurgy, Ontario Research Foundation.

‡ Chief Metallurgist, Edward G. Budd Manufacturing Co.

§ Research Metallurgist, Edward G. Budd Manufacturing Co.

tion taking place) immediately after plastic deformation has occurred. With single crystals of aluminum and with polycrystalline aluminum and copper, however, the reverse of these conditions appears to exist. In other words, at the instant plastic deformation starts in annealed polycrystalline iron and low-carbon steel, a *lower* load can produce a continuation of plastic deformation, whereas in single crystals of aluminum and in polycrystalline aluminum and copper a *greater* load is immediately necessary to produce a continuation of plastic deformation. In the former, the result is a marked nonuniform extension throughout the gauge length, whereas in the latter the extension is practically uniform.

As we see it, however, the phenomenon in the polycrystalline ferrous metals does not resolve itself into a question of the weakness of the metal at the instant plastic deformation starts, but rather into a question of its inordinately high strength before the initiation of plastic deformation. At the top of page 244, for example, the authors suggest that the reason for a different behavior of some metals at the yield point at low temperatures is because the gliding planes have "less tendency to rumple." This infers that the cause of the phenomenon is a result of something that occurs after plastic deformation has occurred. If the cause of the phenomenon lies, as we think it does, simply upon the degree of resistance of the metal to the initiation of plastic deformation, might it not be that a lowered atomic mobility (which decreases as the temperature decreases) simply increases this resistance?

In order to clarify our point of view, it appears that substantial yielding in annealed polycrystalline iron and low-carbon steel should take place at the load *Y* in Fig. 6 and that the load-deformation curve of these metals should be the curve *OYLM* instead of the well-known curve *OALM*. As may readily be seen, it is a curve of the shape *OYLM* that characterizes the load-deformation relations of polycrystalline aluminum and copper. For some reason, however, the load *Y* is "overshot" in annealed polycrystalline iron and low-carbon steel and substantial yielding does not start until the load *A* is reached. When plastic deformation does start, the metal finds itself "overloaded," so to speak, and its subsequent behavior is due to the efforts of the metal to resist this high load. According to our view, then, the load drops because the load-carrying capacity of the metal in the elastic state is greater than its load-carrying capacity at the instant plastic deformation starts and because of a concomitant concentration of the imposed load. The load does not drop to the load *Y*, however, because a balance is reached between these factors and (1) the increase in resistance of the metal undergoing plastic deformation once this has started (work-strengthening); (2) the increase in resistance of the metal undergoing plastic deformation to the high speed of deformation caused by the high load to which it finds itself subjected; (3) by the presence of metal in other parts of the gauge length which must be stressed to a value corresponding to the upper yield point before it can deform plastically. The extremely important point, then, is that at the instant plastic deformation is initiated in annealed polycrystalline iron and low-carbon steel it is not necessary to have present the load to which the metal finds itself subjected in order for further plastic deformation to take place. The potentiality of the metal to withstand this

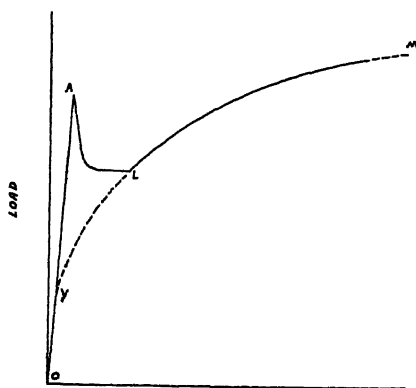


FIG. 6.

high stress while in the elastic state is manifested in the load-deformation curve, as we have described in a recent paper.¹⁴

It is especially worthy of notice that if annealed polycrystalline iron and low-carbon steel have been slightly cold-worked, the load-deformation curve will take the shape of the load-deformation curves of the nonferrous metals. This is because the cold-work puts the steel in a condition in which there is a comparative freedom from metal which can maintain an elastic behavior at loads greater than Y in Fig. 6. That is, it appears as though cold-work produced nuclei from which uniform elongation can take place in a normal manner; i.e., in the same manner as do annealed polycrystalline aluminum and copper. It is, of course, quite clear that such nuclei must be present throughout the whole gauge length for this to occur. For example, if the specimen is slightly cold-worked at only one spot in the gauge length, and the specimen is tested before "aging" has taken place, yielding will occur at a low load because of the cold-work but the remaining parts must still be subjected to a stress corresponding to the "upper" yield point (even though the load at which this occurs is lower) before plastic deformation can take place throughout the gauge length in a normal manner.

It is clear, of course, that if annealed polycrystalline iron and low-carbon steel were tested as the authors have tested their specimens of single crystals of aluminum—that is, under a *constant rate of loading* instead of a *constant rate of deformation*—the load-deformation curve would be somewhat different from Fig. 6. If the metal were tested under a constant rate of loading, the load on the specimen could not, obviously, drop off at A and, further, there could never be a constant load at which plastic deformation could take place. Under these conditions, all of the metal in the gauge length would be deformed at a high speed at the load A and, because of the constantly increasing load, the line Aa would slope slightly upwards. If, however, there is an "overshooting" of the load Y , as we have described, so that the load-carrying capacity of the metal at the instant plastic deformation takes place has been exceeded, the transition at A would always be abrupt and the change of slope at L would always be sudden. The authors' curves do not show the abrupt transitions and sudden changes in slope which we think necessary to indicate the presence of a yield-point elongation similar to that which occurs in annealed polycrystalline iron and low-carbon steel. It is possible that by taking readings only at different increments of extension, as was done by the authors, instead of by an autographic method, the abrupt changes in slope were not observed. And the reference at the bottom of page 236 to an "increase in the speed of deformation at zone 2" of the authors' curves tends to strengthen this possibility. But, until such sudden transitions are obtained, there is some doubt as to whether a real yield-point elongation exists in single crystals of aluminum at any of the temperatures employed by the authors. In our opinion, the authors' interesting load-deformation curves show simply a gradual change in the work-strengthening rate during plastic deformation.

R. F. MILLER (written discussion).—In answer to Mr. Edmunds' question, only specimens XVI to XXVIII were machined and recrystallized from rolled rods. Specimens IV to XIV were cast from ingots, then forged and recrystallized to single crystals. Specimens I and II were grown by the Bridgman method of gradual solidification from the melt. It should be pointed out that for each specimen listed in Table 5, the fraction (F) of the tensile stress acting in shear was calculated for all the $\{111\}$ planes, but only the maximum value was reported in Table 5, since it was on

¹⁴ J. Winlock and R. W. E. Leiter: Some Factors Affecting the Plastic Deformation of Sheet and Strip Steel and Their Relation to the Deep Drawing Properties. *Trans. Amer. Soc. Metals* (March, 1937).

that plane that glide first occurred. There were, of course, other potential glide planes in each crystal, on which F had lower values. The statement made on page 236, that none of these tests were carried to a sufficient extension to cause double glide by rotation of the next most favorable glide plane into a position where it also would begin to slip, referred to the cubic crystals, aluminum and silver. Double glide cannot take place in the ductile zinc single crystals, since there is only one glide plane (the basal plane). It is not conceivable that glide could take place simultaneously in two directions on the basal plane in the zinc single crystals. Such "double glide" would, it seems to us, involve fracturing the crystal. The chance that ϵ for specimen R-4, Table 6, is exactly 30° is exceedingly remote, and even if it were, glide would probably take place in one direction or the other, but not in both directions.

In reply to Professor de Forest's remarks, we would like to state that the deformation of the aluminum and zinc single crystals took place in a discontinuous fashion in the slow tensile tests. The steps were very small, and since the length measurements were made by an observer with a filar micrometer microscope and not with an autographic recorder, the steps do not appear on the published curves. Also, similar discontinuous extension took place during the creep tests on ductile zinc single crystals. The steplike deformation was not evident in the silver single crystals.

Mr. Starr does indeed raise a debatable question. During the deformation of a single crystal below the recrystallization temperature, some fragmentation and loss of perfection of the single crystal probably does occur. However, plastic deformations of ductile zinc single crystals at the temperature of liquid air and of aluminum single crystals at room temperature do not cause the specimens to become polycrystals when annealed; the single-crystal character seems hard to destroy.

The remarks of Dr. Phillips and Mr. Norman concerning the purity of the metals tested brings up a point which cannot be easily disposed of. However, it seems to us that the burden of proof is upon the critic, since until purer material is tested, there is no evidence that the same behavior will not be found. Furthermore, comparison of Figs. 1 and 2 shows that the drop of the yield point above the recrystallization temperature (250°C.) is more marked in the 99.95 per cent than in the 99.90 per cent aluminum.

The remarks of Mr. Winlock and Mr. Leiter have been of much assistance in clarifying the subject of "yield-point elongation." Their reasoning concerning the possibility of a different behavior of annealed low-carbon steel tested under a constant rate of loading leads us to consider the probable results of testing aluminum single crystals under a constant rate of deformation. It may be that such a manner of testing would accentuate the "yield-point elongation" characteristics of the single crystals, and make the similarity to the behavior of the annealed low-carbon steel still more apparent. However, we do not imply that similarities in the load-deformation curves of the two materials necessarily mean that the same process is taking place in each case. The nonuniform deformation and formation of Luder's lines in the low-carbon steel is quite dissimilar to the more uniformly distributed slip which occurs on scattered slip planes throughout the length of the single crystals. The explanation of the phenomenon occurring in the single crystals is probably simpler, and may well deal with changes in the rate of work-strengthening, as has been indicated.

Equipment for Routine Creep Tests on Zinc and Zinc-base Alloys, and an Example of Its Application

By J. RUZICKA*

(New York Meeting, February, 1937)

IN creep testing, material is subjected to a constant load, preferably at a constant temperature, and its rate of deformation is measured. The method of loading can be of various types but in this paper only creep testing under tensile load will be considered.

The ordinary tensile test is essentially a comparison test in conditions that frequently bear little or no relation to those under which the test material is to be used in service. The purpose of creep tests is to measure the strength of the test material at slow rates of deformation that more nearly approach the rates realized in service.

One purpose of this paper is to illustrate that the creep test, in addition to its value as a service test, is superior to the ordinary tensile test as a sensitive tool for the comparison of certain metals in investigative testing. The other purpose is to describe equipment having distinctive features of design that make it especially suitable for such tests.

Representative data obtained with this equipment on a group of rolled zinc-base materials are given. These data are compared with those from practical comparison tests of the creep type on weatherstrip fabricated from the same group of materials. The comparison illustrates the value of the fast creep test and of the equipment.

THE EQUIPMENT

The creep equipment consists essentially of a tank containing a constant-temperature oil bath in which the creep of 14 specimens, loaded by means of levers, is measured by means of one movable extensometer. Figs. 1, 2 and 3 illustrate its general construction and appearance.

Constant-temperature Oil Bath.—A common constant-temperature bath requiring only one temperature-controlling equipment for a number of specimens was chosen as the best means of fulfilling the requirements of low cost and compactness. In addition, this allows the testing of a group of specimens under identical temperature conditions.

Manuscript received at the office of the Institute Nov. 30, 1936.

* Investigator, Rolling Mill Section, Research Division, The New Jersey Zinc Co., Palmerton, Pa.

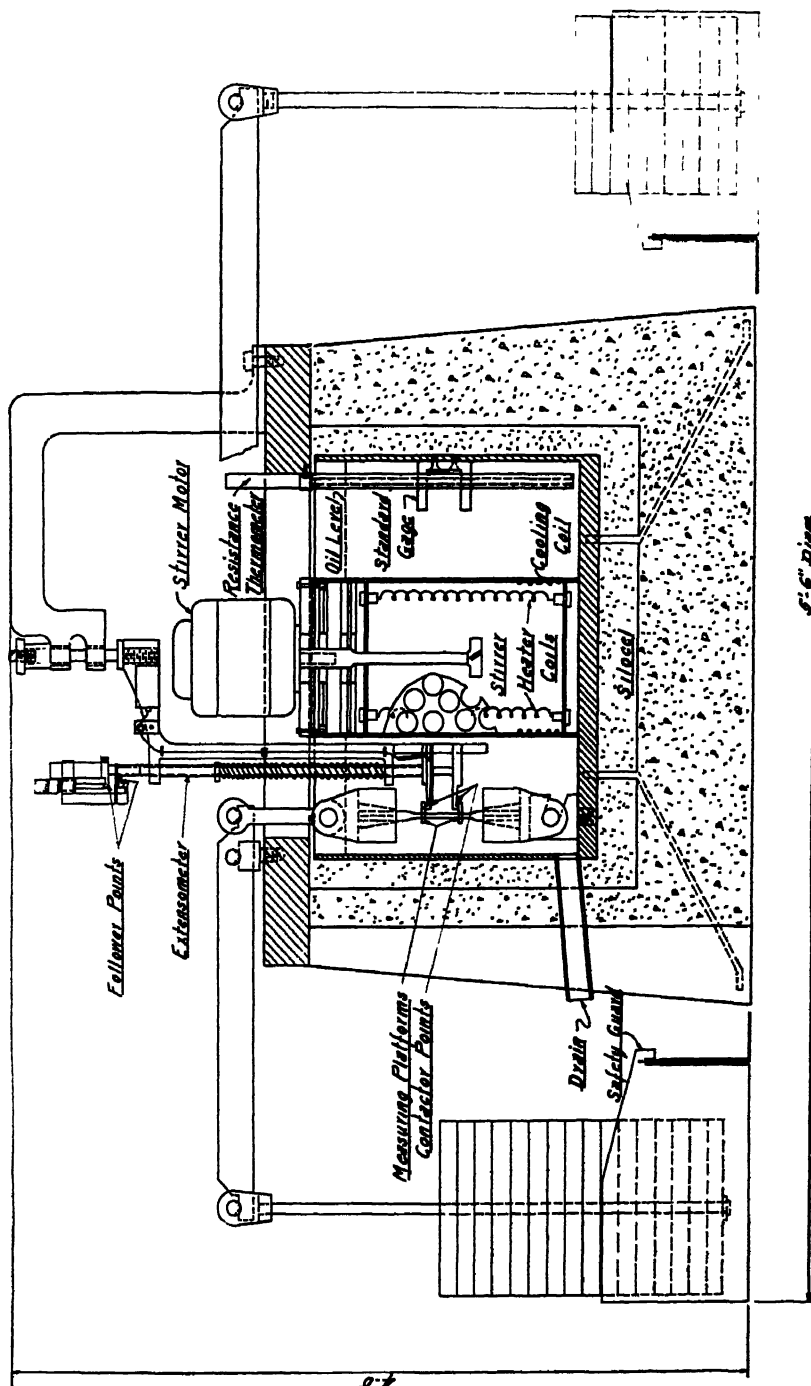


FIG. 1.—GENERAL CROSS-SECTIONAL VIEW OF CREEP EQUIPMENT.

The comparatively low temperatures (25°C. to about 225°C.) of the tests for which this equipment was designed allowed the use of oil as the bath medium. As compared to air, a liquid bath yields better uniformity of temperature control.

The bath is cooled by water, circulating through cooling coils, or heated electrically as required. It is maintained within $\frac{3}{4}^{\circ}\text{C.}$ of the

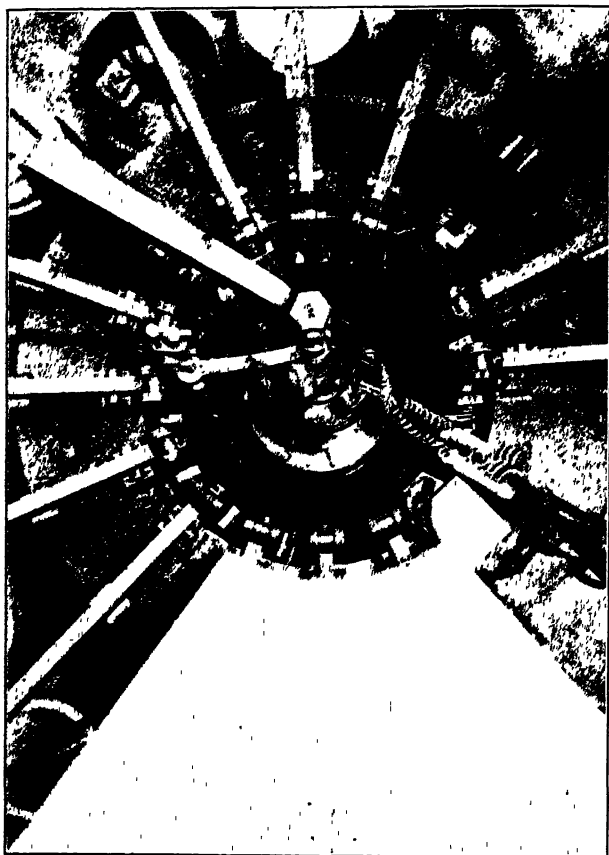


FIG. 2.—TOP VIEW OF CREEP EQUIPMENT.

desired temperature by a resistance thermometer controller. A motor stirrer assures uniformity of temperature throughout the tank. An alarm bell gives a warning whenever the controller fails to function properly. Any possibility of fires is eliminated by a fuse in the heater circuit, which would melt and break the circuit if the bath reached a temperature approaching its flash-point.

The equipment is being used at present at 150°C. but by slight changes and the use of other cooling and bath mediums, tests at tem-

peratures outside the range 25° to 225° C. could be made. In testing at 30° C. only a small fraction of the heating capacity is required.

Gripping and Loading Equipment.—The specimens are held in wedge-type grips in which the gripping force increases with the load on the specimens. Interchangeable grip blocks are available for the testing of

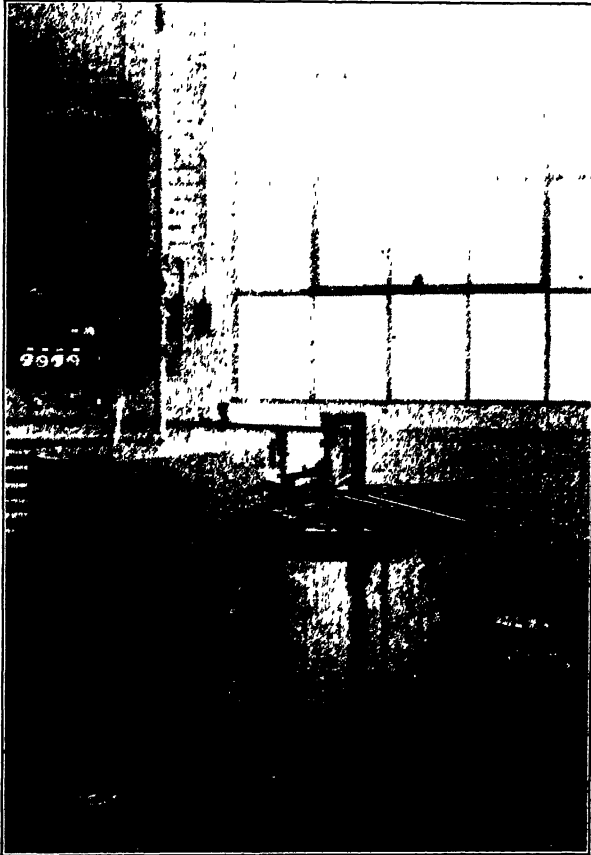


FIG. 3.—FRONT VIEW OF CREEP EQUIPMENT. TEMPERATURE CONTROL IN UPPER LEFT CORNER.

standard die-cast and rolled tensile specimens of 2-in. gauge length. Minor changes in equipment would allow the testing of other sizes and types of specimens. The specimens are loaded by means of accurately calibrated simple levers having multiplying ratios of about 9:1. This system requires little space, avoids the need for handling an excessive number of weights but still is accurate. The equipment is satisfactory for specimen loads of 25 to 2000 lb. The maximum load represents a

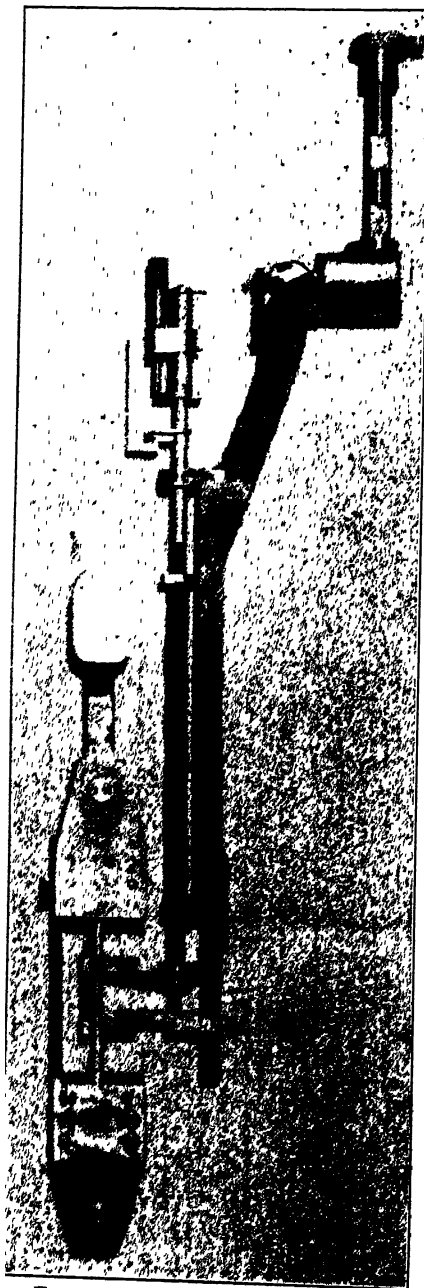


FIG. 4.—SPECIMEN GRIPS, WITH SPECIMEN AND MEASURING PLATFORMS IN PLACE, AND EXTENSOMETER.

load of 40,000 lb. per sq. in. on the largest specimens ordinarily tested, the $\frac{1}{4}$ -in. dia. die-cast specimens.

Extensometer.—The use of a single extensometer for measuring the elongation of 14 specimens is the most important factor in reducing the size and cost of the equipment. The extensometer is movable, mounted on a shaft (Fig. 1) of which the axis passes through the center of the circle of specimens. The extensometer measures the distance between two measuring platforms firmly attached to the specimen (Fig. 4). Two contactor points, like those of an inside caliper, are held against the measuring platforms by spring pressure. Follower points attached to these contactor points extend outside the oil. A micrometer attached to the extensometer frame measures the creep of the specimen in terms of the change in distance between these follower points. All readings are taken at the same degree of pressure between the contactor points and the measuring platforms. This pressure is the minimum required to close an electrical circuit from one contactor point to the other, through the measuring platforms and the specimen. When the circuit is closed, the current from a small dry cell illuminates a flash-light bulb. The contact pressure at which readings are taken is the pressure that causes the light to flicker. The difference between a flickering light and one burning steadily represents a micrometer adjustment of less than the 0.0001-in. sensitivity of the micrometer.

All readings are corrected for wear and changes in adjustment of the equipment by comparison against readings on a standard. The standard (Fig. 1) consists of a hardened steel C-shape rigidly attached to the walls of the tank. The polished surfaces of this standard, on which the standard readings are made, form part of the circle of measuring platforms on the specimens, thus allowing standard readings to be made by exactly the same procedure as is followed in making readings on the specimens.

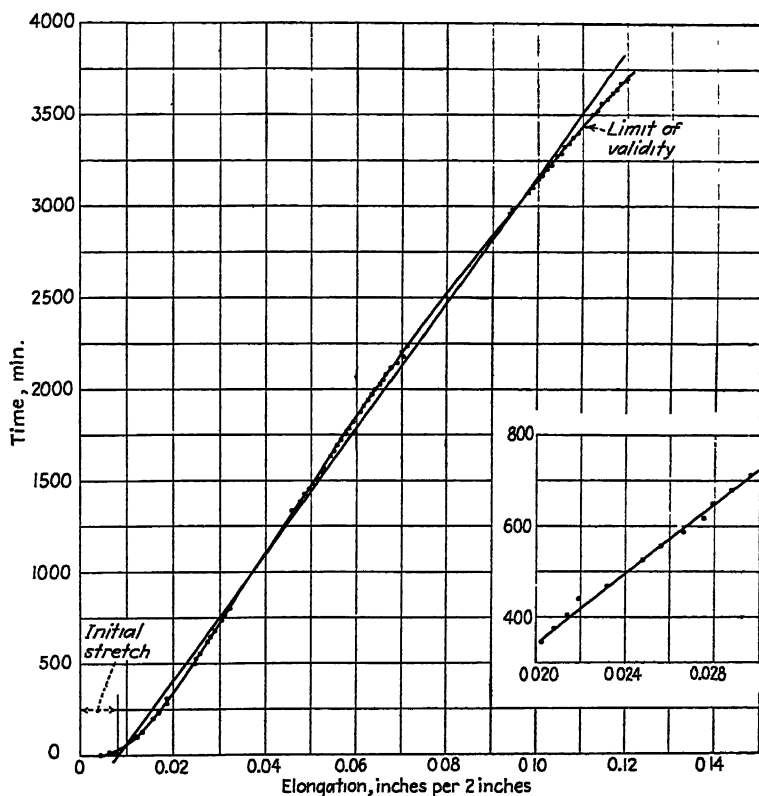


FIG. 5.—REPRESENTATIVE CREEP-TIME CURVE, ILLUSTRATING LOCATING OF CREEP-RATE LINE AND DEGREE OF ACCURACY OF ELONGATION READINGS.

Magnified section of curve at lower right. Ranges of elongation in which no points are shown represent night intervals during which no readings were made.

The usual deviation of any point from the curves is less than 0.0002 inch.

Data Obtained.—Fig. 5 is a curve of typical data obtained with the equipment. This curve illustrates that the accuracy of readings is at least as good as is necessary for such tests.

The behavior of materials in creep is stated in terms of the slope of the constant-rate section of the curve. However, because of the difficulty in

locating this section on some curves on zinc-base metals, an arbitrary method of location has been adopted. This consists in considering as straight the section of the curve that falls within 0.002 in. (0.1 per cent) of a straight line so drawn that as much as possible of the curve will lie within this distance from it. The locating of the line is illustrated in Fig. 5. The slope of this line is reported as the average creep rate in this section.

The inverse rate rather than the direct rate is reported, in units of days per per cent of creep. This method was adopted to avoid the mental

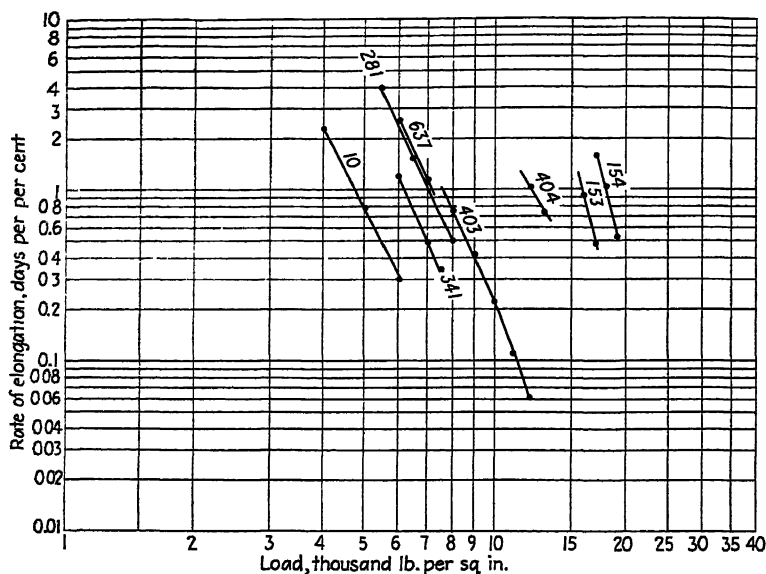


FIG. 6.—REPRESENTATIVE LOAD-CREEP RATE CURVES ON WEATHERSTRIP MATERIALS STRESSED PARALLEL TO ROLLING DIRECTION IN DETERMINATION OF LOAD YIELDING ELONGATION-RATE OF 1 DAY PER 1 PER CENT.

confusion resulting in considering direct-rate data, where low values mean high strength, and vice versa.

The intersection of the rate line with the abscissa is reported as representing the amount of initial rapid elongation (initial stretch in Fig. 5) before the period of comparatively constant rate of elongation. The upper limit of the period of constant elongation rate (limit of validity in Fig. 5) is given as the last point on the curve falling within 0.002 in. of the rate line.

Rough comparisons of the creep strengths of different materials are made by comparison of the rates at the same load. Better comparisons are obtained by determination of the loads yielding the same rate. This is done by interpolating from the rate-load curve of tests at a series of loads. The curves are of the logarithmic type shown in Figs. 6 and 7.

This form was chosen because for zinc-base materials it yields an approximately linear relationship between load and rate over a wide range. This linear relationship allows accurate interpolation between points reasonably close to each other, and also a reasonable amount of extrapolation of curves on materials of which the creep characteristics are known.

Range of Equipment.—Summarizing, the equipment is satisfactory in its present form for tests at temperatures of about 25° to 225° C., at loads of 25 to 2000 lb., and covering total elongations of up to 0.6 in. It is designed especially for tests at rates of several per cent per hour to about 1 per cent per week or month but also is being used for tests at rates of 1 per cent per several years.

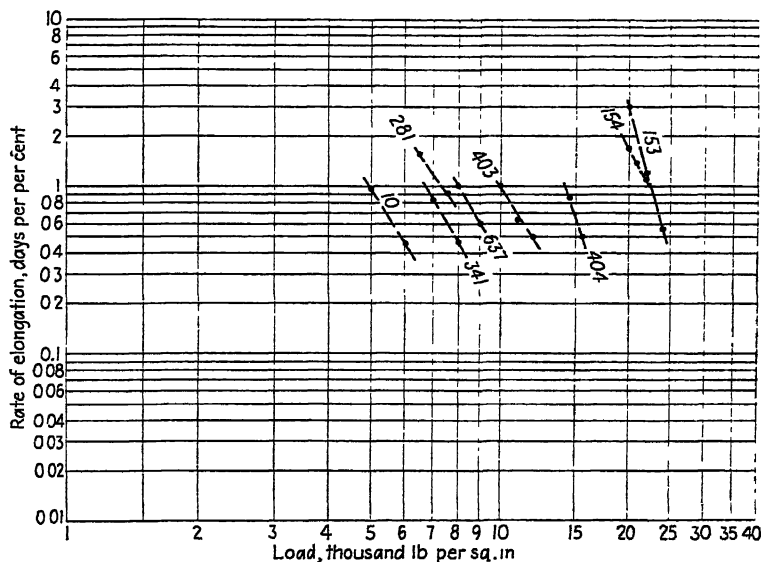


FIG. 7—REPRESENTATIVE LOAD-CREEP RATE CURVES ON WEATHER-STRIP MATERIALS STRESSED AT RIGHT ANGLES TO ROLLING DIRECTION, IN DETERMINATION OF LOAD YIELDING ELONGATION RATE OF 1 DAY PER 1 PER CENT.

General Use of Equipment.—The equipment has ordinarily been used in conjunction with other routine tests, for the comparison of various zinc-base materials. In investigative testing, it is especially valuable because it reveals differences between materials having similar properties in other tests.

As mentioned before, creep tests in general are service tests in purpose, in that they measure strength at rates of deformation approaching those of service. Even tests lasting only a few days or weeks are superior in this respect to ordinary tensile tests. For this reason, the equipment has a particular value for service testing.

An example showing the value of the sensitivity of the equipment in service testing is given in the next section of this paper. It should be

emphasized that this represents only one of many possible applications of the equipment.

APPLICATION OF CREEP EQUIPMENT TO ROUTINE COMPARISON TESTING

The purpose of this section is to show that the creep and practical tests reveal distinctions between materials that are not shown by the more rapid ordinary tensile test. In addition, since the creep test is the only one of the slower tests that yields absolute values and is sufficiently standardized for general use, it is felt that this comparison demonstrates the value of the routine use of creep tests in preference to such practical tests.

Material.—The comparison tests were made on standard weatherstrip fabricated* by roll-forming from the eight rolled-zinc base metals tested in the creep equipment. The general shape of the weatherstrip is indicated in Figs. 8 and 9. The test materials were compared to

TABLE 1.—*Analyzed Compositions of Test Materials*

Zinc Alloy No	Composition, Per Cent					
	Copper	Magnesium	Cadmium	Lead	Iron	Zinc
154	1.1	0.0057	0.0046	0.09	0.012	remainder
153	1.0	0.0036	0.0043	0.09	0.011	remainder
404	1.0	"	0.0049	0.084	0.015	remainder
403	1.1	"	0.0047	0.077	0.012	remainder
637		"	0.13	0.28	0.021	remainder
281		"	0.09	0.80	0.017	remainder
341		"	0.11	0.15	0.017	remainder
10		"	0.12	0.24	0.011	remainder

* Less than 0.0005 per cent. Other elements not present in appreciable proportions, as determined by spectroscopic, qualitative analysis. The results of routine tests on the materials are given in Table 2.

determine their relative suitability not only for weatherstrip but especially for such roll-formed products as window-screen frames, requiring greater stiffness than is needed for weatherstrip. The weatherstrip section was chosen for testing as being representative of the general field of roll-formed products. The analyzed compositions of the materials are given in Table 1. The results of routine tests on the materials are given in Table 2.

Beam, Spreading and Creep-test Procedures

Beam Tests.—In the beam tests, a 20-in. length of weatherstrip was loaded as a simple beam, at the center of a 16-in. span (Fig. 8). The

* Fabricated through the courtesy of the Peerless Metal Weatherstrip Company, Irvington, N. J.

TABLE 2.—*Results of Routine Physical Tests*

Zinc Alloy ^a	Metal Thickness, In.	Shore Scleroscope Hardness	Dynamic ^b Ductility, In.	Temper., Per Cent ^c	Dynamic Cold Bends ^e		Tensile Strength, Lb. per Sq. In. ^e		Elongation, Per Cent in 2 In. ^e	
					With Grain ^d	Across Grain ^e	With Grain ^d	Across Grain ^e	With Grain ^d	Across Grain ^e
154	0.0180	21	0.240	67	5	2	36,700	48,400	21.8	9.3
153	0.0180	19	0.250	62	3.5	2	29,800	36,500	26.0	15.3
404	0.0180	20	0.285	60	3	2	31,300	38,600	32.8	25.0
403	0.0180	17.5	0.300	44	3	2	34,000	30,700	55.8	33.2
637	0.0180	23	0.250	50	/	2	29,200	37,100	27.8	17.3
281	0.0173	22.5	0.255	50	/	2	28,700	36,300	15.5	17.8
341	0.0185	23.5	0.250	49	5	2	29,100	38,400	24.8	26.5
10	0.0180	23.5	0.235	53	/	2	28,800	39,700	23.2	23.2

^a See Table 1 for composition.^b See A.S.T.M. specification for Rolled Zinc B69-29.^c The metal is first bent to a U-shape by hand and then flattened onto itself in a press. The diameter of the most severe bend without failure is the given value times the thickness of the metal.^d Parallel to rolling direction.^e At right angles to rolling direction.

/ Over 5.

^f Tensile-test speed, 0.25 in. per minute.

tests were made at room temperatures of 25° to about 30° C. The materials were compared on the basis of the load yielding an average rate of sag of about 1 in. per day, over the range of $\frac{1}{2}$ to $1\frac{1}{2}$ in. of total sag. In preliminary tests, the load was varied during the test until this rate of sag was obtained. These preliminary results were then checked by final complete tests at these predetermined loads. Fig. 8 represents a final test.

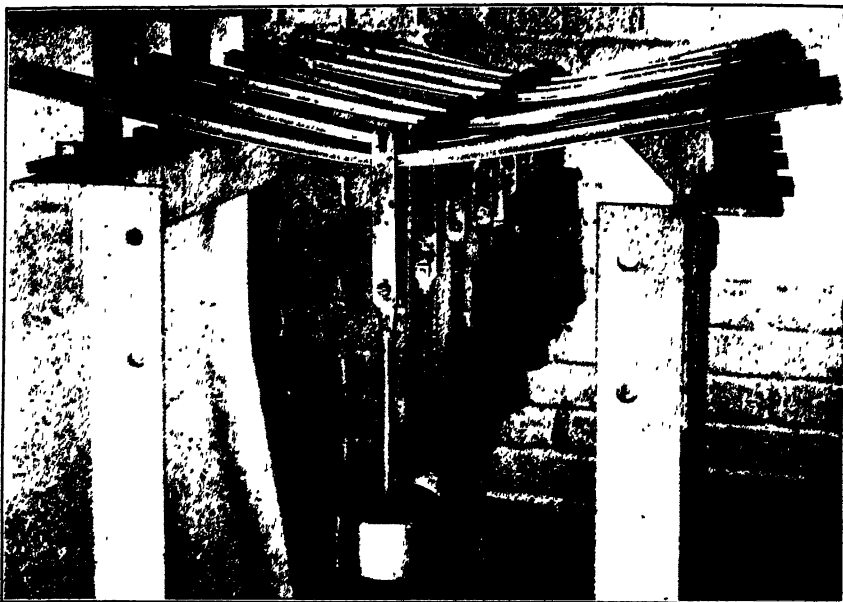


FIG. 8.—BEAM TEST, ILLUSTRATING DIFFERENCE IN LOADS YIELDING SAME RATE OF SAG, 1 INCH PER DAY.

Test photographed after one day under load at room temperature. Reading from front to back:

MATERIAL No.	LOAD, Lb.	MATERIAL No.	LOAD, Lb.
10	4	403	8 $\frac{3}{4}$
281	5 $\frac{3}{4}$	404	10
341	5 $\frac{3}{4}$	15-4	14
637	6 $\frac{3}{4}$	15-3	14 $\frac{3}{4}$

The relative stiffnesses of the materials in this test are shown in Table 3 and Fig. 10.

Spreading Tests.—The spreading test was a measurement of the resistance to spreading of the 180°, 0.08-in. inside diameter bend of a 2-in. length of weatherstrip. The method of loading is shown in Fig. 9. Comparing this photograph with that of the beam test (Fig. 8), it is obvious that in these two tests stiffness was measured in directions at right angles to each other in relation to the original rolling direction.

In the spreading test, the materials were tested at room temperatures of 25° to about 30° C. They were compared in terms of the load, yielding

a total spread of 0.18 in. in 1000 min. This load was determined from a curve of the results of tests at a series of loads, and checked by a test. Fig. 9 represents such a check test.

The relative strengths of the materials in this test are shown in Table 3 and Fig. 10.

Creep Tests.—The creep tests were made on standard rolled-metal tensile specimens of 2-in. gauge length, cut parallel and at right angles to the rolling direction from samples of the flat metal from which the weatherstrip was fabricated.

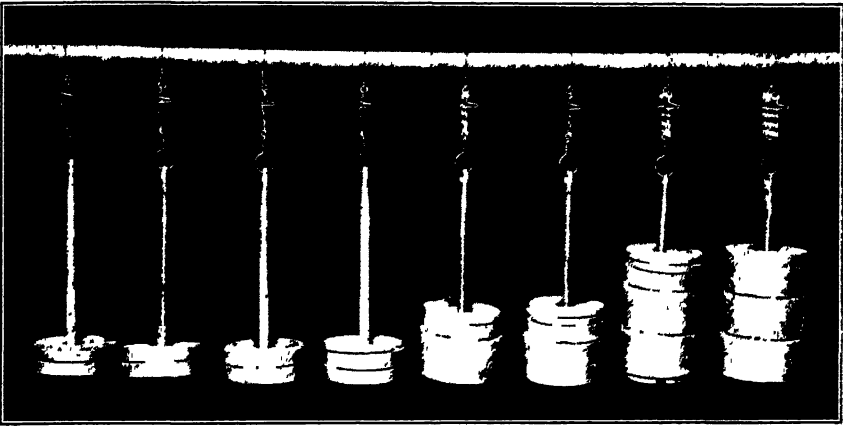


FIG. 9.—SPREADING TEST, ILLUSTRATING DIFFERENCE IN LOADS YIELDING SAME RATE OF SPREAD, 0.18 INCH IN 1000 MINUTES.

Test photographed after 1000 minutes under load at room temperature. Reading from left to right:

MATERIAL No.	LOAD, LB.	MATERIAL No.	LOAD, LB.
341	2.2	403	5.4
10	2.3	404	5.7
281	2.6	154	9.1
637	2.8	153	10.5

The specimens were tested at 30° C. This temperature has been made standard because occasionally during the summer the industrial water used for cooling becomes too warm to maintain a lower temperature.

The testing loads were chosen for a determination of the load at which the materials had a creep rate of one day per one per cent. This rate is used generally for comparisons of zinc-base materials in this equipment, because it is convenient to use and is about the fastest rate that is practically always within the range of the approximately linear relationship between load and rate plotted on the standard logarithmic graph.

The load-rate curves on all the materials are given in Figs. 6 and 7. The interpolated values of the loads yielding a rate of one day per one per cent for each material are included in Table 3 and Fig. 10.

TABLE 3.—*Summary of Comparison of Test Materials*

Zinc Alloy ^a No.	Dynamic Tensile Strength, Lb. per Sq. In.		Creep Strength, Lb. per Sq. In. ^d		Ratio ^c of Strengths to With-grain Strength of Material 404							
	With Grain ^b	Across Grain ^e	With Grain ^b	Across Grain ^e	With-grain Strength ^b				Across-grain Strength ^e			
					Dynamic Tensile	Beam Test	Spreading Test	Creep Test	Dynamic Tensile	Beam Test	Spreading Test	Creep Test
154	36,700	48,400	18,000	22,400	1.2	1.5		1.5	1.5		1.9	1.9
153	29,800	36,500	15,800	22,500	1.0	1.4		1.3	1.2		2.1	1.9
404	31,300	38,600	12,100	14,200	1.0	1.0		1.0	1.2		1.2	1.2
403	24,000	30,700	7,600	9,900	0.8	0.9		0.6	1.0		1.1	0.8
637	29,200	37,100	7,200	8,000	0.9		0.6	0.6	1.2	0.6		0.7
281	28,700	36,300	7,000	7,300	0.9		0.5	0.6	1.2	0.5		0.6
341	29,100	38,400	6,200	6,700	0.9		0.5	0.5	1.2	0.5		0.6
10	28,800	29,700	4,700	5,000	0.9		0.5	0.4	1.3	0.4		0.4

^a See Table 1 for composition.^b Material stressed in direction parallel to original rolling direction.^c Material stressed in direction at right angles to original rolling direction.^d Load yielding elongation rate of 1 day per 1 per cent. From curves of Figs. 6 and 7.^e Ratio of loads yielding same rate of deformation. In spreading test, assumption was made that ratio of across-grain strength of material 404 to its with-grain strength was same as in creep test. Other spreading-test ratios were calculated from this assumed ratio.

It should be emphasized that the tests represented by Figs. 6 and 7 were intended only for the determination of the loads yielding rates of one day per one per cent. Extrapolation is not permissible.

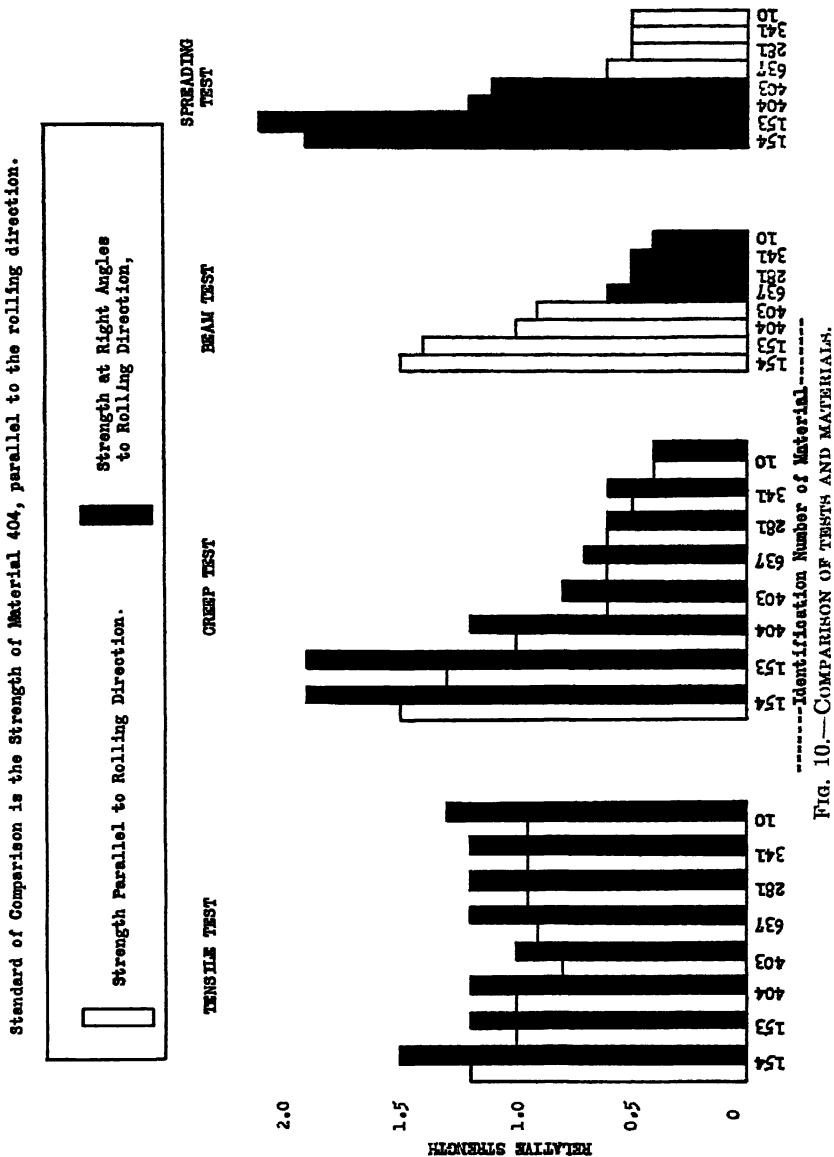


Fig. 10.—COMPARISON OF TESTS AND MATERIALS.

Comparison of Materials and Tests.—It is known that the strength of rolled materials parallel to the rolling direction may differ appreciably from that at right angles to the rolling direction. Of the four tests

(tensile, creep, beam and spreading tests) by which strengths were measured, only the tensile and creep tests measured strengths in both directions on all materials. The beam and spreading tests each measured strength in one of the two directions. Owing to differences in cutting the metal for fabrication, the beam test involved a stress with grain for one group of materials and across grain for the others. The spreading test in each case involved a stress in the grain direction opposite to that in the beam test. Accordingly, in comparing the materials, it was necessary to distinguish between strength differences due to the material and those due to the testing direction.

For convenience in comparison of both the materials and the tests, material 404 was selected as a basis of comparison and its with-grain strength in each test was assigned the value unity. For each test, the strength of each material was then converted to this arbitrary scale.

In the spreading test, material 404 was not tested in the with-grain direction. It was, therefore, necessary to assume that if such a test had been made, the ratio between it and the across-grain test would have been the same as the ratio between the creep tests with and across the grain for this same material.

Table 3 has been arranged with the two "practical tests" bracketed by the conventional, or dynamic tensile test on one side and the creep test on the other. The with-grain and across-grain values are compared separately. The comparison at once shows that except for one material, 403, the practical tests correlate well with the creep test and poorly with the dynamic tensile test. Fig. 10 shows the same comparison graphically.

SUMMARY AND CONCLUSIONS

This paper has described equipment designed especially to allow the routine use of tensile creep tests. Its distinctive features, which make such use possible, are compactness, low cost and simplicity of operation, combined with adequate accuracy.

Compactness and low cost are achieved by the use of one constant-temperature bath (and therefore only one temperature-controlling equipment) and one extensometer for the testing of 14 specimens at a time. A further reduction in original price and the cost of labor for operation results from the simple design of the extensometer, which is essentially an improved ordinary micrometer that can be operated with accuracy by the average laboratory helper.

Fourteen specimens are tested at once in a space $5\frac{1}{2}$ ft. in diameter, at loads of 25 to 2000 lb., at temperatures of about 25° to about 225° C., controlled within $\frac{3}{4}$ ° C. Elongation measurements are accurate within 0.0002 in. The equipment is especially suited to tests at rates in the range of about 1 per cent per hour to 1 per cent per month but is also

being used satisfactorily in tests at rates of 1 per cent for several years. Its limitation is a lack of sufficient sensitivity to measure slow rates except by measurements covering a fairly large range of total creep and long periods of time.

The paper includes representative data obtained with this equipment on a group of rolled zinc-base materials. It illustrates the value of such tests by comparison of these data with those from several routine tests, especially the ordinary tensile test. In addition, a comparison is made with data from "practical" comparison tests on weatherstrip fabricated from the same group of materials. These "practical" tests were considered representative of the general type of test that would be made to determine relative strengths at constant loads if creep equipment were not available.

It is felt that these comparisons and the description of the equipment show that:

1. The ordinary tensile test and other routine tests do not reveal differences in strengths of materials as well as do tests at constant load and slower rates.

2. Constant-load, slow-rate tests are best made in creep equipment on standard specimens. Tests in such equipment, unlike "practical" comparison-tests, are readily standardized and yield absolute data of general value.

3. The particular creep equipment described in this paper offers a means of making such creep tests accurately, conveniently and cheaply.

ACKNOWLEDGMENT

The writer wishes to express his appreciation especially to Mr. G. Edmunds, of the Research Division, The New Jersey Zinc Co., Palmerton, Pa., to whom the basic design of the equipment should be credited. Other members of the same organization have also been extremely helpful, both in this respect and in the preparation of this manuscript.

DISCUSSION

(D. E. Ackerman presiding)

D. E. ACKERMAN, * Bayonne, N. J.—This paper bears on a very practical problem. We have probably all found difficulty in choosing materials for service applications on the basis of nothing better than tensile strength. Mr. Ruzicka has been able, by crossing the long-time creep test with the ordinary tensile test, to devise a test which for applications involving long-time deformation certainly is much more useful than the ordinary tensile test.

A. A. SMITH, JR., † Maurer, N. J.—This paper is of particular interest to us because of the large amount of routine creep testing being done on lead and lead alloys at the Central Research Laboratories of the American Smelting and Refining Co. The

* Research Metallurgist, International Nickel Co.

† Research Metallurgist, American Smelting & Refining Co.

results given by the author are for comparatively short periods of time and the curves are typical time-extension curves as usually found in creep testing.

I should like to know whether Mr. Ruzicka has ever found any sudden changes in creep rates on zinc-base alloys after considerable periods of time. For instance, on certain lead alloys we have found very abrupt changes in rate of extension after test periods of from one to three years, which probably are due to some changes taking place in the alloys. The tests are being conducted in a specially built constant-temperature room and no vibration has ever been detected under the most extreme conditions of shock in the adjacent surroundings. These results on lead alloys indicate the desirability of long-time creep tests and the danger of extrapolating results from comparatively short-time tests.

J. R. DASEN,* Chicago, Ill.—You can find out things in a creep test that do not necessarily bear on what shape the material will be in after a number of years. I am thinking particularly of the condition of strain that may exist in the material. In some uses of other materials there have been serious accidents because the material did not have enough strain in it to yield slightly under load. Perhaps the most interesting example of this is the use of heat-treated steel wire as compared with cold-drawn steel wire in a cable. It is impossible to apply a load on a cable in such a way that each wire of the cable bears its own portion of the load unless those wires have the ability to elongate to some extent under load without cracks. Therefore, the ability of the cold-worked wire to elongate under load without fracture is of great value in effecting uniformity of loading.

In zinc alloys of the type discussed, the method of processing has a great deal to do with whether or not this material will elongate and a short-time test may be completed in only a few days. It is a very good method of finding out the condition of the material with respect to strain. This condition of the material with respect to strain is important in discovering whether or not the alloys will stand mechanical deformation, whether it is a question of slight movement in order to adjust inequalities of stress or a case of standing a relatively severe deformation such as occurs in punching and drawing.

Therefore, I think that this paper on creep tests of zinc should be viewed rather in the light of the information that may be secured on the material with respect to its ability to deform under short-time loads, rather than an indication of the material's condition after a number of years of use.

It would be very interesting to see the effect of zinc containing magnesium without copper as well as the alloys containing copper without magnesium and the alloys containing copper and magnesium. I think it would indicate that the effect by itself is very pronounced in decreasing the creep of zinc alloys.

W. M. PIERCE,† Palmerton, Pa.—The information on the relative creep rates of copper-free magnesium alloys as compared to magnesium-free copper alloys and unalloyed zinc was published in a paper before the A.I.M.E.¹ some years ago and was not repeated here because the copper-free magnesium alloy is not being produced commercially. It is not being produced commercially because if magnesium is to be added to a zinc alloy, it might better be added to an alloy containing copper, because of the much greater effect it yields in the presence of copper.

C. S. BARRETT,‡ Pittsburgh, Pa.—Perhaps a word or two would be in order from the authors and the discussers regarding what might be called the seismographic effect in these dead-load machines.

* Chief Metallurgist, Illinois Zinc Co.

† Research Division, New Jersey Zinc Co.

¹ E. A. Anderson: *Trans. A.I.M.E.* (1930) 89, 481.

‡ Metals Research Laboratory, Carnegie Institute of Technology.

G. EDMUNDS,* Palmerton, Pa.—The comments of Mr. Smith in regard to the rather abrupt changes that take place in lead alloys after long periods of creep loading are particularly interesting. We have had creep tests under way on zinc for a good many years and have not yet observed any phenomena of that type in zinc. We may in the future have such a thing happen, but some of our tests have run, I should say, in the neighborhood of six to eight years without having shown it. Mr. Smith's statement that in some cases the increase in creep rate is as much as 40 to 50 times after two or three years' loading is particularly interesting. Zinc and lead apparently are quite different, then, in their creep properties, as a comparison of our tests with those that Mr. Smith has reported would show.

I am a little at a loss to understand what Mr. Daesen referred to—the use of these tests as a means of prophesying the ability of the material to withstand fabricating operations or something else.

J. R. DAESSEN.—I think that the material that shows very great resistance to creep can be found by actual experience to be less capable of standing certain fabricating operations.

G. EDMUNDS.—That, then, is more or less what I thought you might have meant and I was rather surprised because a few years ago Mr. Kelton and I published a paper² in regard to the drawing properties of strip zinc alloys, at which time we compared drawing properties with the commonly performed tests such as ductility and tensile properties and the like, and we found that there was no correlation—that cupping was a process that could be studied so far as we knew only by cupping tests.

We have made a number of creep tests on materials from the same group as that from which those were taken, and we do not find the correlation between the creep test as we perform it and the ability of the material to withstand fabrication, so that I do not believe we should take these results as significant in that direction. They have been practical tests to determine whether material would withstand a certain stress over a period of time and how much they would deform.

We do find, of course, that the rate of deformation, as shown in Figs. 6 and 7, is approximately a linear function of the logarithm of the load throughout a rather wide range. Extremely small rates of elongation will be observed, then, with low loads. Naturally, for practical purposes we must cut back on our design and use a proper and adequate factor of safety. However, I believe the real significance of these tests is that they do tell us whether one material or another is more suitable where it must be stressed in service. Of course, aside from the description of the equipment given here, the purpose of this paper was to show, and I believe it has been shown that the commercially fabricated articles after fabrication do have very nearly the same properties as the original material from which the fabricated material was made—that is, within certain limits, and if we went to excessive degrees of working in fabrication, that would no longer hold. But for all the normal processes, such as roll fabrication, for example, rolling of screen frames, and many other uses to which the zinc alloys are put in service, the test has real significance in selecting the proper material. So I think we will have to say that that is the useful information obtained from this test, rather than any indication as to the ability of the material to stand fabrication.

From another standpoint it was pointed out that a certain minimum of deformability must be met in the material for it is to be useful in service, in order to take care of the naturally imposed strains set up in service. That is another test. There is,

* Research Division, New Jersey Zinc Co.

² E. H. Kelton and G. Edmunds: Testing the Drawing Properties of Rolled Zinc Alloys. *Trans. A.I.M.E.* (1934) 111, 245.

did not find an endurance limit for a certain sample of Monel metal up to 750,000,000 cycles. On the other hand, R. R. Moore⁴ found an endurance limit for certain extruded magnesium-base alloys at 600,000 cycles. It is characteristic of nonferrous materials to fail after exceedingly long runs; therefore it is necessary, in any study for which only a limited period of time is available, to base the endurance limits on a predetermined number of cycles, and to report all results accordingly.

No accelerated endurance test has been developed that is applicable to all metals. Several of the proposed methods and machines are discussed by Moore².

In the present series of tests, 50,000,000 cycles was arbitrarily set as the limit of the individual tests. The authors feel that the endurance limits of all materials reported in this paper were closely approximated by this procedure.

TESTING MACHINES AND SPECIMENS IN COMMON USE

Testing machines for determining the endurance limits of metals are of various types and forms, depending upon the type of stress they are called upon to develop. They may be classified as three general types: (1) direct tension-compression, (2) flexure or bending, (3) torsion or shear.

Flexure or Bending Machines.—Machines for flexure or bending stresses have been used in more than 90 per cent of the fatigue tests. This type of machine has been popular because of its simplicity of operation, the accuracy with which it can be calibrated, and the fact that it produces a condition of stress that is very commonly met in engineering practice. Two types of machines use cylindrical specimens, the simple rotating-beam machine and the cantilever rotating-beam machine, of which R. R. Moore² gives details.

For tests on flat stock and sheet metal a machine that produces plain bending is commonly used. In most cases these machines have been of the constant-strain type, in which the stress in the specimen is computed from measurements of deflection under static loads. Many machines of this general type have been developed. For most kinds of flat stock the machine developed by Moore and Kommers⁶ is recommended. For tests on thin sheet metal such as spring stock, the design of J. R. Townsend and C. H. Greenall is especially adaptable¹.

Finish on Test Specimens.—In fatigue testing the surfaces of the specimens used must be smooth and free from scratches or other defects. The presence of such surface imperfections produces intensified local stresses and thus affects the test results. Steel specimens may be satisfactorily finished with very fine emery cloth, at least the No. 00 grade. Specimens of the softer metals must be finished more carefully.

All polishing is done by moving the abrasive in a direction parallel to the axis of the specimen, to minimize the scratch effects.

FATIGUE MACHINE

The fatigue machine (Fig. 1) used in these experiments was designed by Townsend and Greenall¹ especially for testing thin sheet metal. It combines simplicity and speed of operation with ease and accuracy of calibration. Fig. 2 shows the assembly at one end of the motor drive,

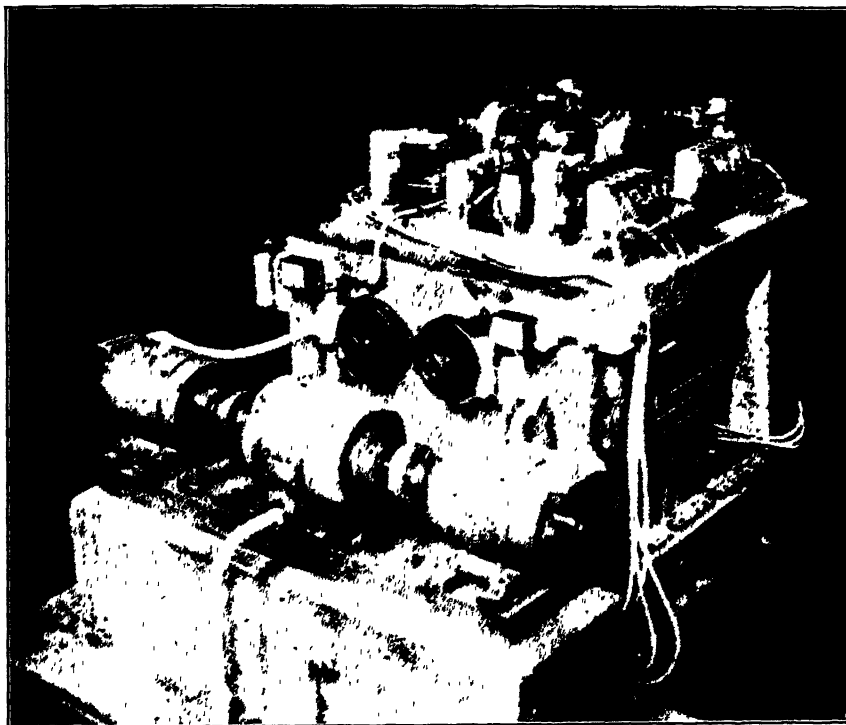


FIG. 1.—FATIGUE MACHINE¹.

and the method of clamping one end of the specimen *S* between phenol fiber blocks *B*, while the free end of the specimen is engaged between two fingers in the reciprocating arm *A*. These fingers have a vertical cylindrical half section, to compensate for the angular movement of the reciprocating arm in relation to the specimen. The deflection of the specimen, and thus the stress, is determined by measuring the movement of the reciprocating arm.

The capacity of the machine permits testing of five specimens of each of four materials at two stresses (20 specimens in each end of the motor drive). The practice of testing five specimens of each material

at each stress yields more accurate results, and the capacity of the machine is large enough to permit this practice.

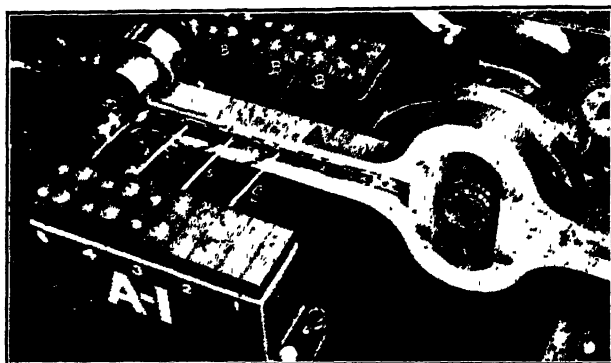


FIG. 2.—ASSEMBLY AT ONE END OF MOTOR DRIVE.

A, reciprocating arm.
B, phenol fiber blocks.
S, specimen.

The machine was designed to operate at 1500 r.p.m., but this series of tests was conducted at 800 r.p.m., to obtain smoother operation and longer life of machine parts.

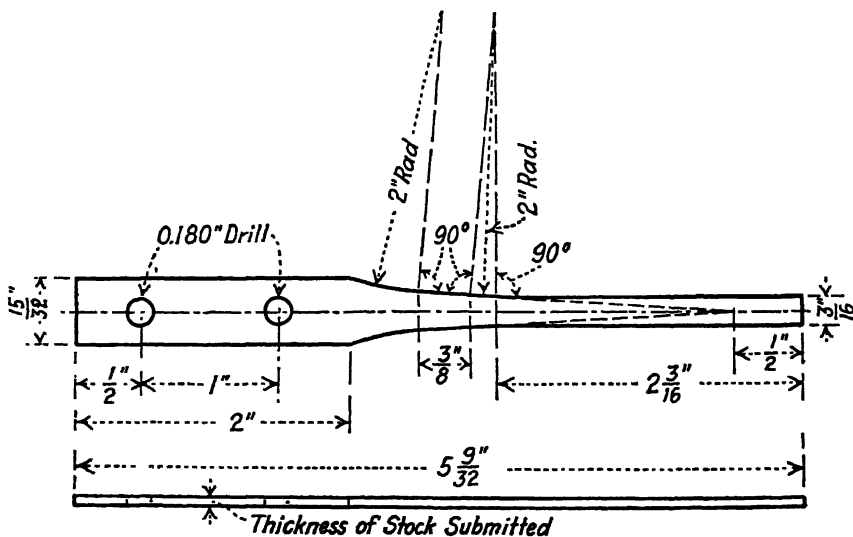


FIG. 3.—TEST SPECIMEN.

The test specimen (Fig. 3) was designed by Townsend and Greenall¹ to approximate the normal dimensions of the springs used in telephone apparatus. It is designed to provide a section of uniform stress for $\frac{3}{8}$ in. at approximately $\frac{1}{2}$ in. from the clamped end of the specimen.

The specimens for this investigation were prepared by cutting pieces of the required length from a coil of carefully prepared flat strip of the desired thickness and width; then the rectangular strips were clamped together and cross-milled with a form milling cutter. The specimens were cut with the direction of rolling parallel to their length. Each set of specimens was examined for surface defects and polished with No. 00 emery cloth before being tested. This additional care is essential to obtain satisfactory correlation of test results.

Obviously this careful surface preparation of the specimens will result in higher endurance-limit values than would be obtained with

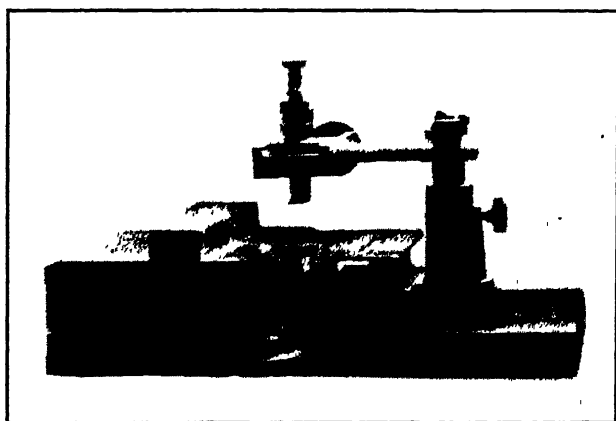


FIG. 4.—APPARATUS FOR DETERMINATION OF LOAD-DEFLECTION CURVES.

specimens tested in the as-rolled condition. This procedure was adopted because it was felt that in this way the relative fatigue properties of the five alloys could be determined with greater certainty, and accidental variables could be eliminated as far as possible.

If these materials are to be used in parts carefully finished and polished, the values as given here will hold. If, however, the materials are used in the as-rolled condition, lower endurance values are to be expected.

APPARATUS FOR DETERMINATION OF LOAD-DEFLECTION CURVES

In determining the deflections corresponding to the range of stresses over which the tests were made, the conditions obtaining in the operation of the fatigue machine, except speed of testing, were duplicated as closely as possible. A small stand, on which the specimen was clamped identically as in the fatigue machine, a balance pan for applying the desired loads, and a comparator for measuring deflections to 0.001 in., comprise the apparatus used in determining the load-deflection curves for the five materials (Fig. 4).

MATERIALS USED

The materials used in the present tests consisted of five rolled alloys of copper, A, B, C, D and E, of the compositions and standard physical properties shown in Table 1. All materials were furnished by the Scovill Manufacturing Co., and were processed there. They were all finished six numbers hard (Brown and Sharpe gauge). Materials A, B and C were annealed before finishing at 600° C. for 2 hr. and 20 min., material E was annealed before finishing at 800° C. in a container, for 2 hr. and 20 min. and material D was also annealed (temperature unrecorded) before finishing.

As the table shows, materials A, B and C are phosphor bronzes; material D is a silicon bronze and material E is the copper-nickel-tin alloy known as "Admic."

TABLE 1.—*Physical Properties and Chemical Compositions of Materials*

Material	A	B	C	D	E
Rockwell hardness (B scale).....	91	92	95	93	90
Tensile strength, lb. per sq. in. . . .	97,900	98,700	104,200	104,300	97,900
Elongation, per cent in 2 in.	2.5	2.0	4.5	5.0	2.5
Gauge.....	0.025	0.025	0.025	0.025	0.025
Cu, per cent.....	95.12	95.16	91.98	96.42	68.47
Sn, per cent.....	4.66	4.70	7.45		1.33
P, per cent.....	0.032	0.106	0.067		
Fe, per cent.....				0.16	0.25
Ni, per cent.....				0.03	29.58
Si, per cent.				3.12	
Zn, per cent.....			0.53	0.22	
C, per cent.....					0.048
Mn, per cent.....					0.32

METHOD OF DETERMINING STRESS

The first step in this investigation was the determination of load-deflection data for the various materials. These data were then converted to stress-deflection curves, so that for any given deflection of the specimen the stress to which it was subjected could be determined.

Specimens representative of each material were clamped identically as in the fatigue machine, on a stand built for this purpose (Fig. 4). Loads were applied by means of a balance pan suspended from a thread passed over a pulley and looped around the free end of the specimen. These loads were applied at the point where the hypothetical beam of uniform bending moment terminates; which was the point at which the reciprocating arm of the machine would bear against the specimen.

Loads were applied in increments of 20 grams (in some cases 40 grams) and the deflections measured to 0.001 in. by means of the comparator. The average of three specimens was taken for each point.

Before the curves were plotted the load values were converted to stresses as follows:

$$S = \frac{6Pl}{bd^2}$$

Where S = stress, lb. per sq. in.

P = load, lb.

l = length, in. from end of hypothetical beam

b = width, in.

d = thickness, in.

The specimens were so designed that $\frac{l}{b} = 9.269$; $d = 0.025$ in.

The stress values so obtained were plotted against the corresponding deflections to give stress-deflection curves.

MANIPULATION

Stresses were chosen that were thought to be above the endurance limits of the various materials, and the corresponding deflections were determined. It was apparent, from the stress-deflection curve, that material E is much more highly stressed at a given deflection than any of the other materials; consequently, it was more expedient to test materials A, B, C and D together (since the capacity of the machine permits testing only four different materials at once).

Material E was tested separately, or was substituted at the lower deflections for one of the other materials wherever possible; for example, at a deflection of 0.540 in., material E was substituted for material B, and at 0.596 in., for material A.

The stroke of the machine was measured by means of the comparator. The first tests were made with one-half of the machine set at 0.830 in. and the other half at 0.755 in.; subsequently each group was operated at lower stresses, until the general forms of the S -log N (stress versus the log of the number of cycles to failure) curves were observed. Then the stresses were chosen that seemed best for completing the curves.

The importance of the surface finish of the specimens was brought out forcibly in the course of this investigation. Several groups of specimens in the as-rolled condition, with no subsequent polishing of edges or flat surfaces, were tested at various stresses. Wide discrepancies were observed in the number of cycles to failure at a given stress; these discrepancies were so great that it seemed quite impossible to determine an endurance limit with such specimens, unless one were to report the stress at which the poorest of the specimens endured 50,000,000 cycles of stress

without failure. Failures were observed, with these specimens, at stresses several thousand pounds below the endurance limits subsequently determined with specimens carefully selected and polished. No attempt was made to determine endurance limits for the as-rolled materials, because the time was not available. The endurance limits determined with such specimens would not represent the true relation between the different materials but would reflect instead the purely accidental differences in the finish of the specimens, or might represent, in a way, the machining qualities of the materials. It was observed, for example, that the

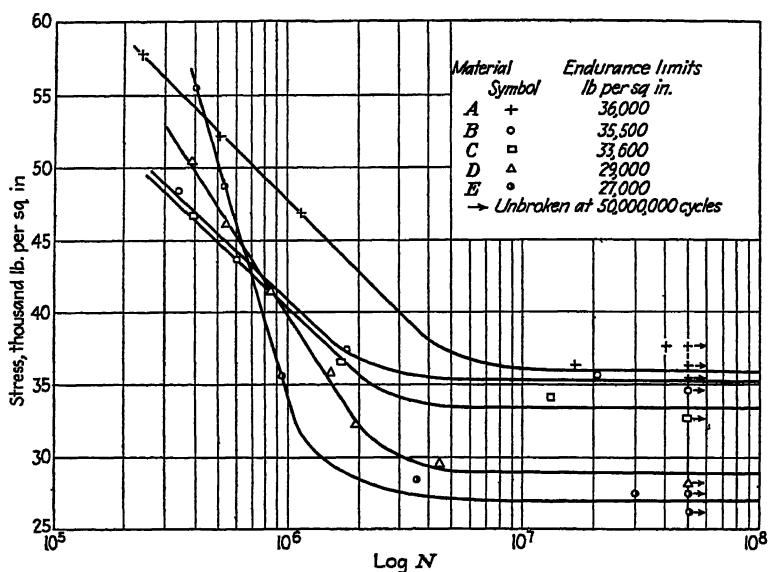


FIG. 5.—STRESS VERSUS LOG N. (N = NUMBER CYCLES TO FAILURE.)

machined edges of the specimens of material D were much "cleaner" than the edges of the specimens of material A; these ragged edges would distort the relation between the two materials.

Consequently, all endurance limits reported in this paper were determined with carefully prepared specimens; thus the authors hope to represent the fatigue properties of the different materials in their true relation to one another.

DISCUSSION OF DATA AND RESULTS OBTAINED IN THIS INVESTIGATION

The summarized data are given in Table 2 and shown plotted in the customary semilogarithmic form for determination of endurance limits in Fig. 5. Well defined curves were obtained, and apparently the true endurance limit for these five alloys is reached below 50,000,000 cycles, since the curves become horizontal below this value.

Certain irregularities were observed in the course of the tests; in some cases several of the five specimens of a given alloy failed at a point removed from the section of uniform stress. These results were valueless, and were discarded. Where the stress value was near the endurance limit, the tests were repeated; otherwise, the point was omitted, since only a limited period of time was available for completing the tests. For the same reason, it was not possible to establish definitely that a true endurance limit was reached. At any rate, the authors feel that the results reported here represent a good approximation to the endurance limits, and are reliable for comparing the different alloys.

TABLE 2.—*Data for Relation of Stress and Number of Cycles*

Stroke, In.	Stress, Lb. per Sq. In.	Number of Cycles
MATERIAL A		
0.830	58,000	245,000
0.755	52,300	518,000
0.686	47,000	1,160,000
0.568	37,800	47,070,000*
0.554	36,500	43,360,000*
0.540	35,500	5 samples unbroken @ 50,000,000
MATERIAL B		
0.755	48,500	340,000
0.686	43,700	605,000
0.596	37,600	1,791,000
0.568	35,800	20,513,000
0.554	34,800	5 samples unbroken @ 50,000,000
MATERIAL C		
0.755	46,800	402,000
0.596	36,700	1,707,000
0.568	34,300	10,300,000
0.540	32,800	4 samples unbroken @ 50,000 000*
MATERIAL D		
0.830	50,600	388,000
0.755	46,200	550,000
0.686	41,600	842,000
0.596	36,000	1,494,000
0.540	32,300	1,972,000
0.500	29,800	4,446,000
0.476	28,300	5 samples unbroken @ 50,000,000

TABLE 2.—(Continued)

Stroke, In.	Stress, Lb. per Sq. In.	Number of Cycles
MATERIAL E		
0.596	55,700	406,000
0.540	48,800	542,000
0.401	35,800	940,000
0.320	28,500	3,563,000
0.310	27,600	29,107,000 ^a
0.294	26,200	4 samples unbroken @ 50,000,000 ^c

SUMMARIZED RESULTS

MATERIAL	ENDURANCE LIMIT, LB. PER SQ. IN.
A	36,000
B	35,500
C	33,600
D	29,000
E	27,000

^a Two samples unbroken @ 50,000,000 cycles.^b Four samples unbroken @ 50,000,000 cycles.^c One sample broke near free end: not counted.^d See Table 1.

These results show well defined differences in the endurance limits of the various alloys, with the exception of the small difference between materials A and B, which is within the possible experimental error and therefore is not conclusive.

Table 1 shows that these two materials differ only in their phosphorus content, material A having 0.032 per cent P while material B has 0.106 per cent P. The effect of the high phosphorus content of material B is appreciable only at stresses above the endurance limit: comparison of the S -log N curves of these two materials (Fig. 5) yields the interesting fact that the "life" of material B is considerably shorter than that of material A at the higher stresses. For example, at a stress of 40,000 lb. per sq. in., material A fails at an average figure of over 3,000,000 cycles, while material B runs only slightly over 1,000,000 cycles. Thus it appears that the increase in phosphorus is definitely detrimental to the fatigue properties of this particular bronze, which is in accordance with the recognized embrittling effect of phosphorus.

Material C, with a higher percentage of tin than either material A or material B, and phosphorus intermediate between that of A and B, has a lower endurance limit, but its S -log N curve follows that of material B fairly closely above the endurance limit. Thus it appears that even 0.067 per cent phosphorus is detrimental, though the difference between materials B and C may be due entirely to the difference in tin content.

Material D, with a still lower endurance limit, is inferior to material A at all stresses within the range of these tests, and is inferior to mate-

rials B and C at stresses up to about 40,000 to 45,000 lb. per sq. in., above which it is somewhat superior to either B or C.

Material E has the lowest endurance limit in this group of alloys, and is inferior to material D at stresses up to about 40,000 to 45,000 lb. per sq. in., above which it is superior to materials B, C and D; at stresses above about 55,000 lb. per sq. in., it is also superior to material A.

Since, at stresses above 40,000 lb. per sq. in., none of these alloys endures more than 1,000,000 cycles (material A, the exception, runs over 3,000,000 cycles), the differences are important only where exceedingly long life is not the major consideration involved in a specific application.

Townsend¹ reports an endurance limit of 24,500 lb. per sq. in. for a phosphor bronze almost identical with material C of this report, for which an endurance limit of 33,600 lb. per sq. in. was determined. While his figures are based on 100,000,000 cycles of stress, it is not logical that this fact alone accounts for the difference. One must assume, instead, that his tests were made on as-rolled specimens, which could account for such a difference. The authors feel that the figure reported here represents more nearly the true endurance limit for this alloy, and shows material C in its true relation to the other alloys.

GENERAL CONCLUSIONS

These tests indicate that phosphorus in the amount of 0.106 per cent in the 95 Cu, 5 Sn bronze is detrimental to the fatigue properties of this alloy at stresses above the endurance limit.

It also seems clear that the phosphor bronzes, materials A, B and C, are definitely superior to the silicon bronze, material D, and to the Admiralty-nickel alloy, material E. Material D is somewhat superior to material E.

The importance of the finish on the test specimens has been emphasized in this report, and the question of finish must always be considered when making recommendations for applications of metal parts where fatigue properties are important.

While great care was taken in all directions to make these results reveal a true comparison of the fatigue properties of the different mixtures tested, unanticipated irregularities may enter into any individual testing program, so that, pending further investigation, the summarized statements of this paper are presented as indications rather than final conclusions concerning the relative merits of phosphor bronzes and silicon bronzes.

REFERENCES

1. J. R. Townsend and C. H. Greenall: Fatigue Tests on Non-Ferrous Sheet Metals. *Proc. Amer. Soc. Test. Mat.* (1929) **29**, pt. II, 353.

2. H. F. Moore: Present Day Knowledge of Fatigue. Committee Reports Amer. Soc. Test. Mat. (1930) **30**, pt. I, 261.
3. R. R. Moore: Resistance of Manganese Bronze Duralumin and Elektron Metal to Alternating Stresses. *Proc. Amer. Soc. Test. Mat.* (1923) **23**, pt. II, 106.
4. R. R. Moore: Resistance of Metals to Repeated Static and Impact Stresses. *Proc. Amer. Soc. Test. Mat.* (1924) **24**, pt. II, 558.
5. J. B. Johnson and T. T. Oberg: Fatigue Resistance of some Aluminum Alloys. *Proc. Amer. Soc. Test. Mat.* (1929) **29**, pt. II, 339.
6. H. F. Moore and J. B. Koppers: The Fatigue of Metals. New York, 1927. McGraw-Hill Book Co.

DISCUSSION

(C. E. Swartz presiding)

H. L. BURGHOFF,* Waterbury, Conn. (written discussion).—With reference to surface finish of endurance test specimens, the authors rightly state that the specimens should be smooth and free from defects. The finishing of steel specimens with fine emery is mentioned, following which it is stated that specimens of softer metals must be finished even more carefully. This presumably refers to stress-concentration effects at the bases of any notches or scratches. These effects are, we believe, much greater in ferrous materials than in nonferrous materials, particularly tough copper-base alloys.

We have made numerous tests of strip materials in machines similar to the one described in this paper. Using metal in the as-rolled condition, tests on specimens carefully machined and with any slight burs removed from the edges have shown little or no difference in number of cycles to fracture among specimens on which the machining marks on the edges have or have not been removed by filing or polishing. The authors refer to distinct differences between their carefully polished specimens and specimens tested simply as rolled and machined. We wonder if they have actual figures at hand to demonstrate their remarks further.

With regard to differences in endurance properties between silicon bronzes and phosphor bronze, it should be remembered that silicon bronzes do have excellent properties and occupy a high place among copper alloys. Furthermore, there is an inherent difference in cost of these alloys, which distinctly favors the use of silicon bronze in many instances.

G. R. BROPHY,† Bayonne, N. J. (written discussion).—It is rather extraordinary to find definite endurance limits for nonferrous alloys such as the authors indicate for fine hard-drawn bronzes. Such results cause one to question their methods of stressing.

Cuthbertson⁷ has shown by dead loading a rotating cantilever beam that the deflection continues with time. This can mean, only, that the modulus is decreasing. Therefore, when a rotating beam is stressed by applying a load through a spring, or, as the authors do, by vibrating a beam through a constant amplitude, it can be expected that the stress is decreasing continuously throughout the test, thereby extending the life considerably. This action would sharpen the knees of the S-N curves as the authors have found, and produce what appears as a definite endurance limit at a stress that if constant would surely result in fracture. The true S-N curves, then, can be expected to lie to the southwest of those of the authors' and to be more typical of nonferrous alloys.

* Chase Brass and Copper Co.

† Research Laboratory, International Nickel Co.

⁷ Iron and Steel Inst. *Carnegie Scholarship Mem.* (1935) **24**.

It would be interesting, too, to know whether alloys A, B and C enjoyed proportionately greater strengthening as a result of rolling 6 to 8 numbers hard than did alloys D and E. If so, might it not be expected that they show longer life at a repeated constant stress when tested as smooth, polished specimens?

A better idea of their performance, and probably a different order of merit, would be obtained if they were tested in the presence of a notch, since some of these alloys show extreme notch sensitivity in their hard-drawn conditions.

A. V. DE FOREST,* Cambridge, Mass.—The copper-base alloys in the cold-worked condition are presumably susceptible of aging and we all know that the elastic properties increase with time, and particularly they increase with a slight degree of reheat. Would it not be an additional point in any discussion of the fatigue limits to know what that aging behavior is? If the aging is improving the fatigue limits, it is probably also changing the notch sensitivity. It appears to me that before trying to compare different materials of anything like the same class to be used for similar purposes, we should have a pretty clear understanding of both the fatigue limit and the notch sensitivity, the notch sensitivity coming in in the practical case where springs are produced in any sort of commercial quantity, unless the surfaces are most carefully polished or ball burnished or some other precaution is taken to keep out tool marks or grinding marks. Practical springs have notches, and spring material that may be excellent as far as fatigue limit is concerned in the perfectly prepared specimen may not be quite as successful under ordinary commercial production.

R. J. WHEELER,† Riverside, N. J. (written discussion).—Since silicon-copper alloys have been offered as a substitute for phosphor bronze and other nonferrous alloys for springs, it is appropriate to compare its fatigue properties with these alloys, which have been used for a great many years. It is unfortunate, however, that the fatigue limits could not be determined on the as-rolled condition, since springs are made from material in this form. The authors noted that the surface finish of the specimens produce wide discrepancies in fatigue values. Their endurance value for material C is much higher than those determined by Townsend and Greenall. If the authors assume that this difference is due to the use of as-rolled instead of polished specimens, how can they explain the apparent consistent results obtained by Townsend and Greenall?

An attempt is made in this paper to show that an increase in phosphorus has a detrimental effect upon the fatigue properties of that particular bronze. Since phosphor bronze is now being made with up to 0.40 per cent P and of the same general tin content as alloys A and B, we believe that these tests should have included specimens covering the range of phosphorus content. We do not feel that the evidence submitted on two low-phosphorus variables should be conclusive.

We believe that the comparison of these alloys could be considerably enhanced by a corrosion-fatigue test. After all, most installations will involve corrosion as well as fatigue. While most ferrous and nonferrous materials show a marked decrease in corrosion-fatigue resistance from fatigue resistance in air, phosphor bronze is considerably higher. This was shown in a recent paper by Gough and Sopwith (*Journal Institute of Metals*). This paper showed that the intrinsic fatigue resistance of a material may be considerably higher than that developed in normal fatigue tests in air.

C. H. GREENALL,‡ New York, N. Y. (written discussion).—The paper by Messrs. Price and Bailey has added considerable information to our knowledge of the fatigue properties of materials that may be used for springs. My comments are of a minor

* Associate Professor of Mechanical Engineering, Massachusetts Institute of Technology.

† Chief Metallurgist, Riverside Metal Co.

‡ Member Technical Staff, Bell Telephone Laboratories, Inc.

nature, but should be considered if the information published in this paper is to be used by design engineers. The specimen shown in Fig. 3 is essentially correct. Our experience, however, during the past five years has shown that it is extremely difficult to obtain a form milling cutter from the dimensions given in this figure. Accordingly, we have developed another method of dimensioning this specimen wherein the basic dimensions for the specimen are referred back to the $1\frac{5}{8}$ -in. end, from which end all specimens are located on the testing machine. This has necessitated a change in the 2-in. dimension shown in Fig. 3 to 2.035 in. The location of the uniformly stressed area, however, remains the same with respect to the point of actuation of the specimen under test. A more thorough mathematical analysis of the shape of the specimen shows that the l/b ratio previously referred to for this specimen should be increased from 9.269 to 9.287, or in the ratio of approximately 19 to 10,000.

In a previous paper by J. R. Townsend and myself,¹ the statement was made that the speed of the machine is approximately 1500 r.p.m. It was pointed out in this paper, however, that it was necessary to adjust the speed of the machine to the material under test in order that the natural frequency of the specimen be not approached by the speed of the machine. The majority of the tests on which we previously reported were made at a speed of 750 to 900 r.p.m. Our present practice is to hold as closely to 750 r.p.m. as possible, which is comparable to the speed used by Messrs. Price and Bailey. In our work, however, we have found that speeds up to approximately 2000 r.p.m. have no noticeable effect on the fatigue properties of the alloys under investigation.

We have checked the stress reported by Messrs. Price and Bailey on the material identified as alloy D. It is reported that the stress for 1 in. deflection is 59,600 lb. per sq. in. The check values we have made approximate 58,320 lb. per sq. in. for the material as received. Mathematically, surface finish should not affect the value of S_i as calculated from the load-deflection data, except as the cross section is reduced in such a manner as to make it difficult to obtain an accurate measurement of b and d . This was checked experimentally on two specimens of material. The values we obtained are as follows:

As received S_i equals 58,320 lb. per sq. in.

Polished with No. 00 French emery, S_i equals 58,400 lb. per sq. in.

Polished with No. 0000 French emery and rouge, S_i equals 58,380 lb. per sq. in.

We agree with Messrs. Price and Bailey that surface finish will affect the endurance limit to a certain extent. For example, on an 8 per cent tin phosphor bronze alloy, rolled 8 numbers hard, the endurance limit for the material as received was 26,000 lb. per sq. in. at 100,000,000 reversals. When a microscopic polish was applied to the specimens the endurance limit (estimated from tests run to 73×10^6 reversals) was raised to 28,500 lb. per sq. in. In the paragraph under "Manipulation," reference is made to the wide spread observed in the number of cycles to failure for the specimens tested at a given stress in the as-rolled condition. This was stated to be due primarily to the surface condition. We do not agree with Messrs. Price and Bailey that the spread in the test results is wider for the unpolished than for the polished specimens. The information we have obtained so far indicates that the spread in test results is as wide for the polished material as for the unpolished material. However, we have noted in our tests on dispersion-hardened alloys that a greater spread occurs with material of this type in the as-rolled condition than with the ordinary commercial tin bronzes.

The data that we have obtained on materials similar to alloy A indicate that the endurance limit is lower for material in the as-rolled condition than that reported by Messrs. Price and Bailey on polished specimens. Our results on a 4 per cent tin phosphor bronze rolled four numbers hard gave an indicated endurance limit of 25,000 lb. per sq. in. at 100,000,000 reversals. When the material was rolled eight

numbers hard the endurance limit approximated 22,000 lb. per sq. in. Both of these materials were in the as-rolled condition. Messrs. Price and Bailey report an indicated endurance limit of 36,000 lb. per sq. in. for similar material rolled six numbers hard, which had been polished. Likewise, on an 8 per cent tin phosphor bronze alloy rolled four numbers hard an indicated endurance limit of 26,000 lb. per sq. in. at 100,000,-000 reversals was obtained for the material as-rolled. Similar material, that was given a microscopic polish before testing had an indicated endurance limit of 28,500 lb. per sq. in., a gain of about 10 per cent resulting from polishing. A second lot of commercial 8 per cent tin phosphor bronze rolled eight numbers hard, in the as-rolled condition, had an indicated endurance limit of 27,000 lb. per sq. in. Another lot, which had been rolled ten numbers hard, had an indicated endurance limit of 24,500 lb. per sq. in. Messrs. Price and Bailey report an indicated endurance limit of 33,600 lb. per sq. in. for similar material rolled six numbers hard but polished.

The results, therefore, as presented by Messrs. Price and Bailey are extremely significant, inasmuch as the importance of surface condition of springs is clearly brought out. The data show that in certain designs it may be necessary to polish the springs in order to take advantage of the increased endurance limit. Likewise, the effect of polished surfaces is more noticeable at the higher stresses, where the difference between the polished and unpolished specimens is much greater than at the endurance limit. In ordinary design work, however, where polished springs are not employed, the lower endurance limit values will, of necessity, have to be used along with suitable factors of safety.

R. W. BAILEY (written discussion).—We realize, as Dr. de Forest has pointed out, that we have not made a comprehensive survey of the fatigue properties of these materials, with regard to different degrees of cold-work, heat-treatment, aging, corrosion, etc., and much remains to be done in this field. Admittedly, the properties of copper-base alloys, especially the proportional elastic limit and the endurance limit^a are affected by a low-temperature heat-treatment, but we are not aware of any significant "aging" characteristics of these particular alloys. We question whether there is enough difference in the heat-treating properties or notch sensitivity of these two types of bronze (phosphor and silicon) to explain the observed differences in fatigue properties.

Mr. Brophy accuses us unjustly of presuming to have shown "definite endurance limits" for these nonferrous alloys. Reference to the paragraph entitled "Discussion of Data and Results" in our paper should clear up this point. The limitations of a fatigue test using a machine of the constant-strain type are recognized, but for tests on spring materials which are used in parts designed for a constant strain, this test is especially suitable.

In reply to Mr. Wheeler, we agree that fatigue tests on materials in the as-rolled condition yield valuable information but, as stated in our paper, we felt that more reliable results could be obtained in the limited time available for these tests if carefully prepared specimens were used, thereby eliminating accidental variables such as poor surface finish, burred edges, etc., which admittedly have a varied and often severe effect upon the fatigue behavior of a given lot of samples. The consistency of Townsend and Greenall's results can, we feel, be attributed to extended experience in fatigue testing and to a careful selection of specimens in the as-rolled condition. We made no definite statement that an increase in phosphorus content is detrimental to the fatigue properties of the phosphor bronze. Our tests indicate that this is true, but unfortunately we were unable to make a more complete investigation, as Mr. Wheeler

^a J. B. Kommers: The Static and Fatigue Properties of Brass. *Trans. A.S.T.M.* (1931) 31, pt. II, 243.

suggests. Corrosion-fatigue tests would be very appropriate, but we could not begin to cover so many variables, in the time available.

We especially thank Mr. Greenall for his comments, and for his checking the stress values on certain of our specimens. His revision of the design of the specimen will be heartily approved by those who work with such specimens.

The question of surface condition has perhaps been unduly stressed, in so far as the difference between carefully rolled and machined specimens in the as-rolled condition and the same carefully prepared specimens with their surfaces polished would be noticeable but not large, as Mr. Greenall shows; but if one were to take a lot of specimens carelessly rolled and machined, with perhaps rolled-in dirt and scale, deep tool marks, badly burned edges, etc., and compare them with carefully prepared specimens, either polished or not polished, real differences would be observed.

Mr. Burghoff's remarks are appreciated, and until further evidence is obtained, we shall feel, as our tests indicate, that the fatigue properties of the phosphor bronzes are superior to those of the silicon bronze tested.

Thermal and Electrical Conductivities of Aluminum Alloys

BY L. W. KEMPF,* C. S. SMITH,† MEMBERS A.I.M.E., AND C. S. TAYLOR‡

(New York Meeting, February, 1937)

THE thermal conductivity of aluminum alloys is of considerable industrial importance. This is particularly true in such applications as internal-combustion engines where one of the principal reasons for the use of these alloys is their relatively higher thermal conductivity. In spite of this, relatively few data are available on this property of aluminum alloys. The reason is quite apparent to anyone concerned with the experimental determination of coefficients of thermal conductivity. This determination, in theory so simple, is extraordinarily difficult if any high degree of precision is desired. Fortunately, some knowledge of the relationship between thermal and electrical conductivity has permitted the use of the latter physical property in deducing the relative approximate values of the thermal conductivities of metals. This fundamental relationship, first enunciated by Wiedemann and Franz¹ as applying to metallic elements and later shown by Lorenz² to be applicable to alloys within a single metallic system, has been of service in the industrial application of metals. The electrical conductivity of metals is easily determined with a high degree of precision. It is, therefore, quite desirable that the relationship between electrical and thermal characteristics be determined with the greatest possible precision.

This paper presents data on the electrical and thermal conductivities of a number of aluminum alloys of industrial importance.

LITERATURE ON THERMAL CONDUCTIVITY OF ALUMINUM ALLOYS

Masumoto³ determined the electrical and thermal conductivities of 18 aluminum alloys. His results indicated a relatively constant relationship between thermal and electrical conductivity.

Manuscript received at the office of the Institute Nov. 27, 1936.

* Aluminum Research Laboratories, Aluminum Company of America, Cleveland, Ohio.

† Copper Alloys Research Laboratory, The American Brass Co., Waterbury, Conn.

‡ Aluminum Research Laboratories, Aluminum Company of America, New Kensington, Pa.

¹ References are at the end of the paper.

Griffith and Schofield⁴ determined the electrical and thermal conductivities of 22 aluminum alloys. They found the Lorentz coefficient to vary from about 5.3 at 80° C. to about 5.5 at 200° C.

Mannchen⁶ determined the conductivities of 15 aluminum alloys. His results show wider variations of thermal conductivity with composition than Masumoto's or those of Griffith and Schofield.

Eurenger and Hanemann⁶ determined the thermal conductivity of seven aluminum alloys in various structural conditions. They gave no data on the electrical conductivity of their materials.

Euken and Warrentrup⁷ determined the conductivities of four specimens, two in the wrought and two in the cast conditions, of 99.7 per cent pure aluminum; of 4 per cent and 8 per cent copper alloys in the wrought and cast conditions; and of three alloys in the wrought condition containing, in addition to 0.5 per cent magnesium, 4, 5 and 7 per cent copper, respectively. Determinations were made at 0° C. in the conditions: (1) as cast; (2) as wrought; (3) solution heat-treated; and (4) solution heat-treated followed by various periods of aging at 0°, 100° and 215° C. A few determinations were also made at -192° C.

The conductivities of similar compositions vary considerably as determined by these various investigators. Generally speaking, however, in any one investigation a fairly constant relationship was found to exist between thermal and electrical conductivity. Numerical values of the ratios, however, vary considerably between various alloys and even vary for the same alloy when the determinations are made by two different investigators. Critical examination of these results suggest that the reason for these variations probably lies in the structural condition of the alloys. Masumoto, for example, indicated considerable variation in conductivities with variation in heat-treatment.

EXPERIMENTAL PROCEDURE

Preparation of Materials.—The alloys chosen for this investigation are compositions in considerable use as materials for the construction of internal-combustion motors. The castings were made in the form of small ingots 2 in. in diameter by about 16 in. long. The metal was cast in iron molds in such a manner as to yield sound castings relatively free from porosity. The wrought material was commercial forging stock hot-rolled from ingots weighing about 1000 lb. to stock 4 to 6 in. in diameter. This stock was reduced by forging in the temperature range 750° to 850° F. to rod about 1 in. square. The initial determinations of thermal conductivity were made on the material in the form in which it is usually placed in service. Exceptions are the three chill-cast alloys, 7542, 7543 and 7544, which were first examined in the chill-cast condition. Determination of the electrical conductivity of these materials prior to the determination of thermal conductivity would have been exceedingly

desirable; however, the magnitude of the change in structure brought about during the determination of the thermal conductivity was considerably underestimated and the electrical conductivity was determined subsequent to the thermal measurements.

Thermal Conductivity.—The procedure utilized in the determination of the thermal characteristics of the alloys has been described and reference should be made to these papers for the details of the procedure^{5,9,10}. It is believed that the determinations are correct to within ± 0.01 cal. per sq. cm. per cm. per sec. per degree centigrade.

Electrical Conductivity.—The electrical conductivities were determined by comparing the potential drop across the specimen, or a specific portion of it, while at a constant temperature with the potential drop across a known resistance standard during the passage of the same small current through the known resistance and the specimen. The resistance unit employed has been standardized by the National Bureau of Standards. It is believed that the electrical measurements are accurate to within ± 0.1 per cent.

RESULTS

The results are tabulated in Table 1. It is immediately apparent from an examination of the thermal and electrical conductivities as determined on the original material, and particularly from the electrical conductivity of the hot and cold ends of the bars, that considerable structural change has been brought about during the determination of the thermal characteristics. Even so the relationship between electrical and thermal conductivity is relatively constant. It is difficult, however, to deduce from these data the correct values of either thermal or electrical conductivity for the initial condition. It was then decided to place the materials in a structural condition that would be relatively stable over the temperature range involved in the determination of the thermal conductivity. As indicated in the table, this was achieved by careful annealing over the range within which the solid solubility of most elements in aluminum changes most rapidly. It was evident from resistivity explorations on the annealed specimens that the treatment had quite satisfactorily achieved its purpose. The thermal conductivity determinations subsequent to the annealing treatment are characterized by much greater uniformity and much lower temperature coefficients than those of the bars in the original condition. The Lorenz constant for the alloys of low silicon content varies over a considerably narrower range for the annealed than for the bars in the original condition.

Subsequent to the determination of thermal conductivity on the annealed bars, an attempt was made to place the specimens in their original structural condition. This was obviously impossible for the as-cast alloys. Experience has indicated, however, that casting in the manner

described for these bars results in a condition not differing greatly from that obtained after quenching from a high-temperature solution treatment. With the remaining specimens, the intervening annealing probably had relatively little effect on the final treatment.

Table 2 gives the electrical conductivities and calculated thermal conductivities of a number of commercial alloys in various conditions of heat-treatment. The specimens for this part of the investigation were machined from standard test bars and the results are representative of commercial fabricating procedures and heat-treatments. It should perhaps be emphasized that the maximum error in these calculated values for thermal conductivity may be as great as ± 6 per cent, as will be evident from the following discussion.

DISCUSSION OF RESULTS

It is now generally accepted that the conduction of heat by metals is effected by two different agencies. The major portion of heat transfer is by means of the free electrons. Heat is also conducted by atomic contact and probably is a function of the frequency and amplitude of vibration of the individual atoms. Electrical conduction is probably entirely an electronic effect. These ideas are expressed mathematically as follows: $K = c\lambda T + k$. Where K is the total thermal conductivity, k is the nonmetallic or atomic part, λ the electrical conductivity, T the absolute temperature, and c a constant, which may be considered as the true Lorenz ratio for the metallic part of the conductivity. This, of course, is the equation of a straight line with a positive intercept on the K axis, if thermal conductivity K is plotted against the product of the electrical conductivity and the absolute temperature. The values in Table 1, with the exception of those for the high-silicon alloys, have been so plotted in Fig. 1 together with many of the data available in the literature. The plotted points from most of the data fall near a straight line, represented by the equation $K = 5.02\lambda T \times 10^{-9} + 0.03$. This line is similar to that determined by the thermal and electrical conductivities of copper alloys as indicated by one of the authors.

Although the values for the annealed alloys of the present investigation lie close to the line, those for the alloys in the as-cast and heat-treated conditions show considerable scatter. It is perhaps to be expected that the ratio between thermal and electrical conductivity in the as-cast and heat-treated conditions should show considerable deviation, because of the structural changes accompanying the determination of the thermal conductivity. These changes in structure are well illustrated by the variation in electrical conductivity from end to end of the specimens subsequent to the determination of the thermal conductivity. The determinations of thermal conductivity had no effect on the structural

condition of the annealed bars and the values for the ratio logically fall on a straight line.

The plotted points for the conductivities of alloys containing more than about 5 per cent silicon fall generally considerably above the line determined by the values for the other alloys. Also, the values determined by Griffith and Schofield for an alloy containing about 7 per cent copper and 1 per cent silver fall above this line. Mannchen's determinations show so much scatter as to suggest, especially in view of the results of the other investigators, that some uncontrolled factor exerted considerable influence on his determinations.

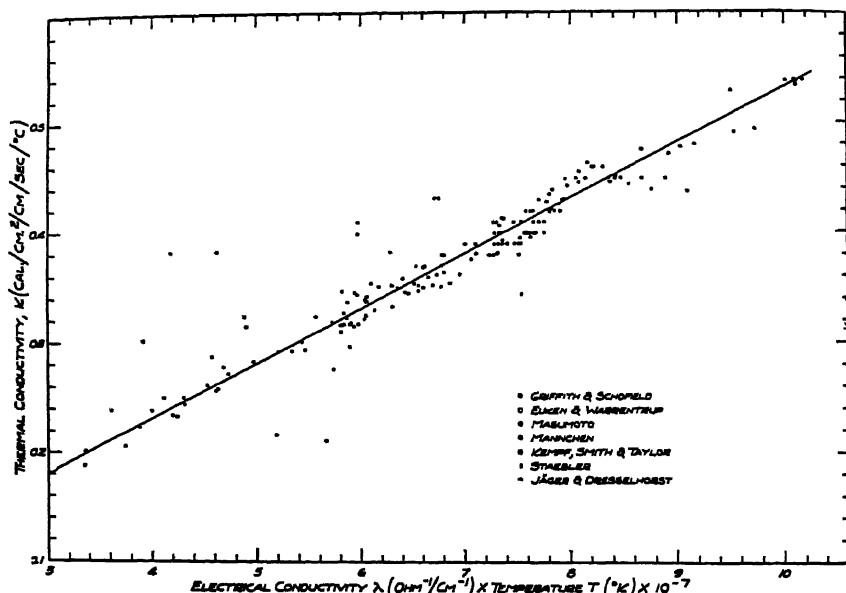


FIG. 1.—RELATION OF THERMAL CONDUCTIVITY AND PRODUCT OF ELECTRICAL CONDUCTIVITY AND ABSOLUTE TEMPERATURE OF ALUMINUM ALLOYS.

When the available data^{7,12} for temperatures below 0° C. are plotted as in Fig. 1, no regular relationship between K and λT is indicated. The curve of Fig. 1, therefore, applies only within the approximate temperature range 0° to 400° C.

Practically all the determinations other than the exceptions noted above fall within ± 6 per cent of the line previously defined. A wide range of temperatures from about 0° to 400° C. is concerned, and it appears evident that some fundamental relationship is involved. It is believed that, with more attention to the structural condition of the specimens and with simultaneous determinations of electrical and thermal conductivities over a narrow range of temperature, the relationship could be much more accurately established.

TABLE 2.—*Electrical and Calculated Thermal Properties of Commercial Alloys*

Sand Cast Alloy		Electrical Resistivity, Ohms $\times 10^4$	Electrical Conductivity, Ohm ⁻¹ $\times 10^{-4}$	Electrical Conductivity, Per Cent I A.C.S.	Approximate Calculated Thermal Con- ductivity, Cal. per Sq. Cm. per Cm. per Sec per Deg C
No.	Condition				
12 . .	As-cast	4 700	21 28	37 4	0 35
	Annealed	3.656	27.35	48.1	0 44
43.	As-cast	4 799	20 84	36 7	0 34
	Annealed	4.190	23.87	42 0	0 39
45	As-cast	5 876	17.02	31.0	0 29
	Annealed	5.299	19.12	33 0	0 32
47 (normal)	As-cast	5 706	17.52	30 8	0 29
	Annealed	5.423	18 45	32.4	0 31
47 (modified)	As-cast	4 352	22.98	40 4	0 37
	Annealed	4 186	23 89	42 0	0 39
108	As-cast	5 680	17.60	31 0	0 29
	Annealed	4 630	21.59	38 0	0 35
109	As-cast	4 874	20 52	36 1	0 34
	Annealed	3 905	25 60	45 0	0 41
112	As-cast	5 826	17.17	30 2	0 29
	Annealed	4 610	21 69	38 1	0 35
	T4 ^a	6 412	15 60	27 4	0 26
	T4, ann	4 389	22.77	40 1	0 37
	T6 ^a	6 056	16.50	29.0	0 28
122	As-cast	5.182	19.31	33 9	0 32
	Annealed	4 090	24 44	43 1	0 40
	T4, ann	3 998	25 00	44 0	0 40
	T2 ^b	4 303	23 26	40 9	0 38
	T54 ^b	4 814	20 79	36.5	0 34
	T61 ^c	5 382	18 59	32 7	0 31
	T551 ^b	4 893	20.45	35.9	0 34
A132...	As-cast	6 480	15 43	27 1	0 26
	Annealed	5 786	17 28	30 4	0 29
	T4, ann.	5 180	19 30	33 9	0 32
	T65 ^c	6 410	15 60	27.4	0 26
	T551	6 354	15 75	27.7	0 26
142	As-cast	4 936	20 24	35.7	0 33
	Annealed	4 019	24 87	43 8	0 40
	T4	5 583	17 92	31 5	0 30
	T4, ann.	3 874	25 80	45.4	0 42
	T6	4 667	21 41	37.7	0 35
195...	T4, ann.	3 457	28 90	50 9	0 46
	T4	5 050	19 80	34 9	0 33
	T7 ^d	3 696	27 03	47.6	0 43
	T62 ^c	4 756	21 01	37.0	0 34
214.	As-cast	5 101	19 61	34 5	0 32
	Annealed	5.091	19 64	34 5	0 32
216.	As-cast	6 303	15 87	27 9	0 27
	Annealed	6 448	15 51	27.3	0 26
220	Annealed	8 329	12 00	21.1	0 21
	T4	8 548	11 70	20.8	0 20
355	T4, ann	3 856	25 94	45 6	0 42
	T4	4.995	20 00	35.2	0 33
	T5 ^b	4.884	20 49	36 0	0 34
	T6	4 906	20 37	35 8	0 33
	T7	4.147	24 10	42.4	0 39
	T51 ^b	4.078	24.51	43.1	0 40
	T59 ^b	4 089	24.45	43.0	0 40
	T61	4.695	21.28	37.4	0 35
A355	Annealed	5 191	19 27	33.9	0 32
	T51	5.531	18 08	31.8	0 31
356.	T4, ann.	3.593	27 85	48.9	0 45
	T4	4.564	21.93	38 6	0 36
	T6	4 495	22.22	39 1	0 36
	T51	4.126	24 21	42 6	0 39
	T59	4.106	24.33	42 8	0 39
654.	As-cast	5.303	18.87	33.2	0 31
	Annealed	5.061	19.76	34.7	0 33

TABLE 2.—(Continued)

Permanent Mold Cast Alloy		Electrical Resistivity, Ohms $\times 10^6$	Electrical Conductivity, Ohms ⁻¹ Cm. ⁻¹ $\times 10^{-4}$	Electrical Conductivity, Per Cent I.A.C.S.	Approximate Calculated Thermal Con- ductivity, Cal. per Sq. Cm. per Cm. per Sec. per Deg. C
No.	Condition				
12...	As-cast	4 607	21 69	38 2	0 35
	Annealed	3 529	28 33	49 8	0 45
43	As-cast	4 280	23 36	41.1	0 38
	Annealed	3 630	27 55	48 4	0 44
A108	As-cast	4 791	20 88	36 7	0 34
	Annealed	3 976	25 15	44 2	0 41
112	As-cast	5 429	18 42	32 4	0 31
	Annealed	4 374	22.88	40 2	0 37
B113	As-cast	6 016	16 61	29 3	0 28
	Annealed	4 798	20.83	36.7	0 34
	T4	5 896	16 95	29.8	0 28
	T4, ann.	4 119	24 27	42 7	0 39
	T6	5 544	18 05	31.7	0 30
C113	As-cast	6 488	15 41	27.1	0 26
	Annealed	5 213	19 19	33 7	0 32
122	As-cast	5 183	19 31	34 0	0 32
	Annealed	4 122	24 27	42.7	0 39
	T55 ^b	4 880	20 49	36 0	0 34
	T65	5 289	18 98	33.4	0 31
	T4, ann.	4.032	24.81	43 6	0 40
A132...	As-cast	5 256	18 97	28.2	0 27
	Annealed	5 400	18 52	32 6	0 31
	T4	5 837	17 12	30.1	0 29
	T4, ann.	4 826	20 72	36.4	0 34
	T7	4 909	20 37	35.8	0 33
	T551	5 982	16 72	29 4	0 28
142	As-cast	5 180	19 38	34.1	0 32
	Annealed	4 189	23 84	42.0	0 39
	T62	5 270	18 98	33.4	0 31
	T571 ^b	5 239	19 08	33.6	0 32
144	As-cast	5 876	17 01	29.9	0 28
	Annealed	4 367	22 90	40.3	0 37
	T4	5 611	17 83	31.3	0 30
	T4, ann.	4.020	24.87	43 7	0 40
151	As-cast	4 221	23 70	41 7	0 38
	Annealed	3 477	28 76	50 6	0 46
B195	T4, ann.	3 524	28 38	49 8	0 45
	T4	5 042	19 84	34.9	0 33
	T62	4 877	20 49	36.1	0 34
355	T4, ann.	3 463	28 87	50 8	0 46
	T4	4 790	20 88	36.7	0 34
	T6	4 508	22 17	39 0	0 36
356	T4, ann.	3 568	28.04	49.3	0 45
	T4	4 484	22 32	39.2	0 36
	T6	4 319	23.15	40.7	0 38

This curve is of considerable practical importance in that it suggests that a comparison of the thermal properties of aluminum alloys in various structural conditions is probably sounder when based on determinations of electrical properties than when based on direct determinations of thermal conductivities, except, of course, when the determinations of thermal conductivity may be made in the annealed condition. The direct determinations of thermal properties in this investigation give a relationship between electrical and thermal conductivities represented by the value for the ratio $\frac{K}{\lambda T}$ of 5.4×10^{-2} . The deviation of the annealed specimens from this ratio is less than ± 3 per cent. If the curve of Fig. 1 is correct, it is not to be expected that $\frac{K}{\lambda T}$ will be constant for any very

TABLE 2.—(Continued)

Forged Alloys		Electrical Resistivity Ohms $\times 10^4$	Electrical Conductivity, Ohms ⁻¹ Cm ⁻¹ $\times 10^{-4}$	Electrical Conductivity, Per Cent I. A. C. S.	Approximate Calculated Thermal Con- ductivity, Cal. per Sq. Cm. per Cm. per Sec. per Deg. C.
No.	Condition				
14S	T ¹ , ann.	3 380	29 59	52 0	0 47
	W ²	4 944	20 24	35 6	0 33
	T	4 407	22 68	39 9	0 37
18S.	T, ann.	3 472	28 80	50 6	0 46
	T	4 359	22 94	40 4	0 37
B18S	T, ann.	3 548	28 18	49 6	0 45
	T	5 050	19 80	34 8	0 33
25S	T, ann.	3 362	29 74	52 3	0 48
	T	4 531	22 08	38 8	0 36
32S	T, ann.	4 111	24 33	42.8	0.39
	T	4 875	20 49	36 1	0 34
A51S	T, ann.	3 160	31 65	55 7	0 50
	T	3 748	26 67	47 0	0 43
52S	Annealed	3 066	32 60	57 3	0 52
	As forged	3 714	26.95	47 3	0 43
53S	T, ann.	3 765	26 56	46.7	0 43
	T	4 131	24 21	42.6	0 39
70S	T, ann.	4 485	22 30	39.2	0 36
	W	5.150	19 42	34.2	0.32
	T	4.891	20 45	36.0	0.34

* T4, solution heat-treatment followed by rapid cooling

¹ T2, T3, T51, T54, T541, T55, T551, T571, T59, precipitation treatment only.

² T6, T61, T62, T65, solution followed by precipitation treatments.

³ T7, solution treatment followed by precipitation and stabilizing treatments.

⁴ W, solution heat-treatment followed by rapid cooling.

⁵ T, precipitation treatment either at ordinary or slightly elevated temperatures.

wide range of conductivity values. Within the range covered by the curve, this ratio varies from about 5.3 to 5.8×10^{-9} . It will require careful experimental work to determine more accurately the relationship between electrical and thermal conductivity in other than the annealed condition. The determination of thermal conductivity involves heating the specimen, which brings about some structural change in most aluminum alloys. Therefore it may be difficult to determine the relationship much more precisely for heat-treated or as-cast specimens.

It has been recognized that, in many ways, aluminum does not behave like a typical metal. Hume-Rothery¹¹ has pointed out some of the anomalous characteristics of aluminum in a consideration of the electron structure of metals. The typical metallic structure characteristic of such metals as copper and gold appears to be an assemblage of positive ions held together by the attraction of generally shared valency electrons. Some of the valency electrons in aluminum appear to have fixed positions; the crystal is apparently not completely ionized and has some of the characteristics of a nonmetal. Silicon is much more nonmetallic in many of its characteristics than aluminum, which may to some extent account for the rather anomalous relationship between thermal and electrical conductivities of aluminum alloys containing relatively high concentrations of silicon. The displacement of the line determined by the silicon alloys to relatively high values for k suggests relatively fewer free electrons in these alloys than in alloys of the other elements.

The conductivity of alloys containing relatively high concentrations of silicon is markedly affected by the particle size and distribution of the silicon. Table 2 shows that the electrical conductivity of aluminum-silicon alloys falls rapidly with increasing silicon concentrations. Surprisingly, though, a 13 per cent silicon alloy modified with sodium has a higher conductivity than a sodium-free 5 per cent silicon alloy. Also, the difference in conductivity of wrought 32-S and cast 132 alloys is greater than would be expected from the difference in composition alone.

TABLE 3.—*For Approximate Conversion of Thermal and Electrical Conductivities of Aluminum-base Alloys at 25° C. from*
 $K = 5.02\lambda T \times 10^{-9} + 0.03$

Electrical Conductivity, Ohm ⁻¹ , Cm ⁻¹ at 25° C. × 10 ⁻⁴	0	0.35	0.69	1.03	1.38	1.72	2.07	2.41	2.76	3.10	Electrical Conductivity, Per Cent I A C.S.
	0	0.02	0.04	0.06	0.08	0.10	0.12	0.14	0.16	0.18	
	Thermal Conductivity, Cal per Sq. Cm. per Sec. per Deg. C. per Cm. at 25° C.										
0	0.03	0.03	0.04	0.04	0.04	0.05	0.05	0.05	0.05	0.06	0
0.2	0.06	0.06	0.07	0.07	0.07	0.08	0.08	0.08	0.08	0.09	3.5
0.4	0.09	0.09	0.10	0.10	0.10	0.11	0.11	0.11	0.11	0.12	6.9
0.6	0.12	0.12	0.13	0.13	0.13	0.14	0.14	0.14	0.14	0.15	10.3
0.8	0.15	0.15	0.16	0.16	0.16	0.17	0.17	0.17	0.17	0.18	13.8
1.0	0.18	0.18	0.19	0.19	0.19	0.20	0.20	0.20	0.20	0.21	17.2
1.2	0.21	0.21	0.22	0.22	0.22	0.23	0.23	0.23	0.23	0.24	20.7
1.4	0.24	0.24	0.25	0.25	0.25	0.26	0.26	0.26	0.26	0.27	24.1
1.6	0.27	0.27	0.28	0.28	0.28	0.29	0.29	0.29	0.29	0.30	27.6
1.8	0.30	0.30	0.31	0.31	0.31	0.32	0.32	0.32	0.32	0.33	31.0
2.0	0.33	0.33	0.34	0.34	0.34	0.35	0.35	0.35	0.35	0.36	34.5
2.2	0.36	0.36	0.37	0.37	0.37	0.38	0.38	0.38	0.38	0.39	37.9
2.4	0.39	0.39	0.40	0.40	0.40	0.41	0.41	0.41	0.41	0.42	41.4
2.6	0.42	0.42	0.43	0.43	0.43	0.44	0.44	0.44	0.44	0.45	44.8
2.8	0.45	0.45	0.46	0.46	0.46	0.47	0.47	0.47	0.47	0.48	48.3
3.0	0.48	0.48	0.49	0.49	0.49	0.50	0.50	0.50	0.50	0.51	51.5
3.2	0.51	0.51	0.52	0.52	0.52	0.53	0.53	0.53	0.53	0.54	55.2
3.4	0.54	0.54	0.55	0.55	0.55	0.56	0.56	0.56	0.56	0.57	58.5
3.6	0.57	0.57	0.58	0.58	0.58	0.59	0.59	0.59	0.59	0.60	62.1
3.8	0.60	0.60	0.61	0.61	0.61	0.62	0.62	0.62	0.62	0.63	65.5
4.0	0.63	0.63	0.63	0.64	0.64	0.64	0.65	0.65	0.65	0.66	69.0

SUMMARY

The thermal and electrical conductivities of a number of commercial aluminum alloys have been determined. The relationship between thermal and electrical conductivity appears to be best defined by the equation $K = 5.02\lambda T \times 10^{-9} + 0.03$ where K is the thermal conductivity, λ the electrical conductivity, and T the absolute temperature. The heating involved in the determination of thermal conductivity brings about changes in structure, except in specimens properly annealed, which

have a profound effect on conductivity. The conductivity of aluminum alloys containing relatively high concentrations of silicon is affected in a marked manner by the particle size and distribution of the silicon, conductivity decreasing with increase in particle size. The $\frac{K}{\lambda T}$ ratio for silicon alloys generally has a larger value than that for the other aluminum alloys.

TABLE 4.—*Chemical Composition of Commercial Alloys*

Alloy Designation	Nominal Composition by Weight, Per Cent							
	Cu	Fe	Si	Cr	Mg	Mn	Ni	Zn
12	8.0							
43			5.0					
45			10.0					
47			12.5					
108	4.0		3.0					
A108	4.5		5.5					
109	12.0							
112	7.5	1.2						1.5
B113	7.0	1.2	1.5					
C113	7.0	1.2	4.0					
122	10.0	1.2			0.2			
A132	0.8	0.8	12.0		1.0		2.5	
142	4.0				1.5			2.0
144	10.0	0.7	4.0		0.25			
195	4.0							
B195	4.5		2.8					
214					3.75			
216					6.0			
220					10.0			
355	1.25		5.0		0.5			
A355	1.4		5.0		0.5	0.75	0.75	
356			7.0		0.3			
645	2.5	1.5						11.0
14S	4.4		0.8			0.75		
18S	4.0				0.5		2.0	
25S	4.5		0.8			0.8		
32S	0.8		12.0		1.0		0.8	
A51S			1.0	0.25	0.6			
52S				0.25	2.5			
53S			0.7	0.25	1.25			
70S	1.0				0.4	0.7		10.0

ACKNOWLEDGMENT

The authors wish to express their indebtedness to the American Brass Co., in whose research laboratory the new thermal conductivity measurements reported herein were made. Some of the determinations

on the cast bars were made by Mr. W. E. Lindlie, but the greater number of the thermal conductivity measurements and the electrical determinations at 200° C. were made by Mr. E. W. Palmer, whose assistance it is a pleasure to acknowledge.

REFERENCES

1. Wiedemann and Franz: *Ann. Physik u. Chem (Pogg. Ann)* (1853) **89**, 497.
2. Lorenz: *Ann. d. Phys.* (1881) **249**, 582.
3. Masumoto: *Sci. Repts. Tohoku Imp. Univ.* (1925) **13**, 229.
4. Griffith and Schofield: *Jnl. Inst. of Metals* (1928) **39**, 337.
5. Mannchen: *Ztsch. f. Metallkunde* (1931) **23**, 193.
6. Euringer and Hanemann: *Metallwirtschaft* (1935) **14**, 389.
7. Euken and Warrentrup: *Ztsch. Elektrochem.* (1935) **41**, 331.
8. Smith: *Trans. A.I.M.E.* (1930) **89**, 84.
9. Smith: *Trans. A.I.M.E.* (1931) **93**, 93.
10. Smith and Palmer: *Trans. A.I.M.E.* (1935) **117**, 225.
11. Hume-Rothery: *Inst. of Metals Monograph and Report Series*, No 1 (1936)
12. Lees: *Phil. Trans. Roy. Soc.* (1908) **A208**, 381.

DISCUSSION

(W. L. Fink presiding)

G. SACHS,* Newark, N. J.—The importance of such investigation as described in this paper is much greater than is usually realized. In metallurgical technique there are many problems of thermal conductivity; for instance, the uniformity of heat (or heat distribution) in furnaces and their contents, the extrusion of metals, materials for use in electrical contacts, etc., all offer problems of thermal conductivity.

As stated in this paper, there is considerable difficulty in obtaining reliable data on thermal conductivity, whereas it is very easy to obtain reliable data on electrical conductivity. Therefore it has been my practice for several years to think and calculate thermal problems on the basis of electric conductivity. It is easier for me to visualize problems like the temperature distribution in heated bars by figuring with electrical conductivity. Many people formerly objected to this method because they did not believe in a simple relation between electric and thermal conductivity. Only in the last few years, and chiefly as a result of papers like this, has it been really proved that the principles of electrical conductivity can be used instead of thermal conductivity to explain the different behavior of various materials in thermal problems. The chief point is that both change in similar manner with alloying, with the structure, with the heat-treatment, and so forth.

C. S. SMITH.—I should like to amplify somewhat the remarks of Dr. Sachs regarding the proportional relationship existing between electrical and thermal conductivity. It has, of course, long been supposed that the two conductivities are directly proportional to each other. This idea is usually attributed to Wiedeman and Franz (1853) but actually it was clearly expressed by Achard 74 years earlier.¹³ The ratio of thermal to electrical conductivity is approximately the same for most pure metals, but many alloys of low conductivity have a higher thermal conductivity than this law requires.

The significance of the present paper is that electrical and thermal conductivities should *not* be considered as directly proportional, but rather that the proportional

* Baker & Co., Inc.

¹³ F. C. Achard: Sur l'analogie qui se trouve entre . . . l'électricité et . . . la chaleur . . . *Mem. Acad. Berlin*, 1779, 27.

relationship applies to only part of the thermal conductivity, and that this part is superimposed on a small constant thermal conductivity. Representing the relationship graphically, this results in a straight line intersecting the thermal conductivity axis at a small value instead of passing through the origin as the Wiedeman-Franz law requires. When this intercept is taken into consideration, the thermal conductivity of many alloys can be calculated more accurately than it can be measured with any but the most refined technique.

P. R. G. KOSTING,* Watertown, Mass.—Have observations been made on the relationship between thermal and electrical conductivities at higher temperatures with aluminum alloys, and does the spread between the two become less? With steel, the lower the temperature at which the measurements are made, the greater the spread, but as the temperature becomes higher, especially approaching 700° C., the relationship between electrical and thermal conductivities becomes very close, and one can use electrical conductivity to calculate thermal conductivity and have greater faith in calculating the value than if he made the same calculations for thermal conductivity at lower temperatures, say around 200°.

A. J. DORNBLATT,† Annapolis, Md.—Having the line drawn so as to pass through the origin (corresponding to zero conductivity) seems to be inconsistent with the fact that even nonconductors such as ceramic materials and other materials nevertheless possess appreciable thermal conductivity. Possibly at the higher resistivities (the lower end of the curve as drawn) there is a condition where the metal may exhibit behavior in some respects analogous to that of nonmetallic material.

L. W. KEMPF.—With regard to Dr. Sach's comments, it really is much easier to use electrical conductivity than thermal conductivity, principally because it is so easy to determine precisely the electrical conductivity of a metal. For most structural applications, it is certainly entirely adequate to use the relationship between the electrical and thermal conductivity for deducing the thermal conductivity.

With regard to the deviation of the values on aluminum alloys from their curve at various temperatures, I suspect that the same thing is true of the aluminum alloys that is true of steel, particularly if the measurements are considered in relation to the melting points of the materials rather than to any specific temperature range. In the low range, that is below room temperature, there have been a few determinations of the thermal and electrical conductivity of aluminum alloys and these, generally speaking, do not fall near enough to the curve to indicate that this relationship expresses the conditions below room temperature. It is true there are relatively few data at temperatures lower than ordinary. In the range we covered, from about room temperature to 300° C., we were not able with the relatively meager data available to note any difference in the deviation with temperature.

* Chemical Engineer, Watertown Arsenal.

† U. S. Naval Academy.

Primary Crystallization of Metals

By F. R. HENSEL*

(New York Meeting, February, 1937)

THE present study was made to determine the laws governing the formation of the primary† crystal structure during solidification. Most of the experiments were carried out on chill castings, but from the results it will be possible to draw certain conclusions as far as sand castings are concerned.

It is necessary to discuss first a number of theories, which are generally adopted for explaining the structure of an ingot. Usually, the structure

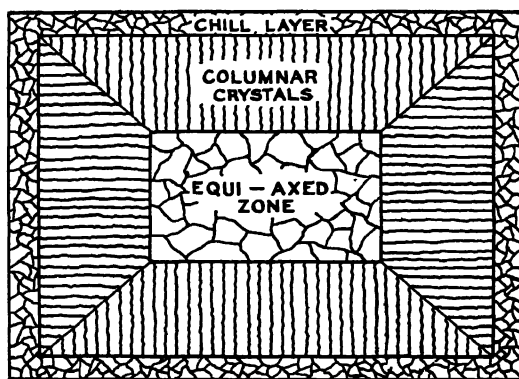


FIG. 1.—VARIOUS ZONES IN A CHILL INGOT.

of an ingot consists of the following three zones (Fig. 1): (1) a chill layer of small at-random oriented crystals; (2) a layer of columnar crystals; (3) a zone of equiaxed crystals.

The tensile properties of the chill layer and the equiaxed range are usually much better than in the columnar range, particularly the planes that are formed by the columnar crystals growing from two sides at right angles have low tensile properties. This is one of the reasons why columnar crystals in ingot structures are undesirable.

Paper presented before the Detroit Foundrymen's Association, Oct. 17, 1935. Manuscript received at the office of the A.I.M.E. Nov. 30, 1936.

* With P. R. Mallory & Co., Indianapolis, Ind.

† So called because there is a secondary crystallization in the solid state in many alloy systems.

In analogy with experiments with organic substances, which also show chill, columnar and equiaxed zones, many investigators have assumed that the degree of undercooling is responsible for the change from an oriented to an at-random structure. Desch assumes that there is a region of metastability within which spontaneous crystallization cannot occur. This region of metastability is supposed to be separated quite distinctly from the labile region. According to this theory, the equiaxed range corresponds to the labile region, while the columnar crystals are formed in the metastable region. A binary diagram showing the stable, metastable and labile regions could be drawn as shown in Fig. 2.

A number of investigators do not believe in this metastable region, but assume that the formation of nuclei is a steady function of the degree of

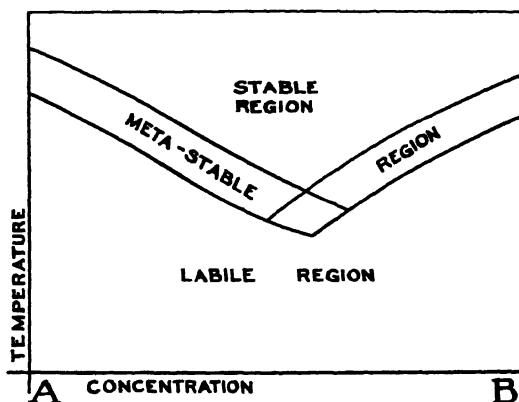


FIG. 2.—UNDERCOOLING DIAGRAM.

undercooling. Tammann has introduced two factors that are used today for the explanation of almost any primary structure: (1) the number of nuclei per unit of weight and time at a definite temperature (K.Z.), (2) the velocity of crystallization (K.G.).

Most of the data available on the "number of nuclei" are based on observations made on organic substances, or inorganic substances of high viscosity, and not on metals. It is of interest, however, to review these data briefly, because there is a definite relation between melts and solutions.

Tammann's theory can be represented in the diagram of Fig. 3. According to this diagram, the number of nuclei increases with undercooling, reaches a maximum and drops to zero at a very high degree of undercooling. At low temperatures, the nuclei very often remain latent. The velocity of crystallization increases rapidly with the undercooling at first and then remains almost constant. According to the kinetic theory, it is necessary for the formation of crystals that the crystallizing molecules assume a definite orientation, the lack of which is characteristic for the

liquid phase. This cannot be accomplished momentarily. Sufficient time is required for a number of molecules to become arranged in the proper directions. The kinetic theory does not seem to apply to metals so much, because metals are built up by atoms, and not molecules. Therefore, theoretically, monatomic substances should not show undercooling, since no time is required for molecular arrangement.

It has been shown that melts that have not been superheated contain anisotropic molecules (showing directional properties like crystals), which may be reduced to a minimum by either prolonging the time or the temperature of superheating. A practical example for this is the refinement in structure by superheating cast iron.

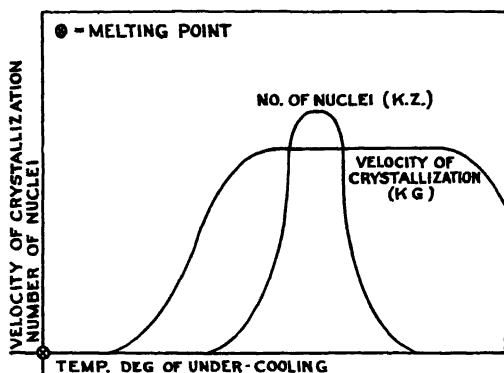


FIG. 3.—EFFECT OF UNDERCOOLING ON NUMBER OF NUCLEI AND VELOCITY OF CRYSTALLIZATION.

It was found that the number of nuclei in nonmetallic substances depends mainly on the following factors: (1) degree of undercooling; (2) degree of superheating the melt, (3) foreign particles, (4) mechanical influences, such as the effects of pressure or shear stresses, (5) the effect of the surface condition of the container holding the melt.

The shape of the crystals is determined by the number, the direction and the magnitude of the vectors of the velocity of crystallization. It is generally assumed that the shape of a crystal depends upon the surface tension, and a simple formula expresses this as follows:

Energy required for crystallization = cross section of crystal \times surface tension (constant) \times velocity of crystallization.

From this formula, it follows that the cross section of the crystals becomes smaller as the velocity of crystallization increases. In other words, the crystals become thin or stringer-like. The crystal uses the shape that provides the least resistance in growing (Fig. 4).

The direction of crystal growth is opposite to the direction of heat flow. The crystals in iron grow in the melt in the form of an octohedron.

The columnar crystals are oriented with respect to one axis. They are not oriented however, with respect to the other two axes. In other words, they can rotate around the elongated axis. A section parallel to the elongated axis, therefore, will expose the three densely packed faces

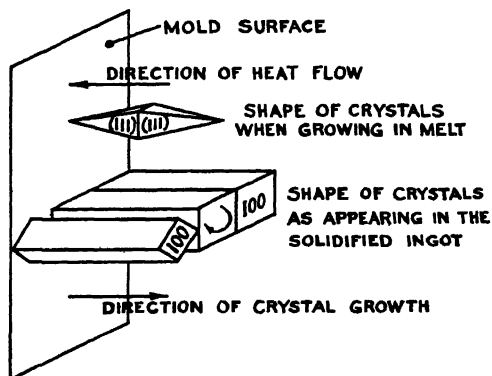


FIG. 4.—GROWTH OF COLUMNAR CRYSTALS.

of the cubic system; that is, the octohedral, the cubic and the dodecahedral face (Fig 5). A section at right angles to the elongated axis will always show a cubic face (Fig. 6). The three different faces of the cubic system are identified by the etching pits.

The degree of undercooling affects the different vectors of the velocity of crystallization. According to Tammann, crystals will grow at a small amount of undercooling as polyhedrons, having many sides and faces,

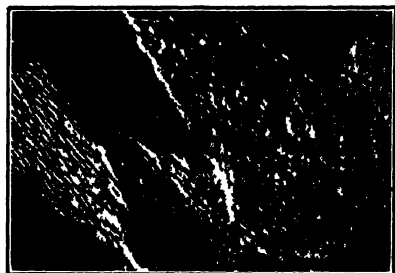


FIG. 5.—COLUMNAR CRYSTALS OF 3.29 PER CENT SILICON STEEL COVERED WITH ETCHING PITS. $\times 30$. A, (001) FACE; B, (111) FACE; C, (101) FACE.

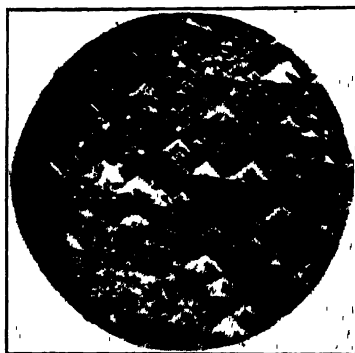


FIG. 6.—ETCHING PITS ON (001) FACE OF 3.27 PER CENT SILICON STEEL.

while at a high degree of undercooling, they will grow as crystal stringers. Differently expressed, we might say that a fast growth of a crystal would lead to stringers, while a slower growth would lead to polyhedrons. In other words, the columnar zone in an ingot would be favored by a fast

crystallization, while slower crystallization would produce polyhedrons, or equiaxed crystals. We shall see that this is quite in agreement with the results determined by experimentation.

The amount of undercooling for metallic crystals is supposed to be approximately 0.1 to 3° C. It should be mentioned here that in the casting process the amount of undercooling of metal will be considerably smaller than this figure. In fact, it will be practically negligible. It should be further pointed out that the velocity of crystallization of different substances depends on how fast the latent heat can be dissipated. The velocity of crystallization can therefore be roughly expressed by a formula of the following type:

Linear velocity of crystallization =

$$\frac{\text{Heat conductivity in kilocalories per unit of area and time}}{\text{Constant} \times \text{the heat of crystallization}}$$

The constant includes such factors as difference of equilibrium temperature between crystal and melt, and temperature of the melt (undercooled), and the thickness of the layer that is attached to the growing face of the crystal. This formula indicates that the velocity of crystallization depends upon the rate at which the heat is dissipated. This is particularly important in metals that have higher heat conductivity than organic substances.

Apart from these theoretical considerations, many factors are mentioned in the metallurgical literature as having influenced the primary structure. Some of these factors are cited below:

1. Alloy composition. Melting characteristics as determined by the constitutional diagram (solidus and liquidus ranges).

2. Factors responsible for the *equiaxed range*: (a) turbulence during pouring, (b) metal cold shots caused in pouring, (c) mechanical influences, (d) decrease of rate of cooling by separation of ingot from ingot molds, (e) degrees of deoxidation in steel, and general shape of solidification diagram.

3. Factors influencing the *columnar range*: (a) casting temperature; (b) rate of cooling influenced by mold temperature, mold dimensions, heat capacity, mold material, and separation of ingot from mold; (c) speed of pouring; (d) temperature differences in melt.

4. Factors influencing the *chill layer*: rapid solidification. The chill layer *disappears* with: (a) very hot material, (b) very thin molds.

5. The reason for formation of the cone-shaped zone on the bottom of the steel ingot: (a) precipitation of crystals of higher specific gravity, (b) type of deoxidation.

It might be well to consider the term "undercooling" somewhat more carefully. Undercooling occurs when at a definite temperature equilibrium conditions are not reached; that is, the solid phase does not occur.

According to the phase law, it is then possible that the temperature will decrease still further. It cannot be assumed that after we have a solid phase present the melt can be further undercooled, because of the good heat conductivity of metals. This is quite different with organic substances. This type of undercooling was found with such metals as gold, copper, bismuth, antimony, lead, tin and a number of alloys. It was found, for instance, that iron-nickel alloys with 1.86 per cent cobalt could be undercooled as much as 100°C .

Undercooling in metals or alloys that exhibit a phase change is also possible in the solid state, and by adding certain alloying elements to steel, for instance, it is possible to suppress the Ar points from 700°C . to below room temperature.

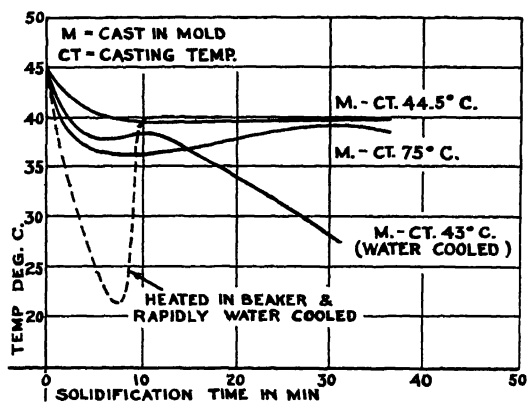


FIG. 7.—UNDERCOOLING EXPERIMENTS WITH SALOL.

Undercooling also exists in the vicinity of a crystal growing in a solution. In analogy with solutions, we might express this for melts as follows: A melt just above the melting point is not saturated. It reaches the saturation point at the melting point. As soon as the temperature drops below this point, saturation occurs, and a part of the solid phase is precipitated. This amount of undercooling is very small for metals and alloys. Only the first explanation of undercooling could be used for explaining the change in orientation in the crystal structure of an ingot.

It should be stated here that very few of the theoretical investigations were carried out under casting conditions. The term "casting condition," means that the material is cast from a container into a mold having usually a somewhat rough surface. It was therefore of interest to make undercooling experiments with an organic compound such as Salol under casting conditions (Fig. 7). The following results were found:

1. Heating in a smooth glass beaker and cooling quickly in water gave an undercooling of 18° to 20°C . Slow cooling decreased this amount of undercooling.

2. Heating in rough containers and cooling in either air or water decreased the undercooling considerably.

3. Casting of Salol in a steel mold prevented the undercooling almost completely. The degree of overheating had only a slight effect on the undercooling. The reason for this is that when the Salol comes in contact with the rough mold, which has a high heat conductivity, nuclei are formed immediately. Very likely nuclei are formed on the outside of the pouring stream during casting. After the first nuclei have appeared, a decrease in temperature below the melting point is impossible. The temperature of the equiaxed zone, therefore, cannot fall into the labile range and solidify spontaneously by the formation of crystal showers, as is often assumed.

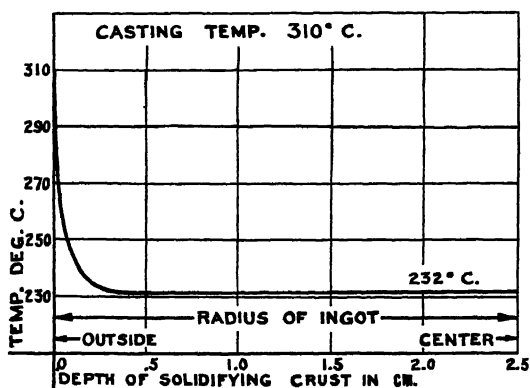


FIG. 8.—TEMPERATURE OF LIQUID DURING SOLIDIFICATION OF TIN INGOT CAST IN STEEL MOLD.

It was of interest to study the actual temperature of the liquid in the mold, since it is frequently assumed that at a higher casting temperature the liquid metal inside of the solidified crust is hotter than when cast at lower temperature. It is further assumed that the temperature of the liquid is considerably above the melting point as long as the formation of columnar crystals occurs, while the equiaxed range is formed after the entire liquid has reached the melting point. The diagram in Fig. 8 shows the results of such a study with tin.

The temperature was measured by means of a thermocouple, which was placed in the center of the mold. It is evident that the superheat is lost immediately with the metal overheated 80° C. Only 5° to 10° C. overheat were measurable after the mold was filled. These few degrees of overheating disappeared rapidly after a small crust formed on the walls of the mold. During the entire time of solidification afterwards, the temperature of the liquid remained constant at 232° C.

Similar experiments were made by casting a superheated melt in a hot sand mold. Crystallization started in this case only after the entire

mass had cooled down to the melting point. In the sand casting, therefore, the time-temperature cooling curves which are known from thermo-analysis hold true. The measurements were checked with melts of over 30 lb., which took about 10 min. to solidify. The results of these tests can be summarized as follows: (1) There is no undercooling that could be measured within one-tenth of a degree; (2) the temperature of the melt drops almost immediately to the temperature of solidification.

Another set of experiments was conducted to find out whether there is a temperature difference between two points in the melt. It was found that the convection currents do not allow any temperature difference to exist between two points of the melt, except at the moment when the hot metal comes in contact with the cold walls of the mold. At this instant the sudden dissipation of heat is greater than the convection currents.

A large number of tests were made in which the pouring time, pouring temperature, mold temperature and mold size were systematically changed and the various zones carefully studied. All these tests indicate that the variation in the primary structure can be fully accounted for by a "thermal" explanation.

Random crystallization of a metal having a cubic or tetragonal structure is caused either by a very quick heat dissipation, or an extremely slow heat dissipation. The fast heat dissipation is therefore responsible for the formation of the chill layer and the slow heat dissipation for the formation of the equiaxed zone.

We may assume that the formation of columnar crystals continues only as long as only one layer of definite thickness solidifies in the unit of time. If the solidification is so fast that in the unit of time not only one but many layers solidify at the same time, the nuclei do not have time to grow and to assume a definite orientation, but must stay in the positions in which they were formed by chance. This phenomenon was particularly noticeable with materials that in casting conditions tend to form a fine grain. In Fig. 9 the change from the chill zone to the columnar zone is illustrated. In this case the change seems rather abrupt but it can be assumed that the columnar crystals grow from the last layer of chill crystals.

The equiaxed zone is formed when the steady heat dissipation in the mold or in the solidified crust of the cast material is disturbed; that is, the ratio of dissipated heat to the heat which is given up during solidifica-



FIG. 9.—TRANSITION FROM CHILL ZONE TO COLUMNAR ZONE OF 4.79 PER CENT SILICON STEEL.

tion* is such that the velocity of heat flow is not in the proper ratio to the velocity of crystallization. The formation of nuclei may then be as large as the tendency of the crystal to grow in the columnar shape. In the equiaxed zone, the heat is dissipated not only perpendicular to the mold surface but also towards the top and bottom of the mold. If the heat dissipation is unequal, a slight crystal orientation will occur in the direction of greatest heat flow.

The effect of the heat capacity of the mold has been studied by many investigators. It has been assumed that the columnar crystals stop growing as soon as the heat capacity of the mold is reached; which means, the

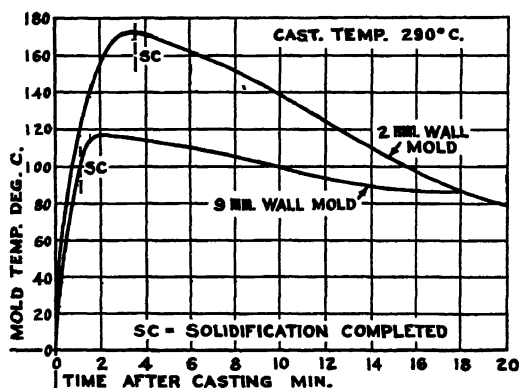


FIG. 10.—HEATING OF MOLD WALLS IN CASTING TIN.

time when the heat is not dissipated by conduction, but by radiation and convection. Small-scale experiments were made, and it was found that the mold temperature had not reached its maximum when the entire ingot was solidified. The ingots showed columnar and equiaxed crystals. This indicates that the columnar crystals stopped growing long before the heat capacity of the mold was reached. Typical temperature-time curves of molds are shown in Fig. 10.

In all cases there is first a rapid increase in mold temperature, then a slow decrease in mold temperature. Similar curves are found in tests on mold temperatures in steel molds. The peak in the curves corresponds to the time when the mold has reached its heat capacity.

The fact that the depth of the columnar range is not alone a function of the mass of the mold, was confirmed by Leitner. He found that an increase of the dimensions of the mold above a certain limit does not influence the primary structure further. The reason for this is that after a certain time the ingot separates from the mold and there is an air space between mold and ingot. In other words, the solidified crust of the ingot

* After the sudden dissipation of the superheat it is necessary only to dissipate the heat of solidification in order to cause crystallization.

acts as a container of the remaining liquid portion and it is quite possible to assume that in such a case solidification may be hastened by removing the billet from the ingot mold.

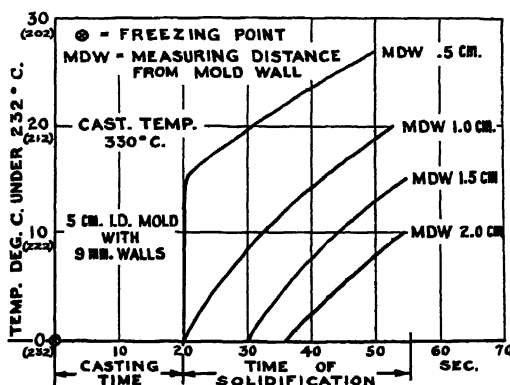


FIG. 11.—TEMPERATURE GRADIENT IN SOLIDIFYING CRUST OF TIN INGOT.

It has been further pointed out that the time after the ingot separates from the mold is responsible for the depth of the columnar crystals. Complete transcrystallization, which occurs rather frequently, cannot be brought into agreement with this explanation, because the separation of ingot and mold occurs after a small crust of the cast material has solidified. This phenomenon, however, is of considerable importance in very large ingots.

A number of tests were made to determine the temperature gradient in the solidified crust of the cast material, because it is important for the steady heat flow and therewith for the crystal formation. A typical set of curves is given in Fig. 11. No irregularities were found. The curves taken at various points of the solidified portion of the ingot are parallel.

It is difficult to calculate the heat dissipation from liquid metal through a mold to the air, because there are not constant conditions during solidification of an ingot. The same is true in calculating the radiation and convection.

The temperature conditions change continuously. In most cases the depths of the columnar crystals increased with increasing casting temperature, and the equiaxed range decreased as shown in Fig. 12.

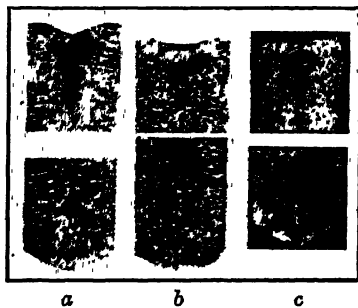


FIG. 12.—CASTING EXPERIMENTS WITH 4.8 PER CENT SILICON STEEL.

A, casting temperature 1580° C. (equiaxed zone of 68 per cent of diameter).

B, casting temperature 1530° C. (equiaxed zone 72 per cent of diameter).

C, casting temperature 1480° C. (equiaxed zone 100 per cent of diameter).

In a high-purity tin (Fig. 13) an equiaxed zone was shown only at a casting temperature of 232°C . It should be noted, however, that the equiaxed zone reappears again when casting at 310°C . The grain size in this high-purity tin is large and does not seem to be much affected by the pouring temperature.

The casting temperature affects greatly the time of solidification and therewith the velocity of crystallization. Casting tin at 232°C . in a mold required 2 min. 20 sec. to solidify (20 sec. casting time). Casting tin at 340°C . in the same type of mold increased this time to 3 min. 50 sec. Increasing the casting time of a tin ingot containing small amounts of copper from 5 to 50 sec. moved the columnar crystals slightly towards the

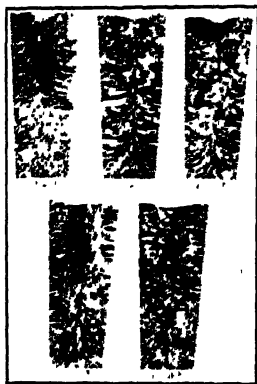


FIG. 13.—CASTING EXPERIMENTS WITH INCREASING CASTING TEMPERATURE, HIGH-PURITY TIN.

Equiaxed zone at 232°C . casting temperature and at 310°C . casting large grains.



FIG. 14.—TIN CAST INTO CHILL MOLD AT 450°C . HEAVY BOTTOM PLATE USED.

Crystals grow perpendicular to bottom plate.

center of the ingot. Tin with small percentages of copper gives a very much smaller grain than a high-purity tin under the same casting conditions. Particularly at low casting temperatures, the impure tin had an extremely fine grain and formed very large equiaxed zones, while a high-purity tin casting under the same conditions would show columnar crystals almost towards the center of the ingot.

In most of the experiments, complete transcrystallization occurred after reaching a certain degree of superheat in the melt. With a still higher superheat, the structure showed irregularities such as formation of localized equiaxed zones, which can be explained by our theory of the effect of disturbances in the heat flow on the primary crystallization.

The chill layer increased at low casting temperatures with the thickness of the molds. At very high casting temperatures, the chill layer disappeared. By casting in a mold that was tilted approximately 30° , a chill layer was formed where the stream hit the mold, and the columnar range was shifted towards the center. The bottom cone showed definite

disturbances in the heat flow with higher temperatures, and a random structure was formed. By pouring tin into a chill mold at 450°C . and by using a heavy bottom plate with the formation of intermediate equiaxed zones as is shown in Fig. 14.

The effect of casting temperature on grain size is well illustrated in Fig. 15 which shows a zinc ingot cast at 435°C . and one cast at 535°C . In the latter, the left half of the mold was preheated to 300°C ., and it can be noticed that the columnar crystals grew faster from the cold half of the mold, which shifted the center of crystallization towards the left half of the mold.

In order to simulate sand-casting conditions, tests were made with preheated molds. It was found that the depths of the columnar crystals is decreased with the preheating of the molds. This type of structure

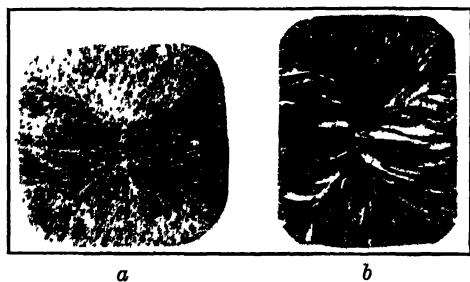


FIG. 15.—ZINC CAST INTO CHILL MOLD.
a, cast at 435°C .; b, at 535°C . (left half of mold preheated to 300°C .)



FIG. 16.—TIN CAST AT 235°C . INTO CHILL MOLD, PREHEATED TO 235°C . AND QUENCHED IN WATER

becomes similar to the equiaxed condition of sand castings and is caused by a slow dissipation of heat.

It was found in the experiments that the preheating of the molds had to be extremely high in order to be effective. In casting tin, for instance, the molds were preheated 150°C . It was also found that the depths of the columnar crystals was increased in preheated molds when an extremely low casting temperature was used. In other words, the velocity of crystallization could be regulated by controlling the heat dissipation.

A typical structure showing columnar and equiaxed zone was formed by quenching a mold preheated to the melting point of tin in water (Fig. 16).

Experiments were also made with sand castings. By casting tin in cold sand molds at 280°C ., the structure was completely at random and coarse-grained. Experiments were made with tin bronzes, and in this material columnar crystals did not occur in sand castings, not even in the chill castings. This points to the fact that the number of nuclei and velocity of crystallization are constants, which vary for each type of material. Typical differences, as in pure tin, were experienced with a 10 per cent aluminum bronze. With a 30-70 brass, the largest columnar

crystals were formed with very slow solidification in hot sand. With a shorter time of crystallization, a definite minimum in the size of the columnar crystals prevailed. Curves showing the influence of the time of solidification upon the grain size of a 5 per cent tin bronze and upon the depths of columnar crystals of 30-70 brass are given in Fig. 17.

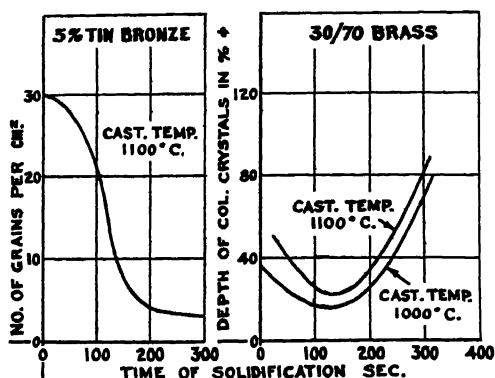


FIG. 17.—INFLUENCE OF TIME OF SOLIDIFICATION UPON (a) GRAIN SIZE OF 5 PER CENT TIN BRONZE, (b) DEPTH OF COLUMNAR CRYSTALS OF 30-70 BRASS.

German silver also shows a typical difference in the grain size between chill and sand castings. That is, the grain increases with increasing time of solidification.

A few tests were made with zinc, which has a hexagonal crystal structure. In this metal, the main axis has such definite thermal characteristics, particularly a higher heat conductivity, and the tendency of the crystals to grow in one preferred direction is so pronounced, that it is

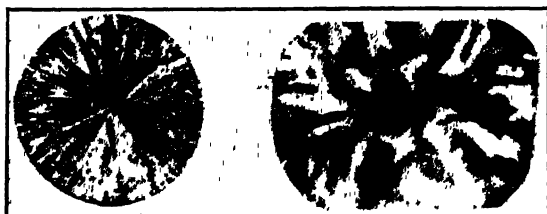


FIG. 18.—(a) ZINC CAST INTO REFRACTORY MOLD AT 435° C. AND (b) ZINC CAST INTO SAND MOLD PREHEATED TO 450° C. CASTING TEMPERATURE 510° C.

almost independent of the thermal conditions (Fig. 18). In all the experiments, there was complete transcrystallization.

CONCLUSIONS

It is hoped that these few fundamental considerations on the primary crystallization of metals will be helpful in explaining and overcoming certain difficulties that are encountered frequently in casting practice.

Segregation in Single Crystals of Solid Solution Alloys

BY ARTHUR PHILLIPS* AND R. M. BRICK,† MEMBERS A.I.M.E.

(New York Meeting, February, 1937)

THE normal method of preparing metallic alloys for commercial use involves the preparation of a melt containing the given components in the chosen proportions and allowing the homogeneous liquid mass to solidify in a mold of the desired form. The solidification is frequently accompanied by a segregation of the alloying elements in different parts of the casting. When the segregation is occasioned primarily by marked differences in density of the solid and liquid phases, it is termed "gravity" segregation. When the segregation conforms to a selective freezing in harmony with the teachings of the equilibrium diagram of the alloy system—i.e., the lower melting phases are concentrated in the regions of the casting last to freeze—it is often referred to as "normal" segregation. However, in many cases the lower-melting part of the system is concentrated in the parts of the casting first to freeze and the result in this case is termed "inverse" segregation. To complete the terminology of the subject, normal segregation in a single phase is usually called "coring" and the word will be used in that sense in this paper. Inverse segregation, particularly when the liquid phase is exuded or sweated out on the surface of the casting, is sometimes called "liquation." Unfortunately, some ambiguity has arisen from the use of this term and it is perhaps advisable to confine its use to the dictionary definition; namely, "The separation of two phases by heat sufficient to melt one but not the other."

The gravity and normal types of segregation are both well understood and to some extent are controllable by taking advantage of the most favorable cooling rate for a given casting condition. Inverse segregation has received considerable attention from several investigators but none of the theories offered seem to account in a convincing way for the many examples of this type. The observations made in the present work on segregation in single crystals, and in some other castings, tend to support one theory of the mechanism of inverse segregation and definitely to

Manuscript received at the office of the Institute Nov. 30, 1936. *

* Professor of Metallurgy, Hammond Laboratory, Yale University, New Haven, Conn.

† Research Assistant in Metallurgy, Hammond Laboratory, Yale University.

preclude the application of others. A different form of gravity segregation has been observed and some data on diffusion within a liquid solution have been obtained.

FACTS AND THEORIES ON INVERSE SEGREGATION

When a molten solution is cast in a mold, several unrelated factors become significant in influencing the progress of solidification and the resultant segregation. First, the freezing characteristics, as described by the slope and spacing of the liquidus and solidus lines of the equilibrium

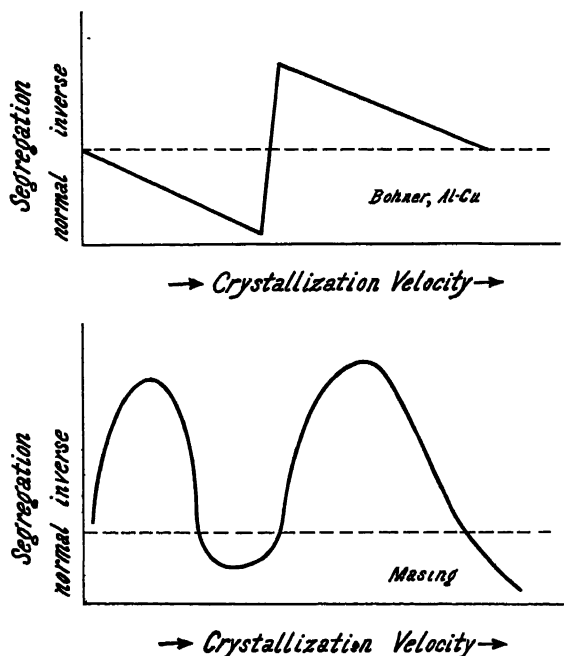


FIG. 1.—INVERSE SEGREGATION IN ALUMINUM-COPPER ALLOYS.

diagram, will influence the segregation, according to Bauer and Arndt¹ and Iokibe². A wide freezing range seems to encourage inverse segregation although it is sometimes found in alloys with a narrow solidification range³; e.g., gold-silver and gold-copper.

Masing⁴, Bohner⁵ (in aluminum-copper alloys), and also Reader⁶ have found that the inverse segregation in most alloys is a function of the cooling rate (Fig. 1). According to Masing, no segregation occurs on extremely slow cooling; segregation increases to a peak at somewhat faster rates, decreases to zero at intermediate speeds, increases again on more rapid cooling and finally disappears for extremely fast chill castings. In view of the cooling-rate factor, the casting temperature of the metal,

the mold temperature, volume and shape are obviously of considerable importance. Other variables will be considered in the discussion of the experimental results obtained in this paper.

It is not proposed to make an exhaustive and critical review of the literature on the subject, since this has been adequately done in several recent articles, notably those by Masing^{7,8} and Genders⁹. The several proposed theories of inverse segregation will be reviewed briefly with a view to establishing a basis for further discussion.

Ludwig-Soret Effect.—The existence of a temperature gradient in a liquid solution of two components should result, according to Benedicks¹⁰ and Smith¹¹, in a composition gradient with the solute atoms concentrated in the cooler portion of the system. The Ludwig-Soret effect, theoretically admissible and experimentally found in aqueous solutions, requires considerable time for atomic movements as well as an absence of agitation. Even under these favorable conditions, Hanson¹² failed to find the effect in low-melting alloys, and there seems to be no reason for believing that this factor operates in any of the common examples of inverse segregation.

Undercooling.—Masing¹³ first proposed that severe undercooling of a liquid solution to a temperature well below the normal solidus would result in inverse segregation, since the first crystals formed would theoretically have a solute concentration greater than that of the melt. Genders⁹ and others have shown that while undercooling undoubtedly decreases normal segregation it cannot cause an "inverse coring" effect because in even a metastable alloy system the liquidus must be above the solidus.

Movement of Primary Crystals.—Some interesting experiments by Watson¹⁴ have shown that primary crystals in a melt may be strongly repelled, even against the force of gravity, by the chilling action of a cold wall. Watson suggests that in a liquid solution, the first crystals formed, lower in solute atom concentration, are repelled towards the center of a casting while the enriched liquid flows outward. This effect is most interesting and probably operates in special cases, but is not applicable as a general explanation. The first dendrites or crystals formed at a cold mold wall quickly become interconnected and fixed, otherwise it would be impossible to make slush castings.

Outward Displacement of Enriched Liquid after Solidification Has Begun.—Generally solidification begins with the growth of dendrites from the cold wall of the mold into the cooling liquid. The dendrites are necessarily below the solidus temperature for crystals of their composition while the liquid phase may be just at or above this temperature. Interdendritic channels must exist, probably up to a point near the surface of the casting. Although it is generally conceded that the remaining liquid, enriched in solute atoms, flows through the dendritic

channels towards the surface of the casting, resulting in a higher average solute concentration at or near the surface, considerable difference of opinion exists as to the dominant cause for the flow. Possible forces acting in this direction are, according to Masing and Scheuer⁷:

1. Gas Pressure.—Genders⁹ first pointed out that during solidification of a melt, the residual liquid is continually enriched in the dissolved gas content as well as in solute atoms. At a late stage in the solidification process, the internal pressure of the supersaturated solution suddenly causes an evolution of gas in the form of bubbles. The hydrostatic pressure of the gas bubbles forces the liquid out through the interdendritic channels, leaving pores or cavities at the center of the casting. Masing suggests that gas pressure is the predominating influence accounting for segregates of the exudation type or for inverse segregation on slow cooling (Fig. 1). Allen^{15,16}, while accepting the gas-pressure effect, ascribes equal importance to contraction pressure. It should be mentioned in this connection that whereas Hoehne¹⁷ and Claus and Bauer^{18,19}

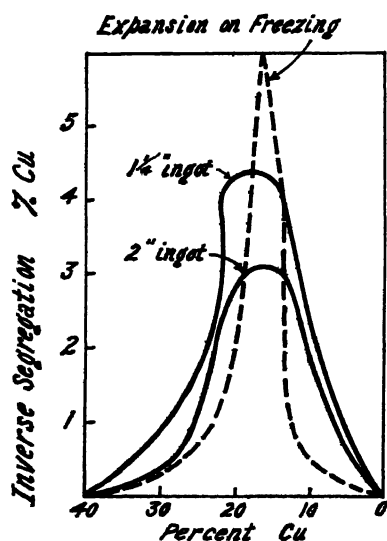


FIG. 2.—CRYSTAL THRUST.

found that hydrogen definitely increased inverse segregation in a Cu-Sn bronze, Fraenkel²⁰ found that degassing in a vacuum did not eliminate the effect in zinc-copper or aluminum-copper alloys. Also, Archbutt²¹ found inverse segregation in the shell (about 0.5 in. thick) of slush castings of aluminum-copper from which the liquid core was drained. It is obvious that gas pressure is not a universal explanation.

2. Contraction Pressure.—Contraction of the solid shell of a casting on the liquid core has been favored by Price and Phillips²² and by Kühnel²³ as an explanation of the effect. However, as pointed out by Genders⁹, liquids have a higher contraction rate in general than do solids. Also, the evidence of Archbutt²¹ is not consistent with this theory. Finally, Masing⁸ has, by calculations, shown that the effect must be very small, particularly on slow cooling.

3. Crystal Thrust.—The experiments of Iokibe^{2,24} have shown, as in Fig. 2, that there is a sharp maximum of expansion on solidification of zinc-copper alloys and a concurrent maximum in inverse segregation. The indicated dilation of these alloys is not real but apparent, since it results in a porous ingot. The expansion and porosity do not seem to be connected with gassing but rather with a sharp crystal thrust; i.e.,

dendrites growing against one another and pushing the metal apart. As they push apart and open up interdendritic spaces, the residual liquid flows into the openings, preferably to the cooler outer zones of lowest energy, with a resultant inverse segregation. The crystal-thrust force here is comparable to the volume increase that occurs on hydration of calcium oxide, in spite of the fact that the hydroxide has a true volume less than the sum of the volumes of calcium oxide and water. The crystallization pressure may explain Watson's results¹⁴, previously mentioned. This theory operates only in specific cases, since Masing^{7,25} has shown that antimony-bismuth alloys, although they expand on solidification without the formation of channels, show inverse segregation.

4. "Lunker-effect."—Finally, the theory of the cause supported by Masing⁷ as dominant particularly on rapid cooling segregation (Fig. 1), is termed by him the "Lunker-effect." He suggests that suction results from the freezing contraction in the dendritic solidifying zone. Employing numerous simplifying assumptions, and with only approximations for many important factors, Masing nevertheless calculated the extent of inverse segregation possible on this basis. He found that in aluminum-copper, silver-copper and zinc-copper alloys the calculated values were from 34 to 200 per cent of the actual observed segregation. This agreement is not unsatisfactory in view of the many uncertainties involved in the calculations and the probability that some other factors might influence the dominant force.

EXPERIMENTAL METHODS

The specimens to be discussed were all obtained under experimental conditions that, although in no way unique, should be described in some detail as essential for proper evaluation of the data. Aluminum-base alloys were melted and alloyed in a gas-fired muffle under a somewhat oxidizing atmosphere, while copper-base and silver-base alloys were melted in a high-frequency furnace under dried charcoal. Melting crucibles were of pure Acheson graphite and the casting molds shown in Fig. 3 were of the same material.

The single-crystal furnace was a vertical 3-in. alundum tube, 24 in. long, wound with Kanthal resistor ribbon, capable of operating at tem-

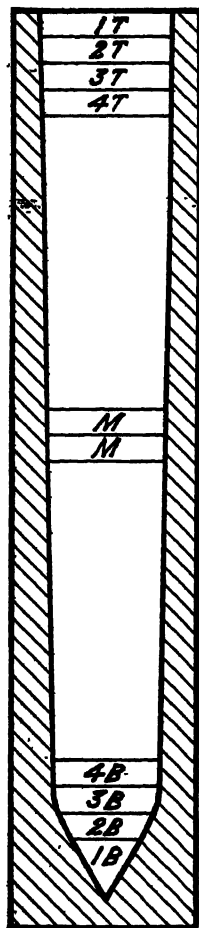


FIG. 3.—CASTING MOLD.

peratures up to 1300° C. The furnace was adequately thermally insulated. A pure nickel seamless tube ran through it, extending to 16 in. below the hot zone, with a connection enabling any chosen gaseous atmosphere to be maintained within the furnace. The top of the nickel tube was closed with a clay plug having a $\frac{3}{8}$ -in. hole. The graphite specimen mold was suspended by a nichrome ribbon, which extended through the clay plug up to the lowering mechanism. The lowering mechanism, separate from the furnace, consisted of an electric motor with suitable gear reductions, which permitted the crucible to be lowered at rates of from $\frac{1}{4}$ to 12 in. per hour. Generally the single-crystal mold was suspended in the furnace and maintained at the operating temperature while the alloy was separately melted and vigorously stirred. The metal was poured into the hot mold, held for an hour to attain temperature equilibrium, and then lowered at the desired rate. Specific variations from this procedure will be described as occasions arise.

Data are presented in the form of chemical analyses, density determinations and photomicrographs. Analyses usually were for one element only, since all alloys were binary and melted from metals of the following purities: Aluminum, 99.95 per cent; copper, 99.99; silver, 99.99; magnesium, 99.5; tin, 99.5; silicon, 99.0; manganese, 98.5. Customary analytical procedures were followed throughout, employing electrolytic methods where possible.

The method of sampling for chemical analyses was usually to cut a slice from the specimen, of such thickness that the entire cross section could be used as a sample. This was necessitated by the fact that some alloys were of two phases, one brittle and one ductile. It was impossible to obtain representative samples from drillings or millings from such material. Generally samples were taken from aluminum alloys as marked in Fig. 3. Copper alloys were analyzed by taking one slice from sections 3B and 3T and dividing the sample into triplicate parts.

The density values were determined with a setup used normally for precision work; i.e., weighing in carefully standardized alcohol with an anodized platinum-wire suspension.

GRAVITY SEGREGATION ON MELTING

Aluminum containing about 5 per cent copper was melted, stirred, cast in the hot graphite mold and solidified by immersing the bottom of the mold in cold water. Under these conditions, solidification took place from the bottom upward and with correct metal and mold temperatures, resulted in a perfectly homogeneous, fine-grained slug with a flat top (spec. 1, Table 1). Solidification was generally complete in about two minutes. The slug was then quietly remelted (without any agitation or stirring) in the single-crystal furnace and lowered at the chosen rate. The resultant single crystal was found to be greatly enriched in copper

at the bottom, where solidification started, rather than at the top (spec. 2, Table 1). Similar results were obtained when after the homogeneous slug had been quietly remelted, it was solidified rapidly from the bottom in water (spec. 9, 10).

TABLE 1.—Gravity Segregation in Alloys Melted Quietly and without Agitation in Furnace at 750° C.

Specimen No.	Alloy	Nominal Concentration, Wt. Per Cent	Remelt	Cooling Rate, In. per Hr.	Analyses, Per Cent (See Fig. 3)								
					Top				M	Bottom			
					1T	2T	3T	4T		4B	3B	2B	Tip
1	Al-Cu	5 0	None	Water-cooled		5 08	5 09		5.08		5 08	5 09	
2	Al-Cu	5 0	Once	$\frac{1}{4}$ in. s.c. ^b		4 56	4 60				6 37	6 51	
3	Al-Cu	5 0	Twice	$\frac{1}{2}$ in. s.c. ^b		4 26	4 28				5 96	6 02	
4	Al-Cu	5 0	Once	$\frac{1}{2}$ in. s.c.	4 82	4 84	4 84		4 36		6 10	6 15	
5	Al-Cu	5 0	Once	$\frac{1}{2}$ in. s.c.	4 39	4 40	4 82	4 83		5 44	5 70	5 76	
6	Al-Cu	5 0	Thrice	$\frac{1}{2}$ in. s.c.	3 69	3 53	3 62	3 88		6 83	7 37	7 65	
7	Al-Cu	5 0	Thrice	$\frac{1}{2}$ in. s.c.	3 50	3 68	3 74	3 73		7 48	8 05	8 17	8.44
8	Al-Cu	5 0	Thrice	2 in. s.c.	3 69	3 74	3 74	3 75	4 40	6 07	6 26	6 58	
9	Al-Cu	5 0	Thrice	Water-cooled	4 08	4 28	4 66		4 65		7 16	8 14	10.14
10	Al-Cu	5 0	Thrice	Water-cooled	3 91	3 94		4 20			7 73	9 42	11.46
11	Al-Cu	5 0	Thrice	Water-cooled*	4 01	4 06	4 16	4 16		6 48	6 67	7 09	7 40
12	Al-Cu	2 5	Thrice	$\frac{1}{2}$ in. s.c.	1 99	2 05	2 07			2 77	2 80	2 87	2 87
13	Al-Cu	2 5	Thrice	$\frac{1}{2}$ in. s.c.	1 88	1 93	1 96	1 98		2 90	2 96	3 00	3 22
14	Al-Cu	2 5	Thrice	$\frac{1}{2}$ in. s.c.	2 13	2 18	2 08			2 78	2 77	2 90	2 90
15	Al-Cu	2 0	Thrice	Water-cooled	1 19	1 34	1 67			2 09	2 27	2 43	
16	Cu-Si	6 5	"	1 in. s.c.	6 68	6 54	6 58			6 01	6 03	5 96	
17	Cu-Si	6 5	Once	1 in. s.c.	7 04	6 86	6 88			6 16	6 18	6 15	

* The alloy only partly solidified in the furnace and then remelted quietly.

^b s.c. designates single crystal and while all specimens so marked were not perfect single crystals, they generally approached that condition.

* This specimen was held quiet and entirely molten at 750° C. for 12 hr. before freezing.

It is evident that the segregation took place on melting rather than on solidification. On relatively slow heating through the range between solidus and liquidus, the first liquid formed is naturally rich in copper. At a certain stage in this temperature range, the heavier copper-rich solution tends to sink in the mold and eventually there are free grain particles low in copper, which tend to rise and float in the solution. By remelting twice more without stirring, it was possible to raise the copper content of the bottom of a slug from 5 to 11.5 per cent copper, while the top might be 3.9 per cent copper (spec. 10, Table 1). A similar gravity segregation on melting was found in the copper-silicon alloys (Fig. 4, also spec. 16 and 17, Table 1).

DIFFUSION IN MOLTEN ALLOYS

It is usually thought that the thermal activity of molten alloys is great enough to enable rapid diffusion in this state. However, specimen 11 of Table 1, otherwise comparable to specimens 9 and 10, indicates that

in 12 hr. at 750° C. diffusion to a homogeneous liquid is far from complete. In a further experiment on the liquid diffusion in aluminum-copper alloys, a composite rod was cast in the single-crystal graphite mold with the lower half of pure aluminum-copper eutectic alloy containing 33 per cent copper. The top half was pure aluminum and the interface was clean and free from oxide. The rod was quietly melted and held at 725° for

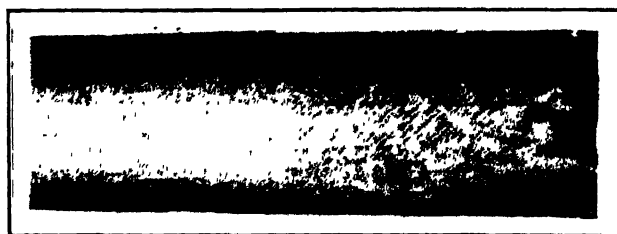


FIG. 4.—COPPER-SILICON ALLOY SHOWING LINES OF ORIGINAL SOLID SOLUTION DENDRITES (TOP, RIGHT) WITH FILLING OF SILICON-RICH SOLUTION.

20 hr. It was then lowered at 8 in. per hour and subsequently analyzed. The results are shown in Fig. 5.

NORMAL SEGREGATION

A consideration of the freezing process based on the conventional constitutional diagram for systems showing limited solid solubility (and consequently a range of solidification temperatures between liquidus and

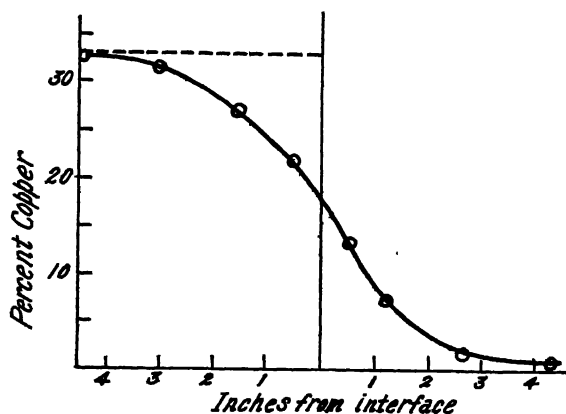


FIG. 5.—DIFFUSION IN ALUMINUM-COPPER ALLOY.

solidus lines), naturally suggests segregation of the "normal" type. Furthermore, knowing that equilibrium between melt and solid is not attained by diffusion in the time available even during the slow cooling of single crystals, it might reasonably be expected that a homogeneous liquid, when formed into a single crystal, would show a vertical coring effect or normal segregation. As a matter of fact, the following alloys

did show normal segregation or coring in single crystals: Al-20 per cent Zn, θ Al-Cu(CuAl_2), Al-6 per cent Mg, β Al-Mg(Mg_2Al_3 or Mg_5Al_8), Cu-7.5 per cent Al, Cu-12.0 per cent Mn, Ag-8 per cent Cu. (Here and elsewhere in the paper, when referring to solid solution alloys, the solvent metal is given first.) As indicated in Table 2, the segregation in all cases was relatively small. In two cases, the aluminum-magnesium and the aluminum-zinc alloys, it is probable that the segregation would have been considerably greater had it not been for the volatility of the solute metals, magnesium and zinc. Some magnesium or zinc continued to distill from the molten top of the specimen during the lowering of the melt, thus reducing the degree of segregation. The distillation of magnesium resulted in a concave top of the specimen, clearly showing the

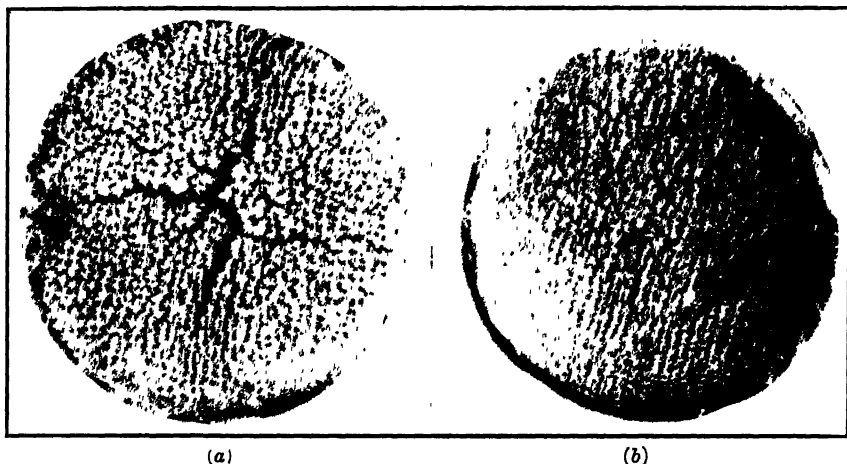


FIG. 6.—NORMAL SEGREGATION: (a) ALUMINUM WITH 5 PER CENT MAGNESIUM; (b) ALUMINUM WITH 1.0 PER CENT MAGNESIUM. $\times 2$.

dendrite axes with nearly idiomorphic crystalline faces (Fig. 6). Usually above this clean face was a large void topped by successive layers of aluminum and magnesium oxides lifted by the vapor pressure of the distilling magnesium.

Density determinations on sections from the rods were made as cast and after 50 per cent cold reduction with the purpose of determining the extent of porosity in the rods. The data show in general a slight amount of porosity in the top of each rod while very little or none is found at the bottom where feeding is complete.

Some of these alloys that showed slight normal segregation on extremely slow cooling formed homogeneous rods on rapid cooling from the bottom in water. The analytical results are detailed in Table 3. The copper-silicon alloys showed no segregation on either rapid or slow cooling.

TABLE 2.—*Alloys Showing Normal Segregation from Homogeneous Liquid When Made into Single Crystals*

Analyses Average of Triplicates from Positions 3T and 3B (Fig. 3)

Specimen No.	Alloy	Solute Nominal Concentration, Per Cent	Furnace Atmosphere	Furnace Temperature, Deg. C.	Lower Rate, In. per Hr.	Analyses, Per Cent		Density, <i>D</i>		<i>D</i> (Rolled 50 Per Cent)	
						Top	Bottom	Top	Bottom	Top	Bottom
18	Al-Mg	2.0	Air	700	$\frac{1}{2}$	1.30	0.74	2.686	2.689	2.686	2.691
19	Al-Mg	11.0	Air	700	$\frac{1}{2}$	5.90	5.59	2.596	2.629	2.628	2.631
20	β (Al-Mg)	37.5	Vacuum	600	$\frac{1}{2}$	32.81	30.75				
21	β (Al-Mg)	41.0	Dry N ₂	600	2	43.76	41.08				
22	Al-Zn	20.0	Air	700	$\frac{1}{2}$	19.47	18.89				
23	Al-Zn	15.0	Dry N ₂	700	1	14.98	14.78				
24	θ (Al ₂ Cu) ^a	52.0	Dry N ₂	700	1	51.57	52.40	4.237	4.267		
25	Ag-Cu	6.0	Air	1000	$\frac{1}{2}$	6.38	5.89				
26	Ag-Cu	6.0	Air	1000	$\frac{1}{2}$	6.45	5.80				
27	Ag-Cu	6.0	Air	1000	$\frac{1}{2}$	7.65	6.35				
28	Ag-Cu	8.0	City gas	1000	1	8.30	8.25				
29	Ag-Cu	8.0	Dry N ₂	1000	1	8.75	7.83	9.318	9.347	9.319	9.336
30	Cu-Al ^a	7.5	Dry N ₂	1100	1	7.81	7.48	7.819	7.853		
31	Cu-Mn	12.0	Dry N ₂	1100	1	12.65	11.98	8.396	8.421	8.407	8.426

^a These were the only complete single crystals. Others usually had one dominant crystal with several smaller ones present.

INVERSE SEGREGATION

It was rather surprising to find a pronounced inverse segregation in some solid solution alloys when they were allowed to solidify into single crystals. The tendency in this direction was most pronounced in the case of aluminum-copper and copper-silver alloys. Table 4 shows data.

TABLE 3.—*Alloys Showing No Segregation from Homogeneous Liquid When Cooled as Indicated*

Specimen No.	Alloy	Cooling	Analyses, Wt. Per Cent Solute		Density, <i>D</i>		<i>D</i> (Rolled 50 Per Cent)		Segregation, Slow Cooling
			Top	Bottom	Top	Bottom	Top	Bottom	
32	Ag-Cu	Water	8.02	8.02					Normal Normal Normal None
33	Cu-Al	Water	6.57	6.57					
34	Cu-Al	Water	7.27	7.16	7.844	7.906	7.903	7.904	
35	Cu-Si	Water	5.93	5.88	8.224	8.251			
36	Cu-Si	s.c. 1 in. per hr.	4.63	4.63	8.409	8.405	8.406	8.406	

on several specimens. All of these alloys were melted under similar conditions using pure metals (except for a few heats of commercial aluminum with copper), pure graphite crucibles and molds and with a dry nitrogen atmosphere maintained in the single-crystal furnace. In some cases, to thoroughly degas the metal it was held molten under a vacuum of one micron for an hour before placing in the single-crystal

furnace. It seems very unlikely that gas pressure could be the factor responsible for the inverse segregation. Under the conditions employed in forming the single crystals, no large internal gas pressure was possible because all bubbles would have time (and be free) to rise through the still molten upper part of the melt. The gas-pressure explanation proposed by Genders and applied by Masing to most cases of inverse segregation on slow cooling is apparently not applicable in this particular case.

TABLE 4.—*Inverse Segregation in Several Solid Solution Alloy Rods Made from Homogeneous Liquid Solutions*

Specimen No.	Alloy	Lower Rate, In per Hr.	Analyses, Wt. Per Cent Solute (Fig. 3)				Density, <i>D</i>		<i>D</i> (Rolled 50 Per Cent)	
			1 <i>T</i>	2 <i>T</i>	2 <i>B</i>	1 <i>B</i>	Top	Bottom	Top	Bottom
37	Al-Cu	½	2.21	2.23	2.27	2.30				
38	Al-Cu ^a	½	4.42	4.45	5.00	5.04				
39	Al-Cu ^a	½	4.34	4.44	4.80	4.80				
40	Al-Cu	½	5.05	5.11	5.80	5.98	2.801	2.812	2.796	2.799
41	Al-Cu	½	5.15	5.16	5.70	5.73	2.803	2.811	(above, specimens heat-treated for rolling)	
42	Al-Cu	¼	5.21	5.26	5.50	5.53	2.797	2.811		
43	Al-Cu	2	5.12	5.20	5.66	5.73				
44	Al-Cu ^b	8	5.44			6.21				
45	Al-Cu ^b	Water	5.44			5.73				
46	Al-Cu ^b	1	(5.40)			6.04				
	Al-Cu (Fe content)		(0.44)			0.47				
	Al-Cu (Si content)		(0.33)			0.36				
	Al-Cu (Mn content)		(0.04)			0.02				
47	Al-Cu	1	15.11	15.18	16.92	16.84				
48	Al-Cu	Water	15.54	15.75	16.59	16.66				
49	Al-Cu	1	32.73	32.76	32.93	32.98	8.515	8.520		
50	Cu-Ag	¼	8.19		8.53					
51	Cu-Ag	1	7.56		8.90		8.785	9.030	8.944	9.046
52	Cu-Sn	1	9.38		9.84					
53	Cu-Sn	1	12.62		12.77		8.916	8.923		
54	Cu-Sn	Water	8.56		9.43		8.632	8.902		(cracked)

^a Melted and stirred under vacuum.

^b Used commercial aluminum, 99.0 per cent.

The conditions prevailing during solidification of the single crystals, sketched in Fig. 7, seem to preclude the acceptance of most of the theories of inverse segregation, certainly in explaining the mechanism of segregation in single crystals. The manner of freezing the specimens eliminates the possibility of a contraction pressure originating in the external layers of the rod. At any stage in the freezing, there is a relatively solid portion at a temperature below the solidus, and above that a certain height of dendrites growing into the melt. The primary dendrites in most specimens probably extended up an inch or more into the liquid solution. At any horizontal level within this zone, the solid and liquid phases coexist at substantially the same temperature. In other words, a temperature gradient probably existed only along the vertical axis of the single-crystal rods.

Although most of the alloy compositions were theoretically single-phase solid solutions at temperatures just under the solidus, the rate of diffusion was too slow to attain equilibrium conditions even during the relatively slow cooling of the alloys. Practically all alloys showed two phases when examined micrographically (Figs. 8 to 11). This condition may be explained on the basis that the solidification and contraction of the dendrites leads to the opening of interdendritic channels. Consequently, feeding into these channels with liquid enriched in the solute element would be possible for a considerable time interval after the bottom portion of the rod had cooled below the nominal solidus temperature. The presence of a second phase at the lower end of a single-

crystal rod is rather positive evidence that a liquid considerably richer in solute atoms than the original melt has filled the interdendritic channels at a temperature below the normal solidus temperature for the given composition.

Masing⁷ used a very much simplified equation to calculate the segregation possible on the basis of zero diffusion and adequate feeding of contraction cavities. Letting Δc represent the concentration difference between top and bottom, s the volume change on freezing, c' the concentration of the liquid phase at a temperature midway between solidus and liquidus and c_0 the initial solute concentration, Masing suggests: $\Delta c = s(c' - c_0)$. On this basis, the aluminum-copper alloys should give about 0.7 per cent copper inverse segregation, which is approximately the maximum result found experimentally. It can be assumed that the

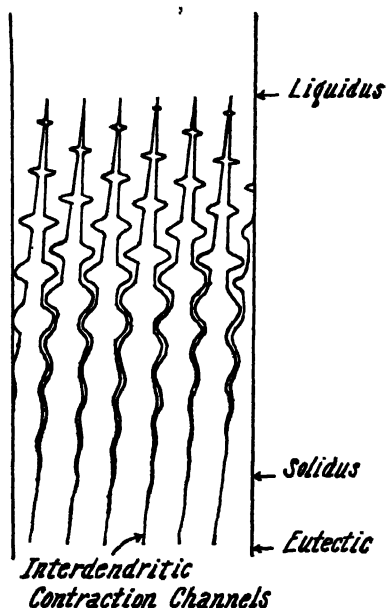
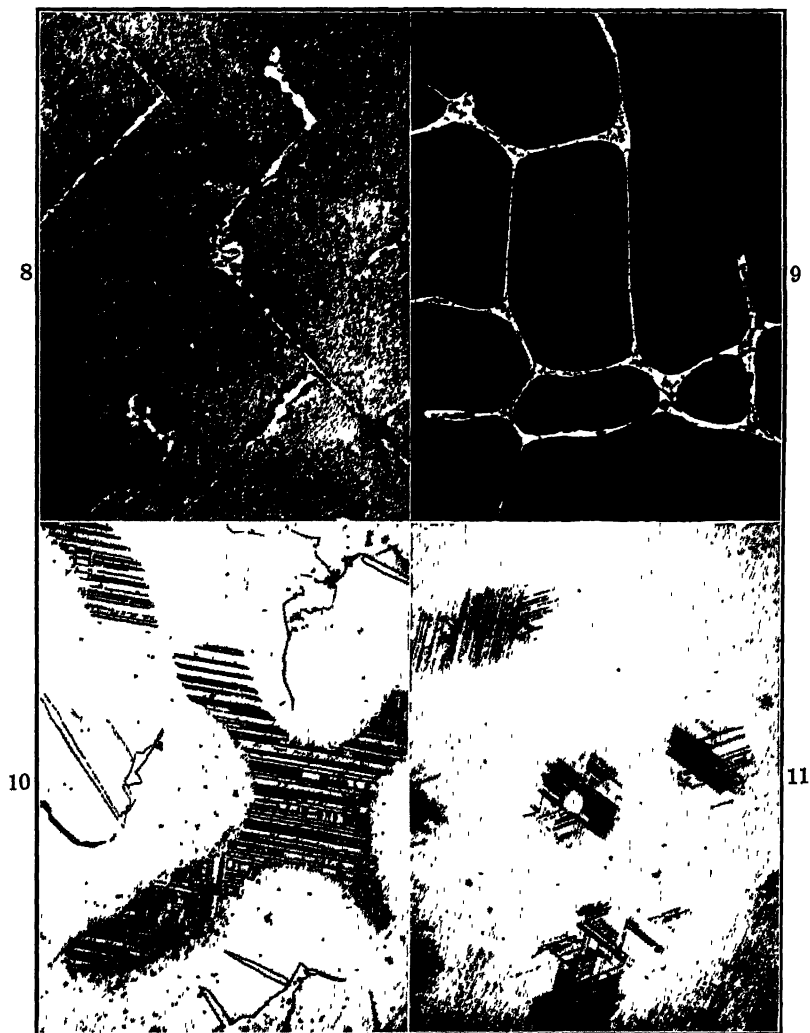


FIG. 7.—CONDITIONS PREVAILING DURING SOLIDIFICATION OF SINGLE CRYSTALS.

assumptions used in setting up the equation were experimentally approximated.

The microstructural examinations and density determinations were made with the hope of obtaining further confirmation of this viewpoint. Porosity generally occurred at points where the second phase was concentrated; i.e., at the places last to freeze, as would be expected. From the structural characteristics of the openings, they appeared to be contraction cavities rather than gas bubbles. It was hoped that density figures on the cast material supplemented by further data on the material after rolling (to completely eliminate the pores) would furnish data on

the relative degree of porosity. However, other troublesome complications arising from structural and composition differences, and particularly the formation of cracks during rolling, etc., made it impossible to rely



FIGS. 8-11.—TWO PHASES IN SOLID SOLUTION ALLOYS. BOTTOMS OF SINGLE CRYSTALS
 Fig. 8. Specimen 24, θ (CuAl₂). Fig. 10. Specimen 17, Cu-6.5 per cent Si.
 Fig. 9. Specimen 51, Cu-8 per cent Ag. Fig. 11. Specimen 36, Cu-4.6 per cent Si.
 Original magnification 150; reduced $\frac{1}{3}$ in reproduction.

on the density data for more than a qualitative estimate of porosity. In general, it appears that the porosity is greater at the top of the single crystal than at the bottom, presumably resulting from the absence of any residual liquid to feed the contraction cavities.

Masing's curve (Fig. 1) for inverse segregation shows two maxima, of which Masing attributes one, on slow cooling, to gas pressure and the other, on rapid cooling, to interdendritic flow. The data in Table 4 show but one maximum in aluminum-copper alloys for the six different cooling speeds employed (Fig. 12).

It is interesting that in the commercial aluminum-copper alloy specimen (No. 46, Table 4), iron and silicon segregate inversely in nearly the same proportion as does the copper. It is known that these three elements with aluminum form a low-melting quaternary eutectic. Manganese, which is present in small quantities, apparently does not enter the eutectic, since it segregated normally. Similar results on the iron, silicon and manganese segregation were obtained on five other comparable rods.

The interpretation of the results obtained on single-crystal rods may not apply generally, since the particular circumstances controlling

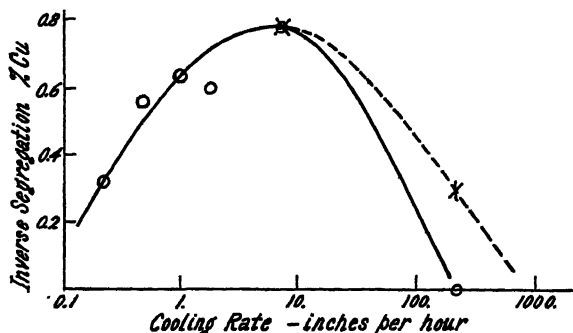


FIG. 12.—INVERSE SEGREGATION IN ALUMINUM-COPPER ALLOYS. Solid lines, pure alloys; dashed line, commercial alloys.

solidification of the rods were peculiar to the present work. It might be expected that the temperature gradient of the single-crystal furnace would affect the results, because it would change the length of the freezing zone (Fig. 11) and perhaps thereby the length of the interdendritic channels. Another factor might well influence the segregation; namely, the viscosity of the liquid feeding the channels. No work was done along this line except the use of commercial aluminum-copper alloys containing iron and silicon contrasted with pure aluminum-copper melts. Both alloys showed nearly the same maximum segregation of copper, although the viscosity of the feeding liquid may have differed somewhat. It is probable, however, that the lower melting point of the quaternary eutectic liquid in the commercial aluminum alloy permitted feeding on even rapid cooling and hence inverse segregation (Fig. 12).

GENERAL REMARKS

The results of the present work on solid solution alloys may be qualitatively summarized as in Table 5.

With the experimental conditions employed in this work, it is possible to explain inverse segregation of aluminum-copper alloys on the basis of slow solid diffusion of copper together with a flow of enriched liquid into interdendritic contraction channels. The absence of noticeable segregation on very rapid cooling may be explained on the basis that the channels were too cold to permit the residual liquid to enter. The decreased segregation on very slow cooling may be attributed to the more complete diffusion. The absence of segregation, as in copper-silicon alloys, may also be caused by a more rapid diffusion of solute atoms, which makes the feeding liquid less rich in the second element. Since a second phase was observed in the bottom of the copper-silicon alloys, it is certain that feeding had occurred with a somewhat enriched liquid phase.

TABLE 5.—*Summary of Results*

Alloy		Segregation		
Solvent	Solute	Slow Cooling	Fast Cooling	Melting
Al	Cu	Inverse	None	Gravity
Al	Mg	Normal		
Al	Zn	Normal		
Cu	Ag	Inverse		
Cu	Al	Normal	None	Gravity
Cu	Mn	Normal		
Cu	Si	None	None	
Cu	Sn	Inverse	Inverse	
Ag	Cu	Normal	None	

Some of the data included in the tables do not appear to support the viewpoint that has been expressed regarding the causes of segregation. Probably no simple fundamental statement can be made that will properly account for all known cases of segregation. In order to obtain a clear picture of the mechanism of segregation, it is necessary to know, and to properly evaluate, the many variables playing a part in the involved processes associated with the solidification and cooling of a solid solution alloy. It is evident that, whatever may be the chief motivating force directed toward segregation, the net results in many cases may be the sum total effect of modifying factors, such as internal gas and external shrinkage pressures, crystallization pressures, inherent variables such as volatility of one component, viscosity of the liquid phase, relative atomic sizes and melting points, extent of freezing range, diffusional characteristics, and so forth.

SUMMARY

1. A special case of gravity segregation was found during the melting of solid solution alloys. It occurs upon heating through the

solidus-liquidus range when the two component elements differ greatly in density.

2. Segregation during slow solidification along a vertical temperature gradient was studied in numerous aluminum-base and copper-base binary solid solution alloys. It is believed that under conditions eliminating gas and contraction pressures, the results show that interdendritic feeding took place in practically all specimens. Whether this feeding overcomes the natural tendency towards normal segregation or coring depends to a large extent on the diffusion rate of the solute element and the temperature conditions along the dendritic contraction channels.

3. The above basic factors are generally modified in ordinary practice by external casting variables and inherent alloy peculiarities.

REFERENCES

1. O. Bauer and H. Arndt: Seigerungserscheinungen. *Ztsch. Metallkunde* (1921) **13**, 497.
2. K. Iokibe: On the Cause of Inverse Segregation. *Sci. Repts. Tohoku Imp. Univ.* (1931) **20**, 608.
3. W. Rosenhain: Discussion. *Met. Ind. (London)* (1933) **43**, 396.
4. G. Masing and C. Haase: *Wiss. Ver. Siemens Konz.* (1927) **6**, 211, 221.
5. H. Bohner: *Haus-Ztsch. Aluminium* (1931) **3**, 3.
6. R. Reader: Effects of Rate of Cooling on the Density and Composition of Metals and Alloys. *Jnl. Inst. Metals* (1923) **30**, 105.
7. G. Masing and E. Scheuer: Untersuchungen über Seigerung. *Ztsch. Metallkunde* (1933) **25**, 173.
8. G. Masing: A Few Problems in Non-Ferrous Castings. *Metals and Alloys* (1933) **4**, 99, 109.
9. R. Genders: The Mechanism of Inverse Segregation in Alloys. *Jnl. Inst. Metals* (1927) **37**, 241.
10. C. Benedicks: Action of Hot Wall. *Trans. A.I.M.E.* (1925) **71**, 597.
11. S. W. Smith: Liquefaction in Molten Alloys. *Trans. Inst. Min. and Met.* (1926) **35**, 254.
12. D. Hanson: Discussion. *Trans. Inst. Min. and Met.* (1926) **35**, 301.
13. G. Masing: Zur Erklärung der umgekehrten Blockseigerung. *Ztsch. Metallkunde* (1922) **14**, 204.
14. J. H. Watson: Liquefaction or Inverse Segregation in the Ag-Cu Alloys. *Jnl. Inst. Metals* (1932) **49**, 347.
15. N. P. Allen: The Distribution of Porosity in Al and Cu Ingots with some Notes on Inverse Segregation. *Met. Ind. (London)* (1933) **43**, 291, 395.
16. N. P. Allen: Further Observations on the Distribution of Porosity in Al and Cu Ingots with some Notes on Inverse Segregation. *Jnl. Inst. Metals* (1933) **52**, 193.
17. F. Hoehne: Beitrag zur Kenntnis der Umgekehrten Blockseigerung. *Die Giesserei* (1933) **20**, 523.
18. W. Claus and W. Bauer: Diss., Berlin (1932).
19. W. Claus and W. Bauer: Umgekehrte Blockseigerung und Gaslöslichkeit studiert an Zinn-Bronzen. *Metallwirtschaft* (1936) **15**, 587.
20. W. Fraenkel and H. Goedecke: Ueber umgekehrte Blockseigerung. *Ztsch. Metallkunde* (1929) **21**, 322.
21. S. Archbutt: Discussion. *Jnl. Inst. Metals* (1927) **37**, 275.

22. W. B. Price and A. J. Phillips: Exudations on Brass and Bronze. *Proc. Inst. Met. Div. A.I.M.E.* (1927) 80.
23. I. Kühnel: Umgekehrte Legierung. *Ztsch. Metallkunde* (1922) 14, 462.
24. K. Iokibe: On the Zn-Cu Alloys which Expand on Solidification. *Jnl. Inst. Metals* (1924) 31, 225.
25. G. Masing: Über die Ursacher der umgekehrten Blockseigerung. *Ztsch. Metallkunde* (1925) 17, 251.

DISCUSSION

(Georg Sachs presiding)

G. SACHS,* Newark, N. J.—These investigations by Phillips and Brick are perhaps the first step toward solving some of the problems of segregation in cast ingots using definite and exact conditions. Previous experimental work has not fully succeeded, as far as I know, in creating conditions that can be completely overlooked. They apparently have not realized that the casting process has at least two phases: filling the mold and solidifying of the material (that which was not solidified during the first phase and filling the pipe in the mold). I think the experimental conditions used by the authors do avoid these difficulties and therefore they show perhaps more clearly results that can never be obtained in practical work, the real features of the process of segregation.

Another interesting point in this paper is that the aluminum alloys show a most pronounced segregation, as they really do in practice.

F. N. RHINES,† Pittsburgh, Pa.—The most striking feature of this investigation lies in the almost insignificant magnitude of the normal and inverse segregation effects observed. Perhaps this is chiefly a result of the method of sampling, and much larger concentration differences might have been found had the analytical samples been drawn from smaller zones. Certainly segregation of a much larger order of magnitude is frequently encountered in aluminum-copper and copper-tin alloys, and I question whether any great difference could exist between single and polycrystalline ingots in this respect.

The authors have found the rate of diffusion of copper in molten aluminum to be small compared to that which would be required to transfer large quantities of copper from one end to the other of an ingot several inches in length within a period of a few hours. It would seem, therefore, that extensive segregation of the normal type could be expected to involve only a relatively small volume of metal unless the rate of cooling was excessively slow, for the mechanism of normal segregation must be mainly one of diffusion. Similarly, the accumulation of low-melting material under physical conditions ultimately leading to inverse segregation could hardly be expected to occur in masses of a size comparable to the size of the ingot itself, but rather in small and widely distributed regions. Thus the true magnitude of the segregation effects could be detected only by taking small samples within more limited zones. For example, the skin of the aluminum-copper ingot should be much higher in copper than the metal just inside if inverse segregation has occurred.

L. W. KEMPF,‡ Cleveland, Ohio.—There is just one thing that has been bothering me during the presentation of the two papers by Phillips and Brick; that is why commercial ingots of our alloys containing magnesium do not act as they are supposed to. Actually, under some conditions, we do get inverse segregation in aluminum-magnesium alloy ingots.

* Baker & Co., Inc.

† Assistant Professor of Metallurgy, Carnegie Institute of Technology.

‡ Aluminum Research Laboratories.

A. PHILLIPS AND R. M. BRICK (written discussion).—The fact that commercial ingots of aluminum-magnesium alloys show inverse segregation, as Mr. Kempf remarks, is not necessarily contradictory to the absence of such segregation in single crystals. The conditions employed in the present work were chosen to eliminate many variables and concentrate on a linear temperature gradient effect. The results may be misleading in systems, such as the aluminum-magnesium alloys, where one component is relatively volatile.

One or two remarks by Dr. Rhines may be somewhat misleading—for example, when it is stated that “the mechanism of normal segregation must be mainly one of diffusion.” It seems probable that very slow or incomplete diffusion is the chief factor in normal segregation. Also in the present work, it was found that the skin of aluminum-copper ingots was not richer in copper than the metal just inside. The segregation effects were along a vertical axis only, probably resulting from the presence of a temperature gradient along a vertical axis with nearly uniform temperature conditions from skin to center of transverse sections of single crystals. There is no doubt, of course, that local microscopic segregations of considerable magnitude occur as suggested by Dr. Rhines. Even during single-crystal formation, diffusion is too slow to form a homogeneous solid solution and localized areas of compound, rich in the solute alloy element, are formed.

Diffusion of Copper and Magnesium into Aluminum

By R. M. BRICK* AND ARTHUR PHILLIPS,† MEMBERS A.I.M.E.

(New York Meeting, February, 1937)

THE Institute of Metals Division Lecture in 1936, given by R. F. Mehl, on diffusion in solid metals¹, was introduced with the statement that "the phenomena of diffusion are intimately related to many basic problems of the metallic state, but in addition to this the process of diffusion is of first importance practically." In view of the scope of that lecture, it does not seem necessary to review the importance, history or present status of diffusion problems.

One aspect of the subject of diffusion that has received little attention became of some immediate importance in the course of a study on segregation. When a solid solution alloy freezes, the familiar mechanism of solidification requires that the first nuclei formed be low in solute concentration, with a resultant normal segregation or coring effect during freezing. Theoretically, diffusion of solute atoms during solidification should result in a homogeneous solid solution. Actually, of course, it is impossible in most binary alloys to obtain a cooling rate that will permit diffusion to eliminate coring in the freezing dendrites. For a given alloy, the extent of diffusion attained up to the point of final solidification will determine the degree of enrichment in solute atoms of the final liquid phase. The flow of this liquid into dendritic contraction channels and the solute concentration of the liquid seem to be the determining factors as to whether the final gross segregation is normal, inverse or absent.

The purpose of the present study of diffusion was to determine to some extent the separate diffusion rates of copper and magnesium into pure aluminum with a view to clarifying previous results on segregation in these alloys; i.e., the fact that under similar freezing conditions aluminum-copper alloys segregate inversely and aluminum-magnesium alloys segregate normally. Of concomitant interest were the questions of the homogenization times required for segregated ingots or partially melted, i.e., "burnt," structures, and the solution heat-treatment times required for cast, hardenable aluminum-copper and aluminum-magnesium alloys, for worked and annealed structures, and so forth.

Manuscript received at the office of the Institute Dec. 21, 1936.

* Research Assistant in Metallurgy, Hammond Laboratory, Yale University, New Haven, Conn.

† Professor of Metallurgy, Hammond Laboratory, Yale University.

¹ References are at the end of the paper.

The diffusion data on aluminum-copper alloys are meager and unreliable. Burkhardt and Sachs² studied the diffusion of copper from aluminum-copper (Lautal) alloys into a pure aluminum coating (e.g., Alclad 24S alloy). They used X-ray lattice-parameter measurements to determine the depth of diffusion but did not express their results in the form of diffusion coefficients. Freche³ studied the diffusion of magnesium on a similar Alclad sample, although in the specimen of the binary magnesium-aluminum diffusion the alloy core was far from being saturated in magnesium at the interface during diffusion. In this work, the depth-concentration relations in the diffusion zone were determined spectrographically. Two studies^{4,5} of the diffusion of copper into aluminum have been made employing aluminum with an electrodeposited coating of copper. Reliable diffusion coefficients were not obtained in either work.

EXPERIMENTAL METHODS

When an alloy melt is cooled through the liquidus-solidus interval, homogeneity depends primarily on diffusion within the solid phase, not on diffusion at the liquid-solid interface. To establish conditions comparable to those operating during the growth of crystal nuclei in a melt, and indeed to obtain diffusion data of any accuracy, it is necessary to have an absolutely clean interface. It is believed that this primary condition was obtained by the following method of specimen preparation.

Rods of pure aluminum, $\frac{1}{2}$ in. in diameter and for the most part rather fine grained, were cleaned and heated to 550° C. for copper-diffusion studies and to 455° C. for magnesium diffusion. In a separate graphite crucible, 1 in. in diameter and 9 in. long, aluminum-copper or aluminum-magnesium eutectic was melted and held at temperatures of 555° C. and 455° C., respectively. The eutectic was covered with a molten flux of mixed chlorides and the hot aluminum rod inserted into the eutectic, first passing through the chloride flux. The flux probably dissolved most of the oxide film from the rod but, in addition, when held at slightly above the eutectic temperature equilibrium relationships demanded that a small amount of aluminum dissolve into the eutectic, thus leaving an absolutely clean diffusion interface. After agitation of the rod in the eutectic for a few minutes, the composite specimen (aluminum rod covered with a thick coating of eutectic) was chilled and solidified from the bottom. Examination of the specimens at this time showed that the initial diffusion zone was always less than 0.0005 centimeter.

The actual diffusion process was performed by reheating the composite specimens at chosen temperatures for various times. The diffusion of copper into aluminum was studied at 540°, 490°, 440° and 400° C.; of magnesium, at 440°, 400° and 365° C. At the conclusion of the diffusion treatment, the concentration of solute atoms in the solid solution in contact with the eutectic was the saturation solubility value at the diffusion

temperature. The concentration of solute atoms decreased with increasing distance from this point into the solvent metal, aluminum. The exact change in concentration with distance was determined micrographically.

The method depends on the known decrease in solid solubility of copper and magnesium, respectively, in pure aluminum. The National Metals Handbook lists the change of solubility of the two metals with temperature as follows:

	548° C	500° C	451° C	400° C	350° C	300° C	250° C.	200° C.
Weight per cent Cu.....	5.65 ^a	4.1	2.6	1.5	1.0	0.7	0.6	0.5
Weight per cent Mg.....			14.9 ^a	11.5	8.7	6.4	4.9	2.9

^a Eutectic temperature.

By reheating the diffusion specimens for relatively short times at temperatures below the actual diffusion temperature, θ Cu-Al(CuAl_2) or β Mg-Al(Mg_2Al_3 or Mg_5Al_8) was precipitated in areas where the solute



FIG. 1.—TYPICAL DIFFUSION ZONE PRECIPITATE STRUCTURES IN ALUMINUM-MAGNESIUM SPECIMENS.

concentration exceeded the solubility saturation value. The edge of the precipitated zone furthest from the eutectic was presumably at the saturation concentration limit. After reheating the specimens at the chosen precipitation temperature, they were polished, etched and examined at a known magnification to determine the depth to which the specified concentration extended. Fig. 1 shows a typical series of diffusion zone precipitates for aluminum-magnesium specimens.

Fig. 1 shows that the original interface between the eutectic and the pure aluminum was displaced during the diffusion process. Magnesium from the solid magnesium-aluminum eutectic formed a saturated solid

solution, which supplied magnesium atoms to be transported into the pure aluminum. An equal number of aluminum atoms diffused into the saturated solid solution and permitted more of the eutectic compound to go into solution. Thus the face of the eutectic did not remain at the original interface but was displaced outward. It was not always possible to see the original interface in the microstructure, although it was necessary to know its true position in calculating the diffusion coefficients. For this reason the specimens were polished before the diffusion heat-treatment, reference marks drilled in the structure and the distance from the marks to the true interface was determined. In this connection, the assumption is made that the interface does not actually move but that through it there is an equal interchange of solute and solvent atoms.

The reheating of specimens for precipitation in the diffusion zone to determine depth-concentration relations will, of course, occasion some further diffusion. However, reheating at the higher temperatures was necessary for only a very short time as compared to the diffusion treatment at a still higher temperature. At the lower temperatures where reheating for relatively longer periods was necessary to clearly define the edge of the precipitate, diffusion was too slow to measurably influence the total depth of diffusion. The error occasioned by this factor is estimated in the next section. It should be remarked, however, that in most cases, the specimens were treated so as to approach equilibrium from both directions; i.e., precipitation from a supersaturated solid solution or partial solution in a completely precipitated structure. The copper-aluminum specimens were usually reheated at the successively decreasing temperatures of 490°, 440°, 350° and 250° C. and then were reheated at the same temperatures on a successively increasing scale. The data used to plot Figs. 2 and 3 were obtained in this manner, averaging the two diffusion-depth values obtained for a given concentration.

CALCULATION OF DIFFUSION COEFFICIENTS

Copper

The data (Fig. 2) for the diffusion of copper into aluminum and the known experimental methods show that the following limiting conditions were approximately true:

Letting x = distance from interface in centimeters for a given

c = atomic per cent copper,

c_0 = saturation solubility of copper in atomic per cent at the diffusion temperature,

t = time in seconds of diffusion,

1. When $x = \infty$ (here the radius of the aluminum rod), $c = 0$.
2. When $t = 0$, $c = 0$ for all values of x greater than 0.
3. When $x = 0$, $c = c_0$ for all values of t .

Simply, these conditions state that diffusion did not proceed to the center of the rod, that there was zero diffusion at the start and that the interface always remained saturated with solute atoms.

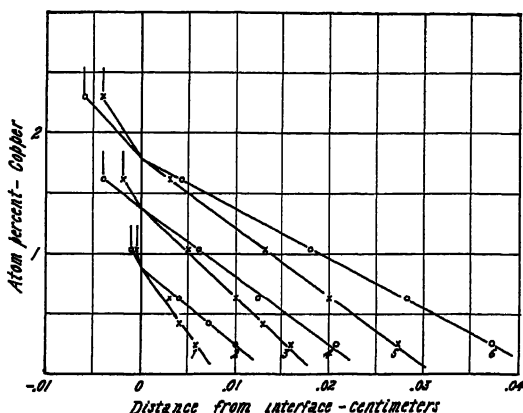


FIG. 2.—DEPTH-PENETRATION (OR $c-x$) CURVES FOR DIFFUSION OF COPPER INTO ALUMINUM.

- | | |
|---------------------|---------------------|
| 1. 78 hr. at 440°. | 4. 151 hr. at 490°. |
| 2. 185 hr. at 440°. | 5. 32 hr. at 540°. |
| 3. 75 hr. at 490°. | 6. 60 hr. at 540°. |

Mehl shows the following equation for the diffusion of solute atoms into a solvent lattice with the limits defined as above:

$$c = c_0 \left[1 - \phi \left(\frac{x}{2\sqrt{Dt}} \right) \right] \quad [1]$$

The letter D represents the diffusion coefficient expressed in square centimeters per second while ϕ is a quantity defined as the Gauss error function, described in mathematical tables as the probability integral. Employing this equation in the same manner as Freche, and using the data from the depth-concentration curves in Fig. 2, we have calculated the diffusion coefficients (Table 1).

The diffusion equation does not provide for any variation of D with concentration although progressively changing values of D with increasing values of x have been found in many diffusion systems. In connection with the diffusion of copper into aluminum, errors in the

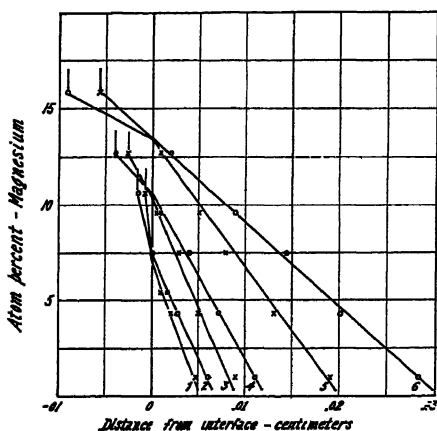


FIG. 3.—DEPTH-PENETRATION (OR $c-x$) CURVES FOR THE DIFFUSION OF MAGNESIUM INTO ALUMINUM.

- | | |
|---------------------|---------------------|
| 1. 110 hr. at 365°. | 4. 110 hr. at 400°. |
| 2. 158 hr. at 365°. | 5. 60 hr. at 440°. |
| 3. 60 hr. at 400°. | 6. 110 hr. at 440°. |

determination of D do not permit an evaluation of the relationship between D and c .

It is known that the value of the diffusion coefficient is related to the temperature of diffusion by the exponential equation:

$$D = Ae^{-\frac{b}{T}} \quad [2]$$

The logarithmic relationship between D and T is usually expressed by plotting the logarithm of D against the reciprocal of the absolute temperature.

TABLE 1.—*Diffusion of Copper into Aluminum*

Specimen No.	Diffusion		Precipitation		Co, Atomic Per Cent	C, Atomic Per Cent	Eutectic to Interface, Cm.	X, Cm.	$\frac{D}{\text{Sq. Cm. per Sec.} \times 10^{-9}}$	Q, Calculated ^a
	Time Hr	Temperature, Deg C	Time, Hr	Temperature, Deg. C.						
3B	32	540	2	490	2.29	1.61	0.004	0.003		
			8	440	2.29	1.02	0.004	0.013	1.26	
			10	400	2.29	0.64	0.004	0.020	1.48	
			50	250	2.29	0.30	0.004	0.027	1.38	31,400
2B	60	540	2	490	2.29	1.61	0.006	0.004		
			8	440	2.29	1.02	0.006	0.018	1.29	
			10	400	2.29	0.64	0.006	(0.028)	1.54	
			50	250	2.29	0.30	0.006	0.037	1.33	
5B	75	490	8	440	1.61	1.02	0.002	0.005		
			10	400	1.61	0.64	0.002	0.010	0.26	
			12	350	1.61	0.42	0.002	0.013	0.25	
			50	250	1.61	0.30	0.002	0.016	0.27	31,400
4B	151	490	8	440	1.61	1.02	0.004	0.006		
			10	400	1.61	0.64	0.004	0.012	0.19	
			50	250	1.61	0.30	0.004	0.021	0.23	
6B	78	440	8	400	1.02	0.64	0.0005	0.003	0.068	
			10	350	1.02	0.42	0.0005	0.004	0.043	
			50	250	1.02	0.30	0.0005	(0.006)	0.059	31,500
7B	185	440	8	400	1.02	0.64	0.001	0.004	0.051	
			10	350	1.02	0.42	0.001	0.007	0.055	
			50	250	1.02	0.30	0.001	(0.010)	0.068	

^a Q from slope of $\ln D$ vs. $1/T = 34,900$.

Langmuir and Dushman have proposed as a general diffusion equation:

$$D = \frac{Q}{Nh} d^2 \cdot e^{-\frac{Q}{RT}} \quad [3]$$

where D = diffusion coefficient, sq. cm. per sec.

Q = heat of diffusion, ergs per gram-mol

N = Avogadro's number = $6.06(10)^{23}$

h = Planck's constant = $6.55(10)^{-27}$ erg. sec.

d = interatomic distance (Al) = $2.85(10)^{-8}$ cm.*

R = gas constant, $8.31(10)^7$ ergs. per deg. C.

T = absolute temperature.

Mehl has employed this equation in numerous systems to calculate Q from one value of D . Comparison of equations 3 and 2 suggests that b , the slope of the $\ln D$ vs. $1/T$ curve, is equal to Q/R and hence Q may also be obtained from diffusion data at several temperatures. Mehl reports that in every case the best diffusion data are in accord with the Langmuir-Dushman equation.

In the present work, Q has been calculated by both methods. The Langmuir-Dushman equation gives a value of about 31,400 at each temperature while the slope of the $\ln D$ vs. $1/T$ line in Fig. 4 indicates a value of 34,900 cal. per gram-mol. It is believed that the former figure is more accurate since, for example, doubling the values of D at lower temperatures would alter the slope of the logarithmic relationship greatly but only very slightly affect the Q calculated from equation 3.

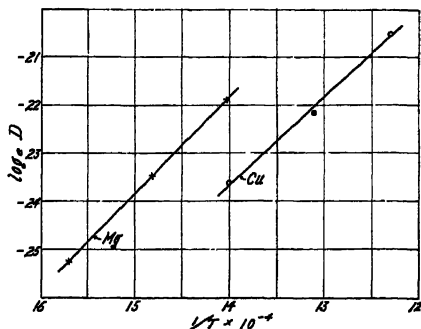


FIG. 4.—PLOT OF NATURAL LOGARITHM OF DIFFUSION COEFFICIENT D OF MAGNESIUM AND COPPER AS A FUNCTION OF THE RECIPROCAL OF THE ABSOLUTE TEMPERATURE T .

Magnesium

The diffusion data for magnesium and aluminum shown in Fig. 3 differ from the copper data in that here the eutectic has moved further away from the interface. Consequently, the interface does not remain at the saturation concentration for the diffusion temperature. This, it will be recalled, was one of the conditions required for the use of equation 1 in calculating the diffusion coefficient.

Some criticism may be directed at the use of this diffusion equation where one condition is not fulfilled. However, Van Orstrand and Dewey proposed the equation specifically for diffusion from a saturated solution containing undissolved solute (the concentration of which thus remains unchanged) into pure solvent. Freche employed the same equation for specimens somewhat similar in physical relationships to those in the present work in that undissolved solute atoms were present on one side of the interface. Although Freche does not plot the $c-x$ values back to

* Use of different values of d , depending on the change in lattice parameter of aluminum with solution of copper or magnesium, does not materially alter the Q values calculated from equation 3.

the interface, it seems certain that at the interface c did not equal c_0 . In all cases, the condition that the interface remain saturated seems to be physically impossible of realization. Excess solute atoms in the form of particles of undissolved compound (or element) cannot dissolve until the surrounding concentration falls below the saturation limit. Following this premise to its logical conclusion, it must be assumed that in all diffusion work it is probably impossible to maintain a saturated solid solution at the interface. With this justification, equation 1 has been employed for the magnesium-diffusion coefficient calculations.

From the results shown in Table 2, it is again impossible to evaluate the change in D with concentration or depth. The values of x for c equal to 1.0 atom per cent at any temperature of diffusion are only estimates based on the appearance of the specimen when polished. The lowest concentration of magnesium that could be determined by precipitation was 4.3 atom per cent. Beyond that, there was a zone hardened sufficiently by magnesium in solution to polish brightly while the pure aluminum was marked by adherent polishing abrasive.

The so-called heat of diffusion, Q , was again calculated both by the Langmuir-Dushman equation and from the slope of the $\ln D$ vs. $1/T$ line (Fig. 4). The values obtained, 29,000 and 38,500 cal., respectively, do not agree as well as in the copper-diffusion data. Again, the Langmuir-Dushman equation probably gives a value closer to the actual figure. A slight increase in the x values, and hence in the diffusion coefficients found at the lower temperatures, 400° and 365°, would bring the two sets of Q values into agreement.

It should be noted that the calculated heat of diffusion, or Q value, for copper is somewhat greater than that for magnesium. In other words, it would seem that magnesium diffuses more readily into aluminum than does copper. This result is contrary to the general rule that elements with the higher melting points will diffuse more readily into a given solvent. However, the diffusion-depth curves of Figs. 2 and 3 for penetration depths at 440° C. substantiate the relative diffusion rates of copper and magnesium as indicated by the Q values.

If magnesium diffuses more readily into aluminum than copper, the higher rate may possibly be attributed to its far greater solubility saturation concentration, 16.5 atom per cent at the eutectic temperature, while the maximum for copper at its eutectic point is only 2.4 atom per cent. At a given diffusion temperature in their respective alpha solution fields, the atomic solubility of magnesium in aluminum exceeds that of copper by a comparable amount. It may be suggested that the greater atomic strain inherent with a high concentration of solute atom, evidenced by a considerably greater change in the lattice parameter of aluminum, would result in a greater driving force towards diffusion between adjacent areas of different solute concentration. In comparing the diffusion of mag-

TABLE 2.—*Diffusion of Magnesium into Aluminum*

Specimen No.	Diffusion		Precipitation		Co, Atomic Per Cent	C, Atomic Per Cent	Eutectic to Interface, Cm.	X, Cm.	D, Sq. Cm. per Sec. $\times 10^{-10}$	Q, Calculated*
	Time, Hr.	Temperature, Deg. C	Time, Hr.	Temperature, Deg. C						
11B	60	440	2	400	15.7	12.7	0.006	0.001		29,000
			8	350	15.7	9.6	0.006	0.005	2.2	
			10	310	15.7	7.6	0.006	0.008	3.0	
			100	225	15.7	4.3	0.006	0.013	3.2	
					15.7	(1.0)	0.006	(0.019)	4.0	
12B	110	440	2	400	15.7	12.7	0.009	0.002		29,600
			8	350	15.7	9.6	0.009	0.009	3.9	
			10	310	15.7	7.6	0.009	0.015	5.8	
			100	225	15.7	4.3	0.009	0.020	4.2	
					15.7	(1.0)	0.009	(0.028)	2.9	
14B	60	400	8	350	12.7	9.6	0.003	0.0005		29,600
			10	310	12.7	7.6	0.003	0.003	0.75	
			100	225	12.7	4.3	0.003	0.005	0.63	
					12.7	(1.0)	0.003	(0.009)	0.60	
13B	110	400	8	350	12.7	9.6	0.004	0.001		30,300
			10	310	12.7	7.6	0.004	0.004	0.73	
			100	225	12.7	4.3	0.004	0.007	0.67	
					12.7	(1.0)	0.004	(0.011)	0.49	
16B	110	365	10	310	10.6	7.6	0.001	0.000		30,300
			50	250	10.6	5.4	0.001	0.001	0.03	
			100	225	10.6	4.3	0.001	0.002	0.07	
					10.6	(1.0)	0.001	(0.005)	0.11	
15B	158	365	10	310	10.6	7.6	0.002	0.000		30,300
			50	250	10.6	5.4	0.002	0.002	0.08	
			100	225	10.6	4.3	0.002	0.003	0.11	
					10.6	(1.0)	0.002	(0.006)	0.11	

* Q from entire slope of $\ln D = 1/T$ curve = 38,500 calories.

nesium and copper into aluminum, this increased driving force apparently somewhat overbalances the atomic size and other factors that tend to make copper diffuse more readily than magnesium.

DISCUSSION OF ERRORS

With reference to the significance of the results of the present study, it would seem appropriate to evaluate the experimental errors in relation to the previous calculations. The depth-concentration curves contain all of the significant data. In obtaining these, the solid solubility and therefore the concentration values in each system are well known for each temperature of reheating. The accuracy of temperature measurement and control during the precipitation treatment will determine, therefore, the extent of errors in the plotted c values. Generally, these

errors may be considered negligible, certainly in relation to others to be discussed.

It seems evident that the determination of the values for x represents the chief source of error. The time of reheating might well affect the completeness of precipitation and certainly the ease of reading the inner edge of the precipitated diffusion zone. Some specimens were reheated for further periods at the same temperature, to test whether precipitation had progressed to a greater depth. The heat-treatment periods listed in Tables 1 and 2 were such that precipitation was apparently complete at each temperature. Next, the accuracy with which the distance from the eutectic to the edge of precipitate could be read varied according to the temperature of precipitation, the quality of the subsequent metallographic polish and similar factors. It is estimated that the error in this reading was, under favorable conditions, about 10 per cent, although generally somewhat larger for low values of x .

Errors in the determination of the position of the original interface were of considerable importance in evaluating x . In most of the aluminum-magnesium diffusion specimens, this point was well marked in the microstructure (Fig. 1) and errors from this source would be about 10 per cent at intermediate points in the concentration range. In the aluminum-copper alloys, the interface was less often structurally marked, and, as determined from the reference marks, a somewhat larger error was encountered. It might be in the neighborhood of 20 per cent at intermediate values of c .

Earlier in the paper, some mention was made of a systematic error occasioned by further diffusion occurring during the precipitation heat-treatments. Obviously, this error does not exist at the highest precipitation temperature but somewhat increases the x values found at lower temperatures; i.e., lower concentrations. Thus the top of the diffusion c - x curves are unaffected but the lower portions may be placed somewhat too far to the right. It would be possible to apply a correction to the curves, knowing the diffusion data at each temperature. However, it was found that the correction would be small and, since this error is in the opposite direction to the normal error encountered in reading the edge of the low-temperature precipitates, no correction was applied to the c - x curves.

Another point of possible significance is the question of impurities. The aluminum used was 99.95 per cent Al for single crystals and 99.90 per cent Al for polycrystalline samples. In both, the chief impurities are iron and silicon. The 99.90 grade of aluminum had slightly more than double the amount of these two elements but there were no very marked differences in the diffusion rates of copper into the two grades of metal. The slight difference found may be attributed to grain size or to the impurities present.

The last source of error in measuring the penetration depth entered from an apparent anisotropy of diffusion encountered in aluminum-copper diffusion specimens. The structures that were found most frequently are reproduced in a later section. With the uncertainty occasioned by this at present unknown factor, the diffusion coefficients for copper must be considered as approximations, since there are unknown errors in the absolute values and a possible error of approximately 50 per cent in the relative values. The data for the diffusion of magnesium into aluminum are somewhat more favorable, in that the depth of the precipitate structures could always be definitely determined. The relative errors in this case may be about 25 per cent.

Always, of course, the calculated values for D depend on the method of calculation; i.e., whether the diffusion equation is appropriate for the given experimental conditions. There is some question about the use of equation 1 for the present diffusion data. The equation gives unsatisfactory D values when x approaches zero, since c does not simultaneously approach c_0 . In Tables 1 and 2, no D values are given for the highest temperatures of precipitation; i.e., when x approaches zero. Another equation similar to equation 1 has been employed for cases of diffusion across an interface in a system where the concentration at the further end of the enriched solution remains unchanged. In this case, $c_0/2$ is substituted for c_0 in equation 1. Again, the use of this equation in the present work leads to impossible results when x approaches zero.

DISCUSSION OF EXPERIMENTAL METHOD

The experimental approach employed in the present work, while based on sound metallographic principles, apparently has not previously been applied to diffusion studies. This is understandable in view of the necessary limitations involved. A good deal of the fundamental work on diffusion has naturally been done on systems exhibiting complete solid solubility at all temperatures. The present method is limited to systems of incomplete solid solubility, in which the solubility decreases markedly with temperature. At the same time, it must be remembered that systems in which this equilibrium condition exists are usually of considerable industrial importance.

The method of specimen preparation provides an unusually clean interface with a supply of solute atoms, which for practical purposes may be termed inexhaustible. The assumption has been made that the solution of solute atoms from excess compound into the momentarily slightly unsaturated solid solution in contact with it proceeds more rapidly than does diffusion from the saturated solid solution into the neighboring unsaturated area. While no proof exists in support of this assumption, similar assumptions as to the relative rates of solution and

diffusion exist in a large part of the data on diffusion for liquid solutions as well as for solid, metallic alloys.

It might seem that the method employed in the determination of depth-concentration curves is crude in comparison to some of the more elaborate methods employed in other work. While spectrographic, lattice-parameter, electron-diffraction and similar measurements are more spectacular, they need not be more accurate than the micrographic method within the experimental limitations of the latter. Furthermore, this method immediately gives information that may be overlooked or undetectable by other approaches. Specific cases that might be mentioned in this connection are data on grain-boundary diffusion, on the possible crystallographic anisotropy of diffusion rates and on recrystallization in diffusion zones under microscopic and macroscopic stresses. Indeed, use of the metallurgical microscope for research should require no defense in view of the significant and accurate micrographic determinations of solid solubility by Dix and collaborators, or the important, fundamental, micrographic studies of transformation rates by Bain, Davenport, Smith and others.

ANISOTROPY OF DIFFUSION

Mehl has remarked that diffusion might be expected to be anisotropic—i.e., the rate should vary with the crystallographic direction of diffusion—but that such an effect has not yet been experimentally observed in a cubic metal. In the present work, the diffusion of magnesium into aluminum seemed to be regular and even regardless of the crystalline orientation. However, the diffusion of copper into aluminum is marked sporadically by a pronounced, apparently anisotropic difference in rate with crystalline orientation. The effect is shown in the depth-concentration diffusion curve of a single crystal (Fig. 5). In the one specimen here represented, the apparent depth of penetration at higher concentrations was found to change gradually as the specimen was rotated. Penetration seemed to be uniform at low concentrations. The exact position of the original interface was not determined.

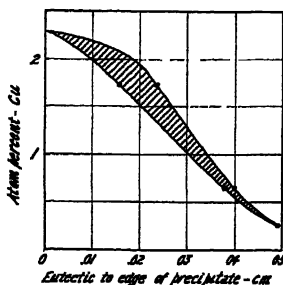


FIG. 5.—LIMITING PENETRATION DEPTH VARIATIONS AROUND THE PERIPHERY OF A SINGLE CRYSTAL OF ALUMINUM. DIFFUSION OF COPPER AFTER 200 HOURS AT 540° C.

was rotated. Penetration seemed to be uniform at low concentrations. The exact position of the original interface was not determined.

Fig. 6 shows a difference in penetration depth of copper into another single crystal of aluminum when reheated to bring out a low concentration level of copper, 0.7 wt. per cent. The direction of the CuAl_2 plates, precipitated on the (110) planes, is approximately parallel to the direction of diffusion in the specimen showing a deep zone and at 60° to the direc-

tion of diffusion in the shallow zone, about 120° around the edge of the specimen.

Similar effects are shown in some polycrystalline specimens (Figs. 7 and 8). Again the difference in penetration depth was found only at



FIG. 6.—DIFFUSION OF COPPER INTO SINGLE CRYSTAL OF ALUMINUM AFTER 20 HOURS AT 550° C. REHEATED AT 300° C. $\times 200$.

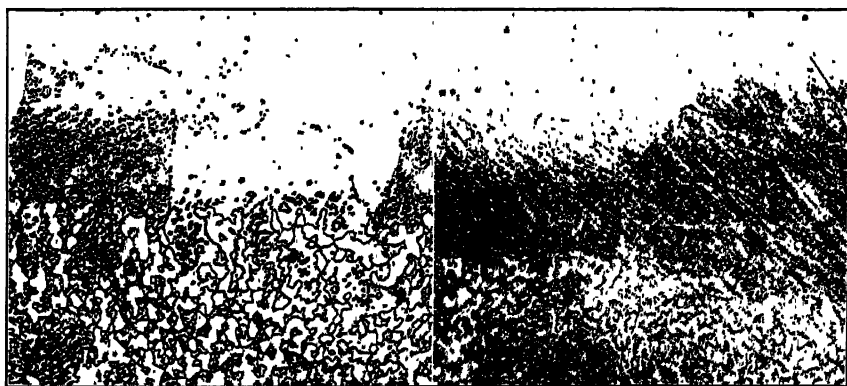


FIG. 7.

FIG. 8.

FIG. 7.—PRECIPITATE STRUCTURE IN COPPER-ALUMINUM DIFFUSION SPECIMENS.

FIG. 8.—PRECIPITATE STRUCTURE IN COPPER-ALUMINUM DIFFUSION SPECIMEN.

higher concentrations. On reheating at low temperatures, the differences were scarcely noticeable.

In spite of the micrographic evidence indicating an anisotropy of diffusion, the suggested effect cannot be evaluated or even definitely supported on these grounds. In single-crystal specimens, it was only occasionally noted. This may have been due to a fortuitous orientation of

the solvent lattice with respect to the interface, a relationship that has not yet been determined. Another source of doubt arises from the polycrystalline specimens. Micrographic fields as shown in Figs. 7 and 8 were found in about 50 per cent of the specimens examined. When similar samples were heat-treated at the same temperatures, some exhibited numerous fields with a peculiar, unresolved microstructure as shown in Fig. 8 but others showed a uniform penetration. Repolishing at a greater depth to eliminate the possibility of a surface effect from previous polishings did not alter the differences. There is a possibility that structures such as these originate in some unknown manner quite separate from actual precipitation. There must be stresses of considerable magnitude in the diffusion zone, originating in marked lattice-parameter variations within a narrow band together with unknown cooling stresses. It is possible that the total stresses are anisotropic and result in a related variation in solubility. At any rate, it is believed the micrographic evidence suggests an anisotropy of diffusion without offering substantial proof of the effect.

DIFFUSION-ZONE MARKINGS

Mehl¹ has pointed out that two types of distortion are created by the solid solution formation accompanying diffusion; a microscopic distortion characteristic of the solid solution state and a macroscopic distortion resulting from gross volume changes accompanying the penetration of solute atoms into regions of low concentration. He reports that the latter type of distortion may lead to some recrystallization and grain growth, and, as an example, shows recrystallization in regions where zinc has diffused into a bi-crystal of copper.

In the present work, when copper diffused into aluminum to a depth of 0.015 in. or more, two types of markings were sometimes found in the diffusion zone after precipitation of the CuAl_2 . They are shown in Fig. 9, where copper has diffused into a single crystal of aluminum, as a series of parallel lines across the diffusion zone and as an apparent recrystallization line at the inner limit of the diffusion zone. Fig. 10, a higher magnification of this latter part, seems to indicate that the directions of the CuAl_2 plates are approximately the same on both sides of the "recrystallization" line. In Fig. 11, another section of the same specimen, a small recrystallized zone is shown. The same area at a higher magnification in Fig. 12 again indicates that the CuAl_2 plate directions have not been altered by the apparent recrystallization. In addition, from the photomicrograph of Fig. 12, it is apparent that the "recrystallization" lines are made up of a series of CuAl_2 plates and that there is no visible grain-boundary line. There does not seem to have been any true recrystallization and the origin of the lines cannot be rationally explained. It seems very possible that these areas may be macromosaics formed by

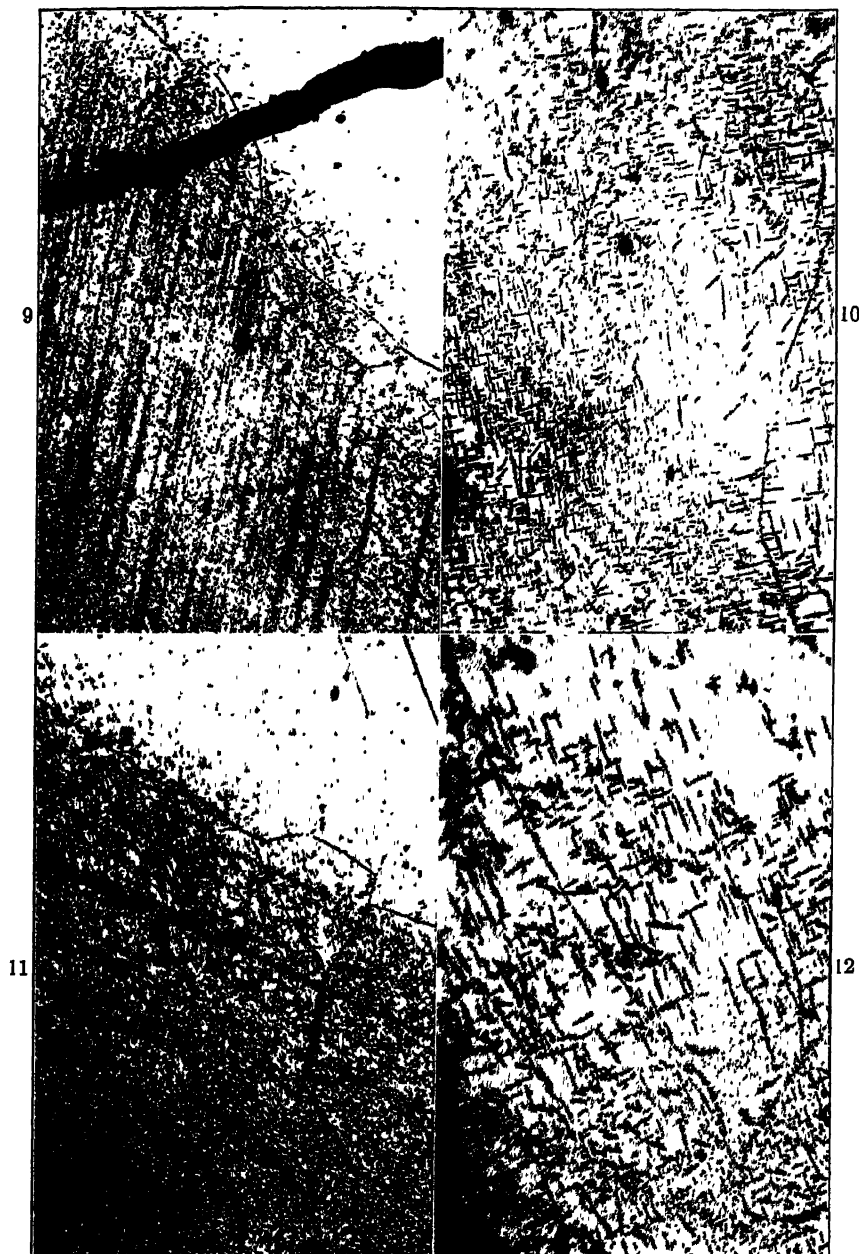


FIG. 9.—DIFFUSION OF COPPER INTO A SINGLE CRYSTAL OF ALUMINUM AFTER 10 DAYS AT 550° C., REHEATED AT 300° C. $\times 100$.

FIG. 10.—SAME AS FIG. 9, ENLARGED. $\times 500$.

FIG. 11.—SAME SPECIMEN AS FIG. 9, ANOTHER FIELD. $\times 100$.

FIG. 12.—SAME AS FIG. 11, ENLARGED. $\times 500$.

deformation under the lattice stresses during diffusion but the areas cannot be more than a few degrees away from the major orientation.

With regard to the straight parallel lines, again there is at present no rational explanation of their origin or presence in the structure, although it seems certain that they are crystallographically related to the matrix. It is apparent from Figs. 10 and 12 that the lines are made up of CuAl_2 plates, closely packed and for the most part at angles of about 55° and 35° to the direction of the lines. Also, when copper diffused into polycrystalline aluminum, parallel lines of closely packed CuAl_2 plates were found to end at the grain boundaries of the aluminum matrix.

One case of recrystallization as a result of diffusion distortion is shown in Fig. 13. A specimen of 5 per cent Cu aluminum alloy with very coarse

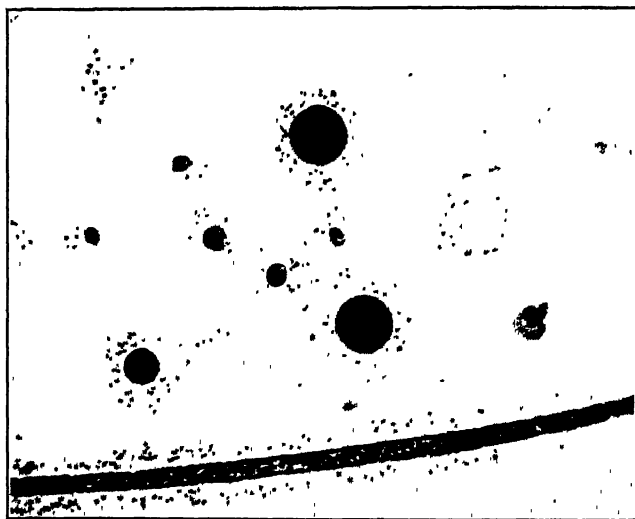


FIG. 13.—A 5 PER CENT COPPER-ALUMINUM ALLOY HOMOGENIZED AT 540° , HEATED 4 HOURS AT 600°C. , 2 HOURS AT 620° , QUENCHED, REHEATED AT 460° (COPPER OVER 3.0 PER CENT PRECIPITATED).

grains was homogenized at 540°C. , raised to 600°C. for 4 hr. and then to 620°C. for 2 hr. It was air-cooled, then reheated to 460°C. , at which temperature copper in solid solution in excess of 3 per cent is precipitated. Aside from the usual grain-boundary melting and pools of eutectic melted within the grains, it should be noted that new grain boundaries have been set up around the eutectic pools at about the 3 per cent Cu concentration limit and also through the grains.

SUMMARY

1. The diffusion of copper and magnesium into aluminum has been studied at various temperatures, employing specimens where a eutectic

of the solute and solvent metals was brought in clean and intimate contact with pure aluminum.

2. The depth-concentration relations in the diffusion zone were determined micrographically by reheating the specimens at temperatures of known solubility limits.

3. The diffusion coefficients were calculated and the change of the coefficient with temperature was noted. The heat of diffusion Q was calculated from the Langmuir-Dushman equation and from the slope of the $\ln D-1/T$ line.

	Copper			Magnesium		
	540° C.	490° C	440° C.	440° C.	400° C.	365° C.
D , sq. cm. per sec. $\times 10^{-10}$	13.8	2.4	0.57	3.2	0.64	0.11
Q (Langmuir-Dushman).....	31,400	31,400	31,500	29,000	29,600	30,300
Q ($\ln D-1/T$ line).....		34,900			38,500	

The relative Q values derived from the Langmuir-Dushman equation are considered to be more accurate.

4. Micrographic evidence was obtained which suggests a possible anisotropy of the diffusion of copper into aluminum. No crystallographic relationships were determined.

5. Several diffusion-zone structures, which showed straight-line markings and apparent lines of recrystallization, were examined, with the conclusion that no true recrystallization had occurred.

REFERENCES

1. R. F. Mehl: Diffusion in Solid Metals. *Trans. A.I.M.E.* (1936) **122**, 11.
2. A. Burkhardt and G. Sachs. Kupferdiffusion in plattier-schichten vergutbarer Aluminiumlegierungen. *Metallwirtschaft* (1935) **14**, 1.
3. H. R. Freche: Diffusion of Magnesium and Silicon into Aluminum. *Trans. A.I.M.E.* (1936) **122**, 324.
4. G. Grube and R. Haefner: *Ztsch. Elektrochem.* (1932) **38**, 835.
5. J. Cournot and E. Perot: *Compt. rend.* (1926) **183**, 1289; (1927) **184**, 1250.

DISCUSSION

(Georg Sachs presiding)

H. R. FRECHE,* New Kensington, Pa. (written discussion).—The subject of diffusion is important and fundamental in metallurgy. Accordingly, a report in which it has been attempted to work out the quantitative elements of diffusion of metal systems should be welcome to the metallurgist. The quantitative data given by Dr. Brick and Dr. Phillips are the only data so far published on the diffusion of magnesium and copper into aluminum from alloys saturated with respect to the diffusing metal.

*Aluminum Research Laboratories.

The method of procedure employed by the authors for the preparation of the diffusion samples, dipping hot aluminum rods into the molten eutectic, may have an appreciable effect on the subsequent diffusion of magnesium and copper into aluminum in the solid state. To be sure, the diffusion that occurred during the dipping of the aluminum rod into the eutectic melt was less than 0.0005 cm., but it was initiated and at a higher temperature than any of the diffusion temperatures studied. It is, of course, possible that the effects of this procedure on the ultimate experimental results are negligible, but it would be most interesting to know how these results would compare with diffusion data obtained from samples produced by effecting adherence between the aluminum and a copper-rich core in the solid state.

The micrographic method does not give directly a quantitative determination of the concentration of the diffusing element but requires interpretation. For example, what was selected as "the edge of the precipitated zone furthest from the eutectic . . ."? Does that edge refer to the particles precipitated within the grains or to the precipitate along the grain boundaries? It is, of course, a known fact and is also apparent from the splendid photomicrographs, illustrated by Fig. 1, that precipitated particles occur at a greater distance from the interface along grain boundaries than elsewhere.

Work done by Mr. Keller⁶ shows that the authors are correct in assuming that the reheating of the specimen effected further diffusion. It was shown that the diffusion zone effected by the migration of the copper, magnesium and silicon from the 17S-T core into the high-purity aluminum coating corresponded to 0.0025 cm. after 15 min. heating at 500° C. and to 0.010 cm. after 4½ hr. heating at the same temperature. In view of this, the amount of diffusion effected during the reheating of the samples to produce precipitation may become appreciable.

Finally, the depth-concentration curves should theoretically approach the x -axis asymptotically. All of the experimental curves in this paper appear to intersect the x -axis at finite values. This may not be the case. The method used by the authors has limited the results to a small range beyond the interface, and it is possible that the slope of the curve may change as the distance from the interface increases.

F. N. RHINES,* Pittsburgh, Pa.—Evidently, as the authors have pointed out, this very ingenious method of measuring diffusion coefficients is not capable of a high degree of precision, but its experimental simplicity is certainly a decided advantage over the schemes previously employed. Whereas the old system of measuring diffusion rates by the analysis of layers involves months of arduous labor, ultimately yielding values of a fairly high degree of accuracy, this new method gives a relatively quick means for obtaining somewhat less accurate diffusion coefficients.

The linear plots of composition versus distance from the interface seem to be a peculiar characteristic of this method of analysis. Other methods of investigation have shown the composition-distance curve to have a modified S form with the ends asymptotic to the distance axis. Where diffusion involves only a single phase the whole of the S-curve is realized, but when a second phase appears at the interface, only the lower half of the S is obtained. It is true, of course, that all of the published diffusion curves are nearly linear near the interface, but they begin to exhibit concavity long before they reach the zero composition value. Perhaps the present observations are the result of some sort of systematic error, such as the formation of precipitate particles too small to be detected at low concentrations of the diffusing element.

It may be of interest also in this connection to mention that the normal S-curves are not exactly symmetrical with respect to the interface. This means that the value

⁶ F. Keller: Diffusion of Zinc into Copper. *Trans. A.I.M.E.* (1929) **83**, 555.

* Metals Research Laboratory, Carnegie Institute of Technology.

of the diffusion coefficient is a function of the concentration of the diffusing element. In the course of measuring diffusion rates in a series of copper-base alloys, I have found that the diffusion coefficient may change as much as 10 or even 100 times over a concentration range of a few per cent. Thus the coefficients reported in the present paper should be understood to apply to only one concentration of copper or magnesium. The actual value of the reference concentration may be somewhat difficult to determine, but probably is not far from the c value selected for the analysis in each case.

I am particularly interested in the observation of what appears to be an anisotropy of the diffusion rate in some of the authors' samples, because I have sought in vain to find evidence of such a phenomenon in a number of the cubic metal systems. Is it not possible that this effect is more apparent than real, and that the appearance of a more advanced front of precipitation in some crystals than in their neighbors may simply be an optical effect resulting from a different orientation of the Widmanstätten pattern in each crystal?

R. F. MEHL,* Pittsburgh, Pa.—I should like to express my admiration for the ingenuity exercised by the authors of this paper. To be sure, their ingenuity has been demonstrated frequently in the past, but any new trick or short-cut method that will facilitate the derivation of diffusion data, even when only approximately, is especially to be welcomed in view of the great labor required for the more usual and direct methods. When the analysis is performed on a bar, and the diffusion occurs between the alloy core and a heavy plated coating—the usual way—a large number of samples for analysis must be machined from the bar and analyzed chemically. In one research program on this subject current in our laboratory, some six hundred analyses were required for a series of samples. Such work requires years to perform.

The depth-penetration curves shown in Figs. 2 and 3 are, of course, anomalous: these should not be straight lines but should approach the abscissas asymptotically as required by equation 1. This may be restated by saying that the concentration (ordinate) values near the abscissas are too low. Is it not possible that the precipitation at the low temperature, which gives these presumably low values, might have produced a precipitate too finely divided to be recognized in the neighborhood of the precipitation boundary measured, and thus an inferior depth of precipitation recorded equivalent to an inferior concentration?

It must be admitted that very little is understood about the factors that determine the relative diffusion coefficients in binary alloy systems. I have recently had occasion to summarize the information available on this point [*Jnl. Applied Physics* (1937) **8**, 174]. Various factors have from time to time been suggested: (1) it has been reasoned that the rate of diffusion should increase with smaller and smaller diffusing atoms; (2) it has been suggested that the rate of diffusion should become greater as the degree of solid solubility decreases; (3) it has been shown that in some systems the rate of diffusion is the greater the higher the melting point of the solute in comparison to that of the solvent; and (4) it has been shown that chemical, electrovalency effects are important. Exceptions obtain in every case except the last. It is certain that the mutual electrovalency effects are highly important, but it is difficult so to characterize the electrovalent properties of the various atoms in the solid state that predictions of relative diffusion coefficients can be made. The best that can be done is to state that the diffusion coefficient tends to increase with increasing distance of removal of the solute and the solvent elements in the periodic table. Many more data will have to be assembled before more definite conclusions can be drawn.

R. M. BRICK AND A. PHILLIPS (written discussion).—It is believed that the method chosen for a study of the relative diffusion rates of copper and magnesium into alumi-

* Metals Research Laboratory and Department of Metallurgy, Carnegie Institute of Technology.

num is a convenient and reasonably reliable approach to a type of investigation which thus far has developed no generally accepted experimental procedure. There are admittedly some factors of unknown significance associated with this plan of attack. These points have been considered in the pertinent discussions offered by Dr. Freche and Dr. Rhines and it seems unnecessary to add anything to their remarks. The subject of diffusion, metallurgically at least, has received its greatest impetus from Dr. Mehl and his co-workers and their future work will probably clarify many of the unanswered questions relating to this important subject.

Effect of Reversed Deformation on Recrystallization*

By PAUL A. BECK,† MEMBER A.I.M.E.

(New York Meeting, February, 1937)

It is well known that the hardness of metallic single crystals, like that of polycrystalline metals, increases during deformation (hardening by cold-work). It is also known that, as a consequence of deformation, the metallic material acquires an evident thermodynamic instability, revealed, for example, by the fact that the increased hardness gradually decreases with time, especially at elevated temperatures (softening by annealing). The temperature at which the stabilizing process begins is different for various metals, and for any metal it depends on the amount of deformation.

Such stabilization of deformed metals may proceed in two different ways: through recovery, and through recrystallization. The former process allows the unstable deformed metal body to approach stability gradually and without visible change in the grain structure; the latter process, like an allotropic transformation, yields directly the undeformed stable "phase" in the form of new undeformed crystals, which, starting out of a certain number of nuclei, grow into and "consume" the deformed hard material.

The extent of stability attainable through recovery is limited, especially if the deformation of the metal crystal or crystals involves not only the gliding along slip planes, but also the bending of the slip lamellae, or at any rate the bending of comparatively large parts of the crystal lattice. In such cases, for instance in bent single crystals or polycrystalline metals subjected to any deformation, recovery will not as a rule be able to restore the "straight" undeformed lattice, and stability can be attained only by recrystallization; that is, by the consumption of the bent crystal lattice parts by new, undeformed crystals—a much more drastic process. It is evident that the part of the surplus free energy stored in deformed crystals, which is present in the form of the elastic energy of the bent lamellae, is in these instances not considerably involved

The experiments were carried out by the author in collaboration with Prof. M. Polanyi, at the Kaiser-Wilhelm Institut für Metallforschung, Berlin-Dahlem, Germany, and some of the results are published in two articles in: (1) *Die Naturwissenschaften* (1931) 19, 505, and (2) *Ztsch. Elektrochem. angew. phys. Chem.* (1931) 37, 521. Manuscript received at the office of the Institute Dec. 23, 1936.

* Research Engineer at the Michigan College of Mining and Technology, Houghton, Mich.

in recovery. However, there has been much controversy among different authors as to the role of such bending in recrystallization.

Polanyi and E. Schmid found¹ that in single crystals of tin that have been deformed by strain in tension, recrystallization occurred preferably in those portions of the specimens where the bending of the lamellae is most pronounced. This observation is of particular interest because the portions of the specimens in which the lamellae were restraughtened in the course of straining in tension did not show recrystallization in spite of their higher deformation and hardening. Consequently, Polanyi considered the bending of the lamellae as specifically responsible for recrystallization. Experiments by Czochralski on aluminum single crystals exposed to torsion and partial retorsion seemed to confirm this view^{2,3}.

A contrary view, however, has resulted from investigations into the recrystallization of polycrystalline metals. The results of these investigations, expressed, for instance, in the well-known Czochralski diagrams and in the "hardening rule" (*Verfestigungsregel*) of van Arkel^{4,5}, show that in polycrystalline metals the number of grains formed by recrystallization increases continuously with increasing deformation (Czochralski) or with the hardening (van Arkel). Furthermore, van Arkel and Ploos van Amstel⁶, repeating the original experiment of Polanyi and Schmid with single crystals of tin, found that nuclei of recrystallized grains are preferably formed in that part of the specimens where *hardening* is most pronounced. This observation is contrary to that of Polanyi and Schmid. On the basis of this experiment van Arkel has maintained that in single crystals, as well as in polycrystalline metals, the number of recrystallization nuclei formed after a certain deformation depends directly on the hardening produced by the deformation.

On the other hand, Polanyi and Beck^{7,8} found, in working with bent single crystals of aluminum, partially restraughtened before recrystallization, that the recrystallization power is diminished, and sometimes nullified, in the restraughtened part even though the hardness in that part is further increased. The *decrease* in recrystallization power is accompanied by an *increase* in hardness in the restraughtened part. This is in apparent contradiction to the views of van Arkel.

Burgers^{9,10} admits Polanyi's explanation—that the decrease of recrystallization power on restraughtening is due to a decrease of stress content in the bent lattice. He believes, however, that the bending here involved is that of the "local curvatures" and not the bending of the comparatively large lattice parts in the lamellae. An attempt to settle this divergence of opinions will be made in the present article.

DEFINITION OF RECRYSTALLIZATION POWER

Some confusion seems to have been due to lack of agreement among authors as to definitions and nomenclature; let us consider first what has

¹ References are at the end of the paper.

really been measured. As mentioned above, recrystallization is similar to the "heterogeneous" type of allotropic transitions in so far as it consists of the formation of nuclei and of their growth. The two characteristic factors of such transformations are: (1) the capacity of the unstable phase to form nuclei of the stable phase (number of nuclei*); (2) the capacity of the unstable phase to be consumed by the stable phase (as measured, for instance, by the velocity of growth of the new crystals). These two factors react very differently to changes in the conditions of transformation, as has been well known since the classical researches of Tammann, and should be determined separately. Now what has actually been determined in the experiments of van Arkel and his collaborators and of Burgers and his collaborators is, strictly speaking, neither of these factors but is the size or number of the fully developed new grains. It is evident, however, that a certain grain size can be obtained by various combinations of factors 1 and 2, and that a certain change in grain size can be accounted for in general by a change in either one or in both. Consequently, without further data or assumptions, no quantitative determination of either of these factors can be made by measuring the grain size alone. In the articles of van Arkel and his collaborators, changes in grain size are referred to as changes in the number of nuclei. Variations in factor 2 are, obviously, assumed to have practically no influence on the grain size.† Karnop and Sachs¹¹ have found that an increase in deformation as small as 1 per cent results in doubling the velocity of growth of the new crystals in deformed polycrystalline aluminum. Even though analogous changes can be expected to be smaller in deformed single crystals, van Arkel's assumption is not at all obvious and should not be made without further examination.

It is clear that "recrystallization power" can be correctly characterized only in terms of data obtained by independent determination of the two factors: number of nuclei, and "consumptibility"‡ of the deformed crystal. Such independent determination has been made by Polanyi and Beck for consumptibility in bent and restraightened single crystals.

* The term "number of nuclei" is applied here in a general sense, and it is doubtful whether it can be interpreted, according to Tammann's usage, as the rate of formation of nuclei. Present evidence tends to show that in recrystallization there is first a definite incubation period during which practically no nuclei are formed, and, second, an apparent recovery which in the later stages of heating decreases the rate of formation of nuclei.

† Neither this assumption nor the reasons for making it seem to have been stated explicitly by van Arkel. Burgers explicitly makes this assumption¹⁰, but does not give the reasons for it.

‡ Consumptibility is used here as a measure of the tendency of the deformed crystals to be consumed by the growing new grains.

In this work the relative thickness of the layer of new crystals formed by recrystallization of the sample is used as a measure of the consumptibility of bent single crystals. It is, of course, not directly equal to the velocity of growth in a homogeneously deformed medium; it is rather an indication of the deformation value* (in terms of per cent of the maximum

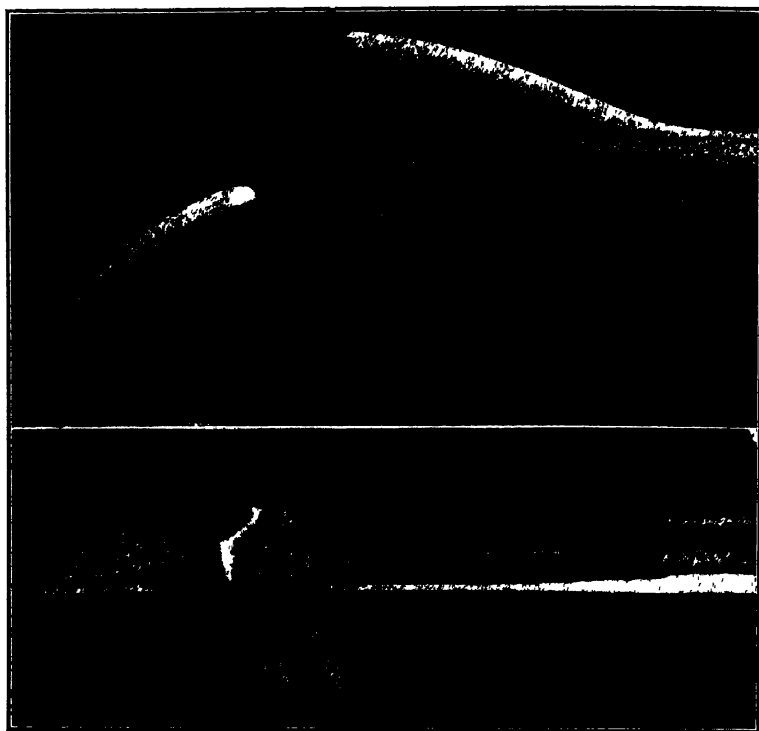


FIG. 1.—PARTLY RESTRAIGHTENED SAMPLE AFTER RECRYSTALLIZATION. RECRYSTALLIZED LAYER PARTLY REMOVED.

Side view (upper picture) shows thickness of recrystallized layer in bent part (left side), in restraightened part (extreme right) and in transition part.

deformation in the outermost part of the sample) at which the velocity of growth becomes practically zero under the specific deformation conditions prevalent in the sample. Important is the fact that *consumptibility*, as defined here, is *entirely independent of the number of nuclei in the above sense*.

* Here deformation value means the percentage of axial elongation, or compression, in a certain layer of the bent crystal. It has been found with aluminum crystals that for all layers of a certain bent crystal this value is approximately proportional to the distance of the layer from the neutral zone. Perpendicular cross sections, marked on the surface of the cylindrical crystal, remain after bending radial plane sections. Maximum elongation occurs in the outermost layer of the crystal and can be calculated from the diameters of the crystal and of the curvature. Hereafter in this paper, the value referred to as deformation is taken to be this maximum elongation.

The physical existence of a well defined, sharp boundary of consumptibility in bent crystals is shown in the following experiments.

Cylindrical single crystals of aluminum (impurities: silicon 0.15 per cent, and iron 0.28 per cent) were produced by the recrystallization method. The crystals were bent to different curvatures, heated for recrystallization, and then etched. Fig. 1 shows such a recrystallized sample; in it the boundary surface between the deformed crystal and the new crystals is made visible by the removal of some of the new crystals. This surface is found to be everywhere perpendicular to the plane of bending (plane containing the middle line of the sample and the radius of curvature of the bending). The cross section of a recrystallized sample, like that of Fig. 1, is shown in Fig. 2. The diameter d of the cylindrical sample was kept constant in all experiments at 4.23 ± 0.02 mm. The consumptibility was calculated according to the formula

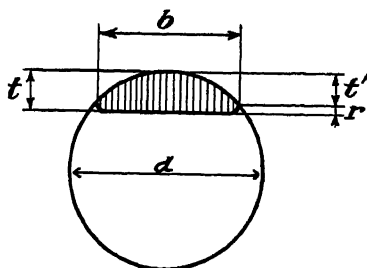


FIG. 2.—CROSS SECTION OF A RECRYSTALLIZED SAMPLE. THE SHADED AREA REPRESENTS THE CROSS SECTION OF THE RECRYSTALLIZED NEW CRYSTAL.



FIG. 3.

$V = t/d$. The depth of the recrystallized layer t was calculated by adding 0.2 mm. to the measured depth t' , in order to correct for the small error due to the rims formed on both sides of the new crystals (Fig. 3). The elevation of this rim, r , was always found to be approximately 0.2 mm. When the depth was very small, the actual measurement was preferably

made of the width, b , of the new crystals; from this width the depth was then calculated.

Fig. 4 shows a typical recrystallized sample, consisting of three distinct layers of uniform thickness. The most severely deformed extreme layers on the inner and on the outer side are recrystallized, and consist of several undeformed individual crystals of different orientations; in the medium layer the deformed lattice of the original bent single crystal still

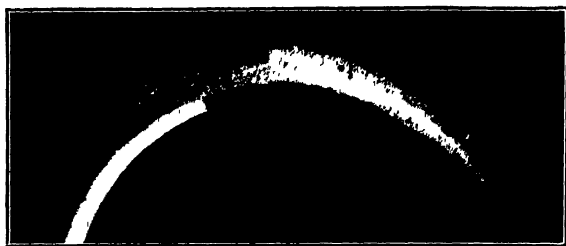


FIG. 4.—TYPICAL RECRYSTALLIZED SAMPLE.

persists. The uniform thickness of the recrystallized layers in such samples shows that the *consumptibility of the bent crystal does not depend on the orientation of the new crystals*.

A crystal 36 cm. long was cut in four parts of 9 cm. each (a , b , c and d). Every crystal part was subjected to the same amount of bending and was heated at 620°C . for 6 to 120 min. The result of this experiment is shown in Table 1. It can be seen that *consumptibility practically does*

TABLE 1.—*Consumptibility as a Function of Time at Temperature of Heating*

Crystal, Part	Duration of Heating, Min.	Consumptibility
a	6	0.43
b	12	0.43
c	34	0.43
d	120	0.45

not depend on the duration of heating; the new crystals grow to full size in less than 6 min. and do not grow further even during a period 20 times as long.

Three pieces of a long crystal were subjected to the same amount of deformation and were recrystallized at different temperatures. Table 2 shows that in a temperature range of approximately 100°C . *consumptibility is practically independent of the recrystallization temperature*.

Three pieces of a long crystal, subjected to the same amount of deformation, were heated to 640°C . at different rates of heating in order to study the effect of the preceding recovery. The specimens were placed in the furnace at the lower temperatures of the intervals indicated in

TABLE 2.—*Consumptibility as a Function of Temperature of Heating*

Crystal	Recrystallization Temperature, Deg C	Consumptibility
<i>a</i>	550	0 26
<i>b</i>	594	0 26
<i>c</i>	646	0 28

Table 3, and heated to the higher temperatures in 30 min. The initial temperature for samples *b* and *c* was well below the recrystallization temperature. The table shows that the *consumptibility is only very slightly decreased by recovery*.

TABLE 3.—*Consumptibility as a Function of Rate of Heating*

Crystal	Temperature Interval, Deg C.	Consumptibility
<i>a</i>	640–640	0.41
<i>b</i>	480–640	0.39
<i>c</i>	320–640	0.38

Another experiment gave the same result. One piece of a crystal was first heated for 30 min. at 400° C. for recovery and was then recrystallized at 640° C. Another piece of the same crystal, which had previously been subjected to the same deformation but not heated for recovery, was also recrystallized at 640° C. These two samples were then compared, and no noticeable difference in the consumptibilities was found. On the other hand, the number of grains seemed to have a tendency to decrease when the recrystallization was preceded by recovery.*

In bent single crystals there is a very well defined, sharp lower limit of the temperature of recrystallization. Fig. 5 shows the result of an experiment carried out with four pieces of a single crystal. After being subjected to the same deformation (10.8 per cent) they were heated to different temperatures for 30 min. Consumptibility rose within an interval of 12° C. from zero to 80 per cent of its final value. It was shown that the

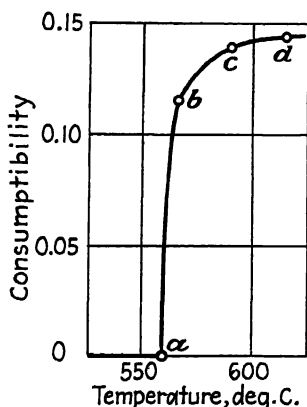


FIG. 5.—CONSUMPTIBILITY AS A FUNCTION OF RECRYSTALLIZATION TEMPERATURE.

* These results are consistent with those of Kornfeld and Pawlow¹². These authors measure the consumptibility of the deformed material as the velocity of growth of the new grains and show that it is practically unchanged by recovery. The effect of recovery is manifested only by an increase of the incubation period of the nuclei (by decrease of the velocity of formation of the nuclei).

absence of recrystallization in sample *a*, heated to 559° C., was not due to the absence of nuclei. In this sample artificial inoculation was made by scratching (a strong deformation confined to a very small part of the specimen);* thus the formation of nuclei upon heating was secured. The observed absence of recrystallization was therefore entirely due to the absence, in this case, of consumptibility. The "artificial" nuclei were unable to grow.

CHANGES DUE TO RESTRAIGHTENING

Let us consider now the changes in these factors due to restraighening. It was shown by Polanyi and Beck^{7,8} that if a part of a bent crystal is restraighened the consumptibility of the restraighened part will be smaller than that of the bent part of the sample. Consumptibility decreases by restraighening, though the hardness, increased by bending, further increases. Fig. 1 shows such a partly restraighened sample after recrystallization, the recrystallized layer having been partly removed. The side view (upper picture) shows the thickness of the recrystallized layer in the bent part (left side), in the restraighened part (extreme right), and in the relatively short transition part between them. These three stages are all incorporated in the long new crystal partly separated from the mother crystal, shown on the right side of Fig. 1. They can be clearly seen as a variation in thickness of this crystal in the side view (upper picture), and as a variation in width of the crystal, in the top view (lower picture).

On the other hand, the interesting investigation by Burgers^{9,10} proves that, although in his conception of a plastically deformed crystal the "local curvatures" are fundamentally connected both with hardening and with recrystallization power, an exact parallelism cannot be expected between these two properties in the sense that for a given crystal a definite shear hardening corresponds to a definite recrystallization power. This result, which was assumed to be in agreement with the experimental results of Polanyi and Beck, actually does not seem to bear any direct relation to them, because what Burgers means by "recrystallization power" is the number of nuclei, whereas the data given by Beck and Polanyi relate to consumptibility. Burgers supported his theoretical results by experiments; in interpreting his experiments he assumed that the number of grains actually measured was equal to the number of nuclei involved in his theory.

The bent and partly restraighened samples of Polanyi and Beck give information about effect of reversed deformation not only on the consumptibility but also on the number of grains formed by recrystallization. While the thickness of the crystals in the recrystallized layer is a measure

* This method of artificial inoculation was first given by van Arkel and van Bruggen¹¹.

of the consumptibility, the length of the new crystals (their dimension in the direction of the axis of the sample) is equal to the grain diameter in the ordinary sense. It has been found in many tests that the number of grains also decreases by restraughtening,* as does the consumptibility. There are, however, certain crystal orientations for which this is not true.† Fig. 6 shows a sample in which the decrease in consumptibility by restraughtening is accompanied by an increase in the number of grains. The photograph represents the inner side of the bent part (at the right) and the corresponding side of the restraughtened part (at the left). It can be seen that the wide, and consequently deep-grown, new crystals in the bent part are long, but that the much thinner new crystals in the

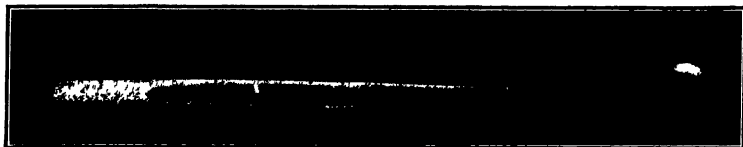


FIG. 6.—SAMPLE IN WHICH DECREASE IN CONSUMPTIBILITY IN RESTRAUGHTENING IS ACCOMPANIED BY INCREASE IN NUMBER OF GRAINS.

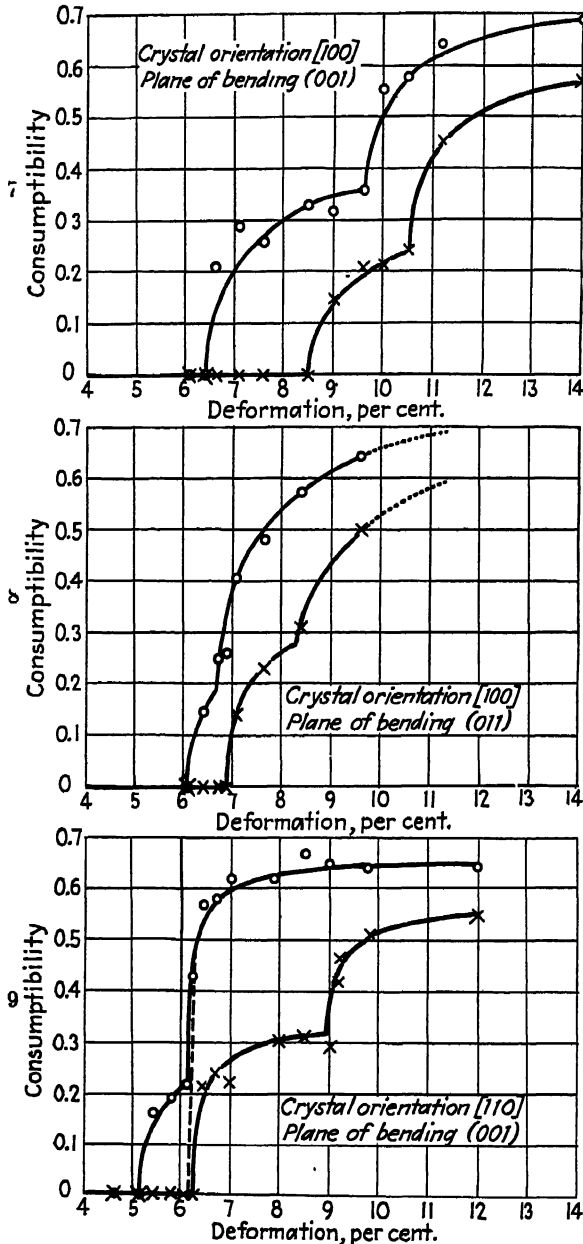
Inner side of bent part (right) and corresponding side of restraughtened part (left).

restraughtened part are short and numerous. This sample proves the necessity for careful discrimination between the two factors of "recrystallization power"—the number of grains and the consumptibility.

While the situation is rather complex with regard to the number of grains, the consumptibility always has decreased in restraughtening. Figs. 7, 8 and 9 show the effect for different orientations of the deformed crystal and of the plane of bending. The crystal orientations were determined by P. W. Bridgman's method. Fig. 7 represents a case where the axis of the samples corresponds to the [100] direction of the crystal, and the plane of bending to the (001) plane; in that shown in Fig. 8 the sample axis is [100] again, but the plane of bending is (011). The samples represented in Fig. 9 are oriented to the [110] direction, and bent in the (001) plane. The orientations here given are "ideal orientations" approximated by the real crystals used. However, the actual orientations of the individual crystals were varying in a certain range, a fact that accounts for the irregularity of the measured values. The irregularity in the data of these experiments is much more pronounced than in those of the experiments described above, where pieces of the same crystal were used. In each figure the points indicated by circles represent the consumptibilities of the bent crystals for different values of the bending. Recrystallization starts first (for small deformations) on only the inner or the outer side of the sample (depending on the orientation), and begins

* This has also been found in torsion and retorsion, by van Arkel and van Bruggen.¹⁴

† The theory of Burgers seems to allow for the dependence upon the orientation of the effect of reversed deformation on the number of "nuclei."



FIGS. 7, 8, 9.—CONSUMPTIBILITY AS A FUNCTION OF DEFORMATION, FOR DIFFERENT CRYSTAL ORIENTATIONS. THE UPPER CURVE, IN EACH FIGURE, REPRESENTS THE CONSUMPTIBILITY OF THE BENT CRYSTALS, THE LOWER CURVE THE CONSUMPTIBILITY OF THE BENT AND RESTRENGTHENED CRYSTALS.

Circles represent consumptibilities of bent crystals, crosses indicate consumptibilities of parts bent and then restrengthened.

on the opposite side at some higher deformation value. For the sake of conciseness the consumptibilities of both sides are added together and represented in a single curve. Each curve, therefore, is composed of two parts, one corresponding to recrystallization on one side only and the other corresponding to recrystallization on both sides, the two being separated by a pronounced break in the curve. The points indicated by crosses represent the consumptibilities of the parts bent to various extent (the abscissas give the deformation values corresponding to the respective bending) and then restraightened. The two curves corresponding to recrystallization on the inner and on the outer side are again united and represent the total effect.

Fig. 7 shows that with that particular orientation there is no recrystallization at all up to a deformation of 6.4 per cent. In the range from 6.4 to 8.5 per cent deformation, the inner side of the bent part of the

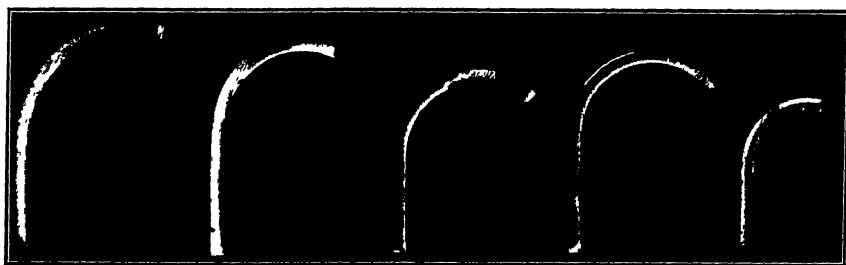


FIG. 10.—FIVE CHARACTERISTIC RANGES.

crystals recrystallizes, but the restraightened parts do not recrystallize at all. In the range between 8.5 and 9.6 per cent deformation the restraightened part also recrystallizes on the same side, though its consumptibility, of course, is still smaller. Between 9.6 and 10.5 per cent, the outer side of the bent part of the crystals also recrystallizes, but there is no recrystallization on the corresponding side of the restraightened part. At still higher deformation values both the inner and the outer sides of both the bent and the restraightened parts recrystallize; but the consumptibilities are smaller in the restraightened part. One sample of each of these five characteristic ranges is shown in Fig. 10. The situation is similar with the two other orientations examined, except that, in these latter, recrystallization starts on both the inner and the outer side of the bent part before it appears in the restraightened part. There are also some differences in the critical deformation values for the three orientations: the $[100] (001)$ needs the largest amount of deformation for recrystallization; the $[110] (001)$, the smallest; and the $[100] (011)$, a deformation value between the two.

The figures show that for all orientations and for all deformation values examined, the consumptibility of the restraightened part is smaller than that of the crystal just bent to the same extent but not restraightened.

The orientation [110], (001) offers a peculiarity worth mentioning: at small deformations, below about 6.2 per cent, recrystallization proceeds only when there is artificial inoculation. In the first experiments, without inoculation, a curve corresponding to the dotted line in Fig. 9 was found. This seems to be the only case of recrystallization so far encountered in which there is a definite consumptibility but no nuclei, a condition similar to that of an undercooled or superheated phase. The difference between the behavior of the two factors—number of nuclei, and consumptibility—should be noted with reference to what has been said earlier in this paper.

It is interesting that where recrystallization occurs only after inoculation, the number of grains appears to have no relation to the number of nuclei. In fact, in almost every such sample the whole recrystallized layer consists of one large crystal only, while in the immediate vicinity of the inoculating scratch an immense number of very small crystals (about 0.1 mm. ϕ) appears, a fact that shows the formation of a large number of nuclei. A great difference between the velocity of growth of the individual nuclei formed seems to exist in this instance.

Finally, mention should here be made of an experiment in which fine-grained polycrystalline samples were subjected to bending, to partial restraughtening and to recrystallization. An analogous decrease in the depth of the recrystallized layer was found as a consequence of restraughtening.* The sharpness of the boundary of consumptibility is smaller in this case than in single crystals, of course, because the consumptibility is different for grains of different orientation, and consequently varies from grain to grain in the polycrystalline sample.

CONCLUSIONS

Considering the results of this investigation, the present status of experimental facts and of basic conceptions in connection with the effect of reversed deformation on recrystallization of single crystals may be summarized, in the author's opinion, as follows:

1. There is no direct physical relation between hardening and recrystallization. While the "hardening rule" of van Arkel is probably a very convenient statistical rule in practical mill operations with polycrystalline metals, it has been shown theoretically by Burgers that hardening bears no direct physical relation to the formation of nuclei, and experimentally by Polanyi and Beck that hardening, as such, is fundamentally unrelated to consumptibility.

2. According to Burgers the formation of nuclei is in immediate physical relation with the "local curvatures" existent in the deformed crystals, especially with those of the highest degree of bending. This

* The effect of inverse deformation in polycrystalline material has been studied by Karnop and Sachs¹⁵ and by van Arkel and van Bruggen¹⁴.

conception involves the dependence of the *number of nuclei*, for a certain value of hardening, on the specific distribution of the total deformation over the different slip systems of the crystal and thus on the orientation of the deformed crystal. Actual experimental determination of the effect of reversed deformation on the number of nuclei has not been made.

3. Experimental evidence (Beck and Polanyi, van Arkel and van Bruggen) relating to the effect of reversed deformation on the *number of grains* shows a general tendency of decrease, but some characteristic exceptions indicate the necessity of a more thorough investigation of these complicated relations.

4. *Consumptibility* is decreased by reversed deformation for all orientations and deformation values examined (Beck-Polanyi).

5. The contradiction between the experimental results obtained by Polanyi-Schmid on the one side and by van Arkel-Ploos van Amstel on the other side, relating to the recrystallization of tin crystals, may be due to differences in the impurities in the metals used, and/or to the complicated laws governing the formation of nuclei referred to above. Consequently these observations, which were limited to a very small number of samples, hardly prove anything at all, and certainly do not allow any conclusion regarding the consumptibility.

6. The apparent contradiction between the view formulated by Polanyi, that "recrystallization power" depends on the bending of the slip lamellae, and the view of Burgers, that it depends on the existence and quality of local curvatures, is not really a contradiction; the term "recrystallization power" is used by Polanyi in the sense of consumptibility, while it is defined by Burgers as the number of nuclei and is measured by him as number of grains. Furthermore, it is quite probable that both Polanyi and Burgers are right, consumptibility depending mainly on the bending of larger parts of the lattice (lamellae) and the formation of nuclei being bound to the existence of local curvatures. In fact, in some characteristic cases the reaction of the consumptibility toward restraighening is very different from that of the number of grains (as reflected in Fig. 6). This fact proves that these two factors are fundamentally related to different structural qualities of the deformed crystal. The independence of consumptibility from recovery supports Polanyi's view that consumptibility is related to the bending of comparatively large lattice parts, or lamellae, because the decrease in the bending of such parts during recovery may be expected to be very small (as pointed out in the introduction to this article). On the other hand, the decrease in the number of grains by recovery can be attributed to a decrease in the number of nuclei, for there is no reason to suppose an increase by recovery of the velocity of growth. The decrease in the number of nuclei by recovery would be in agreement with the view of Burgers that the nuclei are physically related to local curvatures, provided the plausi-

ble assumption is allowed that the effect of recovery on the bending of local curvatures is relatively larger than on the bending of the lamellae.

In certain cases it is evident what is meant by bent lamellae and by local curvatures; however, it should be noted that in others an exact discrimination seems to be much more difficult.

REFERENCES

1. M. Polanyi and E. Schmid: *Ztsch. Physik* (1925) **32**, 684.
2. J. Czochralski: *Proc. Int. Cong. Appl. Mc.*, Delft (1924).
3. J. Czochralski: *Ztsch. Metallkunde* (1925) **17**, 1.
4. Van Arkel: *Ztsch. Physik* (1927) **42**, 795.
5. Van Arkel: *Ztsch. Physik* (1928) **51**, 534.
6. Van Arkel and Ploos van Amstel: *Ztsch. Physik* (1930) **62**, 46.
7. Polanyi and Beck: *Die Naturwissenschaften* (1931) **19**, 505.
8. Polanyi and Beck: *Ztsch. Elektrochem. angew. phys. Chem.* (1931) **37**, 521.
9. W. G. Burgers: *Ztsch. Physik* (1933) **81**, 43.
10. W. G. Burgers: Internat. Conference on Physics, London, 1934.
11. Karnop and Sachs: *Ztsch. Physik* (1930) **60**, 464.
12. Kornfeld and Pawlow: *Physik. Ztsch. Sow.* (1934) **6**, 537.
13. van Arkel and van Bruggen: *Ztsch. Physik* (1927) **42**, 795.
14. van Arkel and van Bruggen: *Ztsch. Physik* (1933) **80**, 804.
15. Karnop and Sachs: *Ztsch. Physik* (1928) **52**, 301.

DISCUSSION

(D. E. Ackerman presiding)

R. F. MEHL,* Pittsburgh, Pa.—There has been a great deal of work on the preferred orientations generated in metal aggregates by cold-work and on the recrystallization orientations that form from these preferred orientations on annealing; but one basic problem remains entirely unsolved—namely, what the relationships of these two orientations are and what mechanism in changing from one to the other may be. In some cases the recrystallization orientations are identical with the initial preferred orientations, but in others, as in copper, the two orientations are quite different. We lack utterly a crystallographic growth mechanism that will explain the latter case; in fact, we are much in need of a basic idea to apply to this problem. It seems likely that experiments on the recrystallization of deformed single crystals might furnish orientation relationships simple enough to lead the observer to the proper basic conception of the mechanism. I should like to ask whether Dr. Beck has determined the orientation relationships between the new grains on the surface of his single-crystal specimens and the original single crystals.

R. F. MILLER,† Kearny, N. J.—In regard to Dr. Mehl's comment, I should like to add that when a zinc single crystal has been deformed to produce twinning and subsequently allowed to recrystallize at 200° C., all the resulting polycrystals disclose one of three types of preferred orientation. One orientation is derived from the original single crystal and the other two are directly inherited from the two sets of twins produced by the drastic deformation. This marked preferred orientation¹² indicates

* Metals Research Laboratory and Department of Metallurgy, Carnegie Institute of Technology.

† Research Laboratory, U. S. Steel Corporation.

¹² R. F. Miller: Creep and Twinning in Zinc Single Crystals. *Trans. A.I.M.E.* (1936) **122**, 188, Fig. 13.

that the nuclei for recrystallization are in the twins and not at random in the twin boundaries.

C. H. MATHEWSON,* New Haven, Conn.—I have been trying to think of some shorter and pleasanter word than consumptibility, but have not been able to find any, so I am led to ask whether it has been possible, by any form of bending or manipulation of the specimen, to induce this "tendency to be consumed" to vanish, so that the awkward word may be removed entirely?

One other thing—I wonder whether the author has any opinion (doubtless he has thought about it) on the bearing of these results on the fundamental question of deformation as to whether something does or does not happen to the atom. Doubtless it is difficult to get a very close connection here, but it would appear that the recrystallization behavior is dependent upon distortion effects that can be removed, by reverse bending, for example, and cannot be explained purely on the basis of the primary slip phenomena of gliding.

C. S. BARRETT,† Pittsburgh, Pa.—I should like to express admiration for the beautiful simplicity of these experiments and the amount of data obtained from them. But at the same time, I wonder whether the nonuniformity of deformation is not a drawback. The magnitude of the difference in consumptibility that is observed in these experiments may be very much limited by the fact that the center of the bent rods receive much less deformation than the outside. Perhaps more homogeneous deformation might be worth while.

R. F. MEHL.—I should like to ask Dr. Beck whether the results of his work are similar to those obtained on the recrystallization of alternately compressed and elongated specimens.

S. L. HOYT,§ Milwaukee, Wis.—I should like to ask if the crystals you have described here have been examined by X-ray methods to at least record the data that are available by X-ray analysis.

R. F. MILLER.—In my experiments on the elongation of aluminum single crystals, from 0 to 5 per cent extension and from room temperature to 300° C., and in creep tests on ductile zinc single crystals in the same temperature range, there was no evidence of recrystallization and the deformation followed the normal laws for crystal glide.

P. A. BECK (written discussion).—There is no doubt as to the fundamental importance of the experiments suggested by Dr. Mehl in his first remark. Some years ago Burgers attempted to determine the orientation relations between the recrystallized grains and the deformed matrix in a compressed aluminum single crystal. He also developed a theory regarding the mechanism of the formation of recrystallization nuclei. References to his work have been given in the paper. We have not attempted to attack this problem in connection with the work described above, since our aim has been a quite different one; namely, *the separate determination of the effect of reversed deformation on the two factors of "recrystallization power"*: on the number of recrystallized grains, and on consumptibility. However, without having made any measurements, and judging merely by looking at the deep-etched specimens, it seems to me that there is no well developed or consistent preferred orientation of the new grains. The orientations of the individual recrystallized grains are scattered over a rather wide

* Professor of Metallurgy, Yale University.

† Metals Research Laboratory, Carnegie Institute of Technology.

§ A. O. Smith Corporation.

range in both the bent and the restraightened parts of our samples; they are different from each other, and also from the orientation of the matrix crystal.

As to the remarks of Dr. Barrett, may I say that our experiments having been directed toward the specific goal described above, the type of deformation was chosen accordingly. I do not believe that the magnitude of the effect was very much (or to any extent at all) limited by the nonuniformity of the deformation, and cannot perceive any serious drawback, for our purposes, due to this nonuniformity. On the other hand the method has considerable advantage—for instance, simplicity—as had been pointed out already by Dr. Barrett. The reversed deformation can be carried out easily, and the samples allow conclusions as regards both factors: the number of grains, and the consumptibility. These questions have been discussed in the paper itself.

The term "consumptibility," to which Professor Mathewson has objected, is certainly not a short and pleasant one, but unfortunately I have not been able as yet to find a better one. As has been shown in the paper, there is a range of deformation for each orientation, in which the consumptibility is entirely nullified by restraightening. This range, however, is not large enough to warrant the entire removal of the clumsy term itself.

I am sorry but obliged to say that our experiments and results do not seem to possess much bearing on the question as to whether something does or does not happen to the atom during deformation.

Concerning Dr. Mehl's second question, I would like to state that, so far as I know, there has been no investigation on the recrystallization of single crystals subjected alternatively to homogeneous compression and elongation. The only recrystallization experiments using homogeneously compressed and elongated samples are those by Karnop and Sachs, referred to in the paper. However these authors used polycrystalline specimens, and consequently their results are, strictly speaking, not comparable with ours.

Karnop and Sachs found that the reversed deformation has: (1) increased the lowest temperature of recrystallization, and (2) increased the number of recrystallized grains. The first effect may be attributed to either one or to both of the following reasons: (a) reversed deformation raises the temperature of the formation of nuclei; (b) reversed deformation raises the temperature at which the nuclei are able to grow—that is, for a given temperature of annealing, it decreases the consumptibility. Of these two explanations, (a) is certainly not contradictory to our results, and (b) would closely correspond to that, what we have found for single crystals.

The second effect found by Karnop and Sachs corresponds to what we have found for a certain crystal orientation (Fig. 6), and it is in disagreement with what has been found for single crystals of other orientations.

The X-ray investigation suggested by Dr. Hoyt has not been carried out with our samples, though this would be interesting to do. An earlier experiment of Czochralski, referred to in the paper, shows that the Laue asterism caused by torsion of an aluminum single crystal is decreased by re-torsion.

Studies upon the Widmanstätten Structure, IX—The Mg-Mg₂Sn and Pb-Sb Systems

BY GERHARD DERGE,* ARTHUR R. KOMMEL,* JUNIOR MEMBERS, AND ROBERT F. MEHL†, MEMBER A.I.M.E.

(New York Meeting, February, 1937)

THE orientation relationships resulting from allotropic transformations and the formation of segregate structures in metals and alloys have been the subject of the eight earlier papers in this series¹. A brief summary of orientation studies has also been given by Sachs². A survey of these papers discloses that the factors that determine the orientation relationship of a precipitated phase to its parent solid solution, as well as the outward form and appearance of the new phase, are not completely understood. It is now evident that crystallographically analogous systems, as a rule, exhibit the same type of Widmanstätten figure and orientation relations, so that useful information is not to be expected from examination of a new alloy involving lattice combinations of which the orientation relationships are already known. Therefore, the determination of the relations existing between lattice types that have not already been studied seems to be the most promising mode of attack upon the problem; both of the systems reported in this paper represent new combinations of lattice types.

A. THE Mg-Mg₂SN SYSTEM

The magnesium-tin equilibrium diagram given by Hansen³ shows the phase Mg₂Sn to be the only intermediate phase. The solid solubility of Sn in Mg decreases from 14.8 weight per cent at the eutectic temperature, 561° C., to 2.3 per cent at 450°, while no solid solubility of Mg in Mg₂Sn has been observed. The crystal structure of Mg is close-packed hexagonal with $a_0 = 3.202 \text{ \AA}$. and $c_0 = 5.199 \text{ \AA}$.⁴, while Mg₂Sn is of the CaF₂ type with $a_0 = 6.78 \text{ \AA}$., with four molecules in a unit cell^{5,6}.

Alloys from two different sources have been used: (1) those supplied by the Dow Chemical Co., which contain 6 and 8 weight per cent Sn, and (2) those prepared in this laboratory, containing 8 and 13.5 per cent Sn. The latter were made from Dow high-purity Mg and Baker chemically

Manuscript received at the office of the Institute Jan. 16, revised May 10, 1937.

* Metals Research Laboratory, Carnegie Institute of Technology, Pittsburgh, Pa.

† Director, Metals Research Laboratory and Head, Department of Metallurgy, Carnegie Institute of Technology, Pittsburgh, Pa.

¹ References are at the end of the paper.

pure Sn, melted in iron crucibles under Dow Flux Number 21; the Sn was added to molten Mg. Large grains suitable for X-ray analysis were prepared by the strain-anneal technique developed for Mg solid solutions by Schmid and Seliger⁷.

The plane of precipitation of Mg_2Sn in the Mg matrix was determined by the usual method of combining direction-frequency counts with X-ray orientations of the matrix on a stereographic projection (see ref. 1, pt. I). The orientation of the matrix was determined by the Davey-Wilson method, using copper radiation.

The most complete study was made with alloys containing 8 per cent Sn, in which the Widmanstätten figure was developed by homogenizing

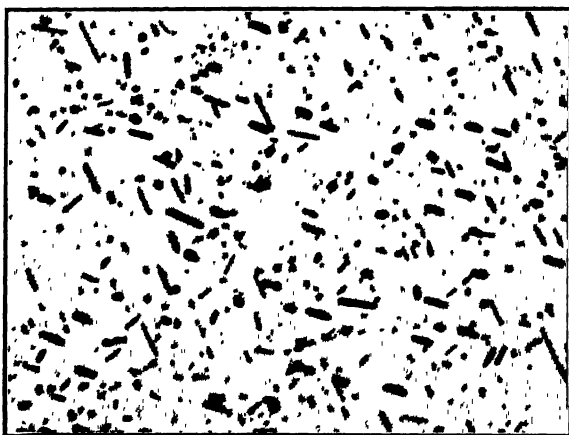


FIG. 1.—WIDMANSTÄTTEN FIGURE OF ALLOY OF MG WITH 8 PER CENT SN. $\times 680$. Heat-treatment: cooled slowly from 560°C . Etchant 0.5 N HCl.

just below the eutectic temperature, cooling to 400° in 8 hr., and furnace-cooling to room temperature in 24 hr. The solid solubility of Mg_2Sn in Mg precludes the possibility of precipitation above 500° in alloys of this composition. The microstructure produced is shown in Fig. 1. Six different grains from alloys of type 2 and one of type 1 were analyzed. Two specimens of type 2 were sectioned so that two perpendicular faces could be examined. Thus a total of nine direction-frequency plots were made, of which four showed seven distinct maxima, four showed six, and one only five. Fig. 2 is the stereographic projection showing the normals to these directions on a surface A (full straight lines), the normals to the directions found on the surface perpendicular to A (dotted great circles), and the $\{10.1\}$ and $\{00.1\}$ poles of the matrix as found by X-rays; the surface A is the plane of the projection. The manipulations involved in such a projection have already been described (ref. 1, pt. I). It is evident that the directions of the precipitate plates can be explained by precipitation on the $\{10.1\}$ and $\{00.1\}$ planes of the matrix. Similar

treatment of the other frequency plots led to the same result, and no other satisfactory solution was found. Precipitation on the basal plane was found in every instance; when fewer than seven directions were observed, traces of two different planes of precipitation were found to be parallel in the polished section.

Two other examples of plate formation on more than one family of planes have been described (ref. 1, pt. III), and in one of these examples it was found that as the alloy content increased the amount of precipitation on the second family of planes also increased. The same effect might therefore be expected in the Mg-Sn system. However, alloys with 6 per cent Sn were identical with the 8 per cent material in this respect.

When alloys containing 13.5 per cent Sn were given the same heat-treatment the Widmanstätten pattern was not as well developed, and the plates were smaller; accordingly, direction-frequency counts were not accurate. In the three grains studied, 8, 12 and 14 directions were observed, and these, with one exception, could be explained by plate formation parallel to the $\{00.1\}$, $\{10.1\}$ and $\{10.2\}$ planes of the matrix. This precipitation on an additional plane led to an investigation of structures developed at other temperatures.

A photomicrograph furnished by Dr. Gann, of the Dow Chemical Co., at the beginning of this research showed plates in one direction only. This was an 8 per cent alloy that had been water-quenched from 470°C . and aged for 72 hr. at 250°C . When the 13.5 per cent Sn alloys were quenched from the eutectic temperature and aged at 250°C ., a very well developed Widmanstätten pattern with practically all plates in one direction was developed (Fig. 3). This structure can be explained only by precipitation on the basal plane, and this was confirmed by X-ray analysis.

It is therefore possible to control the plane of precipitation by heat-treatment; at 250° plate formation is parallel to the $\{00.1\}$ plane only, at temperatures between 250° and 500° plates form parallel to the $\{10.1\}$

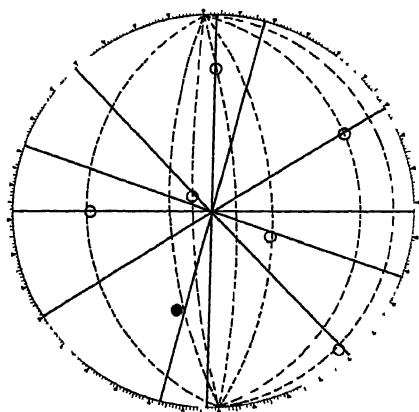


FIG. 2.—STEREOGRAPHIC PROJECTION OF NORMALS TO TRACE DIRECTION IN ALLOY OF Mg WITH 8 PER CENT Sn.

Heat-treatment: cooled slowly from 560°C .

Full lines are normals to trace directions in the surface of the projection.

Dashed great circles are normals to trace directions in surface normal to plane of projection.

Open circles, $\{10.1\}$ poles of matrix.

Filled circle, $\{00.1\}$ pole of matrix.

planes also, while when precipitation begins at 560° (in alloys with higher Sn contents) plates form parallel to the $\{10.2\}$ planes as well as those already listed. The implications of this phenomenon will be discussed later.

The slowly cooled 13.5 per cent alloys were used to determine the orientation relationships between the matrix and the precipitate. Davey-Wilson photograms of 11 large grains were made with a Weissenberg camera, using copper radiation. In solving these complex films the following procedure was used: The matrix orientation was first deter-



FIG. 3.—WIDMANSTÄTTEN FIGURE OF ALLOY OF Mg WITH 13.5 PER CENT Sn. $\times 400$.
Heat-treatment: quenched into ice water from 560° C., aged 80 hr. at 250° C.
Etchant 0.5N HCl.

Polycrystalline specimen, showing a single plate direction in each grain.

mined stereographically, then all the precipitate spots that could be definitely identified on both the stationary and oscillating films were plotted on the same stereographic projection. The interplanar angles between these precipitate poles were then measured from the projection and when two or more poles had the proper angles for a single cubic crystal, the corresponding orientation was plotted in relation to that of the matrix. Results from the 11 films are given in Table 1, in which the first column describes the orientation relationship that was found to exist between the two lattices, the second column lists the number of times this relation was observed, and the third column gives the number of Mg_2Sn reflections upon which each individual Mg_2Sn orientation was based. Thus relation 1 was found for only one precipitate orientation, which was derived from five Mg_2Sn reflections, but it was also found for

four different precipitate orientations which were each derived from four Mg_2Sn reflections. In describing the orientation relationships, the directions are those that lie in the plane specified.* Thus, by relation 1, a (111) plane of Mg_2Sn lies parallel to a (00.1) plane of Mg oriented in such a way that a [110] direction in this (111) plane is parallel to a [10.0] direction in the (00.1) plane.

TABLE 1.—*Orientation Relationships*

Orientation Relationship	Number of Examples	Number of Mg_2Sn Reflections upon Which Each Example Is Based	
ALLOYS COOLED SLOWLY FROM 560° C.			
1	$\{111\} // \{00.1\}$ $[110] // [10.0]$	1	5
		4	4
		3	3
		4	2
2	$\{110\} // \{00.1\}$ $[110] // [10.0]$	2	3
		2	2
3	$\{110\} // \{00.1\}$ $[110] // [11.0]$	1	3
		2	2
4	$\{211\} // \{00.1\}$ $[111] // [10.1]$	2	2
ALLOYS QUENCHED INTO ICE BRINE FROM 560° C., AGED 80 HR. AT 250° C.			
1	$\{111\} // \{00.1\}$ $[110] // [10.0]$	1	2
2	$\{110\} // \{00.1\}$ $[110] // [10.0]$	1	3
5	$\{111\} // \{00.1\}$ $[110] // [11.0]$	2	4
		2	3
		1	2

There can be little question concerning the reality of relationship 1. It is equally certain that another relationship exists in which a (110) plane of Mg_2Sn is parallel to the basal plane of Mg, for this is apparent on several of the films; but whether the complete relationship is that of 2 or 3, or whether both exist, is uncertain. The tabulated X-ray evidence somewhat favors relation 2. Relation 4 will not be considered further,

* The Miller-Bravais system of hexagonal notation has been used. For a description of this notation see E. Schmid and W. Boas⁸.

because the evidence in its favor is so slight. Since precipitation has been found on three different groups of planes, it is to be expected that more than one orientation relationship exists.

Hoping to connect each possible orientation relation with a definite plane of precipitation, four grains of the 13.5 per cent Sn alloy, which had been treated so that all plates were parallel to the basal plane only, were studied. The results from four different grains are given in the lower part of Table 1. Some evidence for both relations 1 and 2 was found, but the new orientation relation 5 was also very prominent. It seems certain that this relation 5 is the correct one for plates parallel to the basal plane when formed by the heat-treatment specified.

DISCUSSION OF RESULTS

Widmanstätten structures already studied have served to emphasize the importance of matching of atomic positions on conjugate planes in determining orientation relationships. The matching resulting from the orientations observed by X-rays has been determined for all three planes upon which plates have been observed, but only those that appear favorable will be described.

Relation 1.—The small, filled circles of Fig. 4 represent the positions of atoms on the basal plane of the Mg lattice, while the open circles represent the Sn atoms on an octahedral plane of the Mg_3Sn lattice, and the open circles marked plus and minus are the Mg atoms in this lattice that lie in planes 0.97 \AA , above and below the (111) plane respectively; all of these Mg_3Sn positions are superimposed on those of the basal plane of the matrix as specified by relation 1. The (111) Mg_3Sn is thus considered as a single warped plane, which really includes three parallel planes of atoms. These arrays are very much the same when aligned in this way. A 12.7 per cent shrinkage of the interatomic distance of 5.5 \AA . to 4.8 \AA . is the largest change of dimensions required and is well within the tolerance limits that have been found in other oriented segregate structures.

This relationship is also such that a $\{201\}$ plane of the precipitate lies within 5° of a $\{10.2\}$ plane of the matrix. When the atomic positions of the two lattices on these planes are plotted, no striking similarity of pattern exists; however, the atomic densities on these planes are very nearly the same, and it is conceivable that the thermal vibrations of the lattice near the eutectic temperature are of sufficient magnitude to allow the formation of nuclei with this orientation relationship.

If this orientation is compared with that found in crystallographically similar systems, it is seen that face-centered cubic lattices are related to hexagonal close-packed lattices by the condition of relation 5, while body-centered cubic lattices are related to hexagonal by the condition of

relation 1. The Mg_2Sn lattice is a face-centered cubic lattice of Sn atoms with eight Mg atoms within each unit cell; evidently with proper heat-treatment these Mg atoms cause precipitation to occur by a body-centered rather than a face-centered cubic mechanism.

Relation 2.—The atomic plot for the conjugate (110) and (00.1) planes of this relation is shown in Fig. 5. It is evident that these arrays are very similar and that very little atomic motion could be required for the

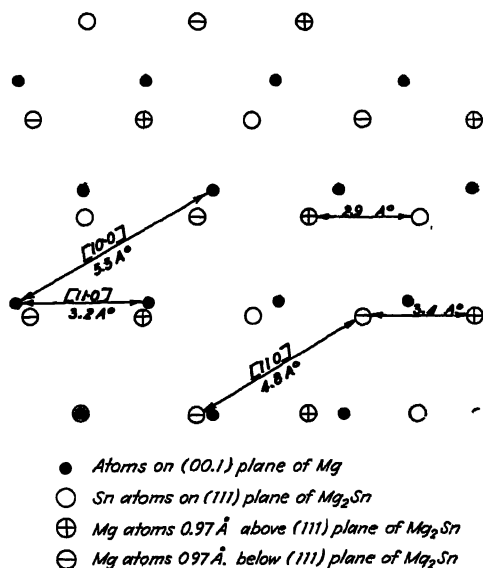


FIG. 4.—ATOMIC MATCHING ON (00.1) PLANE OF Mg BY RELATION 1.

formation of nuclei of the precipitate with this orientation; a 9.4 per cent contraction, from 3.2 Å. to 2.9 Å., is the greatest dimensional change.

This relationship is such that a (110) pole of the Mg_2Sn lattice lies within 5° of a (10.1) pole of the matrix. The corresponding plot of atomic positions, Fig. 6, shows a close similarity between the two planes oriented in this manner, and it is reasonable to account for the plates parallel to the {10.1} planes in this way.

Relation 3.—The plot of atomic positions for this orientation shows no similarity between the two phases on any plane of precipitation. On the basis of atomic matching this orientation is excluded.

Relation 5.—This relation has been found only in specimens aged at 250° after quenching, so that it may definitely be related to plates parallel to the basal plane formed at 250°. The atomic matching is satisfactory.

The combined information derived from X-ray studies and atomic matching therefore indicates that plates may form parallel to the {00.1} planes with orientation relationships 1 and 2, parallel to the {10.1} planes

with relation 2 only, and parallel to the $\{10.2\}$ planes with relation 1 only, when alloys are cooled slowly from the eutectic temperature; but when

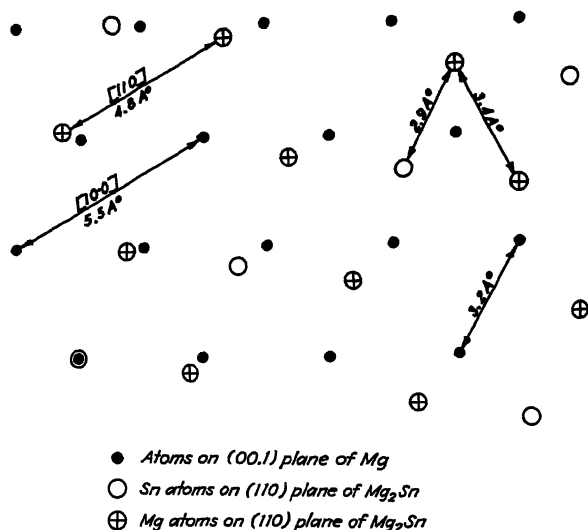


FIG. 5.—ATOMIC MATCHING ON (00.1) PLANE OF Mg BY RELATION 2.

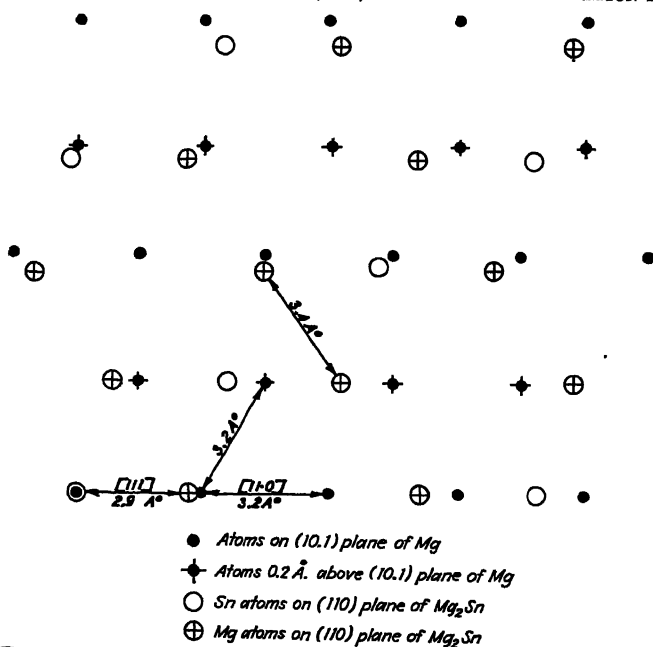


FIG. 6.—ATOMIC MATCHING ON (10.1) PLANE OF Mg BY RELATION 2.

quenched and aged at 250° C. plates form parallel to the basal plane only, predominantly with relation 5.

The formation of plates parallel to different planes of the matrix, varying with the heat-treatment given the sample, is of special interest. It has been observed⁸ that below 200° C. slip in Mg occurs on only the {00.1} planes, while above this temperature slip occurs on the {10.1} and possibly the {10.2} planes, these effects becoming prominent above 400°. Twinning also occurs on the {10.2} planes. It has already been demonstrated¹ that plate formation does not necessarily take place upon the slip planes of the matrix. It should be pointed out, however, that precipitation mechanisms may be described as shearing processes in the matrix lattice. It is probable that when factors of atomic matching are favorable for more than one relation, the mechanism that shall operate will be determined by the shearing properties inherent in the lattice; thus in Mg alloys different mechanisms might be expected to operate at different temperatures, corresponding to the different slip processes effective at these temperatures, and experiments show that this is exactly what happens.

It might be postulated that quenching strains caused slip on the basal plane, which induced plate formation parallel to this plane only in the alloys aged at 250° C. The marked tendency for precipitation to begin on slip planes has often been demonstrated⁹. However, Köster's photomicrographs¹⁰ also establish that precipitation, even though it starts at the slip plane, proceeds by the mechanism characteristic of the unstrained system. It has also been shown that when precipitation is initiated by strains induced by twinning, the normal Widmanstätten mechanism still operates (see ref. 1, pt. I, discussion by C. S. Smith). There is, therefore, justification for believing that the plane of precipitation is controlled by temperature only. Such an influence of temperature upon Widmanstätten mechanism was also observed in Fe-Ni alloys (ref. 1, pt. VIII), and in this case also the effect may possibly be related to the type of shear to be expected at the temperature in question.

The change in the plane of precipitation effected by a change in the temperature of aging suggests interesting possibilities for research. It is possible that the precipitation of a single phase upon different planes may be characterized by different mechanisms whose rates have different temperature coefficients, and, furthermore, that the properties developed in the precipitated (aged) alloy may also be quite different. Differences in the anisotropy of the elastic properties and of tensile strength of single crystals of such alloys might well be observed; the significance of such observations for the slip-interference theory of hardening is obvious. More than one type of slip plane has been reported for Al¹¹, and by inference we might expect to discover that certain aluminum alloys might show a multiple effect such as that reported here for Mg-Sn alloys; furthermore, that such alloys might show interesting variations in aging rates and in physical properties.

B. THE Pb-Sb SYSTEM

Since no Widmanstätten pattern involving a rhombohedral phase has been examined crystallographically, the Pb-Sb system was selected for study. Pb has a face-centered cubic lattice with $a_0 = 4.92 \text{ \AA}$., while Sb is rhombohedral with $a_0 = 4.50 \text{ \AA}$., $\omega = 56^\circ 37'$, and $\mu = 0.466^{12}$. This is a simple eutectic system (ref. 3, 985) with the solid solubility of Sb in Pb decreasing from 2.94 weight per cent at the eutectic temperature, 247° C ., to 0.24 per cent at room temperature. The solid solubility of Pb in Sb has not been well established but is apparently of the same order.

Experiments designed to produce Widmanstätten patterns were successful only with the Pb-rich alloys. Only a very small amount of precipitate was formed in these alloys; consequently there appeared to be little possibility of obtaining complete orientation relationships between the two phases. For this reason only the plane of precipitation of Sb in Pb was determined.

The alloys were made from commercial sheet Pb and C. P. grade Sb from the Fisher Scientific Co. The sample used was a 100-gram melt, 96.65 per cent Pb and 3.35 per cent Sb, prepared in a graphite crucible under a flux of the mixed chlorides of Na, K, Ba and Mg. Slow cooling produced suitably large grains, which subsequently were homogenized for 120 hr. at 242° C ., then cooled to 145° C . over a period of 42 hr. and finally furnace-cooled to room temperature. The Widmanstätten pattern produced by this treatment is shown in Fig. 7.

Direction-frequency counts made on ten of these grains showed four or fewer maxima for a single crystal, which in itself is convincing evidence that the Sb plates have formed on the $\{111\}$ planes of the Pb matrix (ref. 1, pt. I). The orientations of five of these grains were determined by the Davey-Wilson method and then related to the trace directions. Fig. 8 is one example of such a stereographic plot. In all of these cases the precipitate directions could be explained satisfactorily by the $\{111\}$ poles of the matrix, and by no other poles, offering conclusive proof of plate formation on the $\{111\}$ planes.



FIG. 7.—WIDMANSTÄTTEN FIGURE OF ALLOY OF Pb WITH 3.3 PER CENT Sb. $\times 600$. Polished with MgO , not etched. This area includes only a part of one grain.

DISCUSSION

Knowing that Sb precipitates by the formation of plates parallel to the $\{111\}$ planes of the Pb solid solution, it is possible to postulate the orientation relationship between these phases from considerations of atomic matching. The atoms on the $\{111\}$ planes of Pb are disposed in an array of equilateral triangles with an interatomic distance of 3.49 Å. The atoms on the $\{001\}$ planes of Sb are disposed in an array of isosceles triangles with the angle at the vertex equal to $56^\circ 37'$; the interatomic distance on the equal sides is 4.50 Å, while on the base it is 3.56 Å. Therefore, if these two lattices are related to each other so that $(111)\text{Pb} \parallel (001)\text{Sb}$, $[110]\text{Pb} \parallel [100]\text{Sb}$, an Sb nucleus could form on a (111) plane of the solid solution matrix with a very slight displacement of the atoms from their normal positions in the face-centered cubic lattice, and it is highly probable that this is the relationship that exists.

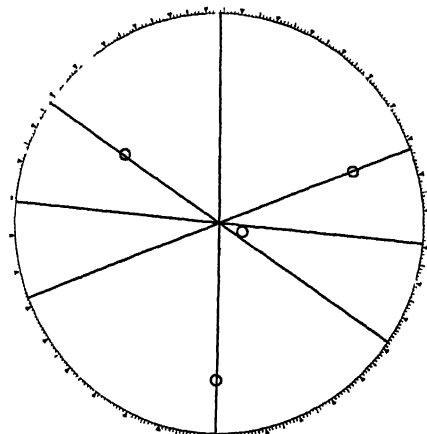


FIG. 8.—STEREOGRAPHIC PROJECTION OF NORMALS TO TRACE DIRECTIONS IN ALLOY OF FIG. 7.

Open circles are $\{111\}$ poles of matrix.

SUMMARY

1. Mg_2Sn with a CaF_2 type of lattice precipitates from its solid solution in the close-packed hexagonal Mg lattice as plates parallel to the $\{00.1\}$, $\{10.1\}$ and $\{10.2\}$ planes of the matrix.

2. It is possible to eliminate the formation of plates on the $\{10.1\}$ and $\{10.2\}$ planes by aging at 250°C . rather than slow cooling from 560°C .

3. Three orientation relationships exist between these lattices:

- a. $\{111\} \parallel \{00.1\}$ and $[110] \parallel [10.0]$
- b. $\{110\} \parallel \{00.1\}$ and $[110] \parallel [10.0]$
- c. $\{111\} \parallel \{00.1\}$ and $[110] \parallel [11.0]$

4. The different precipitation mechanisms are evidently related to the shearing processes that occur at the heat-treating temperature and may have an important bearing on age-hardening processes.

5. Body-centered rhombohedral Sb precipitates from face-centered cubic Pb as plates parallel to the $\{111\}$ planes of Pb, probably by the relation $\{111\}\text{Pb} \parallel \{001\}\text{Sb}$ and $[110]\text{Pb} \parallel [100]\text{Sb}$.

ACKNOWLEDGMENTS

Gerhard Ansel, member of the staff of the Metals Research Laboratory, Carnegie Institute of Technology, Pittsburgh, Pa., assisted with the metallographic work of section A. Dr. John A. Gann, of the Dow Chemical Co., Midland, Mich., very kindly supplied specimens for section A and gave much helpful advice.

REFERENCES

1. R. F. Mehl and collaborators: Studies upon the Widmanstätten Structure, I–VIII. *Trans. A.I.M.E.* (1931–1936) **93**, **99**, **105**, **113**, **117**.
2. G. Sachs: *Praktische Metallkunde*; Dritter Teil, Wärmebehandlung, 25 ff. Berlin, 1935. Julius Springer.
3. M. Hansen: *Der Aufbau der Zweistofflegierungen*, 871. Berlin, 1936. Julius Springer.
4. M. C. Neuburger: Gitterkonstanten 1933. *Ztsch. Krist.* (1933) **A86**, 395–422.
5. L. Pauling: The Crystal Structure of Magnesium Stannide. *Jnl. Amer. Chem. Soc.* (1923) **45**, 2777–80.
6. E. Zintl and H. Kaiser: Über die Fähigkeit der Elemente zur Bildung negativer Ionen. *Ztsch. anorg. allg. Chem.* (1933) **211**, 113–31.
7. E. Schmid and H. Seliger: Untersuchungen an binären Mischkristallen des Magnesiums. *Metallwirtschaft* (1932) **11**, 409–11.
8. E. Schmid and W. Boas: Kristallplastizität, 9–10, 90. Berlin, 1935. Julius Springer.
9. W. L. Fink and D. W. Smith: Age-hardening of Aluminum Alloys, I—Aluminum-copper Alloys. *Trans. A.I.M.E.* (1936) **122**, 284–300.
10. W. Köster: Zur Frage des Stickstoffs im technischen Eisen. *Archiv Eisenhüttenwesen* (1930) **3**, 653.
11. W. Boas and E. Schmid: *Ztsch. Phys.* (1931) **71**, 703.
12. R. W. G. Wyckoff: *The Structure of Crystals*, Ed. 2, 206–207. New York, 1931. Chemical Catalogue Co.

Lattice Relationships Developed by the Peritectic Formation of Beta in the Copper-zinc System

BY ALDEN B. GRENINGER,* MEMBER A.I.M.E.

(New York Meeting, February, 1937)

ALTHOUGH the crystallography of lattice transformations has been studied extensively during the past few years, these studies have been limited, with few exceptions^{1,2}, to specimens in which the transformed lattice appears as a segregate phase. A realization of the technical importance of the segregation mechanism, especially in the formation of martensitic structures and in age-hardening phenomena, has undoubtedly stimulated research in this direction.

In the crystallographic studies of segregation, the general problem has been to relate the orientation of the parent crystal to that of the segregate crystals. The technique has been complicated by the fact that it has been necessary to deal with the presence of as many as 24 ideal segregate orientations within one parent lattice; furthermore, the segregate lattices are invariably scattered (seldom less than $\pm 2^\circ$, often as much as 15° or 20°) about these ideal positions.

It is probable that a more complete picture of phase transformations may result from a study in which complete lattice relationships between individual grains are evaluated, thereby providing an additional parameter which when it is necessary to work with multiple segregate orientations, cannot be evaluated. The present paper presents the results of such a study,[†] wherein a peritectic reaction is made use of to produce the transformed lattices.

MATERIALS AND METHODS

Peritectic Reaction.—In Fig. 1 is reproduced a portion of the copper-zinc equilibrium diagram, which includes the peritectic reaction $\alpha + \text{liq.} \rightarrow \beta$. A liquid of composition between *B* and *D* upon solidifying will

Manuscript received at the office of the Institute Nov. 7, 1936.

* Instructor in Metallurgy, Graduate School of Engineering, Harvard University, Cambridge, Mass.

¹ References are at the end of the paper.

[†] The preliminary results of this study have been announced in *Nature* (April, 1936) 137, 657.

precipitate alpha (f.c.c.*) until the temperature of the peritectic horizontal is reached. At this temperature (900° C.) alpha of composition *B* and the remaining liquid of composition *D* react to produce a new phase, beta (b.c.c.*), of composition *C*. For our purposes it is necessary to note only that the *initial* course of the reaction must involve a diffusion of zinc atoms (or zinc and copper atoms) into the alpha dendrite along the

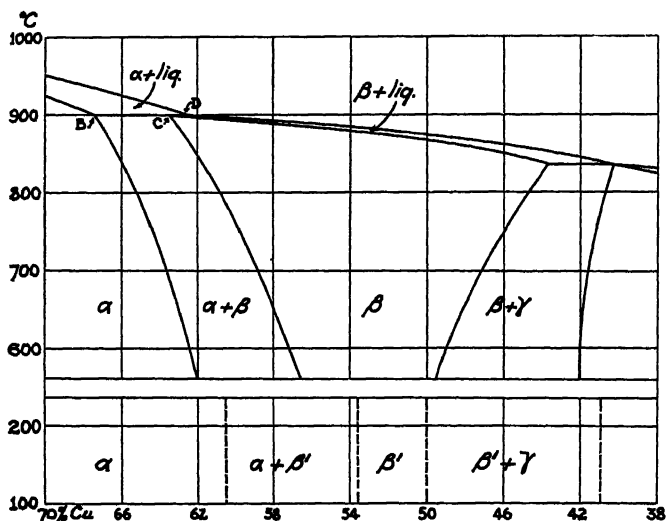


FIG. 1.—A PORTION OF THE COPPER-ZINC EQUILIBRIUM DIAGRAM. Liquidus and peritectic points after Schramm¹². Solid solubilities after Hansen¹³

alpha-liquid interfaces, and that this diffusion is accompanied by a transformation of a thin layer of alpha into beta.

Preparation of Specimens.—In order to preserve at room temperature large grains of beta with nuclei that have been formed by the peritectic reaction, it is necessary to introduce into the specimen a composition gradient extending into the center of the pure beta field. Furthermore, subsequent orientation studies may be facilitated by having only one orientation of alpha present in each specimen.

Specimens having these desired characteristics were prepared by solidifying a beta alloy under a unidirectional temperature gradient, and seeding the crystallization with a copper or alpha brass single crystal. The procedure was as follows: Several single crystals (prepared by a method already described³) were sectioned into two parts with a fine jeweler's saw. The sectioned surface was ground and polished and the crystal was then etched to remove about 0.5 mm. One of these crystals

* F.c.c. designates face-centered cubic lattice; b.c.c. designates body-centered cubic lattice.

(about $\frac{1}{2}$ in. long) was then placed in the bottom of a graphite crucible of which the inside diameter was only slightly larger than the diameter of the crystal (about $\frac{3}{8}$ in.). On top of the crystal were placed several pieces of beta brass (Cu = 52.76 per cent, Zn = 47.19 per cent, Fe = less than 0.01 per cent, Si = 0.006 per cent, Pb = none). The crucible containing the crystal and the beta brass was then placed in a vertical-tube furnace maintained at 1050° C. The crucible (uncovered) was observed through a small opening at the top of the tube; as soon as the beta brass had melted, the crucible was removed from the furnace, placed on an iron block, and allowed to remain there until it had cooled to room temperature. One or two faces (parallel to the cylinder axis) were prepared on each suitable specimen* by grinding and polishing; the specimen was then etched deeply with dilute HNO₃.

Photographs of two of these specimens are shown in Fig. 2. The specimens contain the following phases (in order, from bottom to top): (1) copper (or alpha brass) crystal seed, (2) primary crystallized alpha, having the same orientation as the seed, and (3) beta grains whose nuclei originated in the peritectic reaction; this beta phase has a narrow rim of segregate alpha. This order of crystallization is, of course, a consequence of the composition gradient caused by the diffusion of copper (or alpha brass) into the liquid beta.

Determination of Lattice Relationships.—The orientations of the individual copper and beta-brass crystals were determined by the back-reflection Laue X-ray method⁴. The over-all maximum inaccuracy of this camera amounts to less than 0.1°. The orientations were plotted stereographically (15 $\frac{3}{4}$ -in. circle), and the lattice relationships were evaluated to within either $\frac{1}{2}^\circ$ or $\frac{1}{4}^\circ$, depending upon the perfection of the pattern. A total of 41 lattice relationships were determined from five different specimens.† Specimens I, II and III were seeded with a copper

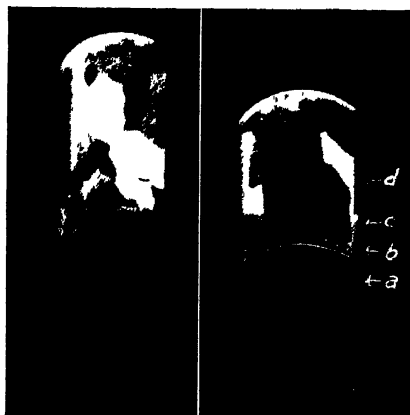


FIG. 2.—SPECIMEN I (LEFT); SPECIMEN II (RIGHT).

Twice natural size, etched with dilute HNO₃. a, copper seed; b, primary alpha and peritectic beta; c, primary beta and segregate alpha; d, primary beta.

* Several specimens were rendered useless by a too extensive diffusion of copper into the liquid beta.

† Two beta crystals at the top of one specimen were found to be randomly oriented with respect to the seed crystal and had evidently not been seeded by the peritectic reaction. These crystals are omitted in the tabulation of results. In general, only

crystal; specimen IV was seeded with an alpha brass (70-30) crystal. Specimen V was seeded with a copper crystal which had a rather pronounced macromosaic structure. Orientations reported for this specimen are averages; actual orientations registered on the X-ray patterns deviate from the mean $\pm 1^\circ$.

RESULTS

The Three Ideal Lattice Relationships.—Each beta crystal was found to be oriented in such a way with respect to its seed crystal that one or more of the following lattice relationships was approximated:

$$\begin{aligned} A & \left\{ \begin{array}{l} (110)_\beta // (111)_\alpha \\ (001)_\beta // (\bar{1}\bar{1}0)_\alpha \end{array} \right. \\ B & \left\{ \begin{array}{l} (110)_\beta // (111)_\alpha \\ (\bar{1}\bar{1}1)_\beta // (\bar{1}\bar{1}0)_\alpha \end{array} \right. \\ C & \left\{ \begin{array}{l} (100)_\beta // (100)_\alpha \\ (011)_\beta // (010)_\alpha \end{array} \right. \end{aligned}$$

Of the 41 grains, 38 closely approximated relationships *A* and *B*; relationship *C* was more closely approximated by only three grains. In both relationships *A* and *B* a dodecahedral beta plane is parallel to an octahedral alpha plane. The two relationships differ slightly ($5^\circ 16'$) in the alignment of directions within these planes. Relationship *A* is the one recently proposed independently by Nishiyama⁵ and Wassermann⁶ for the decomposition of iron-nickel austenite. Before publication of Nishiyama's and Wassermann's results, relationship *B* was generally accepted to hold for all oriented b.c.c. \rightleftharpoons f.c.c. transformations. Relationship *C* has been proposed by Bøggild⁷ to describe the highly scattered orientation relationships between kamacite and the octahedrite structure of meteoric irons. For any one parent lattice there are 24 possible *B* orientations, 12 possible *A* orientations, and only three possible *C* orientations. Each *A* orientation is a geometrical average of two adjacent *B* orientations; each *C* position lies at the geometrical center of ($9^\circ 44'$ removed from) four *A* positions. Each *C* position may be produced by placing the alpha and beta lattices parallel and then rotating the beta lattice 45° about $\langle 100 \rangle_\beta$.

A summary of orientation results is contained in Table 1, wherein the actual orientations are expressed in terms of deviations from the above ideal crystallographic relationships. The data contained in Table 1 may perhaps be more clearly visualized after an inspection of Fig. 3, which represents a stereographic projection of the pertinent poles of one of the evaluated lattice relationships.

the first and second layers of beta grains adjacent to the seed on each specimen face were studied.

TABLE 1.—*Orientation Relationships Developed by the Peritectic Transformation**
Expressed in Terms of Deviations (in Degrees) from Ideal Lattice Relationships

Specimen and Grain No.	Deviations from, Degrees				
	Relationship A and B (110) β //(111) α	Relationship A (001) β //(1 $\bar{1}$ 0) α	Relationship B (1 $\bar{1}$ 1) β //(1 $\bar{1}$ 0) α	Relationship C	
				(100) β //(100) α	(011) β //(010) α
Ia	3 $\frac{1}{4}$	2	2 $\frac{1}{2}$		
b	1	1	4 $\frac{1}{2}$		
c	1	1	4		
d	4 $\frac{1}{2}$	3	5 $\frac{1}{2}$		
e	2 $\frac{1}{2}$	12	6 $\frac{1}{2}$		
f	3	2 $\frac{1}{2}$	5		
g	1	2	2 $\frac{1}{4}$		
h	3	3 $\frac{1}{2}$	3 $\frac{1}{2}$		
i	4 $\frac{1}{2}$	3 $\frac{1}{2}$	5 $\frac{3}{4}$		
j	2	1 $\frac{1}{2}$	4		
k	2	3	3 $\frac{1}{2}$		
l	3 $\frac{1}{4}$	1 $\frac{1}{2}$	4 $\frac{3}{4}$		
m	9 $\frac{1}{2}$	6 $\frac{1}{2}$	7	4	5 $\frac{1}{2}$
n	3	9	2 $\frac{3}{4}$		
o	3 $\frac{3}{4}$	8	2		
Average for specimen.....	2 $\frac{1}{2}$	3 $\frac{3}{4}$	4		
IIa	3	8	3 $\frac{1}{2}$		
b	3	8	4		
c	2 $\frac{1}{2}$	2	4 $\frac{1}{2}$		
d	1 $\frac{1}{2}$	2 $\frac{3}{4}$	3		
e	1 $\frac{1}{2}$	2 $\frac{3}{4}$	3		
f	4	1 $\frac{1}{2}$	5		
g	2	6	2		
Average for specimen.....	2 $\frac{1}{2}$	4 $\frac{1}{2}$	3 $\frac{1}{2}$		
IIIa	2	1 $\frac{1}{2}$	5		
b	1 $\frac{1}{2}$	3 $\frac{1}{2}$	4 $\frac{3}{4}$		
c	1 $\frac{1}{2}$	1	5		
d	2	3 $\frac{1}{2}$	3		
Average for specimen.....	1 $\frac{1}{2}$	1 $\frac{1}{2}$	4 $\frac{1}{2}$		
IVa	3	1	6		
b	3	3 $\frac{1}{4}$	4		
c	1 $\frac{3}{4}$	2 $\frac{3}{4}$	3 $\frac{1}{4}$		
d	2 $\frac{1}{2}$	2 $\frac{3}{4}$	4 $\frac{1}{2}$		
e	1	4	2		
f	1 $\frac{1}{2}$	4	1		
Average for specimen.....	2	3	3 $\frac{1}{2}$		
Va	6	3	5	5	1 $\frac{1}{2}$
b	2	3	4		
c	1	3	3		
d	2	4	4		
e	2	4	3		
f	2	3	3		
g	7	4	10	3	4
h	3	7	3 $\frac{1}{2}$		
i	3	3 $\frac{1}{2}$	3		
Average for specimen.....	2 $\frac{1}{4}$	4	3 $\frac{1}{2}$	4	2 $\frac{1}{4}$
Average for specimens I to V.....	2 $\frac{1}{4}$	3 $\frac{1}{2}$	3 $\frac{3}{4}$	4	3 $\frac{1}{4}$

* The three grains that more closely approximate relationship C are not included in the calculation of averages of the first three columns.

The figures for average deviations, shown in Table 1, do not indicate a preference for either of the two common relationships (*A* and *B*). Thus the average deviation from $(110)_\beta // (111)_\alpha$ is $2\frac{1}{4}^\circ$, from $(001)_\beta // (1\bar{1}0)_\alpha$ is $3\frac{1}{2}^\circ$, and from $(1\bar{1}1)_\beta // (1\bar{1}0)_\alpha$ is $3\frac{3}{4}^\circ$. However, the figures on deviation frequencies (Table 2) favor relationship *A*; deviations of 2° or less were found for twenty-one $(110)_\beta // (111)_\alpha$, twelve $(001)_\beta // (1\bar{1}0)_\alpha$, and only four $(1\bar{1}1)_\beta // (1\bar{1}0)_\alpha$; the corresponding deviation frequencies of 1° or less were, respectively, eight, six and one.

TABLE 2.—Frequency of Deviations^a

Deviations of	From $(110)_\beta // (111)_\alpha$	From $(001)_\beta // (1\bar{1}0)_\alpha$	From $(1\bar{1}1)_\beta // (1\bar{1}0)_\alpha$
1° or less.....	8	6	1
$1\frac{1}{4}^\circ$ to 2°	13	6	3
$2\frac{1}{4}^\circ$ to 3°	12	10	10
$3\frac{1}{4}^\circ$ to 4°	3	9	11
More than 4°	2	7	13

^a The three grains that more closely approximate relationship *C* are not included in this tabulation.

Direction of Deviation.—For deviations from $(110)_\beta // (111)_\alpha$ of 2° or less, the direction of deviation from relationship *A* or *B* appears to be purely random. For deviations greater than $2\frac{1}{2}^\circ$ or 3° , a preferred deviation direction exists, becoming more pronounced the greater the deviation from $(110)_\beta // (111)_\alpha$; this deviation direction is toward the adjacent *C* position.

Any given *A* position is $9^\circ 44'$ removed from a *C* position; that is, the angle between $(100)_\beta$ and $(100)_\alpha$ is $9^\circ 44'$. For the two *B* positions adjacent to the given *A* position, this angle is about $10\frac{1}{2}^\circ$. Consequently, for a lattice relationship which lies between *A* and *B*, the angle between $(100)_\beta$ and $(100)_\alpha$ will be slightly more than 10° ; and for any given lattice relationship that deviates from *A* and *B*, the value of this angle will indicate whether or not the deviation has been in the general direction of the adjacent *C* position.

Of the seventeen grains that deviate from $(110)_\beta // (111)_\alpha$ by $2\frac{1}{2}^\circ$ to $4\frac{1}{2}^\circ$, ten show a decrease in the angle between $(100)_\beta$ and $(100)_\alpha$, six show an increase, and one shows no change, as follows:

Increases (to): 12° , 11° , $11\frac{1}{2}^\circ$, $11\frac{1}{2}^\circ$, $13\frac{1}{2}^\circ$, $14\frac{1}{2}^\circ$,

Decreases (to): $6\frac{1}{2}^\circ$, 7° , 8° , 7° , 8° , $5\frac{1}{2}^\circ$, 7° , 7° , 8° , 8° .

However, five of the six orientations that show increases have angles between $(001)_\beta$ and $(1\bar{1}0)_\alpha$ of 12° , 9° , 8° , 8° and 8° , respectively; hence, might be regarded as exceptions to any generalization. The three grains that deviate from $(110)_\beta // (111)_\alpha$ by 4° to $4\frac{1}{2}^\circ$ all show large decreases in the angle between $(100)_\beta$ and $(100)_\alpha$. Furthermore, the only three grains

found to deviate from $(110)_\beta // (111)_\alpha$ by more than 5° all approximate relationship C more closely than either A or B .

DISCUSSION

Crystallographic studies of the segregation of alpha from beta in copper-zinc alloys have been made by Weerts⁸, Marzke⁹, and Mehl¹⁰. Both Weerts and Marzke conclude that the resulting orientations are best accounted for by relationship B . Mehl's investigation was largely confined to a study of the Widmanstätten structure; lattice relationships were not determined. Thus, the relationship found for alpha-beta segregate structures does not coincide with the relationship statistically favored by the peritectic transformation. The results of the investigation are likewise in disagreement with the theory, currently held by the German investigators in this field (see, for instance, Wassermann⁶), which states that high-temperature transformations (involving nucleation and grain growth) produce randomly oriented structures.

In comparing the above results with those obtained by previous investigators on segregate structures, it should be remembered that these earlier studies dealt with specimens in which the segregate lattices were in the form of a multiple-fiber structure.* The crystallographic relationships that appear in the literature cannot fully describe the orientations that actually exist in these specimens; they merely state which ideal lattice relationship can best account for the composite effect (on the X-ray patterns) due to the presence of both multiple orientations and scattering. Assume, for example, that a specimen were available in which the distribution of segregate lattices conformed with those given in Table 1. The X-ray patterns obtained from this specimen (following the technique employed by Nishiyama, Wassermann, and others) would, according to the tabulation of deviation frequencies, agree nicely with relationship A , notwithstanding the fact that no single segregate lattice would actually be in an A position.

Apparently, then, lattice transformations in general produce structures in which the new lattices are not all in the same position with respect to the parent lattice. Too often this fact is lost sight of, and little attention indeed has been paid to these deviations, which are generally considered as induced by stresses due to the volume change that always accompanies a lattice transformation. Nevertheless, it is possible, indeed probable, that the scattering of orientations is not wholly secondary in origin and that the ideal crystallographic relationship defines only one of many adjacent positions delimited by the transformation. If this is true, relationships A , B and C may be, intrinsically, of small importance, and should be regarded merely as convenient reference positions.

* A composite of several individual fiber structures is described as a multiple-fiber structure.

It has often been remarked that in b.c.c. \rightleftharpoons f.c.c. transformations, relationship *A* (or *B*)* permits a good matching of atomic positions on the most closely packed planes (which are always of about equal spacing) of the two lattices; various shearing movements have been proposed to explain the mechanism by which the atom positions on the transformed lattice are derived from those on the parent lattice. These shearing mechanisms, arbitrarily proposed, are, of course, not to be regarded as giving an "explanation" of lattice relationships. They have, however, permitted certain correlations to be made (in terms of results) between transformations involving phases of different crystal structures. Unfortunately, they are inapplicable to what is geometrically the simplest type of transformation—a transformation in which the two phases are of the same crystal structure but differ in lattice parameter.

It is undoubtedly true that any *general* approach to the explanation of lattice relationships developed by phase transformations must consider the lattice-point interchange in terms of three dimensions; furthermore, the approach logically must be from a statistical viewpoint. As a preliminary step, however, it should be interesting to correlate, for the transformations f.c.c. \rightarrow f.c.c. and f.c.c. \rightarrow b.c.c., the lattice relationships that would allow the best matching of atomic positions in three dimensions with the relationships experimentally determined. It will be necessary to assume that the transformations proceed by a process of nucleation followed by growth. Although the position assumed by a nucleus must be the result of a cooperation of forces between a large number of atoms, and in the final analysis there can be no sharp separation between the end of nucleation and the beginning of growth, for purposes of calculation only it might be assumed that a nucleus may be formed by a coördination number of atoms† moving into their positions on the new lattice.

An f.c.c. \rightarrow f.c.c. transformation has been studied by Barrett, Kaiser and Mehl¹¹; they proved that the lattices of the phase precipitating from both silver-rich and copper-rich copper-silver alloys were always parallel to the lattice of the parent phase. The parameter differences for these transformations were about 10 per cent: judging from the X-ray patterns, deviations must have been extremely small—probably less than 1°. It is evident, then, that the experimentally determined lattice relationship is also that which permits the best matching of atomic positions.‡ For the f.c.c. \rightarrow f.c.c. transformation, the minimum position (in which the sum of all atom displacements needed to reach the new positions, and therefore

* An *A* position permits the best matching in two dimensions; a *B* position the best matching in one dimension.

† The number of nearest atom sites surrounding any given atom site on the nucleus lattice.

‡ This is true no matter how many atoms cooperate in the formation of a nucleus, so long as we assume a reasonable minimum number.

to form a nucleus, is a minimum) is reached only when the lattices are parallel. Under these conditions, all displacements are equal in

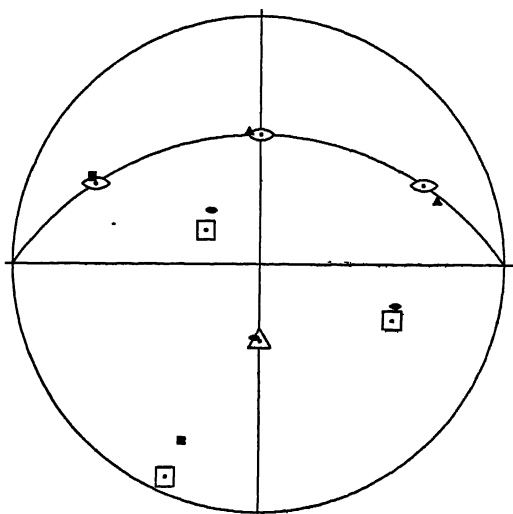


FIG. 3.—STEREOGRAPHIC PLOT OF PERTINENT POLES OF LATTICE RELATIONSHIP DETERMINED FOR GRAIN IVd (TABLE 1).

Large symbols indicate poles of copper seed; small symbols, poles of beta grain IVd.

magnitude and any random deviation from parallelism would involve an increase in each displacement. The proportionate increase in total

TABLE 3.—Displacements Required for Nucleus Formation^a

Relationship	Individual Displacements		Total Displacements Å.
	Number of Displacements	Å.	
<i>C</i>	8	0.443	3.54
<i>A</i>	4	0.246	4.07
	4	0.774	
<i>B</i>	2	0.065	4.18
	2	0.480	
	2	0.642	
	2	0.905	

^a The ratio of displacements *A*:*B*:*C* tends to favor *C* all the more as we include more zones of neighboring atoms in the calculations. Thus, displacement considerations would show a higher ratio in favor of *C* for b.c.c. → f.c.c. (12 atom positions) than the above ratio for f.c.c. → b.c.c.

displacements for a given angular deviation would be a function of the difference in lattice parameter of the two phases. For example, if the

parameter difference is 1 per cent, a deviation from parallelism of about 1° would require (roughly) twice the total displacement needed when the lattices are parallel. For a 10 per cent difference in parameter, displacements would be doubled (roughly) by a deviation from parallelism of about 12° .

For the transformation f.c.c. \rightarrow b.c.c., the minimum position is defined by relationship C (see p. 382). If lattice parameters are assigned to the two crystalline phases involved in the peritectic transformation* as fol-

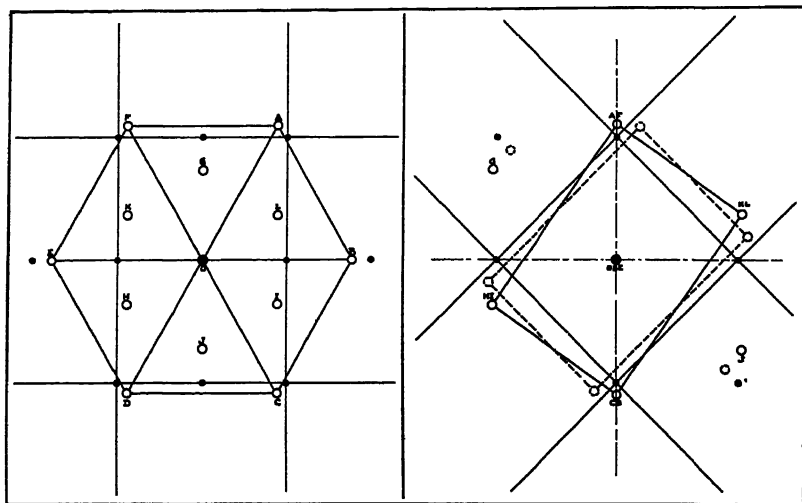


FIG. 4.—*a* (LEFT), CENTER ATOM AND TWELVE COORDINATING ATOMS OF ALPHA (F.C.C.) AND NEAREST CORRESPONDING POSITIONS OF BETA (B.C.C.) PROJECTED ON $(111)_\alpha // (110)_\beta$ ACCORDING TO RELATIONSHIP A.

b (RIGHT), CROSS-SECTIONAL VIEW OF $4a$ ON $(1\bar{1}0)_\alpha // (001)_\beta$, AND ADDITIONAL POINTS (BROKEN CIRCLES) THAT DESIGNATE F.C.C. ATOM POSITIONS ACCORDING TO RELATIONSHIP C.

C positions are derived from A positions by rotating $9^\circ 44'$ about axis BOE .

Dots indicate b.c.c. atom positions; open circles, f.c.c. atom positions (relationship A); broken circles, f.c.c. atom positions (relationship C).

lows: $\beta = 2.945 \text{ \AA}$, and $\alpha = 3.70 \text{ \AA}$, then the actual displacements required for nucleus formation (eight atoms + center atom) according to relationships A, B and C are as shown in Table 3 and Fig. 4. Relationship C, then, defines the position at which the total displacement is a minimum, and in this position all displacements are equal. A deviation from this position would increase the total displacement; but inasmuch as any deviation within limits (up to $\pm 9^\circ 44'$ about $[1\bar{1}0]_\alpha // [001]_\beta$; up^u to $\pm 5^\circ 16'$ about $[111]_\alpha$, etc.—see Fig. 4) would increase some individual displacements and decrease others, the proportionate total increase for a given angular deviation will be much less than for the transformation

* The room-temperature parameters of 52 per cent Cu and 62 per cent Cu, respectively.

f.c.c. \rightarrow f.c.c. Consequently, if nucleus position is delimited by minimum displacement considerations, we should expect considerably larger deviations from the most frequent position for f.c.c. \rightarrow b.c.c. than for f.c.c. \rightarrow f.c.c.

It is evident that the most frequent orientation relationship for the peritectic transformation does not agree with relationship *C*; it does, however, lie amidst relationships *A*, *B* and *C*, although closer to *A* and *B* than to *C*. It is not to be expected, of course, that a complete correlation should be arrived at from such a simple comparison. An important variable, which may have to be considered in a final displacement analysis of the f.c.c. \rightarrow b.c.c. transformation (and not in the f.c.c. \rightarrow f.c.c. transformation), is the multiplicity factor. That is, the final position assumed by *any* number of atoms may be some resultant of three mutually opposing tendencies to assume *C* positions. However, judging from the data now available, it is apparent that a consideration of minimum displacements, although providing a loose explanation of deviations, will not in itself be capable of defining the most probable lattice relationship.

SUMMARY

1. By seeding the crystallization of a 52-48 copper-zinc alloy (β) with a copper crystal, specimens suitable for accurate X-ray study of orientation relationships developed by the peritectic reaction $\alpha + \text{liq.} \rightarrow \beta$ may be prepared.

2. In spite of the fact that the peritectic transformation takes place at the highest temperature possible for an alpha brass \rightleftharpoons beta brass transformation, oriented lattices are developed.

3. The beta lattices are related to the alpha seed in such a way that three lattice relationships (defined on p. 382) are approximated.

4. Considerations of minimum atom displacements would provide a satisfactory explanation of deviations from ideal lattice relationships, but would be incapable, at present, of defining the most probable or mean lattice relationship.

REFERENCES

1. R. F. Mehl, E. L. McCandless and F. N. Rhines: Orientation of Oxide Films on Metals. *Nature* (1934) **134**, 1009.
2. R. F. Mehl and E. L. McCandless: Orientation of Oxide Films on Iron. *Nature* (1936) **137**, 702.
3. A. B. Greninger: The Crystallographic Uniformity of Lineage Structure in Copper Single Crystals. *Trans. A.I.M.E.* (1935) **117**, 75-83.
4. A. B. Greninger: A Back-reflection Laue Method for Determining Crystal Orientation. *Trans. A.I.M.E.* (1935) **117**, 61-74; *Zisch. Krist.* (1935) **A91**, 424-432.
5. Z. Nishiyama: X-ray Investigation of the Mechanism of the Transformation from Face-centered Cubic Lattice to Body-centered Cubic. *Sci. Repts. Tohoku Imp. Univ.* (November, 1934) **22**, 637-664.

6. G. Wassermann: Über den Mechanismus der α - γ Umwandlung des Eisens. *Mitt. K. W. Inst. Eisenforsch.* (1935) **17**, 149-155.
7. O. B. Bøggild: The Meteoric Iron from Savik near Cape York, North Greenland. *Særtryk af Meddelelser om Grønland* (1927) **74**, 1-30.
8. J. Weerts: Über Umwandlungsvorgänge im β -Messing und in β -Silber-Zinklegierungen. *Ztsch. Metallkunde* (1932) **24**, 265-270.
9. O. T. Marzke: Precipitation of Alpha from Beta Brass. *A.I.M.E. Contrib.* **29** (1933).
10. R. F. Mehl and O. T. Marzke: Studies upon the Widmanstätten Structure—The Beta Copper-zinc and Beta Copper-aluminum Alloys. *Trans. A.I.M.E.* (1931) **93**, 123-152.
11. C. S. Barrett, H. F. Kaiser and R. F. Mehl: Studies upon the Widmanstätten Structure, VII—The Copper-silver System. *Trans. A.I.M.E.* (1935) **117**, 39-60.
12. J. Schramm: Beitrag zum Kupfer-Zink-Diagramm. *Metallwirtschaft* (Dec. 6, 1935) **14**, 995-1001.
13. M. Hansen: Der Aufbau der Zweistofflegierungen, 655, 660. Berlin, 1936. Julius Springer.

DISCUSSION

(C. H. Samans presiding)

L. W. McKEEHAN,* New Haven, Conn.—I have two comments, both mathematical in character. The first has to do with the use of vulgar fractions to indicate parts of degrees. I suppose it is an instinct of modesty on the part of the author to underestimate his precision by using such fractions as $\frac{1}{2}$, $\frac{1}{3}$, $\frac{1}{4}$, etc., rather than the more perspicuous decimal fractions, but that is not consistent, of course, with the appearance in the same table of both $\frac{1}{2}$ and $\frac{1}{4}$. The difference between those is only a little over 0.08, so that in effect the author is actually estimating to tenths or better. It seems to me considerably easier for the reader if it is understood that the data are perhaps not precise to tenths but that recording in tenths is the most convenient way to do it.

The second point is in respect to the small change in translations required for considerable deviations from position *C*, as the author has named it. That is, of course, merely a mathematical characteristic of a minimum. If one has a minimum sum, considerable deviations from the minimum state are accompanied by small changes in the sum.

G. DERGE,† Pittsburgh, Pa.—A question arises in my mind in connection with the deviations of orientation the author has found. In an earlier paper² he found that copper crystals grown from the melt were highly imperfect, or, in his terminology, had a pronounced "lineage structure." I wonder if this factor may not be responsible for some of the deviations found in these brasses, which seem to offer a favorable opportunity for the development of this type of imperfection.

R. F. MEHL,‡ Pittsburgh, Pa.—Dr. Greninger has contributed some very excellent new data on the important question of the atomic genesis of metallic phases: data such as these are very welcome in a rapidly expanding field.

* Director, Sloane Physics Laboratory, Yale University.

† Metals Research Laboratory, Carnegie Institute of Technology.

‡ Metals Research Laboratory and Department of Metallurgy, Carnegie Institute of Technology.

The connection between orientation relationships assumed when a new phase appears by a peritectic reaction, and when it appears as a result of a solid-solid precipitation or transformation, is closer than might appear on first sight. Dr. McCandless and I have shown¹⁴ that reaction layers of the oxides of iron formed on iron by direct oxidation are distinctly oriented—just as Dr. Greninger's peritectic reaction layers are oriented, and as crystal overgrowths generally are oriented when lattice dimensions permit. Furthermore it has been shown that the orientation relationships that exist between "FeO" and Fe_2O_4 in oxidation layers are identical with those that obtain when Fe_2O_4 precipitates from "FeO" on cooling. Thus it seems that the orientation relationships between two conjugate phases may perhaps in every case be the same. If this may be assumed, evidently an indirect but much simpler method of solving Widmanstätten relationships is available. Work done recently by Mr. Woo in the Metals Research Laboratory, on the generation of β -brass from α -brass by inward diffusion of zinc vapor, supports this conclusion, for the orientation relationships seem identical with those that occur when α -brass is precipitated from β -brass.

It is generally assumed by the metallurgical profession that papers of this sort are wholly theoretical and therefore of no practical importance. As a matter of fact, there is a confusion in terms here. Dr. Greninger's excellent paper, for instance, is not theoretical; it is experimental scientific, having as its objective an understanding of the atom mechanism in a phenomenon that is familiar to all metallurgists. If Dr. Greninger will pardon a personal reference—which I intrude on his good nature chiefly in support of and to justify such work as he has been doing for some years—I should like to refer to the many occasions when friends have asked me what the practical importance might be of our studies on Widmanstätten mechanisms, inferring that if there is no immediate and easily recognizable importance the metallurgist should not waste his time on mental playthings. I think it would be well to state here the justification of such work.

While it is an obvious truth that the metallurgist must be primarily interested in the engineering production and application of metals and alloys, it is now a well recognized fact in all branches of science and engineering that progress in industry will be the more rapid and the more certain as the development of the science itself is the more rapid and the more certain. Since age-hardening and heat-treatment are matters of prime practical importance, is it not then desirable to understand as much as possible of the basic atom processes that operate in age-hardening and in the heat-treatment of alloys. How much clearer are our notions—our practical notions—of recrystallization as a result of Jeffries' "theoretical" work on this subject, and how much greater is our effectiveness—our effectiveness in practice—in developing age-hardening alloys as a result of Merica's theory! Studies on Widmanstätten figures have as their objective an understanding of the atom mechanisms of precipitation and transformation. When we understand these mechanisms thoroughly, perhaps we shall be able to contribute directly to engineering, in much the same way as studies on the mechanism of chemical reactions, much pursued 30 years ago, now contribute to chemical engineering.

A. B. GRENINGER (written discussion).—The listing of both thirds and quarters of a degree in the same table, when the limit of accuracy has been placed at $\frac{1}{4}$, is, as Dr. McKeehan has stated, unfortunate. Needless to say, the average given at the bottom of Table 1 should read $3\frac{1}{4}$ instead of $3\frac{1}{2}$.

It is probable that no single factor is entirely responsible for the orientation deviations reported. However, judging from the evidence available, it would seem that

¹⁴ R. F. Mehl and E. L. McCandless: Oxide Films on Iron. *A.I.M.E. Tech. Pub.* 780 (1937).

macromosaic structure has little effect. The figures obtained from specimen 5 are similar to those from other specimens, yet No. 5 seed had a pronounced macromosaic structure ($\pm 1^\circ$) and the other crystal seeds were highly perfect in structure.

INDEX

(NOTE: In this index the names of authors of papers and discussions and of men referred to are printed in SMALL CAPITALS, and the title of papers in *italics*)

A

- ACKERMAN, D. E : *Discussion on Equipment for Routine Creep Tests on Zinc and Zinc-base Alloys, and an Example of Its Application*, 267
- Admic: cold-rolled: fatigue properties, 271
- Age-hardening (*See also* Precipitation-hardening and names of metals): effect of aging temperature, 153
- elastic limit of single crystals of aluminum, silver and zinc: influence of temperature, 247
- knot formation: meaning of term, 161, 169
- knot formation and precipitation two consecutive steps, 138
- knot theory: no need for it, 162, 163
- origin, 169, 170
- Aging: double *See* Double Aging
- Alloys: segregation: brief bibliography, 323
- systems: designation of phases, 78
- Aluminum alloys: electrical conductivities, 287
- thermal conductivity, 287
- Aluminum-copper alloys: diffusion in liquid state, 320, 329
- segregation: gravity, on melting, 318
- inverse, 314, 322
- normal, 320
- relation of diffusion rate, 331
- Aluminum-magnesium alloys: age-hardening: microscopic examination, 162
- homogenized sheet containing 10 per cent Mg, 162
- equilibrium relations, 85
- microscopic examination, 163
- segregation: normal, 321
- relation of diffusion rate, 331
- Aluminum-magnesium-zinc alloys: aluminum corner: equilibrium relations, 78
- electrical conductivity, 81, 92, 110
- equilibrium relations: bibliography, 108
- etching characteristics, 100, 109
- high-purity: equilibrium relations, 78
- microscopic examination, 78
- structure, 101
- workability, 78, 109
- X-ray identification of phases, 81
- Aluminum Research Laboratories: study: of age-hardening of aluminum-magnesium alloys, 162
- Aluminum Research Laboratories: study: of equilibrium relations in aluminum-magnesium-zinc alloys of high purity, 78
- of thermal and electrical conductivities of aluminum alloys, 287
- Aluminum-zinc alloys: equilibrium relations, 84
- American Brass Co. Copper Alloys Research Laboratory: study of thermal and electrical conductivities of aluminum alloys, 287
- American Institute of Mining and Metallurgical Engineers: awards: certificate of Institute of Metals Division: list, 10
- Divisions: Institute of Metals: annual award certificate, 10
- officers and committees, 9
- lectures: Institute of Metals: lecturers, 7
- officers and directors, 8
- Antimony: solid solubility in copper, 68
- Arsenic: solid solubility in copper, 64

B

- BAILEY, R. W : *Discussion on Fatigue Properties of Five Cold-rolled Copper Alloys*, 285
- BAILEY, R. W AND PRICE, W. B : *Fatigue Properties of Five Cold-rolled Copper Alloys*, 271
- BARRETT, C. S.: *The Stereographic Projection*, 29
- Discussions on Effect of Reversed Deformation on Recrystallization*, 365
- on Equipment for Routine Creep Tests on Zinc and Zinc-base Alloys, and an Example of Its Application*, 268
- BECK, P. A.: *Effect of Reversed Deformation on Recrystallization*, 351; *discussion*, 365
- Beryllium alloys: use in telephone industry would increase if cost could be reduced, 186
- Bismuth: solid solubility in copper, 75
- BRAY, J. L : *Lead Coating of Steel*, 199; *discussion*, 207
- BRICK, R. M. AND PHILLIPS, A.: *Diffusion of Copper and Magnesium into Aluminum*, 331; *discussion*, 349
- Segregation in Single Crystals of Solid Solution Alloys*, 313; *discussion*, 330
- Bronze: phosphor: cold-rolled: fatigue properties, 271
- vs. silicon for switches and springs, 271
- silicon, 3 per cent: cold-rolled: fatigue properties, 271
- vs. phosphor for switches and springs, 271

- BROPHY, G. R.: *Discussion on Fatigue Properties of Five Cold-rolled Copper Alloys*, 282
 BURGHOFF, H. L.: *Discussion on Fatigue Properties of Five Cold-rolled Copper Alloys*, 282

C

- Carnegie Institute of Technology, Metals Research Laboratory. studies on the Widmanstätten structure, 367
 CHRISTIE, J. L.: *Discussion on Precipitation-hardening and Double Aging*, 187
 COHEN, M.: *Aging Phenomena in a Silver-rich Copper Alloy*, 138; *discussion*, 159, 180
Discussion on Age-hardening of Aluminum Alloys, II—Aluminum-magnesium Alloy, 168, 170
 Cold-work hardening, definition, 187
 Copper, periodic subgroup Vb: effect of quenching strains on lattice-parameter values practically negligible, 59
 solid solubilities of elements, 59
 bibliography, 76
 X-ray analysis, 69
 solid solubility in silver, 159, 160
 Copper alloys: fatigue properties of five cold-rolled, 271
 Copper-antimony alloys: solid solubility, 68
 Copper-arsenic alloys: solid solubility, 64
 Copper-bismuth alloys: solid solubility, 75
 Copper-chromium-beryllium alloys: double aging with intermediate cold-working, 175
 Copper-cobalt-beryllium alloys. precipitation-hardening, 172
 Copper-nickel-tin alloy: Adnic: cold-rolled: fatigue properties, 271
 Copper-phosphorus alloys: solid solubility, 59
 Copper-tin alloys: segregation: inverse, 323
 Copper-silicon alloys: segregation: inverse, 322
 Copper-silver alloys: segregation: inverse, 322
 Copper-zinc alloys: etching: electrolytic, 189
 lattice relationships developed by peritectic formation of beta, 379
 microscopic study, 189
 CRAMPTON, D. K.: *Discussion on Relations between Stress and Reduction in Area for Tensile Tests of Metals*, 227
 Creep test (*See also* names of metals): effect of vibration, 270
 equipment specially designed, 252
 as indication of drawing properties, 268, 269
 superior to tensile test as tool for comparison of certain metals in investigative testing, 252
 Crystallization of metals: casting experiments, 306, 309
 primary: laws governing, 300
 undercooling, 303
 Crystallography: lattice relationships developed by peritectic formation of beta in copper-zinc alloys, 379
 Miller indices, 38
 peritectic formation of beta in copper-zinc system: lattice relationships, 379
 pole figures: interpretation, 54
 plotting, 49
 stereographic projection, 49

- Crystallography stereographic projection *See* Stereographic.
 Crystals, aluminum. single: behavior above and below recrystallization, 242
 elastic limit: temperature influence, slow tensile tests, 229
 yield-point elongation, 236, 243, 247, 251
 yield-point elongation, 236, 243, 247, 251
 Crystals, metallic: cubic system: angles between planes, 40
 lattice relationships developed by peritectic formation of beta in copper-zinc system, 379
 recrystallization *See* Recrystallization
 segregation: meaning, 313
 single: elastic limit, aluminum, silver and zinc: brief bibliography, 245
 elastic limit: temperature influence on aluminum, silver and zinc, slow tensile tests, 229
 solid solution alloys: segregation in, 313
 yield-point elongation, 236, 243, 247, 251
 Crystals, silver: single: elastic limit: temperature influence, slow tensile tests, 229
 Crystals, zinc: single: elastic limit: temperature influence, slow tensile tests, 229

D

- DANSEN, J. R.: *Discussion on Equipment for Routine Creep Tests on Zinc and Zinc-base Alloys, and an Example of Its Application*, 268, 269
 DE FOREST, A. V.: *Discussions: on Fatigue Properties of Five Cold-rolled Copper Alloys*, 283
on Influence of Temperature on Elastic Limit of Single Crystals of Aluminum, Silver and Zinc, 247
on Relations between Stress and Reduction in Area for Tensile Tests of Metals, 227
 DERGE, G.: *Discussion on Lattice Relationships Developed by the Peritectic Formation of Beta in the Copper-zinc System*, 390
 DERGE, G., KOMMEL, A. R. and MEHL, R. F.: *Studies upon the Widmanstätten Structure, IX—The Mg-Mg₂Sn and Pb-Sb Systems*, 367
 Diffusion: copper in pure aluminum: anisotropy, 342
 calculation of coefficients, 334
 rate, 331
 magnesium in pure aluminum: calculation of coefficients, 337
 rate, 331
 molten alloys: aluminum-copper alloy, 320
 structures in diffusion zone: copper and magnesium in aluminum, 344
 DIX, E. H. JR.: *Discussion on Age-hardening of Aluminum Alloys, II—Aluminum-magnesium Alloy*, 170
 DORNBLATT, A. J.: *Discussion on Thermal and Electrical Conductivities of Aluminum Alloys*, 299

- Double aging: definition, 172
with intermediate cold-working, 175
with intermediate thermal strain-hardening, 174

E

- EDMUNDS, G. *Discussions on Equilibrium Relations in Aluminum-magnesium-zinc Alloys of High Purity*, 109
on *Equipment for Routine Creep Tests on Zinc and Zinc-base Alloys, and an Example of Its Application*, 269
on *Influence of Temperature on Elastic Limit of Single Crystals of Aluminum, Silver and Zinc*, 246
- Electrical conductivity: measurements destined for increasing use in studying alloys, 110
proportional relationship to thermal conductivity, 298
- Etching methods: electrolytic, 189
- Etching reagents: for aluminum-copper alloys Keller, 170
for aluminum-magnesium-zinc alloys, 100, 109

F

- Fatigue testing: dimensioning specimens, 284
- FERGUSON, L.: *Discussion on Lead Coating of Steel*, 206, 207
- FETZ, E. AND JETTE, E. R.: *Discussion on Equilibrium Relations in the Nickel-tin System*, 133
- FINK, W. L.: *Discussions: on Age-hardening of Aluminum Alloys, II—Aluminum-magnesium Alloy*, 169, 170, 171
on *Equilibrium Relations in Aluminum-magnesium-zinc Alloys of High Purity*, 109
on *Relations between Stress and Reduction in Area for Tensile Tests of Metals*, 227
- FINK, W. L. AND SMITH, D. W.: *Age-hardening of Aluminum Alloys, II—Aluminum-magnesium Alloy*, 162
Discussion on Aging Phenomena in a Silver-rich Copper Alloy, 158
- FINK, W. L. AND WILLEY, L. A.: *Equilibrium Relations in Aluminum-magnesium-zinc Alloys of High Purity*, 78
- FRECHE, H. R.: *Discussion on Diffusion of Copper and Magnesium into Aluminum*, 347
- Furnaces: thermal efficiencies, various, 15

G

- GATLER, M. L. V.: *Discussion on Aging Phenomena in a Silver-rich Copper Alloy*, 157
- General Electric Co. research laboratory: study of precipitation-hardening and double aging, 172
- GOETZEL, C. G.: *An Investigation to Develop Hard Alloys of Silver for Lining Ring Grooves of Light Alloy Pistons*, 194
- GONSER, B. W.: *Discussion on Precipitation-hardening and Double Aging*, 187

- GREENALL, C. H.: *Discussion on Fatigue Properties of Five Cold-rolled Copper Alloys*, 283
- GRENINGER, A. B.: *Lattice Relationships Developed by the Peritectic Formation of Beta in the Copper-zinc System*, 379; discussion, 391

H

- HARRINGTON, R. H.: *Precipitation-hardening and Double Aging*, 172; discussion, 186, 187, 188
- Harvard University: research on lattice relationships in copper-zinc system, 379
- HENSEL, F. R.: *Primary Crystallization of Metals*, 300
- HOYT, S. L.: *Discussions: on Effect of Reversed Deformation on Recrystallization*, 365
on *Relations between Stress and Reduction in Area for Tensile Tests of Metals*, 227
- HUTTON, R. S.: *Refractories*, 13
photograph, 12

I

- Institute of Metals Division lecture: list with names of lecturers, 7
sixteenth (HUTTON), 13
- Iron: annealed polycrystalline: load deformation, 249

J

- JETTE, E. R. AND FETZ, E.: *Discussion on Equilibrium Relations in the Nickel-tin System*, 133

K

- KEMPF, L. W.: *Discussions: on Relations between Stress and Reduction in Area for Tensile Tests of Metals*, 227
on *Segregation in Single Crystals of Solid Solution Alloys*, 329
on *Thermal and Electrical Conductivities of Aluminum Alloys*, 299
- KEMPF, L. W., SMITH, C. S. AND TAYLOR, C. S.: *Thermal and Electrical Conductivities of Aluminum Alloys*, 287
- Knot formation. See Age-hardening.
- KOMMEL, A. R., MEHL, R. F. AND DERGE, G.: *Studies upon the Widmanstätten Structure, IX—The Mg-Mg₂Sn and Pb-Sb Systems*, 367
- KOSTING, P. R. G.: *Discussion on Thermal and Electrical Conductivities of Aluminum Alloys*, 299

L

- Lattice: See Crystallography.
- Lead: coating for steel: corrosion resistance, 204
dipping sheets, 203
properties necessary, 199
sine as binding agent, 199
- Lead alloys: analysis by electrical-conductivity measurements, 203, 206
- Lead-antimony alloys: Widmanstätten structure, 367

- Lead-zinc alloys. lead-rich: equilibrium diagram, 200, 202
- LEITER, R. W. E. AND WINLOCK, J.: *Discussion on Influence of Temperature on Elastic Limit of Single Crystals of Aluminum, Silver and Zinc*, 248-250
- M
- MACGREGOR, C. W.: *Relations between Stress and Reduction in Area for Tensile Tests of Metals*, 208; discussion, 227
- Magnesium-tin alloys: Widmanstätten structure, 387
- Magnesium-zinc alloys: equilibrium relations, 85
- MATHEWSON, C. H.: *Discussion on Effect of Reversed Deformation on Recrystallization*, 365
- MATHEWSON, C. H. AND MERTZ, J. C.: *Solid Solubilities of the Elements of the Periodic Subgroup Vb in Copper*, 59
- McKEEHAN, L. W.: *Discussion on Lattice Relationships Developed by the Peritectic Formation of Beta in the Copper-zinc System*, 390
- MEHL, R. F.: *Discussions on Diffusion of Copper and Magnesium into Aluminum*, 349
on *Effect of Reversed Deformation on Recrystallization*, 364, 365
on *Lattice Relationships Developed by the Peritectic Formation of Beta in the Copper-zinc System*, 390
- MEHL, R. F., DERGE, G. AND KOMMEL, A. R.: *Studies upon the Widmanstätten Structure, IX—The Mg-Mg₂Sn and Pb-Sb Systems*, 367
- MERTZ, J. C. AND MATHEWSON, C. H.: *Solid Solubilities of the Elements of the Periodic Subgroup Vb in Copper*, 59
- Metallography: stereographic projection. *See* Stereography.
- Microscope: vs. X-ray for studying alloys, 168
- MIKULAS, W.: *Discussion on Equilibrium Relations in the Nickel-tin System*, 136
- MIKULAS, W., THOMASSEN, L. AND UPTREGEV, C.: *Equilibrium Relations in the Nickel-tin System*, 111
- Miller indices of crystal planes, 38
- MILLER, R. F.: *Discussions: on Effect of Reversed Deformation on Recrystallization*, 364, 365
on *Influence of Temperature on Elastic Limit of Single Crystals of Aluminum, Silver and Zinc*, 250
- MILLER, R. F. AND MILLIGAN, W. E.: *Influence of Temperature on Elastic Limit of Single Crystals of Aluminum, Silver and Zinc*, 229
- MILLIGAN, W. E. AND MILLER, R. F.: *Influence of Temperature on Elastic Limit of Single Crystals of Aluminum, Silver and Zinc*, 229
- N
- New Jersey Zinc Co.: creep tests with special equipment, 252
- New Jersey Zinc Co.: equipment for routine creep tests on zinc and zinc-base alloys, 252
notes on etching and microscopical identification of phases in copper-zinc system, 189
- Nickel-tin alloys: equilibrium relations, 111
discussion of previous investigations, 116, 133
solid solubility, 130
X-ray studies, 125
- NORMAN, T. E.: *Discussion on Influence of Temperature on Elastic Limit of Single Crystals of Aluminum, Silver and Zinc*, 248
- NORTON, J. T.: *Discussion on Age-hardening of Aluminum Alloys, II—Aluminum-magnesium Alloy*, 168 et seq
- P
- PEIRCE, W. M.: *Discussion on Equipment for Routine Creep Tests on Zinc and Zinc-base Alloys, and an Example of Its Application*, 268
- Peritectic formation. *See* Crystallography.
- PHILLIPS, A. J.: *Foreword*, 3
Discussions. on Aging Phenomena in a Silver-rich Copper Alloy, 159
on *Influence of Temperature on Elastic Limit of Single Crystals of Aluminum, Silver and Zinc*, 248
- PHILLIPS, ARTHUR AND BRICK, R. M.: *Diffusion of Copper and Magnesium into Aluminum*, 331; discussion, 349
Segregation in Single Crystals of Solid Solution Alloys, 313; discussion, 330
- PHILLIPS, R.: *Discussion on Aging Phenomena in a Silver-rich Copper Alloy*, 159
- Phosphorus: solid solubility in copper, 59
- Piston rings. light alloy: hard silver alloys for lining grooves, 194
- Pole figures. *See* Crystallography.
- Powder metallurgy: quenching, 136, 137
- Precipitation-hardening (*see also* Age-hardening): with double aging: definition, 172
- PRICE, W. B. AND BAILEY, R. W.: *Fatigue Properties of Five Cold-rolled Copper Alloys*, 271
- R
- Recrystallization of metals: changes caused by restraughtening, 358
consumptibility, 353
effect of reversed deformation, 351
no physical relation to hardening, 351
recrystallization power: definition, 352
- Refractories: bibliography, 26
- Degussa: properties, 25
- high-temperature oxides. bibliography, 27
- improvements suggested, 13
- materials used, 17
- melting points, 22
- relation to fuel economy, 16
- requirements, 17
- sintering: benefits, 23
- structure, 21

- Refractories: super-refractories: characteristics, 20
temperatures to be met, 14
thermal conductivities, 19
- RHINES, F. N.: *Discussions on Diffusion of Copper and Magnesium into Aluminum*, 348
on Segregation in Single Crystals of Solid Solution Alloys, 329
- RODDA, J. L.: *Notes on Etching and Microscopical Identification of the Phases Present in the Copper-zinc System*, 189
- RUZICKA, J.: *Equipment for Routine Creep Tests on Zinc and Zinc-base Alloys, and an Example of Its Application*, 252
- S
- SACHS, G.: *Discussions on Segregation in Single Crystals of Solid Solution Alloys*, 329
on Thermal and Electrical Conductivities of Aluminum Alloys, 298
- SCHUMACHER, E. R.: *Discussion on Precipitation-hardening and Double Aging*, 186
- Seovill Mfg Co: fatigue properties of five cold-rolled copper alloys, 271
- Segregation. *See* Crystals, Metallic, or various Alloys.
- Silver alloys. behavior with various metals, 195
hard: for lining ring grooves of light alloy pistons, 194
- Silver-copper alloys: age-hardening: knot formation, 155, 157, 158
pre-precipitation hardening, 151
silver-rich. age-hardening. effect of temperature, 153
aging phenomena, 138
bibliography, 156
electrical resistance, 149
gradual precipitation, 155
hardness changes during aging, 142
microstructure, 148
two-stage aging process, 138, 160
X-ray study, 147
solid solubility, 139, 159
- SMITH, A. A. JR.: *Discussion on Equipment for Routine Creep Tests on Zinc and Zinc-base Alloys, and an Example of Its Application*, 267
- SMITH, C. S.: *Discussion on Thermal and Electrical Conductivities of Aluminum Alloys*, 298
- SMITH, C. S., TAYLOR, C. S. AND KEMPF, L. W.: *Thermal and Electrical Conductivities of Aluminum Alloys*, 287
- SMITH, D. W. AND FINK, W. L.: *Age-hardening of Aluminum Alloys, II—Aluminum-magnesium Alloy*, 162
Discussion on Aging Phenomena in a Silver-rich Copper Alloy, 158
- Solid solubility: copper. elements of periodic subgroup Vb, 59
bibliography, 76
silver-copper alloys: influence of rate of cooling, 159
- STARR, C.: *Discussion on Influence of Temperature on Elastic Limit of Single Crystals of Aluminum, Silver and Zinc*, 247
- Steel lead coating. *See* Lead.
low-carbon: lead deformation, 249
- Stereographic nets, 34
- Stereographic projection. applications to metallography, 41
bibliography, 56
nets, 34
orientation relationships in twinned crystals, 47
pole figures in orientation studies, 49
principles and methods, 29
properties, 37
- Strain-hardening: definition, 187
would stress-hardening be better term? 187
- Stress-hardening: is this more descriptive than strain-hardening? 187
- T
- TAYLOR, C. S., KEMPF, L. W. AND SMITH, C. S.: *Thermal and Electrical Conductivities of Aluminum Alloys*, 287
- Tensile tests of metals: relations between stress and reduction in area: bibliography, 226
($S - q'$) method of determining, 208
- Thermal conductivity: proportional relationship to electrical conductivity, 298
- THOMASSEN, L., UPTHEGROVE, C. AND MIKULAS, W.: *Equilibrium Relations in the Nickel-tin System*, 111
- Tin: crystallization phenomena, 306
solid solubility in nickel, 130
- U
- UPTHEGROVE, C.: *Discussion on Equilibrium Relations in the Nickel-tin System*, 137
- UPTHEGROVE, C., MIKULAS, W. AND THOMASSEN, L.: *Equilibrium Relations in the Nickel-tin System*, 111
- W
- Weatherstrip: zinc alloy: beam tests, 260
creep tests, 252
spreading tests, 260
- WHEELER, R. J.: *Discussion on Fatigue Properties of Five Cold-rolled Copper Alloys*, 283
- Widmanstätten structure: lead-antimony alloys, 367
magnesium-tin alloys, 367
magnesium-tin and lead-antimony alloys: brief bibliography, 378
- WILLEY, L. A. AND FINK, W. L.: *Equilibrium Relations in Aluminum-magnesium-zinc Alloys of High Purity*, 78
- WINLOCK, J. AND LUTHER, R. W. E.: *Discussion on Influence of Temperature on Elastic Limit of Single Crystals of Aluminum, Silver and Zinc*, 248

Wise, E. M.: *Discussions on Aging Phenomena in a Silver-rich Copper Alloy*, 159
on Precipitation-hardening and Double Aging, 188

X

X-ray: advantage in study of alloys, 134, 137
 identification of phases aluminum-magnesium-zinc alloys, 81
 lattice relationships developed by peritectic formation of beta in copper-zinc system, 379
 limitations in study of alloys, 168
 study of nickel-tin systems, 125, 133
 study of silver-copper alloys during aging, 147

X-ray vs. microscopic method of studying alloys, 168

Y

Yale University: research on diffusion of copper and magnesium into aluminum, 331
 on segregation in single crystals of solid solution alloys, 313

Z

Zinc-base alloys: rolled: creep tests, as indication of drawing properties, 268, 269
 with specially designed equipment, 252
 weatherstrip. *See* Weatherstrip

